ISSN 2307-8960 (online)

World Journal of *Clinical Cases*

World J Clin Cases 2023 February 6; 11(4): 719-978

Published by Baishideng Publishing Group Inc

World Journal of Clinical Cases

Contents

Thrice Monthly Volume 11 Number 4 February 6, 2023

MINIREVIEWS

ORIGINAL ARTICLE

Clinical and Translational Research

Retrospective Study

Clinical Trials Study

Observational Study

World Journal of Clinical Cases

Thrice Monthly Volume 11 Number 4 February 6, 2023

Contents

World Journal of Clinical Cases

Thrice Monthly Volume 11 Number 4 February 6, 2023

Contents

World Journal of Clinical Cases

Thrice Monthly Volume 11 Number 4 February 6, 2023

Contents

ABOUT COVER

Editorial Board Member of *World Journal of Clinical Cases*, Sahand Samieirad, DDS, MS, MSc, Associate Professor, Oral and Maxillofacial Surgery Department, Mashhad Dental School, Mashhad University of Medical Sciences, Mashhad 9178613111, Iran. samieerads@mums.ac.ir

AIMS AND SCOPE

The primary aim of *World Journal of Clinical Cases* (*WJCC*, *World J Clin Cases*) is to provide scholars and readers from various fields of clinical medicine with a platform to publish high-quality clinical research articles and communicate their research findings online.

WJCC mainly publishes articles reporting research results and findings obtained in the field of clinical medicine and covering a wide range of topics, including case control studies, retrospective cohort studies, retrospective studies, clinical trials studies, observational studies, prospective studies, randomized controlled trials, randomized clinical trials, systematic reviews, meta-analysis, and case reports.

INDEXING/ABSTRACTING

The *WJCC* is now abstracted and indexed in Science Citation Index Expanded (SCIE, also known as SciSearch®), Journal Citation Reports/Science Edition, Current Contents®/Clinical Medicine, PubMed, PubMed Central, Scopus, Reference Citation Analysis, China National Knowledge Infrastructure, China Science and Technology Journal Database, and Superstar Journals Database. The 2022 Edition of Journal Citation Reports® cites the 2021 impact factor (IF) for *WJCC* as 1.534; IF without journal self cites: 1.491; 5-year IF: 1.599; Journal Citation Indicator: 0.28; Ranking: 135 among 172 journals in medicine, general and internal; and Quartile category: Q4. The *WJCC*'s CiteScore for 2021 is 1.2 and Scopus CiteScore rank 2021: General Medicine is 443/826.

RESPONSIBLE EDITORS FOR THIS ISSUE

NAME OF JOURNAL
World Journal of Clinical Cases

ISSN
ISSN 2307-8960 (online)

LAUNCH DATE
April 16, 2013

FREQUENCY
Thrice Monthly

PUBLICATION DATE
February 6, 2023

World Journal of Clinical Cases

Submit a Manuscript: https://www.f6publishing.com

World J Clin Cases 2023 February 6; 11(4): 719-724

DOI: 10.12998/wjcc.v11.i4.719

ISSN 2307-8960 (online)

MINIREVIEWS

Development and refinement of diagnostic and therapeutic strategies for managing patients with cardiogenic stroke: An arduous journey

Ze-Xin Fan, Ri-Xia Liu, Guang-Zhi Liu

Specialty type: Medicine, research and experimental

Provenance and peer review: Invited article; Externally peer reviewed.

Peer-review model: Single blind

Peer-review report's scientific quality classification

Grade A (Excellent): 0
Grade B (Very good): B
Grade C (Good): C
Grade D (Fair): 0
Grade E (Poor): 0

P-Reviewer: Alkhatib AJ, Jordan; Teramoto-Matsubara OT, Mexico

Received: October 6, 2022
Peer-review started: October 6, 2022
First decision: December 13, 2022
Revised: December 22, 2022
Accepted: January 12, 2023
Article in press: January 12, 2023
Published online: February 6, 2023

Ze-Xin Fan, Ri-Xia Liu, Guang-Zhi Liu, Department of Neurology, Beijing Anzhen Hospital, Beijing 100029, China

Corresponding author: Guang-Zhi Liu, MD, Chief Doctor, Professor, Department of Neurology, Beijing Anzhen Hospital, No. 2 Anzhen Road, Chaoyang District, Beijing 100029, China. guangzhi2002@hotmail.com

Abstract

Cardioembolic stroke, referred to as cardiogenic stroke, is a clinical syndrome in which emboli from the heart pass through the circulatory system and cause cerebral artery embolism and corresponding brain dysfunction. Compared to other subtypes of ischemic stroke, cardiogenic stroke presents with more etiologies, greater severity, worse prognosis, and a higher recurrence rate. In this minireview, we provide new insights into the etiological classification, diagnostic methods, and interventions of cardiogenic stroke.

Key Words: Cardiogenic stroke; Diagnostic methods; Therapeutic strategies

Core Tip: There are many reviews focused on the diagnosis and treatment strategies of cardiogenic stroke. However, in clinical practice, there are still many problems such as non-standard diagnosis and large differences in treatment measures. In this minireview, we introduce the latest Chinese expert consensus on cardiogenic stroke-based diagnostic criteria and provide some new insights into the etiological classification and interventions of cardiogenic stroke.

Citation: Fan ZX, Liu RX, Liu GZ. Development and refinement of diagnostic and therapeutic strategies for managing patients with cardiogenic stroke: An arduous journey. *World J Clin Cases* 2023; 11(4): 719-724

URL: https://www.wjgnet.com/2307-8960/full/v11/i4/719.htm

DOI: https://dx.doi.org/10.12998/wjcc.v11.i4.719

INTRODUCTION

Stroke is a disease that can seriously endanger human health. The 2019 Global Burden of Disease study showed that stroke is the second leading cause of death worldwide after ischemic heart disease (11.6% of total deaths), and the third leading cause of death and disability combined (5.7% of total disability-adjusted life years) with ischemic strokes accounting for the majority of strokes (62.4%)[1]. Cardiogenic stroke, also known as cardioembolic stroke, constitutes 20% to 30% of all ischemic strokes. It is a clinical syndrome in which emboli from the heart pass through the circulatory system and cause cerebral artery embolism and corresponding brain dysfunction[2,3]. With the strengthening of community medical management, atherosclerosis risk factors were significantly reduced (*e.g.*, low-density lipoprotein-cholesterol and blood pressure levels were better controlled than before). As a result, stroke/transient ischemic attacks caused by large-artery atherosclerosis (LAA) and small-vessel occlusion were remarkably decreased; conversely, cardiogenic stroke/transient ischemic attack increased significantly [4]. Compared to other subtypes of ischemic stroke, cardiogenic stroke presents with more etiologies, greater severity, worse prognosis, and a higher recurrence rate[5,6]. Although the diagnosis and treatment of cardiogenic stroke has substantially improved worldwide in recent years, there are still plenty of shortcomings, such as insufficient understanding of this disease and significant differences in treatment strategies[3,4]. Therefore, further strengthening the understanding of the etiological classification, diagnostic methods, and intervention measures of cardiogenic stroke, and uniformly improving the diagnosis and treatment of cardiogenic stroke, have become the top priority in the neurology community.

AS YET CLARIFIED ETIOLOGICAL CLASSIFICATION OF CARDIOGENIC STROKE

According to the definite (or potential) cause of cardiogenic stroke in the A-S-C-O (phenotype) classification and its epidemiological characteristics, the relatively common causes are divided into atrial fibrillation (AF), heart failure, acute coronary syndromes, patent foramen ovale (PFO), rheumatic heart disease, artificial heart valve, infectious endocarditis (IE), dilated cardiomyopathy, and cardiac myxoma. In most cases, the intracardiac wall thrombus, tumor surface thrombus/debris, shedding of vegetations on the valve intima or aortic arch plaque, or paradoxical embolism (derived from veins), underlie the pathogenesis, thereby contributing to the obstruction of cerebral blood vessels[7].

To date, the etiological attribution of cardiogenic stroke remains elusive. Firstly, the boundary between cardiogenic stroke and cryptogenic stroke, especially embolic stroke of undetermined source (ESUS), is blurred. Strokes that do not clearly meet the diagnostic criteria of the known ischemic stroke subtypes are classified as cryptogenic strokes[8,9], and cryptogenic stroke is further defined as ESUS when the clinical and neuroimaging features suggest a distant thrombus origin, the absence of lacunar infarcts, a high-risk source of cardiac embolism, or high-degree stenosis of the responsible vessel at the site of the infarction[10,11] (Figure 1). Regarding the etiology of embolism in ESUS, some cases may originate from arterial-arterial embolism caused by large atherosclerotic plaques in the brain, while other cases may result from some cardiac diseases (*e.g.*, paroxysmal AF, PFO, atrial cardiomyopathy, *etc.*)[3,12], strongly suggesting the existence of an overlap between ESUS and cardiogenic stroke. Hence, for ESUS cases, once the above causes are found through adequate standard evaluation, we recommend that, after multi-disciplinary discussion and confirmation of a cardiac cause, cardiogenic stroke should be considered so that treatment can be initiated as soon as possible. Secondly, there is still controversy over whether aortic arch atheroma (AAA)-related stroke should be classified as cardiogenic strokes, as some clinicians have categorized it as an ESUS subgroup of cryptogenic strokes[12]; however, the latest guideline for the prevention of stroke in patients with stroke and transient ischemic attack from the American Heart Association (AHA)/American Stroke Association (ASA) classified it as a subtype of LAA[13]. In view of this, we propose that while the classification of AAA-related strokes as LAA subtypes may reflect its exact pathogenesis, it is still more appropriate to attribute it to cardiogenic strokes. A strong reason for this is that its mechanisms and clinical manifestations are very similar to those of cardiogenic stroke, and studies have shown that attributing it to cardiogenic stroke has no significant impact on the choice of treatment measures and patient prognosis[14].

URGENCY TO DEVELOP A STANDARDIZED DIAGNOSTIC SYSTEM FOR CARDIOGENIC STROKE

The diagnosis of cardiogenic stroke is frequently made based on its clinical and neuroimaging features, combined with other elements such as vascular and cardiac evaluation. With improvements in disease awareness and detection methods (*e.g.*, long-term electrocardiogram monitoring, echocardiography), the detection rate of cardiogenic stroke has greatly increased in recent years when compared with other subtypes of ischemic stroke[15]. Nonetheless, several lines of clinical and radiological evidence to

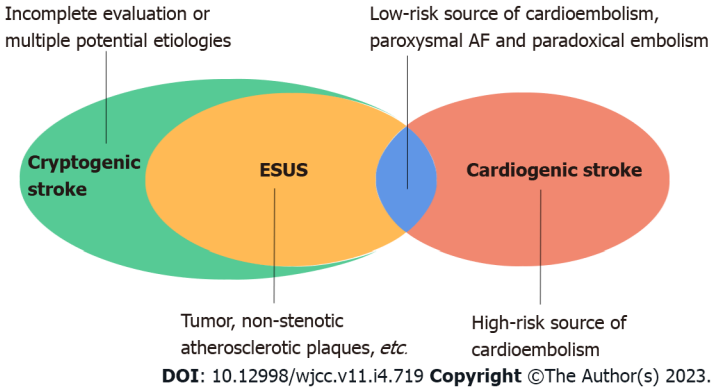

DOI: 10.12998/wjcc.v11.i4.719

Figure 1 Relationship between cryptogenic stroke, embolic stroke of undetermined source, and cardiogenic stroke. AF: Atrial fibrillation; ESUS: Embolic stroke of undetermined source.

support cardiogenic stroke have been proposed in this regard since the 1990s[8,16,17], but there are no well-established diagnostic criteria. Additionally, there is also controversy over the specific examination protocol used to identify the etiology of cardiogenic stroke. Finally, there are many other problems, such as inconsistent diagnosis and treatment levels across different medical institutions, misdiagnosis, and mistreatment.

In an attempt to solve these problems, we first proposed new clinical diagnostic criteria for cardiogenic stroke[7]. According to the Chinese expert consensus on the diagnosis of cardiogenic stroke (2019) (Table 1), cardiogenic stroke is categorized into definite cardiogenic stroke, probable cardiogenic stroke, and possible cardiogenic stroke: Definite cardiogenic stroke = 2 of (A) + at least 1 of (B) + C; probable cardiogenic stroke = 2 of (A), or at least 1 of (A) + at least 1 of (B); possible cardiogenic stroke = at least 1 of (A). Clinical validation of the diagnostic criteria is currently underway.

URGENT NEED FOR THE DEVELOPMENT OF A STANDARDIZED AND REFINED INTERVENTION STRATEGY FOR CARDIOGENIC STROKE

Even though the treatment principles of cardiogenic stroke are generally similar to other subtypes of ischemic stroke, more emphasis is placed on anticoagulation therapy. However, when to start or restart anticoagulation therapy and the choice of anticoagulants are mostly based on personal experience, mainly due to the lack of clinical evidence or clinical guidelines. Although the principle of using intravenous thrombolysis in the acute phase is similar of all subtypes, cardiogenic stroke also has its own specificity. In light of the above issues, the standardization of treating cardiogenic stroke has become an urgent issue which needs to be addressed.

For most stroke patients with AF, the guidelines for the early management of acute ischemic stroke from the 2018 AHA/ASA recommend that oral anticoagulation therapy should be initiated within 4 to 14 d after onset[17]. Nevertheless, in a recent multicenter real-world cohort study, initiation of oral anticoagulation within 4 to 14 d did not significantly reduce the incidence of ischemic and hemorrhagic stroke compared to that initiated within zero to three days[18]. Additionally, regarding the best time to restart oral anticoagulation after acute stroke, Hindricks *et al*[19] suggests that anticoagulation be restarted as soon as possible within 2 wk of onset under the guidance of a multi-disciplinary team (neurologist and cardiologist), in combination with the patient's willingness to treat; however, so far there are no reliable data to support this viewpoint. Regarding the anticoagulant choice, results from four randomized controlled trials involving anticoagulation for stroke or systemic embolism in AF showed that, novel oral anticoagulants (NOACs) are noninferior to warfarin in reducing the risk of stroke or systemic embolism in patients with AF but are safer in terms of adverse reactions, such as risk of intracranial hemorrhage[20-23]. Due to this, we recommend that the risk of hemorrhagic transformation in cardiogenic stroke be taken into account, regardless of indications for anticoagulation (*e.g.*, AF, valvular disease), and treatment should be started or restarted several days to several weeks after the onset of the disease, in consideration of the severity of the disease, the size of the acute cerebral infarction, and the risk of bleeding. It is also necessary to fully consider the faster effect and higher safety characteristics of NOACs compared with warfarin.

With regard to intravenous thrombolysis in cardiogenic stroke, to date, most studies were observational or small sample studies[24-26]; in addition, the consensus on efficacy and adverse reactions such as bleeding were different, mainly owing to differences in inclusion criteria and patient characteristics. It should be kept in mind that the use of intravenous thrombolysis is also limited or complicated under special circumstances, such as with prior anticoagulation therapy[27-32], recent valve surgery or

Table 1 Diagnostic criteria for cardiogenic stroke[7]

Criteria	Element
A: Essential criteria	Typical clinical manifestations
	Characteristic neuroimaging (brain CT/MRI) findings
B: Supportive criteria	Cardiogenic embolus on echocardiography[1]
	Arrhythmia on electrocardiogram, especially atrial fibrillation
	Characteristic vascular neuroimaging/cerebral angiography findings[2]
C: Exclusion of other diseases	

[1]Intracardiac thrombus, intracardiac vegetation, intracardiac tumor and right-to-left intracardiac shunt.
[2]An abrupt cut-off of the main trunk or branch of an intracranial large-vessel, in the absence of significant atherosclerotic plaques which cause narrowing of the upstream vessels (*e.g.*, internal carotid artery).
CT: Computed tomography; MRI: Magnetic resonance imaging.

percutaneous coronary intervention[33,34], and IE-related stroke[35]. Accordingly, a variety of guidelines and expert consensus have provided corresponding individualized treatment advice or recommendations[18,36-38]. Chinese neurologists have also recently reported a case of cardiogenic stroke successfully treated by intravenous thrombolysis with alteplase after reversal of dabigatran by idacilizumab[39]. Hence, for patients with acute cardiogenic stroke, especially those who received anticoagulation before disease onset, we recommend the treatment strategy should be individualized according to the specific situation, and intravenous thrombolytic therapy can be performed after multi-disciplinary consultation to improve patient outcomes.

CONCLUSION

In summary, three major issues are raised in this review: The etiology classification; the boundary between cardiogenic stroke, cryptogenic stroke and ESUS; as well as the attribution of AAA-related stroke all need to be clarified. Regarding the diagnosis, given the fact that currently no well-established diagnostic standard is available, we hence developed a new diagnostic system for cardiogenic stroke. Additionally, we recommend that anticoagulant therapy should be initiated or restarted several days to weeks after the onset of stroke, based on the patients' specific situation, and treatment for acute phase and prevention of recurrent stroke should be actively carried out after multidisciplinary consultation. Despite substantial progress in the diagnosis and treatment of cardiogenic stroke worldwide, there is still a long way to go to address all issues. In particular, the development of a standard protocol for management of the acute phase and recovery phase should be determined as soon as possible. Thus, we look forward to seeing additional evidence-based research, real-world research, and health economics evidence in the future in order for clinicians to gain a more comprehensive understanding of cardiogenic stroke and precise prevention and treatment measures, thereby maximizing the clinical benefit and improving the prognosis of patients.

FOOTNOTES

Author contributions: Liu GZ conceived the outline and performed the majority of the writing; Fan ZX and Liu RX performed part of writing and prepared the figures and tables.

Conflict-of-interest statement: All the authors report no relevant conflicts of interest for this article.

Country/Territory of origin: China

ORCID number: Ze-Xin Fan 0000-0002-6321-9179; Ri-Xia Liu 0000-0002-7006-2579; Guang-Zhi Liu 0000-0001-8953-0005.

S-Editor: Wang JJ

L-Editor: A
P-Editor: Wang JJ

REFERENCES

1 **GBD 2019 Stroke Collaborators**. Global, regional, and national burden of stroke and its risk factors, 1990-2019: a systematic analysis for the Global Burden of Disease Study 2019. *Lancet Neurol* 2021; **20**: 795-820 [PMID: 34487721 DOI: 10.1016/S1474-4422(21)00252-0]
2 **Bogiatzi C**, Hackam DG, McLeod AI, Spence JD. Secular trends in ischemic stroke subtypes and stroke risk factors. *Stroke* 2014; **45**: 3208-3213 [PMID: 25213343 DOI: 10.1161/STROKEAHA.114.006536]
3 **Kamel H**, Healey JS. Cardioembolic Stroke. *Circ Res* 2017; **120**: 514-526 [PMID: 28154101 DOI: 10.1161/CIRCRESAHA.116.308407]
4 **Spence JD**. Cardioembolic stroke: everything has changed. *Stroke Vasc Neurol* 2018; **3**: 76-83 [PMID: 30022801 DOI: 10.1136/svn-2018-000143]
5 **Lin HJ**, Wolf PA, Kelly-Hayes M, Beiser AS, Kase CS, Benjamin EJ, D'Agostino RB. Stroke severity in atrial fibrillation. The Framingham Study. *Stroke* 1996; **27**: 1760-1764 [PMID: 8841325 DOI: 10.1161/01.str.27.10.1760]
6 **Bjerkreim AT**, Khanevski AN, Thomassen L, Selvik HA, Waje-Andreassen U, Naess H, Logallo N. Five-year readmission and mortality differ by ischemic stroke subtype. *J Neurol Sci* 2019; **403**: 31-37 [PMID: 31185434 DOI: 10.1016/j.jns.2019.06.007]
7 **Liu GZ**, Hu R, Peng DT; Geriatric Neurology Group, Geriatric Branch of Chinese Medical Association; Writing Group of Chinese expert consensus on diagnosis of cardiogenic stroke. Chinese expert consensus on the diagnosis of cardiogenic stroke (2019). *Chin Med J (Engl)* 2021; **134**: 505-507 [PMID: 33652457 DOI: 10.1097/CM9.0000000000001217]
8 **Adams HP Jr**, Bendixen BH, Kappelle LJ, Biller J, Love BB, Gordon DL, Marsh EE 3rd. Classification of subtype of acute ischemic stroke. Definitions for use in a multicenter clinical trial. TOAST. Trial of Org 10172 in Acute Stroke Treatment. *Stroke* 1993; **24**: 35-41 [PMID: 7678184 DOI: 10.1161/01.str.24.1.35]
9 **Ay H**, Benner T, Arsava EM, Furie KL, Singhal AB, Jensen MB, Ayata C, Towfighi A, Smith EE, Chong JY, Koroshetz WJ, Sorensen AG. A computerized algorithm for etiologic classification of ischemic stroke: the Causative Classification of Stroke System. *Stroke* 2007; **38**: 2979-2984 [PMID: 17901381 DOI: 10.1161/STROKEAHA.107.490896]
10 **Hart RG**, Diener HC, Coutts SB, Easton JD, Granger CB, O'Donnell MJ, Sacco RL, Connolly SJ; Cryptogenic Stroke/ESUS International Working Group. Embolic strokes of undetermined source: the case for a new clinical construct. *Lancet Neurol* 2014; **13**: 429-438 [PMID: 24646875 DOI: 10.1016/S1474-4422(13)70310-7]
11 **Hart RG**, Catanese L, Perera KS, Ntaios G, Connolly SJ. Embolic Stroke of Undetermined Source: A Systematic Review and Clinical Update. *Stroke* 2017; **48**: 867-872 [PMID: 28265016 DOI: 10.1161/STROKEAHA.116.016414]
12 **Ntaios G**. Embolic Stroke of Undetermined Source: JACC Review Topic of the Week. *J Am Coll Cardiol* 2020; **75**: 333-340 [PMID: 31976872 DOI: 10.1016/j.jacc.2019.11.024]
13 **Kleindorfer DO**, Towfighi A, Chaturvedi S, Cockroft KM, Gutierrez J, Lombardi-Hill D, Kamel H, Kernan WN, Kittner SJ, Leira EC, Lennon O, Meschia JF, Nguyen TN, Pollak PM, Santangeli P, Sharrief AZ, Smith SC Jr, Turan TN, Williams LS. 2021 Guideline for the Prevention of Stroke in Patients With Stroke and Transient Ischemic Attack: A Guideline From the American Heart Association/American Stroke Association. *Stroke* 2021; **52**: e364-e467 [PMID: 34024117 DOI: 10.1161/STR.0000000000000375]
14 **Amarenco P**, Davis S, Jones EF, Cohen AA, Heiss WD, Kaste M, Laouénan C, Young D, Macleod M, Donnan GA; Aortic Arch Related Cerebral Hazard Trial Investigators. Clopidogrel plus aspirin versus warfarin in patients with stroke and aortic arch plaques. *Stroke* 2014; **45**: 1248-1257 [PMID: 24699050 DOI: 10.1161/STROKEAHA.113.004251]
15 **Pepi M**, Evangelista A, Nihoyannopoulos P, Flachskampf FA, Athanassopoulos G, Colonna P, Habib G, Ringelstein EB, Sicari R, Zamorano JL, Sitges M, Caso P; European Association of Echocardiography. Recommendations for echocardiography use in the diagnosis and management of cardiac sources of embolism: European Association of Echocardiography (EAE) (a registered branch of the ESC). *Eur J Echocardiogr* 2010; **11**: 461-476 [PMID: 20702884 DOI: 10.1093/ejechocard/jeq045]
16 **Kelley RE**, Kelley BP. Heart-Brain Relationship in Stroke. *Biomedicines* 2021; **9** [PMID: 34944651 DOI: 10.3390/biomedicines9121835]
17 **Powers WJ**, Rabinstein AA, Ackerson T, Adeoye OM, Bambakidis NC, Becker K, Biller J, Brown M, Demaerschalk BM, Hoh B, Jauch EC, Kidwell CS, Leslie-Mazwi TM, Ovbiagele B, Scott PA, Sheth KN, Southerland AM, Summers DV, Tirschwell DL; American Heart Association Stroke Council. 2018 Guidelines for the Early Management of Patients With Acute Ischemic Stroke: A Guideline for Healthcare Professionals From the American Heart Association/American Stroke Association. *Stroke* 2018; **49**: e46-e110 [PMID: 29367334 DOI: 10.1161/STR.0000000000000158]
18 **Yaghi S**, Trivedi T, Henninger N, Giles J, Liu A, Nagy M, Kaushal A, Azher I, Mac Grory B, Fakhri H, Brown Espaillat K, Asad SD, Pasupuleti H, Martin H, Tan J, Veerasamy M, Liberman AL, Esenwa C, Cheng N, Moncrieffe K, Moeini-Naghani I, Siddu M, Scher E, Leon Guerrero CR, Khan M, Nouh A, Mistry E, Keyrouz S, Furie K. Anticoagulation Timing in Cardioembolic Stroke and Recurrent Event Risk. *Ann Neurol* 2020; **88**: 807-816 [PMID: 32656768 DOI: 10.1002/ana.25844]
19 **Hindricks G**, Potpara T, Dagres N, Arbelo E, Bax JJ, Blomström-Lundqvist C, Boriani G, Castella M, Dan GA, Dilaveris PE, Fauchier L, Filippatos G, Kalman JM, La Meir M, Lane DA, Lebeau JP, Lettino M, Lip GYH, Pinto FJ, Thomas GN, Valgimigli M, Van Gelder IC, Van Putte BP, Watkins CL; ESC Scientific Document Group. 2020 ESC Guidelines for the diagnosis and management of atrial fibrillation developed in collaboration with the European Association for Cardio-Thoracic Surgery (EACTS): The Task Force for the diagnosis and management of atrial fibrillation of the European Society of Cardiology (ESC) Developed with the special contribution of the European Heart Rhythm Association (EHRA) of the

ESC. *Eur Heart J* 2021; **42**: 373-498 [PMID: 32860505 DOI: 10.1093/eurheartj/ehaa612]
20 **Connolly SJ**, Ezekowitz MD, Yusuf S, Eikelboom J, Oldgren J, Parekh A, Pogue J, Reilly PA, Themeles E, Varrone J, Wang S, Alings M, Xavier D, Zhu J, Diaz R, Lewis BS, Darius H, Diener HC, Joyner CD, Wallentin L; RE-LY Steering Committee and Investigators. Dabigatran versus warfarin in patients with atrial fibrillation. *N Engl J Med* 2009; **361**: 1139-1151 [PMID: 19717844 DOI: 10.1056/NEJMoa0905561]
21 **Patel MR**, Mahaffey KW, Garg J, Pan G, Singer DE, Hacke W, Breithardt G, Halperin JL, Hankey GJ, Piccini JP, Becker RC, Nessel CC, Paolini JF, Berkowitz SD, Fox KA, Califf RM; ROCKET AF Investigators. Rivaroxaban versus warfarin in nonvalvular atrial fibrillation. *N Engl J Med* 2011; **365**: 883-891 [PMID: 21830957 DOI: 10.1056/NEJMoa1009638]
22 **Granger CB**, Alexander JH, McMurray JJ, Lopes RD, Hylek EM, Hanna M, Al-Khalidi HR, Ansell J, Atar D, Avezum A, Bahit MC, Diaz R, Easton JD, Ezekowitz JA, Flaker G, Garcia D, Geraldes M, Gersh BJ, Golitsyn S, Goto S, Hermosillo AG, Hohnloser SH, Horowitz J, Mohan P, Jansky P, Lewis BS, Lopez-Sendon JL, Pais P, Parkhomenko A, Verheugt FW, Zhu J, Wallentin L; ARISTOTLE Committees and Investigators. Apixaban versus warfarin in patients with atrial fibrillation. *N Engl J Med* 2011; **365**: 981-992 [PMID: 21870978 DOI: 10.1056/NEJMoa1107039]
23 **Giugliano RP**, Ruff CT, Braunwald E, Murphy SA, Wiviott SD, Halperin JL, Waldo AL, Ezekowitz MD, Weitz JI, Špinar J, Ruzyllo W, Ruda M, Koretsune Y, Betcher J, Shi M, Grip LT, Patel SP, Patel I, Hanyok JJ, Mercuri M, Antman EM; ENGAGE AF-TIMI 48 Investigators. Edoxaban versus warfarin in patients with atrial fibrillation. *N Engl J Med* 2013; **369**: 2093-2104 [PMID: 24251359 DOI: 10.1056/NEJMoa1310907]
24 **Vaclavik D**, Vilionskis A, Jatuzis D, Karlinski MA, Gdovinova Z, Kõrv J, Tsivgoulis G, Mikulik R. Clinical outcome of cardioembolic stroke treated by intravenous thrombolysis. *Acta Neurol Scand* 2018; **137**: 347-355 [PMID: 29218699 DOI: 10.1111/ane.12880]
25 **Anticoli S**, Bravi MC, Perillo G, Siniscalchi A, Pozzessere C, Pezzella FR, Tanzi P, Gallelli L, Cartoni D. Effect of Cardioembolic Etiology on Intravenous Thrombolysis Efficacy for Acute Ischemic Stroke. *Curr Neurovasc Res* 2016; **13**: 193-198 [PMID: 27149937 DOI: 10.2174/1567202613666160506125426]
26 **Wang XG**, Zhang LQ, Liao XL, Pan YS, Shi YZ, Wang CJ, Wang YL, Liu LP, Zhao XQ, Wang YJ, Li D, Wang CX; Thrombolysis Implementation and Monitoring of acute ischemic Stroke in China (TIMS-China) Investigators. Unfavorable Outcome of Thrombolysis in Chinese Patients with Cardioembolic Stroke: a Prospective Cohort Study. *CNS Neurosci Ther* 2015; **21**: 657-661 [PMID: 26096605 DOI: 10.1111/cns.12421]
27 **Xian Y**, Liang L, Smith EE, Schwamm LH, Reeves MJ, Olson DM, Hernandez AF, Fonarow GC, Peterson ED. Risks of intracranial hemorrhage among patients with acute ischemic stroke receiving warfarin and treated with intravenous tissue plasminogen activator. *JAMA* 2012; **307**: 2600-2608 [PMID: 22735429 DOI: 10.1001/jama.2012.6756]
28 **Toyoda K**, Yamagami H, Koga M. Consensus Guides on Stroke Thrombolysis for Anticoagulated Patients from Japan: Application to Other Populations. *J Stroke* 2018; **20**: 321-331 [PMID: 30309227 DOI: 10.5853/jos.2018.01788]
29 **Agosti S**, Casalino L, Rocci E, Zaccone G, Rota E. Successful intravenous thrombolysis for ischemic stroke after reversal of dabigatran anticoagulation with idarucizumab: a case report. *J Med Case Rep* 2017; **11**: 224 [PMID: 28806993 DOI: 10.1186/s13256-017-1404-2]
30 **Barber PA**, Wu TY, Ranta A. Stroke reperfusion therapy following dabigatran reversal with idarucizumab in a national cohort. *Neurology* 2020; **94**: e1968-e1972 [PMID: 32079737 DOI: 10.1212/WNL.0000000000009155]
31 **Mazya MV**, Lees KR, Markus R, Roine RO, Seet RC, Wahlgren N, Ahmed N; Safe Implementation of Thrombolysis in Stroke Investigators. Safety of intravenous thrombolysis for ischemic stroke in patients treated with warfarin. *Ann Neurol* 2013; **74**: 266-274 [PMID: 23744571 DOI: 10.1002/ana.23924]
32 **Frank B**, Grotta JC, Alexandrov AV, Bluhmki E, Lyden P, Meretoja A, Mishra NK, Shuaib A, Wahlgren NG, Weimar C, Lees KR; VISTA Collaborators. Thrombolysis in stroke despite contraindications or warnings? *Stroke* 2013; **44**: 727-733 [PMID: 23391774 DOI: 10.1161/STROKEAHA.112.674622]
33 **Manoukian SV**, Feit F, Mehran R, Voeltz MD, Ebrahimi R, Hamon M, Dangas GD, Lincoff AM, White HD, Moses JW, King SB 3rd, Ohman EM, Stone GW. Impact of major bleeding on 30-day mortality and clinical outcomes in patients with acute coronary syndromes: an analysis from the ACUITY Trial. *J Am Coll Cardiol* 2007; **49**: 1362-1368 [PMID: 17394970 DOI: 10.1016/j.jacc.2007.02.027]
34 **Kamel H**, Johnston SC, Kirkham JC, Turner CG, Kizer JR, Devereux RB, Iadecola C. Association between major perioperative hemorrhage and stroke or Q-wave myocardial infarction. *Circulation* 2012; **126**: 207-212 [PMID: 22679143 DOI: 10.1161/CIRCULATIONAHA.112.094326]
35 **Brownlee WJ**, Anderson NE, Barber PA. Intravenous thrombolysis is unsafe in stroke due to infective endocarditis. *Intern Med J* 2014; **44**: 195-197 [PMID: 24528816 DOI: 10.1111/imj.12343]
36 **Demaerschalk BM**, Kleindorfer DO, Adeoye OM, Demchuk AM, Fugate JE, Grotta JC, Khalessi AA, Levy EI, Palesch YY, Prabhakaran S, Saposnik G, Saver JL, Smith EE; American Heart Association Stroke Council and Council on Epidemiology and Prevention. Scientific Rationale for the Inclusion and Exclusion Criteria for Intravenous Alteplase in Acute Ischemic Stroke: A Statement for Healthcare Professionals From the American Heart Association/American Stroke Association. *Stroke* 2016; **47**: 581-641 [PMID: 26696642 DOI: 10.1161/STR.0000000000000086]
37 **Diener HC**, Bernstein R, Butcher K, Campbell B, Cloud G, Davalos A, Davis S, Ferro JM, Grond M, Krieger D, Ntaios G, Slowik A, Touzé E. Thrombolysis and thrombectomy in patients treated with dabigatran with acute ischemic stroke: Expert opinion. *Int J Stroke* 2017; **12**: 9-12 [PMID: 27694315 DOI: 10.1177/1747493016669849]
38 **Berge E**, Whiteley W, Audebert H, De Marchis GM, Fonseca AC, Padiglioni C, de la Ossa NP, Strbian D, Tsivgoulis G, Turc G. European Stroke Organisation (ESO) guidelines on intravenous thrombolysis for acute ischaemic stroke. *Eur Stroke J* 2021; **6**: I-LXII [PMID: 33817340 DOI: 10.1177/2396987321989865]
39 **Xie D**, Wang X, Li Y, Chen R, Zhao Y, Xu C, Zhang Q, Zhang Y. Intravenous Thrombolysis After Reversal of Dabigatran With Idarucizumab in Acute Ischemic Stroke: A Case Report. *Front Aging Neurosci* 2021; **13**: 765037 [PMID: 34970137 DOI: 10.3389/fnagi.2021.765037]

World Journal of Clinical Cases

Submit a Manuscript: https://www.f6publishing.com

World J Clin Cases 2023 February 6; 11(4): 725-737

DOI: 10.12998/wjcc.v11.i4.725

ISSN 2307-8960 (online)

MINIREVIEWS

Portal vein aneurysm-etiology, multimodal imaging and current management

Admir Kurtcehajic, Enver Zerem, Ervin Alibegovic, Suad Kunosic, Ahmed Hujdurovic, Jasmin A Fejzic

Specialty type: Gastroenterology and hepatology

Provenance and peer review: Invited article; Externally peer reviewed.

Peer-review model: Single blind

Peer-review report's scientific quality classification

Grade A (Excellent): 0
Grade B (Very good): 0
Grade C (Good): C
Grade D (Fair): D
Grade E (Poor): 0

P-Reviewer: Ding X, China; Sripongpun P, Thailand

Received: November 6, 2022
Peer-review started: November 6, 2022
First decision: December 11, 2022
Revised: December 24, 2022
Accepted: January 12, 2023
Article in press: January 12, 2023
Published online: February 6, 2023

Admir Kurtcehajic, Department of Gastroenterology and Hepatology, Plava Medical Group, Tuzla 75000, Tuzla Kanton, Bosnia and Herzegovina

Enver Zerem, Department of Medical Sciences, The Academy of Sciences and Arts of Bosnia and Herzegovina, Sarajevo 71000, Bosnia and Herzegovina

Ervin Alibegovic, Department of Gastroenterology and Hepatology, University Clinical Center Tuzla, Tuzla 75000, Tuzla Kanton, Bosnia and Herzegovina

Suad Kunosic, Department of Physics, Faculty of Natural Sciences and Mathematics, University of Tuzla, Tuzla 75000, Tuzla Kanton, Bosnia and Herzegovina

Ahmed Hujdurovic, Department of Internal Medicine, Plava Medical Group, Tuzla 75000, Tuzla Kanton, Bosnia and Herzegovina

Jasmin A Fejzic, Department of Internal Medicine, General Hospital Tesanj, Tesanj 74260, Bosnia and Herzegovina

Corresponding author: Admir Kurtcehajic, PhD, Academic Research, Research Assistant, Research Scientist, Department of Gastroenterology and Hepatology, Plava Medical Group, No. 10 Crnogorcevica, Tuzla 75000, Tuzla Kanton, Bosnia and Herzegovina.
admircg7@gmail.com

Abstract

Portal vein aneurysm (PVA) is a rare vascular abnormality, representing 3% of all venous aneurysms in the human body, and is not well understood. It can be congenital or acquired, located mainly at the level of confluence, main trunk, branches and bifurcation. A PVA as an abnormality of the portal venous system was first reported in 1956 by Barzilai and Kleckner. A review from 2015 entitled "Portal vein aneurysm: What to know" considered fewer than 200 cases. In the last seven years, there has been an increase in the number of PVAs diagnosed thanks to routine abdominal imaging. The aim of this review is to provide a comprehensive update of PVA, including aetiology, epidemiology, and clinical assessment, along with an evaluation of advanced multimodal imaging features of aneurysm and management approaches.

Key Words: Aneurysm; Portal vein; Abdominal imaging; Treatment; Follow-up

Core Tip: The number of reported portal vein aneurysms (PVAs) across the world with this review stands at about 280. In relation to a new acquired aetiology of PVA, the following conditions are noted: Budd-Chiari syndrome, splenomegaly in thalassaemia major, giant splenic artery aneurysm and a long-term cholelithiasis. Percentage of 30 to 50 of patients experienced non-specific abdominal pain, the most frequent complications of PVA are thrombosis and biliopathy. Recently, endoscopic ultrasound and intraductal ultrasonography, as an additional tool have also been used for assessment of PVA in more detail. With this review we have highlighted treatment of PVA with comorbidities based on the transjugular intrahepatic portosystemic shunt, percutaneous approach, and endoscopic approach.

Citation: Kurtcehajic A, Zerem E, Alibegovic E, Kunosic S, Hujdurovic A, Fejzic JA. Portal vein aneurysm-etiology, multimodal imaging and current management. *World J Clin Cases* 2023; 11(4): 725-737
URL: https://www.wjgnet.com/2307-8960/full/v11/i4/725.htm
DOI: https://dx.doi.org/10.12998/wjcc.v11.i4.725

INTRODUCTION

A portal vein aneurysm (PVA) is the abnormal focal saccular or fusiform dilatation of the portal venous system, and it is defined as a PV diameter exceeding 19 mm in cirrhotic patients and 15 mm in a normal liver. It is a rare vascular abnormality, representing 3% of all venous aneurysms in the human body, and is not well understood[1-7].

Douglass *et al*[8] studied 92 autopsies and reported that the diameter of the PV was between 0.64 mm and 12.1 mm in patients without cirrhosis and those without portal hypertension. In 1976, Doust *et al*[9] conducted a vascular study of 53 patients to assess the size of the PV and underlying liver status through abdominal ultrasound, and they detected that the maximum calibre of the PV was 19 mm in cirrhotic patients and 15 mm in patients with normal livers. Hence, a portal vein diameter of > 20 mm is universally regarded as the threshold for diagnosis of a PVA.

In a retrospective study by Koc *et al*[10], involving 4186 patients who had undergone routine abdominal contrast-enhanced computed tomography (CT), the prevalence of PVAs was 0.43%. The location of a PVA can be extrahepatic or intrahepatic. Extrahepatic PVAs often occur in the main trunk of the PV, the splenomesenteric confluence, at the level of the PV bifurcation, the main branches of the PV, the splenic vein (SV) and the superior mesenteric vein (SMV). A study by Doust *et al*[9] characterized intrahepatic PVAs as having a diameter measuring more than 7 mm in normal patients and 8.5 mm in cirrhotic patients. PVA as an abnormality of portal venous system firstly was reported 1956 by Barzilai and Kleckner[11]. A review from 2015 entitled "*Portal vein aneurysm: What to know*" considered 96 reports and included 190 patients[1].

Aiming to clarify novelty as regards this visceral vascular abnormality, we performed a literature search of the PubMed database for all articles relating to PVA between January 2015 and July 2022[12-68]. We collected 57 reports, involving 62 patients with a PVA[3-7,12-16,19,21-25,27,29-68]; we also found one retrospective study with 18 PVA patients[2], and three cases of PV pseudoaneurysm[69-71].

ETIOLOGY, MULTIMODAL IMAGING AND CURRENT MANAGEMENT

Epidemiological characteristics

Of the 62 patients in the review, 33 (53%) were male; the patients were between 1 (youngest) and 95 (oldest) years of age, and the mean patient age at diagnosis was 54.85 years (± 21.72). A number of reported PVA cases per year is shown in Figure 1.

In terms of aetiology, the frequency of congenital PVAs was 29 (46.7%), and it was 17 (27.4%) for acquired PVAs. In 16 (25.8%) patients, the aetiology of the PVAs was unclear. Regarding the location of PVAs, 27.41% were at the level of the splenomesenteric confluence; 19.35% were at the main trunk; 17.74% were at branches; 6.45% were at the PV bifurcation; 6.45% were at the SV; and 4.83% were at the SMV; 14.51% were classified as intrahepatic PVAs. A retrospective study by Ahmed *et al*[2] included 18 patients [13 of whom were female (72.2%)], aged between 20 years and 101 years, with an average age of 56 years. Our review also covered three patients (all male) with a PV pseudoaneurysm resulting from trauma.

Etiopathogenesis

The aetiology of PVA is not clear. Postulated origins include both congenital and acquired causes. It is well known that the main cause of acquired PVA is chronic liver disease (cirrhosis and fibrosis) with portal hypertension. Long-standing portal hypertension causes intimal thickening with compensatory

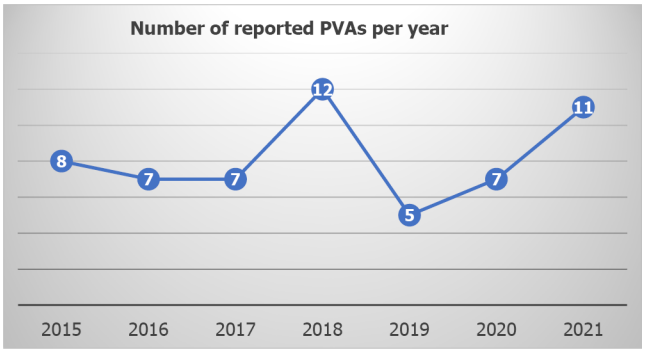

DOI: 10.12998/wjcc.v11.i4.725

Figure 1 Number of reported portal vein aneurysms per year, from January 2015 until December 2021. PVA: Portal vein aneurysms.

medial hypertrophy of the PV. Over time, medial hypertrophy is replaced by fibrous tissue, leading to weakening of the vein wall, thus making it susceptible to aneurysmal dilatation[12,13]. However, the incidence of portal hypertension and PVA is disproportionate, suggesting the existence of other contributory factors.

Acquired PVA can also be part of severe acute pancreatitis, likely to be due to leakage of digestive enzymes, causing localized inflammation of the PV. Malignancy was also noted as a cause of acquired PVA[1].

In several reports[69-71] a pseudoaneurysm of the PV is defined as post-traumatic (surgical pancreatic procedure, liver transplantation, or other rare clinical situations) uncommon finding (dilation) of the portal venous system. It is a serious condition followed life-threatening complications requiring an interventional approach.

In relation to a new acquired aetiology of PVA, the following conditions were noted: Budd-Chiari syndrome[14], splenomegaly in thalassaemia major[15] and giant splenic artery aneurysm[16]. Long-term cholelithiasis was also considered as a possible cause of PVA[17].

Some PVAs are congenital. During gestation, three pairs of veins are developed: The cardinal veins, umbilical veins and vitelline veins. The PV, hepatic veins and part of the inferior cava vein (ICV) come from umbilical veins and vitelline veins. Generally, cranial segments of the left vitelline vein and caudal segments of the right vitelline vein regress during the foetal period, and the SV and SMV are derived from the left vitelline vein[18].

Evidence supporting a congenital cause includes reported cases of *in utero* diagnosis of PVA, evidence of PVA in patients with histologically proven normal livers (particularly in children and young adults), normal portal venous pressure in the presence of a PVA, and the frequent stability of aneurysms at follow-up imaging. Theories for a congenital cause involve inherent weakness in the vessel wall or incomplete regression of the distal right primitive vitelline vein, leading to a vascular diverticulum that ultimately develops into an aneurysm. Congenital PVAs are usually incidentally diagnosed later in life (not in neonatal or paediatric age groups) when an abdominal ultrasound is carried out because of some other indication[4,6,19]. Burdall *et al*[20] evaluated the relation between trisomy 21 (Down's syndrome) and congenital vascular malformation of the liver in a study of 45 children, seven of whom had vascular malformation and two of whom had evidence of a PVA.

Clinical presentation of patients with a PVA

The clinical presentation of PVA is controversial and poorly understood. According to the review article by Laurenzi *et al*[1], 30% of patients with a PVA were asymptomatic, and 50% experienced non-specific abdominal pain. In our review, we found that up to 25% of patients were asymptomatic; for 15% of patients, the authors did not provide clear presenting symptoms relating to the PVA, and approximately 30% of patients experienced non-specific abdominal pain. In patients with a PVA, the nature of non-specific abdominal pain should be clarified. The main question is whether PVA low-pressure truly the source of the pain; gastritis, duodenitis and cholecystitis, *etc.*, should be ruled out. A retrospective study by Ahmed *et al*[2] showed that in eight (44.4%) patients with abdominal pain, a PVA was actually the source of the pain in only one patient.

Up to 10% of cases involve portal hypertension, gastrointestinal bleeding (varices) or presenting symptoms related to compression of adjacent organs (abdominal swelling or jaundice)[1]. With a PVA, presenting symptoms or complications such as portal hypertension and bleeding are discussible. One thing that should be clarified is whether a PVA is a consequence of portal hypertension or whether the PVA is causing portal hypertension. Khan *et al*[16] found coexistence of a giant splenic artery aneurysm, portal hypertension without liver cirrhosis and a PVA at the level of bifurcation. In this case, the PVA and portal hypertension were presumed to be secondary to the pressure effect from the splenic artery aneurysm. Güngör *et al*[21] presented an 11-mo-old girl with a congenital PVA, and oesophageal and

fundal varices with bleeding. This was the only case in our review where PVA caused portal hypertension complications.

Clinical presentation has a close relation with morphology, size and location of the PVA. When it grows, there can be contact with the biliary tract, the ICV and duodenum, *etc*., and complications can arise from compression of these organs. Six patients in our review (9.67%) had compression complications, including four biliopathies[22-25], one thrombosis in the ICV[7] and one intestinal obstruction [19].

Laurenzi *et al*[1] reported PVA complications such as thrombosis (which happened in 20% of cases) and a rupture (which occurred twice). A recent retrospective study by Ahmed *et al*[2] reported 18 patients with a PVA; 22.22% of patients had thrombosis, and no ruptures were reported. PVA with a complication of thrombosis is reported in the literature as nearly always being symptomatic, with 91% of patients reporting abdominal pain, 53% reporting fever and 38% presenting with ascites[26].

In our review, thrombosis occurred in 12 (19.35%) patients (six of whom were female), with a median age of 38.33 years. Abdominal pain was reported in 10 of 12 patients; in a one-year-old girl, the symptoms manifested as haematemesis and melena[21]; a 69-year-old female with a congenital PVA followed by thrombosis did not experience any symptoms[5]. In five patients, treatment was based on anticoagulation medication; seven patients underwent open surgery or invasive radiology procedures. In our review, a rupture as a complication of a PVA was not reported.

Patients with a PVA have a normal laboratory results, including complete blood count, inflammatory parameters, basic metabolic profile and liver function tests[1].

Imaging of PVA

Increased use of abdominal cross-sectional imaging in recent years has led to a growing number of cases describing PVA, and as such, proper handling of this lesion is increasingly relevant to both diagnostic and interventional radiologists. Evaluation of PVA by multiple imaging modalities is important because a PVA can mimic solid, cystic or hypervascular abdominal masses[1-7].

Sonography assessment can be performed for differential diagnosis to determine whether anechoic area or cyst at porta hepatis are PVA, hepatic artery aneurysm or choledochal cyst. Abdominal ultrasound based on the greyscale of the PVA produces an anechoic structure with a "*smoke effect*" within, which simulates a natural contrast agent, determined by slowed venous flow (Figure 2A). Spectral Doppler sonography reveals the presence of a monophasic, non-pulsatile venous flow pattern inside the aneurysm (Figure 2B). With colour Doppler sonography of a PVA, anechoic areas will be completely filled, looking like the Korean flag or a "y*in-yang*" sign. Hepatic artery aneurysms show a colour flow with arterial waveform, but choledochal cysts do not show such colour flow and are connected to biliary channels[6,15].

Contrast-enhanced CT with angiography shows the filling of PVA. On a CT and magnetic resonance imaging (MRI) scan, a PVA will appear as a well-defined contrast-enhanced focal saccular anomaly or fusiform dilatation of the portal venous system during the portal venous phase[4,27].

In one case, CT angiography facilitated better assessment of the portal venous system, which contained some thin calcifications in the aneurysmal wall and the main portal trunk[13]. Iimuro *et al*[28] presented "*computational fluid dynamics software*", analyzing the haemodynamics of the portal venous system, including congenital saccular PVA at the level of confluence. Turbulent flow was obvious in PVA, and the wall shear stress against the upper-posterior part of the aneurysm wall was greater than in other parts of the aneurysm. In order to prevent the PVA from growing and avoid thrombosis or a rupture, an aneurysmectomy of the PVA was performed.

The diagnostic role of endoscopic ultrasound (EUS) was highlighted in congenital PVA at the level of the splenomesenteric confluence. EUS confirmed the presence of anechoic lesions adjacent to the neck of the pancreas[29]. EUS as a diagnostic tool was also used for assessment of an intrahepatic aneurysmal portosystemic venous shunt[30].

"*Intraductal ultrasonography*" (IDU) was used for the first time to identify an adjacent PVA as the cause of a common hepatic duct stricture, showing a lobulated hypoechoic mass containing a mobile echogenic substance, outside of the biliary tract, highly suggestive of a vascular lesion[24].

Management and treatment of PVA

Because of their rarity, the natural history of PVA remains unclear, and the optimal strategy for management is controversial. Following diagnosis of a PVA, treatment will depend on the size, presenting symptoms and location of the PVA, and comorbidities.

If the PVA is asymptomatic (as in 30% of cases), it does not require any active treatment, and monitoring (a policy of "wait and see") should be adopted[1]. While asymptomatic aneurysms smaller than 30 mm can be clinically observed, surgical intervention may be necessary in large asymptomatic aneurysms (> 30 mm)[1,10]. The origin, morphology and symptomatology of a PVA, along with comorbidities and conservative treatment, are shown in Table 1.

Where there is thrombosis due to a PVA, anticoagulation treatment should be considered. In a recently published case, a 10-year-old boy with PVA thrombosis was treated with enoxaparin. The thrombosis disappeared completely after 6 mo[31]. In a case involving biliopathy, where the PVA comprised hepatic ducts, ursodeoxycholic acid was used to decrease the level of conjugated bilirubin

Table 1 Clinical features of the patients with portal vein aneurysm, regards the conservative treatment

Year	Ref.	Gender	Age	Etiology	Location	Morphology/size	Symptomatology	Complications	Comorbidity	Imaging	Treatment	Follow-up
2015	Prabhakar *et al*[48]	Male	47	None	Intrahepatic, left br	18 mm			Shunt	CT	Surveillance	Alive
2015	Srikanth *et al*[49]	Female	12	Congenital	Right branch	Saccular				US, CT	Surveillance	
2015	Starikov *et al*[50]	Male	27	None	SMV aneurysm	86 mm	Abdominal pain	Thrombosis CTPV	Acute pancreatitis	CT, MRI	Anticoagulation	24 mo
2016	Gaba *et al*[3]	Female	61	None	Confluence	50 mm			Ca colon; surgery	US, CT	Surveillance	
2016	Hanafiah *et al*[12]	Male	70	Acquired	Right branch	Fusiform, 22 mm			HBV; cirrhosis, HCC	US, CT	No treatment	Died
2016	Nayman *et al*[51]	Female	48	Congenital	Intrahepatic, two br	Right 43, left 13 mm	Abdominal pain			US, CT	Surveillance	
2016	Kurtcehajic *et al*[22]	Female	75	Congenital	Bifurcation	Saccular	Jundice	Biliopathy		US, CT, MRI	Usodeoxolic acid	Alive
2016	Khairallah *et al*[13]	Female	68	Acquired	Bifurcation	Fusiform, 40 mm	Bleeding		Cirrhosis; portal Hyp	US, CT	No treatment	
2017	Jaiswal *et al*[52]	Female	59	Congenital	Confluence	53.7 mm	Abdominal pain		Cholelithias	US, CT	Surveillance	18 mo
2017	Guilbaud *et al*[53]	Male	88	Congenital	Main trunk	Saccular, 59 mm			Cholecystectomy	CT	Surveillance	
2018	Maia *et al*[54]	Female	67	Congenital	Main trunk	35 mm	Abdominal pain		Diabetes, arterial Hyp	US, CT	Surveillance	12 mo
2018	Ashmore *et al*[55]	Female	62	None	Confluence		Abdominal pain			CT	Surveillance	
2018	Martínez *et al*[56]	Female	29	Congenital	Left branch	Saccular, 28 mm				US, CT	Surveillance	
2018	Hirji *et al*[57]	Male	62	Congenital	Confluence	50 mm			Diabetes, Parkinson	CT	Surveillance	6 mo
2018	Alur *et al*[58]	Female	45	Congenital	Left branch	21.5 mm				US, MRI	Surveillance	
2018	Chaubard *et al*[59]	Male	66	Congenital	Confluence	Saccular, 40 mm	Abdominal pain		T-cell hemopathy	US, CT	Surveillance	
2019	Ramamoorthy *et al*[60]	Female	42	Congenital	Confluence	Fusiform, 26 mm	Abdominal pain			US, MRI	Surveillance	Alive
2019	De Vloo *et al*[4]	Male	67	None	Confluence	Fusiform, 55 mm	Abdominal pain	Thrombosis CTPV	Neuroendocrine tm	US, CT	Anticoagulation	
2020	Kabir *et al*[61]	Male	77	Congenital	Intrahepatic, left br	28 mm	Abdominal pain		Abd. aortic aneurysm	US, MRI	Surveillance	3 mo
2020	Rana *et al*[29]	Female	51	Congenital	Confluence	38 mm	Abdominal pain			US, EUS, CT	Surveillance	30 mo
2020	Shams *et al*[62]	Male	67	None	SMV aneurysm		Abdominal pain	Thrombosis			Anticoagulation	12 mo
2020	Watanabe *et al*[5]	Female	69	Congenital	Right branch	35 mm		Thrombosis		US, CT	Surveillance	120 mo
2020	Schilardi *et al*[6]	Male	86	Congenital	Right branch	55 mm			Heart failure; COPD	US, CT	Surveillance	24 mo
2021	Hernando *et al*[63]	Female	51	Congenital	Right branch	25 mm	Abd. pain, jundice		Choledocholithiasis	US, MRI	Surveillance	

2021	Priadko *et al*[32]	Male	81	Acquired		48 mm			HBV, cirrhosis	US	Surveillance	36 mo
		Female	52	None		Saccular, 42.3 mm				US, CT, MRI	Surveillance	60 mo
		Male	73	None	Intrahepatic, right br	27 mm				US	Surveillance	12 mo
2021	Tan *et al*[64]	Male		Congenital	Main trunk	26 mm				CT	Surveillance	Alive
2021	López *et al*[65]	Female	41	None	SMV aneurysm	43 mm	Abdominal pain		Splenorenal shunt	CT	Surveillance	
2022	Tri *et al*[31]	Male	10	Congenital	Main trunk	36 mm	Abdominal pain	Thrombosis		CT	Anticoagulation	6 mo
2022	Villani *et al*[66]	Male	73	Acquired	Main trunk	Saccular, 40 mm			Cirrhosis, ascites	US, CT	Surveillance	
2022	Mortazavi *et al*[67]	Male	49	Congenital	Main trunk	21 mm	Abdominal pain		Cholelithias	CT	Surveillance	
2022	Mohamadnejad *et al*[30]	Female	76	None	Intrahepatic, left br	25 mm			Aneurysm, shunt	CT, EUS	Surveillance	
2022	Kanamalla *et al*[7]	Male	95	Congenital	Confluence	Saccular, 35 mm		Thrombosis of ICV	Diabetes, arterial Hyp	CT	Anticoagulation	

Abd: Abdominal; br: Branch; Ca: Carcinoma; COPD: Chronic obstructive pulmonary disease; CT: Computed tomography; CTPV: Cavernous transformation of the portal vein; EUS: Endoscopic ultrasound; HBV: Hepatitis B virus; HCC: Hepatocellular carcinoma; Hyp: Hypertensio; ICV: Inferior cava vein; MRI: Magnetic resonance imaging; SMV: Superior mesenteric vein; tm: tumor; US: Ultrasound.

[22].

While, in some studies, a CT scan every 12 mo was the preferred monitoring strategy, most published studies indicate that sonography is the preferred imaging technique for monitoring PVA growth, as it is relatively inexpensive and does not involve radiation exposure[32].

Open surgery approach: If the PVA is growing and constricting adjacent organs, thrombosis occurs, aiming to prevent potential rupture, open surgery methods should be considered. An aneurysmectomy for fusiform aneurysms (aneurysm resection, followed by insertion of a synthetic or cadaveric graft as a replacement conduit) and an aneurysmorrhaphy for saccular aneurysms (restores the normal diameter of the portal vein, if the remaining venous wall is of good quality) are considered for symptomatic aneurysms and to prevent a negative PVA prognosis.

The origin, morphology, PVA symptomatology and comorbidities as regards invasive treatment are shown in Table 2.

Fleming *et al*[33] demonstrated the efficacy of open surgery (aneurysmectomy) in three cases (two patients with an autograft and one with ePTFE). The two women with an autogenous graft remained asymptomatic at 85 mo and 65 mo, respectively; the third woman with ePTFE got thrombosis during pregnancy. The same report also included an aneurysmorrhaphy as the chosen treatment in one woman with a PVA.

Kim *et al*[34] presented a case with a PVA at the level of the main trunk, growing and with thrombosis complications. An aneurysm excision with an interposition bypass was successfully performed. The patient's postoperative recovery was rapid and uneventful, with normal portal flow revealed by colour Doppler ultrasonography and a contrast-enhanced CT scan.

Table 2 Clinical features of the patients with portal vein aneurysm, regards the surgery/invasive treatment

Year	Ref.	Gender	Age	Etiology	Location	Morphology /size	Symptomatology	Complications	Comorbidity	Imaging	Treatment	Follow-up
2015	Fleming *et al*[33]	Female	70	None	Confluence, SMV	From 30 mm to 50 mm				CT	Aneurysmectomy	85 mo
		Female	47	None	Confluence, SMV	From 35 mm to 60 mm	Abdominal pain		HCV	US, CT	Aneurysmectomy	65 mo
		Female	29	None		40 mm	Abdominal pain	Thrombosis/CTPV		CT	Aneurysmectomy	144 mo
		Female	49	None	Confluence, SMV	40 mm	Abdominal pain				Aneurysmorrhaphy	17 mo
2015	Tsauo *et al*[14]	Female	65	Acquired	Right branch	Saccular, 32 mm	Abdominal pain		Budd Chiari Sy	CT	TIPS	12 mo
2016	Khan *et al*[16]	Female	40	Acquired	Bifurcation	34 mm			Splenic artery aneurysm	US, CT	Aneurysmectomy	Alive
2016	Ierardi *et al*[69]	Male	42	Car accident	Confluence	PSA, 23 mm	Abdominal pain		Liver trauma	CT	Expanding stent graft	13 d
2016	Shukla *et al*[39]	Male	55	None	Intrahepatic, right br	Saccular, 30 mm			Sigmoid hemicolectomy	CT	Percut embolisation	Alive
2017	Shrivastava *et al* [27]	Male	55	Acquired	Intrahepatic, right br	62 mm			Portal Hyp, pancre-atitis	US, CT	Percut embolisation	12 mo
2017	Ding *et al*[45]	Male	48	Acquired	Bifurcation	70 mm			HBV, cirrhosis	CT	TIPS	72 mo
2017	Kim *et al*[34]	Female	34	Congenital	Main trunk	Fusiform, from 57 mm to 62 mm	Abdominal pain	Thrombosis	Celiac artery dissection	US, CT	Aneurysmectomy	6 mo
2017	Das *et al*[15]	Female	18	None	Confluence	Fusiform, 30 mm			Thalassemia major	US, CT	Splenectomy	
2017	Ding *et al*[23]	Male	80	Acquired	Left branch	Fusiform	Abd. pain, jaundice	Biliopathy	Cirrhosis, portal Hyp.	US, CT, MRI	ERCP, biliary stent	3 mo
2018	Walton *et al*[70]	Male	42	Percut Biopsy	Main trunk	PSA, 13 mm	Haemobilia		Lymphomatosus of pancreas		Percut, covered stent	
2018	Kimura *et al*[44]	Male	62	Acquired	Branch	40 mm			HCV, HCC, art portal fistula	MRI	Selective embolisation	
2018	Sun *et al*[24]	Male	85	Congenital	Main trunk	32 mm	Abdominal pain	Cholangitis	Diabetes, ulcer disease	IDUS, CT	ERCP, biliary stent	42 mo
2018	Chandran *et al* [19]	Male	1	Congenital				Colonic obstruction			Ligation of PVA	3 mo
2018	Chadha *et al*[35]	Male	66	Acquired	SV aneurysm	39 mm			HCV, cirrhos		External Sundt carotid shunt	6 mo

2018	Güngör *et al*[21]	Female	1	Congenital	Intrahepatic, right br	Fusiform	Hematemesis, melena	Portal Hyp, thrombosis		US, CT	Sugiura oper	
2018	Ktenidis *et al*[36]	Male	43	Acquired	SV aneurysm	98 mm			Splenectomy, AV shunt	CT	Open surgery	Alive
2019	Cleveland *et al*[71]	Male	68	Vehicle collision		PSA	Abdominal pain	Shock bowel		CT		Dead
2019	Juscafresa *et al*[40]	Female	77	Acquired	SV aneurysm	45 mm			Pancreatitis	CT	Percut, Viabahn stent	12 mo
2019	Bremer *et al*[42]	Male	65	Acquired	Intrahepatic, right br	64 mm	Abdominal pain		Cirrhosis, transplantation		TAE, stent graft exclusion	6 mo
2019	Oguslu *et al*[43]	Female	58	Acquired	Left branch	Saccular, 130 mm	Abdominal pain	Thrombosis	Art. portal fistula, portal Hyp	US, CT	Percut embolisation	9 mo
2020	Field *et al*[25]	Male	25	Congenital	Main trunk	55 mm	Abdominal pain	Biliopathy, thrombosis		CT, MRI	Thrombolysis, thrombectomy	12 mo
2021	Sura *et al*[38]	Male	80	Congenital	Main trunk	Saccular, 37 mm			Diaphragmatic hernia	CT	Open surgery	6 mo
2021	Marmor *et al*[41]	Male	67	Congenital	SV aneurysm	Saccular, 40 mm			Ca bladder	CT	Balloon expandable stent	12 mo
2021	Matsumoto *et al*[68]	Male	75	Acquired	Main trunk	42 mm	Abdominal pain		Ca pancreas	CT	Open surgery, omental graft	3 mo
2021	Gorolay *et al*[37]	Female	36	Congenital	Confluence	Saccular, from 45 mm to 65 mm	Abdominal pain	Thrombosis		US, CT	Hybrid operative repair	36 mo
2021	Dunlap *et al*[46]	Male	32	Acquired	Confluence	From 52 mm to 57 mm			Cirrhosis, portal Hyp		TIPS	6 mo
2022	Kohlbrenner *et al*[47]	Male	37	Congenital	Confluence	Fusiform, 51 mm	Abdominal pain	Thrombosis, ischemia		CT	Thrombolysis, TIPS	24 mo

Abd: Abdominal; art: Artery; br: Branch; Ca: Carcinoma; CT: Computed tomography; CTPV: Cavernous transformation of the portal vein; ERCP: Endoscopic retrograde cholangiopancreatography; HBV: Hepatitis B virus; HCC: Hepatocellular carcinoma; HCV: Hepatitis C virus; Hyp: Hypertensio; IDUS: Intraductal ultrasonography; MRI: Magnetic resonance imaging; percut: percutaneous; PSA: Pseudoaneurysm; PVA: Portal vein aneurysm; SMV: Superior mesenteric vein; SV: Splenic vein; Sy: Syndrome; TAE: Transarterial embolisation; TIPS: Transjugular intrahepatic portosystemic shunt; US: Ultrasound.

Khan *et al*[16] presented a case where splenomegaly, a giant splenic artery aneurysm and a PVA were found to coexist. The patient underwent a splenectomy and excision of the splenic artery aneurysm. It was determined that her PVA shrank considerably. Das *et al*[15] presented a case with thalassaemia major, splenomegaly and a PVA. After a splenectomy (necessitated by the existence of hypersplenism), the PVA significantly reduced.

Chadha *et al*[35] reported the case of a 66-year-old male with an acquired SV aneurysm and described novel use of a "*Sundt external carotid endarterectomy shunt*" as a temporary portacaval shunt to control portomesenteric hypertension, before transplantation of the liver. A giant SV aneurysm 98 mm in size

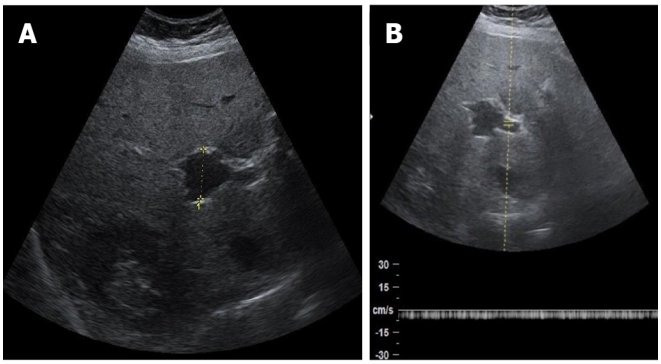

DOI: 10.12998/wjcc.v11.i4.725

Figure 2 Sonography assessment of portal vein aneurysm. A: Abdominal ultrasound shows portal vein aneurysm (PVA) at the level of bifurcation; B: Spectral Doppler sonography shows nonpulsatile blood flow through the portal venous system with PVA.

developed as a consequence of a splenectomy, an arteriovenous fistula and portal hypertension; this aneurysm was treated successfully with open surgery[36].

Male and female patients, both of whom had a congenital PVA and subsequent thrombosis complications, were treated with a hybrid operative repair involving a transhepatic catheter thrombectomy, and their aneurysms were operated on in open surgery[25,37].

The limited number of PVAs that have been reported means that there are no clear indications for open surgery on PVA. Koc *et al*[10] studied the size of PVA and concluded that aneurysms larger than 30 mm should be surgically treated with the aim of preventing thrombosis or rupture. On the other hand, a recently reported case of a patient with a congenital PVA 35 mm in size, with subsequent thrombosis complications, showed spontaneous resolution after 10 years[5].

Sura *et al*[38] reported the case of an 80-year-old man who had open surgery on a 37-mm PVA at the level of the main trunk. The reasons for PVA surgery were not postulated, but given the congenital origin, advanced age of the patient and absence of symptoms or thrombosis, it is our view that surgery was not the best treatment choice.

Interventional radiology procedures: In cases where a PVA is a consequence of portal hypertension and/or coexists with life-threatening conditions (injuries), the high risk associated with open surgery methods means that interventional radiology procedures *via* a percutaneous approach, endovascular approach and even more endoscopic approach should be considered[1,2].

Percutaneous approach: Shukla *et al*[39] successfully demonstrated percutaneous embolization of a saccular intrahepatic PVA, which prevented further growth or other clinical sequelae. Shrivastava *et al*[27] presented the largest intrahepatic PVA and the first case where the endovascular technique was used for treatment of the same. Under sonography and fluoroscopy guidance, the PVA was directly punctured with an 18G needle and embolized with a Lipiodol-Glue combination.

Juscafresa *et al*[40] reported the case of an elderly female treated for an acquired SV aneurysm 45 mm in size, through a transhepatic percutaneous approach, using a Viabahn covered stent. Marmor *et al*[41] presented the case of a patient with a congenital SV aneurysm 40 mm in size. Because the aneurysm was getting larger, it was treated with an expandable stent *via* a transhepatic approach.

In one case, after liver transplantation necessitated by HCV cirrhosis, the patient subsequently developed an arterioportal fistula with an intrahepatic PVA. The first step of the treatment was transarterial embolization, and the second step was stent graft exclusion of the PVA. As there was leakage, the patient underwent liver re-transplantation[42]. Oguslu *et al*[43] demonstrated two techniques for treatment of an arterioportal fistula with a giant saccular PVA at the level of the left branch. After failure of an endovascular approach due to tortuosity and angulation of the celiac artery, access to the hepatic artery was obtained directly *via* a percutaneous transhepatic route, and the fistula site was embolized with an Amplatzer Vascular Plug II and coils.

Treatment of portal vein pseudoaneurysm: Our review covered three patients (all males) with a PV pseudoaneurysm, all of which were a consequence of abdominal trauma or injury. In a patient with a traumatic pseudoaneurysm at the level of the splenomesenteric confluence, Ierardi *et al*[69] demonstrated a novel management strategy with a percutaneous transhepatic self-expanding stent graft.

A patient with a PV pseudoaneurysm at the level of the main trunk, resulting from invasive medical procedures [*e.g.*, a percutaneous biopsy or endoscopic retrograde cholangiopancreatography (ERCP)] to address lymphomatosus infiltration of the pancreatic head (with symptoms of haemobilia), was treated using percutaneous transhepatic covered stenting[70].

In the last case, involving a patient with a pseudoaneurysm of the portal venous system resulting from a motor vehicle collision, the patient was brought into the emergency department with diffuse abdominal pain and bowel shock. Unfortunately, the patient soon succumbed to his injuries[71].

Endovascular approach: Gaining access to the treatment zone can be challenging, and the target vessel may have tortuosity and elongation due to haemodynamic changes created by the hyperdynamic flow. Kimura *et al*[44] presented a case involving a hepatectomy (hepatocellular carcinoma), where the patient subsequently developed an arterioportal fistula with hepatofugal flow and a 40-mm-diameter PVA. After selective embolization of the anterior hepatic artery, the PVA disappeared, and portal flow was normalized.

An endovascular approach includes creation of a transjugular intrahepatic portosystemic shunt (TIPS). In patients with portal hypertension, an attempt may be made to decrease portal venous pressure in order to reduce the size of the aneurysm. Our review covered four patients with a PVA where the treatment of choice was a TIPS. Tsauo *et al*[14] presented a case involving a PVA resulting from portal hypertension associated with Budd-Chiari syndrome. For the first time, a TIPS was created without complications. The patient's abdominal pain completely ceased within two days, and she remained asymptomatic during the one-year follow-up. Ding *et al*[45] presented a case with a PVA at the level of bifurcation, with comorbidities such as portal hypertension, liver cirrhosis and HBV chronica. A TIPS successfully decreased the patient's portal hypertension and reduced the size of the PVA from 53 mm × 76 mm to 23 mm × 25 mm. Two years later, a CT scan and digital subtraction angiography revealed that the aneurysm had disappeared. The patient remained asymptomatic for 72 mo[45]. Dunlap *et al*[46] also used a TIPS successfully to treat a PVA resulting from portal hypertension and liver cirrhosis. Kohlbrenner *et al*[47] demonstrated transhepatic pharmacomechanical thrombolysis of a large thrombosed PVA. This was followed by insertion of a TIPS, along with an additional trans-TIPS thrombectomy to improve sluggish portal outflow and prevent re-thrombosis. Nine months later, an MRI showed complete resolution of the thrombosis.

Endoscopic approach *via* ERCP: In older patients with a PVA and complication of biliopathy and jaundice, ERCP with biliary stenting can be an appropriate treatment choice. In an 80-year-old male with liver cirrhosis and portal hypertension, an acquired PVA at the level of the left branch was found. The patient had developed biliopathy due to compression of the common bile duct; this complication was successfully treated endoscopically *via* ERCP with a biliary stent[23]. Sun *et al*[24] reported the case of an 85-year-old man with cholangitis complications from PVA-induced compression. Given the age of the patient, surgery was not considered, and instead an ERCP biliary stent was deployed several times.

CONCLUSION

PVA is a rare morphological abnormality of the portal venous system, accounting for 3% of all venous aneurysms in the human body. The number of reported PVAs across the world now stands at about 280: The 200 PVAs covered in the previous review published in 2015[1], the 18 cases in the retrospective study[2] and the 62 PVAs in our review covering the last seven years. PVA can be congenital or acquired, located mainly at the level of confluence, main trunk, branches and bifurcation. Up to 30% of patients can be asymptomatic, and non-specific abdominal pain should be investigated to exclude other pathological causes, such as cholecystitis or peptic ulcer disease, *etc.* Thrombosis complications occur in approximately 19%-23% of patients, and biliopathy occurs in approximately 4%-6% of patients. Other complications can also arise from compression due to a PVA, including thrombosis of the ICV and intestinal obstruction. Diagnosis of a PVA is based on spectral and colour Doppler sonography, and CT and MRI. EUS and IDU have also been used as a diagnostic tool. If a PVA is asymptomatic, it does not require any active treatment, and monitoring (a policy of "wait and see") should be adopted. The first choice for treatment of PVA thrombosis is anticoagulation medication. If the PVA is getting larger and compressing adjacent organs, thrombosis will occur, so to prevent a potential rupture, open surgery methods such as an aneurysmectomy or an aneurysmorrhaphy should be considered. Given the risk associated with open surgery methods, interventional radiology procedures *via* a percutaneous approach, endovascular approach or, better still, an endoscopic approach should be considered for cases where a PVA is a consequence of portal hypertension and/or coexists with life-threatening conditions (injuries).

FOOTNOTES

Author contributions: Kurtcehajic A, Alibegovic E, and Fejzic AJ designed, edited and wrote the manuscript; Kunosic S and Hujdurovic A performed the collection of the data and designed appearance of the tables; Zerem E contributed to the critical revision and editing of the paper; all authors wrote, read, and approved the final version of the manuscript.

Conflict-of-interest statement: There are no conflicts of interest to report.

Country/Territory of origin: Bosnia and Herzegovina

ORCID number: Admir Kurtcehajic 0000-0002-6445-4090; Enver Zerem 0000-0001-6906-3630; Suad Kunosic 0000-0002-5211-4099.

S-Editor: Chen YL
L-Editor: A
P-Editor: Chen YL

REFERENCES

1 **Laurenzi A**, Ettorre GM, Lionetti R, Meniconi RL, Colasanti M, Vennarecci G. Portal vein aneurysm: What to know. *Dig Liver Dis* 2015; **47**: 918-923 [PMID: 26188840 DOI: 10.1016/j.dld.2015.06.003]
2 **Ahmed O**, Ohman JW, Vachharajani N, Yano M, Sanford DE, Hammill C, Fields RC, Hawkins WG, Strasberg SM, Doyle MB, Chapman WC, Khan AS. Feasibility and safety of non-operative management of portal vein aneurysms: a thirty-five year experience. *HPB (Oxford)* 2021; **23**: 127-133 [PMID: 32561177 DOI: 10.1016/j.hpb.2020.05.006]
3 **Gaba RC**, Hardman JD, Bobra SJ. Extrahepatic Portal Vein Aneurysm. *Radiol Case Rep* 2009; **4**: 291 [PMID: 27307811 DOI: 10.2484/rcr.v4i2.291]
4 **De Vloo C**, Matton T, Meersseman W, Maleux G, Houthoofd S, Op de Beeck K, Laleman W, Van Malenstein H, Nevens F, Verbeke L, Van der Merwe S, Verslype C. Thrombosis of a portal vein aneurysm: a case report with literature review. *Acta Clin Belg* 2019; **74**: 115-120 [PMID: 30147008 DOI: 10.1080/17843286.2018.1511298]
5 **Watanabe Y**, Takase K, Okada K, Aikawa M, Okamoto K, Koyama I. Portal vein aneurysm with complete spontaneous regression after 10 years using conservative treatment. *Clin J Gastroenterol* 2020; **13**: 940-945 [PMID: 32449089 DOI: 10.1007/s12328-020-01131-6]
6 **Schilardi A**, Ciavarella A, Carbone M, Antonica G, Berardi E, Sabbà C. A large asymptomatic portal vein aneurysm in an old man. *Clin Case Rep* 2021; **9**: 15-18 [PMID: 33489127 DOI: 10.1002/ccr3.3365]
7 **Kanamalla K**, Alwakkaa H. Thrombosis of the inferior vena cava secondary to incidental portal vein aneurysm. *Radiol Case Rep* 2022; **17**: 1532-1535 [PMID: 35282317 DOI: 10.1016/j.radcr.2022.02.006]
8 **Douglass BE**, Baggenstoss AH, Hollinshead WH. The anatomy of the portal vein and its tributaries. *Surg Gynecol Obstet* 1950; **91**: 562-576 [PMID: 14787850]
9 **Doust BD**, Pearce JD. Gray-scale ultrasonic properties of the normal and inflamed pancreas. *Radiology* 1976; **120**: 653-657 [PMID: 948601 DOI: 10.1148/120.3.653]
10 **Koc Z**, Oguzkurt L, Ulusan S. Portal venous system aneurysms: imaging, clinical findings, and a possible new etiologic factor. *AJR Am J Roentgenol* 2007; **189**: 1023-1030 [PMID: 17954635 DOI: 10.2214/AJR.07.2121]
11 **BARZILAI R**, KLECKNER MS Jr. Hemocholecyst following ruptured aneurysm of portal vein; report of a case. *AMA Arch Surg* 1956; **72**: 725-727 [PMID: 13301133 DOI: 10.1001/archsurg.1956.01270220173023]
12 **Hanafiah M**, Johari B, Koshy M, Misni MN. Intrahepatic Portal Vein Aneurysm with Concurrent Hepatocellular Carcinoma. *Sultan Qaboos Univ Med J* 2016; **16**: e115-e116 [PMID: 26909202 DOI: 10.18295/squmj.2016.16.01.023]
13 **Khairallah S**, Elmansouri A, Jalal H, Idrissi MO, Ganouni NC. Calcified wall portal venous aneurysm: a case report. *Pan Afr Med J* 2016; **25**: 93 [PMID: 28292056 DOI: 10.11604/pamj.2016.25.93.9896]
14 **Tsauo J**, Li X. Portal vein aneurysm associated with Budd-Chiari syndrome treated with transjugular intrahepatic portosystemic shunt: a case report. *World J Gastroenterol* 2015; **21**: 2858-2861 [PMID: 25759562 DOI: 10.3748/wjg.v21.i9.2858]
15 **Das S**, Dey M, Kumar V, Lal H. Portal vein aneurysm in thalassaemia. *BMJ Case Rep* 2017; **2017** [PMID: 28801322 DOI: 10.1136/bcr-2016-218551]
16 **Khan A**, Ayub M, Haider I, Humayun M, Shah Z, Ajmal F. Coexisting giant splenic artery and portal vein aneurysms leading to non-cirrhotic portal hypertension: a case report. *J Med Case Rep* 2016; **10**: 270 [PMID: 27686495 DOI: 10.1186/s13256-016-1059-4]
17 **Kurtcehajic A**, Alibegovic E, Hujdurovic A, Vele E, Kurtcehajic D. Role of Cholelithiasis in Development of Portal Vein Aneurysm. *Am J Med* 2018; **131**: e119 [PMID: 29454428 DOI: 10.1016/j.amjmed.2017.09.004]
18 **Kim SH**, Yu HW, Kim HY, Jo HS. Neonatal vitelline vein aneurysm with thrombosis: prompt treatment should be needed. *Ann Surg Treat Res* 2015; **89**: 334-337 [PMID: 26665130 DOI: 10.4174/astr.2015.89.6.334]
19 **Chandran S**, Kumar M, Jacob TJK, Mohamed F. Intestinal obstruction with a twist: a rare case of congenital portal vein aneurysm causing intestinal obstruction. *BMJ Case Rep* 2018; **2018** [PMID: 30244223 DOI: 10.1136/bcr-2018-225689]
20 **Burdall OC**, Grammatikopoulos T, Sellars M, Hadzic N, Davenport M. Congenital Vascular Malformations of the Liver: An Association With Trisomy 21. *J Pediatr Gastroenterol Nutr* 2016; **63**: e141-e146 [PMID: 27602703 DOI: 10.1097/MPG.0000000000001405]

21 **Güngör Ş**, Varol Fİ, Kutlu R, Yılmaz S, Selimoğlu MA. An intrahepatic Portal Vein Aneurysm Presenting with Esophageal Variceal Bleeding in a Pediatric Patient: A Rare Clinical Entity. *Balkan Med J* 2018; **35**: 442-444 [PMID: 29966998 DOI: 10.4274/balkanmedj.2017.1776]

22 **Kurtcehajic A**, Vele E, Hujdurovic A. Portal vein aneurysm and portal biliopathy. *J Hepatobiliary Pancreat Sci* 2016; **23**: 658 [PMID: 27561886 DOI: 10.1002/jhbp.383]

23 **Ding F**, Li Q, Duan X, Ye J. Hepatobiliary and Pancreatic: Ruptured aneurysm of intra-hepatic portal vein causing obstructive jaundice. *J Gastroenterol Hepatol* 2017; **32**: 1666 [PMID: 28948704 DOI: 10.1111/jgh.13837]

24 **Sun J**, Sun CK. Repeated Plastic Stentings of Common Hepatic Duct for Portal Vein Aneurysm Compression in a Patient Unsuitable for Surgery. *Case Rep Gastroenterol* 2018; **12**: 570-577 [PMID: 30323732 DOI: 10.1159/000492812]

25 **Field Z**, Madruga M, Carlan SJ, Abdalla R, Carbono J, Al Salihi H. Portal vein aneurysm with acute portal vein thrombosis masquerading as a pancreatic mass. *Hematol Oncol Stem Cell Ther* 2020 [PMID: 32561224 DOI: 10.1016/j.hemonc.2020.05.010]

26 **Chawla YK**, Bodh V. Portal vein thrombosis. *J Clin Exp Hepatol* 2015; **5**: 22-40 [PMID: 25941431 DOI: 10.1016/j.jceh.2014.12.008]

27 **Shrivastava A**, Rampal JS, Nageshwar Reddy D. Giant Intrahepatic Portal Vein Aneurysm: Leave it or Treat it? *J Clin Exp Hepatol* 2017; **7**: 71-76 [PMID: 28348475 DOI: 10.1016/j.jceh.2016.08.013]

28 **Iimuro Y**, Suzumura K, Ohashi K, Tanaka H, Iijima H, Nishiguchi S, Hao H, Fujimoto J. Hemodynamic analysis and treatment of an enlarging extrahepatic portal aneurysm: report of a case. *Surg Today* 2015; **45**: 383-389 [PMID: 24633932 DOI: 10.1007/s00595-014-0882-8]

29 **Rana SS**, Dhalaria L, Sharma R, Gupta R. Extra-hepatic portal vein aneurysm diagnosed by EUS. *Endosc Ultrasound* 2020; **9**: 270-271 [PMID: 32687073 DOI: 10.4103/eus.eus_40_20]

30 **Mohamadnejad M**, Al-Haddad M. Intrahepatic aneurysmal portosystemic venous shunt diagnosed on EUS. *VideoGIE* 2022; **7**: 138-139 [PMID: 35937191 DOI: 10.1016/j.vgie.2021.12.010]

31 **Tri TT**, Duy HP, Trung BH, Thuan LA, Thach PN, Hien NX, Duc NM. A rare pediatric case of portal vein aneurysm thrombosis. *Radiol Case Rep* 2022; **17**: 286-289 [PMID: 34876951 DOI: 10.1016/j.radcr.2021.10.065]

32 **Priadko K**, Romano M, Vitale LM, Niosi M, De Sio I. Asymptomatic portal vein aneurysm: Three case reports. *World J Hepatol* 2021; **13**: 515-521 [PMID: 33959231 DOI: 10.4254/wjh.v13.i4.515]

33 **Fleming MD**, Lall P, Nagorney DM, Gloviczki P, Kalra M, Duncan A, Oderich G, Toomey B, Bower TC. Operative interventions for extrahepatic portomesenteric venous aneurysms and long-term outcomes. *Ann Vasc Surg* 2015; **29**: 654-660 [PMID: 25770384 DOI: 10.1016/j.avsg.2015.01.029]

34 **Kim HJ**, Ha TY, Ko GY, Noh M, Kwon TW, Cho YP, Lee SG. A Case of Extrahepatic Portal Vein Aneurysm Complicated by Acute Thrombosis. *Ann Vasc Surg* 2017; **43**: 311.e9-311.e13 [PMID: 28478175 DOI: 10.1016/j.avsg.2017.01.020]

35 **Chadha RM**, Dougherty MK, Musto KR, Harnois DM, Nguyen JH. Temporary Portomesenteric Decompression for Splenic Vein Aneurysm During Orthotopic Liver Transplant. *Liver Transpl* 2018; **24**: 1485-1488 [PMID: 30129118 DOI: 10.1002/lt.25295]

36 **Ktenidis K**, Manaki V, Kapoulas K, Kourtellari E, Gionis M. Giant Splenic Aneurysm with Arteriovenous (A-V) Shunt, Portal Hypertension, and Ascites. *Am J Case Rep* 2018; **19**: 1410-1415 [PMID: 30478253 DOI: 10.12659/AJCR.911106]

37 **Gorolay V**, Nguyen D, Samra J, Neale M. Asymptomatic thrombosis of extrahepatic portal vein aneurysm necessitating hybrid operative repair. *Vascular* 2021; **29**: 762-766 [PMID: 33270525 DOI: 10.1177/1708538120976977]

38 **Sura TA**, Boutrous ML, Ruiz MI, Williams MS. Operative management of an incidental portal vein aneurysm in the setting of an incarcerated congenital diaphragmatic hernia. *J Vasc Surg Cases Innov Tech* 2021; **7**: 64-67 [PMID: 33665534 DOI: 10.1016/j.jvscit.2020.10.009]

39 **Shukla PA**, Kolber MK, Kumar A, Patel RI. Percutaneous Embolization of an Intrahepatic Portal Vein Aneurysm. *J Vasc Interv Radiol* 2016; **27**: 1747-1749 [PMID: 27926409 DOI: 10.1016/j.jvir.2016.01.132]

40 **Juscafresa LC**, Alfaro MP, Grochowicz L, Lorenzo JIL, Jaureguizar JIB. Endovascular treatment of a splenic vein aneurysm through a transhepatic approach. *Diagn Interv Radiol* 2019; **25**: 166-168 [PMID: 30774093 DOI: 10.5152/dir.2019.18057]

41 **Marmor RA**, Goodman S, Parsa P. Endovascular Repair of Splenic Vein Aneurysm with Balloon Expandable Stent Placement. *Ann Vasc Surg* 2021; **73**: 554-556 [PMID: 33556510 DOI: 10.1016/j.avsg.2020.12.051]

42 **Bremer WA**, Lokken RP, Gaba RC, Bui JT. Arterial-portal fistula treated with hepatic arterial embolization and portal venous aneurysm stent-graft exclusion complicated by type 2 endoleak. *Radiol Case Rep* 2019; **14**: 1301-1305 [PMID: 31467626 DOI: 10.1016/j.radcr.2019.08.005]

43 **Oguslu U**, Uyanik SA, Gümüş B. Endovascular treatment of hepatic arterioportal fistula complicated with giant portal vein aneurysm *via* percutaneous transhepatic US guided hepatic artery access: a case report and review of the literature. *CVIR Endovasc* 2019; **2**: 39 [PMID: 32026997 DOI: 10.1186/s42155-019-0084-y]

44 **Kimura Y**, Hori T, Machimoto T, Ito T, Hata T, Kadokawa Y, Kato S, Yasukawa D, Aisu Y, Takamatsu Y, Kitano T, Yoshimura T. Portal vein aneurysm associated with arterioportal fistula after hepatic anterior segmentectomy: Thought-provoking complication after hepatectomy. *Surg Case Rep* 2018; **4**: 57 [PMID: 29904893 DOI: 10.1186/s40792-018-0465-9]

45 **Ding PX**, Han XW, Hua ZH. Extrahepatic Portal Vein Aneurysm at the Portal Bifurcation Treated with Transjugular Intrahepatic Portosystemic Shunt. *J Vasc Interv Radiol* 2017; **28**: 764-766 [PMID: 28431653 DOI: 10.1016/j.jvir.2016.12.1228]

46 **Dunlap R**, Golden S, Lyons GR. Portal Vein Aneurysm Treated With Trans-Jugular Intrahepatic Porto-Systemic Shunt. *Vasc Endovascular Surg* 2021; **55**: 885-888 [PMID: 34114524 DOI: 10.1177/15385744211023291]

47 **Kohlbrenner R**, Schwertner AB, Vogel AR, Conrad M, Lokken RP. Large thrombosed portomesenteric venous aneurysm treated with pharmacomechanical thrombolysis combined with TIPS placement. *CVIR Endovasc* 2022; **5**: 11 [PMID: 35133515 DOI: 10.1186/s42155-022-00288-0]

48 **Prabhakar N**, Vyas S, Taneja S, Khandelwal N. Intrahepatic aneurysmal portohepatic venous shunt: what should be done?

Ann Hepatol 2015; **14**: 118-120 [PMID: 25536649]
49 **Srikanth KP**, Thapa BR. Aneurysm of Right Branch of Portal Vein in a Child. *Indian Pediatr* 2015; **52**: 440 [PMID: 26061939]
50 **Starikov A**, Bartolotta RJ. Massive superior mesenteric venous aneurysm with portal venous thrombosis. *Clin Imaging* 2015; **39**: 908-910 [PMID: 26001660 DOI: 10.1016/j.clinimag.2015.05.001]
51 **Nayman A**, Guler I, Koplay M, Erdogan H, Cebeci H. Intrahepatic Portal Vein Aneurysm : An Unusual Entity. *Acta Gastroenterol Belg* 2016; **79**: 385 [PMID: 27821039]
52 **Jaiswal P**, Yap JE, Attar BM, Wang Y, Devani K, Jaiswal R, Basu A, Mishra S. Massive Asymptomatic Extrahepatic Portal Vein Aneurysm. *Am J Med* 2017; **130**: e383-e386 [PMID: 28454904 DOI: 10.1016/j.amjmed.2017.04.002]
53 **Guilbaud T**, Birnbaum DJ, Duconseil P, Soussan J, Moutardier V. Portal vein aneurysm incidentaloma. *Surgery* 2017; **162**: 1177-1178 [PMID: 27871687 DOI: 10.1016/j.surg.2016.10.016]
54 **Maia L**, Castro-Poças FM, Pedroto I. Portal Vein Aneurysm Mimicking a Liver Nodule. *GE Port J Gastroenterol* 2018; **25**: 105-106 [PMID: 29662938 DOI: 10.1159/000480244]
55 **Ashmore S**, Stacy K. Aneurysm of the Splenomesenteric Portal Venous Confluence: A Case Report. *S D Med* 2018; **71**: 199-201 [PMID: 29999605]
56 **Martínez D**, Belmonte MT, Kosny P, Gómez MR, Hellìn D. Aneurysm of the Left Portal Branch. *Eur J Case Rep Intern Med* 2018; **5**: 000868 [PMID: 30756043 DOI: 10.12890/2018_000868]
57 **Hirji SA**, Robertson FC, Casillas S, McPhee JT, Gupta N, Martin MC, Raffetto JD. Asymptomatic portal vein aneurysms: To treat, or not to treat? *Phlebology* 2018; **33**: 513-516 [PMID: 28950753 DOI: 10.1177/0268355517733375]
58 **Alur İ**, Us M. An incidental intrahepatic portal vein aneurysm. *Turk Gogus Kalp Damar Cerrahisi Derg* 2018; **26**: 681-682 [PMID: 32082819 DOI: 10.5606/tgkdc.dergisi.2018.16454]
59 **Chaubard S**, Lacroix P, Kennel C, Jaccard A. [Aneurysm of the portal venous system: A rare and unknown pathology]. *Rev Med Interne* 2018; **39**: 946-949 [PMID: 30146175 DOI: 10.1016/j.revmed.2018.07.007]
60 **Ramamoorthy E**, Kumar H, Gupta P. An Uncommon Portal Vein Abnormality. *Clin Gastroenterol Hepatol* 2019; **17**: e19-e20 [PMID: 29360510 DOI: 10.1016/j.cgh.2018.01.010]
61 **Kabir T**, Choke ETC, Kam JH. Unusual discovery in the liver: intrahepatic portal vein aneurysm. *ANZ J Surg* 2020; **90**: E28-E29 [PMID: 30977216 DOI: 10.1111/ans.15113]
62 **Shams T**, Hug M, Wolff T, Roduit J. [Superior mesenteric vein aneurysm, a rare case]. *Rev Med Suisse* 2020; **16**: 1652-1655 [PMID: 32914597]
63 **Hernando Sanz A**, Navarro-Aguilar V, López-Andújar R. Portal vein aneurysm, an update on the subject. A case report. *Rev Esp Enferm Dig* 2021; **113**: 77-78 [PMID: 33226247 DOI: 10.17235/reed.2020.6842/2019]
64 **Tan RLW**, Ng ZQ. Portal venous aneurysm. *BMJ Case Rep* 2021; **14** [PMID: 34330734 DOI: 10.1136/bcr-2021-244704]
65 **López-Fernández J**, García Plaza G, García Quesada SM, Hernández Hernández JR. Superior mesenteric vein aneurysm. *Rev Esp Enferm Dig* 2021; **113**: 615-616 [PMID: 33761751 DOI: 10.17235/reed.2021.7932/2021]
66 **Villani R**, Lupo P, Angeletti AG, Sacco AF, Macarini L, Serviddio G. Asymptomatic saccular portal vein aneurysm: a case report and review of the literature. *J Ultrasound* 2022; **25**: 799-803 [PMID: 35113392 DOI: 10.1007/s40477-022-00659-2]
67 **Mortazavi S**, Trinder M, Li R, Abdul Aziz F. Extrahepatic portal vein aneurysm identification during cholecystectomy. *ANZ J Surg* 2022; **92**: 921-922 [PMID: 34559442 DOI: 10.1111/ans.17206]
68 **Matsumoto T**, Aoki T, Kubota K. Pancreatic Head Adenocarcinoma Complicated by Portal Venous Aneurysm. *J Gastrointest Surg* 2021; **25**: 1628-1630 [PMID: 33169326 DOI: 10.1007/s11605-020-04865-3]
69 **Ierardi AM**, Berselli M, Cuffari S, Castelli P, Cocozza E, Carrafiello G. Uncommon Case of a Post-Traumatic Portal Vein Pseudoaneurysm Treated with Percutaneous Transhepatic Stent Grafting. *Cardiovasc Intervent Radiol* 2016; **39**: 1506-1509 [PMID: 27230514 DOI: 10.1007/s00270-016-1373-7]
70 **Walton H**, Yu D, Imber C, Webster G. Portal vein pseudoaneurysm secondary to pancreatic lymphoma and biliary stent insertion: a rare cause of haemobilia. *CVIR Endovasc* 2018; **1**: 5 [PMID: 30652138 DOI: 10.1186/s42155-018-0011-7]
71 **Cleveland NC**, Nguyen DN, Tran CD, Maheshwary RK, Hartman MS. Traumatic Injury to the Portal Vein With Shock Bowel. *Curr Probl Diagn Radiol* 2019; **48**: 97-99 [PMID: 29107397 DOI: 10.1067/j.cpradiol.2017.09.011]

World Journal of Clinical Cases

Submit a Manuscript: https://www.f6publishing.com

World J Clin Cases 2023 February 6; 11(4): 738-755

DOI: 10.12998/wjcc.v11.i4.738

ISSN 2307-8960 (online)

ORIGINAL ARTICLE

Clinical and Translational Research

CD93 serves as a potential biomarker of gastric cancer and correlates with the tumor microenvironment

Zheng Li, Xiao-Jie Zhang, Chong-Yuan Sun, He Fei, Ze-Feng Li, Dong-Bing Zhao

Specialty type: Gastroenterology and hepatology

Provenance and peer review: Unsolicited article; Externally peer reviewed.

Peer-review model: Single blind

Peer-review report's scientific quality classification

Grade A (Excellent): A
Grade B (Very good): B
Grade C (Good): 0
Grade D (Fair): 0
Grade E (Poor): 0

P-Reviewer: Dilek ON, Turkey; Koganti SB, United States

Received: October 12, 2022
Peer-review started: October 12, 2022
First decision: December 13, 2022
Revised: December 13, 2022
Accepted: January 3, 2023
Article in press: January 3, 2023
Published online: February 6, 2023

Zheng Li, Xiao-Jie Zhang, Chong-Yuan Sun, He Fei, Ze-Feng Li, Dong-Bing Zhao, Department of Pancreatic and Gastric Surgical Oncology, National Cancer Center/National Clinical Research for Cancer/Cancer Hospital, Chinese Academy of Medical Sciences and Peking Union Medical College, Beijing 100021, China

Corresponding author: Dong-Bing Zhao, MD, Professor, Department of Pancreatic and Gastric Surgical Oncology, National Cancer Center/National Clinical Research for Cancer/Cancer Hospital, Chinese Academy of Medical Sciences and Peking Union Medical College, No. 17 Pan-Jia-Yuan South Lane, Chaoyang District, Beijing 100021, China. dbzhao@cicams.ac.cn

Abstract

BACKGROUND

The tumor microenvironment (TME) plays an important role in the growth and expansion of gastric cancer (GC). Studies have identified that CD93 is involved in abnormal tumor angiogenesis, which may be related to the regulation of the TME.

AIM

To determine the role of CD93 in GC.

METHODS

Transcriptomic data of GC was investigated in a cohort from The Cancer Genome Atlas. Additionally, RNA-seq data sets from Gene Expression Omnibus (GSE118916, GSE52138, GSE79973, GSE19826, and GSE84433) were applied to validate the results. We performed the immune infiltration analyses using ESTIMATE, CIBERSORT, and ssGSEA. Furthermore, weighted gene co-expression network analysis (WGCNA) was conducted to identify the immune-related genes.

RESULTS

Compared to normal tissues, CD93 significantly enriched in tumor tissues (t = 4.669, 95%CI: 0.342-0.863, P < 0.001). Higher expression of CD93 was significantly associated with shorter overall survival (hazard ratio = 1.62, 95%CI: 1.09-2.4, P = 0.017), less proportion of CD8 T and activated natural killer cells in the TME (P < 0.05), and lower tumor mutation burden (t = 4.131, 95%CI: 0.721-0.256, P < 0.001). Genes co-expressed with CD93 were mainly enriched in angiogenesis. Moreover, 11 genes were identified with a strong relationship between CD93 and the immune microenvironment using WGCNA.

CONCLUSION
CD93 is a novel prognostic and diagnostic biomarker for GC, that is closely related to the immune infiltration in the TME. Although this retrospective study was a comprehensive analysis, the prospective cohort studies are preferred to further confirm these conclusions.

Key Words: Gastric cancer; CD93; Tumor microenvironment; Immunotherapy; Prognosis; Biomarker

Core Tip: Gastric cancer (GC) is an aggressive malignancy, with a 5-year survival rate lower than 20%. The disease burden caused by GC remains heavy worldwide. In this study, various analyses were performed using transcriptomic profiles from the Gene Expression Omnibus databases and The Cancer Genome Atlas. Finally, enrichment analysis and protein-protein interaction network were constructed. CD93 is identified as a diagnostic and prognostic biomarker of GC, which is closely related to the immune infiltration in the tumor microenvironment. Then, Immune-related gene modules were identified to further reveal the relationship between CD93 and immune characteristics.

Citation: Li Z, Zhang XJ, Sun CY, Fei H, Li ZF, Zhao DB. CD93 serves as a potential biomarker of gastric cancer and correlates with the tumor microenvironment. *World J Clin Cases* 2023; 11(4): 738-755
URL: https://www.wjgnet.com/2307-8960/full/v11/i4/738.htm
DOI: https://dx.doi.org/10.12998/wjcc.v11.i4.738

INTRODUCTION

As a common malignancy of the digestive tract tumor, gastric cancer (GC) is the fourth leading cause of cancer-related mortality worldwide, and the 5-year survival rate of GC is lower than 20%[1]. Treatments for GC include endoscopic resection, surgery (D2 lymphadenectomy), perioperative or adjuvant chemotherapy, targeted therapy, immunotherapy, and so on. Among them, immunotherapy for GC has attracted more attention in recent years[2,3]. The tumor microenvironment (TME) refers to tumor cells and their surrounding cellular matrix, including blood vessels, and immune cells, and is an important factor influencing the effect of immunotherapy on GC[4]. Targeting and suppressing the immunosuppressive properties of the TME can enhance the overall response rate (ORR) to immunotherapy, including immune checkpoint inhibitors (ICIs)[5-7]. CD93 is known as a C1q receptor that is involved in a variety of biological processes, such as the inflammatory response, tumor angiogenesis, matrix regulation, and innate lymphoid cell function [8-10], which suggests that CD93 may participate in the regulation of the TME. A recent study has found that blocking the CD93 pathway contributes to drug transport and immunotherapy efficacy by normalizing the vasculature of tumors. CD93 pathway blockade can improve the efficacy of chemotherapy and immunotherapy[11]. Although the roleof CD93 in some tumors has been explored, the specific role of CD93 in GC is still unclear.

Given these considerations, we were deeply interested in the relationship between CD93 and immune infiltration in the TME and the value of CD93 in the diagnosis, prognosis, and immunotherapy of GC. Therefore, the RNA-seq transcriptome profiles of stomach adenocarcinoma (STAD) within The Cancer Genome Atlas (TCGA) and Gene Expression Omnibus (GEO) were investigated. We first performed a pan-cancer analysis to identify the general significance of CD93 in cancers. Then, we divided patients with GC in this study into two groups according to the expression of CD93, and we compared the groups in terms of immune cell infiltration, gene mutation landscape, tumor mutational burden, and so on.

MATERIALS AND METHODS

Data sources and processing

Gene expression RNA-seq (HTSeq-Counts, HTSeq-FPKM) and survival data in a cohort of TCGA Stomach Cancer were downloaded from UCSC Xena[12]. HTSeq-FPKM of 375 tumor samples and 32 normal samples were used for further analysis. HTSeq-Counts data were used to identify the differential expressed genes (DEGs) of low and high CD93 expression groups using the R package DESeq2 [13] (|log2FoldChange| > 1 and adjusted $P < 0.05$). Expression profiling data in 5 datasets (GSE118916, GSE52138, GSE79973, GSE19826, and GSE84433) from GEO[14] were downloaded as validation sets.

Mutation data (MuTect2) including 414 patients with STAD from TCGA were processed using R package maftools[15]. The waterfall plot was used to show the genetic mutation using the R package ComplexHeatmap[16].

Pan-cancer analysis

To understand the general significance of CD93 in cancers, we compared the expression levels of CD93 between tumor tissues and normal tissues in various cancer types using TIMER2.0[17]. Additionally, TISIDB[18] was also used to obtain the relationship between CD93 expression and the OS of these cancer types.

Diagnostic and prognostic value analysis

We compared CD93 expression levels of GC and normal tissues in both unpaired and paired samples and visualize outcomes using R package ggplot2. Receiver operating characteristic (ROC) curves and Kaplan-Meier survival analysis were conducted to further explore the diagnostic and prognostic value of CD93, and R packages pROC[19] and survminer were used for visualization, respectively. Univariate and multivariate COX proportional hazards models were established for better understanding. In addition, Immunohistochemistry and Immunofluorescence of CD93 were obtained from Human Protein Atlas[20].

Functional enrichment analysis

Genes that were significantly positively or negatively related to CD93 were identified using LinkedOmics[21]. Heatmaps were used to show the top 50 positively and the top 50 negatively correlated genes. Then, we constructed a protein-protein interaction (PPI) network of positively correlated genes *via* GeneMANIA[22]. Gene Ontology (GO) and Kyoto Encyclopedia of Genes and Genomes (KEGG) enrichment analyses of these genes were performed using the R package clusterProfiler[23].

Immune infiltration analysis

A plot from the TIMER[24] was used to show the correlations between the CD93 expression level and B cell, CD8+T Cell, CD4+T cell, macrophage, neutrophil, and dendritic cell. ESTIMATE is a method to identify the proportions of stromal and immune cells, which can bring the in-depth exploration of TME. We evaluated the immune score (immune component), stromal score (stromal component), and ESTIMATE score (comprehensive score of immunity and matrix) of each sample from TCGA and GEO using the R package estimate[25]. CIBERSORT[26] is a tool to characterize the cell composition of various tissues. We calculate the proportion of 22 immune cells in each sample with STAD using this method. Then, we conducted the ssGSEA to evaluate the infiltration level of 28 immune cell types based on the published immune gene sets[27] using the R package GSVA[28].

Weighted gene co-expression network analysis

Weighted gene co-expression network analysis (WGCNA) was applied to identify the module genes related to CD93 and the immunity of patients with STAD using the R package WGCNA[29] (softPower = 4). Nine modules were obtained to calculate their relationships with stromal score, immune score, ESTIMATE score, and tumor purity. Finally, we identified 11 hub genes based on the value of module membership (MM) > 0.80 and gene significance (GS) > 0.85.

Analysis of hub genes

The PPI network and GO enrichment analysis of 11 hub genes were performed using the R package clusterProfiler and STRING[30], respectively. Then, we calculated Spearman's correlation of 11 hub genes, hub gene-ESTIMATE, and hub gene-ssGSEA using the R package corrplot.

Statistical analysis

All statistical analyses mentioned in this article were conducted by R (version 4.2.0) and SPSS (version 25.0). Weltch't test and Spearman's coefficient were used for box plots and correlation analysis, respectively. We evaluated statistical significance using two-sided t-tests and defined it as $^{a}P < 0.05$, $^{b}P < 0.01$, and $^{c}P < 0.001$.

RESULTS

Pan-cancer analysis of CD93

The expression of CD93 between tumor and normal tissues in various cancers was compared using TIMER2.0, suggesting that CD93 expression was significantly different between tumor and normal tissues in various types of cancers ($P < 0.05$) (Figure 1A). We further investigated the effect of CD93 on OS across human cancers *via* the TISIDB. It showed that high CD93 expression led to shorter overall

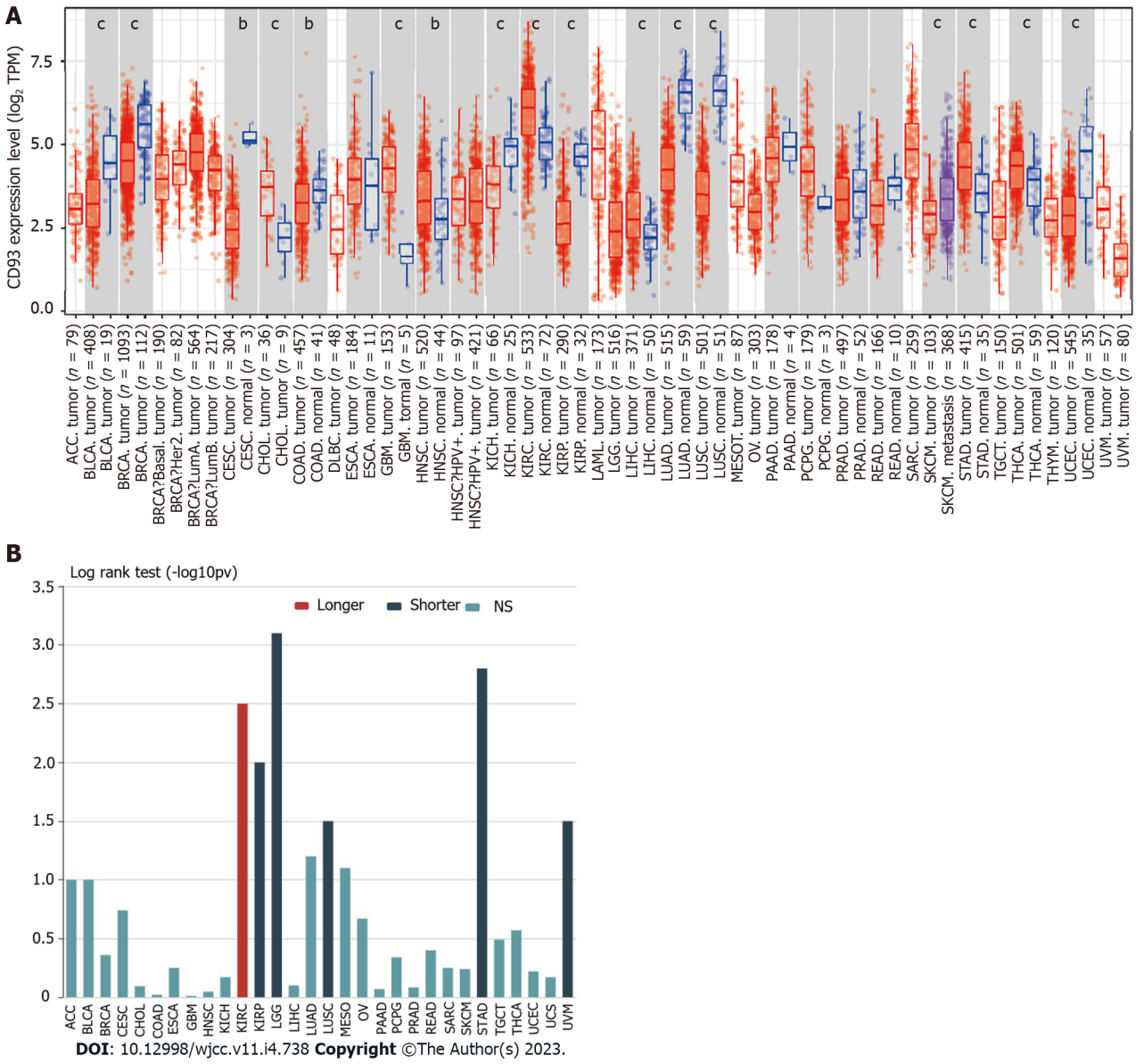

Figure 1 Pan-cancer analysis of CD93. A: Differential expression of CD93 between normal and tumor tissues in pan-cancer based on the TIMER2.0; B: Associations between CD93 expression and overall survival in pan-cancer. The *P* values are labeled as $^{a}P < 0.05$, $^{b}P < 0.01$, $^{c}P < 0.001$.

survival in STAD, kidney renal papillary cell carcinoma, brain lower-grade glioma, lung squamous cell carcinoma, and uveal melanoma, while leading to a longer one in kidney renal clear cell carcinoma (Figure 1B).

Diagnostic value for GC of CD93

The CD93 expression levels of unpaired and paired samples from TCGA were both significantly higher in GC than in normal tissues ($t = 4.669$, 95%CI: 0.342-0.863, $P < 0.001$; $t = 3.238$, 95%CI: 0.196-0.877, $P = 0.003$) (Figure 2A and B). In addition, expression data obtained from GEO (GSE118916, GSE52138, GSE79973, and GSE19826) was applied for verification (Figure 2H-K). All datasets from TCGA and GEO showed a significantly higher expression of CD93 in GC tissues than in normal tissues ($P < 0.05$). Immunohistochemistry indicated higher CD93 expression in GC tissues than in normal tissues from the protein level (Figure 2E). Immunofluorescence indicated that CD93 mainly expressed in vesicles, plasma membrane, and toggle channels (Figure 2F). Furthermore, ROC curves were performed using the datasets mentioned above to evaluate the diagnostic value of CD93, the area under the curve was 0.695, 0.876, 0.806, 0.750, and 0.771, respectively (Figure 2C and L-O).

Prognostic value for GC of CD93

Samples from the TCGA STAD dataset were divided into two groups by the CD93 expression level, including the low CD93 expression group (low, $n = 114$) and the high CD93 expression group (high, $n = 220$). Kaplan-Meier analysis of two groups was conducted, suggesting that patients with high

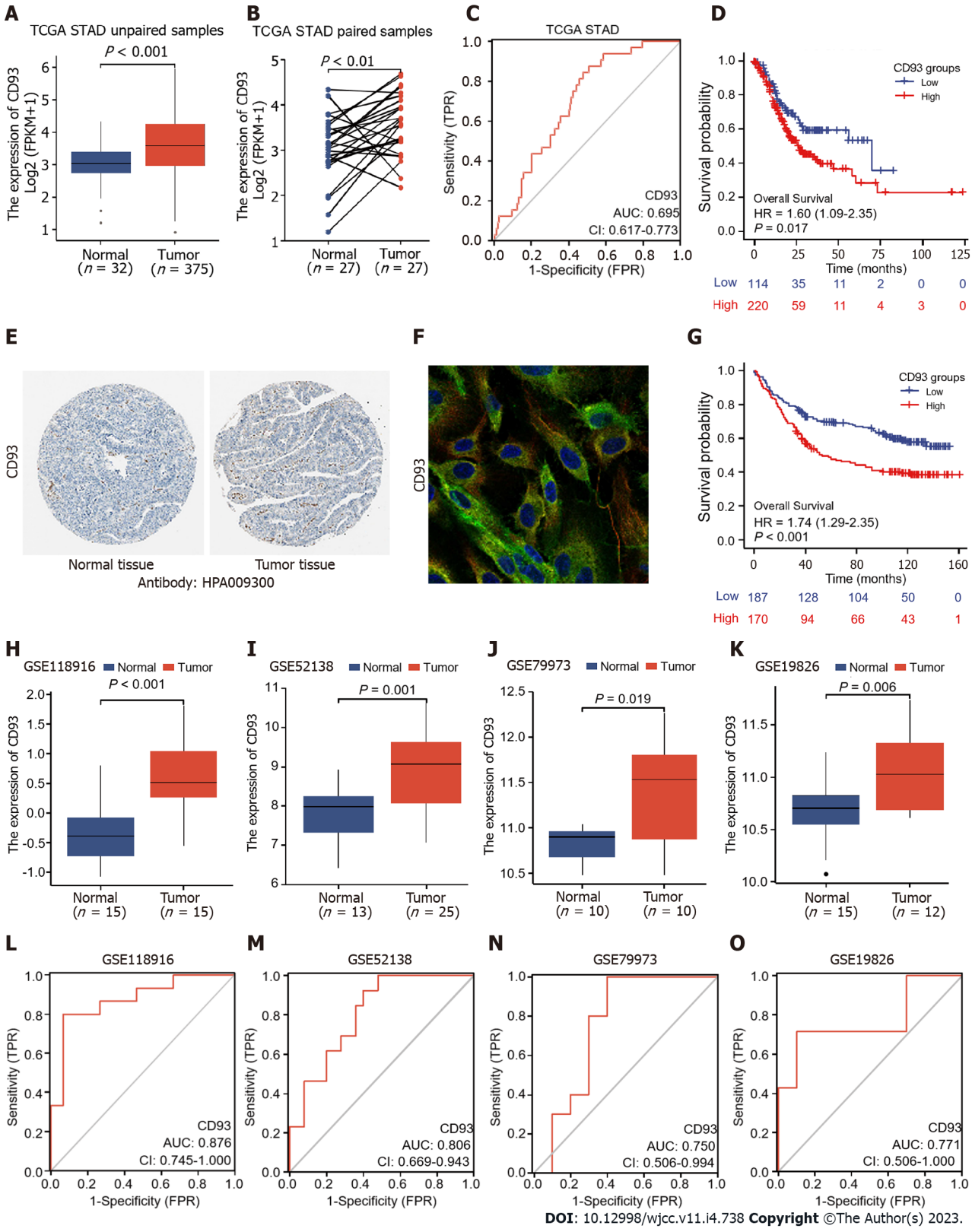

DOI: 10.12998/wjcc.v11.i4.738

Figure 2 Diagnostic and prognostic value analysis. A and B: Differential expression of CD93 between gastric cancer (GC) and normal tissues in unpaired samples (A), paired samples (B); C: Receiver operating characteristic (ROC) curve of overall survival based on CD93 in The Cancer Genome Atlas stomach adenocarcinoma; D: Kaplan-Meier analysis of OS between two groups; E: Immunohistochemistry of CD93 between GC and normal tissues; F: Immunofluorescence of CD93; H-K: Differential expression of CD93 in 4 validation datasets (GSE118916, GSE52138, GSE79973, and GSE19826); L-O: ROC curves of 4 validation datasets based on CD93.

expression of CD93 had significantly shorter OS [hazard ratio (HR) = 1.60, 95%CI: 1.09-2.35, P = 0.017] (Figure 2D). In addition, we set GSE84433 with 357 GC patients as an external independent validation dataset and divided these patients into low-CD93 (low, n = 178) and high-CD93 (high, n = 179)

Table 1 Univariate and multivariate Cox regression analysis of overall survival

Characteristics	Univariate analysis			Multivariate analysis		
	HR	95%CI	*P* value	HR	95%CI	*P* value
Age	1.02	1.01-1.04	0.002	1.03	1.02-1.05	< 0.001
Grade						
G1	Reference					
G2	2.64	0.36-19.18	0.337			
G3	3.53	0.49-25.38	0.209			
G4	3.54	0.37-34.07	0.274			
Gender	1.31	0.91-1.9	0.145			
Stage						
I	Reference			Reference		
II	1.45	0.75-2.8	0.268	1.41	0.73-2.74	0.307
III	2.11	1.14-3.91	0.018	1.99	1.07-3.71	0.03
IV	3.65	1.81-7.39	< 0.001	4.97	2.41-10.22	< 0.001
CD93 (high *vs* low)	1.6	1.09-2.35	0.017	1.62	1.09-2.4	0.017

HR: Hazard ratio.

expression groups. A similar result could be drawn from the Kaplan–Meier analysis that patients in the high-CD93 expression group had a shorter OS (HR: 1.74, 95%CI: 1.29-2.35, $P < 0.001$) (Figure 2G). Univariate and multivariate COX regression analysis were conducted as Table 1, indicating CD93 was a significant independent prognostic risk factor for GC (HR = 1.62, 95%CI: 1.09-2.40, $P = 0.017$). The baseline patient characteristics were summarized in Table 2.

Identification and enrichment analysis of correlation genes

Correlation analysis with CD93 based on the Pearson test was conducted using LinkedOmics. The result was visualized by a volcano plot (Figure 3A). We obtained 7026 significantly positively correlated genes (red dots) and 5308 significantly negatively ones (green dots), respectively. In addition, we showed heatmaps of the top 50 positively correlated and the top 50 negatively correlated genes (Figure 3B and C). PPI network of the top 10 positive CD93 co-expressed genes was further constructed using GeneMANIA, suggesting functions of "angiogenesis", "endothelium development", and "regulation of angiogenesis" (Figure 3D). GO enrichment analysis of positive CD93 co-expressed genes mainly enriched in "ameboidal-type cell migration" (biological process), "collagen-containing extracellular matrix" (cell component), and "growth factor binding" (molecular function) (Figure 3E). KEGG pathway enrichment analysis indicated that these genes mainly participated in the "PI3K-Akt signaling pathway", "Focal adhesion", and "Pathways in cancer" (Figure 3F).

Immune-related analysis in the TME

The expression of CD93 was positively proportional to CD8+T Cell, CD4+T cell, macrophage, neutrophil, and dendritic cell ($P < 0.05$) (Figure 4A). Furthermore, CD93 expression tended to have a positive correlation with ESTIMATE results (immune score, stromal score, and ESTIMATE score) ($P < 0.05$) (Figure 4B-D). Then, we performed the CIBERSORT for determining the proportion of 22 immune cells in each sample with STAD (Figure 4E). The proportion of 22 immune cells in two groups was compared using CIBERSORT, suggesting the proportion of CD8 T cells, follicular helper T cells, and activated NK cells in the high CD93 expression group was significantly lower than that in the low CD93 expression group, whereas Monocytes, Dendritic cells resting, and Mast cells resting had just the reverse ($P < 0.05$) (Figure 4F). ssGSEA showed that 24 types of immune cell (such as activated B cell, activated CD8 T cell, activated dendritic cell, central memory CD4 T cell, and central memory CD8 T cell) had a significantly higher expression in the high CD93 expression group, while CD56 bright natural killer (NK) cell had a lower expression in this group ($P < 0.05$) (Figure 4G).

Gene mutation analysis and tumor mutation burden comparison

Gene mutation of GC is closely related to its therapeutic efficacy. Accordingly, a waterfall plot was used to identify the top 15 significant gene mutations (such as *TTN*, *MUC16*, and *LRP1B*) between two groups ($P < 0.05$) (Figure 5A). Furthermore, we made a comparison of tumor mutation burden (TMB) between

Table 2 Baseline patient characteristics

Characteristics	high-CD93 (*n* = 220)	low-CD93 (*n* = 114)	Overall (*n* = 334)
Age, yr (mean ± SD)	64.8 ± 12.8	64.1 ± 10.3	64.5 ± 12.0
Gender, *n* (%)			
Female	72 (32.7)	48 (42.1)	120 (35.9)
Male	148 (67.3)	66 (57.9)	214 (64.1)
Grade, *n* (%)			
G1	4 (1.8)	4 (3.5)	8 (2.4)
G2	66 (30.0)	50 (43.9)	116 (34.7)
G3	143 (65.0)	59 (51.8)	202 (60.5)
GX	7 (3.2)	1 (0.9)	8 (2.4)
pT, *n* (%)			
T1	5 (2.3)	10 (8.8)	15 (4.5)
T2	45 (20.5)	25 (21.9)	70 (21.0)
T3	103 (46.8)	53 (46.5)	156 (46.7)
T4	67 (30.5)	26 (22.8)	93 (27.8)
pN, *n* (%)			
N0	63 (28.6)	40 (35.1)	103 (30.8)
N1	62 (28.2)	24 (21.1)	86 (25.7)
N2	43 (19.5)	26 (22.8)	69 (20.7)
N3	48 (21.8)	22 (19.3)	70 (21.0)
NX	4 (1.8)	2 (1.8)	6 (1.8)
pM, *n* (%)			
M0	194 (88.2)	105 (92.1)	299 (89.5)
M1	17 (7.7)	4 (3.5)	21 (6.3)
MX	9 (4.1)	5 (4.4)	14 (4.2)
Stage, *n* (%)			
Stage I	24 (10.9)	22 (19.3)	46 (13.8)
Stage II	75 (34.1)	35 (30.7)	110 (32.9)
Stage III	96 (43.6)	48 (42.1)	144 (43.1)
Stage IV	25 (11.4)	9 (7.9)	34 (10.2)

low and high CD93 expression groups, which indicated that patients with high CD93 expression had a lower TMB (t = 4.131, 95%CI: 0.721-0.256, P < 0.001) (Figure 5B). The mutation rate of CD93 in GC ranked fourth in pan-cancer (Figure 5C).

Identification of hub genes in the immune microenvironment of GC

A total of 1679 DEGs (966 upregulated and 713 downregulated) were obtained between low and high CD93 expression groups. Then, we visualize the results using a volcano plot (Figure 6A). WGCNA was conducted to identify a module related to CD93 expression and immune infiltration (Figure 6B-D). The Yellow module was screened out because of its high correlation with immunity (r = 0.89, $P = 5 \times 10^{-122}$), hence we acquired 11 hub genes (*MPEG1*, *IL10RA*, *SRGN*, *SLA*, *DOCK2*, *NCKAP1L*, *IKZF1*, *PTPRC*, *SIGLEC10*, *PLEK*, *P2RY10*) from the yellow module based on MM > 0.80 and GS > 0.85 (Figure 6E).

Analysis of 11 hub genes

GO enrichment analysis identified these genes were mainly enriched in "positive regulation of phagocytosis" (biological process), "cytoplasmic side of plasma membrane" (cell component), and "interleukin-10 binding" (molecular function) (Figure 7A). Furthermore, we constructed a PPI network and made a correlation analysis of these genes (Figure 7B and C). Correlation analysis between these

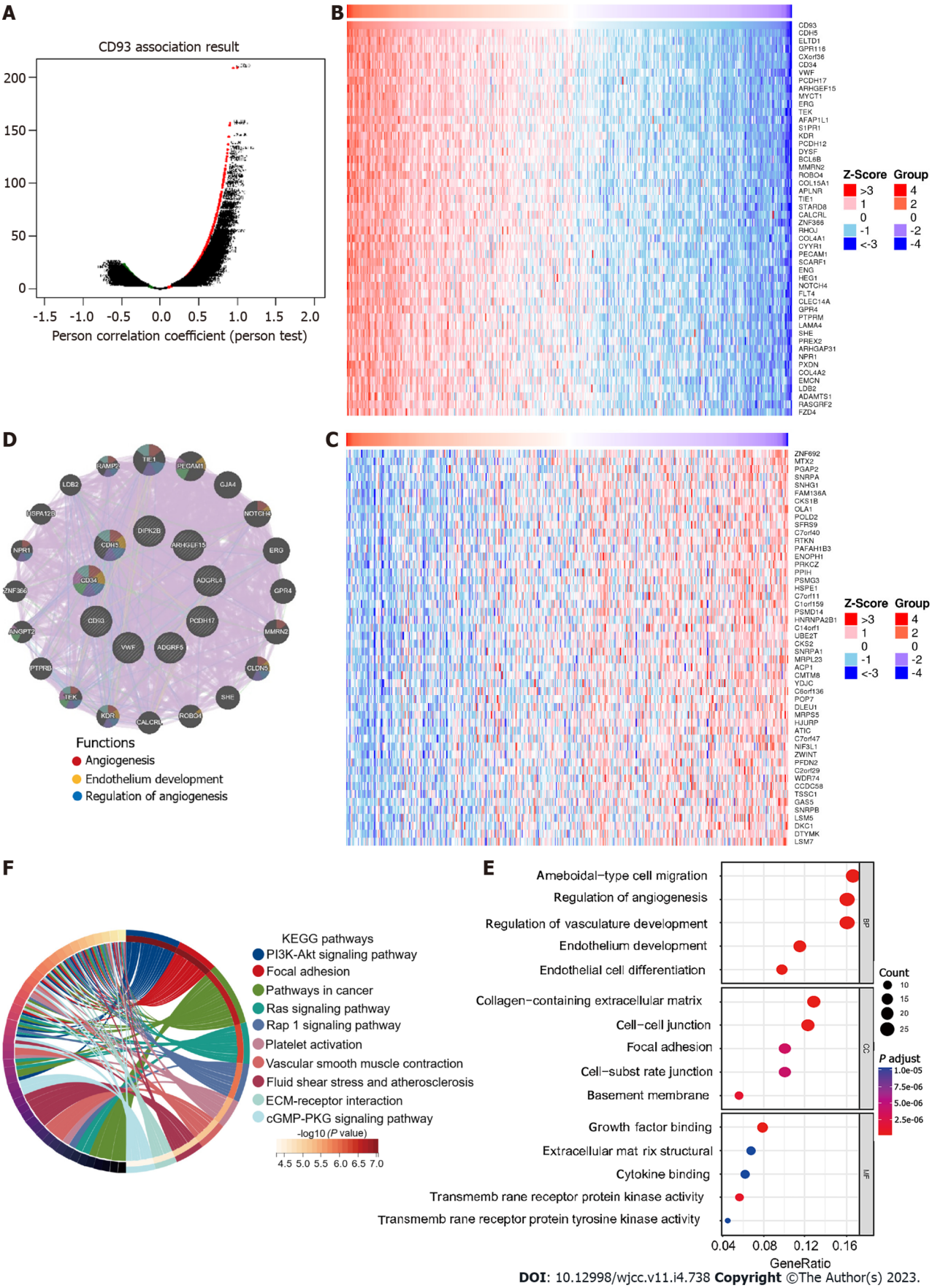

DOI: 10.12998/wjcc.v11.i4.738

Figure 3 Function and pathway analysis. A: Genes are highly correlated with CD93; B: Heatmap of the top 50 positive correlation genes; C: Heatmap of the top 50 negative correlation genes; D: Protein-protein interaction of the top positive correlation genes; E: The Gene Ontology enrichment analysis; F: The Kyoto Encyclopedia of Genes and Genomes pathways enrichment analysis.

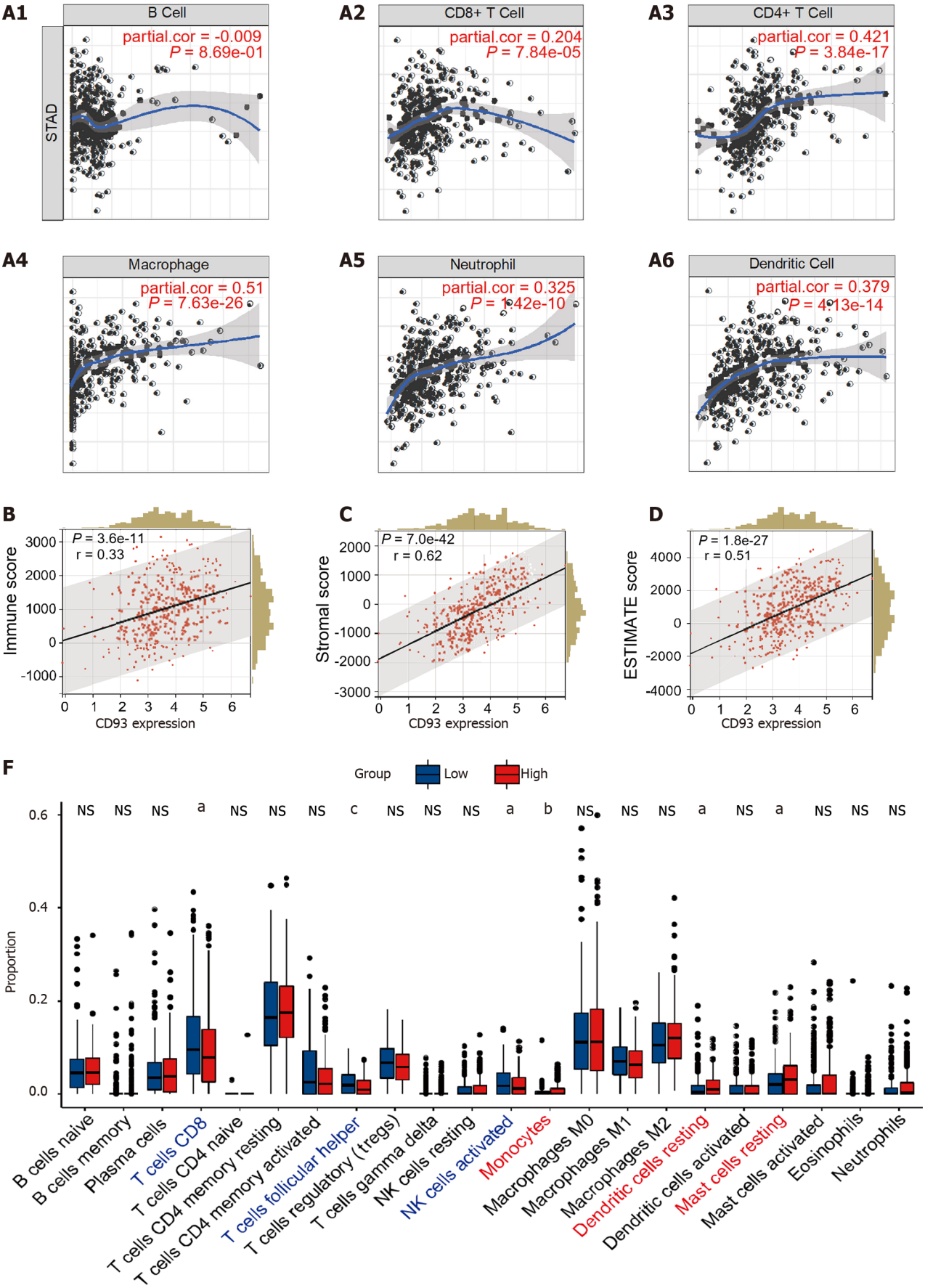
A1
B Cell
STAD
partial.cor = -0.009
P = 8.69e-01
A2
CD8+ T Cell
partial.cor = 0.204
P = 7.84e-05
A3
CD4+ T Cell
partial.cor = 0.421
P = 3.84e-17
A4
Macrophage
partial.cor = 0.51
P = 7.63e-26
A5
Neutrophil
partial.cor = 0.325
P = 1.42e-10
A6
Dendritic Cell
partial.cor = 0.379
P = 4.13e-14
B
P = 3.6e-11
r = 0.33
Immune score
CD93 expression
C
P = 7.0e-42
r = 0.62
Stromal score
CD93 expression
D
P = 1.8e-27
r = 0.51
ESTIMATE score
CD93 expression
F
Group
Low
High
Proportion
B cells naive
B cells memory
Plasma cells
T cells CD8
T cells CD4 naive
T cells CD4 memory resting
T cells CD4 memory activated
T cells follicular helper
T cells regulatory (tregs)
T cells gamma delta
NK cells resting
NK cells activated
Monocytes
Macrophages M0
Macrophages M1
Macrophages M2
Dendritic cells resting
Dendritic cells activated
Mast cells resting
Mast cells activated
Eosinophils
Neutrophils

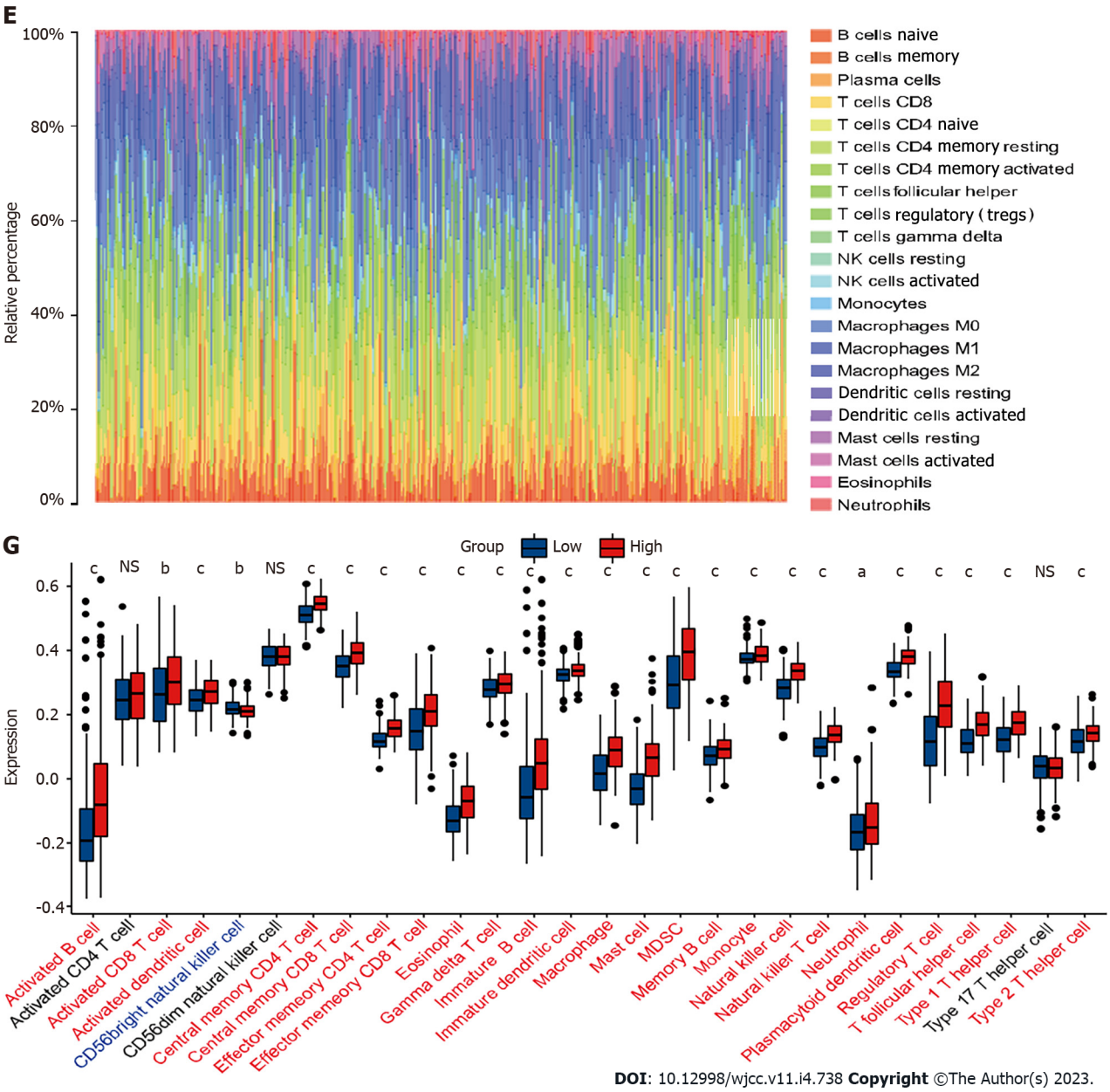

DOI: 10.12998/wjcc.v11.i4.738

Figure 4 Immune characteristics in tumor microenvironment. A: Correlation between CD93 and six types of immune cells based on TIMER; B-D: Correlation between CD93 and immune score (B), stromal score (C), ESTIMATE score (D); E: The proportion of immune cell infiltration; F: Different proportions of immune cells infiltration between two groups; G: Expression of immune cells between two groups *via* ssGSEA. The *P* values are labeled as $^{a}P < 0.05$, $^{b}P < 0.01$, $^{c}P < 0.001$, NS: No significance.

genes and TME (ESTIMATE and ssGSEA) suggested that these genes were closely related to both stromal components and immune infiltration in GC (Figure 7D and E).

Validation of immune-related characteristics in TME

GSE84433 (357 samples) was set as an external independent validation dataset. We performed ESTIMATE, CIBERSORT, and ssGSEA to evaluate the immune-related characteristics of CD93 in TME again. Then, several similar results as before could be obtained. CD93 expression was positively correlated with the ESTIMATE results (Figure 8A-C). CIBERSORT showed the proportion of various immune cell types in each sample (Figure 8D). The proportion of follicular helper T cells and activated NK cells in the high-CD93 expression group was lower compared to that in the low-CD93 expression group (Figure 8E). ssGSEA indicated that 24 immune cell types (including activated B cell, activated CD8 T cell, and activated dendritic cell) expressed significantly higher in the high-CD93 expression group (Figure 8F). Accordingly, CD93 was identified to be closely related to immune infiltration in TME of GC.

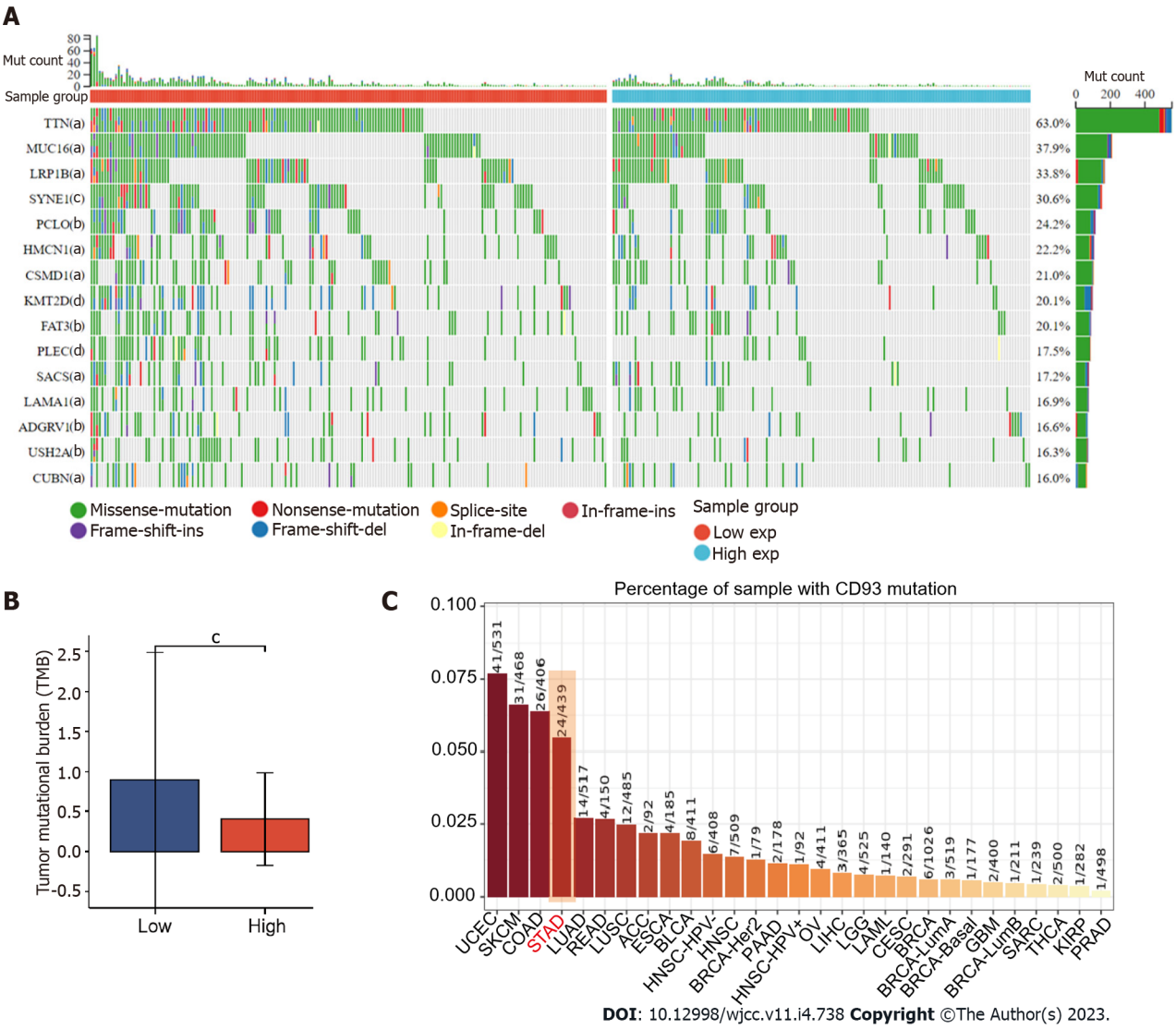

DOI: 10.12998/wjcc.v11.i4.738

Figure 5 Gene mutation and tumor mutational burden comparison. A: Comparison of mutational landscapes between two groups; B: Comparison of tumor mutational burden between two groups; C: The mutation rate of CD93 in gastric cancer ranked fourth in pan-cancer. The *P* values are labeled as $^{a}P < 0.05$, $^{b}P < 0.01$, $^{c}P < 0.001$.

DISCUSSION

In this study, we applied bioinformatics technology to determine the specific role of CD93 in GC. Various analytical methods identified that CD93 is a biomarker for the diagnosis and prognosis of GC. Concerning the potential mechanisms of CD93, enrichment analysis was performed. Consistent with previous studies[11], CD93 was found to be involved in the formation of tumor blood vessels in GC. Such disordered, immature, and impermeable blood vessels can lead to poor tumor blood perfusion. The resulting hypoxic microenvironment can promote the production of more aggressive tumor cells and limit the killing effect of immune cells[31]. In addition to regulating angiogenesis, GO enrichment analysis suggested that CD93 is involved in matrix formation including cell junction, focal adhesion, and regulation of cytokine production, which further demonstrates the important status of CD93 in TME. Also worth noting is that CD93 plays a critical role in the PI3K-Akt signaling pathway. The PI3K-Akt pathway is constantly found to be activated in various cancers and has been considered a promising target for therapy. Multiple activators of this pathway have been proved to possess oncogenic potentials *in vivo* and *in vitro* with diverse mechanisms, including stimulation of metabolic reprogramming, proliferation, and so on[32]. These tend to be part of the reasons for the poor prognosis of patients with GC induced by CD93.

As important components of the TME, immune cells can inhibit or promote tumor progression by interacting with tumor cells[33]. The investigation of immune components in TME brings a deeper understanding of the biological characteristics, prognosis, and other information of tumors. Based on ESTIMATE, CIBERSORT, and ssGSEA, a comparison of immune cell infiltration between low and high CD93 expression groups was conducted. According to the result of ESTIMATE, we found that CD93

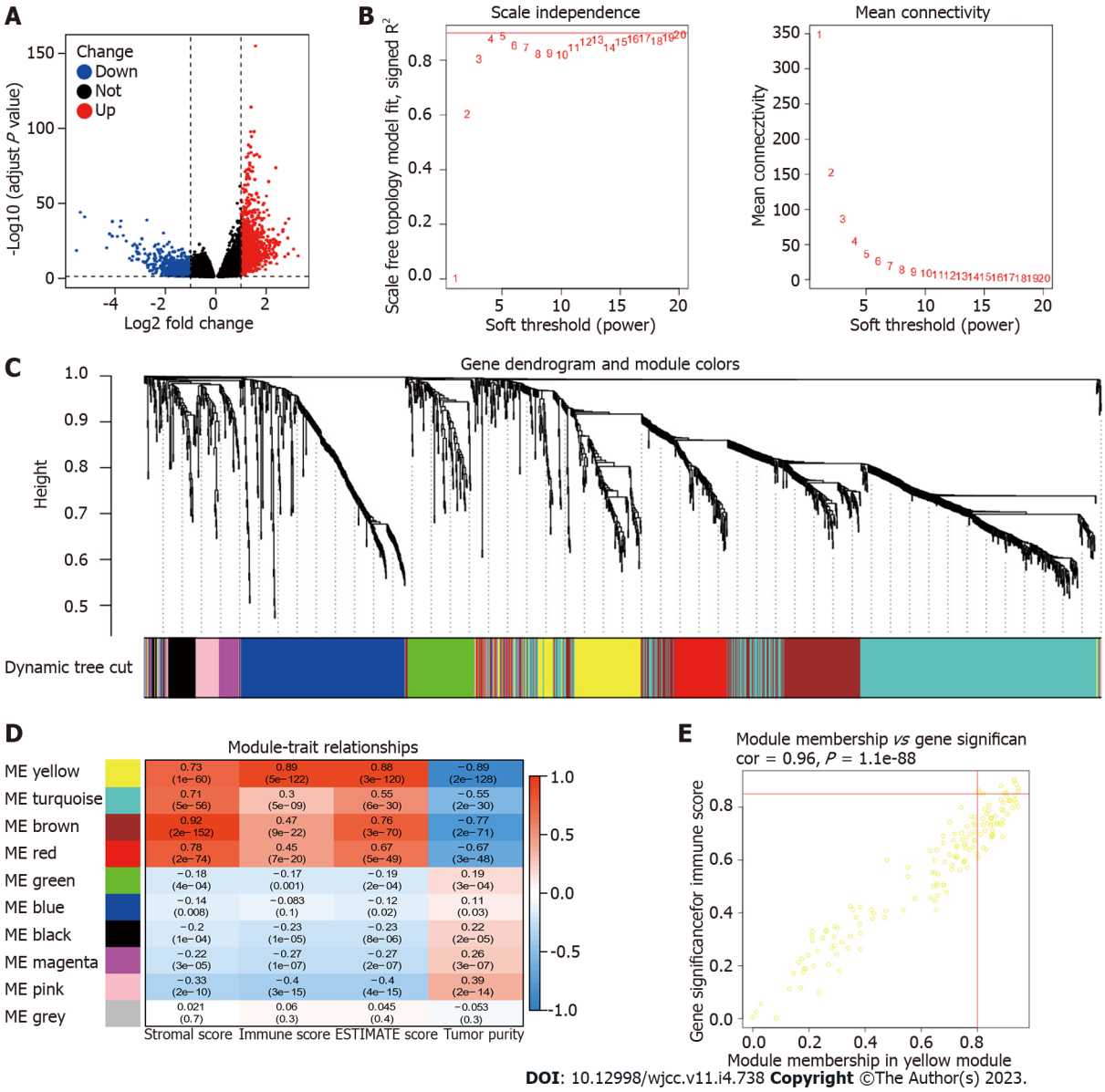

DOI: 10.12998/wjcc.v11.i4.738 **Copyright** ©The Author(s) 2023.

Figure 6 Identification of the key genes related to CD93 in the tumor immune microenvironment. A: Volcano plot of variance analysis; B: Analysis of network topology for soft powers; C: Gene dendrogram and module colors; D: Heatmap between modules and ESTIMATE results; E: Scatter plot of genes in the yellow module.

was significantly proportional to immunity. Previous studies could give reasonable explanations for this result. The blood vessel wall mainly consists of endothelial cells, pericytes, and smooth muscle cells. On the one hand, these cells can activate T cells by expressing MHCI, MHCII, and some costimulatory factors such as CD80, and CD86 to participate in the immune response[34]. On the other hand, a variety of immune cell subsets, including NK cells, T helper 17 cells, regulatory T lymphocytes, and functional subsets of macrophages can act as regulators of arteriogenesis[35]. The crosstalk between the vascular system and immunity explains the high correlation between CD93 and immunity.

From the proportion of immune cell expression, CD8 T cells, Follicular helper T cells, and activated NK cells showed a lower proportion in the high CD93 expression group, while monocytes, resting dendritic cells, and resting mast cells had just the reverse. This is probably caused by local microenvironment hypoxia and accumulation of metabolic end-products induced by abnormal vascular proliferation due to high expression of CD93. CD8 T cells and NK cells are important effector cells involved in anti-tumor immune response in TME and are related to tumor progression and prognosis[36,37]. At present, CD8 T cells have been described as a variety of subtypes, including Tc1, Tc2, Tc9, Tc17, and Tc22, each with different cytotoxicity and effects. Among these cell subtypes, Tc17 and Tc22 are the main T cell subtypes in gastric tissue. Tc17 has no cytotoxicity, and its high expression is negatively correlated with the survival time of GC, while Tc22 is just the opposite. Besides, follicular helper T cells are the key to the production of germinal center formation[38]. They interact with tumor-specific B cells to enhance the anti-tumor effect of CD8 T cells. In summary, the reduced proportion of these important

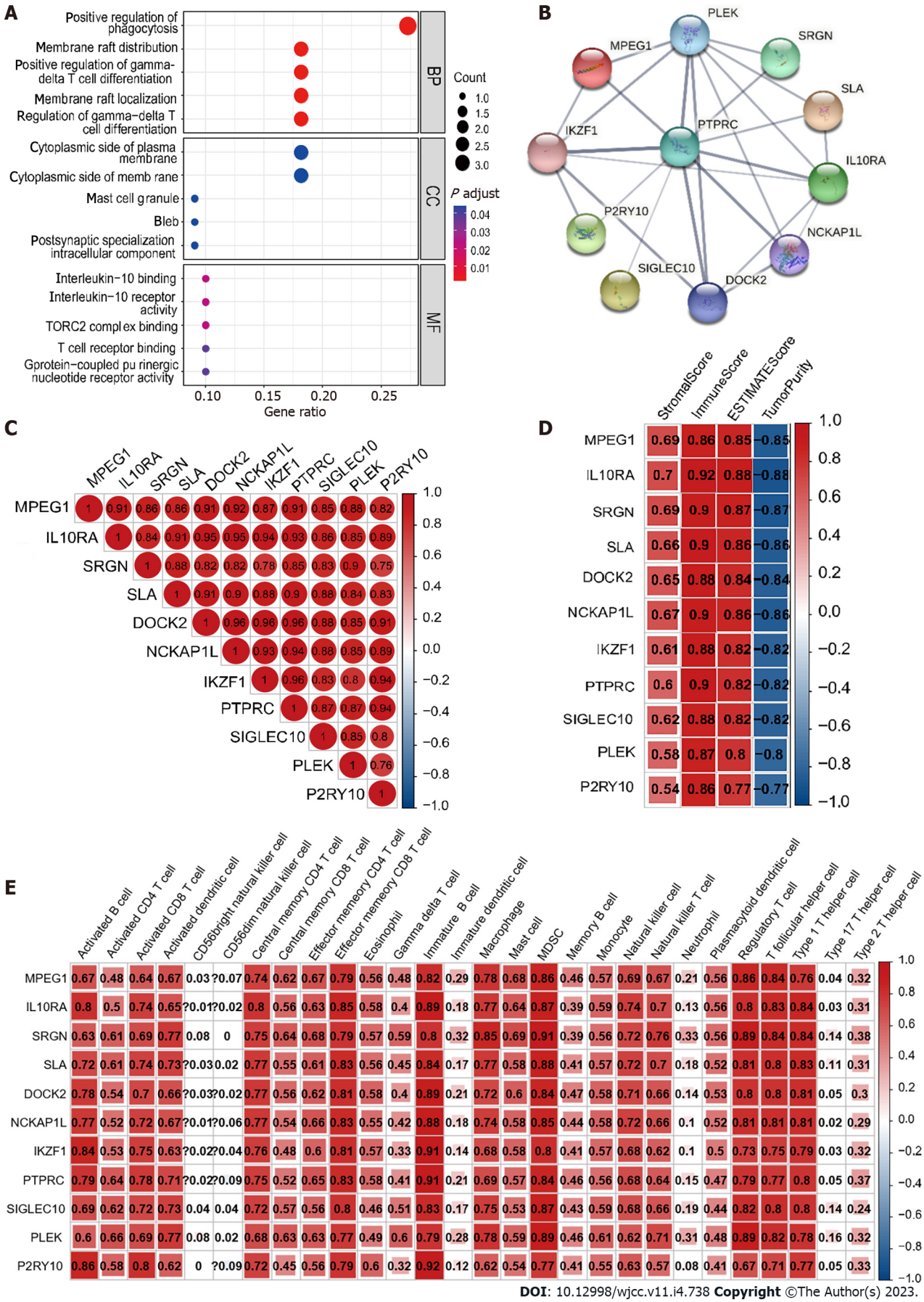

DOI: 10.12998/wjcc.v11.i4.738

Figure 7 Analysis of 11 hub genes. A: The Gene Ontology analysis of hub genes; B: Protein-protein interaction network of hub genes; C: Relevance between hub genes; D: Correlation between hub genes and ESTIMATE results; E: Correlation between hub genes and expression of immune cells.

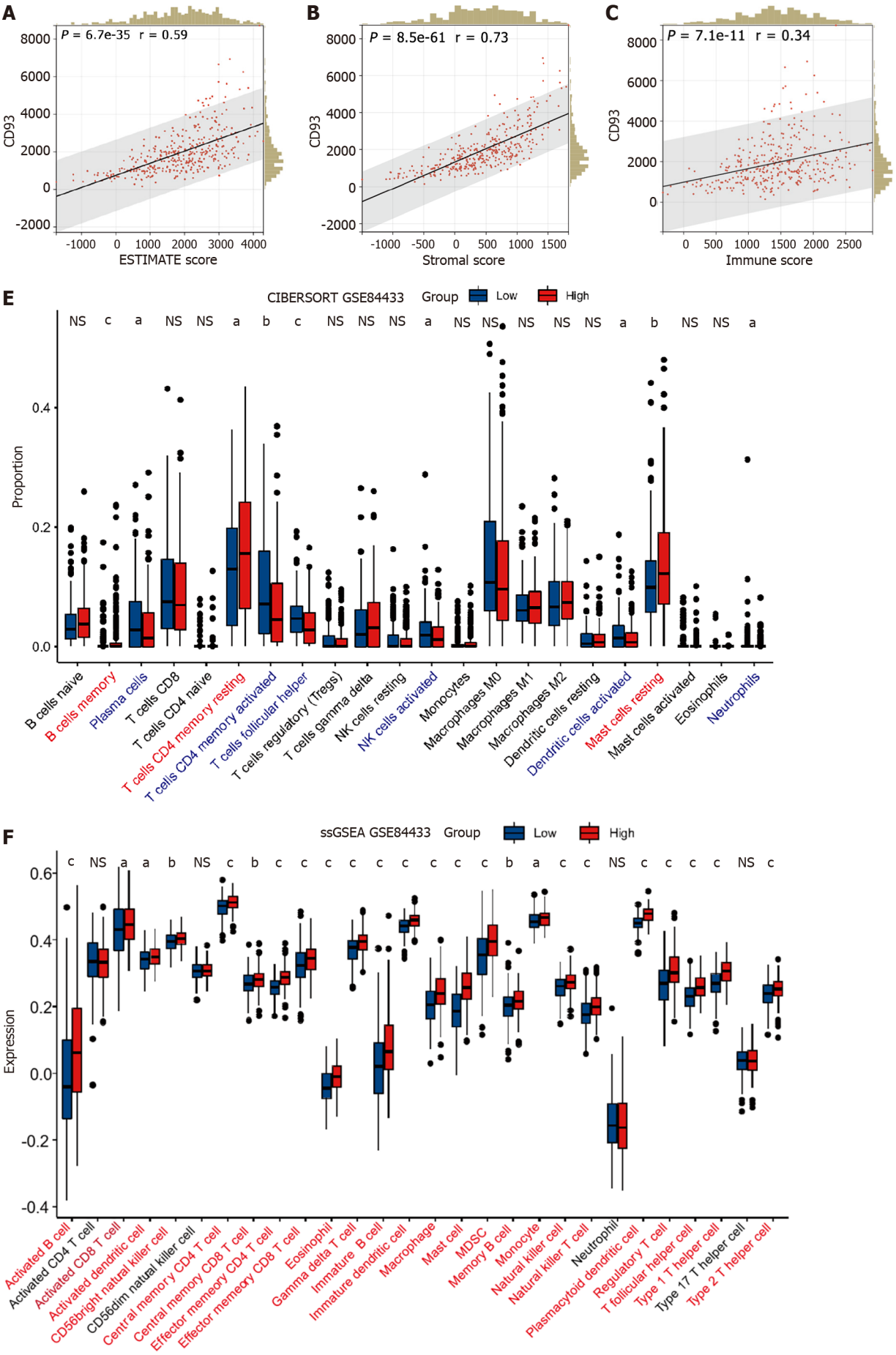
A
P = 6.7e-35 r = 0.59
CD93
ESTIMATE score
B
P = 8.5e-61 r = 0.73
CD93
Stromal score
C
P = 7.1e-11 r = 0.34
CD93
Immune score
E
CIBERSORT GSE84433 Group Low High
Proportion
B cells naive
B cells memory
Plasma cells
T cells CD8
T cells CD4 naive
T cells CD4 memory resting
T cells CD4 memory activated
T cells follicular helper
T cells regulatory (Tregs)
T cells gamma delta
NK cells resting
NK cells activated
Monocytes
Macrophages M0
Macrophages M1
Macrophages M2
Dendritic cells resting
Dendritic cells activated
Mast cells resting
Mast cells activated
Eosinophils
Neutrophils
F
ssGSEA GSE84433 Group Low High
Expression
Activated B cell
Activated CD4 T cell
Activated CD8 T cell
Activated dendritic cell
CD56bright natural killer cell
CD56dim natural killer cell
Central memory CD4 T cell
Central memory CD8 T cell
Effector memeory CD4 T cell
Effector memeory CD8 T cell
Eosinophil
Gamma delta T cell
Immature B cell
Immature dendritic cell
Macrophage
Mast cell
MDSC
Memory B cell
Monocyte
Natural killer cell
Natural killer T cell
Neutrophil
Plasmacytoid dendritic cell
Regulatory T cell
T follicular helper cell
Type 1 T helper cell
Type 17 T helper cell
Type 2 T helper cell

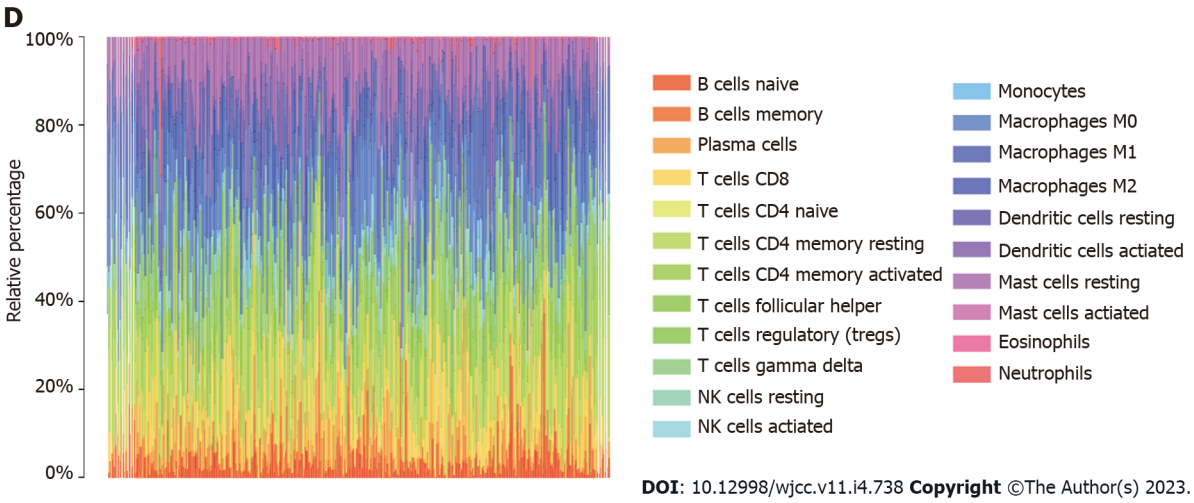

DOI: 10.12998/wjcc.v11.i4.738

Figure 8 Validation of immune characteristics. A-C: Correlation between CD93 and ESTIMATE score (A), stromal score (B), immune score (C). D: Cibersort; E: Different proportions of immune cells infiltration between two groups; F: ssGSEA. The *P* values are labeled as $^{a}P < 0.05$, $^{b}P < 0.01$, $^{c}P < 0.001$, NS: No significance.

immune cells in the TME may be the main reason for the poor prognosis caused by CD93. However, analysis of the expression of immune cells in two groups suggested that various types of immune cells were highly expressed in the high CD93 expression group. Although blood vessels are conducive to tissue growth and immune response, they can contribute to inflammation and malignant diseases. Abnormal angiogenesis induced by CD93 in TME can promote tumor growth and form an immune-hostile microenvironment[39], and this effect exceeds its immune enhancement effect, which makes the prognosis of the high CD93 expression group with high immune infiltration still poor.

In recent years, the ICIs represented by PD-1, PD-L1, and CTLA-4 bring considerable disease relief to tumor patients, playing an important role in tumor immunotherapy. However, not all patients can benefit from ICIs. A series of studies have shown that TMB is a potential biomarker for predicting the response to ICIs and patients with high TMB possess a better immunotherapeutic effect of ICIs[40,41]. In this study, we made a comparison of gene mutational landscape and TMB between two groups. The results showed that GC patients with high expression of CD93 had a lower TMB, indicating that the effect of immunotherapy in GC patients with high expression of CD93 is poor. Then, we performed WGCNA to identify the key genes related to CD93 in the tumor immune microenvironment of GC. We obtained 11 genes from the yellow module. Among them, SRGN overexpression has been previously shown to promote colorectal cancer metastasis and predict a poor prognosis of hepatocellular carcinoma [42,43]. This time, the identification of these 11 genes can help us further understand the immune microenvironment of GC and suggest potential methods for immunotherapy of GC in the future.

Although we have taken a variety of methods to obtain a comprehensive understanding of the relationship between CD93 and GC, we use 5 cohorts (GSE118916, GSE52138, GSE79973, GSE19826, and GSE84433) as external validation sets, some limitations of this study should be recognized. First, this is a retrospective study. Selection bias, loss of follow-up bias, recall bias, and other biases exist in the study. Thus, a prospective study is required to avoid these biases. Furthermore, limited by TCGA and GEO, we only performed research and analysis from the genetic level. A study that can demonstrate CD93 expression from the protein level or reveal the direct mechanism needs to be conducted in the future.

CONCLUSION

All in all, comprehensive analyses were applied using transcriptomic profiles and survival information from the GEO and TCGA databases, suggesting that CD93 is a biomarker of diagnosis and prognosis for GC, which closely correlates with immune infiltration in TME. These data help us further comprehend the role of CD93 in the immune microenvironment and may suggest potential strategies for immunotherapy of GC in the future.

ARTICLE HIGHLIGHTS

Research background

Gastric cancer (GC) is a common malignancy with poor 5-year survival rate. Tumor microenvironment (TME) containing intricate interaction between immune and non-immune cells produces significant impact of the survival of GC. Additionally, CD93 was proved to be associated with abnormal angiogenesis, which could be involved in TME of GC.

Research motivation

This study was conducted to determine the specific role of CD93 in GC in order to provide insights for the discovery of novel therapeutic target of GC in the feature.

Research objectives

Cohorts data of GC patients was investigated from The Cancer Genome Atlas and Gene Expression Omnibus (GSE118916, GSE52138, GSE79973, GSE19826, and GSE84433).

Research methods

We performed a series of immune infiltration analyses using ESTIMATE, CIBERSORT, and ssGSEA. Furthermore, weighted gene co-expression network analysis was conducted to identify the immune-related genes.

Research results

CD93 significantly enriched in tumor tissues. Additionally, higher expression of CD93 was significantly associated with shorter overall survival, less proportion of CD8 T and activated nature killer cells in the TME, and lower tumor mutational burden.

Research conclusions

CD93 is a novel prognostic and diagnostic biomarker for GC, which is closely related to the immune infiltration in TME.

Research perspectives

CD93 can serve as a potential therapeutic target for the immunotherapy of GC in the feature.

FOOTNOTES

Author contributions: Li Z and Zhang XJ contributed to the conceptualization; Li Z contributed to the methodology; Sun CY contributed to the software; Li Z and Zhang XJ contributed to the validation; Li Z and Fei H contributed to the formal analysis; Li ZF contributed to the investigation; Zhao DB contributed to the resources; Li Z and Sun CY contributed to the writing-original draft preparation; All authors contributed to the writing-review and editing; Zhao DB contributed to the project administration. All authors have reviewed and agreed to the published version of the manuscript.

Conflict-of-interest statement: All authors declare no conflict of interest.

Data sharing statement: All data analyzed in this study can be available in XENA (http://xena.ucsc.edu), GEO (https://www.ncbi.nlm.nih.gov/geo/).

Country/Territory of origin: China

ORCID number: Zheng Li 0000-0003-4415-6552; Xiao-Jie Zhang 0000-0001-9850-9806; Chong-Yuan Sun 0000-0003-1354-2063; He Fei 0000-0003-4831-4028; Ze-Feng Li 0000-0002-5345-3527; Dong-Bing Zhao 0000-0002-6770-2694.

S-Editor: Zhang H
L-Editor: A
P-Editor: Zhang H

REFERENCES

1 **Sung H**, Ferlay J, Siegel RL, Laversanne M, Soerjomataram I, Jemal A, Bray F. Global Cancer Statistics 2020: GLOBOCAN Estimates of Incidence and Mortality Worldwide for 36 Cancers in 185 Countries. *CA Cancer J Clin* 2021; **71**: 209-249 [PMID: 33538338 DOI: 10.3322/caac.21660]

2 **Smyth EC**, Nilsson M, Grabsch HI, van Grieken NC, Lordick F. Gastric cancer. *Lancet* 2020; **396**: 635-648 [PMID: 32861308 DOI: 10.1016/S0140-6736(20)31288-5]

3 **Zhao Q**, Cao L, Guan L, Bie L, Wang S, Xie B, Chen X, Shen X, Cao F. Immunotherapy for gastric cancer: dilemmas and prospect. *Brief Funct Genomics* 2019; **18**: 107-112 [PMID: 30388190 DOI: 10.1093/bfgp/ely019]

4 **Rojas A**, Araya P, Gonzalez I, Morales E. Gastric Tumor Microenvironment. *Adv Exp Med Biol* 2020; **1226**: 23-35 [PMID: 32030673 DOI: 10.1007/978-3-030-36214-0_2]

5 **Kim J**, Hong J, Lee J, Fakhraei Lahiji S, Kim YH. Recent advances in tumor microenvironment-targeted nanomedicine delivery approaches to overcome limitations of immune checkpoint blockade-based immunotherapy. *J Control Release* 2021; **332**: 109-126 [PMID: 33571549 DOI: 10.1016/j.jconrel.2021.02.002]

6 **Xiao Y**, Yu D. Tumor microenvironment as a therapeutic target in cancer. *Pharmacol Ther* 2021; **221**: 107753 [PMID: 33259885 DOI: 10.1016/j.pharmthera.2020.107753]

7 **Lei Q**, Wang D, Sun K, Wang L, Zhang Y. Resistance Mechanisms of Anti-PD1/PDL1 Therapy in Solid Tumors. *Front Cell Dev Biol* 2020; **8**: 672 [PMID: 32793604 DOI: 10.3389/fcell.2020.00672]

8 **Lugano R**, Vemuri K, Yu D, Bergqvist M, Smits A, Essand M, Johansson S, Dejana E, Dimberg A. CD93 promotes β1 integrin activation and fibronectin fibrillogenesis during tumor angiogenesis. *J Clin Invest* 2018; **128**: 3280-3297 [PMID: 29763414 DOI: 10.1172/JCI97459]

9 **Huang J**, Lee HY, Zhao X, Han J, Su Y, Sun Q, Shao J, Ge J, Zhao Y, Bai X, He Y, Wang X, Dong C. Interleukin-17D regulates group 3 innate lymphoid cell function through its receptor CD93. *Immunity* 2021; **54**: 673-686.e4 [PMID: 33852831 DOI: 10.1016/j.immuni.2021.03.018]

10 **Nativel B**, Ramin-Mangata S, Mevizou R, Figuester A, Andries J, Iwema T, Ikewaki N, Gasque P, Viranaïcken W. CD93 is a cell surface lectin receptor involved in the control of the inflammatory response stimulated by exogenous DNA. *Immunology* 2019; **158**: 85-93 [PMID: 31335975 DOI: 10.1111/imm.13100]

11 **Sun Y**, Chen W, Torphy RJ, Yao S, Zhu G, Lin R, Lugano R, Miller EN, Fujiwara Y, Bian L, Zheng L, Anand S, Gao F, Zhang W, Ferrara SE, Goodspeed AE, Dimberg A, Wang XJ, Edil BH, Barnett CC, Schulick RD, Chen L, Zhu Y. Blockade of the CD93 pathway normalizes tumor vasculature to facilitate drug delivery and immunotherapy. *Sci Transl Med* 2021; **13** [PMID: 34321321 DOI: 10.1126/scitranslmed.abc8922]

12 **Goldman MJ**, Craft B, Hastie M, Repečka K, McDade F, Kamath A, Banerjee A, Luo Y, Rogers D, Brooks AN, Zhu J, Haussler D. Visualizing and interpreting cancer genomics data *via* the Xena platform. *Nat Biotechnol* 2020; **38**: 675-678 [PMID: 32444850 DOI: 10.1038/s41587-020-0546-8]

13 **Love MI**, Huber W, Anders S. Moderated estimation of fold change and dispersion for RNA-seq data with DESeq2. *Genome Biol* 2014; **15**: 550 [PMID: 25516281 DOI: 10.1186/s13059-014-0550-8]

14 **Barrett T**, Wilhite SE, Ledoux P, Evangelista C, Kim IF, Tomashevsky M, Marshall KA, Phillippy KH, Sherman PM, Holko M, Yefanov A, Lee H, Zhang N, Robertson CL, Serova N, Davis S, Soboleva A. NCBI GEO: archive for functional genomics data sets--update. *Nucleic Acids Res* 2013; **41**: D991-D995 [PMID: 23193258 DOI: 10.1093/nar/gks1193]

15 **Mayakonda A**, Lin DC, Assenov Y, Plass C, Koeffler HP. Maftools: efficient and comprehensive analysis of somatic variants in cancer. *Genome Res* 2018; **28**: 1747-1756 [PMID: 30341162 DOI: 10.1101/gr.239244.118]

16 **Gu Z**, Eils R, Schlesner M. Complex heatmaps reveal patterns and correlations in multidimensional genomic data. *Bioinformatics* 2016; **32**: 2847-2849 [PMID: 27207943 DOI: 10.1093/bioinformatics/btw313]

17 **Li T**, Fu J, Zeng Z, Cohen D, Li J, Chen Q, Li B, Liu XS. TIMER2.0 for analysis of tumor-infiltrating immune cells. *Nucleic Acids Res* 2020; **48**: W509-W514 [PMID: 32442275 DOI: 10.1093/nar/gkaa407]

18 **Ru B**, Wong CN, Tong Y, Zhong JY, Zhong SSW, Wu WC, Chu KC, Wong CY, Lau CY, Chen I, Chan NW, Zhang J. TISIDB: an integrated repository portal for tumor-immune system interactions. *Bioinformatics* 2019; **35**: 4200-4202 [PMID: 30903160 DOI: 10.1093/bioinformatics/btz210]

19 **Robin X**, Turck N, Hainard A, Tiberti N, Lisacek F, Sanchez JC, Müller M. pROC: an open-source package for R and S+ to analyze and compare ROC curves. *BMC Bioinformatics* 2011; **12**: 77 [PMID: 21414208 DOI: 10.1186/1471-2105-12-77]

20 **Asplund A**, Edqvist PH, Schwenk JM, Pontén F. Antibodies for profiling the human proteome-The Human Protein Atlas as a resource for cancer research. *Proteomics* 2012; **12**: 2067-2077 [PMID: 22623277 DOI: 10.1002/pmic.201100504]

21 **Vasaikar SV**, Straub P, Wang J, Zhang B. LinkedOmics: analyzing multi-omics data within and across 32 cancer types. *Nucleic Acids Res* 2018; **46**: D956-D963 [PMID: 29136207 DOI: 10.1093/nar/gkx1090]

22 **Warde-Farley D**, Donaldson SL, Comes O, Zuberi K, Badrawi R, Chao P, Franz M, Grouios C, Kazi F, Lopes CT, Maitland A, Mostafavi S, Montojo J, Shao Q, Wright G, Bader GD, Morris Q. The GeneMANIA prediction server: biological network integration for gene prioritization and predicting gene function. *Nucleic Acids Res* 2010; **38**: W214-W220 [PMID: 20576703 DOI: 10.1093/nar/gkq537]

23 **Yu G**, Wang LG, Han Y, He QY. clusterProfiler: an R package for comparing biological themes among gene clusters. *OMICS* 2012; **16**: 284-287 [PMID: 22455463 DOI: 10.1089/omi.2011.0118]

24 **Li T**, Fan J, Wang B, Traugh N, Chen Q, Liu JS, Li B, Liu XS. TIMER: A Web Server for Comprehensive Analysis of Tumor-Infiltrating Immune Cells. *Cancer Res* 2017; **77**: e108-e110 [PMID: 29092952 DOI: 10.1158/0008-5472.CAN-17-0307]

25 **Yoshihara K**, Shahmoradgoli M, Martínez E, Vegesna R, Kim H, Torres-Garcia W, Treviño V, Shen H, Laird PW, Levine DA, Carter SL, Getz G, Stemke-Hale K, Mills GB, Verhaak RG. Inferring tumour purity and stromal and immune cell admixture from expression data. *Nat Commun* 2013; **4**: 2612 [PMID: 24113773 DOI: 10.1038/ncomms3612]

26 **Newman AM**, Liu CL, Green MR, Gentles AJ, Feng W, Xu Y, Hoang CD, Diehn M, Alizadeh AA. Robust enumeration of

cell subsets from tissue expression profiles. *Nat Methods* 2015; **12**: 453-457 [PMID: 25822800 DOI: 10.1038/nmeth.3337]

27 **Bindea G**, Mlecnik B, Tosolini M, Kirilovsky A, Waldner M, Obenauf AC, Angell H, Fredriksen T, Lafontaine L, Berger A, Bruneval P, Fridman WH, Becker C, Pagès F, Speicher MR, Trajanoski Z, Galon J. Spatiotemporal dynamics of intratumoral immune cells reveal the immune landscape in human cancer. *Immunity* 2013; **39**: 782-795 [PMID: 24138885 DOI: 10.1016/j.immuni.2013.10.003]

28 **Hänzelmann S**, Castelo R, Guinney J. GSVA: gene set variation analysis for microarray and RNA-seq data. *BMC Bioinformatics* 2013; **14**: 7 [PMID: 23323831 DOI: 10.1186/1471-2105-14-7]

29 **Langfelder P**, Horvath S. WGCNA: an R package for weighted correlation network analysis. *BMC Bioinformatics* 2008; **9**: 559 [PMID: 19114008 DOI: 10.1186/1471-2105-9-559]

30 **Szklarczyk D**, Gable AL, Nastou KC, Lyon D, Kirsch R, Pyysalo S, Doncheva NT, Legeay M, Fang T, Bork P, Jensen LJ, von Mering C. The STRING database in 2021: customizable protein-protein networks, and functional characterization of user-uploaded gene/measurement sets. *Nucleic Acids Res* 2021; **49**: D605-D612 [PMID: 33237311 DOI: 10.1093/nar/gkaa1074]

31 **Viallard C**, Larrivée B. Tumor angiogenesis and vascular normalization: alternative therapeutic targets. *Angiogenesis* 2017; **20**: 409-426 [PMID: 28660302 DOI: 10.1007/s10456-017-9562-9]

32 **Aoki M**, Fujishita T. Oncogenic Roles of the PI3K/AKT/mTOR Axis. *Curr Top Microbiol Immunol* 2017; **407**: 153-189 [PMID: 28550454 DOI: 10.1007/82_2017_6]

33 **Choi KY**, Kim JH, Park IS, Rho YS, Kwon GH, Lee DJ. Predictive gene signatures of nodal metastasis in papillary thyroid carcinoma. *Cancer Biomark* 2018; **22**: 35-42 [PMID: 29562496 DOI: 10.3233/CBM-170784]

34 **Pober JS**, Tellides G. Participation of blood vessel cells in human adaptive immune responses. *Trends Immunol* 2012; **33**: 49-57 [PMID: 22030237 DOI: 10.1016/j.it.2011.09.006]

35 **la Sala A**, Pontecorvo L, Agresta A, Rosano G, Stabile E. Regulation of collateral blood vessel development by the innate and adaptive immune system. *Trends Mol Med* 2012; **18**: 494-501 [PMID: 22818027 DOI: 10.1016/j.molmed.2012.06.007]

36 **Terrén I**, Orrantia A, Vitallé J, Zenarruzabeitia O, Borrego F. NK Cell Metabolism and Tumor Microenvironment. *Front Immunol* 2019; **10**: 2278 [PMID: 31616440 DOI: 10.3389/fimmu.2019.02278]

37 **St Paul M**, Ohashi PS. The Roles of CD8(+) T Cell Subsets in Antitumor Immunity. *Trends Cell Biol* 2020; **30**: 695-704 [PMID: 32624246 DOI: 10.1016/j.tcb.2020.06.003]

38 **Cui C**, Wang J, Fagerberg E, Chen PM, Connolly KA, Damo M, Cheung JF, Mao T, Askari AS, Chen S, Fitzgerald B, Foster GG, Eisenbarth SC, Zhao H, Craft J, Joshi NS. Neoantigen-driven B cell and CD4 T follicular helper cell collaboration promotes anti-tumor CD8 T cell responses. *Cell* 2021; **184**: 6101-6118.e13 [PMID: 34852236 DOI: 10.1016/j.cell.2021.11.007]

39 **Lamplugh Z**, Fan Y. Vascular Microenvironment, Tumor Immunity and Immunotherapy. *Front Immunol* 2021; **12**: 811485 [PMID: 34987525 DOI: 10.3389/fimmu.2021.811485]

40 **Chan TA**, Yarchoan M, Jaffee E, Swanton C, Quezada SA, Stenzinger A, Peters S. Development of tumor mutation burden as an immunotherapy biomarker: utility for the oncology clinic. *Ann Oncol* 2019; **30**: 44-56 [PMID: 30395155 DOI: 10.1093/annonc/mdy495]

41 **Cristescu R**, Mogg R, Ayers M, Albright A, Murphy E, Yearley J, Sher X, Liu XQ, Lu H, Nebozhyn M, Zhang C, Lunceford JK, Joe A, Cheng J, Webber AL, Ibrahim N, Plimack ER, Ott PA, Seiwert TY, Ribas A, McClanahan TK, Tomassini JE, Loboda A, Kaufman D. Pan-tumor genomic biomarkers for PD-1 checkpoint blockade-based immunotherapy. *Science* 2018; **362** [PMID: 30309915 DOI: 10.1126/science.aar3593]

42 **He L**, Zhou X, Qu C, Tang Y, Zhang Q, Hong J. Serglycin (SRGN) overexpression predicts poor prognosis in hepatocellular carcinoma patients. *Med Oncol* 2013; **30**: 707 [PMID: 23996242 DOI: 10.1007/s12032-013-0707-4]

43 **Xu Y**, Xu J, Yang Y, Zhu L, Li X, Zhao W. SRGN Promotes Colorectal Cancer Metastasis as a Critical Downstream Target of HIF-1α. *Cell Physiol Biochem* 2018; **48**: 2429-2440 [PMID: 30121667 DOI: 10.1159/000492657]

World Journal of Clinical Cases

Submit a Manuscript: https://www.f6publishing.com

World J Clin Cases 2023 February 6; 11(4): 756-763

DOI: 10.12998/wjcc.v11.i4.756

ISSN 2307-8960 (online)

ORIGINAL ARTICLE

Retrospective Study

Chest computed tomography findings of the Omicron variants of SARS-CoV-2 with different cycle threshold values

Wei-Feng Ying, Qiong Chen, Zhi-Kui Jiang, Da-Guang Hao, Ying Zhang, Qian Han

Specialty type: Infectious diseases

Provenance and peer review: Unsolicited article; Externally peer reviewed.

Peer-review model: Single blind

Peer-review report's scientific quality classification

Grade A (Excellent): 0
Grade B (Very good): B
Grade C (Good): 0
Grade D (Fair): 0
Grade E (Poor): 0

P-Reviewer: Shahid M, Pakistan

Received: September 1, 2022
Peer-review started: September 1, 2022
First decision: November 22, 2022
Revised: November 29, 2022
Accepted: January 12, 2023
Article in press: January 12, 2023
Published online: February 6, 2023

Wei-Feng Ying, Qiong Chen, Da-Guang Hao, Ying Zhang, Department of Radiology, Shanghai Xuhui Dahua Hospital, Shanghai 200237, China

Zhi-Kui Jiang, Qian Han, Department of Clinical Laboratory, Shanghai Xuhui Dahua Hospital, Shanghai 200237, China

Corresponding author: Qiong Chen, MSc, Chief Doctor, Department of Radiology, Shanghai Xuhui Dahua Hospital, No. 901 Lao'humin Road, Xuhui District, Shanghai 200237, China. cq1444@sina.com

Abstract

BACKGROUND

The Omicron variant of severe acute respiratory syndrome coronavirus 2 (SARS-CoV-2) mainly infects the upper respiratory tract. This study aimed to determine whether the probability of pulmonary infection and the cycle threshold (Ct) measured using the fluorescent polymerase chain reaction (PCR) method were related to pulmonary infections diagnosed *via* computed tomography (CT).

AIM

To analyze the chest CT signs of SARS-CoV-2 Omicron variant infections with different Ct values, as determined *via* PCR.

METHODS

The chest CT images and PCR Ct values of 331 patients with SARS-CoV-2 Omicron variant infections were retrospectively collected and categorized into low (< 25), medium (25.00-34.99), and high (≥ 35) Ct groups. The characteristics of chest CT images in each group were statistically analyzed.

RESULTS

The PCR Ct values ranged from 13.36 to 39.81, with 99 patients in the low, 155 in the medium, and 77 in the high Ct groups. Six abnormal chest CT signs were detected, namely, focal infection, patchy consolidation shadows, patchy ground-glass shadows, mixed consolidation ground-glass shadows, subpleural interstitial changes, and pleural changes. Focal infections were less frequent in the low Ct group than in the medium and high Ct groups; these infections were the most common sign in the medium and high Ct groups. Patchy consolidation shadows and pleural changes were more frequent in the low Ct group than in the other two groups. The number of patients with two or more signs was greater in the low Ct

group than in the medium and high Ct groups.

CONCLUSION
The chest CT signs of patients with pulmonary infection caused by the Omicron variants of SARS-CoV-2 varied depending on the Ct values. Identification of the characteristics of Omicron variant infection can help subsequent planning of clinical treatment.

Key Words: COVID-19; SARS-CoV-2; Omicron variant; Computed tomography; Cycle threshold; Polymerase chain reaction

Core Tip: Pulmonary infections caused by the Omicron variant of severe acute respiratory syndrome coronavirus 2 were highly correlated with cycle threshold (Ct) values. Lower Ct values were associated with a higher incidence and degree of pulmonary damage.

Citation: Ying WF, Chen Q, Jiang ZK, Hao DG, Zhang Y, Han Q. Chest computed tomography findings of the Omicron variants of SARS-CoV-2 with different cycle threshold values. *World J Clin Cases* 2023; 11(4): 756-763
URL: https://www.wjgnet.com/2307-8960/full/v11/i4/756.htm
DOI: https://dx.doi.org/10.12998/wjcc.v11.i4.756

INTRODUCTION

Since the emergence of the Omicron variant of severe acute respiratory syndrome coronavirus 2 (SARS-CoV-2) on November 24, 2021[1], it has spread in most countries and caused infection in numerous individuals worldwide[2]. Although the virulence of Omicron appears to be weaker than that of previous SARS-CoV-2 variants, the large-scale use of vaccines against SARS-CoV-2, particularly with enhanced needles, has reduced the mortality rate associated with SARS-CoV-2[3]. Omicron is more infectious and transmissible than other variants[4,5] and causes damage to the lungs of some patients to different degrees[6]. Therefore, determining the degree of pulmonary damage caused by different Omicron viral load levels is key to understanding the characteristics of Omicron variant infection and its inhibition[7].

Fluorescent polymerase chain reaction (PCR) is the gold standard for diagnosing SARS-CoV-2 infection, and its cycle threshold (Ct) values can help achieve a reliable assessment and comparison of viral loads in patients[8-10]. Ct diagnosis has an extremely high diagnostic efficiency for determining the degree of pulmonary damage in patients with SARS-CoV-2 infections[11,12]. So far, only a few studies have attempted to correlate Ct values and pulmonary damage evidenced on chest computed tomography (CT) images obtained from patients with Omicron variant infection. The author's hospital is a designated treatment facility for symptomatic patients with Omicron variant infection. This study aimed to assess the chest CT signs of patients with Omicron variant infection with different Ct values for determining the severity of the infection and providing guidance for subsequent clinical treatments.

MATERIALS AND METHODS

Clinical data

Chest CT scans of patients with Omicron variant infection admitted to Shanghai Xuhui Dahua Hospital were collected from April to May 2022. The inclusion criteria were patients with PCR-positive results (Ct value of < 40) and those with viral infection signs on chest CT within 48 h after PCR. The exclusion criteria were patients with bacterial infections, as determined using laboratory indexes, or those with a clinical or CT diagnosis of other basic pulmonary infectious diseases. This study complied with the ethical standards and was approved by the Ethics Committee of Shanghai Xuhui Dahua Hospital (approval No. 20220804).

Examination method

All CT scans were obtained using a Siemens 64-slice spiral CT scanner (SOMATOM sensation) from the pulmonary apex to the pulmonary bottom using the following scanning parameters: Detector collimation, 64.0 mm × 0.6 mm; tube voltage, 120 KV; tube current, automatic milliampere; slice thickness, 5 mm; reconstructed slice thickness, 1.5 mm; reconstructed slice spacing, 1.5 mm; and matrix,

512 × 512.

Image analysis

The lower Ct value between the ORF and N genes was selected as the PCR Ct value. The patients were divided into three groups based on their Ct values: Low (< 25), medium (25.00-34.99), and high (≥ 35) Ct groups. Double-blind analysis was conducted using the CT data of each group by two physicians with > 10 years of experience in radiological diagnosis. In cases of disagreement, consensus was achieved after mutual consultation. When patients exhibited pulmonary infection foci with a long diameter (≤ 20 mm), it was considered as a focal infection. Other infection signs, including patchy consolidation shadows, patchy ground-glass density shadows, subpleural interstitial changes, mixed consolidation ground-glass shadows, and pleural changes, were judged based on their characteristics.

Statistical methods

Statistical analysis of the data was performed using SPSS 23.0. Normally distributed data are expressed as mean ± SD, whereas enumeration data are expressed as case numbers or percentages. Within- and between-group comparisons of CT signs were performed using χ^2 test. A P value of < 0.05 was considered to indicate statistical significance.

RESULTS

Baseline characteristics

Chest CT images of 331 patients [143 men and 188 women; age: 76 ± 12 (range: 25-102) years] with Omicron variant infection were collected. All patients showed respiratory symptoms of varying degrees, mainly including fever (n = 247, 74.62%), cough (n = 203, 61.33%), and chest tightness (n = 49, 14.8%). Among them, 187 (56.5%) patients were vaccinated thrice against SARS-CoV-2, 74 (22.36%) were vaccinated twice, 12 (3.63%) were vaccinated once, and 58 (17.52%) were not vaccinated. Additionally, 236 (71.3%) patients had a history of close or secondary contact with patients with SARS-CoV-2 infection, 65 (19.64%) had a definite history of gathering in public places, and 30 (9.06%) had no definite history of close contact with patients with SARS-CoV-2 infection.

The PCR Ct values ranged from 13.36 to 39.81 (average, 28.85 ± 6.68), with 99 (29.91%) patients in the low, 155 (46.83%) in the medium, and 77 (23.26%) in the high Ct groups.

General distribution of abnormal chest CT characteristics

Among all patients, the most common CT sign was focal infection (n = 178, 45.18%), followed by subpleural interstitial changes (n = 81, 20.56%), patchy ground-glass density shadows (n = 76, 19.29%), patchy consolidation shadows (n = 27, 6.85%), pleural changes (n = 20, 5.08%), and mixed consolidation ground-glass shadows (n = 12, 3.04%).

Analysis of the differences in the distribution of abnormal chest CT characteristics within and between different Ct groups

Focal infections were less frequent in the low Ct group (30%) than in the medium (52.27%, χ^2 = 10.004, P = 0.002) and high (53.41%, χ^2 = 10.895, P = 0.002) Ct groups. Focal infection was the most common sign in the medium and high Ct groups (compared with the second most common sign in the groups: The medium Ct group, χ^2 = 23.780, P < 0.001 and the high Ct group, χ^2 = 19.100, P < 0.001), with statistically significant differences (Figure 1A-C).

The frequency of patchy consolidation shadows (Figure 1D-F) was the highest in the low Ct group (14.62%), less in the medium Ct group (3.98%; χ^2 = 7.037, P = 0.014), and the lowest in the high Ct group (1.14%), with statistically significant between-group differences (χ^2 = 13.315, P < 0.001).

There were no statistically significant differences in the frequency of patchy ground-glass density shadows (Figure 1G and H) among the low (16.92%), medium (19.32%), and high (22.73%) Ct groups (χ^2 = 0.136, χ^2 = 1.125, and χ^2 = 0.482; P = 0.854, P = 0.377, and P = 0.603, respectively).

Furthermore, no statistically significant differences were observed in subpleural interstitial changes among the low (25.38%), medium (17.61%), and high (19.32%) Ct groups (χ^2 = 1.452, χ^2 = 1.049, and χ^2 = 0.033; P = 0.302, P = 0.394, and P = 1.000, respectively).

In addition, mixed consolidation ground-glass shadows showed no statistically significant differences among the low (2.31%), medium (3.98%), and high (2.27%) Ct groups (χ^2 = 0.687, χ^2 = 0.000, and χ^2 = 0.687; P = 0.683, P = 1.000, and P = 0.683, respectively).

The frequency of pleural changes (Figure 1D-F) was the highest in the low Ct group (10.77%), less frequent in the medium Ct group (2.84%; χ^2 = 4.916, P = 0.049), and the lowest in the high Ct group (1.13%; χ^2 = 8.865, P < 0.005), with statistically significant between-group differences.

Among the three groups, the number of patients with two or more abnormal chest CT signs was the highest in the low Ct group (30.3%, 30/99), less in the medium Ct group [12.26% (19/155), χ^2 = 9.765, P = 0.003], and the lowest in the high Ct group [12.99% (10/77), χ^2 = 8.562, P = 0.005], with statistically

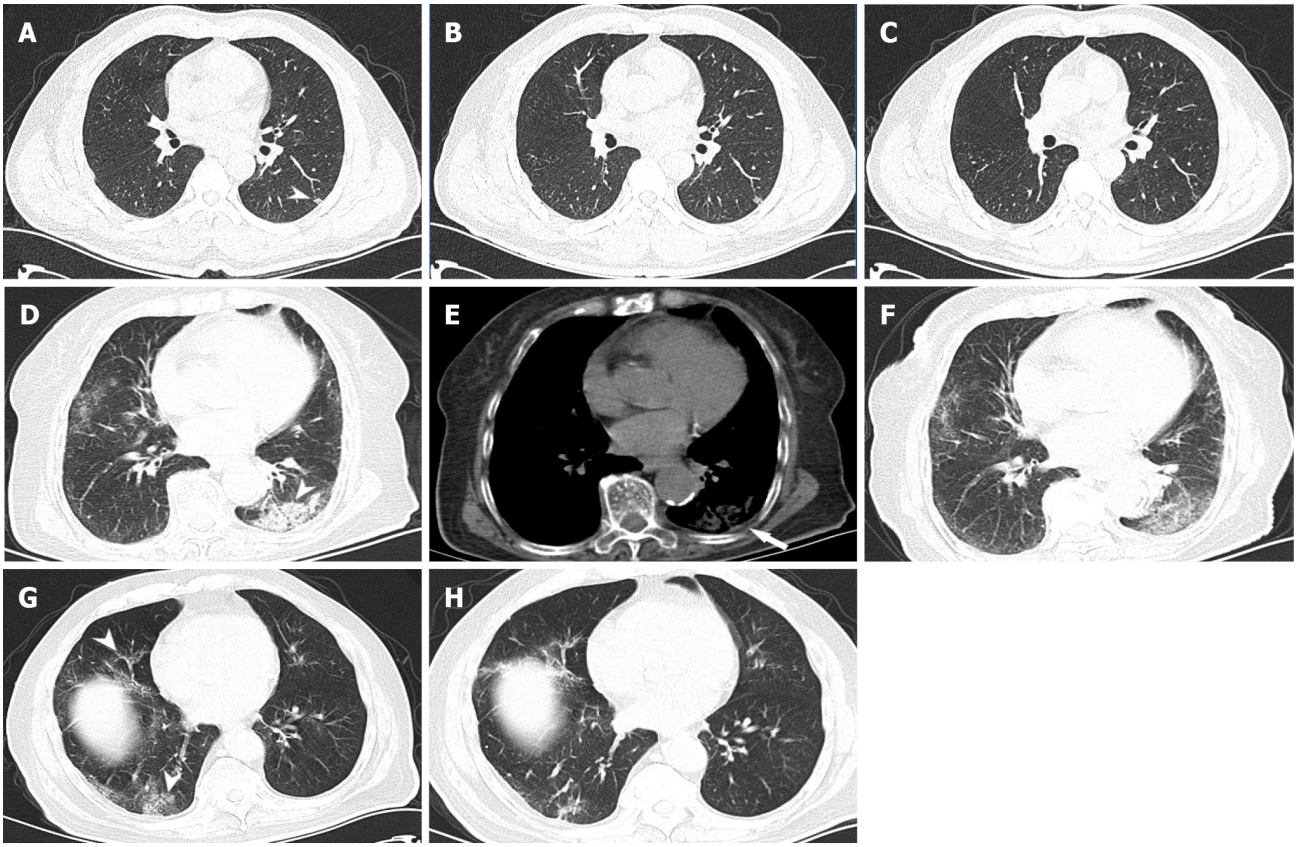

DOI: 10.12998/wjcc.v11.i4.756 **Copyright** ©The Author(s) 2023.

Figure 1 Computed tomography. A and B: A 48-year-old man had a history of close contact with patients mildly infected with SARS-CoV-2 Omicron variant. He had fever and mild cough for 3 d, with nucleic acid polymerase chain reaction positivity [cycle threshold (Ct) value, 35.43], leukocyte count of 7.26 × 10^9/L, neutrophil proportion of 58.8%, lymphocyte proportion of 32.9%, hypersensitive C-reactive protein content of < 0.5 mg/L (reference range, 0-8), and serum amyloid A (rapid method) content of < 5.0 mg/L (reference value < 10). The pulmonary window of the chest computed tomography (CT) scan revealed a focal high-density infection in the long diameter of the dorsal segment of the left lower lobe (< 2 cm) (A, short arrow); CT re-examination after 4 d revealed a decreased lesion density and slightly increased volume in the dorsal segment of the left lower lobe (B); 1 wk later, CT images showed that most of the lesions were dissipated and absorbed (C); D-F: A 93-year-old woman had a history of close contact with asymptomatic patients infected with SARS-CoV-2 Omicron variant. She had a high fever, cough, and expectoration for 4 d, with nucleic acid polymerase chain reaction positivity (Ct value, 23.97), leukocyte count of 7.41 × 10^9/L, neutrophil proportion of 63.3%, lymphocyte proportion of 22.25% (close to the lower limit of normal value), hypersensitive C-reactive protein content of 31.48 mg/L↑, serum amyloid A (rapid method) content of > 200 mg/L↑, partial pressure of carbon dioxide of 4.65↓, and D-dimer content of 4.25↑. The pulmonary window of the chest CT scan revealed consolidation shadows in the dorsal segment of the left lower lobe (short arrow) accompanied with a small amount of effusion in the adjacent pleural cavity, and scattered patchy, slightly high-density infection foci in both lungs, suggestive of an infection (D); the mediastinal window of the same CT revealed a small amount of effusion in the left pleural cavity (long arrow) (E); CT re-examination after 5 d revealed a decreased density of the consolidation infection foci in the dorsal segment of the left lower lobe and partial absorption of other infection foci in both lungs (F); G and H: An 81-year-old man had a history of close contact with his wife who had asymptomatic SARS-CoV-2 Omicron infection. He had fever, cough, and expectoration for 4 d, with nucleic acid polymerase chain reaction positivity (Ct value, 26.3), leukocyte count of 7.73 × 10^9 /L, neutrophil proportion of 61.9%, lymphocyte proportion of 20.1% (close to the lower limit of normal value), hypersensitive C-reactive protein content of 7.42 mg/L, and serum amyloid A (rapid method) content of 16.6 mg/L↑. The pulmonary window of the chest CT scan revealed scattered patchy ground-glass density shadows in the right middle and lower lobes (short arrows) (G); CT re-examination after 6 d revealed shrinkage and partial absorption of most of the infected foci in the right lung (H).

significant between-group differences (Table 1).

DISCUSSION

SARS-CoV-2 is constantly mutating. A recent report in Lancet confirmed that the viral genomes of the current round of local viral epidemics in Shanghai (present since late February) consist of the SARS-CoV-2 BA.2.2 variant, which is a subpopulation of the SARS-CoV-2 Omicron variant (B.1.1.159)[13]. Although its virulence is weaker than that of previous variants (including the Delta variant), it exhibits higher infectivity and stronger ability to escape the immune system, resulting in large-scale infections, high Ct values among symptomatic patients, and high mortality rates, which have an impact on the society. Therefore, it is particularly important to understand the clinical manifestations and imaging characteristics of patients with Omicron variant infection.

Table 1 Differences in the distribution of abnormal chest computed tomography imaging characteristics in each cycle threshold group, *n* = 394

Group	CT sign						
	Focal infection	Patchy consolidation shadows	Patchy ground-glass density shadows	Mixed consolidation ground-glass shadows	Subpleural interstitial changes	Pleural changes	Total
Low Ct group (< 25)	39[1]	19[2]	22	3	33	14[2]	130
Medium Ct group (25.00-34.99)	92[1]	7	34	7	31	5	176
High Ct group (≥ 35)	47[1]	1	20	2	17	1	88
Total	178	27	76	12	81	20	394

[1]Statistically significant difference in the group;
[2]Statistically significant difference between groups.
CT: Computed tomography; Ct: Cycle threshold.

Currently, the autopsy reports of patients with Omicron variant infection are rarely reported; therefore, the pathological mechanism of this infection remains unclear. According to the autopsy reports of other SARS-CoV-2 subtypes abroad[14-16], SARS-CoV-2 directly infects target cells, including bronchial and alveolar epithelial cells, vascular epithelial and endothelial cells, and immune cells. The formation of early vasculitis leads to vascular wall and perivascular inflammation, immune cell infiltration, vascular stenosis, thrombosis, and secondary bleeding. In the later stage of SARS-CoV-2 infection, interstitial fibrosis and diffuse alveolar injury of the perivascular lung parenchyma can often occur secondary to infection with various bacteria and mucor, consolidation, and complications, such as mucus plugs formed by airway mucus secretion and peripheral pleural changes. Viruses can travel through the blood and induce pathological changes in other parts of the body.

PCR Ct values indicate the number of amplifications required for detecting SARS-CoV-2. The lower the Ct value, the higher the viral load in a nucleic acid sample and vice versa. A previous study reported a linear correlation between Ct values and viral loads. Accordingly, Ct values can reflect the viral levels in patients to a certain extent[8,10]. Some studies have considered Ct values of < 25 to indicate high viral loads; these patients required a longer viral clearance time[17]. We included patients with Ct values of < 25 in the low Ct group. According to the Diagnosis and Treatment Protocol for Novel Coronavirus Pneumonia (Trial Version 9) of China, the standard for dissolution in our region was a Ct value of ≥ 35. Moreover, another study reported that the virus can no longer be isolated from samples at Ct values ≥ 35[18]. Thus, we included patients with Ct values ≥ 35 and < 25 in the high and low Ct groups, respectively. Patients with Ct values of 25.00-34.99 were included in the medium Ct group. Along with chest CT features, Ct values can help improve our understanding of the pathological characteristics of patients with Omicron variant infection.

In this study, among all groups, the most common abnormal chest CT sign was focal infection (30.00%-53.41%, all $P < 0.05$), which was observed as blurred shadows, consolidation shadows, ground-glass density shadows with a long diameter (≤ 2 cm), and small nodule-like shadows with fuzzy edges, most of which were located under the pleura. These findings differ from the most common abnormal sign (patchy ground-glass density shadows) observed in patients with other previously identified SARS-CoV-2 subtype infection[19]. This suggests that the virulence of the Omicron variant is weaker than that of other SARS-CoV-2 variants. In addition, the large-scale use of vaccines leads to the most infection-caused vasculitis being replaced by peripheral vasculitis, more limited secondary peripheral pathological changes, and more common focal infections in the medium and high Ct groups. These findings indicate that lower viral loads in patients with Omicron variant infection result in fewer pulmonary infection foci and improved prognosis.

Among all Ct groups, patchy ground-glass density shadows (16.92%-22.73%) and subpleural interstitial changes (17.61%-25.38%) were also common (but not the most common) chest CT signs. Mixed consolidation ground-glass shadows were less common (2.27%-3.98%). In addition, the above abnormal signs were not significantly different among the three groups (all $P > 0.05$). These abnormal signs were consistent with the chest CT findings of pneumonia caused by other SARS-CoV-2 variants [20-22], however, their proportions were significantly decreased, indicating that the virulence of Omicron is weaker than that of previously identified variants.

The number of patients with patchy consolidation shadows (14.62%), pleural changes (10.77%), and two or more abnormal signs (30.3%) was higher in the low Ct group than in the other two groups (all *P*

< 0.05). Overall, Omicron infection showed fewer signs of pulmonary consolidation than other SARS-CoV-2 variant infections[23]. Consolidation shadows may result from vasculitis, hemorrhage, and peripheral serous exudation caused by high viral loads attacking blood vessels, secondary or direct alveolar inflammation, massive immune cell filling, and small airway mucus plugs. In addition, exudative and inflammatory stimulation of some lesions induces changes such as pleural thickening and pleural effusion. These results suggest that high viral loads can lead to severe and complex pulmonary injuries in some patients.

We used a Ct value of ≥ 35 as an inclusion criterion for patients in the high Ct group. Ct values of ≥ 35 in two consecutive tests is a criterion for patient discharge from mobile cabin hospitals, according to the Diagnosis and Treatment Plan for SARS-CoV-2 Pneumonia (trial version 9) issued by the National Health Commission of the People's Republic of China. Although such patients are noninfectious, their lungs might show abnormal signs to different degrees. Therefore, follow-up observations and treatment of such patients is important.

The sample size of this study was reasonable. Although future studies should be conducted with larger sample sizes, considering the urgent epidemic situation, the sample size of this study was adequate. It is expected that studies with a large sample size will further validate our findings.

CONCLUSION

In this study, patients with SARS-CoV-2 Omicron variant infection were grouped based on their Ct values. We found that the chest CT signs of patients with different viral loads varied to a certain extent. Focal infection was the most common abnormal chest CT sign in the medium and high Ct groups. Patients in the high Ct group more commonly presented with patchy consolidation shadows, pleural changes, and two or more abnormal CT signs than those in the other two groups. The results of this study can effectively enhance our understanding of the characteristics of Omicron variant infections and provide guidance for subsequent clinical treatments of patients with such infections.

ARTICLE HIGHLIGHTS

Research background

The Omicron variant of severe acute respiratory syndrome coronavirus 2 (SARS-CoV-2) mainly infects the upper respiratory tract. Chest computed tomography (CT) can reveal the presence of pulmonary infection. The measured cycle threshold (Ct) was related to pulmonary infections diagnosed *via* CT.

Research motivation

To explore the relationship between chest CT characteristics and Ct value using the fluorescent polymerase chain reaction (PCR) method.

Research objectives

Pulmonary infections caused by the Omicron variant of severe acute respiratory syndrome coronavirus 2 were highly correlated with Ct values. Lower Ct values were associated with a higher incidence and degree of pulmonary damage.

Research methods

The chest CT images and PCR Ct values of 331 patients with Omicron variant infections were retrospectively collected; categorized into low (< 25), moderate (25.00-34.99), and high (≥ 35) Ct groups; and analyzed statistically.

Research results

Focal infections were less frequent in the low Ct group than in the medium and high Ct groups. Patchy consolidation shadows and pleural changes were more common in the low Ct group than in the other two groups. The number of patients with two or more signs was greater in the low Ct group than in the medium and high Ct groups.

Research conclusions

Pulmonary infection and the Ct measured using the fluorescent PCR method were related to pulmonary infections diagnosed *via* CT.

Research perspectives

Future studies with large sample sizes and multiple centers will further validate our findings.

FOOTNOTES

Author contributions: Chen Q designed the research study; Jiang ZK and Han Q performed the research; Hao DG and Zhang Y contributed new reagents and analytic tools; Ying WF analyzed the data and wrote the manuscript; All authors have read and approved the final manuscript.

Institutional review board statement: This study was reviewed and approved by the Ethics Committee of Shanghai Xuhui Dahua Hospital (Approval No. 20220804).

Informed consent statement: All study participants or their legal guardian provided informed written consent about personal and medical data collection prior to study enrolment.

Conflict-of-interest statement: The authors state that there are no conflicts of interest to report.

Data sharing statement: Technical appendix, statistical code, and dataset available from the corresponding author at cq1444@sina.com upon reasonable request.

Country/Territory of origin: China

ORCID number: Wei-Feng Ying 0000-0002-8877-6828; Qiong Chen 0000-0001-7167-1897; Zhi-Kui Jiang 0000-0003-2716-2790; Da-Guang Hao 0000-0002-1386-8189; Ying Zhang 0000 0002 1386 8189; Qian Han 0000-0002-1138-3284.

Corresponding Author's Membership in Professional Societies: Member of tumor imaging special committee of Shanghai anticancer association Member of Shanghai radiologist Association.

S-Editor: Chen YL
L-Editor: Filipodia
P-Editor: Chen YL

REFERENCES

1 **Meo SA**, Meo AS, Al-Jassir FF, Klonoff DC. Omicron SARS-CoV-2 new variant: global prevalence and biological and clinical characteristics. *Eur Rev Med Pharmacol Sci* 2021; **25**: 8012-8018 [PMID: 34982465 DOI: 10.26355/eurrev_202112_27652]
2 **Nyberg T**, Ferguson NM, Nash SG, Webster HH, Flaxman S, Andrews N, Hinsley W, Bernal JL, Kall M, Bhatt S, Blomquist P, Zaidi A, Volz E, Aziz NA, Harman K, Funk S, Abbott S; COVID-19 Genomics UK (COG-UK) consortium, Hope R, Charlett A, Chand M, Ghani AC, Seaman SR, Dabrera G, De Angelis D, Presanis AM, Thelwall S. Comparative analysis of the risks of hospitalisation and death associated with SARS-CoV-2 omicron (B.1.1.529) and delta (B.1.617.2) variants in England: a cohort study. *Lancet* 2022; **399**: 1303-1312 [PMID: 35305296 DOI: 10.1016/S0140-6736(22)00462-7]
3 **Pérez-Then E**, Lucas C, Monteiro VS, Miric M, Brache V, Cochon L, Vogels CBF, Malik AA, De la Cruz E, Jorge A, De Los Santos M, Leon P, Breban MI, Billig K, Yildirim I, Pearson C, Downing R, Gagnon E, Muyombwe A, Razeq J, Campbell M, Ko AI, Omer SB, Grubaugh ND, Vermund SH, Iwasaki A. Neutralizing antibodies against the SARS-CoV-2 Delta and Omicron variants following heterologous CoronaVac plus BNT162b2 booster vaccination. *Nat Med* 2022; **28**: 481-485 [PMID: 35051990 DOI: 10.1038/s41591-022-01705-6]
4 **Garcia-Beltran WF**, St Denis KJ, Hoelzemer A, Lam EC, Nitido AD, Sheehan ML, Berrios C, Ofoman O, Chang CC, Hauser BM, Feldman J, Roederer AL, Gregory DJ, Poznansky MC, Schmidt AG, Iafrate AJ, Naranbhai V, Balazs AB. mRNA-based COVID-19 vaccine boosters induce neutralizing immunity against SARS-CoV-2 Omicron variant. *Cell* 2022; **185**: 457-466.e4 [PMID: 34995482 DOI: 10.1016/j.cell.2021.12.033]
5 **Chen J**, Wang R, Gilby NB, Wei GW. Omicron Variant (B.1.1.529): Infectivity, Vaccine Breakthrough, and Antibody Resistance. *J Chem Inf Model* 2022; **62**: 412-422 [PMID: 34989238 DOI: 10.1021/acs.jcim.1c01451]
6 **Kozlov M**. Omicron's feeble attack on the lungs could make it less dangerous. *Nature* 2022; **601**: 177 [PMID: 34987210 DOI: 10.1038/d41586-022-00007-8]
7 **Ren SY**, Wang WB, Gao RD, Zhou AM. Omicron variant (B.1.1.529) of SARS-CoV-2: Mutation, infectivity, transmission, and vaccine resistance. *World J Clin Cases* 2022; **10**: 1-11 [PMID: 35071500 DOI: 10.12998/wjcc.v10.i1.1]
8 **Garrett N**, Tapley A, Andriesen J, Seocharan I, Fisher LH, Bunts L, Espy N, Wallis CL, Randhawa AK, Ketter N, Yacovone M, Goga A, Bekker LG, Gray GE, Corey L. High Rate of Asymptomatic Carriage Associated with Variant Strain Omicron. *medRxiv* 2022 [PMID: 35043118 DOI: 10.1101/2021.12.20.21268130]
9 **Osterman A**, Badell I, Basara E, Stern M, Kriesel F, Eletreby M, Öztan GN, Huber M, Autenrieth H, Knabe R, Späth PM, Muenchhoff M, Graf A, Krebs S, Blum H, Durner J, Czibere L, Dächert C, Kaderali L, Baldauf HM, Keppler OT. Impaired detection of omicron by SARS-CoV-2 rapid antigen tests. *Med Microbiol Immunol* 2022; **211**: 105-117 [PMID: 35187580

DOI: 10.1007/s00430-022-00730-z]

10 **Juanola-Falgarona M**, Peñarrubia L, Jiménez-Guzmán S, Porco R, Congost-Teixidor C, Varo-Velázquez M, Rao SN, Pueyo G, Manissero D, Pareja J. Ct values as a diagnostic tool for monitoring SARS-CoV-2 viral load using the QIAstat-Dx® Respiratory SARS-CoV-2 Panel. *Int J Infect Dis* 2022; **122**: 930-935 [PMID: 35840097 DOI: 10.1016/j.ijid.2022.07.022]

11 **Tsakok MT**, Watson RA, Saujani SJ, Kong M, Xie C, Peschl H, Wing L, MacLeod FK, Shine B, Talbot NP, Benamore RE, Eyre DW, Gleeson F. Reduction in Chest CT Severity and Improved Hospital Outcomes in SARS-CoV-2 Omicron Compared with Delta Variant Infection. *Radiology* 2023; **306**: 261-269 [PMID: 35727150 DOI: 10.1148/radiol.220533]

12 **Yoon SH**, Lee JH, Kim BN. Chest CT Findings in Hospitalized Patients with SARS-CoV-2: Delta versus Omicron Variants. *Radiology* 2023; **306**: 252-260 [PMID: 35762887 DOI: 10.1148/radiol.220676]

13 **Zhang X**, Zhang W, Chen S. Shanghai's life-saving efforts against the current omicron wave of the COVID-19 pandemic. *Lancet* 2022; **399**: 2011-2012 [PMID: 35533708 DOI: 10.1016/S0140-6736(22)00838-8]

14 **Goussard P**, Schubert P, Parker N, Myburgh C, Rabie H, van der Zalm MM, Van Zyl GU, Preiser W, Maponga TG, Verster J, Gie AG, Andronikou S. Fatal SARS-CoV-2 Omicron variant in a young infant: Autopsy findings. *Pediatr Pulmonol* 2022; **57**: 1363-1365 [PMID: 35243813 DOI: 10.1002/ppul.25881]

15 **Martín-Martín J**, Martín-Cazorla F, Suárez J, Rubio L, Martín-de-Las-Heras S. Comorbidities and autopsy findings of COVID-19 deaths and their association with time to death: a systematic review and meta-analysis. *Curr Med Res Opin* 2022; **38**: 785-792 [PMID: 35254193 DOI: 10.1080/03007995.2022.2050110]

16 **Calabrese F**, Pezzuto F, Fortarezza F, Hofman P, Kern I, Panizo A, von der Thüsen J, Timofeev S, Gorkiewicz G, Lunardi F. Pulmonary pathology and COVID-19: lessons from autopsy. The experience of European Pulmonary Pathologists. *Virchows Arch* 2020; **477**: 359-372 [PMID: 32642842 DOI: 10.1007/s00428-020-02886-6]

17 **Aranha C**, Patel V, Bhor V, Gogoi D. Cycle threshold values in RT-PCR to determine dynamics of SARS-CoV-2 viral load: An approach to reduce the isolation period for COVID-19 patients. *J Med Virol* 2021; **93**: 6794-6797 [PMID: 34264527 DOI: 10.1002/jmv.27206]

18 **Ke R**, Martinez PP, Smith RL, Gibson LL, Mirza A, Conte M, Gallagher N, Luo CH, Jarrett J, Zhou R, Conte A, Liu T, Farjo M, Walden KKO, Rendon G, Fields CJ, Wang L, Fredrickson R, Edmonson DC, Baughman ME, Chiu KK, Choi H, Scardina KR, Bradley S, Gloss SL, Reinhart C, Yedetore J, Quicksall J, Owens AN, Broach J, Barton B, Lazar P, Heetderks WJ, Robinson ML, Mostafa HH, Manabe YC, Pekosz A, McManus DD, Brooke CB. Daily longitudinal sampling of SARS-CoV-2 infection reveals substantial heterogeneity in infectiousness. *Nat Microbiol* 2022; **7**: 640-652 [PMID: 35484231 DOI: 10.1038/s41564-022-01105-z]

19 **Solomon JJ**, Heyman B, Ko JP, Condos R, Lynch DA. CT of Post-Acute Lung Complications of COVID-19. *Radiology* 2021; **301**: E383-E395 [PMID: 34374591 DOI: 10.1148/radiol.2021211396]

20 **Chinese Research Hospital Association**; Respiratory Council. [Expert recommendations for the diagnosis and treatment of interstitial lung disease caused by novel coronavirus pneumonia]. *Zhonghua Jie He He Hu Xi Za Zhi* 2020; **43**: 827-833 [PMID: 32992435 DOI: 10.3760/cma.j.cn112147-20200326-00419]

21 **Hu Q**, Guan H, Sun Z, Huang L, Chen C, Ai T, Pan Y, Xia L. Early CT features and temporal lung changes in COVID-19 pneumonia in Wuhan, China. *Eur J Radiol* 2020; **128**: 109017 [PMID: 32387924 DOI: 10.1016/j.ejrad.2020.109017]

22 **Yan S**, Chen H, Xie RM, Guan CS, Xue M, Lv ZB, Wei LG, Bai Y, Chen BD. Chest CT Evaluation of 11 Persistent Asymptomatic Patients with SARS-CoV-2 Infection. *Jpn J Infect Dis* 2021; **74**: 1-6 [PMID: 32611980 DOI: 10.7883/yoken.JJID.2020.264]

23 **Granata V**, Fusco R, Villanacci A, Magliocchetti S, Urraro F, Tetaj N, Marchioni L, Albarello F, Campioni P, Cristofaro M, Di Stefano F, Fusco N, Petrone A, Schininà V, Grassi F, Girardi E, Ianniello S. Imaging Severity COVID-19 Assessment in Vaccinated and Unvaccinated Patients: Comparison of the Different Variants in a High Volume Italian Reference Center. *J Pers Med* 2022; **12** [PMID: 35743740 DOI: 10.3390/jpm12060955]

World Journal of Clinical Cases

Submit a Manuscript: https://www.f6publishing.com

World J Clin Cases 2023 February 6; 11(4): 764-779

DOI: 10.12998/wjcc.v11.i4.764

ISSN 2307-8960 (online)

ORIGINAL ARTICLE

Retrospective Study

Major depressive disorders in patients with inflammatory bowel disease and rheumatoid arthritis

Maryam Bilal Haider, Brinda Basida, Jasleen Kaur

Specialty type: Medicine, research and experimental

Provenance and peer review: Unsolicited article; Externally peer reviewed.

Peer-review model: Single blind

Peer-review report's scientific quality classification

Grade A (Excellent): 0
Grade B (Very good): B
Grade C (Good): C
Grade D (Fair): D
Grade E (Poor): 0

P-Reviewer: Liu XQ, China; Xiao J, China

Received: September 21, 2022
Peer-review started: September 21, 2022
First decision: November 30, 2022
Revised: December 14, 2022
Accepted: January 12, 2023
Article in press: January 12, 2023
Published online: February 6, 2023

Maryam Bilal Haider, Department of Internal Medicine, Detroit Medical Center, Wayne State University, Sinai Grace Hospital, Detroit, MI 48235, United States

Brinda Basida, Department of Geriatrics, Rohde Island Hospital/Brown University, Providence, RI 02903, United States

Jasleen Kaur, Department of Rheumatology, St. Mary's Ascension/Central Michigan University, Saginaw, MI 48601, United States

Corresponding author: Maryam Bilal Haider, MD, Doctor, Department of Internal Medicine, Detroit Medical Center, Wayne State University, Sinai Grace Hospital, 6071 Outer Dr W, Detroit, MI 48235, United States. maryambilalhaider@yahoo.com

Abstract

BACKGROUND

Various immune-mediated inflammatory diseases consisting of inflammatory bowel disease (IBD) and rheumatoid arthritis (RA), are found to have a substantial societal burden, increased healthcare costs, and progressive disability. Studies suggest that patients with *vs* without comorbid depression have a more significant disability, a lower likelihood of remission, and reduced adherence to therapy. Elevated interleukin (IL)-1β, tumor necrosis factor-α, and IL-6 contribute to developing depression by the impaired physiological responses to stress, resulting in increased pain, fever, fatigue, and lack thereof of interest, and thus poor long-term outcomes. This study emphasizes the timely recognition of the prevalence of major depressive disorder (MDD) in patients with RA and IBD combined, thus preventing disability.

AIM

To identify the prevalence level and temporal trends of depression in hospitalized IBD-RA patients.

METHODS

All adult hospitalized patients from January 2000 to December 2019 in the nationwide inpatient sample (NIS) were captured. The study population included all patients with a primary or secondary IBD-RA overlap disease using corresponding international classification of diseases (ICD)-9 and ICD-10 codes. IBD includes Crohn's disease and ulcerative colitis. The study population was divided into IBD-RA without MDD (controls) and IBD-RA with MDD (cases). For group

comparison between MDD *vs* no MDD, we used Student's *t*-test for continuous variables and Rao-Scott Chi-square tests for categorical variables. For univariate analyses, we used logistic regression, and for multivariate analysis, we used a weighted multi-level mixed-effects model. We attested all hypotheses with two-tailed significance level of 0.05 ($P < 0.05$ was considered significant). The outcome is to examine the temporal trends and prevalence of depression in patients with IBD-RA by gender, race, and age.

RESULTS

A total of 133315 records were identified with IBD-RA overlap, of which 26155 patients (19.62%) had MDD. Among the IBD-RA patients, those who had MDD were younger [mean age of 56 years (SD ± 15)] to IBD-RA without MDD patients with a $P < 0.0001$, more females (80% among cases *vs* 73% among controls) than males with a $P < 0.0001$, frequent in the white race (79% among cases *vs* 73% among controls) than black race. Over the 19 years, the number of patients with MDD in IBD-RA increased from 153 (the year 2000) to 2880 (the year 2019) in weighted NIS, representing a 1782% increase compared to the year 2000 with a $P < 0.001$. Factors associated with higher MDD included younger age, female gender, white race, alcohol, opioids, esophageal disorders, peptic ulcer disease, chronic pancreatitis, paralysis, dementia, menopausal disorders, obesity, nutritional deficiencies, diabetes mellitus with chronic complications, and osteoarthritis.

CONCLUSION

There is a rise in the prevalence of depression in younger patients with IBD-RA combined compared to their counterparts. These patients are also at higher risk for the increased cost of care and poor treatment compliance. It is crucial to educate the involved clinicians to identify the early signs and symptoms of depression in patients with IBD or RA or IBD-RA combined and treat them to have a better overall prognosis.

Key Words: Inflammatory bowel disease; Rheumatoid arthritis; Depression; Multimorbidity; Epidemiology; Demographics

Core Tip: Our study is a nationwide inpatient sample-based study of the two decades in which we aim to analyze inflammatory bowel disease (IBD) and rheumatoid arthritis (RA) patients' characteristics, temporal trends, sociodemographic characteristics, and predictors of major depressive disorders in the IBD-RA cohort. There is an increasing trend in the prevalence of IBD-RA, especially in younger patients. We believe this study will open the door for further research and educate the involved physicians to identify the early signs and symptoms of depression in patients with IBD or RA or IBD-RA combined and treat them or have them treated to have a better overall prognosis.

Citation: Haider MB, Basida B, Kaur J. Major depressive disorders in patients with inflammatory bowel disease and rheumatoid arthritis. *World J Clin Cases* 2023; 11(4): 764-779
URL: https://www.wjgnet.com/2307-8960/full/v11/i4/764.htm
DOI: https://dx.doi.org/10.12998/wjcc.v11.i4.764

INTRODUCTION

The coexistence between immune-mediated inflammatory diseases (IMID) with depression has long been studied[1,2]. Rheumatoid arthritis (RA) is a chronic systemic autoimmune disorder that primarily targets the synovial joints leading to inflammation (synovitis), joint erosion, and damage to the cartilage [3]. Inflammatory bowel disease (IBD) is broadly subdivided into ulcerative colitis and Crohn's disease. Crohn's disease is a relapsing systematic immune-mediated chronic IBD, and Ulcerative colitis is an idiopathic, chronic IBD with bloody diarrhea[4].

The global prevalence of RA is estimated at 460 *per* 100000 population, while its prevalence in the United States is 700 *per* 100000 population[5,6]. Both depression and RA contribute substantially to global disability, and the diseases often coexist. The global prevalence rate of IBD is 84.3 *per* 100000 population, while that in the United States is 464.5 *per* 100000 population[7].

Patients with RA suffer twice from depression than the general population[8], with 41%-66% reported lifetime prevalence[1,3]. The prevalence of major depressive disorders (MDDs) was 17% in patients with RA[3]. IBD patients have more than 25% lifetime diagnosis of depression[9,10].

Not many studies have identified the impact of depression in patients with both RA and IBD combined. Our study is researched using the national inpatient sampling database sought to evaluate the co-existence of depression in patients with RA and IBD. The role of the Brain-Gut axis and Brain-Joint axis in the development of depression has been illustrated before[11,12], but there is not enough literature demonstrating the combined Brain-Gut-Joint axis. Our study discusses the clinical data on this combined axis and emphasizes potentially valuable strategies for managing these patients. Our primary aim was to identify a pooled prevalence level and temporal trends of depression in hospitalized IBD-RA patients. To have a multimorbidity approach, which is more patient-focused, we aimed to investigate various comorbidities as predictors of depression.

MATERIALS AND METHODS

We analyzed the nationwide inpatient sample (NIS) database from January 2000 to December 2019. The NIS is the largest all-payer publicly available database of hospitalizations in the United States, designed to produce national and regional inpatient utilization, cost, quality, and outcomes[13]. We used the international classification of diseases (ICD)-9, diagnosis and procedures before October 1, 2015, and ICD-10 afterward[14]. In this study, we used the latest available datasets. The NIS dataset is very suitable for temporal trends, but the dataset has undergone several changes over time. We used the Healthcare Cost and Utilization Project (HCUP) recommendation to use trend weights before 2012 to make estimates comparable to the 2012 NIS design[15]. The dataset was de-identified to protect the privacy of individual patients, physicians, and hospitals. As the dataset lacks patient information, this study was exempted from Institutional Review Board-IRB approval from Wayne State University under the Health Insurance Portability and Accountability Act[16].

The study population included patients with a primary or secondary IBD-RA overlap disease using corresponding ICD-9 and ICD-10 codes. For IBD, we included Crohn's disease and ulcerative colitis patients. We used the clinical classification software refined to determine the ICD codes of depressive disorders[17,18]. The study population was divided into IBD-RA without MDD (controls) and IBD-RA with MDD (cases).

Outcomes and variables

The outcomes included temporal trends and predictors of MDDs in the IBD-RA cohort. In the first part, we performed a trend analysis of weighted prevalence, the percentage change in prevalence compared to the year 2000, mean age, gender and ethnicity, length of stay, and total hospital charges. Next, we compared baseline patient and hospital characteristics and comorbidities between cases (IBD-RA with MDD) and controls (IBD-RA without MDD). We also evaluated predictors for MDD in IBD-RA patients.

Patient demographics included gender, age, ethnicity, socioeconomic status, and primary health insurance. Socioeconomic status was defined as the median household income in the patient's zip code and was divided into quartiles by year (2019): Less than $47999, $48000–$60999, $61000–$81999, $82000 or more). Hospitalization care costs were adjusted using the United States Bureau of Labor and Statistics' consumer price index[19]. In addition, we used NIS characterization for hospital factors. The complete list of comorbidities is shown in Table 1.

Statistical analysis

The statistical analyses are performed in SAS software (SAS Institute Inc., Cary, NC, United States). The HCUP NIS database was redesigned beginning in 2012 to improve national estimates. We deployed HCUP recommendations for trend analysis and used survey sampling and analysis procedures for weighted analysis. Continuous variables such as age, total charges, and length of stay are represented with a mean ± SD, and categorical variables are presented with frequency and computed percentages. For group comparison between MDD *vs* no MDD, we used Student's *t*-test for continuous variables and Rao-Scott Chi-square tests for categorical variables. We used the Cochran-Armitage trend test for categorical variables and poison regression with a log link for continuous variables for temporal trends analysis. The univariate analysis is performed with logistic regression. The multivariate analysis is achieved with a weighted multi-level mixed-effects model using the Glimmix procedure with maximum likelihood estimation and Gauss-Hermite quadrature likelihood approximation. We categorized age into five sub-categories *per* HCUP standard categories (< 18, 18-44, 45-64, 65-84, and ≥ 85) for group-level comparison. The missing values are categorized as either missing or unknown. All hypothesis testing is performed with two-tailed significance level of 0.05 ($P < 0.05$ was considered significant).

RESULTS

Baseline characteristics of the study population

The baseline characteristics of the study population with and without MDD are described in Table 2.

Table 1 Comorbidities comparison in inflammatory bowel disease-rheumatoid arthritis overlap patients with and without major depressive disorders, national inpatient sample year 2000 to 2019

	IBD-RA without depressive disorders, weighted, *n* (%)	IBD-RA with depressive disorders, weighted, *n* (%)	*P* value
Liver disease, mild	6400 (5.97)	2130 (8.14)	< 0.0001[a]
Liver disease, moderate to severe	786 (0.73)	230 (0.88)	0.2871[a]
Peptic ulcer disease	1709 (1.59)	632 (2.41)	< 0.0001[a]
Esophageal disorders	30712 (28.65)	10569 (40.40)	< 0.0001[a]
Gastritis	3781 (3.52)	1124 (4.30)	0.0095[a]
Diabetes mellitus with chronic complications	6367 (5.94)	2005 (7.66)	< 0.0001[a]
Diabetes mellitus without chronic complications	14014 (13.07)	3533 (13.50)	0.4244[a]
Hypertension	40782 (38.05)	10493 (40.12)	0.0080[a]
Heart Failure	12798 (11.94)	2908 (11.11)	0.1176[a]
Coronary artery disease	16644 (15.53)	3549 (13.57)	0.0007[a]
Cardiac dysrhythmias	16114 (15.04)	3299 (12.61)	< 0.0001[a]
Myocardial infarction	1316 (1.23)	224 (0.86)	0.0237[a]
Stroke	1530 (1.42)	230 (0.88)	0.0018[a]
Iron Deficiency Anemia	9298 (8.68)	2296 (8.78)	0.8167[a]
Nutritional deficiencies	4062 (3.79)	1494 (5.71)	< 0.0001[a]
Lipid Metabolism disorders	24990 (23.32)	7036 (26.90)	< 0.0001[a]
Thyroid disorders	18029 (16.82)	5531 (21.15)	< 0.0001[a]
Chronic Pancreatitis	1165 (1.09)	507 (1.94)	< 0.0001[a]
Renal failure, moderate	8563 (7.99)	2132 (8.15)	0.7113[a]
Renal failure, severe	2965 (2.77)	767 (2.93)	0.5434[a]
Menopausal disorders	536 (0.50)	222 (0.84)	0.0033[a]
Osteoporosis	11752 (10.97)	3544 (13.55)	< 0.0001[a]
Osteoarthritis	15084 (14.07)	4562 (17.44)	< 0.0001[a]
Obesity	11706 (10.92)	4062 (15.53)	<.0001[1]
Weight Loss	1201 (1.12)	365 (1.39)	0.1101[a]
Protein-calorie malnutrition	8479 (7.91)	2370 (9.06)	0.0085[a]
Leukemia	558 (0.52)	134 (0.51)	0.9401[a]
Lymphoma	838 (0.78)	181 (0.69)	0.5132[a]
Metastatic cancer	1381 (1.29)	329 (1.26)	0.8524[a]
Solid tumor without metastasis, malignant	3785 (2.84)	850 (0.64)	0.8524[a]
Paralysis	1498 (1.40)	495 (1.89)	0.0114[a]
Dementia	2291 (2.14)	886 (3.39)	< 0.0001[a]
AIDS	212 (0.19)	45 (0.17)	0.6818[a]
Smoking	32336 (30.17)	9893 (37.82)	< 0.0001[a]
Alcohol	1747 (1.63)	950 (3.63)	< 0.0001[a]
Opioids	3180 (2.97)	1797 (6.87)	< 0.0001[a]

[a]Rao-Scott Chi-Square 2-tailed Test for the association of two Categorical Variables.

IBD-RA: Inflammatory bowel disease-rheumatoid arthritis; AIDS: Acquired immunodeficiency syndrome.

From January 2000 to December 2019, we found 133315 IBD-RA overlap patients in weighted settings, of which 26155 patients (19.62%) had MDD. Among the IBD-RA patients, those who had MDD were younger [mean age of 56 years (SD ± 15) as compared to mean age of 59 years (SD ± 17)] in IBD-RA without MDD patients with $P < 0.0001$, more females (80% among cases *vs* 73% among controls) than males (20% for cases *vs* 17% for controls) with $P < 0.0001$, frequent in the white race (79% among cases *vs* 73% among controls) than black race (7% for cases *vs* 10% for controls) and Hispanic (4.00% among cases *vs* 4.63% among controls) with $P < 0.0001$, and more frequent in patients with Medicaid (12% among cases *vs* 9% among controls) than patients with private insurance (28% among cases *vs* 31% among controls) $P < 0.0001$. A comparison of comorbidities of the study population with and without MDD is described in Table 1.

Temporal trends

Over the 19 years, the number of patients with MDD in IBD-RA increased from 153 (the year 2000) to 2880 (the year 2019) in weighted NIS (Figure 1), representing a 1782% increase (Figure 2) compared to the year 2000 with $P < 0.001$. The mean age of IBD-RA in MDD patients was 56.36 years in 2000 compared with 59.8 years in 2019, with a $P < 0.001$ (Figure 3A). There was no significant change in the male *vs* female trend of MDD in the IBD-RA cohort (Figure 3B). Overall, the white race among IBD-RA with MDD is 78.80%. We observed a decreasing trend in the white race with $P = 0.03$. The black race is 7.07%, and no change is followed over time. The Hispanic ethnicity is 3.99%, and we noted an increasing trend with $P = 0.02$ (Figure 3C). In terms of hospital burden, the mean length of stay of IBD-RA with MDD patients decreased from 5.69 d in 2000 to 5.35 d in 2019 with a $P < 0.001$ (Figure 3D), and the mean total cost of care (inflation-adjusted) increased from $20564 in 2000 to $60428 in 2019 with $P < 0.001$ (Figure 3E).

Predictors for MDDs

The univariate and multivariate analyses for IBD-RA patients with MDD are shown in Table 3. The multivariate analyses showed that demographic factors associated with higher MDD included female gender [adjusted odds ratios (aOR): 1.52; 95%CI: 1.46-1.58; $P < 0.0001$], patients aged 18-44 (aOR: 1.89; 95%CI: 1.79-1.99; $P < 0.0001$) and patients aged 45-64 (aOR: 1.69; 95%CI: 1.63-1.76; $P < 0.0001$) as compared to the reference group (patients aged 65-84), white (aOR: 1.83; 95%CI: 1.73-1.94; $P < 0.0001$) and Hispanic race (aOR: 1.39; 95%CI: 1.27-1.52; $P < 0.0001$) as compared to the black race, and median socioeconomic status in the second quartile (aOR: 1.07; 95%CI: 1.03-1.12; $P = 0.002$) as compared to quartile 1.

Comorbidities associated with higher MDD in IBD-RA patients included alcohol (aOR: 2.11; 95%CI: 1.93–2.31; $P < 0.0001$), opioids (aOR: 2.00; 95%CI: 1.83–2.15; $P < 0.0001$), smoking (aOR: 1.23; 95%CI: 1.19–1.27; $P < 0.0001$), esophageal disorders (aOR: 1.53; 95%CI: 1.48-1.58; $P < 0.0001$), peptic ulcer disease (PUD) (aOR: 1.26; 95%CI: 1.13-1.39; $P < 0.0001$), chronic pancreatitis (aOR: 1.36; 95%CI: 1.21-1.53; $P < 0.0001$), mild liver disease (aOR: 1.16; 95%CI: 1.09-1.23; $P < 0.0001$), gastritis (aOR: 1.10; 95%CI: 1.09-1.18; $P = 0.02$), paralysis (aOR: 1.48; 95%CI: 1.32-1.66; $P < 0.0001$), dementia (aOR: 2.08; 95%CI: 1.91–2.27; $P < 0.0001$), menopausal disorders (aOR: 1.43; 95%CI: 1.21-1.70; $P < 0.0001$), obesity (aOR: 1.29; 95%CI: 1.18-1.28; $P < 0.0001$), nutritional deficiencies (aOR: 1.28; 95%CI: 1.20-1.37; $P < 0.0001$), weight loss (aOR: 1.21; 95%CI: 1.07-1.38; $P < 0.0001$), protein-calorie malnutrition (aOR: 1.10; 95%CI: 1.05-1.16; $P = 0.0002$),thyroid disorders (aOR: 1.25; 95%CI: 1.20-1.30; $P < 0.0001$), osteoarthritis (aOR: 1.22; 95%CI: 1.17-1.27; $P < 0.0001$), osteoporosis (aOR: 1.21; 95%CI: 1.16-1.27; $P < 0.0001$), diabetes mellitus with chronic complications (aOR: 1.20; 95%CI: 1.13-1.28; $P < 0.0001$), lipid metabolism disorders (aOR: 1.19; 95%CI: 1.15-1.24; $P < 0.0001$), and severe renal failure (aOR: 1.12; 95%CI: 1.02-1.23; $P < 0.0001$).

DISCUSSION

Various studies have been done in the past, which show a higher rate of depression in patients with IMIDs like RA and IBD than in the general population[20,21]. Patients with coexisting IMID and depression tend to have higher disease activity[1], more fatigue[22], distressing symptoms of pain[23], lower health-related quality of life, and increasing health care costs[24] than patients without depression [1]. Depression as a comorbidity negatively impacts IMID patients' physical function, mental health, symptom severity, overall morbidity, and mortality[24].

RA is an autoimmune-mediated disease leading to joint destruction, directed mainly by the action of T cells and inflammatory cytokines[3,22]. There is a lack of complete understanding of the biological mechanism responsible for this association of depression with these autoimmune inflammatory disorders. It is mainly attributed to chronic inflammation caused by elevated cytokines like interleukin (IL)-1β, tumor necrosis factor-α, and IL-6. These cytokines decrease neurogenesis and influence the

Table 2 Comparison of Patients' demographics and hospital Characteristics of inflammatory bowel disease-rheumatoid arthritis overlap patients with and without depressive disorders, national inpatient sample year 2000 to 2019

	IBD-RA without MDD, weighted, *n* (%)	IBD-RA with MDD, weighted, *n* (%)	*P* value
Weighted total, *n* (%)	107160 (80.38)	26155 (19.62)	
Sex			< 0.0001[a]
Female	78088 (72.87)	21052 (80.49)	
Male	29073 (27.13)	5103 (19.51)	
Age (yr), mean ± SD	58.70 ± 16.89	56.36 ± 15.47	< 0.0001[b]
Age groups (yr)			< 0.0001[c]
< 18	319 (0.29)	25 (0.10)	
18-44	22215 (20.73)	5887 (22.50)	
45-64	40363 (37.67)	11544 (44.14)	
65-84	39111 (36.50)	7902 (30.21)	
≥ 85	5152 (4.81)	798 (3.05)	
Ethnicity			< 0.0001[c]
White	77818 (72.62)	20612 (78.80)	
Black	10543 (9.83)	1850 (7.07)	
Hispanic	4963 (4.63)	1045 (3.99)	
Asian or Pacific Islander	741 (0.69)	94 (0.36)	
Native American	500 (0.47)	91 (0.35)	
Other	12596 (11.75)	2464 (9.42)	
Primary payer status			< 0.0001[c]
Medicare	59738 (55.75)	14522 (55.52)	
Medicaid	10128 (9.45)	3257 (12.45)	
Private	32808 (30.62)	7239 (27.68)	
Self-Pay	2034 (1.89)	505 (1.93)	
No charge	186 (0.17)	40 (0.15)	
Other	2266 (2.11)	592 (2.26)	
Median socioeconomic status by national quartiles			0.0008[c]
0-25	24484 (22.85)	6111 (23.37)	
25-50	26531 (24.75)	6690 (25.58)	
50-75	27857 (26.00)	7171 (27.42)	
75-100	26431 (24.66)	5876 (22.46)	
Other	1857 (1.73)	307 (1.17)	
Hospital bed size			0.0147[c]
Small	16789 (15.67)	4496 (17.19)	
Medium	28359 (26.46)	7067 (27.02)	
Large	62012 (57.87)	14592 (55.79)	
Location/teaching status of the hospital			< 0.0001[c]
Rural	10398 (9.70)	2299 (8.79)	
Urban nonteaching	36576 (34.13)	7801 (29.83)	
Urban teaching	60186 (56.17)	16055 (61.38)	

Hospital region			< 0.0001[c]
Northeast	21819 (20.36)	4601 (17.59)	
Midwest or North Central	27596 (25.75)	7636 (29.19)	
South	40204 (37.52)	9583 (36.64)	
West	17541 (16.36)	4335 (16.57)	
Discharge outcomes			
Routine Discharge	69143 (64.52)	16289 (62.28)	< 0.0031[a]
Transfer to Short-term Hospital	2240 (2.09)	475 (1.82)	0.2013[a]
Transfer to other facilities	16349 (15.26)	4612 (17.63)	< 0.0001[a]
HHC	17635 (16.45)	4536 (17.34)	0.1373[a]
In-hospital mortality	1792 (1.67%)	243 (0.93%)	< 0.0001[a]
Length of stay (days), mean ± SD	5.49 ± 5.75	5.65 ± 5.79	0.0738[a]
Total charges (USD), mean ± SD	43881 ± 61300	45157 ± 60859	0.1762[a]

[a]Two-sample Student *t*-test, 2-tailed for comparing means of two Continuous Variables.
[b]Rao-Scott Chi-Square 2-tailed Test for the association of two Categorical Variables.
[c]Rao-Scott Chi-square, 2-tailed Test for two by *n* table. Statistical significance illustrates that the two groups differ.
IBD-RA: Inflammatory bowel disease-rheumatoid arthritis; HHC: Home health care.

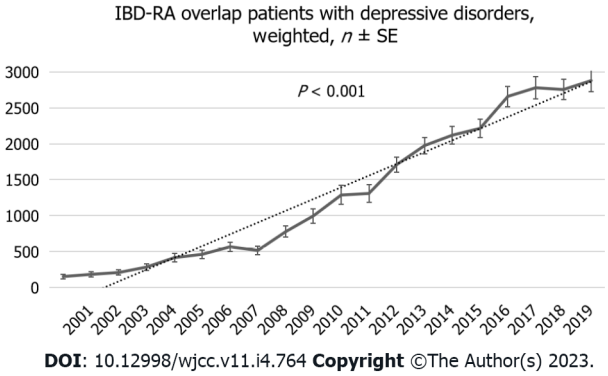

DOI: 10.12998/wjcc.v11.i4.764 **Copyright** ©The Author(s) 2023.

Figure 1 Weighted trend of inflammatory bowel disease-rheumatoid arthritis overlap patients with major depressive disorders, national inpatient sample year 2000 to 2019. IBD-RA: Inflammatory bowel disease-rheumatoid arthritis.

homeostasis of the neurotransmission axis, like glutamate-dependent pathways, monoaminergic pathways, and the hypothalamic-pituitary-adrenal (HPA) axis[8]. Hence, these factors contribute to the development of depression by the impaired physiological responses to stress, resulting in increased pain, fever, fatigue, lack of interest, and thus poor long-term outcomes[3].

Due to the bidirectional communication *via* the gut-brain axis, reduced social functioning, and impaired quality of life, patients with IBD have increased rates of psychiatric disorders as compared to the general population. Walker *et al*[10] demonstrated that individuals with IBD have more than double the lifetime prevalence of MDD compared to the general population[10]. Marrie *et al*[25] showed that the incidence and prevalence of depression, anxiety, and bipolar disorders are elevated in RA patients compared to a matched population[25]. The prevalence of depression in patients with RA is approximately 19%, with conservative estimates, most common in females and younger age groups[5]. In our study, the prevalence of depression in the IBD-RA cohort is approximately 20%, females have 50% more odds of depression than males, and younger patients have higher odds of depression (patients aged 18-44 have 88% higher odds of depression than patients aged 65-84 years). We noted an increasing trend of MDD in the IBD-RA cohort (Figure 1) and an increasing trend in the mean age (Figure 3A). We also exhibited a growing trend in hospital charges (Figure 3E) with a decreasing trend in the length of stay (Figure 3D).

Pezzato *et al*[26] assessed 490 Italian patients with RA and found that depression was more frequent in females and unemployed patients[26]. In our study, patients with private insurance have lower odds of depression than patients with Medicare. Physicians should be aware that women and those of lower socioeconomic status are at increased risk of these disorders.

Table 3 Univariate and multivariate analyses of demographics and comorbidities associated with major depressive disorders in the inflammatory bowel disease-rheumatoid arthritis cohort, national inpatient sample year 2000 to 2019

Variables	Univariate analysis		Multivariate analysis	
	Unadjusted odds ratio[1] (95%CI)	*P* value	Adjusted odds ratio[2] (95%CI)	*P* value
Gender, Female *vs* Male	1.533 (1.424–1.651)	< 0.0001	1.518 (1.463-1.575)	< 0.0001
Age groups (yr)				
< 18	0.380 (0.153–0.944)	0.0371	0.793 (0.523-1.203)	0.2842
18-44	1.320 (1.214-1.434)	< 0.0001	1.888 (1.790-1.991)	< 0.0001
45-64	1.418 (1.321-1.521)	< 0.0001	1.693 (1.625-1.764)	< 0.0001
65-84	Reference	NA	Reference	NA
≥ 85	0.773 (0.649-0.920)	0.0037	0.749 (0.688-0.814)	< 0.0001
Race				
White	1.500 (1.338-1.682)	< 0.0001	1.830 (1.728-1.939)	< 0.0001
Black	Reference	NA	Reference	NA
Hispanic	1.193 (0.993-1.434)	0.0598	1.391 (1.272-1.521)	< 0.0001
Asian or Pacific Islander	0.720 (0.441-1.174)	0.1876	0.856 (0.679-1.078)	0.1876
Native American	1.029 (0.616-1.720)	0.9120	0.937 (0.733-1.198)	0.6120
Other	1.109 (0.959-1.282)	0.1627	1.456 (1.351-1.568)	< 0.0001
Primary payer status				
Medicare	Reference	NA	Reference	NA
Medicaid	1.327 (1.205-1.462)	< 0.0001	1.043 (0.99-1.10)	0.1148
Private	0.911 (0.850-0.977)	0.0085	0.774 (0.744-0.805)	< 0.0001
Self-Pay	1.035 (0.831-1.289)	0.7616	0.892 (0.800-0.994)	0.0382
No charge	0.853 (0.398-1.827)	0.6825	0.698 (0.485-1.005)	0.0555
Other	1.069 (0.871-1.311)	0.5255	0.974 (0.88-1.077)	0.5930
Median socioeconomic status by national quartiles				
0-25	Reference	NA	Reference	NA
25-50	1.006 (0.923-1.097)	0.8836	1.031 (0.988-1.075)	0.1595
50-75	1.026 (0.943-1.117)	0.5455	1.071 (1.025-1.118)	0.0019
75-100	0.890 (0.814-0.972)	0.0095	0.998 (0.952-1.045)	0.9323
Other	0.664 (0.505-0.873)	0.0034	0.697 (0.61-0.795)	< 0.0001
Hospital bed size				
Small	Reference	NA	Reference	NA
Medium	1.061 (0.967-1.164)	0.2109	0.956 (0.913-1.002)	0.0585
Large	0.936 (0.873-1.005)	0.0669	0.926 (0.888-0.966)	0.0004
Location/teaching status of the hospital				
Rural	Reference	NA	Reference	NA
Urban nonteaching	1.028 (0.917-1.152)	0.6376	0.994 (0.938-1.054)	0.8450
Urban teaching	1.253 (1.172-1.339)	< 0.0001	1.235 (1.168-1.306)	< 0.0001
Hospital region				
Northeast	Reference	NA	Reference	NA
Midwest or North Central	1.312 (1.199-1.437)	< 0.0001	1.223 (1.162-1.286)	< 0.0001

South	1.124 (1.031-1.225)	0.0078	1.083 (1.032-1.137)	0.0015
West	1.179 (1.065-1.306)	0.0015	1.148 (1.085-1.213)	< 0.0001
Comorbidities				
Liver disease, mild	1.401 (1.251-1.569)	< 0.0001	1.156 (1.091-1.224)	< 0.0001
Liver disease, moderate to severe	1.206 (0.867-1.677)	0.2655	0.976 (0.827-1.152)	0.7708
Peptic ulcer disease	1.532 (1.247-1.881)	< 0.0001	1.254 (1.133-1.387)	< 0.0001
Esophageal disorders	1.684 (1.582-1.792)	< 0.0001	1.528 (1.481-1.576)	< 0.0001
Gastritis	1.236 (1.063-1.436)	0.0059	1.096 (1.018-1.18)	0.0145
Diabetes mellitus with chronic complications	1.326 (1.181-1.489)	< 0.0001	1.201 (1.131-1.274)	< 0.0001
Diabetes mellitus without chronic complications	1.033 (0.946-1.128)	0.4688	1.064 (1.018-1.113)	0.0059
Hypertension	1.082 (1.018-1.151)	0.0115	1.091 (1.055-1.128)	< 0.0001
Heart Failure	0.922 (0.839-1.014)	0.0943	1.005 (0.955-1.058)	0.8505
Coronary artery disease	0.858 (0.787-0.936)	0.0005	0.901 (0.861-0.944)	< 0.0001
Cardiac dysrhythmias	0.811 (0.742-0.887	< 0.0001	0.884 (0.844-0.925)	< 0.0001
Myocardial infarction	0.703 (0.512-0.965)	0.0295	0.684 (0.587-0.797)	< 0.0001
Stroke	0.604 (0.443-0.825)	0.0015	0.564 (0.484-0.656)	< 0.0001
Iron Deficiency Anemia	1.009 (0.908-1.122)	0.8635	1.017 (0.966-1.071)	0.5143
Nutritional deficiencies	1.539 (1.344-1.762)	< 0.0001	1.282 (1.199-1.37)	< 0.0001
Lipid Metabolism disorders	1.210 (1.130-1.296)	< 0.0001	1.192 (1.15-1.237)	< 0.0001
Thyroid disorders	1.327 (1.231-1.430)	< 0.0001	1.247 (1.201-1.295)	< 0.0001
Chronic Pancreatitis	1.788 (1.415-2.259)	< 0.0001	1.356 (1.207-1.524)	< 0.0001
Renal failure, moderate	1.026 (0.919-1.145)	0.6530	1.04 (0.981-1.102)	0.1839
Renal failure, severe	1.072 (0.897-1.282)	0.4445	1.117 (1.02-1.223)	0.0172
Menopausal disorders	1.716 (1.211-2.432)	0.0024	1.433 (1.206-1.702)	< 0.0001
Osteoporosis	1.280 (1.171-1.399)	< 0.0001	1.21 (1.157-1.265)	< 0.0001
Osteoarthritis	1.287 (1.187-1.395)	< 0.0001	1.215 (1.167-1.264)	< 0.0001
Obesity	1.500 (1.377-1.635)	< 0.0001	1.228 (1.176-1.283)	< 0.0001
Weight Loss	1.253 (0.964-1.628	0.0913	1.212 (1.067-1.378)	0.0032
Protein-calorie malnutrition	1.162 (1.045-1.291)	0.0054	1.103 (1.047-1.162)	0.0002
Leukemia	0.980 (0.643-1.492)	0.9237	1.05 (0.856-1.288)	0.6351
Lymphoma	0.875 (0.610-1.255)	0.4685	1.014 (0.852-1.207)	0.8744
Metastatic cancer	0.975 (0.744-1.277)	0.8532	1.095 (0.948-1.265)	0.2168
Solid tumor without metastasis, malignant	0.917 (0.775-1.085)	0.3140	0.944 (0.863-1.034)	0.2131
Paralysis	1.391 (1.110-1.744)	0.0042	1.48 (1.32-1.659)	< 0.0001
Dementia	1.601 (1.344-1.908)	< 0.0001	2.082 (1.906-2.274)	< 0.0001
AIDS	0.866 (0.422-1.776)	0.6938	0.826 (0.58-1.178)	0.2847
Smoking	1.410 (1.325-1.502)	< 0.0001	1.231 (1.193-1.271)	< 0.0001
Alcohol	2.296 (1.922-2.743)	< 0.0001	2.109 (1.927-2.308)	< 0.0001
Opioids	2.430 (2.128-2.774)	< 0.0001	2.009 (1.882-2.145)	< 0.0001

[1]Univariate analysis is performed with logistic regression.
[2]Multivariate analysis is performed with weighted multi-level mixed effect models.
NA: No application; AIDS: Acquired immunodeficiency syndrome.

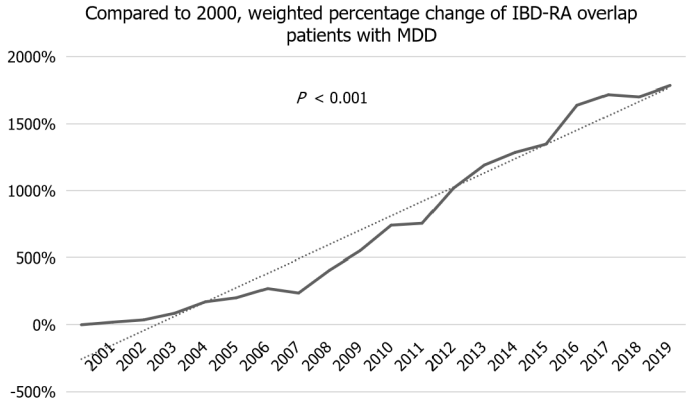

DOI: 10.12998/wjcc.v11.i4.764

Figure 2 Percentage change of inflammatory bowel disease-rheumatoid arthritis overlap patients with major depressive disorder, compared to baseline 2000, national inpatient sample year 2000 to 2019. MDD: Major depressive disorder; IBD-RA: Inflammatory bowel disease-rheumatoid arthritis.

Multimorbidity, defined as the coexistence of multiple health conditions, is a growing public health challenge[27]. EULAR considers comorbidities like cardiovascular diseases, malignancy, osteoporosis, infection, and depression in rheumatic diseases[28]. Depression screening may be a valuable tool for interventions to improve health-related quality of life in individuals with IMIDs. In our study, various comorbidities are independently linked with depression.

GI diseases are closely linked with depression, possibly due to the gut-brain axis. A literature review showed a positive correlation between the severity of reflux esophagitis with depression[29]. In our study, patients with esophageal disorders are at 1.5 times increased risk of MDDs. Kim *et al*[30] demonstrated that patients with PUD have 1.47 times higher odds of depression. Alkhayyat *et al*[31] showed that chronic pancreatitis patients are at an increased risk of depression than those without it. Our study showed a 1.3 times increase in risk with chronic pancreatitis and 1.2 times with PUD. Kim *et al*[30] mentioned the bidirectional relationship between PUD and depression, as depression causes consistent activation of the HPA axis, leading to immune dysfunction and elevating the risk of PUD. Conversely, PUD increases the risk of depression by increasing neuropeptide expression of substance P and its receptors.

Among the elderly, malnourished subjects were 31% more likely to have symptoms of depression than those with normal nutritional status[32,33]. Our results showed that nutritional deficiencies are 1.3 times higher in the depression cohort. There is growing evidence of the crucial necessity of neuron membrane cholesterol in the organization and function of the 5-HT1A serotonin receptor. Hence, low cholesterol level is associated with depression and suicidality[34]. Our study also found lipid metabolism disorders as an independent predictor of depression.

In our study, severe renal failure is an independent predictor of depression in IBD-RA subjects. The literature review showed that about one-quarter of dialysis patients suffer from a MDD. Medications reduced physical function, and dietary restrictions are the main contributing factors[35]. The prevalence of depression in chronic kidney disease (CKD) stage 5 was 39 times higher than in CKD stages 1-5[36].

Depression has also been associated with elevated pain and enhanced functional disability in patients with osteoarthritis. Depression affects the HPA axis by altering the release of hypothalamic corticotropin-releasing hormone, increasing its levels in the cerebrospinal fluid and changing the set point threshold for negative feedback, which results in hypercortisolism and thus increased bone loss[37]. Stubbs *et al*[38] meta-analysis showed that patients with depression had lower bone mass than controls [38]. Our study showed 1.2 times higher odds of having depression with both osteoporosis and osteoarthritis. Our study results agree with Stubbs *et al*[38] findings that showed a 1.17% relative risk of depression in osteoarthritis patients compared with the non-osteoarthritis group[38].

Obesity at baseline increased the risk of the onset of depression at follow-up. However, depression increased the odds of developing obesity (OR: 1.58; 95%CI: 1.33-1.87; $P < 0.001$)[39]. Our study also exhibited increased odds of depression with obesity (aOR: 1.29; 95%CI: 1.18-1.28; $P < 0.0001$). Interestingly, our study also increased the odds of depression with weight loss (aOR: 1.21; 95%CI: 1.07-1.38; $P < 0.0001$). Dietary effects on mental health can be explained by the anti-inflammatory effect (*i.e.*, omega-3 polyunsaturated fatty acids), antioxidant effect (anthocyanins, *etc.*), or functional modulation (group B vitamins, L-ornithine, tryptophan amino acids, glycine, *etc.*)[40,41]. A National Health and Nutrition Examination Survey study reported that using even a single unhealthy weight-loss strategy was significantly linked with depression[42]. In our study, the odds of depression are 28% higher in patients with nutritional deficiencies.

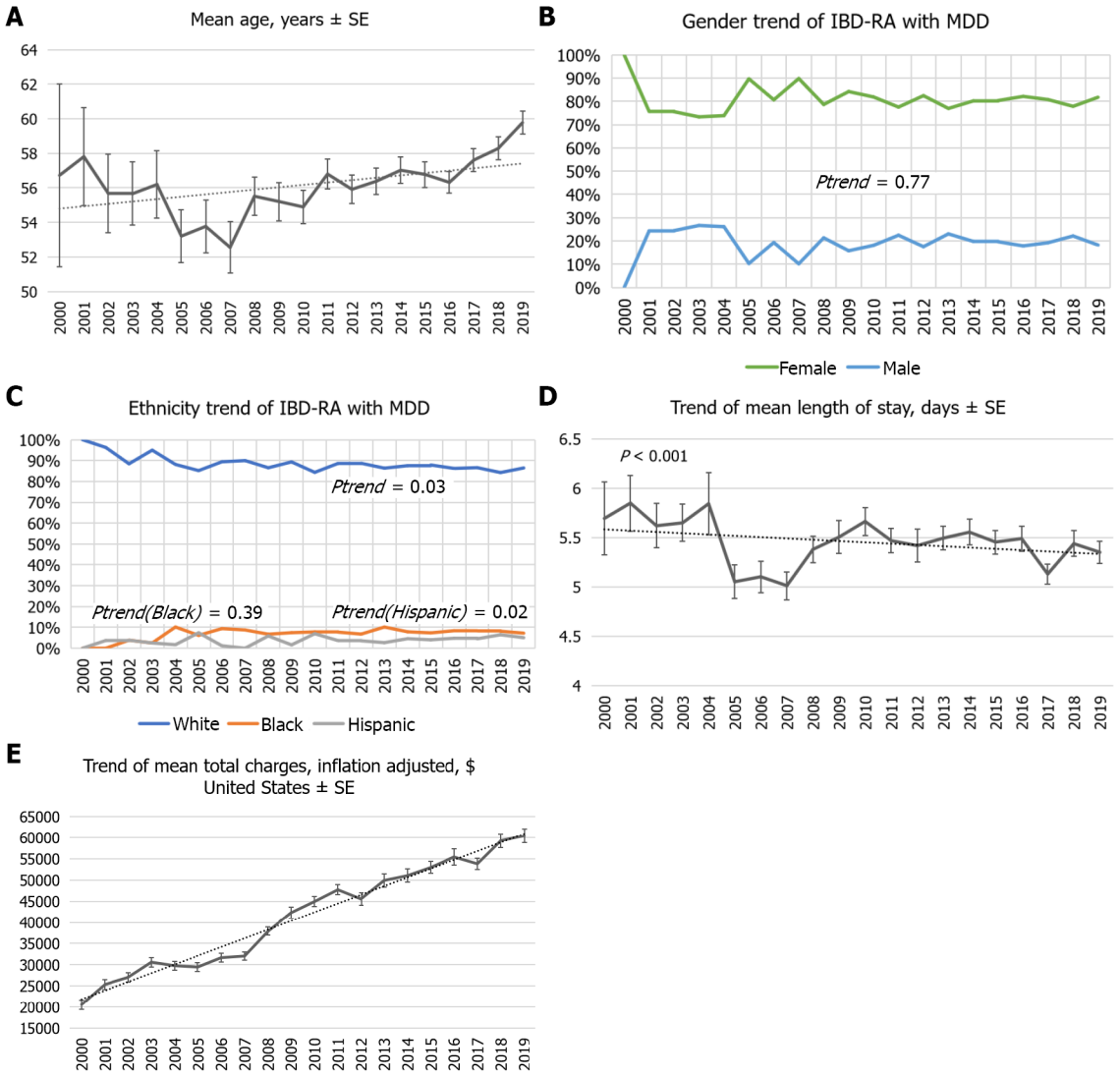

DOI: 10.12998/wjcc.v11.i4.764

Figure 3 Inflammatory bowel disease-rheumatoid arthritis overlap patients identified with depressive disorders, national inpatient sample year 2000 to 2019. A: Trend of mean age (years) inflammatory bowel disease-rheumatoid arthritis (IBD-RA) overlap patients identified with depressive disorders; B: Trend of male and female (percentages) of IBD-RA overlap patients identified with depressive disorders; C: Trend of ethnicity (percentages) of IBD-RA overlap patients identified with depressive disorders; D: Mean hospital stay (days) of IBD-RA overlap patients with depressive disorders; E: Mean total cost of care (the United States$) of IBD-RA overlap patients with depressive disorders. IBD-RA: Inflammatory bowel disease-rheumatoid arthritis.

Depression can be both a risk factor and a prodrome for dementia. Amongst all the proposed mechanisms, trophic, inflammatory, and cerebrovascular factors may contribute, along-with monoamine deficiency and severity of plaques and tangle pathology[43]. In a meta-analysis that included 5897 subjects with dementia from 20 studies, the prevalence rates of depression in mild, moderate, and severe dementia were 38%, 41%, and 37%, respectively[44]. In our study, patients with dementia have two times increased likelihood of depression.

Nearly one-third of patients with MDD also have substance use disorders. It yields a higher risk of suicide and greater social and personal impairment[45]. Alcohol use disorder is notable in our society (lifetime prevalence of 29.1%) and is associated with MDD[46]. We also found alcohol an independent predictor of depression in patients with RA-IBD. Other Substance abuses include nicotine; its withdrawal is known to cause a marked increase in negative affect among smokers in the general population[47]. A group of cross-sectional studies showed that current smokers were more depressed than never-smokers and former smokers[48]. In our study, smoking is independently associated with 1.2 times higher odds of depression. Similarly, the literature review showed that opioids were associated with higher odds of new-onset major depressive symptoms without baseline symptoms of MDD[49]. These findings correspond with our results that showed opioid use doubled the risk of depression in the IBD-RA group.

Another vital study finding includes thyroid disorders as an independent predictor of depression. A literature search showed depression is associated with a functional interruption of the hypothalamus,

causing dysregulation of the hippocampal inhibitory glucocorticoid feedback pathway to the hypothalamus. This results in increased cortisol levels and impaired dexamethasone suppression. A similar situation exists with the thyroid axis. An increased T4 and blunted thyrotropin response to exogenous thyrotropin-releasing hormone (TRH) in depression. This is due to the glucocorticoid activation of the TRH neuron that increases TRH secretion and down-regulates the TRH receptor on the thyrotrope[50,51]. In our study, patients with lipid disorders have an increased likelihood of depression. It correlates with a meta-analysis Wei *et al*[52] that showed that hyperlipidemia patients have 1.7 times more odds of MDD than the general population[52].

Strengths and limitations

To our best knowledge, this is the first large study performed in the United States, analyzing twenty years of inpatient sample data (n = 26155) of patients with depression affected by RA and IBD. This study's biggest strength is identifying the prevalence of depression among patients with dual autoimmune diseases and a motivation to incorporate such values of depression screening in outpatient clinics. Our analysis also recommends the possibility of a Rheumatology-Gastroenterology Comorbidity clinic initiative, which could identify various comorbidities like depression and substance use disorder among IMID patients. This is an area that requires more attention. Most rheumatologists and gastroenterologists do not routinely screen their RA patients for depression which was evident during the verbal surveys taken at the various conferences. It could be related to time limitations, inadequate psychiatry referral services, lack of training, or even lack of confidence in managing mental health problems. A simple Patient Health Questionnaire (PHQ-2) or PHQ-9 questionnaire can be incorporated into the clinic outflow, especially at the onset of the diagnosis. Such efforts are pivotal in identifying depression in our patients, ensuring patient-mental health support system interrelation, and hence normalizing the discussion around their mental health. This study's biggest strength is identifying the prevalence of depression among patients with dual autoimmune diseases and a motivation to incorporate such values in our outpatient clinics. This is pivotal for healthcare delivery systems and economies in the global context of treating chronic diseases like RA and IBD, especially in the era of the coronavirus disease 2019 pandemic as we understand that the standard care for these conditions, particularly immunomodulators, is extremely costly.

This study has several limitations using the NIS dataset, including the inability to access laboratory values, treatment options, and testing conditions, including colonoscopy findings and severity of IBD based on histology. We intended to investigate the prevalence of IMIDs and depression; it's challenging to know the clinical correlates of depression regarding RA/IBD disease activity and disability. This study is performed on the inpatient population. However, IBD/RA and MDD are outpatient diagnoses except for IBD flare-ups. Individuals with fibromyalgia, connective tissue diseases (Sjogren, scleroderma, dermatomyositis, polymyositis), vasculitis, gout, infective arthritis, polymyalgia rheumatica, or other IBDs were excluded or not chosen as comorbidity which could also be a reason for depressive symptoms. However, these ailments were not selected as they have been known from previous studies, and other co-morbidities mentioned in our research could be highlighted. NIS entry is equivalent to one hospitalization. If a patient is admitted more than once, one patient may contribute multiple entries. Finally, inherent database limitations include a lack of disease process-specific variables and coding errors without formal validation.

CONCLUSION

This study offers the opportunity to increase our knowledge of the various comorbidities by investigating depression and its clinical correlates as part of the routine clinical monitoring in the outpatient clinic setting and, hence, a multimorbidity approach that is more patient-focused. There is an inevitable rise in the prevalence of depression in younger patients with IBD-RA combined autoimmune disease compared to their counterparts. These patients are also at higher risk of the increased cost of care, disability, and poor treatment adherence. It is crucial to educate the involved physicians to identify the early signs and symptoms of depression in patients with IBD or RA or IBD-RA combined and treat them or have them treated to have a better overall prognosis. As physicians, we can play an important role as part of social determinants of health by giving good quality of care. Timely recognition of depression in these patients is critical to preventing disability.

ARTICLE HIGHLIGHTS

Research background

Inflammatory bowel disease (IBD) and rheumatoid arthritis (RA), are found to have a substantial societal burden, increased healthcare costs, and progressive disability. Studies suggest that patients with *vs* without depression have a more significant disability, a lower likelihood of remission, and reduced

adherence to therapy.

Research motivation

The role of the Brain-Gut axis and Brain-Joint axis in the development of depression has been discussed, but there is not enough literature demonstrating the combined Brain-Gut-Joint axis.

Research objectives

Our primary aim is to identify a pooled prevalence level and temporal trends of depression in hospitalized IBD-RA patients. We aimed to investigate clinical factors associated with depression in these patients.

Research methods

All adult hospitalized patients from January 2000 to December 2019 in the nationwide inpatient sample were captured. The study population included all patients with a primary or secondary IBD-RA overlap disease using corresponding international classification of diseases (ICD)-9 and ICD-10 codes.

Research results

Other factors associated with higher major depressive disorder included younger age, female gender, white race, alcohol, opioids, esophageal disorders, peptic ulcer disease, chronic pancreatitis, paralysis, dementia, menopausal disorders, obesity, nutritional deficiencies, diabetes mellitus with chronic complications, and osteoarthritis.

Research conclusions

There is an inevitable rise in the prevalence of depression in younger patients with IBD-RA combined autoimmune diseases. As physicians, we can play an important role in social determinants of health by giving good quality care. Timely recognition of depression in these patients is critical to preventing disability.

Research perspectives

Our study discusses the clinical data on this combined axis and emphasizes potentially valuable strategies for managing these patients. This study will open the door for further research and educate the involved physicians to identify the early signs and symptoms of depression in patients with IBD or RA or IBD-RA combined and treat them or have them treated to have a better overall prognosis.

FOOTNOTES

Author contributions: Haider MB, Basida B and Kaur J contributed equally to this work; Haider MB and Kaur J designed the research study; Kaur J and Basida B performed the research; Haider MB analyzed the data; Haider MB, Basida B and Kaur J wrote the manuscript; All authors have read and approve the final manuscript.

Institutional review board statement: Data from this study used de-identified data from the National Inpatient Sample Database (NIS) 2000-2019. A publicly available all-payer inpatient care database in the United States. Institutional Review Board Approval Form or Document is not required.

Informed consent statement: Data from this study used de-identified data from the National Inpatient Sample Database. A publicly available all-payer inpatient care database in the United States. Informed patient consent is not required.

Conflict-of-interest statement: All the authors report no relevant conflicts of interest for this article.

Data sharing statement: Data that support the findings of this study are publicly available at https://www.hcup-us.ahrq.gov/db/nation/nis/nisdbdocumentation.jsp.

Country/Territory of origin: United States

ORCID number: Maryam Bilal Haider 0000-0002-4157-8576.

S-Editor: Fan JR

L-Editor: A
P-Editor: Fan JR

REFERENCES

1 **Enns MW**, Bernstein CN, Kroeker K, Graff L, Walker JR, Lix LM, Hitchon CA, El-Gabalawy R, Fisk JD, Marrie RA; CIHR Team in Defining the Burden and Managing the Effects of Psychiatric Comorbidity in Chronic Immunoinflammatory Disease. The association of fatigue, pain, depression and anxiety with work and activity impairment in immune mediated inflammatory diseases. *PLoS One* 2018; **13**: e0198975 [PMID: 29879231 DOI: 10.1371/journal.pone.0198975]
2 **Englbrecht M**, Alten R, Aringer M, Baerwald CG, Burkhardt H, Eby N, Flacke JP, Fliedner G, Henkemeier U, Hofmann MW, Kleinert S, Kneitz C, Krüger K, Pohl C, Schett G, Schmalzing M, Tausche AK, Tony HP, Wendler J. New insights into the prevalence of depressive symptoms and depression in rheumatoid arthritis - Implications from the prospective multicenter VADERA II study. *PLoS One* 2019; **14**: e0217412 [PMID: 31136632 DOI: 10.1371/journal.pone.0217412]
3 **Lwin MN**, Serhal L, Holroyd C, Edwards CJ. Rheumatoid Arthritis: The Impact of Mental Health on Disease: A Narrative Review. *Rheumatol Ther* 2020; **7**: 457-471 [PMID: 32535834 DOI: 10.1007/s40744-020-00217-4]
4 **Ordás I**, Eckmann L, Talamini M, Baumgart DC, Sandborn WJ. Ulcerative colitis. *Lancet* 2012; **380**: 1606-1619 [PMID: 22914296 DOI: 10.1016/S0140-6736(12)60150-0]
5 **Almutairi K**, Nossent J, Preen D, Keen H, Inderjeeth C. The global prevalence of rheumatoid arthritis: a meta-analysis based on a systematic review. *Rheumatol Int* 2021; **41**: 863-877 [PMID: 33175207 DOI: 10.1007/s00296-020-04731-0]
6 **Pryce CR**, Fontana A. Depression in Autoimmune Diseases. *Curr Top Behav Neurosci* 2017; **31**: 139-154 [PMID: 27221625 DOI: 10.1007/7854_2016_7]
7 **GBD 2017 Inflammatory Bowel Disease Collaborators**. The global, regional, and national burden of inflammatory bowel disease in 195 countries and territories, 1990-2017: a systematic analysis for the Global Burden of Disease Study 2017. *Lancet Gastroenterol Hepatol* 2020; **5**: 17-30 [PMID: 31648971 DOI: 10.1016/S2468-1253(19)30333-4]
8 **Isnardi CA**, Capelusnik D, Schneeberger EE, Bazzarelli M, Berloco L, Blanco E, Benítez CA, Luján Benavidez F, Scarafía S, Lázaro MA, Pérez Alamino R, Colombres F, Kohan MP, Sosa J, Gonzalez Lucero L, Barbaglia AL, Maldonado Ficco H, Citera G. Depression Is a Major Determinant of Functional Capacity in Rheumatoid Arthritis. *J Clin Rheumatol* 2021; **27**: S180-S185 [PMID: 32732521 DOI: 10.1097/RHU.0000000000001506]
9 **Barberio B**, Zamani M, Black CJ, Savarino EV, Ford AC. Prevalence of symptoms of anxiety and depression in patients with inflammatory bowel disease: a systematic review and meta-analysis. *Lancet Gastroenterol Hepatol* 2021; **6**: 359-370 [PMID: 33721557 DOI: 10.1016/S2468-1253(21)00014-5]
10 **Walker JR**, Ediger JP, Graff LA, Greenfeld JM, Clara I, Lix L, Rawsthorne P, Miller N, Rogala L, McPhail CM, Bernstein CN. The Manitoba IBD cohort study: a population-based study of the prevalence of lifetime and 12-month anxiety and mood disorders. *Am J Gastroenterol* 2008; **103**: 1989-1997 [PMID: 18796096 DOI: 10.1111/j.1572-0241.2008.01980.x]
11 **Peppas S**, Pansieri C, Piovani D, Danese S, Peyrin-Biroulet L, Tsantes AG, Brunetta E, Tsantes AE, Bonovas S. The Brain-Gut Axis: Psychological Functioning and Inflammatory Bowel Diseases. *J Clin Med* 2021; **10** [PMID: 33498197 DOI: 10.3390/jcm10030377]
12 **Süß P**, Rothe T, Hoffmann A, Schlachetzki JCM, Winkler J. The Joint-Brain Axis: Insights From Rheumatoid Arthritis on the Crosstalk Between Chronic Peripheral Inflammation and the Brain. *Front Immunol* 2020; **11**: 612104 [PMID: 33362800 DOI: 10.3389/fimmu.2020.612104]
13 **Introduction to the NIS**. Healthcare Cost and Utilization Project (HCUP). February 2018. Agency for Healthcare Research and Quality, Rockville, MD. [cited 10 August 2022]. Available from: www.hcup-us.ahrq.gov/db/nation/nis/NIS_Introduction_2015.jsp
14 **HCUP National Inpatient Sample (NIS)**. Healthcare Cost and Utilization Project (HCUP). 2012. Agency for Healthcare Research and Quality, Rockville, MD. [cited 3 February 2022]. Available from: www.hcup-us.ahrq.gov/nisoverview.jsp
15 **HCUP NIS Trend Weights**. Healthcare Cost and Utilization Project (HCUP). October 2021. Agency for Healthcare Research and Quality, Rockville, MD. [cited 3 February 2022]. Available from: www.hcup-us.ahrq.gov/db/nation/nis/trendwghts.jsp.
16 **DUA Training - Accessible Version**. Healthcare Cost and Utilization Project (HCUP). April 2020. Agency for Healthcare Research and Quality, Rockville, MD. [cited 3 February 2022]. Available from: www.hcup-us.ahrq.gov/DUA/dua_508/DUA508version.jsp
17 **HCUP Clinical Classifications Software Refined (CCSR) for ICD-10-CM diagnoses**, v2021. 2. Healthcare Cost and Utilization Project (HCUP). Agency for Healthcare Research and Quality, Rockville, MD. [cited 4 April 2022]. Available from: www.hcup-us.ahrq.gov/toolssoftware/ccsr/dxccsr.jsp
18 **HCUP Clinical Classifications Software Refined (CCSR) for ICD-10-PCS procedures**, v2021. 1. Healthcare Cost and Utilization Project (HCUP). Agency for Healthcare Research and Quality, Rockville, MD. [cited 15 January 2022]. Available from: www.hcup-us.ahrq.gov/toolssoftware/ccsr/prccsr.jsp
19 **US Bureau of Labor Statistics**. Consumer price index for all urban consumers: Hospital services. [cited 15 January 2022]. Available from: https://data.bls.gov/timeseries/CUUR0000SA0
20 **Matcham F**, Rayner L, Steer S, Hotopf M. The prevalence of depression in rheumatoid arthritis: a systematic review and meta-analysis. *Rheumatology (Oxford)* 2013; **52**: 2136-2148 [PMID: 24003249 DOI: 10.1093/rheumatology/ket169]
21 **Neuendorf R**, Harding A, Stello N, Hanes D, Wahbeh H. Depression and anxiety in patients with Inflammatory Bowel Disease: A systematic review. *J Psychosom Res* 2016; **87**: 70-80 [PMID: 27411754 DOI: 10.1016/j.jpsychores.2016.06.001]
22 **van Hoogmoed D**, Fransen J, Bleijenberg G, van Riel P. Physical and psychosocial correlates of severe fatigue in rheumatoid arthritis. *Rheumatology (Oxford)* 2010; **49**: 1294-1302 [PMID: 20353956 DOI: 10.1093/rheumatology/keq043]

23 **Anderson KO**, Bradley LA, McDaniel LK, Young LD, Turner RA, Agudelo CA, Keefe FJ, Pisko EJ, Snyder RM, Semble EL. The assessment of pain in rheumatoid arthritis. Validity of a behavioral observation method. *Arthritis Rheum* 1987; **30**: 36-43 [PMID: 3814196 DOI: 10.1002/art.1780300105]

24 **Li N**, Chan E, Peterson S. The economic burden of depression among adults with rheumatoid arthritis in the United States. *J Med Econ* 2019; **22**: 372-378 [PMID: 30663460 DOI: 10.1080/13696998.2019.1572015]

25 **Marrie RA**, Hitchon CA, Walld R, Patten SB, Bolton JM, Sareen J, Walker JR, Singer A, Lix LM, El-Gabalawy R, Katz A, Fisk JD, Bernstein CN; Canadian Institutes of Health Research Team in Defining the Burden and Managing the Effects of Psychiatric Comorbidity in Chronic Immunoinflammatory Disease. Increased Burden of Psychiatric Disorders in Rheumatoid Arthritis. *Arthritis Care Res (Hoboken)* 2018; **70**: 970-978 [PMID: 29438604 DOI: 10.1002/acr.23539]

26 **Pezzato S**, Bonetto C, Caimmi C, Tomassi S, Montanari I, Gnatta MG, Fracassi E, Cristofalo D, Rossini M, Carletto A, Tosato S. Depression is associated with increased disease activity and higher disability in a large Italian cohort of patients with rheumatoid arthritis. *Adv Rheumatol* 2021; **61**: 57 [PMID: 34526144 DOI: 10.1186/s42358-021-00214-3]

27 **Johnston MC**, Crilly M, Black C, Prescott GJ, Mercer SW. Defining and measuring multimorbidity: a systematic review of systematic reviews. *Eur J Public Health* 2019; **29**: 182-189 [PMID: 29878097 DOI: 10.1093/eurpub/cky098]

28 **Baillet A**, Gossec L, Carmona L, Wit Md, van Eijk-Hustings Y, Bertheussen H, Alison K, Toft M, Kouloumas M, Ferreira RJ, Oliver S, Rubbert-Roth A, van Assen S, Dixon WG, Finckh A, Zink A, Kremer J, Kvien TK, Nurmohamed M, van der Heijde D, Dougados M. Points to consider for reporting, screening for and preventing selected comorbidities in chronic inflammatory rheumatic diseases in daily practice: a EULAR initiative. *Ann Rheum Dis* 2016; **75**: 965-973 [PMID: 26984008 DOI: 10.1136/annrheumdis-2016-209233]

29 **Wang R**, Wang J, Hu S. Study on the relationship of depression, anxiety, lifestyle and eating habits with the severity of reflux esophagitis. *BMC Gastroenterol* 2021; **21**: 127 [PMID: 33743601 DOI: 10.1186/s12876-021-01717-5]

30 **Kim SY**, Min C, Oh DJ, Choi HG. Reciprocal association between depression and peptic ulcers: Two longitudinal follow-up studies using a national sample cohort. *Sci Rep* 2020; **10**: 1749 [PMID: 32020020 DOI: 10.1038/s41598-020-58783-0]

31 **Alkhayyat M**, Abou Saleh M, Coronado W, Abureesh M, Al-Otoom O, Qapaja T, Mansoor E, Simons-Linares CR, Stevens T, Chahal P. Increasing Prevalence of Anxiety and Depression Disorders After Diagnosis of Chronic Pancreatitis: A 5-Year Population-Based Study. *Pancreas* 2021; **50**: 153-159 [PMID: 33565791 DOI: 10.1097/MPA.0000000000001746]

32 **Wei J**, Fan L, Zhang Y, Li S, Partridge J, Claytor L, Sulo S. Association Between Malnutrition and Depression Among Community-Dwelling Older Chinese Adults. *Asia Pac J Public Health* 2018; **30**: 107-117 [PMID: 29514465 DOI: 10.1177/1010539518760632]

33 **García-Montero C**, Ortega MA, Alvarez-Mon MA, Fraile-Martinez O, Romero-Bazán A, Lahera G, Montes-Rodríguez JM, Molina-Ruiz RM, Mora F, Rodriguez-Jimenez R, Quintero J, Álvarez-Mon M. The Problem of Malnutrition Associated with Major Depressive Disorder from a Sex-Gender Perspective. *Nutrients* 2022; **14** [PMID: 35268082 DOI: 10.3390/nu14051107]

34 **Segoviano-Mendoza M**, Cárdenas-de la Cruz M, Salas-Pacheco J, Vázquez-Alaniz F, La Llave-León O, Castellanos-Juárez F, Méndez-Hernández J, Barraza-Salas M, Miranda-Morales E, Arias-Carrión O, Méndez-Hernández E. Hypocholesterolemia is an independent risk factor for depression disorder and suicide attempt in Northern Mexican population. *BMC Psychiatry* 2018; **18**: 7 [PMID: 29334911 DOI: 10.1186/s12888-018-1596-z]

35 **Natale P**, Palmer SC, Ruospo M, Saglimbene VM, Rabindranath KS, Strippoli GF. Psychosocial interventions for preventing and treating depression in dialysis patients. *Cochrane Database Syst Rev* 2019; **12**: CD004542 [PMID: 31789430 DOI: 10.1002/14651858.CD004542.pub3]

36 **Palmer S**, Vecchio M, Craig JC, Tonelli M, Johnson DW, Nicolucci A, Pellegrini F, Saglimbene V, Logroscino G, Fishbane S, Strippoli GF. Prevalence of depression in chronic kidney disease: systematic review and meta-analysis of observational studies. *Kidney Int* 2013; **84**: 179-191 [PMID: 23486521 DOI: 10.1038/ki.2013.77]

37 **Cizza G**, Primma S, Coyle M, Gourgiotis L, Csako G. Depression and osteoporosis: a research synthesis with meta-analysis. *Horm Metab Res* 2010; **42**: 467-482 [PMID: 20455194 DOI: 10.1055/s-0030-1252020]

38 **Stubbs B**, Aluko Y, Myint PK, Smith TO. Prevalence of depressive symptoms and anxiety in osteoarthritis: a systematic review and meta-analysis. *Age Ageing* 2016; **45**: 228-235 [PMID: 26795974 DOI: 10.1093/ageing/afw001]

39 **Luppino FS**, de Wit LM, Bouvy PF, Stijnen T, Cuijpers P, Penninx BW, Zitman FG. Overweight, obesity, and depression: a systematic review and meta-analysis of longitudinal studies. *Arch Gen Psychiatry* 2010; **67**: 220-229 [PMID: 20194822 DOI: 10.1001/archgenpsychiatry.2010.2]

40 **Grosso G**. Nutritional Psychiatry: How Diet Affects Brain through Gut Microbiota. *Nutrients* 2021; **13** [PMID: 33919680 DOI: 10.3390/nu13041282]

41 **Chaitoff A**, Swetlik C, Ituarte C, Pfoh E, Lee LL, Heinberg LJ, Rothberg MB. Associations Between Unhealthy Weight-Loss Strategies and Depressive Symptoms. *Am J Prev Med* 2019; **56**: 241-250 [PMID: 30661572 DOI: 10.1016/j.amepre.2018.09.017]

42 **Enache D**, Winblad B, Aarsland D. Depression in dementia: epidemiology, mechanisms, and treatment. *Curr Opin Psychiatry* 2011; **24**: 461-472 [PMID: 21926624 DOI: 10.1097/YCO.0b013e32834bb9d4]

43 **Leung DKY**, Chan WC, Spector A, Wong GHY. Prevalence of depression, anxiety, and apathy symptoms across dementia stages: A systematic review and meta-analysis. *Int J Geriatr Psychiatry* 2021; **36**: 1330-1344 [PMID: 33905138 DOI: 10.1002/gps.5556]

44 **Davis L**, Uezato A, Newell JM, Frazier E. Major depression and comorbid substance use disorders. *Curr Opin Psychiatry* 2008; **21**: 14-18 [PMID: 18281835 DOI: 10.1097/YCO.0b013e3282f32408]

45 **Grant BF**, Goldstein RB, Saha TD, Chou SP, Jung J, Zhang H, Pickering RP, Ruan WJ, Smith SM, Huang B, Hasin DS. Epidemiology of DSM-5 Alcohol Use Disorder: Results From the National Epidemiologic Survey on Alcohol and Related Conditions III. *JAMA Psychiatry* 2015; **72**: 757-766 [PMID: 26039070 DOI: 10.1001/jamapsychiatry.2015.0584]

46 **Mathew AR**, Hogarth L, Leventhal AM, Cook JW, Hitsman B. Cigarette smoking and depression comorbidity: systematic review and proposed theoretical model. *Addiction* 2017; **112**: 401-412 [PMID: 27628300 DOI: 10.1111/add.13604]

47 **Luger TM**, Suls J, Vander Weg MW. How robust is the association between smoking and depression in adults? *Addict*

Behav 2014; **39**: 1418-1429 [PMID: 24935795 DOI: 10.1016/j.addbeh.2014.05.011]

48 **Li X**, Fu Q, Scherrer JF, Humphrey D, Leigh I. A temporal relationship between nonmedical opioid Use and major depression in the U.S.: A Prospective study from the National Epidemiological Survey on Alcohol and Related Conditions. *J Affect Disord* 2020; **273**: 298-303 [PMID: 32421616 DOI: 10.1016/j.jad.2020.04.047]

49 **Jackson IM**. The thyroid axis and depression. *Thyroid* 1998; **8**: 951-956 [PMID: 9827665 DOI: 10.1089/thy.1998.8.951]

50 **Williams MD**, Harris R, Dayan CM, Evans J, Gallacher J, Ben-Shlomo Y. Thyroid function and the natural history of depression: findings from the Caerphilly Prospective Study (CaPS) and a meta-analysis. *Clin Endocrinol (Oxf)* 2009; **70**: 484-492 [PMID: 18681859 DOI: 10.1111/j.1365-2265.2008.03352.x]

51 **Chien IC**, Lin CH, Chou YJ, Chou P. Increased risk of hyperlipidemia in patients with major depressive disorder: a population-based study. *J Psychosom Res* 2013; **75**: 270-274 [PMID: 23972417 DOI: 10.1016/j.jpsychores.2013.06.003]

52 **Wei YG**, Cai DB, Liu J, Liu RX, Wang SB, Tang YQ, Zheng W, Wang F. Cholesterol and triglyceride levels in first-episode patients with major depressive disorder: A meta-analysis of case-control studies. *J Affect Disord* 2020; **266**: 465-472 [PMID: 32056914 DOI: 10.1016/j.jad.2020.01.114]

World Journal of Clinical Cases

Submit a Manuscript: https://www.f6publishing.com

World J Clin Cases 2023 February 6; 11(4): 780-787

DOI: 10.12998/wjcc.v11.i4.780

ISSN 2307-8960 (online)

ORIGINAL ARTICLE

Retrospective Study

Selective laser trabeculoplasty as adjunctive treatment for open-angle glaucoma *vs* following incisional glaucoma surgery in Chinese eyes

Jing Zhu, Juan Guo

Specialty type: Medicine, research and experimental

Provenance and peer review: Unsolicited article; Externally peer reviewed.

Peer-review model: Single blind

Peer-review report's scientific quality classification

Grade A (Excellent): 0
Grade B (Very good): 0
Grade C (Good): C, C
Grade D (Fair): 0
Grade E (Poor): 0

P-Reviewer: Bravetti GE, Switzerland; Liu Q, China

Received: October 15, 2022
Peer-review started: October 15, 2022
First decision: November 16, 2022
Revised: November 30, 2022
Accepted: January 9, 2023
Article in press: January 9, 2023
Published online: February 6, 2023

Jing Zhu, Juan Guo, Department of Ophthalmology, The Third People's Hospital of Chengdu, Affiliated Hospital of Southwest Jiao Tong University, Affiliated Chengdu Second Clinical College of Chongqing Medical University, Chengdu 610031, Sichuan Province, China

Corresponding author: Juan Guo, MD, Chief Physician, Doctor, Department of Ophthalmology, The Third People's Hospital of Chengdu, Affiliated Hospital of Southwest Jiao Tong University, Affiliated Chengdu Second Clinical College of Chongqing Medical University, NO. 82, Qing Long Street, Chengdu 610031, Sichuan Province, China. guojuan869@163.com

Abstract

BACKGROUND

Selective laser trabeculoplasty (SLT) is a relatively safe and effective therapy in lowering intraocular pressures (IOP) for glaucoma.

AIM

To study the long-term effects of SLT on IOP and number of glaucoma medications used in Chinese eyes.

METHODS

This is a retrospective study in which 75 eyes of 70 patients with open-angle glaucoma (OAG, n =36) and eyes with prior glaucoma surgery (PGS, n =39) were included. Changes in mean IOP and number of glaucoma medications used evaluated at 1 d, 1 wk, 1 mo, 3 mo, 6 mo, 12 mo, and 36 mo after laser treatment.

RESULTS

All patients (33 male, 37 female) were Chinese. The mean age was 44.34 ± 16.14 years. Mean pre-SLT IOP was 22.75 ± 2.08 mmHg in OAG and 22.52 ± 2.62 mmHg in PGS. Mean IOP was significantly reduced 1 d, 1 wk, 1 mo and 3 mo after laser treatment (P < 0.05, respectively). Whereas, there were no significant differences between baseline and SLT treated groups at the 6th month both in OAG (P = 0.347, P > 0.05) and in PGS (P = 0.309, P > 0.05). Six months after SLT treatment, some patients received retreatment of SLT or were given more topical IOP-lowering medication to control the IOP. By the end of our study, the average IOP decreased to 20.73 ± 1.82 mmHg in OAG and 20.49 ± 1.53 mmHg in PGS groups. The number of glaucoma medications used was significantly reduced until the end of 3 years compared to baseline.

CONCLUSION
SLT could reduce IOP as adjunctive treatment both in OAG and PGS groups. SLT significantly reduced the number of glaucoma medications used 3-years following treatment in glaucoma patients.

Key Words: Selective laser trabeculoplasty; Open-angle glaucoma; Intraocular pressure; Prior glaucoma surgery; Adjunctive treatment

Core Tip: Selective laser trabeculoplasty (SLT) could reduce intraocular pressure as adjunctive treatment both in open-angle glaucoma and prior glaucoma surgery groups of patients. SLT significantly reduced the number of glaucoma medications used 3-years following treatment in glaucoma patients.

Citation: Zhu J, Guo J. Selective laser trabeculoplasty as adjunctive treatment for open-angle glaucoma *vs* following incisional glaucoma surgery in Chinese eyes. *World J Clin Cases* 2023; 11(4): 780-787
URL: https://www.wjgnet.com/2307-8960/full/v11/i4/780.htm
DOI: https://dx.doi.org/10.12998/wjcc.v11.i4.780

INTRODUCTION

Selective laser trabeculoplasty (SLT) is a relatively safe and effective therapy in lowering intraocular pressures (IOP) for glaucoma which was first described in 1995 by Latina and Park[1]. This is an Nd: YAG laser improves aqueous outflow by selectively targeting the pigmented trabecular meshwork (TM) cells and presumably does not produce any damage to the microstructure of the TM[2].

SLT could be offered as initial treatment at decreasing IOP for open-angle glaucoma (OAG) and ocular hypertension. The Laser in Glaucoma and ocular Hyper Tension (LiGHT) study demonstrated that SLT could be offered as a first-line treatment of decreasing IOP without the adverse effects and costs of long-term medication use[3]. However, in the LiGHT study, nearly 15% of patients treated with SLT required additional IOP lowering interventions within 1 year, and some patients require retreatment to maintain IOP lowering[3]. SLT treatment can be particularly helpful for patients with poor compliance and drug intolerance[3]. A randomized clinical trial reported that there was no statistically significant difference between the SLT treated group and the drug therapy group after 1 year[4]. Ang *et al*[5] demonstrated that the rate of successful IOP reduction was higher in the medication group compared with SLT group at 24 mo. However, SLT did not cause any changes affecting ocular blood flow as does tropic intraocular pressure drugs[3]. It has been reported that repeated treatment of SLT safely provides significant IOP reductions in OAG through nearly 8 years of follow-up[6].

SLT could be used to reduce the IOP of patients who failed to achieve target IOP after receiving maximally tolerated medical therapy (MTMT). Previous studies have demonstrated significant reductions in mean IOP and the number of glaucoma medications used in patients who received SLT as a secondary treatment after receiving MTM[7]. A 5-year study showed that although the long-term decrease of IOP after SLT treatment may not be obvious, the numbers of drug use were reduced[8].

SLT could reduce the uncontrolled intraocular pressure after glaucoma surgery. There are many anti-glaucoma surgeries including trabeculectomy, Ahmed glaucoma drainage valve, trabeculectomy combined with cataract extraction and other surgical methods[9]. In patients with prior glaucoma surgery (PGS), the IOP rises again due to glaucoma filtering bleb scar, inflammatory reaction, and other reasons. A prospective study reported that the IOP of 18 patients with uncontrolled IOP after trabeculectomy decreased by 24% treated with SLT for 9 mo[10]. Previous studies have also demonstrated that two groups of patients with PGS (n =53) and without operation history (n =53), the IOP reduction rates were 7.3% and 10.8% respectively after SLT treatment at 6 mo of follow-up (P = 0.42, P > 0.05)[11].

Therefore, our aim was to determine the efficacy of SLT as adjunctive treatment in patients with previous incisional glaucoma surgery whose IOP remains or becomes uncontrolled, and the number of medications used up to 3 years.

MATERIALS AND METHODS

Outpatients who underwent SLT were reviewed retrospectively at the Department of Ophthalmology, Third People's Hospital of Chengdu, Affiliated Hospital of Southwest Jiao Tong University from

September 2016 to January 2020. This is a single-center study. During this research, the ethical use of human subjects was approved by the Ethics and Research Committee of Chengdu Third People's hospital (Approval No. [2022]-S-5). All the patients signed written informed consent.

In our study, 75 consecutive eyes of 70 patients (33 male, 37 female) with OAG (n = 36), and PGS (n = 39) were enrolled. The information of patients is shown in Table 1.

Inclusion criteria: Age ≥ 18 years, an increased IOP (> 21 mmHg), open atrial angle and scleral process can be seen by gonioscopy, OAG diagnostic criteria are met. OAG diagnostic criteria: Glaucomatous optic nerve damage (cup-to-disc ratio, C/D > 0.5, or difference in the C/D > 0.2), visual field defect, mean defect of visual field < -1.00 DB[12]. Inclusion criteria of PGS group: Those diagnosed as OAG, who have undergone trabeculectomy, drainage nail implantation, Ahmed glaucoma valve implantation or trabeculectomy combined with cataract extraction (Table 2); These patients have been treated with MTMT, but fail to reach the target IOP[11]. Exclusion criteria consisted of patients who were, unable to have SLT successfully performed, history of uveitis, or lost to follow up before 1 mo. Also, patients with other prior major incisional eye surgeries were excluded apart from cataract surgery alone.

All patients received SLT more than 1 year after anti-glaucoma surgery. These patients agreed to SLT treatment and signed the consent form for laser surgery.

Eyes were pretreated with topical anesthesia of 0.4% obucaine hydrochloride (Benoxil). And Latina anterior chamber gonioscope was placed after anesthesia. SLT was performed with a q-switched, frequency-doubled 532 nm Nd: YAG laser (selecta duet, Lumenis, Israel) which has a spot size of 400 μm and pulse duration of 3ns. Nonoverlapping 100 ± 10 Laser spots were applied to 360 degrees of the TM. The initial energy level was set at 0.8 mJ. The energy was increased or decreased until cavitation bubbles within the TM were just noted. In this study, the therapeutic energy was 0.6-1.2 mJ. Pranoprofen eye drops were used as postoperative medications.

Detailed ophthalmic examinations including visual acuity, intraocular pressure, slit lamp microscope, gonioscopy, visual field, Optical Coherence tomography for retinal nerve fiber layer thickness, funduscopic examination was conducted both before SLT. After SLT, the patients were followed up regularly (1 d, 1 wk, 1 mo, 3 mo, 6 mo, 1 year and 3 year). Complications, IOP and C/D were observed at each follow-up time point. The IOP was measured by Goldmann applanation in all patients. The 3 years follow-up were monitored by National Institute for Health and Care Excellence guidance to avoid bias in clinical decision-making.

Statistical analysis

SPSS 23.0 (version 23.0; IBM Corporation, Armonk, NY, USA) statistical software was used for statistical analysis. The means and standard deviation of IOP at different time points before and after SLT treatment was calculated. The paired t-test of two independent samples was used to compare the IOP between baseline and post treatment at different time points for statistical analysis; The statistical analysis of the number of medications used were analyzed using Wilcoxon signed rank test and tested using Generalized Estimating Equations and Poisson regression models. The variables that did not meet the normal distribution were analyzed using the Mann Whitney U test. The comparative evaluation of treatment effects between and within different types of glaucoma after SLT was tested by analysis of variance. The success rate was calculated with Kaplan-Meier survival curve analysis. $P < 0.05$ was considered statistically significant.

RESULTS

In this study, SLT was performed on 75 eyes from 70 OAG patients (33 males and 37 females) included. Before SLT treatment, all eyes were given glaucoma medications (1 to 4 drugs). The average age of patients receiving SLT was 44.34 ± 16.14 yr (Table 1). The mean IOP before treatment was 22.75 ± 2.08 mmHg in OAG and 22.52 ± 2.62 mmHg in PGS (Table 3).

The average number of medications used before SLT treatment was 3.39 ± 0.69 in OAG and 2.97 ± 0.74 in PGS group (Table 4). The course of IOP over the 36 mo of the study is shown in Table 3. 75 eyes were followed up for longer than 1 year, and 58 eyes were followed up for more than 3 years.

In the OAG group, IOP began to rise at the 6th month (P = 0.3465, P > 0.05). The mean IOP was 22.59 ± 2.26 mmHg at the 6th month and there was no significant difference compared to baseline.

Six months after SLT treatment, 6 eyes undertook retreatment of SLT, 4 eyes were given more topical IOP-lowering medications to control the IOP in the OAG group.

In the PGS group, there was a statistically significant lower IOP in the study compared with pretreatment levels after SLT treatment at all points (P < 0.001; Table 3) except for the 6th month (P =0.309, P > 0.05). The average IOP was 21.94 ± 2.11 mmHg at 6 mo and there was no significant difference compared to the baseline. At the 6th month, 4 eyes undertook retreatment of SLT and 2 eyes were given more topical IOP-lowering medications to control the IOP.

In this retrospective study, there was no statistically significant difference between the OAG and PGS groups at all time intervals (P > 0.05; Table 3) except for the 3rd month (P = 0.0039, P < 0.05; Table 3).

Table 1 Demographic and clinical characteristics of patients

Characteristics	
Age (yr, mean ± SD)	44.34 ± 16.14
Gender	
Male (*n*)	33 (3 both eyes)
Female (*n*)	37 (2 both eyes)
Diagnosis	
OAG (*n*)	36
PGS (*n*)	39
Total	75

OAG: Open angle glaucoma; PGS: Prior glaucoma surgery.

Table 2 Type of prior glaucoma surgery group

Type of PGS	Trabeculectomy	Drainage nail implantation	Ahmed glaucoma valve implantation	Trabeculectomy combined with cataract extraction
Number of patients	18	2	4	15

PGS: Prior glaucoma surgery.

Table 3 Evaluation of intraocular pressures and cumulative proportion of selective laser trabeculoplasty success

Groups	Baseline	1 d	1 wk	1 mo	3 mo	6 mo	12 mo	36 mo
Eyes (*n*)	36	36	36	36	36	36	35	28
OAG	22.75 ± 2.08	16.29 ± 3.62	18.97 ± 5.42	18.62 ± 4.39	21.32 ± 2.19	22.59 ± 2.26	20.13 ± 1.8	20.73 ± 1.82
*P*1 value		< 0.0001	0.0005	0.0005	0.0020	0.3465	< 0.0001	0.0009
Cumulative proportion of SLT success (%)				87.13	76.81	68.27	47.66	24.96
Eyes (*n*)	39	39	39	39	39	39	33	29
PGS	22.52 ± 2.62	16.45 ± 4.16	18.51 ± 5.09	18.80 ± 4.99	19.21 ± 3.82	21.94 ± 2.11	20.28 ± 1.61	20.49 ± 1.53
*P*1 value		< 0.0001	0.0002	0.0002	0.0002	0.3086	< 0.0001	0.0002
Cumulative proportion of SLT success (%)				84.70	67.40	59.39	42.15	27.61
*P*2 value	0.517	0.785	0.517	0.696	0.006	0.433	0.987	0.594

OAG: Open-angle glaucoma; SLT: Selective laser trabeculoplasty; PGS: Prior glaucoma surgery. *P*1: Repetitive measure analysis of variance (ANOVA), difference of intraocular pressures (IOP) between selective laser trabeculoplasty treatment and baseline group at different time points. *P*2: One way ANOVA, Comparison within groups, difference of IOP between open angle glaucoma and prior glaucoma surgery groups at different time points.

During the first 3 mo of follow-up, the IOP in the PGS group was 18.76 ± 3.92 mmHg and that in the OAG group was 21.32 ± 2.19 mmHg. The PGS group had a better and longer effect on IOP than the OAG group.

On the Kaplan-Meier survival analysis, the success rates after 1, 3, 6, 12, and 36 mo were 87.13%, 76.81%, 68.27%, 47.66% and 24.96% in the OAG group, and 84.70%, 67.40%, 59.39%, 42.15% and 27.61% in the PGS group, respectively ($P = 0.320$; Log-rank test) (Figure 1 and Table 3).

Table 4 presented the number of glaucoma medications used. There were no statistical differences on the 1st day after SLT treatment compared with the baseline ($P = 0.083$, $P > 0.05$). As the ocular spike was observed in part of patients at the 1st day after laser treatment, the number of anti-glaucoma drugs were not changed. The number of drugs was gradually reduced 1 wk after treated by laser and lasted for 36 mo.

Table 4 Number of glaucoma medications used in patients undergoing selective laser trabeculoplasty

Number of medications	Baseline	1 d	1 wk	1 mo	3 mo	6 mo	12 mo	36 mo
OAG	3.39 ± 0.69	3.31 ± 0.82	2.75 ± 0.5	2.06 ± 0.79	2.19 ± 0.71	2.39 ± 0.64	2.34 ± 0.64	2.5 ± 0.69
*P*1 value		0.083	< 0.001	< 0.001	< 0.001	< 0.001	< 0.001	< 0.001
PGS	2.97 ± 0.74	2.85 ± 0.67	2.51 ± 0.56	1.33 ± 1.28	1.44 ± 1.23	1.77 ± 0.99	1.79 ± 1.02	1.9 ± 0.82
*P*1 value		0.025	< 0.001	< 0.001	< 0.001	< 0.001	< 0.001	< 0.001
*P*2 value	0.015	0.005	0.048	0.004	0.003	0.006	0.008	0.007

OAG: Open angle glaucoma; PGS: Prior glaucoma surgery. *P*1: Wilcoxon signed rank test, difference of medication quantity between selective laser trabeculoplasty treatment and baseline group at different time points. *P*2: Mann-Whitney test, Comparison within groups, difference of medication quantity between open angle glaucoma and prior glaucoma surgery group at different time points.

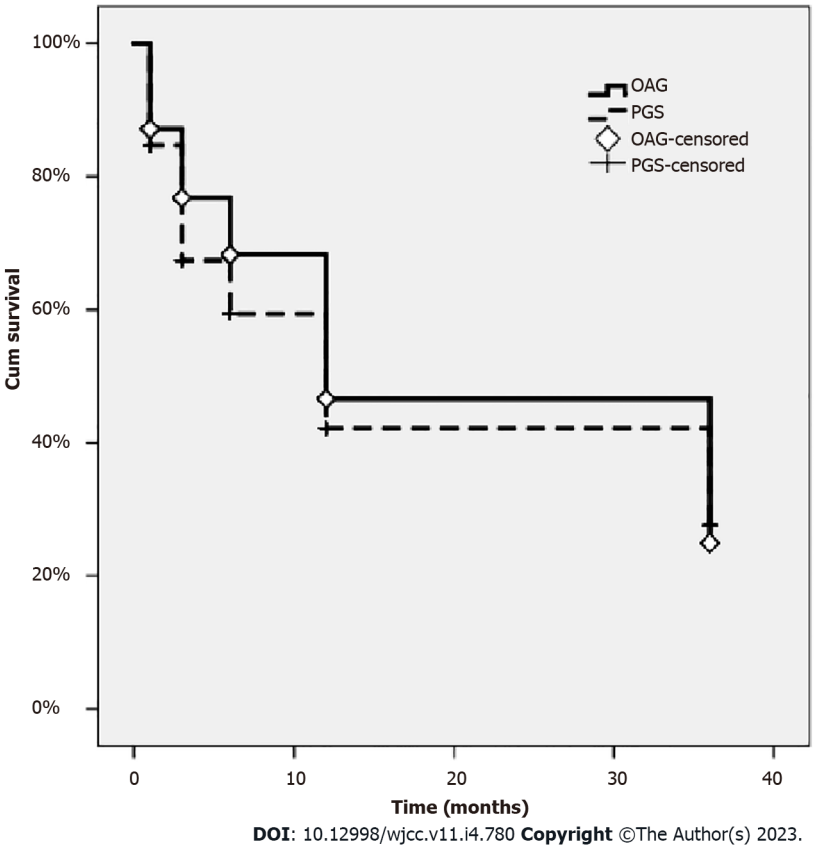

DOI: 10.12998/wjcc.v11.i4.780

Figure 1 A graph revealing the cumulative success rate in selective laser trabeculoplasty using the Kaplan-Meier method. Log Rank (Mantel-Cox), *P* = 0.591.

Of the 70 patients, 5 had both eyes treated. Six eyes experienced IOP spikes on the 1st day after SLT. In these eyes, the IOP returned to baseline after the appropriate intervention. No other complications after SLT therapy occurred in any eye. In the span of 3 years, 10 eyes (12.99%) underwent a repeat SLT, 5 eyes (6.49%) underwent glaucoma surgery. At the 6th months point, two patients in the PGS group had been excluded because of the progression of visual field, and they underwent glaucoma surgery again.

Conjunctival hyperemia occurred in 56 eyes (72.7%), which disappeared after 1 d. There was an anterior chamber reaction in 49 eyes (50.51%). Tyndall (±) ~ (+) in the anterior chamber was observed in 1 ~ 2 h after SLT and disappeared after 1 wk. A transient IOP elevation (spike) was observed 1 h after SLT, IOP ≥ 5 mmHg in 6 eyes (7.79%) and IOP ≥ 1 ~ 4 mmHg in 15 eyes (19.48%).

There were no severe complications in these patients, such as ocular inflammation, hyphemia, choroidal effusion, or retinal detachment.

DISCUSSION

Due to the IOP spike after treatment, the number of drugs used on the 1st day after SLT treatment did not decrease. Whereas, on the 1st day after SLT treatment, the IOP was greatly reduced. The difference was statistically significant at different time points until the 6th month after SLT treatment. Two prospective studies have reported that SLT can effectively reduce IOP 4 years and 6 years after treatment in patients who have used the maximum dose of IOP reducing drugs. 44% and 59% of patients have at least 20% of an IOP reduction, respectively[6,13]. However, our results showed that the action time of SLT lasted about 6 mo. After the 6th month, the IOP of some patients increased again. Therefore, at the 6th month after SLT treatment, some patients underwent SLT treatment again or added the numbers of anti-glaucoma drugs to control IOP. This result is not consistent with the published results, which may be related to race, trabecular meshwork structure or the distribution of trabecular meshwork pigment. The effectiveness and safety of SLT was affected by pigmentation of trabecular meshwork and laser energy[14].

In our study, the PGS group was included. These patients had a history of previous glaucoma surgery, 39 eyes, including 18 eyes after trabeculectomy, 2 eyes after drainage nail implantation, 4 eyes after glaucoma valve implantation and 15 eyes after trabeculectomy combined with cataract extraction. The chamber angular structure was not changed except for the surgical site in the PGS group, which provided the conditions for the SLT treatment. As there was no significant difference in IOP after SLT treatment between OAG and PGS groups, the history of glaucoma surgery might have little impact on the results of SLT laser treatment. The residual function in the trabecular meshwork pathway still has potential to be modulated in a post-surgical eye, which provided the conditions for the SLT treatment.

The energy used was between 0.6-1.2 mJ in our study. High energy laser could cause transient high intraocular pressure. For patients with heavy pigmentation in trabecular meshwork, high energy laser may lead to continuous IOP[15]. It was reported that SLT with appropriate high energy (1.2-1.5 mJ) can effectively reduce IOP in patients with steroid-induced glaucoma[16]. It is also reported that low-energy SLT treatment is also effective. The results show that low-energy laser could also effectively reduce IOP in OAG patients for 2 years after 360° SLT with initial energy of 0.3 mJ[17]. In the future research, we could further analyze the impact on IOP with different laser energy.

Our study shows that SLT could reduce the number of drugs as an adjunctive therapy. Juzych reported that in another study of OAG, SLT could effectively reduce IOP and reduce the number of drugs used after 5 years[18]. In a prospective randomized controlled study, the number of drugs decreased in varying degrees 1, 3 and 5 years after SLT treatment[19]. These results suggest that SLT can be used in the treatment of glaucoma patients with poor drug or surgical control.

A limitation of this study is a retrospective study which may have selection bias. It would be a better control for this potential selection bias in a prospective study. There are more types of glaucoma that could be treated by SLT, such as glaucoma secondary to silicone oil eye after vitrectomy, steroid-induced glaucoma and so on[16].

CONCLUSION

In summary, SLT may be efficacious in eyes with prior incisional glaucoma surgery and it provides an effective treatment option to lower IOP to avoid or postpone subsequent incisional glaucoma procedures.

ARTICLE HIGHLIGHTS

Research background

Selective laser trabeculoplasty (SLT) is a relatively safe and effective therapy in lowering intraocular pressures (IOP) for glaucoma. SLT could be offered as an initial treatment at decreasing IOP for open-angle glaucoma (OAG) and ocular hypertension. SLT could be used to reduce the IOP of patients who failed to achieve target IOP after receiving maximally tolerated medical therapy. SLT could reduce the uncontrolled intraocular pressure after glaucoma surgery.

Research motivation

To find out whether SLT could reduce IOP in patients with prior glaucoma surgery.

Research objectives

Our aim was to determine the efficacy of SLT as adjunctive treatment in patients with previous incisional glaucoma surgery whose IOP remains or becomes uncontrolled, and the number of medications used up to 3 years.

Research methods

Outpatients who underwent SLT were reviewed retrospectively at the Department of Ophthalmology, Third People's Hospital of Chengdu, Affiliated Hospital of Southwest Jiao Tong University from September 2016 to January 2020. 75 consecutive eyes of 70 patients (33 male, 37 female) with OAG (n = 36), and PGS (n = 39) were enrolled. The IOP was measured both before and after SLT and followed up to 3 years.

The means and standard deviations of IOP at different time points before and after SLT treatment was calculated. The statistical analysis of the number of medications used were analyzed using the Wilcoxon signed rank test. The comparative evaluation of treatment effects between and within different types of glaucoma after SLT was tested by the analysis of variance. The success rate was calculated with the Kaplan-Meier survival curve analysis.

Research results

The average age of patients receiving SLT was 44.34 ± 16.14 yr (Table 1). The mean IOP before treatment was 22.75 ± 2.08 mmHg in the OAG group and 22.52 ± 2.62 mmHg in the PGS group (Table 3). The average number of medications used before SLT treatment was 3.39 ± 0.69 in the OAG group and 2.97 ± 0.74 in the PGS group (Table 4). 75 eyes were followed up for longer than 1 year, and 58 eyes were followed up for more than 3 years. There was no statistically significant difference between the OAG and PGS groups. The success rates after 1, 3, 6, 12, and 36 mo were 87.13%, 76.81%, 68.27%, 47.66% and 24.96% in the OAG group, and 84.70%, 67.40%, 59.39%, 42.15% and 27.61% in the PGS group, respectively. The number of drugs was gradually reduced 1 wk after being treated by laser and lasted for 36 mo.

Research conclusions

SLT could reduce IOP as an adjunctive treatment both in the OAG and PGS groups. The residual function in the trabecular meshwork pathway still has potential to be modulated in a post-surgical eye, which provided the conditions for the SLT treatment. SLT significantly reduced the number of glaucoma medications used 3-years following treatment in glaucoma patients.

Research perspectives

SLT may be efficacious in eyes with prior incisional glaucoma surgery and it provides an effective treatment option to lower IOP to avoid or postpone subsequent incisional glaucoma procedures.

ACKNOWLEDGEMENTS

We thank all patients for their participation and trust in our study.

FOOTNOTES

Author contributions: Zhu J collected and analyzed the data; Guo J conceived and supervised the project; All authors have read and approved the article.

Supported by Natural Science Foundation of Sichuan Province of China, No. 2022NSFSC1400, and Youth Innovation Project of Sichuan Medical Association, No. Q15045.

Institutional review board statement: The study was reviewed and approved by the Third People's Hospital of Chengdu Institutional Review Board (Approval No. [2022]-S-5).

Informed consent statement: Patients were not required to give informed consent to the study because the analysis used anonymous clinical data that were obtained after each patient agreed to treatment by written consent.

Conflict-of-interest statement: The authors have no conflict of interest to declare. The authors alone are responsible for the content and writing of the paper.

Data sharing statement: The data that support the findings of this study are available on request from the corresponding author.

Country/Territory of origin: China

ORCID number: Jing Zhu 0000-0002-1677-7848; Juan Guo 0000-0003-2243-8903.

S-Editor: Liu GL
L-Editor: Filipodia
P-Editor: Liu GL

REFERENCES

1 **Latina MA**, Park C. Selective targeting of trabecular meshwork cells: *in vitro* studies of pulsed and CW laser interactions. *Exp Eye Res* 1995; **60**: 359-371 [PMID: 7789416 DOI: 10.1016/s0014-4835(05)80093-4]
2 **Latina MA**, Tumbocon JA. Selective laser trabeculoplasty: a new treatment option for open angle glaucoma. *Curr Opin Ophthalmol* 2002; **13**: 94-96 [PMID: 11880722 DOI: 10.1097/00055735-200204000-00007]
3 **Gazzard G**, Konstantakopoulou E, Garway-Heath D, Garg A, Vickerstaff V, Hunter R, Ambler G, Bunce C, Wormald R, Nathwani N, Barton K, Rubin G, Morris S, Buszewicz M. Selective laser trabeculoplasty versus drops for newly diagnosed ocular hypertension and glaucoma: the LiGHT RCT. *Health Technol Assess* 2019; **23**: 1-102 [PMID: 31264958 DOI: 10.3310/hta23310]
4 **Apolostolski S**, Susaković N, Lavrnić S, Stolić I, Trikić R. HLA antigens and immunoglobulin allotypes in myasthenia gravis. *Neurologija* 1987; **36**: 41-49 [PMID: 3509808 DOI: 10.14744/bej.2020.85866]
5 **Ang GS**, Fenwick EK, Constantinou M, Gan ATL, Man REK, Casson RJ, Finkelstein EA, Goldberg I, Healey PR, Pesudovs K, Sanmugasundram S, Xie J, McIntosh R, Jackson J, Wells AP, White A, Martin K, Walland MJ, Crowston JG, Lamoureux EL. Selective laser trabeculoplasty versus topical medication as initial glaucoma treatment: the glaucoma initial treatment study randomised clinical trial. *Br J Ophthalmol* 2020; **104**: 813-821 [PMID: 31488427 DOI: 10.1136/bjophthalmol-2018-313396]
6 **Weinand FS**, Althen F. Long-term clinical results of selective laser trabeculoplasty in the treatment of primary open angle glaucoma. *Eur J Ophthalmol* 2006; **16**: 100-104 [PMID: 16496252 DOI: 10.1177/112067210601600116]
7 **Sayin N**, Alkin Z, Ozkaya A, Demir A, Yazici AT, Bozkurt E, Demirok A. Efficacy of selective laser trabeculoplasty in medically uncontrolled glaucoma. *ISRN Ophthalmol* 2013; **2013**: 975281 [PMID: 24558611 DOI: 10.1155/2013/975281]
8 **Patel V**, El Hawy E, Waisbourd M, Zangalli C, Shapiro DM, Gupta L, Hsieh M, Kasprenski A, Katz LJ, Spaeth GL. Long-term outcomes in patients initially responsive to selective laser trabeculoplasty. *Int J Ophthalmol* 2015; **8**: 960-964 [PMID: 26558209 DOI: 10.3980/j.issn.2222-3959.2015.05.19]
9 **Stein JD**, Khawaja AP, Weizer JS. Glaucoma in Adults-Screening, Diagnosis, and Management: A Review. *JAMA* 2021; **325**: 164-174 [PMID: 33433580 DOI: 10.1001/jama.2020.21899]
10 **Zhang H**, Yang Y, Xu J, Yu M. Selective laser trabeculoplasty in treating post-trabeculectomy advanced primary open-angle glaucoma. *Exp Ther Med* 2016; **11**: 1090-1094 [PMID: 26998042 DOI: 10.3892/etm.2015.2959]
11 **Sharpe RA**, Kammerdiener LL, Williams DB, Das SK, Nutaitis MJ. Efficacy of selective laser trabeculoplasty following incisional glaucoma surgery. *Int J Ophthalmol* 2018; **11**: 71-76 [PMID: 29375994 DOI: 10.18240/ijo.2018.01.13]
12 **Francis BA**, Loewen N, Hong B, Dustin L, Kaplowitz K, Kinast R, Bacharach J, Radhakrishnan S, Iwach A, Rudavska L, Ichhpujani P, Katz LJ. Repeatability of selective laser trabeculoplasty for open-angle glaucoma. *BMC Ophthalmol* 2016; **16**: 128 [PMID: 27464887 DOI: 10.1186/s12886-016-0299-9]
13 **Gracner T**, Falez M, Gracner B, Pahor D. [Long-term follow-up of selective laser trabeculoplasty in primary open-angle glaucoma]. *Klin Monbl Augenheilkd* 2006; **223**: 743-747 [PMID: 16986084 DOI: 10.1055/s-2006-926725]
14 **Kinori M**, Hostovsky A, Skaat A, Schwartsman J, Melamed S. A novel method for quantifying the amount of trabecular meshwork pigment in glaucomatous and nonglaucomatous eyes. *J Glaucoma* 2014; **23**: e13-e17 [PMID: 24370807 DOI: 10.1097/IJG.0b013e3182a0758c]
15 **Leahy KE**, White AJ. Selective laser trabeculoplasty: current perspectives. *Clin Ophthalmol* 2015; **9**: 833-841 [PMID: 26005327 DOI: 10.2147/OPTH.S53490]
16 **Xiao J**, Zhao C, Liang A, Zhang M, Cheng G. Efficacy and Safety of High-Energy Selective Laser Trabeculoplasty for Steroid-Induced Glaucoma in Patients with Quiescent Uveitis. *Ocul Immunol Inflamm* 2021; **29**: 766-770 [PMID: 31902258 DOI: 10.1080/09273948.2019.1687730]
17 **Xu L**, Yu RJ, Ding XM, Li M, Wu Y, Zhu L, Chen D, Peng C, Zeng CJ, Guo WY. Efficacy of low-energy selective laser trabeculoplasty on the treatment of primary open angle glaucoma. *Int J Ophthalmol* 2019; **12**: 1432-1437 [PMID: 31544039 DOI: 10.18240/ijo.2019.09.10]
18 **Juzych MS**, Chopra V, Banitt MR, Hughes BA, Kim C, Goulas MT, Shin DH. Comparison of long-term outcomes of selective laser trabeculoplasty versus argon laser trabeculoplasty in open-angle glaucoma. *Ophthalmology* 2004; **111**: 1853-1859 [PMID: 15465546 DOI: 10.1016/j.ophtha.2004.04.030]
19 **Bovell AM**, Damji KF, Hodge WG, Rock WJ, Buhrmann RR, Pan YI. Long term effects on the lowering of intraocular pressure: selective laser or argon laser trabeculoplasty? *Can J Ophthalmol* 2011; **46**: 408-413 [PMID: 21995983 DOI: 10.1016/j.jcjo.2011.07.016]

World Journal of Clinical Cases

Submit a Manuscript: https://www.f6publishing.com

World J Clin Cases 2023 February 6; 11(4): 788-796

DOI: 10.12998/wjcc.v11.i4.788

ISSN 2307-8960 (online)

ORIGINAL ARTICLE

Retrospective Study

Efficacy of transvaginal ultrasound-guided local injections of absolute ethanol for ectopic pregnancies with intrauterine implantation sites

Toshiyuki Kakinuma, Kaoru Kakinuma, Yoshio Matsuda, Kaoru Yanagida, Michitaka Ohwada, Hirotsune Kaijima

Specialty type: Obstetrics and gynecology

Provenance and peer review: Unsolicited article; Externally peer reviewed.

Peer-review model: Single blind

Peer-review report's scientific quality classification

Grade A (Excellent): A
Grade B (Very good): 0
Grade C (Good): 0
Grade D (Fair): D
Grade E (Poor): 0

P-Reviewer: Maglic R, Serbia; Zhang F, China

Received: November 18, 2022
Peer-review started: November 18, 2022
First decision: December 13, 2022
Revised: December 27, 2022
Accepted: January 12, 2023
Article in press: January 12, 2023
Published online: February 6, 2023

Toshiyuki Kakinuma, Kaoru Kakinuma, Yoshio Matsuda, Kaoru Yanagida, Michitaka Ohwada, Department of Obstetrics and Gynecology, International University of Health and Welfare Hospital, Nasushiobara 329-2763, Japan

Hirotsune Kaijima, Minatomirai Yume Clinic, Yokohama 2200012, Japan

Corresponding author: Toshiyuki Kakinuma, MD, PhD, Doctor, Department of Obstetrics and Gynecology, International University of Health and Welfare Hospital, 537-3, Iguchi, Nasushiobara-City, Tochigi, Nasushiobara 329-2763, Japan. tokakinuma@gmail.com

Abstract

BACKGROUND

Cervical pregnancies, interstitial tubal pregnancies, and cesarean scar pregnancies, which are ectopic pregnancies with intrauterine implantation sites exhibit increasing trends with the recent widespread use of assisted reproductive technologies and increased rate of cesarean deliveries. The development of high-sensitivity human chorionic gonadotropin testing reagents and the increased precision of transvaginal ultrasonic tomography have made early diagnosis possible and have enabled treatment. Removal of ectopic pregnancies using methotrexate therapy and/or uterine artery embolization has been reported. However, delayed resumption of infertility treatments after methotrexate therapy is indicated, and negative effects on the next pregnancy after uterine artery embolization have been reported.

AIM

To examine the efficacy and safety of ultrasound-guided topical absolute ethanol injection in ectopic pregnancies with an intrauterine implantation site.

METHODS

In this study, we retrospectively examined the medical records of 21 patients who were diagnosed with an ectopic pregnancy with an intrauterine implantation site at our hospital, between April 2010 and December 2018, and underwent transvaginal ultrasound-guided local injections of absolute ethanol to determine the treatment outcomes. We evaluated the treatment methods, treatment outcomes,

presence of bleeding requiring hemostasis measures and blood transfusion, complications, and treatment periods. Successful treatment was defined as the completion of treatment using transvaginal ultrasound-guided local injections of absolute ethanol alone.

RESULTS

There were 21 total cases comprising 10 cervical pregnancies, 10 interstitial tubal pregnancies, and 1 cesarean scar pregnancy. All patients completed treatment with this method. No massive hemorrhaging or serious adverse reactions were observed during treatment. The mean gestation ages at the time of diagnosis were 5.9 wk (SD, ± 0.9 wk) for cervical and 6.9 wk (SD, ± 2.1 wk) for interstitial tubal pregnancies. The total ethanol doses were 4.8 mL (SD, ± 2.2 mL) for cervical pregnancies and 3.3 mL (SD, ± 2.2 mL) for interstitial pregnancies. The treatment period was 28.5 days (SD, ± 11.7 d) for cervical pregnancies and 30.0 ± 8.1 d for interstitial pregnancies. Positive correlations were observed between the blood β- human chorionic gonadotropin level at the beginning of treatment and the total ethanol dose (r = 0.75; P = 0.00008), as well as between the total ethanol dose and treatment period (r = 0.48; P = 0.026).

CONCLUSION

Transvaginal ultrasound-guided local injections of absolute ethanol could become a new option for intrauterine ectopic pregnancies when fertility preservation is desired.

Key Words: Embryo transfer; Fertility; Fertilization in vitro; Pregnancy complications; Prenatal care; Ectopic pregnancy

Core Tip: Transvaginal ultrasound-guided local injections of absolute ethanol for ectopic pregnancies such as cervical pregnancies, interstitial tubal pregnancies, and cesarean scar pregnancies can preserve the uterus without serious adverse reactions. This treatment avoids the complications caused by methotrexate therapy and uterine artery embolization. This treatment may become a new treatment option for intrauterine ectopic pregnancy when fertility preservation is desired.

Citation: Kakinuma T, Kakinuma K, Matsuda Y, Yanagida K, Ohwada M, Kaijima H. Efficacy of transvaginal ultrasound-guided local injections of absolute ethanol for ectopic pregnancies with intrauterine implantation sites. *World J Clin Cases* 2023; 11(4): 788-796
URL: https://www.wjgnet.com/2307-8960/full/v11/i4/788.htm
DOI: https://dx.doi.org/10.12998/wjcc.v11.i4.788

INTRODUCTION

Ectopic pregnancy occurs in approximately 1% of all pregnancies and the majority of these are tubal pregnancies. Although cervical, interstitial tubal, and cesarean scar pregnancy, which are ectopic pregnancies with intrauterine implantation sites, are rare, they have exhibited an increasing trend with the recent widespread use of assisted reproductive technologies and the increased rate of cesarean delivery[1-3]. Ectopic pregnancies are serious conditions prone to massive hemorrhaging, and surgical treatments such as total hysterectomy and focal excision have been the primary standard treatment options. However, early diagnosis has become possible with the development of high-sensitivity human chorionic gonadotropin (hCG) testing reagents and the increased precision of transvaginal ultrasonic tomography, which enable treatment before clinical manifestation. Therefore, uterine preservation for the purpose of fertility preservation has become more feasible after early therapeutic intervention. There have been reports of ectopic pregnancy removal using methotrexate (MTX) therapy and uterine artery embolization (UAE), or a combination of these, when fertility preservation is desired[4-8]. However, for patients desiring fertility preservation, MTX therapy is concerning because of the associated delay in resumption of infertility treatment to avoid the possibility of decreased ovarian function and the necessary washout period[9]. Moreover, increased rates of miscarriage and placenta accreta during the next pregnancy have been associated with UAE[10]. Furthermore, MTX administration is often unsuccessful when there is fetal heart movement or when the blood hCG value is high[11-14]. Additionally, there are concerns that massive hemorrhaging may occur during treatment[15-17]. Therefore, it is important to consider the effects of treatment on fertility for those who desire uterine preservation and future pregnancies.

We have previously reported the efficacy and safety of ultrasound-guided topical injection of absolute ethanol as an alternative to topical MTX treatment for ectopic pregnancy[18]. Because this treatment has a local effect, there is no effect on ovarian function and no need for a washout period, which is required with MTX therapy. Moreover, this therapy can help the avoid negative effects on subsequent pregnancies that are otherwise associated with UAE.

The purpose of this study was to examine the efficacy and safety of ultrasound-guided topical injection of absolute ethanol in ectopic pregnancies with an implantation site within the uterus.

MATERIALS AND METHODS

All procedures performed in studies involving human participants were in accordance with the ethical standards of the institutional and/or national research committee and with the 1964 Helsinki Declaration and its later amendments or comparable ethical standards. This study was approved by the International University of Health and Welfare Hospital Ethics Committee (referral number: 21-B-34). Written informed consent was obtained from all individual participants included in the study. We retrospectively collected and examined the medical records of patients diagnosed with ectopic pregnancy with an implantation site within the uterus (interstitial tubal pregnancy, cervical pregnancy, cesarean scar pregnancy) and who underwent transvaginal ultrasound-guided local injections of absolute ethanol at our hospital from April 2010 to December 2018. Transvaginal ultrasound-guided local injections of absolute ethanol were administered after obtaining informed consent from the patients.

The diagnostic methods for ectopic pregnancies with intrauterine implantation sites included the confirmation of fetal heart movement using transvaginal ultrasonography, evaluation of the blood flow around the gestation sac using color Doppler imaging, and performing a β-hCG assay. We evaluated the treatment methods, treatment outcomes, presence of bleeding requiring hemostasis measures and blood transfusion, complications, and treatment periods. Successful treatment was defined as the completion of treatment using transvaginal ultrasound-guided local injections of absolute ethanol alone. The treatment period was defined as the time from the initiation of treatment until a negative blood β-hCG level (detection sensitivity limit: 1.2 mIU/mL) was confirmed.

Transvaginal ultrasound-guided local injections of absolute ethanol were administered to inpatients, and analgesia was administered using a nonsteroidal anti-inflammatory drug suppository or peri-cervical block 15 min before treatment. Using transvaginal ultrasound guidance, anhydrous ethanol (anhydrous ethanol injection, Fuso; Fuso Pharmaceutical Industries, Ltd., Osaka, Japan) was locally injected through the myometrium into the guide sheath (GS) periphery of the intrauterine ectopic pregnancy site using a 21-gauge oocyte collection needle (KITAZATO OPU NEEDLE; Kitazato Corporation, Tokyo, Japan). Absolute ethanol was locally injected in the site, where the GS peripheral blood flow was confirmed using the transvaginal ultrasound color Doppler method, until blood flow was interrupted and the GS periphery changed to a highly echoic image (Figure 1). When the blood β-hCG level at 2 h after local ethanol injection exhibited a 10% to 30% decrease compared to that before treatment, the treatment was deemed effective. Additionally, when the blood β-hCG level had decreased after transvaginal ultrasound-guided local injections of absolute ethanol but increased again at a later date, an inadequate response was considered; thereafter, additional local injections of absolute alcohol were administered at a suitable time. The blood β-hCG level was measured using the chemiluminescent immunoassay method (CLIA method; Abbott Japan LLC, Chiba, Japan).

Continuous variables are presented as the mean ± standard deviation (SD). To investigate the correlations among the blood β-hCG level at the beginning of treatment, the treatment period, and the total absolute ethanol dose, Pearson's product-moment correlation coefficient was derived (Microsoft Excel 2019; Microsoft, Redmond, WA, United States) and $P < 0.05$ was considered significant.

RESULTS

There were 21 total cases comprising 10 cervical pregnancies, 10 interstitial tubal pregnancies, and 1 cesarean scar pregnancy (Table 1). All these cases were treated with transvaginal ultrasound-guided local injections of absolute ethanol. The mean patient age for those with cervical pregnancies was 37.4 years (SD, ± 3.9 years). The mean patient age for those with interstitial tubal pregnancies was 36.4 years (SD, ± 5.5 years). Of the women with cervical pregnancies, eight were nulliparous and two were parous. Nine of the 10 women with interstitial tubal pregnancies were nulliparous. Of the 10 cervical pregnancies, 8 (80%) were attributable to *in vitro* fertilization with embryo transfer. Seven (70%) of the 10 interstitial tubal pregnancies were attributable to *in vitro* fertilization with embryo transfer. The mean gestation ages at the time of diagnosis were 5.9 wk (SD, ± 0.9 wk) for cervical pregnancies and 6.9 wk (SD, ± 2.1 wk) for interstitial tubal pregnancies. The blood β-hCG levels at the beginning of treatment were 13352.0 mIU/mL (SD, ± 8004.1 mIU/mL) for cervical pregnancies and 7485.7 mIU/mL (SD, ± 9647.8 mIU/mL) for interstitial pregnancies. Fetal heart movement was observed during two of the

Table 1 Patient background

Case	Implantation site	Age, yr	Pregnancies, no.	Live birth, no.		Gestation age at diagnosis	Fetal heartbeat	Blood β-hCG (mIU/mL) at the beginning of treatment	Blood β-hCG (mIU/mL) at the final visit	Local ethanol injections, no.	Total ethanol dose, mL	Treatment period, d
1	Cervix	32	2	0	IVF-ET	Week 5 Day 0	-	17760	< 1.2	3	5	51
2	Cervix	37	1	0	IVF-ET	Week 5 Day 6	-	20795	< 1.2	1	4.8	16
3	Cervix	36	0	0	Spontaneous pregnancy	Week 6 Day 5	-	12585	< 1.2	3	6.8	39
4	Cervix	36	1	1	IVF-ET	Week 6 Day 1	-	2326	< 1.2	2	3	36
5	Cervix	39	0	0	IVF-ET	Week 5 Day 1	-	6480	< 1.2	2	4	19
6	Cervix	35	1	0	IVF-ET	Week 5 Day 2	-	4835	< 1.2	1	3.2	22
7	Cervix	39	1	0	IVF-ET	Week 5 Day 5	+	16346	< 1.2	3	10	39
8	Cervix	41	1	0	IVF-ET	Week 5 Day 3	-	7807	< 1.2	1	2	22
9	Cervix	33	1	1	Spontaneous pregnancy	Week 7 Day 6	+	26930	< 1.2	1	5	21
10	Cervix	37	1	0	IVF-ET	Week 5 Day 3	-	19356	< 1.2	2	4.5	20
11	Fallopian tube interstitium	41	0	0	IVF-ET	Week 8 Day 2	-	2384	< 1.2	4	4.7	28
12	Fallopian tube interstitium	35	3	0	IVF-ET	Week 6 Day 1	-	853	< 1.2	1	0.6	16
13	Fallopian tube interstitium	39	1	0	IVF-ET	Week 5 Day 4	-	2933	< 1.2	3	4	24
14	Fallopian tube interstitium	37	3	0	IVF-ET	Week 7 Day 0	-	1170	< 1.2	2	1.5	26
15	Fallopian tube interstitium	36	0	0	IVF-ET	Week 7 Day 3	-	2198	< 1.2	4	4.9	30
16	Fallopian tube interstitium	25	0	0	Spontaneous pregnancy	Week 12 Day 0	-	2420	< 1.2	2	1.5	26
17	Fallopian tube interstitium	38	2	0	IVF-ET	Week 7 Day 0	-	11147	< 1.2	3	3.6	31
18	Fallopian tube interstitium	33	1	0	Spontaneous pregnancy	Week 5 Day 2	-	6715	< 1.2	3	4.6	45
19	Fallopian tube interstitium	34	0	0	Spontaneous pregnancy	Week 5 Day 1	-	12836	< 1.2	1	1.3	36
20	Fallopian tube interstitium	46	2	1	IVF-ET	Week 5 Day 3	-	32201	< 1.2	3	8	38

21	Cesarean delivery scar	35	1	1	Spontaneous pregnancy	Week 7 Day 1	+	91798	< 1.2	3	12	41	

IVF-ET: *In vitro* fertilization – embryo transfer; hCG: human chorionic gonadotropin.

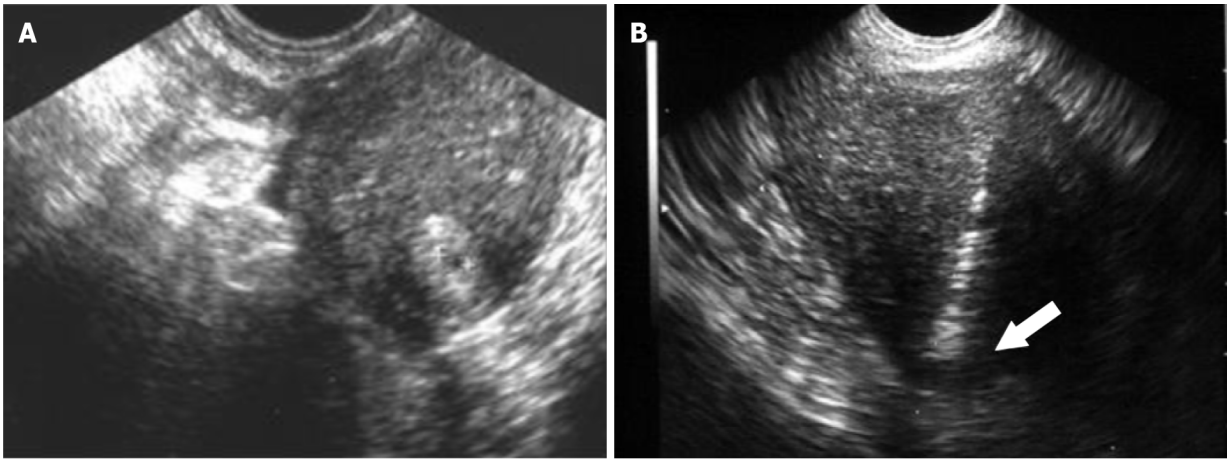

DOI: 10.12998/wjcc.v11.i4.788 **Copyright** ©The Author(s) 2023.

Figure 1 Transvaginal ultrasonography findings (case 11: interstitial tubal pregnancy) and transvaginal ultrasonography findings after local injections of absolute ethanol. A: Although a 20-mm gestation sac was observed in the interstitial portion of the left fallopian tube separated from the endometrium, no fetal heartbeat was observed; B: Absolute ethanol local injection site using a 21-gauge oocyte collection needle. Local absolute ethanol injections were performed in the guide sheath periphery of the interstitial tubal pregnancy site using transvaginal ultrasound guidance.

cervical pregnancies and one cesarean scar pregnancy. For cervical pregnancies, 1.9 (SD, ± 0.9) transvaginal ultrasound-guided local injections of absolute ethanol were administered. For interstitial pregnancies, 2.6 (SD, ± 1.1) transvaginal ultrasound-guided local injections of absolute ethanol were administered. The total ethanol doses were 4.8 mL (SD, ± 2.2 mL) for cervical pregnancies and 3.3 mL (SD, ± 2.2 mL) for interstitial pregnancies. The treatment period was 28.5 d (SD, ± 11.7 d) for cervical pregnancies; for interstitial pregnancies, it was 30.0 ± 8.1 d. Positive correlations were observed between the blood β-hCG level (mIU/mL) at the beginning of treatment and the total ethanol dose (r = 0.75; P = 0.00008), as well as between the total ethanol dose and the treatment period (r = 0.48; P = 0.026). No correlation was observed between the blood β-hCG level (mIU/mL) at the beginning of treatment and the treatment period (r = 0.31; P = 1.41).

No massive hemorrhaging occurred during observation, and no patients required blood transfusions. Additionally, no complications attributable to this treatment were observed. Menses resumed for all women after treatment. Furthermore, case 1 achieved spontaneous pregnancy 5 mo after undergoing ultrasound-guided local injections of absolute ethanol. The course of her pregnancy was normal, the placental attachment site was problem-free, and normal delivery occurred at 41+0 wk of gestation. There was no abnormal postpartum bleeding and the postpartum course was good.

DISCUSSION

In this study, we studied the efficacy and safety of transvaginal ultrasound-guided local injections of absolute ethanol as a new conservative treatment for ectopic pregnancy with an implantation site within the uterus.

Although cervical pregnancy, interstitial tubal pregnancy, and cesarean scar pregnancy, which are ectopic pregnancies with intrauterine implantation sites, are serious conditions prone to massive hemorrhaging, early diagnosis has become possible with the development of high-sensitivity hCG testing reagents and the increased precision of transvaginal ultrasonic tomography. However, there is no consensus regarding uterus-preserving treatments for ectopic pregnancies when the attachment site is within the uterus.

MTX therapy is associated with the possibility of decreased ovarian function and delayed resumption of infertility treatment because of the washout period[9]. Therefore, MTX therapy has possible negative effects on fertility preservation. An investigation on oocyte yields before and after MTX therapy for 35 cervical pregnancy patients with a history of MTX therapy reported that the oocyte yield of *in vitro* fertilization was 7.8 (SD, ± 3.6) after treatment; however, it was 10.1 (SD, ± 3.9) before treatment[9].

Therefore, MTX therapy was considered to reduce the oocyte yield. This reduction in oocytes was associated with a subsequent decrease in the number of eggs collected[9]. Therefore, the possible negative effects of MTX treatment on the ovaries must be considered for women who desire future pregnancies.

Additionally, because a washout period is necessary when MTX is used, a contraception period of 4 to 6 mo postoperatively is recommended[19,20] before infertility therapy can be resumed. Most of the cases that have been studied involved pregnancy as a result of *in vitro* fertilization. Therefore, a treatment method that enables early resumption of infertility treatments is desirable because the patients are often of advanced age. Furthermore, it has been reported that MTX administration is often unsuccessful when there is either fetal heart movement or high blood hCG values[11-14], and there are concerns that massive hemorrhaging may occur during treatment[15-17].

Complications after UAE include fever, pain, endometriosis, intrauterine adhesions, uterine necrosis, and reduced ovarian function[21-23]. Regarding postoperative fertility, Hardeman *et al*[24] studied 14 of 53 patients who had undergone UAE for obstetrical bleeding and desired to become pregnant and reported that 12 were able to achieve pregnancy and live birth. Therefore, fertility after UAE is considered relatively good. However, pregnancies after UAE are affected by significantly increased rates of miscarriage, postpartum hemorrhage, premature birth, and malpresentation; furthermore, intrauterine growth restriction has been observed after UAE[10]. Therefore, careful management during the perinatal period is necessary for pregnancies after UAE.

In this study, we performed transvaginal ultrasound-guided local injections of absolute ethanol as an alternative to MTX therapy and UAE. We previously reported the efficacy and safety of this treatment method for ectopic pregnancy[18]. This treatment method involves local injections of absolute ethanol into the GS periphery of the pregnancy site under ultrasonic guidance. The therapeutic effect of absolute ethanol can be judged within a shorter time than that of MTX therapy because it is possible to confirm a blood hCG decrease of 10% to 30% at 2 h after local injection. Absolute ethanol is thought to dewater and denature the chorionic tissue, resulting in acute tissue changes that reduce the blood hCG within a short time. Therefore, among the cases that we have studied, transvaginal ultrasound-guided local injections of absolute ethanol have been considered effective even with high blood hCG levels and fetal heart movement, which cannot be successfully treated with MTX therapy. Additionally, because transvaginal ultrasound-guided local injections of absolute ethanol did not result in massive hemorrhaging, it was surmised that hemostatic action is involved; therefore, it is likely an effective treatment for intrauterine ectopic pregnancies accompanied by genital bleeding, even when fertility preservation is desired. Additionally, because of the characteristics of absolute ethanol, including its low probability of associated infection, it is effective for transvaginal procedures. Moreover, because a fine-gauge needle is used, there is little blood loss and pain, and general anesthesia is unnecessary. Because absolute ethanol is less expensive than MTX, there are fewer economic burdens on the patients. When repeated administration is required for persistent trophoblastic disease, local treatment with absolute ethanol is suitable because it produces a local effect, whereas anticancer drugs such as MTX produce adverse reactions. Multiple local injections of absolute ethanol were administered for persistent trophoblastic disease among 15 of the cases examined, and no adverse reactions attributable to this treatment were observed.

Although we observed a cervical pregnancy after spontaneous conception and normal delivery after this treatment among our target cases, few reports have described the pregnancy prognosis and uterine preservation for those who desire to have children and have experienced an intrauterine ectopic pregnancy. No consensus has been reached regarding such cases. Pregnancy and delivery courses were recorded for women with cervical pregnancies who desired pregnancy and fertility-preserving treatment and underwent MTX therapy and UAE[17,25-29]. Of the 110 women examined, approximately half (n = 51) wished to become pregnant; of those 110 women, 32 (62.7%) became pregnant and 22 (43.1%) achieved live birth[17,25-29]. Although the background characteristics of the individual women differed, approximately half became pregnant; therefore, it is important to proactively study conservative treatments for cervical pregnancies of women who desire fertility preservation. Additionally, there have been reports of an increased risk of uterine rupture during pregnancies after surgical treatment of the pregnancy site of interstitial tubal pregnancies[30-32]. Therefore, conservative treatments are thought to be highly significant from the perspective of fertility preservation. For women who have undergone treatment for cesarean scar pregnancies, approximately half became pregnant after cesarean scar pregnancy treatment, and their outcomes varied. Although some women have achieved live birth by cesarean delivery at full term, others experienced another cesarean scar pregnancy, stillbirth, or maternal death caused by uterine rupture even though implantation occurred in the uterine body, and some required a total hysterectomy because of massive hemorrhaging caused by placenta accreta[7,33]. During pregnancy management after cesarean scar pregnancy treatment, careful examination is necessary during early pregnancy. Even in cases of normal pregnancy, it may be necessary to be cautious of uterine rupture and placenta accreta.

Since intrauterine ectopic pregnancy is a relatively rare disease, further examination of an accumulated number of cases and long-term follow-up after transvaginal ultrasound-guided local injections of absolute ethanol are required. There are many unknowns regarding the effects of fertility preservation treatments on future pregnancies. Therefore, investigations of the treatment methods used

for intrauterine ectopic pregnancies and long-term follow-up are necessary.

CONCLUSION

Transvaginal ultrasound-guided local injections of absolute ethanol for ectopic pregnancies with an intrauterine implantation site can preserve the uterus without serious adverse reactions. This treatment method avoids the complications caused by MTX therapy and UAE. Therefore, it may become a new treatment option for intrauterine ectopic pregnancy when fertility preservation is desired.

ARTICLE HIGHLIGHTS

Research background

Ectopic pregnancy at cervical pregnancy, caesarean scar pregnancy, and interstitial pregnancy are rare; therefore, it is challenging to say that a standard treatment has been established.

Research motivation

Removal of ectopic pregnancies using methotrexate therapy and/or uterine artery embolization has been reported. However, delayed resumption of infertility treatments after methotrexate therapy is indicated, and negative effects on the next pregnancy after uterine artery embolization have been reported. To avoid these problems, we will establish a new treatment method for Cervical pregnancies, interstitial tubal pregnancies, and cesarean scar pregnancies, which are ectopic pregnancies with intrauterine implantation sites.

Research objectives

The purpose of this study was to examine the efficacy and safety of ultrasound-guided topical injection of absolute ethanol in ectopic pregnancies with an implantation site within the uterus.

Research methods

We retrospectively examined the medical records of 21 patients who were diagnosed with an ectopic pregnancy with an intrauterine implantation site at our hospital, between April 2010 and December 2018, and underwent transvaginal ultrasound-guided local injections of absolute ethanol to determine the treatment outcomes. We evaluated the treatment methods, treatment outcomes, presence of bleeding requiring hemostasis measures and blood transfusion, complications, and treatment periods.

Research results

All patients completed treatment with transvaginal ultrasound-guided local injections of absolute ethanol. No massive hemorrhaging or serious adverse reactions were observed during treatment.

Research conclusions

Transvaginal ultrasound-guided local injections of absolute ethanol could become a new option for intrauterine ectopic pregnancies when fertility preservation is desired.

Research perspectives

Ectopic pregnancy at cervical pregnancy, caesarean scar pregnancy, and interstitial pregnancy are rare; therefore, it is challenging to say that a standard treatment has been established. Transvaginal ultrasound-guided local injections of absolute ethanol for ectopic pregnancies such as cervical pregnancies, interstitial tubal pregnancies, and cesarean scar pregnancies can preserve the uterus without serious adverse reactions. This treatment avoids the complications caused by methotrexate therapy and uterine artery embolization. This treatment may become a new treatment option for intrauterine ectopic pregnancy when fertility preservation is desired.

FOOTNOTES

Author contributions: Kakinuma T conceived, designed, and performed the analysis, and wrote the paper; all authors collected and contributed data/analysis tools; all authors have read and approved the final manuscript.

Institutional review board statement: This study was approved by the International University of Health and Welfare Hospital Ethics Committee (referral number: 21-B-34).

Informed consent statement: Written informed consent was obtained from all individual participants included in the

study.

Conflict-of-interest statement: The authors have no relevant financial or non-financial interests to disclose.

Data sharing statement: The data are available upon reasonable request to the corresponding author.

Country/Territory of origin: Japan

ORCID number: Toshiyuki Kakinuma 0000-0001-7853-4860; Kaoru Kakinuma 0000-0003-4647-9582; Yoshio Matsuda 0000-0002-2890-2802; Kaoru Yanagida 0000-0002-5348-3603; Michitaka Ohwada 0000-0002-0396-6228; Hirotsune Kaijima 0000-0002-1932-4780.

S-Editor: Liu JH
L-Editor: A
P-Editor: Liu JH

REFERENCES

1 **Londra L**, Moreau C, Strobino D, Garcia J, Zacur H, Zhao Y. Ectopic pregnancy after *in vitro* fertilization: differences between fresh and frozen-thawed cycles. *Fertil Steril* 2015; **104**: 110-118 [PMID: 25956363 DOI: 10.1016/j.fertnstert.2015.04.009]
2 **Clayton HB**, Schieve LA, Peterson HB, Jamieson DJ, Reynolds MA, Wright VC. Ectopic pregnancy risk with assisted reproductive technology procedures. *Obstet Gynecol* 2006; **107**: 595-604 [PMID: 16507930 DOI: 10.1097/01.AOG.0000196503.78126.62]
3 **Bouyer J**, Coste J, Fernandez H, Pouly JL, Job-Spira N. Sites of ectopic pregnancy: a 10 year population-based study of 1800 cases. *Hum Reprod* 2002; **17**: 3224-3230 [PMID: 12456628 DOI: 10.1093/humrep/17.12.3224]
4 **Adabi K**, Nekuie S, Rezaeei Z, Rahimi-Sharbaf F, Banifatemi S, Salimi S. Conservative management of cervical ectopic pregnancy: systemic methotrexate followed by curettage. *Arch Gynecol Obstet* 2013; **288**: 687-689 [PMID: 23525594 DOI: 10.1007/s00404-013-2807-y]
5 **Martinelli P**, Maruotti GM, Oppedisano R, Agangi A, Mazzarelli LL, Votino C, Quarantelli M, Iaccarino V. Is uterine artery embolization for cervical ectopic pregnancy always safe? *J Minim Invasive Gynecol* 2007; **14**: 758-763 [PMID: 17980340 DOI: 10.1016/j.jmig.2007.05.017]
6 **Ushakov FB**, Elchalal U, Aceman PJ, Schenker JG. Cervical pregnancy: past and future. *Obstet Gynecol Surv* 1997; **52**: 45-59 [PMID: 8994238 DOI: 10.1097/00006254-199701000-00023]
7 **Ash A**, Smith A, Maxwell D. Caesarean scar pregnancy. *BJOG* 2007; **114**: 253-263 [PMID: 17313383 DOI: 10.1111/j.1471-0528.2006.01237.x]
8 **Hafner T**, Aslam N, Ross JA, Zosmer N, Jurkovic D. The effectiveness of non-surgical management of early interstitial pregnancy: a report of ten cases and review of the literature. *Ultrasound Obstet Gynecol* 1999; **13**: 131-136 [PMID: 10079493 DOI: 10.1046/j.1469-0705.1999.13020131.x]
9 **McLaren JF**, Burney RO, Milki AA, Westphal LM, Dahan MH, Lathi RB. Effect of methotrexate exposure on subsequent fertility in women undergoing controlled ovarian stimulation. *Fertil Steril* 2009; **92**: 515-519 [PMID: 18829004 DOI: 10.1016/j.fertnstert.2008.07.009]
10 **Goldberg J**, Pereira L, Berghella V. Pregnancy after uterine artery embolization. *Obstet Gynecol* 2002; **100**: 869-872 [PMID: 12423843 DOI: 10.1016/s0029-7844(02)02347-5]
11 **Hung TH**, Shau WY, Hsieh TT, Hsu JJ, Soong YK, Jeng CJ. Prognostic factors for an unsatisfactory primary methotrexate treatment of cervical pregnancy: a quantitative review. *Hum Reprod* 1998; **13**: 2636-2642 [PMID: 9806299 DOI: 10.1093/humrep/13.9.2636]
12 **Lipscomb GH**, McCord ML, Stovall TG, Huff G, Portera SG, Ling FW. Predictors of success of methotrexate treatment in women with tubal ectopic pregnancies. *N Engl J Med* 1999; **341**: 1974-1978 [PMID: 10607814 DOI: 10.1056/NEJM199912233412604]
13 **Watanabe K**, Chigusa Y, Kondoh E, Mogami H, Horie A, Baba T, Mandai M. Human chorionic gonadotropin value and its change prior to methotrexate treatment can predict the prognosis in ectopic tubal pregnancies. *Reprod Med Biol* 2019; **18**: 51-56 [PMID: 30655721 DOI: 10.1002/rmb2.12247]
14 **Pulatoglu C**, Dogan O, Basbug A, Kaya AE, Yildiz A, Temizkan O. Predictive factors of methotrexate treatment success in ectopic pregnancy: A single-center tertiary study. *North Clin Istanb* 2018; **5**: 227-231 [PMID: 30688925 DOI: 10.14744/nci.2017.04900]
15 **Cok T**, Kalayci H, Ozdemir H, Haydardedeoglu B, Parlakgumus AH, Tarim E. Transvaginal ultrasound-guided local methotrexate administration as the first-line treatment for cesarean scar pregnancy: Follow-up of 18 cases. *J Obstet Gynaecol Res* 2015; **41**: 803-808 [PMID: 25491022 DOI: 10.1111/jog.12627]
16 **Zhang S**, Yan H, Ji WT. Uterine artery embolization combined with intra-arterial MTX infusion: its application in

treatment of cervical pregnancy. *Arch Gynecol Obstet* 2016; **293**: 1043-1047 [PMID: 26525692 DOI: 10.1007/s00404-015-3929-1]

17 **Yamaguchi M**, Honda R, Erdenebaatar C, Monsur M, Honda T, Sakaguchi I, Okamura Y, Ohba T, Katabuchi H. Treatment of cervical pregnancy with ultrasound-guided local methotrexate injection. *Ultrasound Obstet Gynecol* 2017; **50**: 781-787 [PMID: 27943496 DOI: 10.1002/uog.17384]

18 **Kaijima H**, Osada H, Kato K, Segawa T, Takehara Y, Teramoto S, Kato O. The efficacy and safety of managing ectopic pregnancies with transvaginal ultrasound-guided local injections of absolute ethanol. *J Assist Reprod Genet* 2006; **23**: 293-298 [PMID: 16832599 DOI: 10.1007/s10815-006-9037-1]

19 **Gougeon A**. Dynamics of follicular growth in the human: a model from preliminary results. *Hum Reprod* 1986; **1**: 81-87 [PMID: 3558758 DOI: 10.1093/oxfordjournals.humrep.a136365]

20 **Strauss J**, Barbieri R, Gargiulo A. The ovarian life cycle. In: Yen & Jaffe's reproductive endocrinology: physiology, pathophysiology, and clinical management. 5th edn. Philadelphia: Elsevier Saunders, 2004; 213

21 **Badawy SZ**, Etman A, Singh M, Murphy K, Mayelli T, Philadelphia M. Uterine artery embolization: the role in obstetrics and gynecology. *Clin Imaging* 2001; **25**: 288-295 [PMID: 11566093 DOI: 10.1016/s0899-7071(01)00307-2]

22 **Vegas G**, Illescas T, Muñoz M, Pérez-Piñar A. Selective pelvic arterial embolization in the management of obstetric hemorrhage. *Eur J Obstet Gynecol Reprod Biol* 2006; **127**: 68-72 [PMID: 16229935 DOI: 10.1016/j.ejogrb.2005.09.008]

23 **Hong TM**, Tseng HS, Lee RC, Wang JH, Chang CY. Uterine artery embolization: an effective treatment for intractable obstetric haemorrhage. *Clin Radiol* 2004; **59**: 96-101 [PMID: 14697382 DOI: 10.1016/j.crad.2003.08.007]

24 **Hardeman S**, Decroisette E, Marin B, Vincelot A, Aubard Y, Pouquet M, Maubon A. Fertility after embolization of the uterine arteries to treat obstetrical hemorrhage: a review of 53 cases. *Fertil Steril* 2010; **94**: 2574-2579 [PMID: 20381035 DOI: 10.1016/j.fertnstert.2010.02.052]

25 **Xiaolin Z**, Ling L, Chengxin Y, Yiqing T, Jun W, Yan C, Guangxi T. Transcatheter intraarterial methotrexate infusion combined with selective uterine artery embolization as a treatment option for cervical pregnancy. *J Vasc Interv Radiol* 2010; **21**: 836-841 [PMID: 20400332 DOI: 10.1016/j.jvir.2010.02.013]

26 **Wang Y**, Xu B, Dai S, Zhang Y, Duan Y, Sun C. An efficient conservative treatment modality for cervical pregnancy: angiographic uterine artery embolization followed by immediate curettage. *Am J Obstet Gynecol* 2011; **204**: 31.e1-31.e7 [PMID: 20889136 DOI: 10.1016/j.ajog.2010.08.048]

27 **Krissi H**, Hiersch L, Stolovitch N, Nitke S, Wiznitzer A, Peled Y. Outcome, complications and future fertility in women treated with uterine artery embolization and methotrexate for non-tubal ectopic pregnancy. *Eur J Obstet Gynecol Reprod Biol* 2014; **182**: 172-176 [PMID: 25300059 DOI: 10.1016/j.ejogrb.2014.09.026]

28 **Uludag SZ**, Kutuk MS, Aygen EM, Sahin Y. Conservative management of cervical ectopic pregnancy: Single-center experience. *J Obstet Gynaecol Res* 2017; **43**: 1299-1304 [PMID: 28586112 DOI: 10.1111/jog.13362]

29 **Chen H**, Yang S, Fu J, Song Y, Xiao L, Huang W, Zhang H. Outcomes of Bilateral Uterine Artery Chemoembolization in Combination with Surgical Evacuation or Systemic Methotrexate for Cervical Pregnancy. *J Minim Invasive Gynecol* 2015; **22**: 1029-1035 [PMID: 26037963 DOI: 10.1016/j.jmig.2015.05.018]

30 **Imai S**, Kondoh E, Kawasaki K, Mogami H, Ueda A, Umeoka S, Konishi I. Placental blood flow disappears coincident with a fall in human chorionic gonadotropin to undetectable levels in conservative management of placenta accreta. *Eur J Obstet Gynecol Reprod Biol* 2014; **180**: 199-201 [PMID: 24916034 DOI: 10.1016/j.ejogrb.2014.05.020]

31 **Weissman A**, Fishman A. Uterine rupture following conservative surgery for interstitial pregnancy. *Eur J Obstet Gynecol Reprod Biol* 1992; **44**: 237-239 [PMID: 1607064 DOI: 10.1016/0028-2243(92)90105-8]

32 **Downey GP**, Tuck SM. Spontaneous uterine rupture during subsequent pregnancy following non-excision of an interstitial ectopic gestation. *Br J Obstet Gynaecol* 1994; **101**: 162-163 [PMID: 7864910 DOI: 10.1111/j.1471-0528.1994.tb13086.x]

33 **Ben Nagi J**, Helmy S, Ofili-Yebovi D, Yazbek J, Sawyer E, Jurkovic D. Reproductive outcomes of women with a previous history of Caesarean scar ectopic pregnancies. *Hum Reprod* 2007; **22**: 2012-2015 [PMID: 17449510 DOI: 10.1093/humrep/dem078]

World Journal of Clinical Cases

Submit a Manuscript: https://www.f6publishing.com

World J Clin Cases 2023 February 6; 11(4): 797-808

DOI: 10.12998/wjcc.v11.i4.797

ISSN 2307-8960 (online)

ORIGINAL ARTICLE

Clinical Trials Study

Efficacy of incremental loads of cow's milk as a treatment for lactose malabsorption in Japan

Matsuri Hasegawa, Kazuko Okada, Satoru Nagata, Shigetaka Sugihara

Specialty type: Gastroenterology and hepatology

Provenance and peer review: Unsolicited article; Externally peer reviewed.

Peer-review model: Single blind

Peer-review report's scientific quality classification

Grade A (Excellent): 0
Grade B (Very good): B
Grade C (Good): C
Grade D (Fair): 0
Grade E (Poor): E

P-Reviewer: Pavlovic M, Serbia; Rocha R, Brazil; Zhang F, China

Received: October 17, 2022
Peer-review started: October 17, 2022
First decision: November 11, 2022
Revised: December 2, 2022
Accepted: January 5, 2023
Article in press: January 5, 2023
Published online: February 6, 2023

Matsuri Hasegawa, Shigetaka Sugihara, Department of Pediatrics, Tokyo Women's Medical University Medical Center East, Arakawa-ku 116-8561, Tokyo, Japan

Kazuko Okada, Department of Pediatrics, Okada Pediatric Clinic, Shinjuku-ku 169-0072, Tokyo, Japan

Satoru Nagata, Department of Pediatrics, Tokyo Women's Medical University, Shinjuku-ku 162-8666, Tokyo, Japan

Corresponding author: Matsuri Hasegawa, MD, Doctor, Department of Pediatrics, Tokyo Women's Medical University Medical Center East, 2-1-10, Nishiogu, Arakawa-ku 116-8561, Tokyo, Japan. hasegawa.matsuri@twmu.ac.jp

Abstract

BACKGROUND

Lactose intolerance (LI) is commonly seen in East Asian countries. Several studies showed that lactose or milk loading has been used as a treatment for lactose malabsorption (LM) in Western countries, but there have been no reports regarding this type of treatment in Japan. As lactose or milk loading requires ingestion of large amounts of lactose within a short period, this is considered to be too harsh for Japanese people because of their less habitual milk consumption (175 mL per day in average) than Western people. In this study, we demonstrated lactose tolerance acquisition in a suitable way for Japanese.

AIM

To examine the efficacy of lactose (cow's milk) loading treatment in patients with LM.

METHODS

Individuals with abdominal symptoms induced by milk or dairy products (LI symptoms) were identified with a questionnaire. A 20 g lactose hydrogen breath test (LHBT) was carried out to confirm LM diagnosis and to evaluate co-existence of small intestinal bacterial overgrowth (SIBO). Respondents diagnosed with LM were selected as study subjects and were treated with incremental loads of cow's milk, starting from 30 mL and increasing up to 200 mL at 4-7 d intervals. After the treatment, changes in symptoms and LM diagnostic value of 20 g LHBT were investigated. Stool samples pre- and post-treatment were examined for changes in intestinal microbiota using 16S rRNA sequencing. Informed consent was obtained

prior to each stage of the study.

RESULTS

In 46 subjects with LI symptoms (10-68 years old, mean age 34 years old) identified with the questionnaire, 35 (76.1%) were diagnosed with LM by 20 g LHBT, and 6 had co-existing SIBO. The treatment with incremental cow's milk was carried out in 32 subjects diagnosed with LM (14-68 years old, median age 38.5 years old). The mean period of the treatment was 41 ± 8.6 d. Improvement of symptoms was observed in 29 (90.6%; 95% confidence interval: 75.0%-98.0 %) subjects. Although 20 g LHBT indicated that 10 (34.5%) subjects had improved diagnostic value of LM, no change was observed in 16 (55.2%) subjects. Analysis of the fecal intestinal microbiota showed a significant increase in *Blautia* in 7 subjects who became symptom-free after the treatment (P = 0.0313).

CONCLUSION

LM was diagnosed in approximately 75% of the subjects who had LI. Incremental loads of cow's milk is regarded as a useful treatment for LM without affecting everyday life.

Key Words: Lactose Intolerance; Lactose Malabsorption; lactose loading treatment; Intestinal bacterial flora; Fecal microbiota

Core Tip: The incidence of lactose malabsorption (LM) is high in East Asians such as Japan. Colonic adaptation by daily consumption of milk or lactose has been known as a method to treat LM, reducing symptoms of lactose intolerance (LI). However, reports regarding such treatment have not been found in Japan. In this study, we clarified the prevalence of LM diagnosed among the Japanese patients who had LI symptoms, and evaluated the efficacy of incremental loads of cow's milk as a treatment for LM without affecting everyday life.

Citation: Hasegawa M, Okada K, Nagata S, Sugihara S. Efficacy of incremental loads of cow's milk as a treatment for lactose malabsorption in Japan. *World J Clin Cases* 2023; 11(4): 797-808
URL: https://www.wjgnet.com/2307-8960/full/v11/i4/797.htm
DOI: https://dx.doi.org/10.12998/wjcc.v11.i4.797

INTRODUCTION

Self-reported lactose intolerance (LI) affects approximately 45% of the Japanese population, according to a survey in 2015[1]. The average daily milk consumption by Japanese people was found to be around 175 mL, indicating less habitual milk consumption than that of Western countries, in spite of the nutritional benefit[2]. Current adjuvant treatment for lactose intolerance is self-administration of commercialized lactose-degrading enzyme before consuming milk or dairy products, yet its effect has been limited. Literature from other countries reported that colonic adaptation by daily milk or lactose consumption reduced LI symptoms in patients who also suffered lactose malabsorption (LM)[3], but patients who underwent this treatment were required to ingest large volumes of milk within a short period, which is considered to be too harsh for Japanese.

On the contrary, the abdominal symptoms can also be induced by psychological conditions, which should be ruled out from the lactose-induced symptoms[4,5]. To resolve this issue, LM is diagnosed non-invasively by the lactose hydrogen breath test (LHBT). In order to distinguish psychogenic symptoms, a single-blind comparative study (SBCS) was conducted on subjects with self-reported LI, as well as LHBT to diagnose LM. For subjects diagnosed with LM, lactose tolerance acquisition treatment is conducted in a suitable way for Japanese, followed by the assessment of the treatment efficacy.

As other studies have reported intestinal microbiota changes when clinical symptoms are alleviated by daily milk intake[6], the analysis of the intestinal microbiota was also conducted to assess the changes before and after the treatment.

MATERIALS AND METHODS

Subjects

A questionnaire survey was undertaken by Japanese people aged between 10 and 70 years to identify subjects with abdominal symptoms due to cow's milk and dairy products consumption. The questionnaire asked for the amount of milk and dairy products that caused abdominal symptoms and the severity of the symptoms, and people with milk allergy or other underlying diseases were excluded from the study (Figure 1).

This study was approved by the Tokyo Women's Medical University Ethics Committee. Informed consent was obtained from subjects prior to beginning each stage of the study.

Clinical examinations

Diagnostic studies: A 200 mL SBCS was conducted in order to identify abdominal symptoms caused by cow's milk (Study A), and 20 g LHBT was performed to diagnose LM in these subjects (Study B). Study A and Study B were carried out separately, with a minimum 1-wk interval.

Study A (200 mL SBCS): Lactose-reduced milk (LRM) (containing approximately 1.9 g of lactose/200 mL) and general milk (GM) (unadjusted milk: Containing approximately 9.8 g of lactose/200 mL), were used as the test materials of the study. The subjects started from ingesting 200 mL of the test material (LRM or GM) after fasting, and abdominal symptoms, including bloating, abdominal pain, borborygmi, gas, and diarrhea, were recorded for up to 3 h after the intake. Symptom severity was recorded and classified into five grades, using visual analog scales (0: Absence; 1: Trivial; 2: Mild; 3: Moderate; 4: Severe).

These two trial tests were separately performed with an at least 1-wk interval. Outcomes of this study were evaluated and classified into three groups based on the characteristic of symptoms as follows: (1) More obvious symptoms induced by GM than with LRM; (2) symptoms induced by LRM or unclear difference between the two materials (unevaluable group); and (3) no symptoms induced by either material.

Study B (lactose challenge test: 20 g LHBT): The subjects were requested to fast overnight, at least 5 h prior to the lactose challenge. At the start of LHBT, the subject exhaled into a gas collection bag, followed by ingestion of 20 g lactose dissolved in approximately 150 mL of water. Breath samples were then collected at 30-min intervals for 3 h (7 times in total). Abdominal symptom severity was recorded during the test. The breath hydrogen concentration was measured by using MicroLyzer 12i (QuinTron Inst. Co. Inc., United States).

The diagnostic criterion for LM was set as 20 ppm or more hydrogen level from the baseline. In addition, diagnostic evaluation of small intestinal bacterial overgrowth (SIBO) was considered to indicate that the elevated breath hydrogen concentration and abdominal symptoms coexisted within 60 min from the start of the test.

Stool collection for analysis of intestinal microbiota: Stool samples were collected from the subjects before and after the treatment to evaluate changes in the intestinal microbiota. The stool samples were appropriately stored frozen until DNA extraction and microbiota profiling by sequencing the V4 region of the 16S rRNA[7], which was performed by Bioengineering Lab. Co., Ltd. An increase or decrease of intestinal microbiota population change before and after the treatment was evaluated by comparing each bacterium occupancy rate out of total bacteria.

Treatment method for LM: Incremental loads of cow's milk

The subjects identified with LM were requested to start the treatment immediately after completing the diagnostic studies. Subjects began taking 30 mL of general milk around the same time every day on an empty stomach, and the amount of milk was gradually increased by 30 mL after 4-7 d. If they were anxious about abdominal symptoms, they were allowed to maintain the same volume up to 7 d. During the treatment period, subjects were required to record their general conditions, amount of milk ingested, and symptoms. Subjects were instructed to avoid taking any other milk or dairy products on an empty stomach, except for the milk supplied for the study, otherwise dairy products were allowed in small amounts during or after meals. Throughout the treatment, subjects were also instructed to avoid taking confounding medicines such as antibiotics, probiotics, prebiotics, antidiarrheal agents, and intestinal regulators.

All subjects were informed about LM treatment protocol and consent was obtained prior to starting the treatment. Participants were also given the right to withdraw from the study at any time.

Doctors (authors) routinely monitored the progress of each subject fortnightly during the treatment period *via* phone or e-mail correspondence. Study participants were obliged to report any decline in their physical condition and follow care instructions from the physician where needed.

After the subjects succeeded in taking 200 mL of milk for more than 4 d, a final examination was conducted to evaluate the efficacy of the treatment, described as below.

Questionnaire form to
persons who recognize abdominal symptoms due to intake of milk and dairy products

1) Do you have abdominal symptoms from intake of milk or dairy products?
( )YES ( )NO
If "Yes", please write down the frequency.
( ) Every time ( )Sometimes ( )Less frequent

2) What kind of symptoms did you have at the time? Please circle all that apply.
Diarrhea Abdominal pain Abdominal bloating
Borborygmus (rumbling stomach) Exhaust gas (farts) Nausea (feel sick)
Others ( )

3) What kind of dairy products did you take when you had abdominal symptoms?
Please circle all that apply. (Please write down the amount, if possible.)
Milk (mL) Whipped cream (tablespoon/scoop)
Soft serve ice cream (scoop) Ice cream (scoop) Yogurt (scoop)
Cheese (slices) Others ( )

4) Do you have milk allergy?
( ) NO ( ) I think "no" but never have taken the test
( ) YES ( ) I think "yes" but never have taken the test

5) Do you have any underlying diseases other than allergic diseases such as bronchial asthma and hay fever?
( ) NO ( ) YES (Please name the disease)

****

You may have lactose intolerance, meaning the enzyme that digests lactose contained in milk in the small intestine is insufficient, and such a condition is common in Japanese people. We are currently conducting a study to investigate a useful treatment method.
Should you be interested in our research, please contact us anytime.
We would love to explain in detail.

DOI: 10.12998/wjcc.v11.i4.797

Figure 1 Questionnaire form to persons who recognize abdominal symptoms due to intake of milk and dairy products. The questionnaire asks for the frequency and severity of LI symptoms, milk allergy, or other underlying diseases. There is also a brief introduction of our study to the subjects.

Evaluation of therapeutic effect of incremental cow's milk treatment

The subjects were requested to return their completed questionnaire to their doctor after the completion of the treatment. Degree of symptom improvement after the treatment was rated as follows: 0: No symptoms; 1: Trivial symptoms; 2: Mild symptoms but improved; 3: Moderate symptoms but improved, and 4: No improvement. Capable volume of milk tolerated without anxiety about abdominal symptoms was also rated: 1: Up to 50 mL; 2: Up to 100 mL; 3: Up to 150 mL; 4: Up to 200 mL.

Final examinations immediately after the treatment

After completion of the treatment, 20 g LHBT was performed to examine changes in lactose tolerance before and after the treatment.

In addition, stool was also collected at the end of the study from participants, in order to identify changes in the intestinal microbiota by methods described previously.

Statistical analysis

Values were presented as mean ± standard deviation (SD). Fisher's exact test, paired *t*-test, or Wilcoxon test was applied wherever appropriate. A two-sided *P* value of < 0.05 was considered statistically significant. Logistic regression analysis was also applied to the 95% confidence interval (CI). All statistical analyses were performed using JMP.

RESULTS

Subjects

Following the questionnaire survey conducted between July 2017 and December 2019 regarding abdominal symptoms caused by lactose consumption, 55 subjects were recruited and 9 subjects were excluded according to the exclusion criteria, some of whom refused to participate to this study (Figure 2). Hence, 46 subjects aged 10-68 years (mean age: 34.0 years; males/females: 16/30)

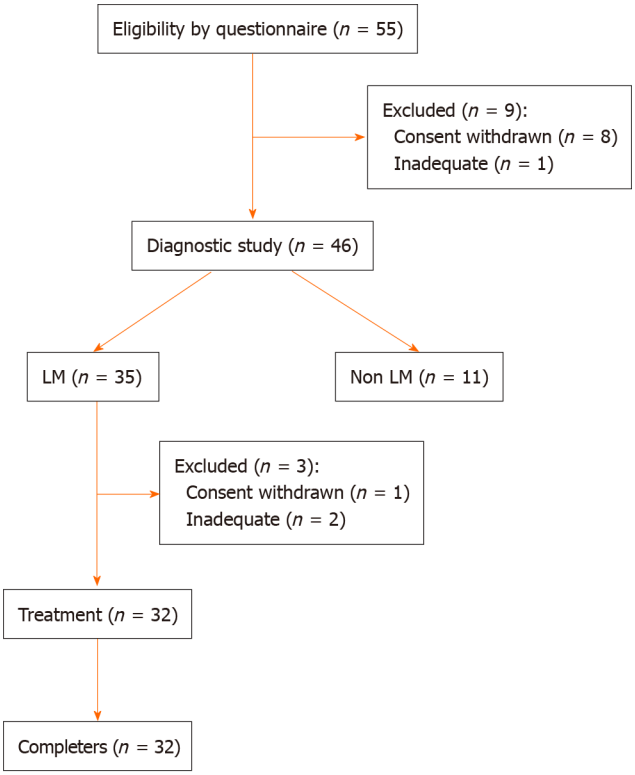

DOI: 10.12998/wjcc.v11.i4.797

Figure 2 Flowchart of participant recruitment and study processes. A questionnaire survey was conducted on 55 participants, and 20 g lactose hydrogen breath test was performed on 46 subjects who were assumed to have lactose intolerance symptoms. Thirty-five subjects were diagnosed with lactose malabsorption, of which 32 underwent and completed the treatment study without dropping out. LM: Lactose malabsorption.

participated in the study upon informed consent.

The amount of milk at which the subjects recognized abdominal symptoms during their daily lives was found to be: 100 mL in 9 (19.6%) subjects, 150 mL in 4 (8.7%), 200 mL in 19 (41.3%), and 250 mL or more in 7 (15.2%). Five (10.9%) subjects did not answer as they were avoiding milk consumption. The remaining 2 (4.3%) subjects had abdominal symptoms induced by other dairy products, such as fresh cream.

Results of clinical examination

Diagnostic studies: For study A, namely, 200 mL single-blind comparative study (200 mL SBCS), the results consisted of: (1) More obvious symptoms induced by general milk than lactose-reduced milk (tested positive) in 22 (47.8%) subjects; (2) unevaluable symptoms in 20 (43.5%) subjects (symptoms induced by lactose-reduced milk in 16 subjects and unclear difference between two materials in 4); and (3) no symptoms induced by either material (tested negative) in 4 subjects (8.7%) (Figure 3). For study B (diagnosis with LM from 20 g LHBT and evaluation of SIBO), 35 (76.1%) out of 46 subjects were diagnosed with LM. Moreover, abdominal symptoms appeared at early stage (within 60 min from the start of the test) in 6 out of 35 subjects, suggesting that SIBO correlated with the rise of breath-hydrogen.

Furthermore, the reliability of the LM diagnosis by SBCS was also assessed. Setting the LM diagnosis by 20 g LHBT as the gold standard, the diagnosis precision by SBCS was 80.8% (sensitivity 86.4%, specificity 50.0%).

Characteristics seen in LHBT among the group of unevaluable subjects classified based on the result of SBCS: The onset of abdominal symptoms during the LHBT in the unevaluable group was investigated, and the results are summarized in Tables 1 and 2.

Abdominal symptoms appeared within 30 min after lactose ingestion (early onset of symptoms) in 9 (64.3%) out of 14 unevaluable subjects diagnosed with LM (tested positive in LHBT) (Table 1). On the other hand, early onset of symptoms was found in 5 (83.3%) out of 6 unevaluable subjects diagnosed with non-LM (tested negative in LHBT) (Table 2). Overall, 14 (70.0%) out of 20 subjects in the unevaluable group had early onset of abdominal symptoms from LHBT.

Results of treatment with incremental loads of milk for LM

The treatment study was conducted on 32 out of 35 subjects who received a definitive diagnosis of LM, after excluding 3 subjects: 2 subjects were regarded as inappropriate and 1 did not agree to the informed

Table 1 Relation between results of the two tests: 200 mL single-blind comparative study and 20 g lactose hydrogen breathe test (LHBT) in LHBT positive subjects (*n* = 35)

SBCS		Time of abdominal symptom onset during LHBT (min)							
Result	***n***	**0**	**30**	**60**	**90**	**120**	**150**	**180**	**No appearance**
Positive	19	1	7	6	1	1	3		
Unevaluable	14		9	1	2	1			1
Negative	2		1						1
Total	35	1	17	7	3	2	3		2

SBCS: 200 mL single-blind comparative study. LHBT: 20 g lactose hydrogen breathe test. Positive: More obvious symptoms induced by general milk than by lactose-reduced milk. Unevaluable: Symptoms induced by lactose-reduced milk, or unclear difference between the two materials. Negative: No symptoms induced by either material. LHBT: Lactose hydrogen breathe test; SBCS: Single-blind comparative study.

Table 2 Relation between results of the two tests: 200 mL single-blind comparative study and 20 g lactose hydrogen breathe test (LHBT) in LHBT negative subjects (*n* = 11)

SBCS		Time when symptoms appeared during LHBT (min)							
Result	***n***	**0**	**30**	**60**	**90**	**120**	**150**	**180**	**No appearance**
Positive	3		1		1				1
Unevaluable	6		5						1
Negative	2				1				1
Total	11		6		2				3

SBCS: 200 mL single-blind comparative study. LHBT: 20 g lactose hydrogen breathe test. Positive: More obvious symptoms induced by general milk than by lactose-reduced milk. Unevaluable: Symptoms induced by lactose-reduced milk, or unclear difference between the two materials. Negative: No symptoms induced by either material. LHBT: Lactose hydrogen breathe test; SBCS: Single-blind comparative study.

consent.

The age distribution was 14-68 years, with a median age of 38.5 years (males: females = 8:24). The treatment period was 29-66 d (mean 41 ± 8.6 d). All 32 subjects were compliant with the treatment regimen and completed the study schedule.

Evaluation of symptom improvement: After the treatment, "no symptoms", "trivial symptoms", "mild symptoms but improved", "moderate symptoms but improved", and "no improvement" indicated in 7 (21.9%), 9 (28.1%), 8 (25.0%), 5 (15.6%), and 3 subjects (9.4%), respectively (Figure 4). Thus, symptoms were estimated to have improved in 29 (90.6%; 95%CI: 75.0%-98.0%) out of 32 subjects in total.

Volume of milk which could be tolerated without anxiety of abdominal symptoms was classified into 3 capacity volumes: 200 mL in 15 (51.8%) subjects, 150 mL in 7 (24.1%), and 100 mL in 7 (24.1%).

Comparison of diagnostic values for LM by 20 g LHBT before and after the treatment: Therapeutic effect was also evaluated by using objective data of LHBT on 29 subjects who showed symptom improvement (Figure 5). Changes were defined based on 15 ppm difference in diagnostic value before and after the treatment.

A decrease of more than 15 ppm was seen in 10 (34.5%) subjects, indicative of an improvement after the treatment. An increase of more than 15 ppm was observed in 3 (10.3%) subjects, whereas a difference of 15 ppm or less, meaning no change, was seen in 16 (55.2%) subjects.

Result of intestinal microbial analysis before and after the treatment

Fecal microbiota was assessed on 29 subjects who had therapeutic effects. There was no significant change in total bacterial occupancy before and after the treatment. However, there was a trending increase in *Lachnospiraceae Blautia* (median +0.65, $P = 0.0789$), and a trending decrease in *Lachnospiraceae [Ruminococcus]* (median -0.50, $P = 0.0773$). However, there was a significant change in bacterial occupancy rate based on the degree of symptom improvement. There was a significant increase of *Blautia* in 7 subjects who became symptom-free after the treatment ($P = 0.0313$) (Figure 6).

On the other hand, the change of diagnostic values of LHBT on the 7 subjects after the treatment varied: Decreased (improved) in 2 subjects, unchanged in 3, and increased in 2.

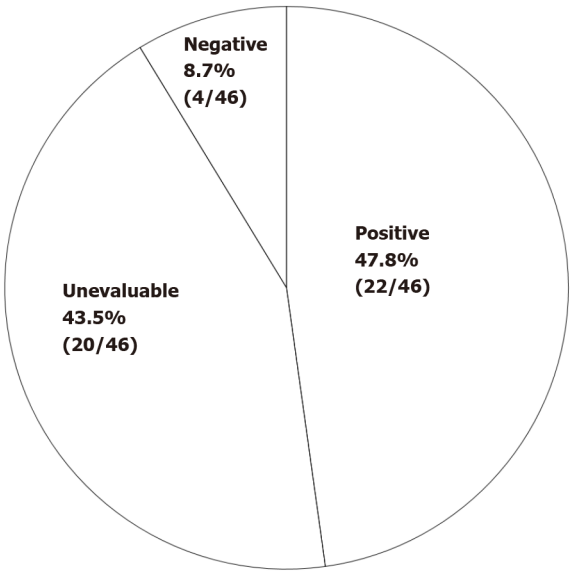

DOI: 10.12998/wjcc.v11.i4.797 **Copyright** ©The Author(s) 2023.

Figure 3 Outcomes of 200 mL single-blind comparative study. Positive: More obvious symptoms induced by general milk than by lactose-reduced milk. Unevaluable: Symptoms induced by lactose-reduced milk, or unclear difference between the two materials. Negative: No symptoms induced by either material.

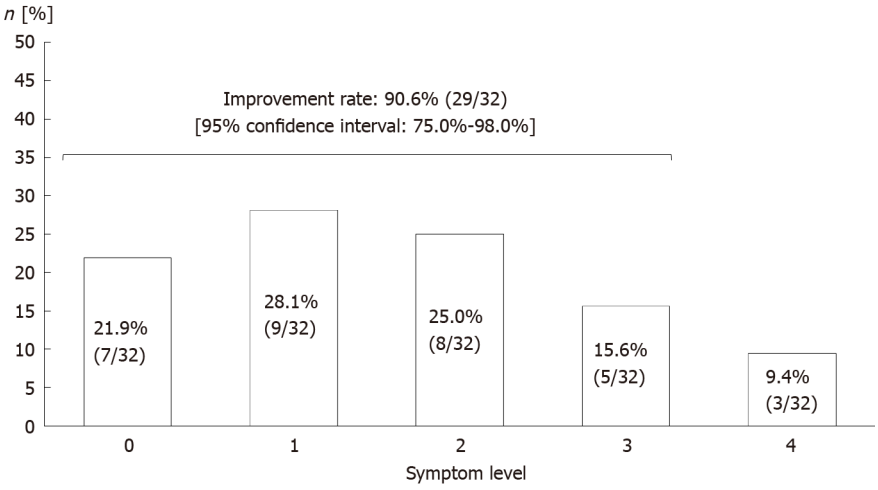

DOI: 10.12998/wjcc.v11.i4.797 **Copyright** ©The Author(s) 2023.

Figure 4 Evaluation of symptom improvement after the incremental milk treatment of lactose malabsorption subjects. Grades of symptom level: 0 = no symptoms; 1 = trivial symptoms; 2 = mild symptoms but improved; 3 = moderate symptoms but improved; 4 = no improvement. Symptom improvement was defined in grades from 0-3.

DISCUSSION

It has only been 50 years since LI was recognized and scientifically analyzed. Recently, LI was defined as a clinical syndrome characterized by abdominal symptoms after lactose consumption. However, LI needs to be distinguished from lactose maldigestion or malabsorption, which are also subclinical conditions, where LM can also be indicative of inefficient absorption of lactose caused by primary and secondary decrease of lactase activity or other intestinal conditions. Diagnosis of LI requires comparison with inert placebo, endorsed by a National Institute of Health conference[3,6,8,9].

LHBT is currently considered as the gold standard for diagnosing LM, and symptoms in this test are observed in a dosage-dependent manner. Recently, there have been many studies that apply a 20-25 g lactose dosage, as a more realistic dosage in LHBT for diagnosing LM[10]. Thus, 20 g of lactose was used in this study.

Our previous study showed that the prevalence of LM diagnosed by 20 g LHBT was 52% among 31 subjects (Japanese adults), regardless of the presence of subjective symptoms caused by milk or dairy product consumption[11]. Of all the subjects with self-reported LI symptoms, 76.1% were diagnosed with LM, suggesting that one quarter of the subjective symptoms may not be directly linked to LM.

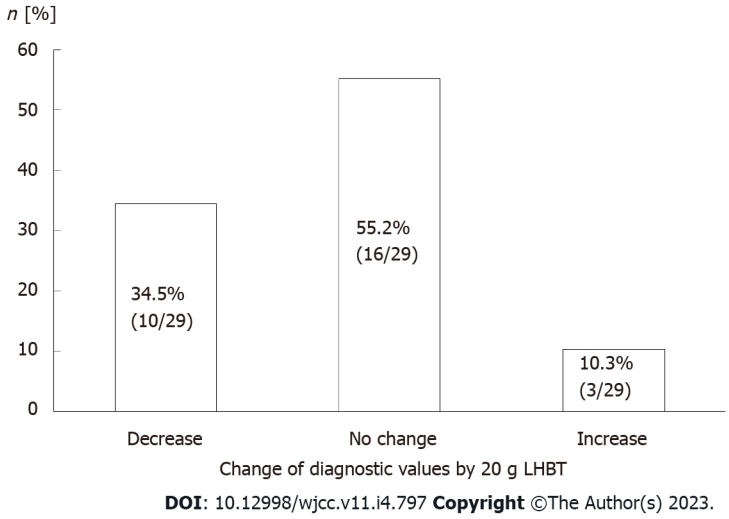

DOI: 10.12998/wjcc.v11.i4.797 **Copyright** ©The Author(s) 2023.

Figure 5 Comparison of diagnostic values of lactose malabsorption by 20 g lactose hydrogen breath test before and after the incremental milk treatment in subjects with improved symptoms. Decrease (improved): More than 15 ppm decrease; No change: Within 15 ppm difference; Increase: More than 15 ppm increase. LHBT: Lactose hydrogen breath test.

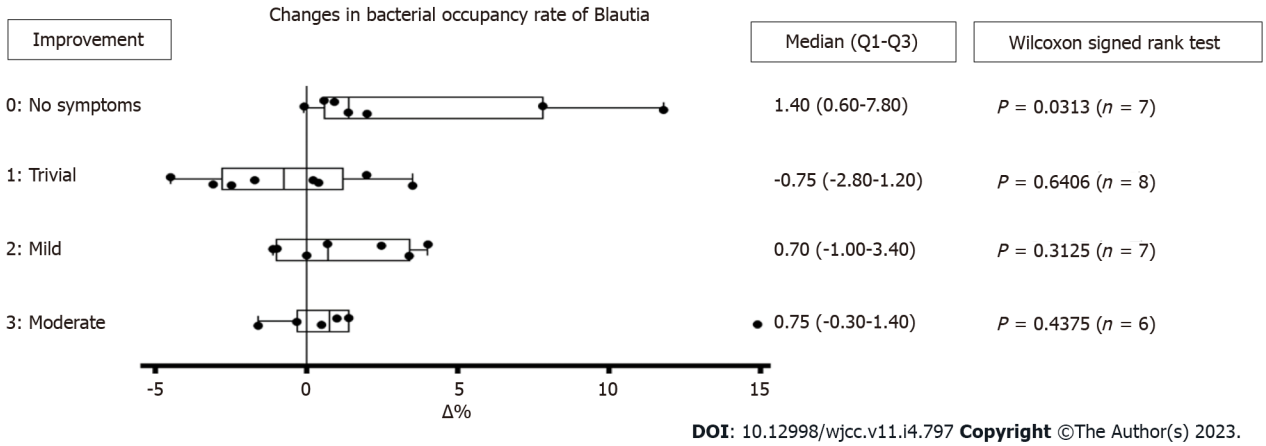

DOI: 10.12998/wjcc.v11.i4.797 **Copyright** ©The Author(s) 2023.

Figure 6 Analysis of *Blautia* in fecal microbiota before and after the incremental milk treatment. Change in bacterial occupancy rate of *Blautia* based on the degree of symptom improvement was observed in 28 subjects. *Blautia* was not detected in one out of 29 subjects. Degree of improvement: 0 = no symptoms; 1 = trivial symptoms; 2 = mild symptoms but improved; 3 = moderate symptoms but improved.

Furthermore, LM was distinguished from symptoms of self-reported LI by 200 mL SBCS. In our study, 43.5% of the subjects were found to be unevaluable, revealing that abdominal symptoms are often influenced by psychogenic conditions.

On diagnosing LM by LHBT in cases where oro-cecal transit time is within a normal range, the symptoms are believed to appear in 50-100 min after lactose ingestion. An increase in breath hydrogen is observed at least 60 min after lactose intake, peaking at around 120-150 min, indicating that breath hydrogen correlates with symptom onsets[12]. The "early onset of symptoms" was defined as appearance of abdominal symptoms within 30 min after lactose ingestion in LHBT, and accordingly, 70% of subjects in the unevaluable group tested by SBCS, had early onset of symptoms, suggesting a brain-gut interaction.

Moreover, this study showed that 6 out of 35 subjects diagnosed with LM were also suspected to have SIBO. Lactulose hydrogen breath test has been widely used to detect SIBO, while it does not have indicative criteria for SIBO. LHBT, on the other hand, can be useful for SIBO detection as an increase in breath hydrogen can be detected within 90 min after lactose ingestion. Thus, LM with SIBO can be distinguished from LM alone (by observing a peak of hydrogen after 90 min)[13]. However, a study of patients with chronic diarrhea in China, which applied hydrogen breath test with 10 g-lactulose loading and 20 g-lactose loading, reported that SIBO was more prevalent in patients with LI than those with LM. In this case, several overlapping pathological conditions were suspected[6,14].

Irritable bowel syndrome (IBS) is a common functional gastrointestinal (GI) disorder classified by Rome IV. IBS is characterized by abdominal pain associated with abnormal bowel habit, but IBS patients

can also suffer from other GI and non-GI symptoms, including psychological symptoms and psychiatric comorbidity[15]. Some studies in China reported that 80%-85% of the patients with diarrhea-predominant IBS also had LM[16,17].

Despite some limitations in evaluating IBS or SIBO, the LHBT provides many key pieces of information, such as transition of breath hydrogen and symptom onset during the test. Therefore, non-invasive 20 g LHBT is believed to be useful not only for diagnosing LM, but also for examining the cause of LI symptoms.

In Western countries, there are various methods of lactose load to treat LM, such as daily dose of 34 g lactose for 2 wk[5], incremental milk intake starting from 118 mL (4 oz) up to 708 mL (8 oz) in 6 d[18], and incremental lactose intake starting from 0.3-0.6 g/kg with adding 0.2 g/kg/d (max 1.0 g/kg) for 10-17 d[19]. In these studies, some participants refused to continue the treatments due to severe abdominal symptoms from lactose intake. In some reports from Europe, 12 g or less lactose was reported to be well tolerated with minimal or no symptoms[8,9,20], though even this low amount of lactose may still be intolerable for Japanese people. In our study, 9 out of 46 subjects had subjective symptoms caused by drinking 100 mL of milk (approximately 10 g of lactose), according to the questionnaire of self-reported LI symptoms. Hence, we started from 30 mL of milk intake and gradually increased the amount in every 4-7 d until 200 mL could be ingested successively. As a result, all subjects completed the treatment schedule without dropping out.

The mean treatment period was 41 d. After the treatment, 91% of the subjects showed improvement in their abdominal symptoms and 76% were able to drink 150-200 mL of milk at a time without anxiety of abdominal symptoms. These outcomes suggested that our original treatment for LM with ordinary milk was effective for Japanese patients without affecting quality of life. In addition, this treatment could be widely applied to Asian and African people suffering from LM[6].

Comparing the diagnostic values of LM by 20 g LHBT, undertaken before and after the treatment, abdominal symptoms improved only in one-third of the subjects and no change was seen in half of the subjects, suggesting that colonic adaptation was insufficient to see changes in diagnostic values regardless of improved symptoms. This could be due to limitations of this study such as lack of dietary restrictions except for milk, maximum amount of milk set at 200 mL, and insufficient sample size.

Some reports hypothesized that reduced symptoms were related to lactose adaptation of colonic bacteria, while other clinical studies reported that lactose induced growth of *Bifidobacteria* and *Lactobacillues* in intestinal microbiota[21,22]. Even though such bacteria were not observed in our study, it was interesting that there was a significant increase of fecal *Blautia* in 7 subjects who became symptom-free after the treatment. It is known that fecal *Blautia* is likely to decrease in patients who have obesity, liver diseases, and diabetes[23]. A fecal microbiota analysis in another study also had an interesting finding that *Blautia* significantly increased among subjects with LM after daily intake of 250 mL of whole milk for 4 wk[24]. Therefore, an increase of fecal *Blautia* found in our study indicated a favorable intestinal environment.

CONCLUSION

The treatment by incremental loads of ordinary cow's milk was useful in treating LM without affecting quality of life. As three-fourths of the subjects with LI symptoms in our study were further diagnosed with LM and showed improved lactose tolerance post-treatment, this treatment may also benefit people with LI symptoms but unknown LM status.

ARTICLE HIGHLIGHTS

Research background

Self-reported lactose intolerance (LI) has been known to have a high prevalence in Asian people. However, there has been no recent report in Japan regarding the prevalence of lactose malabsorption (LM). Some literature shows that colonic adaptation by daily milk or lactose ingestion reduces LI symptoms in patients with LM, but such treatment has not been reported in Japan.

Research motivation

According to the literature from Western countries, patients with LM who underwent milk or lactose loading therapy were required to ingest large volumes of milk within a short period. Applying the same treatment to Japanese people is considered to carry a high risk for abdominal symptoms during the treatment, due to less habitual consumption of milk than Western people. In this study, we implemented an original method of milk loading without affecting daily life of study subjects.

Research objectives

The aim of this study was to examine the efficacy of incremental cow's milk loading for treating patients with LM.

Research methods

We selected subjects with LI symptoms using a questionnaire, and the selected subjects underwent a 20 g lactose hydrogen breath test (LHBT) for diagnosis of LM. We then conducted the treatment of incremental loads of cow's milk on the subjects diagnosed with LM, starting from 30 mL and increasing up to 200 mL at 4-7 d intervals. After the treatment, improvement of symptoms and LM diagnostic value of LHBT were investigated. Stool samples pre- and post-treatment were examined for changes in the intestinal microbiota using 16S rRNA sequencing.

Research results

By LHBT, LM was diagnosed in 35 (76%) out of 46 subjects with LI selected using the questionnaire. Improvement of abdominal symptoms after the treatment was seen in 29 (91%) out of 35 subjects with LM. The diagnostic value measured in LHBT before and after the treatment improved in 10 (35%) out of 29 subjects with reduced symptoms, and no change was observed in 16 (55%) subjects. Analysis of fecal microbiota showed a significant increase of *Blautia* in 7 subjects who became symptom-free after the treatment.

Research conclusions

Incremental loads of cow's milk that are commercially available is a useful treatment for LM without affecting daily lives of Japanese people.

Research perspectives

The incremental loads of cow's milk can be widely utilized for LM patients, as well as improve their quality of life. We would like to further verify the efficacy of the same treatment in a longer term study.

ACKNOWLEDGEMENTS

The authors thank Naoki Shimojo, Department of Pediatrics, Graduate School of Medicine, Chiba University, for his excellent advice. We also thank Sadako Nakamura, PhD, Jumonji University, and Yasushi Kawai, PhD, Nihon University, for their support in recruiting volunteers and for giving us useful comments throughout the study.

FOOTNOTES

Author contributions: Okada K and Nagata S conceptualized and designed the study outline; Hasegawa M and Okada K acquired, analyzed, and interpreted the data, as well as drafted the manuscript; Nagata S advised the interpretation of the data and the critical revision of the manuscript for important intellectual content; Sugihara S obtained funding and supervised the critical revision of the manuscript for important intellectual content; all authors have reviewed and approved the final manuscript.

Supported by Grants of J-milk (Japan Dairy Association).

Institutional review board statement: This work was approved by Tokyo Women's Medical University Hospital Ethics Committee (approval number 160506).

Clinical trial registration statement: The trial described in this work was registered at https://center6.umin.ac.jp/cgi-open-bin/ctr/ctr_view.cgi?recptno=R000026742 under trial number: UMIN 000023298.

Informed consent statement: All study participants, or their legal guardian, provided informed written consent prior to study enrollment.

Conflict-of-interest statement: All the authors declare that they have no conflicts of interest for this article.

Data sharing statement: No additional date are available.

CONSORT 2010 statement: The authors have read the CONSORT 2010 statement, and the manuscript was prepared and revised according to the CONSORT 2010 statement.

Country/Territory of origin: Japan

ORCID number: Matsuri Hasegawa 0000-0001-9304-6849.

S-Editor: Liu JH
L-Editor: Wang TQ
P-Editor: Liu JH

REFERENCES

1 **J-milk (Japan Dairy Association)**. The investigation about eating habit trend of milk, dairy products in 2015. March 31, 2016. Available from: https://www.j-milk.jp/report/trends/f13cn00000000x9t-att/hn0mvm0000000tv1.pdf
2 The information of livestock: Investigation and Information Department, Agriculture & Livestock Industries Corporation. The investigation about consumption trend of milk, dairy products in 2015. 2016 May. Available from: https://www.alic.go.jp/content/000124597.pdf
3 **Szilagyi A**. Adaptation to Lactose in Lactase Non Persistent People: Effects on Intolerance and the Relationship between Dairy Food Consumption and Evalution of Diseases. *Nutrients* 2015; **7**: 6751-6779 [PMID: 26287234 DOI: 10.3390/nu7085309]
4 **Zheng X**, Chu H, Cong Y, Deng Y, Long Y, Zhu Y, Pohl D, Fried M, Dai N, Fox M. Self-reported lactose intolerance in clinic patients with functional gastrointestinal symptoms: prevalence, risk factors, and impact on food choices. *Neurogastroenterol Motil* 2015; **27**: 1138-1146 [PMID: 26095206 DOI: 10.1111/nmo.12602]
5 **Briet F**, Pochart P, Marteau P, Flourie B, Arrigoni E, Rambaud JC. Improved clinical tolerance to chronic lactose ingestion in subjects with lactose intolerance: a placebo effect? *Gut* 1997; **41**: 632-635 [PMID: 9414969 DOI: 10.1136/gut.41.5.632]
6 **Fassio F**, Facioni MS, Guagnini F. Lactose Maldigestion, Malabsorption, and Intolerance: A Comprehensive Review with a Focus on Current Management and Future Perspectives. *Nutrients* 2018; **10** [PMID: 30388735 DOI: 10.3390/nu10111599]
7 **von Ahsen U**, Noller HF. Identification of bases in 16S rRNA essential for tRNA binding at the 30S ribosomal P site. *Science* 1995; **267**: 234-237 [PMID: 7528943 DOI: 10.1126/science.7528943]
8 **Shaukat A**, Levitt MD, Taylor BC, MacDonald R, Shamliyan TA, Kane RL, Wilt TJ. Systematic review: effective management strategies for lactose intolerance. *Ann Intern Med* 2010; **152**: 797-803 [PMID: 20404262 DOI: 10.7326/0003-4819-152-12-201006150-00241]
9 **Suchy FJ**, Brannon PM, Carpenter TO, Fernandez JR, Gilsanz V, Gould JB, Hall K, Hui SL, Lupton J, Mennella J, Miller NJ, Osganian SK, Sellmeyer DE, Wolf MA. National Institutes of Health Consensus Development Conference: lactose intolerance and health. *Ann Intern Med* 2010; **152**: 792-796 [PMID: 20404261 DOI: 10.7326/0003-4819-152-12-201006150-00248]
10 **Gasbarrini A**, Corazza GR, Gasbarrini G, Montalto M, Di Stefano M, Basilisco G, Parodi A, Usai-Satta P, Vernia P, Anania C, Astegiano M, Barbara G, Benini L, Bonazzi P, Capurso G, Certo M, Colecchia A, Cuoco L, Di Sario A, Festi D, Lauritano C, Miceli E, Nardone G, Perri F, Portincasa P, Risicato R, Sorge M, Tursi A; 1st Rome H2-Breath Testing Consensus Conference Working Group. Methodology and indications of H2-breath testing in gastrointestinal diseases: the Rome Consensus Conference. *Aliment Pharmacol Ther* 2009; **29** Suppl 1: 1-49 [PMID: 19344474 DOI: 10.1111/j.1365-2036.2009.03951.x]
11 **Kosuge N**, Yoshimatsu M, Tsukada K. Investigation into lactose absorption in Japanese children and adults- Relation to intake of milk and dairy products-. *J Jpn Pediatr Soc* 1998; **102**: 1090-1097
12 **Law D**, Conklin J, Pimentel M. Lactose intolerance and the role of the lactose breath test. *Am J Gastroenterol* 2010; **105**: 1726-1728 [PMID: 20686460 DOI: 10.1038/ajg.2010.146]
13 **Pimentel M**, Saad RJ, Long MD, Rao SSC. ACG Clinical Guideline: Small Intestinal Bacterial Overgrowth. *Am J Gastroenterol* 2020; **115**: 165-178 [PMID: 32023228 DOI: 10.14309/ajg.0000000000000501]
14 **Zhao J**, Fox M, Cong Y, Chu H, Shang Y, Fried M, Dai N. Lactose intolerance in patients with chronic functional diarrhoea: the role of small intestinal bacterial overgrowth. *Aliment Pharmacol Ther* 2010; **31**: 892-900 [PMID: 20132150 DOI: 10.1111/j.1365-2036.2010.04252.x]
15 **Mearin F**, Lacy BE, Chang L, Chey WD, Lembo AJ, Simren M, Spiller R. Bowel Disorders. *Gastroenterology* 2016 [PMID: 27144627 DOI: 10.1053/j.gastro.2016.02.031]
16 **Yang JF**, Fox M, Chu H, Zheng X, Long YQ, Pohl D, Fried M, Dai N. Four-sample lactose hydrogen breath test for diagnosis of lactose malabsorption in irritable bowel syndrome patients with diarrhea. *World J Gastroenterol* 2015; **21**: 7563-7570 [PMID: 26140004 DOI: 10.3748/wjg.v21.i24.7563]
17 **Wang Y**, Xiong L, Gong X, Li W, Zhang X, Chen M. Small intestinal bacterial overgrowth as an uncommon cause of false positive lactose hydrogen breath test among patients with diarrhea-predominant irritable bowel syndrome in Asia. *J Gastroenterol Hepatol* 2015; **30**: 995-1000 [PMID: 25470082 DOI: 10.1111/jgh.12862]
18 **Mummah S**, Oelrich B, Hope J, Vu Q, Gardner CD. Effect of raw milk on lactose intolerance: a randomized controlled pilot study. *Ann Fam Med* 2014; **12**: 134-141 [PMID: 24615309 DOI: 10.1370/afm.1618]
19 **Hertzler SR**, Savaiano DA. Colonic adaptation to daily lactose feeding in lactose maldigesters reduces lactose intolerance. *Am J Clin Nutr* 1996; **64**: 232-236 [PMID: 8694025 DOI: 10.1093/ajcn/64.2.232]
20 **Misselwitz B**, Butter M, Verbeke K, Fox MR. Update on lactose malabsorption and intolerance: pathogenesis, diagnosis

and clinical management. *Gut* 2019; **68**: 2080-2091 [PMID: 31427404 DOI: 10.1136/gutjnl-2019-318404]

21 **Szilagyi A**, Shrier I, Heilpern D, Je J, Park S, Chong G, Lalonde C, Cote LF, Lee B. Differential impact of lactose/Lactase phenotype on colonic microflora. *Can J Gastroenterol* 2010; **24**: 373-379 [PMID: 20559580 DOI: 10.1155/2010/649312]

22 **Ito M**, Kimura M. Influence of lactose on faecal microflora in lactose maldigestors. *Microb Ecol Health Dis* 1993; **6**: 73-76 [DOI: 10.3109/08910609309141564]

23 **Liu X**, Mao B, Gu J, Wu J, Cui S, Wang G, Zhao J, Zhang H, Chen W. Blautia-a new functional genus with potential probiotic properties? *Gut Microbes* 2021; **13**: 1-21 [PMID: 33525961 DOI: 10.1080/19490976.2021.1875796]

24 **Li X**, Yin J, Zhu Y, Wang X, Hu X, Bao W, Huang Y, Chen L, Chen S, Yang W, Shan Z, Liu L. Effects of Whole Milk Supplementation on Gut Microbiota and Cardiometabolic Biomarkers in Subjects with and without Lactose Malabsorption. *Nutrients* 2018; **10** [PMID: 30279333 DOI: 10.3390/nu10101403]

World Journal of Clinical Cases

Submit a Manuscript: https://www.f6publishing.com

World J Clin Cases 2023 February 6; 11(4): 809-820

DOI: 10.12998/wjcc.v11.i4.809

ISSN 2307-8960 (online)

ORIGINAL ARTICLE

Observational Study

Transdiagnostic considerations of mental health for the post-COVID era: Lessons from the first surge of the pandemic

Sari Goldstein Ferber, Gal Shoval, Rodolfo Rossi, Viviana Trezza, Giorgio Di Lorenzo, Gil Zalsman, Aron Weller, J John Mann

Specialty type: Medicine, research and experimental

Provenance and peer review: Invited article; Externally peer reviewed.

Peer-review model: Single blind

Peer-review report's scientific quality classification

Grade A (Excellent): 0
Grade B (Very good): 0
Grade C (Good): C, C
Grade D (Fair): 0
Grade E (Poor): 0

P-Reviewer: Di Meglio L, Italy; Nithiyaraj E, India

Received: September 4, 2022
Peer-review started: September 4, 2022
First decision: October 30, 2022
Revised: November 28, 2022
Accepted: January 16, 2023
Article in press: January 16, 2023
Published online: February 6, 2023

Sari Goldstein Ferber, Aron Weller, Department of Psychology, Bar Ilan University, Ramat Gan 5290002, Israel

Gal Shoval, Department of Neuroscience, Princeton University, Princeton NJ 08544, United States

Gal Shoval, Gil Zalsman, Geha Mental Health Center, Petah Tiqva, Israel and Sackler Faculty of Medicine, Tel Aviv University, Tel Aviv 77096, Israel

Rodolfo Rossi, Department of Systems Medicine, University of Rome Tor Vergata, Rome 00133, Italy

Viviana Trezza, Department of Science, Rome Tre University, Rome 00154, Italy

Giorgio Di Lorenzo, Department of Psychiatry, Rome University Tor Vergata, Rome 00179, Italy and IRCCS—Fondazione Santa Lucia, Rome 00179, Italy

Gil Zalsman, J John Mann, Division of Molecular Imaging and Neuropathology, Department of Psychiatry, Columbia University, NY, 10032, United States

Corresponding author: Sari Goldstein Ferber, PhD, Additional Professor, Department of Psychology, Bar Ilan University, Geha St, Ramat Gan 5290002, Israel. sari.goldstein@biu.ac.il

Abstract

BACKGROUND

The Coronavirus disease 19 (COVID-19)-related psychiatric burden partly results from prolonged social stress world-wide. Studies have examined the psychiatric impact of COVID-19 on Diagnostic and Statistical Manual of Mental Disorders, Fifth Edition (DSM 5) and International Classification of Diseases 11th Revision (ICD-11) categories, implicating multiple diagnoses, complicating clinical management.

AIM

To verify whether COVID-19-related psychopathology spans multiple DSM-5 and ICD-11 diagnoses, but not in a random pattern. Consequently, empirical analysis of the multiple associated symptoms will better describe COVID-19-related psychopathology.

METHODS

We conducted a bi-national study during the first surge of the pandemic: an Italian sample (n = 21217, studied March-April 2020); and three representative longitudinal samples from Israel (n = 1276, 1189, and 1432 respectively, studied May-July 2020). Data in Italy were collected by a national internet-based survey with an initially approached sample of about one million persons and in Israel by the Israeli Central Bureau of Statistics using probability-based national representative sampling. Data analysis focused on the frequency and patterns of reported multiple mental health symptoms.

RESULTS

Combinations with all symptoms were more prevalent than combinations with fewer symptoms, with no majorities-minorities differences in both countries, demonstrating the generalizability of the transdiagnostic pattern of mental health issues in both nations. A history of previous mental disorder (Italian study) and an increase in symptom prevalence over time (Israel study) were associated with an increased number of symptoms. Conclusions: Based on finding correlated symptom diversity spanning conventional diagnostic categories, we suggest that the pattern of mental health issues associated with the COVID-19 pandemic is transdiagnostic.

CONCLUSION

The findings have implications for improving prevention and treatment of COVID-19 related psychopathology and for post-pandemic times in conditions resulting from multiplicity of stressors with mixed symptomatology in the clinical picture.

Key Words: Post-COVID-19; Diagnosis; Stress; Mental disorders; Transdiagnosis; Reactive psychiatric disorders

Core Tip: The unique clinical picture that characterizes the reaction to the pandemic as shown in our findings may raise broader thoughts on diagnostic considerations regarding a new category beyond pandemic mental health symptomatology. This suggested category as outlined in our recently published review in the World Journal of Psychiatry may involve transdiagnostic criteria resulting from multiplicity of stressors. This type of condition may be apparent in the post-coronavirus disease (COVID) era although not recognized to date. Our findings showing this type of complex transdiagnostic symptomatology in two countries indicate a need for a new understanding of the COVID-19 pandemic's psychopathological consequences in the post-COVID era.

Citation: Goldstein Ferber S, Shoval G, Rossi R, Trezza V, Di Lorenzo G, Zalsman G, Weller A, Mann JJ. Transdiagnostic considerations of mental health for the post-COVID era: Lessons from the first surge of the pandemic. *World J Clin Cases* 2023; 11(4): 809-820

URL: https://www.wjgnet.com/2307-8960/full/v11/i4/809.htm

DOI: https://dx.doi.org/10.12998/wjcc.v11.i4.809

INTRODUCTION

Prolonged stressful situations erode coping capacity[1,2]. The pervasive and persistent stress of the Coronavirus disease 19 (COVID-19) pandemic resulted in psychopathology afflicting millions worldwide. The unique impact of the pandemic on mental health is still pervasive and a significant burden on society[3], including the difficulties in diagnosis[4], which span diagnostic boundaries in Diagnostic and Statistical Manual of Mental Disorders, Fifth Edition (DSM-5) and International Classification of Diseases 11th Revision (ICD-11) defined disorders[5,6]. Past pandemics have raised similar concerns regarding mental health[7,8]. This highlights the concern regarding multiple diagnoses being given to a single patient and excessive use of the term "comorbidity", with confusing implications for prevention and treatment[9].

A debate about diagnosis has commenced[10-13] and a transdiagnostic approach has been suggested by previous studies[12,14,15]. To examine the transdiagnostic hypothesis, we conducted two independent studies of psychiatric data collected during the first surge of the COVID-19 pandemic, one in Italy and one in Israel. We further hypothesized that the resultant pattern of symptom complexity will be robust enough to be detected in two different countries with different survey methodologies.

MATERIALS AND METHODS

Study 1: A Representative Sample of the Israeli Population - Three Surveys.

Methods: The Israeli Central Bureau of Statistics (CBS) collected data on mental health at three different time points during the early months of the COVID-19 pandemic: 1st survey: 26/4/-1/5/2020; and 2nd survey: 11-14/5/2020; 3rd survey: 12-16/7/2020. Informed consent was obtained verbally, and this was a prerequisite for continuing with the survey questions. The survey was conducted under the Ethical Code, a section on the CBS ethical requirements and commitments, which is part of the Israeli Law of Statistics 1972 regulating the CBS functions. This study complies with the Declaration of Helsinki.

The sampling sought to represent all the Israeli population age 21 years and above except for dispersed rural Bedouins in the South and institutionalized individuals.

The 1st survey sample included 2,279 people, of whom 56% responded by phone. The 2nd survey sample included 2,271 people of whom 52% responded by phone. The 3rd survey sample included 2,291 people of whom 62.5% responded by phone. The Arab minority participants were 15.1% of the sample in the 1st survey, 15.3% in the 2nd, and 17.7% in the 3rd survey.

Sample characteristics: Gender and age distributions (see Table 1).

To correct for potential non-responder biases, respondent distributions were weighted by the CBS according to their known gender, age, and geographical distributions in the Israeli general population. CBS also tested for data reliability in their standard methods.

Mental health outcome measures: In the 1st survey, 3 mental health symptoms were assessed: Perceived depression, perceived anxiety and perceived loneliness. In the 2nd and 3rd surveys, an additional symptom was added: COVID-19-related phobia.

Data analysis: From these reports, we calculated the proportion of people that reported suffering from a combination of 2, 3, or 4 symptoms. We compared these proportions over the three surveys to assess progression over the ongoing pandemic. To test statistically whether there was a change in the proportion of people that suffer from a combination of symptoms, we used a 2-sample equality of proportions test. We compared the estimated proportion of people suffering from at least 2, 3, or 4 symptoms to that observed in previous surveys (i.e., Survey 2 *vs* Survey 1, and Survey 3 *vs* Survey 1 and 2).

In addition, we identified the most common combination of 3 symptoms (in the 2nd and 3rd surveys).

The major ethnic minority group in Israel is Israeli Arab and the majority group is Israeli Jew. We compared the two groups on the relative proportions of 3- and 4-combined symptoms.

To understand the associations between the four mental health symptoms studied, we performed a Pearson product-moment correlation matrix for them in each survey, separately.

Bonferroni corrections for multiple comparisons were conducted.

Study 2: A survey in Italy during the peak of the COVID-19 pandemic

Study Design: This cross-sectional web-based observational study is a part of a long-term project monitoring mental health outcomes in the general population. The survey was anonymous, and confidentiality was assured. Three weeks after the beginning of the lockdown in Italy, the survey was conducted using convenient sampling. Every person living in Italy ≥ 18 years was eligible. The study was approved by the local Institutional Review Board (IRB) at the University of L'Aquila. Online written consent was obtained from all participants. Participants could terminate the survey at any time as approved by the IRB. This study complies with the Declaration of Helsinki.

Sampling strategy and online questionnaire dissemination: An online questionnaire was presented to the Italian population between March 25th and April 7th. The investigated timeframe corresponded to Italy's first contagion peak (https://who.sprinklr.com/). This general population questionnaire was disseminated using sponsored adverts on Facebook®. The questionnaire asked participants to re-share the questionnaire link. Using the Facebook Ads app, it was estimated that the number of link clicks was about 100,000, and the advertisement reached one million people.

Sample characteristics: The demographic characteristics of the sample are presented in Table 2. Briefly, about 80% were women, 48% were 40 years old or older, 2.5% were foreigners and 28% reported previous psychiatric history.

Outcome Measures: The following psychometric scales were used and covered the previous two weeks: The Global Psychotrauma Screen (GPS) post-traumatic stress symptoms (PTSS) subscale (GPS-PTSS)[16, 17]: The validated version of PTSS was used. PTSS were considered of clinical relevance if more than 3 out of five 5 symptoms were reported as present.

The 9-item Patient Health Questionnaire (PHQ-9)[18], using the cut-off for severe depression symptoms at ≥ 15. The validated version of this questionnaire was used.

The 7-item Generalized Anxiety Disorder scale (GAD-7)[19], using the cut-off for severe anxiety symptoms at ≥ 15. The validated version of this scale was used.

Table 1 Gender and age distributions of the Israeli samples

Gender distribution		
Survey 1		
Gender	Count	Frequency
Men	541	47.10%
Women	607	52.90%
Survey 2		
Gender	Count	Frequency
Men	528	46.70%
Women	602	53.30%
Survey 3		
Gender	Count	Frequency
Men	684	48.75%
Women	719	51.25%
Age-group distribution		
Survey 1		
Age	Count	Frequency
21-44	509	44.30%
45-64	351	30.60%
65 +	288	25.10%
Survey 2		
Age	Count	Frequency
21-44	507	44.90%
45-64	345	30.50%
65 +	278	24.20%
Survey 3		
Age	Count	Frequency
21-44	664	47.30%
45-64	419	29.90%
65 +	320	22.80%

GPS- Post-Traumatic Stress Disorder-Negative Affect (PTSD-NA): 11 items, including symptoms related to disturbances in self-organization, anxiety, depression, self-harm, substance abuse, and other physical, emotional, or social problems. This cluster of symptoms is related to the Disturbance in Self Organization dimension of Complex PTSD.

The 10-item Perceived Stress Scale (PSS)[20], using quartiles such that the upper quartile was separated from the rest.

Data analysis: We analyzed the frequency of all combinations of symptoms, to determine the most frequent combinations of 3, 4, and 5 symptoms. We also identified the pattern of the most prevalent combination of symptoms. In addition, we used proportion tests to compare Italians and foreigners, and separately people with and without previous psychiatric history, on the frequency of reporting a combination of 3, 4, and 5 symptoms. Bonferroni corrections for multiple comparisons were conducted.

RESULTS

Study 1 The Israeli surveys

The Pearson correlations between pairs of symptoms were significant in all 3 surveys; see Table 3.

Table 2 Gender, age, nationality, and previous psychiatric history distributions of the Italian sample

Gender	Frequency	Percentage
Men	4122	19.40%
Women	17095	80.60%
Age	Frequency	Percentage
20-39	10894	51.30%
40-64	10118	47.70%
65-74	180	0.85%
75 +	25	0.10%
Foreign	Frequency	Percentage
Foreigner	516	2.40%
Italian	20701	97.60%
Psychiatric history	Frequency	Percentage
No	15160	71.40%
Yes	6075	25.88%

Table 3 The association between the three symptoms in the Israeli sample

	Loneliness	Depression	Anxiety
Survey 1			
Loneliness	1		
Depression	0.6364[1]	1	
Anxiety	0.5027[1]	0.581[1]	1
Survey 2			
Loneliness	1		
Depression	0.6364[1]	1	
Anxiety	0.5027[1]	0.577[1]	1
Phobia	0.1638[1]	0.1684[1]	0.3145[1]
Survey 3			
Loneliness	1		
Depression	0.7172192[1]	1	
Anxiety	0.4570808[1]	0.5448582[1]	1
Phobia	0.1467067[1]	0.1770808[1]	0.3177728[1]

[1]P < 0.0001.

Analysis of symptom patterns: Table 4 shows that in the 1st survey, 22.1% (95%CI: 19.7-24.5) reported all three symptoms, Depression, Loneliness, and Anxiety, significantly more than those reporting the most frequent 2-symptom pattern (Depression and Anxiety; 6.4%, 95%CI: 4.9-7.8; $P < 0.001$).

In the 2nd survey, 13.3% reported three symptoms and an additional 20.1% reported all four symptoms, totaling about one-third of the population. The prevalence of the four-symptom combination (95%CI: 17.8-22.4) was greater than the most prevalent 3-symptom combination (Phobia, Anxiety and Depression, 5.58%, 95%CI: 4.2-6.9, $P < 0.001$).

In the 3rd survey, 12.8% reported three symptoms, and an additional 24.3%, reported all four symptoms. The prevalence of the four-symptom combination (95%CI: 21.8-26.3) was greater than the most prevalent 3-symptom combination (Phobia, Anxiety and Depression, 7.32%, 95%CI: 6.0-8.7, $P < 0.001$).

Table 4 Frequency of reported symptoms in all three Israeli surveys

Number of symptoms	Count	Frequency
Survey 1		
0	512	44.6%
1	239	20.8%
2	143	12.5%
3	254	22.1%
Survey 2		
0	175	15.5%
1	359	31.8%
2	219	19.4%
3	150	13.3%
4	227	20.1%
Survey 3		
0	159	11.3%
1	396	28.2%
2	328	23.4%
3	179	12.8%
4	341	24.3%

Analysis of quantitative progression of symptom complexity over time: Survey 2 produced a significantly greater prevalence of 2 or 3 combined symptoms, compared to Survey 1 ($P < 0.0001$ and $P < 0.001$, respectively).

Survey 3 produced a greater prevalence of 4 combined symptoms, compared to Survey 2 ($P < 0.01$), attesting to the increase in the prevalence of a complex of symptoms over time.

The frequency of 3 and 4 combined complaints in the Arab compared with the Jewish sub-populations did not differ in any of the 3 surveys (data not shown).

Study 2 Italian general population

All Pearson correlations between pairs of symptoms were significant ($P < 0.001$; Table 5).

Analysis of symptom patterns: Table 6 presents all combinations of symptoms reported in the Italian sample. The most frequent 3-symptom combination was PTSS, Depression, and PTSD-NA (3.3%), compared to the other 3-symptom combinations. The most frequent 4-symptom combination was Anxiety, PTSS, Depression, and PTSD-NA (3.2%), compared to the other 4-symptom combinations. The prevalence of the 5-symptom combination, Anxiety, Perceived stress, PTSS, Depression, and PTSD-NA (9.0%, 95%CI: 8.5-9.3) was greater than of the most prevalent 3- (95%CI: 3.0-3.5) and 4-symptom combinations (95%CI: 2.9-3.4, $P < 0.001$).

This combination of prevalence was comparable in Italians and foreigners. In addition, there were no differences detected between Italians and foreigners in the most frequent symptom combinations.

A proportion test was performed to compare Italians and foreigners that suffered from a combination of three symptoms: 11.3% of Italians (2332 out of 20701) and 14.9% of foreigners (77 out of 516) experienced 3 symptoms. There was a higher rate in foreigners ($P = 0.0119$).

Nine point three percent of Italians (1918 out of 20701) and 10.7% of foreigners (55 out of 516) experienced four symptoms. There was no significant difference between the two populations' proportions, $P = 0.3173$.

Nine percent of Italians (1860 out of 20701) and 8.9% of foreigners (46 out of 516) experienced five symptoms. There was no significant difference between the two populations' proportions, P value = 1.

Quantitative analysis of the prevalence of symptom complexity: The role of psychiatric history: A psychiatric history, compared to no psychiatric history, increased the likelihood of multiple symptoms, with an identical pattern of symptom combinations as described above.

Specifically, regarding the differences between people with psychiatric history (PH) and without PH (NoPH) - a history of psychiatric symptoms (Table 7), proportion tests were performed to compare the groups.

Table 5 Correlations between the mental health features in the Italian sample (*n* = 21217)

Mental health issue	Anxiety	Perceived stress	PTSS	Depression	PTSD-NA
Anxiety	1				
Perceived stress	0.522	1			
PTSS	0.3521	0.3423	1		
Depression	0.5866	0.4867	0.3301	1	
PTSD-NA	0.2097	0.213	0.3636	0.2228	1

Note: All correlations: $P < 0.001$. PTSS: Post-traumatic stress symptoms; PTSD-NA: Post-traumatic stress disorder-negative affect.

Table 6 Italian sample

Combination	Count	Frequency	Percentage
None	0	3500	16.5%
PTSD-NA	1	6725	31.7%
Depression	1	147	0.7%
Perceived stress	1	59	0.3%
Anxiety	1	22	0.1%
Depression, PTSD-NA	2	771	3.6%
PTSS, PTSD-NA	2	2995	14.1%
Perceived stress, PTSD-NA	2	424	2.0%
Perceived stress, Depression	2	31	0.2%
Anxiety, PTSD-NA	2	202	1.0%
Anxiety, Depression	2	45	0.2%
Anxiety, Perceived stress	2	8	0.0%
PTSS, Depression, PTSD-NA	3	693	3.3%
Perceived stress, Depression, PTSD-NA	3	292	1.4%
Perceived stress, PTSS, PTSD-NA	3	586	2.8%
Anxiety, Depression, PTSD-NA	3	357	1.7%
Anxiety, PTSS, PTSD-NA	3	301	1.4%
Anxiety, Perceived stress, PTSD-NA	3	137	0.7%
Anxiety, Perceived stress, Depression	3	43	0.2%
Perceived stress, PTSS, Depression, PTSD-NA	4	480	2.3%
Anxiety, PTSS, Depression, PTSD-NA	4	657	3.2%
Anxiety, Perceived stress, Depression, PTSD-NA	4	537	2.5%
Anxiety, Perceived stress, PTSS, PTSD-NA	4	281	1.3%
Anxiety, Perceived stress, PTSS, Depression, PTSD-NA	5	1906	9.0%

PTSS: Post-traumatic stress symptoms; PTSD-NA: Post-traumatic stress disorder-negative affect.

Thirteen point three percent of PH (805 out of 6057) and 10.6% of NoPH (1604 out of 15160) experienced 3 symptoms. There is a significant difference between the two populations' proportions, P value < 0.0001.

Twelve point nine percent of PH (782 out of 6057) and 7.9% of NoPH (1191 out of 15160) experienced 4 symptoms. There is a significant difference between the two populations' proportions, P value < 0.0001.

Table 7 The most frequent symptom combinations per number of symptoms, for people with and without Psychiatric history

Combination	Count	Frequency	Percentage
Psychiatric history			
PTSS, Depression, PTSD-NA	3	257	4.2%
Anxiety, PTSS, Depression, PTSD-NA	4	291	4.8%
Anxiety, Perceived stress, PTSS, Depression, PTSD-NA	5	885	14.6%
No Psychiatric history			
Perceived stress, PTSS, PTSD-NA	3	439	2.9%
Anxiety, PTSS, Depression, PTSD-NA	4	384	2.5%
Anxiety, Perceived stress, PTSS, Depression, PTSD-NA	5	1021	6.7%

PTSS: Post-traumatic stress symptoms; PTSD-NA: Post-traumatic stress disorder-negative affect.

Fourteen point six percent of PH (885 out of 6057) and 6.7% of NoPH (1021 out of 15160) experienced 5 symptoms. There is a significant difference between the two populations' proportions, P value < 0.0001.

DISCUSSION

We report evidence from studies in two different countries, on the presentation of complex symptomatology that crosses diagnostic boundaries, during the first surge of the COVID-19 pandemic. The complex of symptoms that we found correlated in severity. This suggests a common relationship or a single overarching disorder. This offers an alternative and perhaps more complete characterization of psychopathology compared with employing multiple diagnoses for the same patient[9]. Moreover, this pattern is observed within each of the two countries studied, despite different survey methods, and is found within ethnic subpopulations of both countries, attesting to the generalizability of the pattern. The more the number of symptoms or diagnostic categories reported, the greater the proportion of subjects with past psychiatric history, suggesting that the identified complex of symptoms is related to psychiatric vulnerability. The greater proportion of subjects reporting this pattern over time indicates a cumulative effect of prolonged stress conditions driving individuals towards this more complex combination of symptoms.

Because our findings span different diagnostic categories, we propose that this argues for the need for a broader, transdiagnostic perspective[4,21,22]. We note that even prior to the pandemic others suggested a transdiagnostic approach for better treatment[23-26]. Given these earlier considerations, the current study may support the implementation of the treatment and organizational guidelines published by the WPA[27]. Thus, our large binational study provides more robust support for a new perspective, termed by some researchers "COVID Stress Syndrome"[12,28], which crosses DSM 5 and ICD 11 boundaries. In addition, transdiagnostic considerations may be helpful for post-COVID-19 concerns, if multiple stressors are identified as triggers and complex symptomatology characterizes the clinical picture.

"Transdiagnostic" in the context of the COVID-19 pandemic

We searched the literature using Reference Citation analysis, PubMed and Google Scholar, focusing on the term "transdiagnostic" in the context of the COVID-19 pandemic. For the term "transdiagnostic" we identified 1284 references from 2019 to 2022. For the same years, in PubMed, 84 references were identified by the search "transdiagnostic and COVID-19". In Google Scholar, with the same terms and range of years, 5670 references were identified. In reviewing the literature found, we conclude that the "transdiagnostic" term is very popular and used in a too general manner, not specifying exactly which symptoms are associated with a more accurate diagnosis. From our literature search it appears that the term "transdiagnostic" is used for conventional categories (DSM-5 and ICD-11) and for non-conventional (other psychological) phenotypes too, making it hard to understand what the term truly means. Most of the transdiagnostic research papers that uses diagnosis for treatment intervention, relate to the association between depression and anxiety, *e.g.*[29], which is a known comorbidity and not directly related particularly to the COVID-19 mental health symptomatology. In our search we found just a few papers that diagnose three associated symptoms or more[15,30-33], as in our study.

It seems from the literature that the traditional approach of developing programs for prevention and treatment derived from an accurate specific research-based diagnosis as uniquely shown in our research

is not included in most papers that used the "transdiagnostic" perspective. Additionally, unlike the methodology and rational for the present study, general use of this term is related to treatment, not necessarily explained and derived from an accurate, transdiagnostic, research based new diagnosis or a group of symptoms that span conventional categories[34,35] as shown in our findings.

Moreover, the transdiagnostic approach is presented in the literature with the promise to unravel better prevention and treatment of mental health disorders. The novelty of our current paper lies in analyzing the COVID-19 situation with its multiplicity of stressors to identify a more accurate diagnosis spanning more than 2 or 3 conventional categories. In our search, a few cutting-edge papers were found, in which associations between conventional categories were investigated with sound methodology *e.g.* [29,31,32]. The benefit of these cutting-edge papers is in showing the long-term impact of the COVID-19 pandemic on mental health. The identification of such a long-term effect emphasizes the relevance of our paper at this time, in learning lessons from the first surge towards the post-pandemic era. We note however, that these cutting-edge papers, too, focus on treatment, and not on the investigation of a more accurate diagnosis of the mental health reaction during the COVID-19 epidemic, as we suggest in the present paper.

Limitations

One limitation of our bi-national research is that we did not assess the full range of the possible neuropsychiatric spectrum, including neuropsychiatric symptoms and patterns evident in individuals recovering from infection. This extended transdiagnostic approach is discussed in our recent review published in the World Journal of Psychiatry, suggesting a neuropsychiatric syndrome, Complex Stress Reaction Syndrome, combining emotional-psychological symptoms (Type A) with neuropsychiatric (the non-systemic portion of Long-COVID) symptoms (Type B)[4]. Although the Israeli sample size is modest compared to the Italian sample, the Israeli data were collected by national probability-based representative sampling. We note that the fact that two differently designed studies in two different countries show similar results is a strength of this study and not a limitation. While the data analyzed are from the first surge of the pandemic, the pattern of results provides a novel perspective on diagnostic considerations in the post-COVID era.

CONCLUSION

In sum, our data and the literature suggest multiple symptoms that characterize the mental health reaction to the pandemic, and that the clinical picture during the first surge of the pandemic was transdiagnostic in terms of DSM/ICD diagnostic systems. This occurred more frequently in individuals with prior psychiatric illness and with the continued duration of the pandemic. This unique clinical picture that characterizes the reaction to the pandemic may raise broader thoughts on diagnostic considerations regarding a new category beyond pandemic mental health symptomatology[4]. This suggested category may involve transdiagnostic criteria resulting from multiplicity of stressors. This type of condition may be apparent in the post-COVID era although not recognized to date. Our findings indicate a need for an empirical unbiased approach for reaching a true understanding of the COVID-19 pandemic's psychopathologic consequences in the post-COVID era. Further international studies are essential. Accordingly, we are currently conducting a multi-national study, based on the present empirical paper's findings. This understanding needs to be extended to encompass psychopathology more comprehensively including neuropsychiatric effects. Without a more complete diagnosis, the treatment plan and organizational modifications cannot be complete.

ARTICLE HIGHLIGHTS

Research background

From early stages of the COVID-19 pandemic up to the current post-COVID era there are accumulating reports of a mix clinical picture of the related mental health symptomatology.

Research motivation

We hypothesized that the clinical picture of the COVID-19 related mental health symptomology span several conventional diagnostic categories and therefore there is a growing risk for misdiagnosing suffering individuals thus reducing the option of developing more accurate research -based programs for prevention and treatment.

Research objectives

To show that the association between 3 or more symptoms from different conventional diagnostic categories are more prevalent.

Research methods

Three consecutive representative samples in Israel has been compared to a very large sample in Italy for 3 or more associated symptoms from different conventional categories using proportion analyses.

Research results

The most frequent 4-symptom combination was Anxiety, post-traumatic stress symptoms (PTSS), Depression, and Post-Traumatic Stress Disorder-Negative Affect (PTSD-NA) (3.2%), compared to the other 4-symptom combinations. The prevalence of the 5-symptom combination, Anxiety, Perceived stress, PTSS, Depression, and PTSD-NA (9.0%, 95%CI: 8.5-9.3) was greater than that of the most prevalent 3- (95%CI: 3.0-3.5) and 4-symptom combinations (95%CI: 2.9-3.4, $P < 0.001$) In Italy.

The prevalence of the four-symptom combination (95%CI: 21.8-26.3) was greater than that of the most prevalent 3-symptom combination (Phobia, Anxiety and Depression, 7.32%, 95%CI: 6.0-8.7, $P < 0.001$) in Israel with an increase over time.

Research conclusions

We report evidence from studies in two different countries, on the presentation of complex symptomatology that crosses diagnostic boundaries, during the first surge of the COVID-19 pandemic. The complex of symptoms that we found correlated in severity. This suggests a common relationship or a single overarching disorder that we termed previously Complex Stress Reaction Syndrome. This offers an alternative and perhaps more complete characterization of psychopathology compared with employing multiple diagnoses for the same patient. Moreover, this pattern is observed within each of the two countries studied, despite different survey methods, and is found within ethnic subpopulations of both countries, attesting to the generalizability of the pattern.

Research perspectives

Further international studies are essential. Accordingly, we are currently conducting a multi-national study, based on the present empirical paper's findings. This understanding needs to be extended to encompass psychopathology more comprehensively including neuropsychiatric effects. Without a more complete diagnosis, the treatment plan and organizational modifications cannot be complete.

ACKNOWLEDGEMENTS

The authors thank Tal Kozlovski for statistical analyses. The Israeli data were collected by Nurit Dobrin and Avishai Cohen from the Israeli Central Bureau of Statistics with the support of Timna Ferber.

FOOTNOTES

Author contributions: Goldstein Ferber S and Mann JJ contributed to conceptualization; Di Lorenzo G, Rossi R and Trezza V verified the Italian data; Weller A and Goldstein Ferber S verified the Israeli data; Weller A, Goldstein Ferber Trezza V, Di Lorenzo G and Rossi R contributed to data curation; Weller A, Goldstein Ferber Trezza V, Di Lorenzo G and Rossi R contributed to formal analysis; Zalsman G and Shoval G contributed to investigation; Trezza V, Di Lorenzo G, Rossi R, Goldstein Ferber S and Mann JJ contributed tomethodology; Weller A, Goldstein Ferber S, Di Lorenzo G, and Rossi R contributed to project administration; Zalsman G, Shoval G, Mann JJ, Weller A, Goldstein Ferber S, Trezza V, Rossi R, and Di Lorenzo G contributed to validation; Goldstein Ferber S contributed to writing - original draft; Mann JJ, Trezza V, Rossi R, Di Lorenzo G, Zalsman G, Shoval G, Weller A and Goldstein Ferber S contributed to writing, review & editing; All authors contributed substantially to the final version of the manuscript.

Institutional review board statement: The Israeli representative samples were obtained according to the Israel Law of Statistics. The Italian study was reviewed and approved by the University of L'Aquila Institutional Review Board.

Informed consent statement: Informed consent was obtained in Israel verbally by a telephone call, and in Italy by an online click for virtual recruitment to this internet-based study.

Conflict-of-interest statement: All the authors report no relevant conflicts of interest for this article.

Data sharing statement: No additional data are available.

STROBE statement: The authors have read the STROBE Statement—checklist of items, and the manuscript was prepared and revised according to the STROBE Statement—checklist of items.

Country/Territory of origin: Israel

ORCID number: Sari Goldstein Ferber 0000-0001-6843-3695.

S-Editor: Liu GL
L-Editor: A
P-Editor: Liu GL

REFERENCES

1 **Lazarus R**, Folkman S. Stress, Appraisal, and Coping. Encyclopedia of Behavioral Medicine. Springer, New York, NY. 2013. Available from: https://link.springer.com/referenceworkentry/10.1007/978-1-4419-1005-9_215
2 **Ding Y**, Dai J. Advance in Stress for Depressive Disorder. Adv Exp Med Biol 2019; 1180: 147–178. [PMID: 31784962 DOI: 10.1007/978-981-32-9271-0_8]
3 **Malik P**, Patel K, Pinto C, Jaiswal R, Tirupathi R, Pillai S, Patel U. Post-acute COVID-19 syndrome (PCS) and health-related quality of life (HRQoL)-A systematic review and meta-analysis. J Med Virol 2022; 94: 253–262. [PMID: 34463956 DOI: 10.1002/jmv.27309]
4 **Goldstein Ferber S**, Shoval G, Zalsman G, Weller A. Does COVID-19 related symptomatology indicate a transdiagnostic neuropsychiatric disorder? *World J Psychiatry* 2022; **12**: 1004-1015 [PMID: 36158308 DOI: 10.5498/wjp.v12.i8.1004]
5 **Rossi R**, Socci V, Pacitti F, Di Lorenzo G, Di Marco A, Siracusano A, Rossi A. Mental Health Outcomes Among Frontline and Second-Line Health Care Workers During the Coronavirus Disease 2019 (COVID-19) Pandemic in Italy. *JAMA Netw Open* 2020; **3**: e2010185 [PMID: 32463467 DOI: 10.1001/jamanetworkopen.2020.10185]
6 **Gao J**, Zheng P, Jia Y, Chen H, Mao Y, Chen S, Wang Y, Fu H, Dai J. Mental health problems and social media exposure during COVID-19 outbreak. *PLoS One* 2020; **15**: e0231924 [PMID: 32298385 DOI: 10.1371/journal.pone.0231924]
7 **Perrin PC**, McCabe OL, Everly GS Jr, Links JM. Preparing for an influenza pandemic: mental health considerations. *Prehosp Disaster Med* 2009; **24**: 223-230 [PMID: 19618359 DOI: 10.1017/S1049023X00006853]
8 **Troyer EA**, Kohn JN, Hong S. Are we facing a crashing wave of neuropsychiatric sequelae of COVID-19? *Brain Behav Immun* 2020; **87**: 34-39 [PMID: 32298803 DOI: 10.1016/j.bbi.2020.04.027]
9 **Maj M**. "Psychiatric comorbidity": an artefact of current diagnostic systems? *Br J Psychiatry* 2005; **186**: 182-184 [PMID: 15738496 DOI: 10.1192/bjp.186.3.182]
10 **Xiang YT**, Yang Y, Li W, Zhang L, Zhang Q, Cheung T, Ng CH. Timely mental health care for the 2019 novel coronavirus outbreak is urgently needed. *Lancet Psychiatry* 2020; **7**: 228-229 [PMID: 32032543 DOI: 10.1016/S2215-0366(20)30046-8]
11 **Brooks SK**, Webster RK, Smith LE, Woodland L, Wessely S, Greenberg N, Rubin GJ. The psychological impact of quarantine and how to reduce it: rapid review of the evidence. *Lancet* 2020; **395**: 912-920 [PMID: 32112714 DOI: 10.1016/S0140-6736(20)30460-8]
12 **Taylor S**, Landry CA, Paluszek MM, Fergus TA, McKay D, Asmundson GJG. COVID stress syndrome: Concept, structure, and correlates. *Depress Anxiety* 2020; **37**: 706-714 [PMID: 32627255 DOI: 10.1002/da.23071]
13 **Hossain MM**, Tasnim S, Sultana A, Faizah F, Mazumder H, Zou L, McKyer ELJ, Ahmed HU, Ma P. Epidemiology of mental health problems in COVID-19: a review. *F1000Res* 2020; **9**: 636 [PMID: 33093946 DOI: 10.12688/f1000research.24457.1]
14 **Spencer-Laitt D**, Eustis EH, Barlow DH, Farchione TJ. The Impact of COVID-19 Related Social Distancing on Mental Health Outcomes: A Transdiagnostic Account. *Int J Environ Res Public Health* 2022; **19** [PMID: 35682179 DOI: 10.3390/ijerph19116596]
15 **Kachadourian L**, Murrough J, Kaplan C, Kaplan S, Feingold J, Feder A, Charney D, Southwick S, Peccoralo L, DePierro J, Ripp J, Pietrzak R. A prospective study of transdiagnostic psychiatric symptoms associated with burnout and functional difficulties in COVID-19 frontline healthcare workers. *J Psychiatr Res* 2022; **152**: 219-224 [PMID: 35753241 DOI: 10.1016/j.jpsychires.2022.05.034]
16 **Olff M**, Bakker A, Frewen P, Aakvaag H, Ajdukovic D, Brewer D, Elmore Borbon DL, Cloitre M, Hyland P, Kassam-Adams N, Knefel M, Lanza JA, Lueger-Schuster B, Nickerson A, Oe M, Pfaltz MC, Salgado C, Seedat S, Wagner A, Schnyder U; Global Collaboration on Traumatic Stress (GC-TS). Screening for consequences of trauma - an update on the global collaboration on traumatic stress. *Eur J Psychotraumatol* 2020; **11**: 1752504 [PMID: 32489523 DOI: 10.1080/20008198.2020.1752504]
17 **Rossi R**, Socci V, Talevi D, Niolu C, Pacitti F, Di Marco A, Rossi A, Siracusano A, Di Lorenzo G, Olff M. Trauma-spectrum symptoms among the Italian general population in the time of the COVID-19 outbreak. *Eur J Psychotraumatol* 2021; **12**: 1855888 [PMID: 34992741 DOI: 10.1080/20008198.2020.1855888]
18 **Spitzer RL**, Kroenke K, Williams JB. Validation and utility of a self-report version of PRIME-MD: the PHQ primary care study. Primary Care Evaluation of Mental Disorders. Patient Health Questionnaire. *JAMA* 1999; **282**: 1737-1744 [PMID: 10568646 DOI: 10.1001/jama.282.18.1737]
19 **Spitzer RL**, Kroenke K, Williams JB, Löwe B. A brief measure for assessing generalized anxiety disorder: the GAD-7. *Arch Intern Med* 2006; **166**: 1092-1097 [PMID: 16717171 DOI: 10.1001/archinte.166.10.1092]
20 **Cohen S**, Kamarck T, Mermelstein R. A global measure of perceived stress. *J Health Soc Behav* 1983; **24**: 385-396 [PMID: 6668417 DOI: 10.1111/j.1559-1816.1983.tb02325.x]

21 **Ferber SG**, Weller A, Maor R, Feldman Y, Harel-Fisch Y, Mikulincer M. Perceived social support in the social distancing era: the association between circles of potential support and COVID-19 reactive psychopathology. *Anxiety Stress Coping* 2022; **35**: 58-71 [PMID: 34652983 DOI: 10.1080/10615806.2021.1987418]

22 **Ferber SG**, Shoval G, Zalsman G, Mikulincer M, Weller A. Between Action and Emotional Survival During the COVID-19 era: Sensorimotor Pathways as Control Systems of Transdiagnostic Anxiety-Related Intolerance to Uncertainty. *Front Psychiatry* 2021; **12**: 680403 [PMID: 34393847 DOI: 10.3389/fpsyt.2021.680403]

23 **McEvoy PM**, Hyett MP, Shihata S, Price JE, Strachan L. The impact of methodological and measurement factors on transdiagnostic associations with intolerance of uncertainty: A meta-analysis. *Clin Psychol Rev* 2019; **73**: 101778 [PMID: 31678816 DOI: 10.1016/j.cpr.2019.101778]

24 **Gillett CB**, Bilek EL, Hanna GL, Fitzgerald KD. Intolerance of uncertainty in youth with obsessive-compulsive disorder and generalized anxiety disorder: A transdiagnostic construct with implications for phenomenology and treatment. *Clin Psychol Rev* 2018; **60**: 100-108 [PMID: 29426573 DOI: 10.1016/j.cpr.2018.01.007]

25 **Fernandez KC**, Jazaieri H, Gross JJ. Emotion regulation: a transdiagnostic perspective on a new RDoC domain. *Cognit Ther Res* 2016; **40**: 426-440 [PMID: 27524846 DOI: 10.1007/s10608-016-9772-2]

26 **Einstein DA**. Extension of the Transdiagnostic Model to Focus on Intolerance of Uncertainty: A Review of the Literature and Implications for Treatment. *Clin Psychol (New York)* 2014; **21**: 280-300 [PMID: 25400336 DOI: 10.1111/cpsp.12077]

27 **Carpiniello B**, Tusconi M, Zanalda E, Di Sciascio G, Di Giannantonio M; Executive Committee of The Italian Society of Psychiatry. Psychiatry during the Covid-19 pandemic: a survey on mental health departments in Italy. *BMC Psychiatry* 2020; **20**: 593 [PMID: 33327940 DOI: 10.1186/s12888-020-02997-z]

28 **Paluszek MM**, Asmundson AJN, Landry CA, McKay D, Taylor S, Asmundson GJG. Effects of anxiety sensitivity, disgust, and intolerance of uncertainty on the COVID stress syndrome: a longitudinal assessment of transdiagnostic constructs and the behavioural immune system. Cogn Behav Ther 2021; 50: 191–203. [PMID: 33576712 DOI: 10.1080/16506073.2021.1877339]

29 **Heckendorf H**, Lehr D, Boß L. Effectiveness of an Internet-Based Self-Help Intervention versus Public Mental Health Advice to Reduce Worry during the COVID-19 Pandemic: A Pragmatic, Parallel-Group, Randomized Controlled Trial. *Psychother Psychosom* 2022; **91**: 398-410 [PMID: 35051939 DOI: 10.1159/000521302]

30 **Guzick AG**, Leong AW, Dickinson EM, Schneider SC, Zopatti K, Manis J, Meinert AC, Barth AM, Perez M, Campo DM, Weinzimmer SA, Cepeda SL, Mathai D, Shah A, Goodman WK, Salloum A, Kennedy S, Ehrenreich-May J, Storch EA. Brief, parent-led, transdiagnostic cognitive-behavioral teletherapy for youth with emotional problems related to the COVID-19 pandemic. J Affect Disord 2022; 301: 130-137 [PMID: 35031335 DOI: 10.1016/j.jad.2022.01.034]

31 **Ehrenreich-May J**, Halliday ER, Karlovich AR, Gruen RL, Pino AC, Tonarely NA. Brief Transdiagnostic Intervention for Parents With Emotional Disorder Symptoms During the COVID-19 Pandemic: A Case Example. *Cogn Behav Pract* 2021; **28**: 690-700 [PMID: 34629841 DOI: 10.1016/j.cbpra.2021.01.002]

32 **Muñoz-Navarro R**, Cano Vindel A, Schmitz F, Cabello R, Fernández-Berrocal P. Emotional Disorders During the COVID-19 Outbreak in Spain: The Role of Sociodemographic Risk Factors and Cognitive Emotion Regulation Strategies. *Health Educ Behav* 2021; **48**: 412-423 [PMID: 34008452 DOI: 10.1177/10901981211014101]

33 **Warren AM**, Zolfaghari K, Fresnedo M, Bennett M, Pogue J, Waddimba A, Zvolensky M, Carlbring P, Powers MB. Anxiety sensitivity, COVID-19 fear, and mental health: results from a United States population sample. *Cogn Behav Ther* 2021; **50**: 204-216 [PMID: 33595414 DOI: 10.1080/16506073.2021.1874505]

34 **Cassiello-Robbins C**, Rosenthal MZ, Ammirati RJ. Delivering Transdiagnostic Treatment Over Telehealth During the COVID-19 Pandemic: Application of the Unified Protocol. *Cogn Behav Pract* 2021; **28**: 555-572 [PMID: 34108830 DOI: 10.1016/j.cbpra.2021.04.007]

35 **Amici P**. Intolerance of Uncertainty: From Transdiagnostic Model to Clinical Management. *Psychiatr Danub* 2021; **33**: 22-25 [PMID: 34559773]

World Journal of Clinical Cases

Submit a Manuscript: https://www.f6publishing.com

World J Clin Cases 2023 February 6; 11(4): 821-829

DOI: 10.12998/wjcc.v11.i4.821

ISSN 2307-8960 (online)

ORIGINAL ARTICLE

Observational Study

Effect of patient COVID-19 vaccine hesitancy on hospital care team perceptions

Inbar Caspi, Ophir Freund, Omer Pines, Odelia Elkana, Jacob N Ablin, Gil Bornstein

Specialty type: Medicine, general and internal

Provenance and peer review: Invited article; Externally peer reviewed.

Peer-review model: Single blind

Peer-review report's scientific quality classification

Grade A (Excellent): 0
Grade B (Very good): 0
Grade C (Good): C, C
Grade D (Fair): 0
Grade E (Poor): 0

P-Reviewer: Lee S, South Korea; Tiejun W, China

Received: October 27, 2022
Peer-review started: October 27, 2022
First decision: November 30, 2022
Revised: December 12, 2022
Accepted: January 16, 2023
Article in press: January 16, 2023
Published online: February 6, 2023

Inbar Caspi, Ophir Freund, Gil Bornstein, Internal Medicine Department B, Tel-Aviv Sourasky Medical Center and Sackler Faculty of Medicine, Tel Aviv University, Tel Aviv 6423906, Israel

Omer Pines, Odelia Elkana, Behavioral Sciences Department, Academic College of Tel Aviv-Yaffo, Tel Aviv 6818211, Israel

Jacob N Ablin, Internal Medicine Department H, Tel Aviv Sourasky Medical Center and Sackler School of Medicine, Tel Aviv 6423906, Israel

Corresponding author: Ophir Freund, MD, Doctor, Internal Medicine Department B, Tel-Aviv Sourasky Medical Center and Sackler Faculty of Medicine, Tel Aviv University, Weizman 6, Tel Aviv 6423906, Israel. ophir068@gmail.com

Abstract

BACKGROUND

The coronavirus disease 2019 (COVID-19) pandemic posed new challenges in patient care worldwide. Vaccinations, which have proven efficacious in lowering the COVID-19 hospital burden, are still avoided by large populations. We, therefore, hypothesized that hospital care teams would have worse perceptions regarding the characteristics and care of patients with vaccine hesitancy.

AIM

To evaluate whether patient vaccine hesitancy affected the hospital care team (HCT) perceptions.

METHODS

We performed a prospective clinical study using structured questionnaires. We approached physicians and nurses with previous experience caring for COVID-19 patients from 11 medical centers across Israel during the fourth COVID-19 surge (September and October 2021). The participants completed a questionnaire with the following parts: (1) Sociodemographic characteristics; (2) Assessment of anger (STAXI instrument) and chronic workplace stress (Shirom-Melamed burnout measure); and (3) Three tools to assess the effect of patient vaccine hesitancy on the HCT perceptions (the difficult doctor-patient relation questionnaire, the medical staff perception of patient's responsibility questionnaire and the characterological derogation questionnaire). Results were evaluated according to each part of the questionnaire and the questionnaire as a whole. Associations between

HCT perceptions and their baseline characteristics, anger or chronic workplace stress were assessed.

RESULTS

The HCT experienced their relationship with unvaccinated patients as more difficult ($P < 0.001$, Cohen's $d = 0.85$), perceived unvaccinated patients as responsible for their medical condition ($P < 0.001$, $d = 1.39$) and perceived vaccinated patients as having a higher character value ($P < 0.001$, $d = 1.03$). Unvaccinated patients were considered selfish ($P < 0.001$), less mature ($P < 0.001$) and less satisfying to care for ($P < 0.001$). The relationship with unvaccinated patients was more difficult among HCT with higher burnout ($r = 0.37$, $n = 66$, $P = 0.002$). No correlations with baseline characteristics were found. All three study tools showed high internal consistency (α between 0.72 and 0.845).

CONCLUSION

Our results should raise awareness of the possible effects of vaccine hesitancy on HCT perceptions regarding unvaccinated patients. In order to minimize the potential negative impact on patient care, designated departments should promote specific patient-centered preparations. Further investigations should assess whether vaccine hesitancy directly affects patient quality of care.

Key Words: COVID-19; Vaccination; Hesitancy; Patient care; Doctor-patient relationship; Attitudes

Core Tip: Coronavirus disease 2019 (COVID-19) vaccine hesitancy is common around the world. We considered that patient vaccine hesitancy could affect the hospital care team perceptions. To test that possibility, we implemented a questionnaire during the Delta variant surge among physicians and nurses with prior experience in caring for COVID-19 patients. We found that patient vaccine hesitancy negatively affected how the medical care team perceived these patients and their care. Vaccine hesitancy can negatively affect the physician-patient relationship and raising awareness of this important issue is crucial for proper interventions.

Citation: Caspi I, Freund O, Pines O, Elkana O, Ablin JN, Bornstein G. Effect of patient COVID-19 vaccine hesitancy on hospital care team perceptions. *World J Clin Cases* 2023; 11(4): 821-829
URL: https://www.wjgnet.com/2307-8960/full/v11/i4/821.htm
DOI: https://dx.doi.org/10.12998/wjcc.v11.i4.821

INTRODUCTION

Medical care team beliefs and practices are impacted by patient characteristics[1]. Such characteristics also have the potential to intervene with the shared decision-making process by changing physicians' perceptions of their patients[2,3]. The coronavirus disease 2019 (COVID-19), which continues to affect millions of people globally since 2019, poses new challenges regarding patient care[4,5]. Severe COVID-19 infection has the potential for hospitalization due to possible complications that result in a high burden on the hospital care team (HCT)[6]. Caring for hospitalized COVID-19 patients requires functioning with full personal protective equipment and caring for patients who may rapidly deteriorate. This environment creates obvious stressful triggers.

The introduction of the mRNA COVID-19 vaccines was a crucial step in preventing the spread of the virus, limiting disease transmission and infectivity[7,8]. COVID-19 vaccines dramatically reduced the rate of hospitalizations due to severe disease as well as complications among hospitalized patients regardless of any comorbidities or age[9,10]. Despite its obvious benefits, several large populations avoided vaccination for various reasons, demonstrating distrust against the vaccines[11]. Therefore, it is not surprising that many studies focused on attitudes toward COVID-19 vaccines themselves and specifically on vaccine hesitancy for both patients and medical teams[11-13]. However, it is still unknown whether patient vaccine hesitancy influences the HCT's perceptions of them. We hypothesized that HCTs would have negative perceptions towards the characteristics and care of vaccine-hesitant patients. Our aim was to evaluate this hypothesis and to raise awareness in order to promote early intervention, hopefully preventing potential negative effects on patient care.

MATERIALS AND METHODS

Study design

This is a prospective clinical study conducted at 11 medical centers throughout Israel between September and October 2021 using standardized questionnaires. We held the study during the fourth surge of the COVID-19 pandemic when the Delta variant was predominant, and the hospital disease burden reached its peak. We approached physicians and nursing staff that treated COVID-19 patients to participate in the study. Invitations to participate in the study were offered personally or *via* social networks and whenever needed were followed by a text message with an active link to the questionnaire. Consenting participants were enrolled using an online interface. All participants accepted an informed consent form, agreed to participate by pressing "continue" within the questionnaire electronically and had the ability to drop out at any stage. Only participants who completed at least one of the three study tools (described below) were included in our final cohort. The study was approved by the ethics committee of The Academic College of Tel Aviv-Yaffo (Authorization number 2021142).

Study instrument

We created a computerized questionnaire *via* the Qualtrics platform. The design of our study instrument appears in Figure 1. The first set of questions discussed sociodemographic information, such as age, sex, profession (physician, nurse, *etc.*) and prior experience with treating COVID-19. The second part included questions about participant anger (4-point Likert scale, using the STAXI instrument[14]) and their chronic workplace stress (7-point Likert scale, using the Shirom-Melamed Burnout Measure[15]). The third part of the questionnaire assessed the effect of patient COVID-19 vaccine hesitancy on the participants. To properly assess this aspect, we used three validated tools that together created a comprehensive review of the topic. For comparison purposes, the third part (including the three tools) appeared twice, first regarding unvaccinated patients and second regarding vaccinated patients. The three selected tools used were as follows.

Tool 1-difficult doctor-patient relation questionnaire: A well-established questionnaire, consisting of 10 items answered on a 6-point Likert scale, with values ranging from 1 ("Not at all") to 6 ("A great deal")[16]. Higher scores indicate that the physician experiences the relationship with the patient as more difficult. In our study, we made a minor modification by using a 1 to 7 scale, to give participants an option of expressing a neutral (middle range) opinion, which is achieved by an uneven number of items.

Tool 2-medical staff perception of patient's responsibility questionnaire: This questionnaire was previously used in similar studies evaluating physician perception of illness, with a variety of patient populations[17,18]. It is written as a 10-item questionnaire, answered on a 7-point Likert scale, with values ranging from 1 ("Not at all") to 7 ("A great deal"). A higher score indicates that the participant perceives the patient as more responsible for his own medical condition.

Tool 3-characterological derogation questionnaire: This questionnaire was written by Brouns[19], as part of a thesis regarding negative attitudes towards refugees and based on previous questionnaires by Correia *et al*[20]. It is a nine-item questionnaire, relating to the question: "In your opinion, what represents 'X' best?". Five items include positive characteristics, *e.g.*, polite, responsible, mature, warm and nice, and four items include negative characteristics *e.g.*, stupid, selfish, untrue and unaware. The scoring was by a 7-point Likert scale, with values ranging from 1 ("Not at all") to 7 ("A great deal"). A high score indicates that the participant perceives the patient's character as a high-value character.

Statistical analysis

Categorical variables were described using frequencies and percentages. Continuous variables were described by mean and standard deviation. Comparison between answers regarding vaccinated and unvaccinated patients was utilized using paired samples *t*-test. $P < 0.05$ was defined as statistically significant. The effect size of significant results was calculated using Cohen's d test. The internal consistency of each tool in the study instrument was measured using the alpha Cronbach score (alpha above 0.7 is considered high). Correlations were examined using the Pearson correlation coefficient. The analysis was performed using SPSS 26.0 for Windows.

RESULTS

Participants

During the study period, we approached more than 500 active physicians and nursing staff from 11 different medical centers. In total, 138 participants agreed to enroll in the study, and of them 66 (48%) completed at least one of the three study tools and were included in our cohort. Participant character-

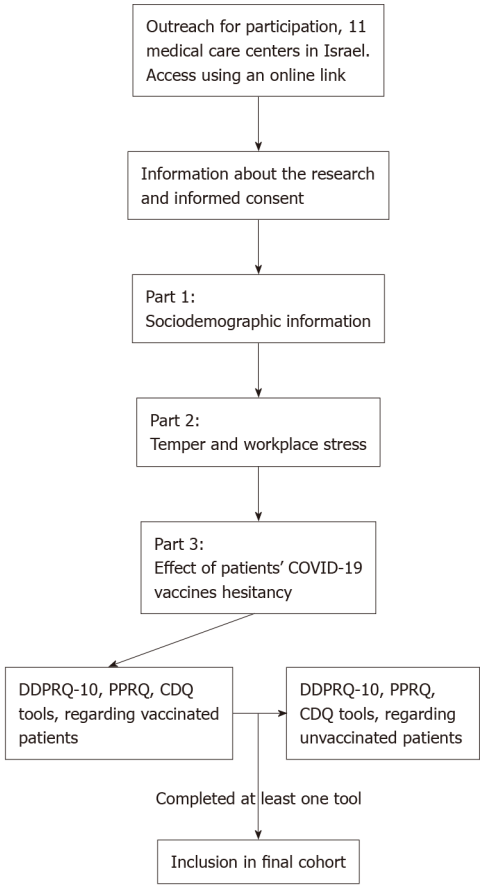

DOI: 10.12998/wjcc.v11.i4.821

Figure 1 Design of study instrument and inclusion process. CDQ: Characterological derogation questionnaire; COVID-19: Coronavirus disease 2019; DDPRQ-10: Difficult doctor-patient relation questionnaire; PPRQ: Perception of patient's responsibility questionnaire.

istics are presented in Table 1. In total, 38 (58%) participants were women, mean age was 40.5 ± 10, 37 (56%) were physicians (senior doctors, residents and interns), and 29 (44%) participants were staff of internal medicine departments. All but two were vaccinated (97%), and 12 (18%) had prior COVID-19.

Effect of patient vaccine hesitancy on the HCT perceptions

The three tools used for this study [difficult doctor-patient relation questionnaire (DDPRQ-10), medical staff perception of patient's responsibility questionnaire (PPRQ) and characterological derogation questionnaire (CDQ)] showed a high internal consistency based on our results (α between 0.72 and 0.845). Table 2 presents the mean scores of selected questions from each tool comparing vaccinated and unvaccinated patients. Based on tool 1 (DDPRQ-10), the HCT considered caring for unvaccinated patients to be more frustrating ($P < 0.001$), time-consuming ($P < 0.001$) and less satisfying ($P < 0.001$). Answers in tool 2 (PPRQ) revealed that the HCT perceived unvaccinated patients to be responsible for their illness ($P < 0.001$), to consciously endanger their surroundings ($P < 0.001$) and as less deserving of occupying beds in the intensive care unit than vaccinated patients ($P = 0.002$). The HCT also believed that social and economic sanctions should be imposed on unvaccinated people (mean scores 4.2 and 4.1, respectively, $P < 0.001$ for both). Tool 3 (CDQ) indicated that unvaccinated patients were perceived as less mature, more selfish and more ignorant ($P < 0.001$).

The mean total scores for each tool are presented in Figure 2. Based on these results, the HCT experienced their relationship with unvaccinated patients as more difficult (DDPRQ-10 tool, $P < 0.001$, Cohen's d = 0.85), perceived unvaccinated patients as more responsible for their medical condition (PPRQ tool, $P < 0.001$, Cohen's d = 1.39) and perceived the character of vaccinated patients as a higher value character (CDQ tool, $P < 0.001$, Cohen's d = 1.03).

None of the participants' baseline characteristics correlated with results in any of the above tools. HCTs with higher workplace burnout (Shirom-Melamed Burnout Measure tool) perceived the relationship with unvaccinated patients as more difficult (DDPRQ-10 tool, $r = 0.37$, $n = 66$, $P = 0.002$). No other correlations were found between workplace burnout or anger (STAXI tool) and any of the other tools.

Table 1 Baseline characteristics of study cohort and responses on anger and stress tools, *n* = 66 (%)

Variable	Study cohort
Age, mean ± SD	40.5 ± 10.1
Male sex	28 (42)
Occupation	
Physicians	37 (56)
Nursing staff	22 (33)
Department managers/vice	7 (11)
Medical field	
Internal or general medicine	36 (54)
Psychiatry	7 (11)
Intensive care unit	4 (6)
Emergency department	5 (8)
Other	14 (21)
Vaccinated to COVID-19	64 (97)
Prior COVID-19 disease	12 (18)
Anger, mean ± SD[a]	1.8 ± 0.4
Workplace stress, mean ± SD[b]	3.1 ± 1

[a]Mean score in the STAXI instrument, 4-point Likert scale.
[b]Mean score Shirom-Melamed bournout measure, 7-point Likert scale.
COVID-19: Coronavirus disease 2019.

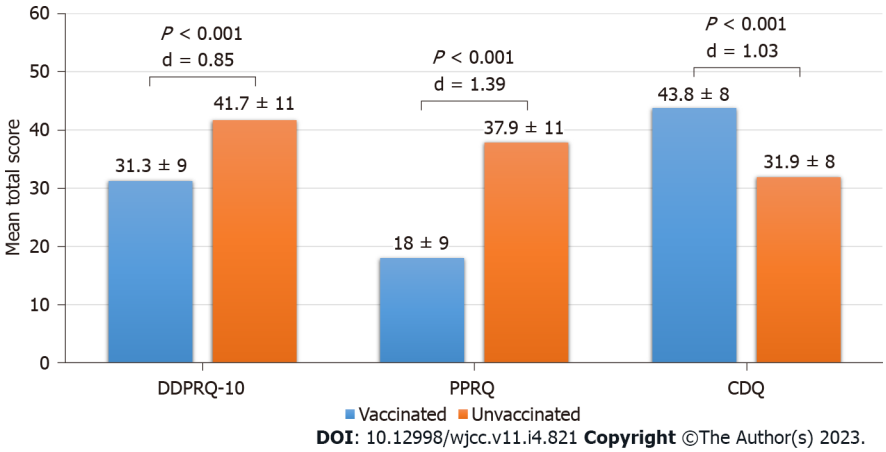

DOI: 10.12998/wjcc.v11.i4.821 **Copyright** ©The Author(s) 2023.

Figure 2 Mean total scores for each of the three tools used in the study questionnaire compared by addressing vaccinated and unvaccinated patients. CDQ: Characterological derogation questionnaire; DDPRQ-10: Difficult doctor-patient relation questionnaire; PPRQ: Perception of patient's responsibility questionnaire.

DISCUSSION

This study explored our hypothesis that patient COVID-19 vaccine hesitancy can have a negative effect on HCT perceptions. Our results showed that vaccine hesitancy had a negative impact on how the HCT perceived patients' character, their care and their responsibility for their disease. We specifically addressed active physicians and nursing staff working in medical centers that treated COVID-19 patients, as they were directly affected by the pandemic. By approaching 11 different centers, our results may reflect the effect on HCT perceptions on a national scale. As stated above, several previous studies described the attitude of patients and medical personnel toward COVID-19 vaccines[12,13,21]. However, whether patients' beliefs on this issue affect their treating team have yet to be described.

Table 2 Comparison of responses to selected questions regarding unvaccinated and vaccinated coronavirus disease 2019 patients

Questions[a]	Unvaccinated, mean ± SD	Vaccinated, mean ± SD	*P* value
Tool 1-difficult doctor-patient relation questionnaire (7-point Likert scale)[b]			
Do you expect to see clinical improvement in a COVID-19 patient?	3.8 ± 1.6	5.5 ± 1.3	< 0.001
How frustrating is a patient with COVID-19?	4.8 ± 2.0	3.2 ± 2.0	< 0.001
How frustrated are you with treating a COVID-19 patient?	4.7 ± 2.0	2.8 ± 1.8	< 0.001
Are you satisfied when you care for COVID-19 patients?	3.9 ± 2.0	4.6 ± 1.8	0.001
How time consuming is caring for COVID-19 patients?	5.0 ± 1.6	4.1 ± 1.5	< 0.001
How enthusiastic do you feel about caring for a COVID-19 patient?	2.8 ± 1.8	3.2 ± 1.8	0.09
How difficult is it to communicate with a COVID-19 patient?	3.4 ± 1.8	2.4 ± 1.5	< 0.001
Tool 2-perception of patient's responsibility questionnaire (7-point Likert scale)[b]			
I believe a COVID-19 patient is responsible for his illness	5.1 ± 1.8	2.1 ± 1.5	< 0.001
COVID-19 patients consciously endanger their family and environment	5.4 ± 1.9	2.3 ± 1.7	< 0.001
COVID-19 patients have a bad influence on my personal life	3.6 ± 2.2	1.6 ± 1.2	< 0.001
COVID-19 patients deserve to occupy beds in the ICU	5.1 ± 1.9	5.9 ± 1.8	0.002
I believe that social sanctions should be imposed on people un/vaccinated to COVID-19	4.2 ± 2.1	1.4 ± 1.1	< 0.001
I believe that economic sanctions should be imposed on people un/vaccinated to COVID-19	4.1 ± 2.2	1.4 ± 1.0	< 0.001
Un/vaccinated COVID-19 patients make it impossible to eradicate the pandemic	5.0 ± 2.2	1.8 ± 1.2	< 0.001
Tool 3-characterological derogation questionnaire (7-point Likert scale)[b]			
A patient with COVID-19 is polite	3.4 ± 1.4	3.9 ± 1.3	0.001
A patient with COVID-19 is responsible	2.5 ± 1.6	5.2 ± 1.8	< 0.001
A patient with COVID-19 is mature	2.7 ± 1.6	4.9 ± 1.7	< 0.001
A patient with COVID-19 is nice	3.4 ± 1.4	3.9 ± 1.4	0.01
A patient with COVID-19 is selfish	4.6 ± 2.1	2.4 ± 1.7	< 0.001
A patient with COVID-19 is ignorant	4.8 ± 1.9	2.6 ± 1.7	< 0.001

[a]All questions were answered twice, first regarding vaccinated patients and second regarding unvaccinated patients.
[b]Answers ranged from 1 ("not at all") to 7 ("highly agree").
COVID-19: Coronavirus disease 2019; ICU: Intensive care unit.

Our study was conducted during the fourth surge of the COVID-19 pandemic. Despite multiple studies demonstrating the safety and efficacy of mRNA vaccines[7,9,22], large populations still refuse to get vaccinated. Vaccination hesitancy continues to be a serious concern worldwide[23,24], with amplification of the discussion in social media settings[25]. During the fourth surge, most hospitalized patients were unvaccinated, showing worse clinical outcomes[10]. This situation created a fertile ground for the development of frustration among medical staff, particularly in the context of the highly stressful work environment in COVID-19 departments. We hypothesized that this confluence of factors might aggravate negative feelings while taking care of unvaccinated patients, as presented in our results. This trend was reflected in our study by the strong correlation between higher workplace burnout and the perception of more difficult relationships with unvaccinated patients.

In Israel, vaccines were free for every citizen and available in multiple centers all over the country with the option for home visits when needed. Therefore, it is not surprising that the unvaccinated COVID-19 patients in our study were considered responsible for their own medical predicament (P < 0.001) and were blamed for allowing the pandemic to spread, thus endangering others (P < 0.001). This dynamic can conceivably lead to more strain on the doctor-patient relationship. The results of the current study demonstrated the strong effect that vaccine status has on the HCT perceptions of their patients.

The use of three different study tools emphasized the internal consistency of the results since the negative attitude was consistent in three independent instruments. Additionally, the results of all three

questionnaires were statistically significant, demonstrating a large effect, despite a relatively small sample size. It is important to note that 97% of the participants were vaccinated for COVID-19. While it may seem like a potential selection bias, it is important to remember that in Israel vaccination was obligatory for hospital medical teams, and therefore the vaccine status does not reflect the participants' attitudes towards the COVID-19 vaccines[21].

Throughout the history of medicine, physicians have handled situations in which the patient may be held responsible for his condition due to various health behavior (*e.g.*, obesity, diabetes, chronic obstructive pulmonary disease). Some medical conditions have even been stigmatized due to moral failure (*e.g.*, venereal disease). Although it remains difficult to establish whether such perceptions play a role in the doctor–patient relationship, in all such cases medical professionalism and ethics call for a non-judgmental and unbiased approach toward patients. Additionally, the treating HCT must be familiar with variables that might influence their perceptions or interaction with their patients[26,27]. As shown by Mateo *et al*[28], there is a high prevalence of harmful bias and discrimination within the health professions, with a proven negative impact on patient care. It was argued that addressing these biases is the professional responsibility of every provider and essential to effective and equitable care. In light of this, we assumed that ongoing negative perceptions can eventually lead to a harmful effect on the quality of care of unvaccinated patients. We believe that our findings should raise awareness for potentially harmful biases in medical practice and hopefully lead to the establishment of specific measures in designated COVID-19 departments to combat this issue. For example, departments should be able to offer the staff a reassuring environment to express their feelings and prevent their aggravation.

This study has several limitations. We used questionnaires, which can cause report bias. Only participants who completed the questionnaire were included, which can cause selection bias. To avoid those biases, further research should aim to assess the effect of patient COVID-19 vaccine hesitancy on HCT perceptions in a direct manner. Observational prospective studies with consecutive patients are needed for this purpose and to assess any effect on patient quality of care. Furthermore, it can be assumed that since the reporting bias is a concern in both study groups, it has a relatively negligible influence on our results. Although we approached a variety of medical personnel in multiple centers, our cohort size is relatively small. A potential reason could be the timing of the study during the peak of an outbreak, finding the medical staff extremely busy and therefore less responsive to participate in online surveys, especially considering the multiple tools included in our questionnaire. Furthermore, even though the survey was anonymous, medical staff might have been hesitant to reveal negative attitudes toward patients. This study was designed as a "snapshot" study, capturing the essence of medical staff perceptions of COVID-19 patients during the peak of the outbreak.

CONCLUSION

Our study demonstrated that patient vaccine hesitancy had a strong negative effect on the HCT perceptions regarding these patients. We aimed to raise awareness and promote preventive interventions. Early detection might prevent negative feelings from escalating and mitigate the feared consequence of harming patient care.

ARTICLE HIGHLIGHTS

Research background

Patient characteristics can affect their medical care team practice and intervene in the shared decision-making process. The coronavirus disease 2019 (COVID-19) pandemic posed new challenges to patient care, especially severe infections with high rates of deterioration and adverse outcomes. COVID-19 vaccines have proven highly efficacious in reducing the disease severity and as a result its burden. We, therefore, hypothesized that patient vaccine hesitancy would influence the hospital care team (HCT) perceptions.

Research motivation

Many studies focused on the attitudes toward COVID-19 vaccines themselves and specifically on vaccine hesitancy for both patients and medical teams. However, it is still unknown whether patient vaccine hesitancy influences HCT perceptions.

Research objectives

To study the effect of patient vaccine hesitancy on HCT perceptions towards these patients' characteristics and care.

Research methods

We conducted a prospective study at 11 medical centers during the Delta variant surge using standardized questionnaires. Hospital physicians and nursing staff treating COVID-19 patients (n = 66) were recruited and completed a questionnaire, which included three validated tools to assess the effect of patient vaccine hesitancy. We analyzed the questionnaire results in all different items and evaluated their associations with patients' characteristics.

Research results

Our data demonstrated that HCT experienced their relationship with vaccine-hesitant patients as more difficult, perceived them as responsible for their disease and as having a lower character. The relationship with unvaccinated patients was more difficult among HCTs with higher workplace burnout.

Research conclusions

We concluded that patient vaccine hesitancy had a negative impact on how the HCT perceived patient character, their care and their responsibility for their disease.

Research perspectives

Our results should raise awareness of the potentially harmful biases in medical practice and hopefully lead to the establishment of specific measures in designated COVID-19 departments to combat this issue. Early detection might prevent negative feelings from escalating and mitigate the feared consequence of harming patient care.

FOOTNOTES

Author contributions: Ablin JN and Bornstein G designed and supervised the study; Freund O, Pines O, Elkana O and Caspi I performed data acquisition, analysis and interpretation; Caspi I and Freund O drafted the manuscript; All authors reviewed and confirmed the final version of the manuscript and critically revised it.

Institutional review board statement: The study was approved by the ethics committee of The Academic College of Tel Aviv-Yaffo (Authorization No. 2021142).

Informed consent statement: All participants accepted an informed consent form, agreed to participate by pressing to continue with the questionnaire electronically and had the ability to drop out at any stage.

Conflict-of-interest statement: The authors declare having no conflicts of interest, real or perceivable, to report.

Data sharing statement: No additional data are available.

STROBE statement: The authors have read the STROBE Statement-checklist of items, and the manuscript was prepared and revised according to the STROBE Statement-checklist of items.

Country/Territory of origin: Israel

ORCID number: Inbar Caspi 0000-0001-9538-3865; Ophir Freund 0000-0002-7272-5284; Odelia Elkana 0000-0003-1862-4930; Jacob N Ablin 0000-0003-2523-4850; Gil Bornstein 0000-0002-4720-1577.

S-Editor: Zhang H
L-Editor: Filipodia
P-Editor: Zhang H

REFERENCES

1 **van Ryn M**, Burke J. The effect of patient race and socio-economic status on physicians' perceptions of patients. *Soc Sci Med* 2000; **50**: 813-828 [PMID: 10695979 DOI: 10.1016/S0277-9536(99)00338-X]

2 **Keij SM**, de Boer JE, Stiggelbout AM, Bruine de Bruin W, Peters E, Moaddine S, Kunneman M, Pieterse AH. How are patient-related characteristics associated with shared decision-making about treatment? *BMJ Open* 2022; **12**: e057293

[PMID: 35613791 DOI: 10.1136/bmjopen-2021-057293]
3 **Shepherd HL**, Butow PN, Tattersall MH. Factors which motivate cancer doctors to involve their patients in reaching treatment decisions. *Patient Educ Couns* 2011; **84**: 229-235 [PMID: 21112174 DOI: 10.1016/j.pec.2010.10.018]
4 **Wu JT**, Leung K, Leung GM. Nowcasting and forecasting the potential domestic and international spread of the 2019-nCoV outbreak originating in Wuhan, China: a modelling study. *Lancet* 2020; **395**: 689-697 [PMID: 32014114 DOI: 10.1016/S0140-6736(20)30260-9]
5 **Krishnan A**, Hamilton JP, Alqahtani SA, Woreta TA. COVID-19: An overview and a clinical update. *World J Clin Cases* 2021; **9**: 8-23 [PMID: 33511168 DOI: 10.12998/wjcc.v9.i1.8]
6 **Çelik MY**, Kiliç M. Family relationship of nurses in COVID-19 pandemic: A qualitative study. *World J Clin Cases* 2022; **10**: 6472-6482 [PMID: 35979301 DOI: 10.12998/wjcc.v10.i19.6472]
7 **Haas EJ**, Angulo FJ, McLaughlin JM, Anis E, Singer SR, Khan F, Brooks N, Smaja M, Mircus G, Pan K, Southern J, Swerdlow DL, Jodar L, Levy Y, Alroy-Preis S. Impact and effectiveness of mRNA BNT162b2 vaccine against SARS-CoV-2 infections and COVID-19 cases, hospitalisations, and deaths following a nationwide vaccination campaign in Israel: an observational study using national surveillance data. *Lancet* 2021; **397**: 1819-1829 [PMID: 33964222 DOI: 10.1016/S0140-6736(21)00947-8]
8 **Chen LP**, Zeng QH, Gong YF, Liang FL. Should people with chronic liver diseases be vaccinated against COVID-19? *World J Clin Cases* 2021; **9**: 7959-7962 [PMID: 34621852 DOI: 10.12998/wjcc.v9.i26.7959]
9 **Bar-On YM**, Goldberg Y, Mandel M, Bodenheimer O, Freedman L, Kalkstein N, Mizrahi B, Alroy-Preis S, Ash N, Milo R, Huppert A. Protection of BNT162b2 Vaccine Booster against Covid-19 in Israel. *N Engl J Med* 2021; **385**: 1393-1400 [PMID: 34525275 DOI: 10.1056/NEJMoa2114255]
10 **Freund O**, Tau L, Weiss TE, Zornitzki L, Frydman S, Jacob G, Bornstein G. Associations of vaccine status with characteristics and outcomes of hospitalized severe COVID-19 patients in the booster era. *PLoS One* 2022; **17**: e0268050 [PMID: 35536849 DOI: 10.1371/journal.pone.0268050]
11 **Vergara RJD**, Sarmiento PJD, Lagman JDN. Building public trust: a response to COVID-19 vaccine hesitancy predicament. *J Public Health (Oxf)* 2021; **43**: e291-e292 [PMID: 33454769 DOI: 10.1093/pubmed/fdaa282]
12 **Pogue K**, Jensen JL, Stancil CK, Ferguson DG, Hughes SJ, Mello EJ, Burgess R, Berges BK, Quaye A, Poole BD. Influences on Attitudes Regarding Potential COVID-19 Vaccination in the United States. *Vaccines (Basel)* 2020; **8** [PMID: 33022917 DOI: 10.3390/vaccines8040582]
13 **El-Elimat T**, AbuAlSamen MM, Almomani BA, Al-Sawalha NA, Alali FQ. Acceptance and attitudes toward COVID-19 vaccines: A cross-sectional study from Jordan. *PLoS One* 2021; **16**: e0250555 [PMID: 33891660 DOI: 10.1371/journal.pone.0250555]
14 **Lievaart M**, Franken IH, Hovens JE. Anger Assessment in Clinical and Nonclinical Populations: Further Validation of the State-Trait Anger Expression Inventory-2. *J Clin Psychol* 2016; **72**: 263-278 [PMID: 26766132 DOI: 10.1002/jclp.22253]
15 **Lundgren-Nilsson Å**, Jonsdottir IH, Pallant J, Ahlborg G Jr. Internal construct validity of the Shirom-Melamed Burnout Questionnaire (SMBQ). *BMC Public Health* 2012; **12**: 1 [PMID: 22214479 DOI: 10.1186/1471-2458-12-1]
16 **Hahn SR**, Kroenke K, Spitzer RL, Brody D, Williams JB, Linzer M, deGruy FV 3rd. The difficult patient: prevalence, psychopathology, and functional impairment. *J Gen Intern Med* 1996; **11**: 1-8 [PMID: 8691281 DOI: 10.1007/BF02603477]
17 **Aloush V**, Niv D, Ablin JN, Yaish I, Elkayam O, Elkana O. Good pain, bad pain: illness perception and physician attitudes towards rheumatoid arthritis and fibromyalgia patients. *Clin Exp Rheumatol* 2021; **39** Suppl 130: 54-60 [PMID: 33338002 DOI: 10.55563/clinexprheumatol/u1nbxz]
18 **Kelly JA**, St Lawrence JS, Smith S Jr, Hood HV, Cook DJ. Stigmatization of AIDS patients by physicians. *Am J Public Health* 1987; **77**: 789-791 [PMID: 3592030 DOI: 10.2105/AJPH.77.7.789]
19 **Brouns M**. To what extent does the Belief in a Just World Theory offer insight in prevailing positive and negative attitudes toward Islamic and non-Islamic refugees in the Netherlands? *Master Thesis Victomology Criminal Justice* 2016
20 **Correia I**, Vala J, Aguiar P. The Effects of Belief in a Just World and Victim's Innocence on Secondary Victimization, Judgements of Justice and Deservingness. *Soc Justice Res* 2001; **14**: 327-342 [DOI: 10.1023/A:1014324125095]
21 **Gesser-Edelsburg A**, Badarna Keywan H. Physicians' Perspective on Vaccine-Hesitancy at the Beginning of Israel's COVID-19 Vaccination Campaign and Public's Perceptions of Physicians' Knowledge When Recommending the Vaccine to Their Patients: A Cross-Sectional Study. *Front Public Health* 2022; **10**: 855468 [PMID: 35356022 DOI: 10.3389/fpubh.2022.855468]
22 **Tartof SY**, Slezak JM, Fischer H, Hong V, Ackerson BK, Ranasinghe ON, Frankland TB, Ogun OA, Zamparo JM, Gray S, Valluri SR, Pan K, Angulo FJ, Jodar L, McLaughlin JM. Effectiveness of mRNA BNT162b2 COVID-19 vaccine up to 6 months in a large integrated health system in the USA: a retrospective cohort study. *Lancet* 2021; **398**: 1407-1416 [PMID: 34619098 DOI: 10.1016/S0140-6736(21)02183-8]
23 **Khubchandani J**, Sharma S, Price JH, Wiblishauser MJ, Sharma M, Webb FJ. COVID-19 Vaccination Hesitancy in the United States: A Rapid National Assessment. *J Community Health* 2021; **46**: 270-277 [PMID: 33389421 DOI: 10.1007/s10900-020-00958-x]
24 **Yang R**, Penders B, Horstman K. Addressing Vaccine Hesitancy in China: A Scoping Review of Chinese Scholarship. *Vaccines (Basel)* 2019; **8** [PMID: 31861816 DOI: 10.3390/vaccines8010002]
25 **Jiang X**, Su MH, Hwang J, Lian R, Brauer M, Kim S, Shah D. Polarization Over Vaccination: Ideological Differences in Twitter Expression About COVID-19 Vaccine Favorability and Specific Hesitancy Concerns. *Soc Media Soc* 2021; **7** [DOI: 10.1177/20563051211048413]
26 **Hall JA**, Stein TS, Roter DL, Rieser N. Inaccuracies in physicians' perceptions of their patients. *Med Care* 1999; **37**: 1164-1168 [PMID: 10549618 DOI: 10.1097/00005650-199911000-00008]
27 **Street RL Jr**, Haidet P. How well do doctors know their patients? *J Gen Intern Med* 2011; **26**: 21-27 [PMID: 20652759 DOI: 10.1007/s11606-010-1453-3]
28 **Mateo CM**, Williams DR. Addressing Bias and Reducing Discrimination: The Professional Responsibility of Health Care Providers. *Acad Med* 2020; **95**: S5-S10 [PMID: 32889919 DOI: 10.1097/ACM.0000000000003683]

World Journal of Clinical Cases

Submit a Manuscript: https://www.f6publishing.com

World J Clin Cases 2023 February 6; 11(4): 830-843

DOI: 10.12998/wjcc.v11.i4.830

ISSN 2307-8960 (online)

ORIGINAL ARTICLE

Randomized Clinical Trial

Improvement of inflammatory response and gastrointestinal function in perioperative of cholelithiasis by Modified Xiao-Cheng-Qi decoction

Bao-Fang Sun, Fan Zhang, Qiang-Pu Chen, Qiang Wei, Wen-Tao Zhu, Hai-Bin Ji, Xing-Yuan Zhang

Specialty type: Medicine, research and experimental

Provenance and peer review: Unsolicited article; Externally peer reviewed.

Peer-review model: Single blind

Peer-review report's scientific quality classification

Grade A (Excellent): 0
Grade B (Very good): 0
Grade C (Good): C, C
Grade D (Fair): D
Grade E (Poor): 0

P-Reviewer: Pan J, China; Zamani M, Iran

Received: October 1, 2022
Peer-review started: October 1, 2022
First decision: November 26, 2022
Revised: December 15, 2022
Accepted: January 9, 2023
Article in press: January 29, 2023
Published online: February 6, 2023

Bao-Fang Sun, Fan Zhang, Qiang-Pu Chen, Qiang Wei, Wen-Tao Zhu, Hai-Bin Ji, Xing-Yuan Zhang, Department of Hepatobiliary Surgery, Binzhou Medical University Hospital, Binzhou 256603, Shandong Province, China

Corresponding author: Qiang-Pu Chen, Doctor, Full Professor, Department of Hepatobiliary Surgery, Binzhou Medical University Hospital, No. 661 Huanghe Second Road, Binzhou 256603, Shandong Province, China. chenqiangpu@bzmc.edu.cn

Abstract

BACKGROUND

In the perioperative period of biliary surgery, various factors can induce the release of a large number of inflammatory factors, leading to an imbalance in pro-inflammatory and anti-inflammatory responses and resulting in gastrointestinal (GI) dysfunction. Enhanced Recovery After Surgery protocols in biliary surgery have been shown to reduce the stress response and accelerate postoperative recovery. It is crucial to reduce the inflammatory response and promote the recovery of GI function after biliary surgery, both of which are the basis and key for perioperative care and postoperative recovery.

AIM

To better understand the effects of Modified Xiao-Cheng-Qi decoction (MXD) on inflammatory response and GI function in the perioperative management of cholelithiasis and their correlation.

METHODS

This was a prospective randomized placebo-controlled trial, in which 162 patients who received biliary tract surgery were randomly assigned to three groups: MXD group, XD group, and placebo-control group. The observed parameters included frequency of bowel sounds, time of first flatus and defecation, time of diet, and amount of activity after surgery. The serum levels of C-reactive protein (CRP), interleukin (IL)-6, IL-10, serum amyloid A protein (SAA), and substance P were measured by the enzyme-linked immunosorbent assay. Then, the spearman correlation coefficient was used to analyze the relationship between the indicators of GI function and inflammation.

RESULTS

Compared to the placebo-control, improvements in GI function were observed in the MXD groups including reduced incidence of nausea, vomiting, and bloating; and earlier first exhaust time, first defecation time, and feeding time after surgery ($P < 0.05$). On the 1st and 2nd d after surgery, IL-6, CRP and SAA levels in MXD group were lower than that in placebo control, but substance P level was higher, compared to the control ($P < 0.05$). Functional diarrhea occurred in both MXD and XD groups without any other adverse effects, toxic reactions, and allergic reactions. Diarrhea was relieved after the discontinuation of the investigational remedies. Bowel sounds at 12 h after surgery, the occurring time of the first flatus, first defecation, postoperative liquid diet and semi-liquid diet were significantly correlated with levels of IL-6, CRP, SAA and substance P on second day after surgery ($P < 0.05$).

CONCLUSION

Treatment with MXD can relieve inflammatory response and improve GI function after surgery. Moreover, there are significant correlations between them. Furthermore, it does not cause serious adverse reactions.

Key Words: Modified Xiao-cheng-qi Decoction; Cholelithiasis; Inflammatory response; Gastrointestinal function; Enhanced Recovery After Surgery; Perioperative

Core Tip: It is crucial to reduce the inflammatory response and promote the recovery of gastrointestinal (GI) function after biliary surgery, as both are the basis and key for perioperative care and postoperative recovery. Treatment with Modified Xiao-Cheng-Qi decoction can reduce the inflammatory response and improve GI function after surgery. Moreover, a close correlation between them was found in our study. Our findings provide insights into the possible role of inflammatory stress response in the pathogenesis of postoperative GI tract dysfunction (PGID) and support the development of novel therapeutic strategies for the prevention and treatment of postoperative inflammatory stress response and PGID.

Citation: Sun BF, Zhang F, Chen QP, Wei Q, Zhu WT, Ji HB, Zhang XY. Improvement of inflammatory response and gastrointestinal function in perioperative of cholelithiasis by Modified Xiao-Cheng-Qi decoction. *World J Clin Cases* 2023; 11(4): 830-843
URL: https://www.wjgnet.com/2307-8960/full/v11/i4/830.htm
DOI: https://dx.doi.org/10.12998/wjcc.v11.i4.830

INTRODUCTION

In the perioperative period of biliary surgery, various factors such as starvation, tissue injury, anesthesia, and pain can induce the release of a large number of inflammatory factors[1-4], leading to an imbalance in pro-inflammatory and anti-inflammatory responses and result in gastrointestinal (GI) dysfunction[5-7]. Enhanced Recovery After Surgery (ERAS) is a multimodal perioperative care pathway designed to achieve early recovery after surgical procedures by maintaining pre-operative organ function and reducing the profound stress response following surgery[8-11]. ERAS protocols in biliary surgery have been shown to reduce the stress response and accelerate postoperative recovery[12-14]. It is crucial to reduce the inflammatory response and promote the recovery of GI function after biliary surgery, both of which are the basis and key for perioperative care and postoperative recovery[15-17]. Therefore, it is necessary to develop novel interventions to reduce the inflammatory response and improve the recovery of GI function after biliary surgery. However, the relationship between inflammatory response and postoperative GI tract dysfunction (PGID) is complex and also there is less report on the correlation between the inflammatory response and GI function recovery after biliary surgery.

Modified Xiao-Cheng-Qi decoction (MXD) is a new remedy with traditional Chinese medicine (TCM), which has the addition of Huangqi (Astragalus), Ruxiang (Frankincense) and Moyao (Myrrh) compared to the classic XD. It is notable that MXD was primarily designed by the author based on the characteristics of biliary tract surgery, which have been applied to therapy according to "clinical differentiation" for several years. To better understand the effects of MXD on the inflammatory response and GI function recovery in perioperative of cholelithiasis, also their correlation, we conducted this prospective randomized controlled study.

MATERIALS AND METHODS

Study design

This study was a prospective randomized, double-blind, and placebo-controlled trial. In this study, three treatment groups were randomized in a 1:1:1 ratio (test:control:control). To obtain statistically significant results, the estimated sample size in both the test group and control group was at least 45 patients per group, according to ERAS. Participants were stratified according to the presence or absence of common bile duct stones. Considering the possibility of dropping out of the trial (10%), at least 50 patients were needed in each group, *i.e.*, our study needed a total of 150 patients in the three groups. Actually, 185 patients were assessed for eligibility, and finally 170 patients were recruited during the period from January 2017 to January 2018. All participants were randomly assigned to the three groups (MXD, XD, and control). Among them, 162 subjects (95.3%) finally completed the treatment. Four patients in the MXD group and four in the XD group dropped out because they could not tolerate the taste of the TCM or were unwilling to complete this study. The reasons and dates of withdrawal were recorded in detail. The general situation and indicators of those patients were also evaluated. A flow diagram of the patient enrollment and study phase schedule was shown in Figure 1.

The study procedures were approved by the ethics committee of Binzhou Medical University Hospital [No. Ethical research (2017-026-01)]. This study was registered at the Chinese Clinical Trial Registry (ChiCTR2000033125). The statistical methods of this study were reviewed by Qiang-Pu Chen from Binzhou Medical University Hospital. An investigator who was unaffiliated with this study created the randomization list. The randomization was completed by SAS 9.4 software to generate a random sequence. The participants were randomly allocated at a 1:1:1 ratio to three groups: (1) MXD group: ERAS + MXD [Dahuang (rhubarb) 6 g, Houbu (Magnolia officinalis) 6 g, Zhishi (Immature Bitter Orange) 12 g, Huangqi (Astragalus) 20 g, Ruxiang (Frankincense) 6 g, Moyao (Myrrh) 6 g]; (2) XD group: ERAS + XD [Dahuang (rhubarb) 6 g, Houbu (Magnolia officinalis) 6 g, Zhishi (Immature Bitter Orange) 12 g]; and (3) Placebo-control group: ERAS + warm water (Table 1). All patients underwent ERAS protocol during the perioperative period. Rhubarb, Magnolia officinalis, Immature Bitter Orange, Astragalus, Frankincense and Myrrh are Chinese Medicine Granules and all produced by Yifang Pharmaceutical Corporation (Guangdong, China). For one dose of MXD or XD, all herb ingredients were extracted with 100 mL warm boiled water to make an aqueous extract. Then 50 mL of investigational drug was administered orally at 14-16 and 6-8 h before surgery; and at 6-8, 14-16, 22-24, and 30-32 h after surgery. The control group was given 50 mL warm water at the same time.

Inclusion and exclusion criteria

The inclusion criteria were: (1) Confirmed diagnosis of cholelithiasis, surgical indications; (2) Written informed consent for surgery; (3) Underwent elective laparoscopic choledocholithotomy and cholecystectomy or laparoscopic cholecystectomy; > 18 years and ≤ 75 years; (4) Had no severe cardiopulmonary complications and American Society of Anesthesiologists grade (ASA) I or II; and (5) Underwent primary biliary tract surgery. Exclusion criteria were: (1) Patients with acute inflammation, fever, or other diseases that might seriously impact the body's stress and inflammatory responses, accompanied by immune diseases, metabolic diseases, or use of some drugs that affect the immune system; ≤ 18 years and > 75 years; (2) Had undergone an emergency operation; (3) Had undergone reoperation of the biliary tract; (4) Had severe cardiopulmonary complications; or (5) ASA III or IV. Randomization was achieved by a computer-generated list of numbers for group allocation.

ERAS protocols

The ERAS protocols were implemented as follows: (1) Preoperative preparation included admission education, nutritional risk screening, disease assessment, detailed introduction of the treatment plan, preemptive analgesia, Visual Analogue Scale (VAS) pain score; (2) Intraoperative management included sedative analgesia before anesthesia, general anesthesia, intraoperative warming, controlled infusion, and minimally invasive surgery; and (3) Postoperative management included postoperative continuous monitoring of vital signs, VAS pain score, early ambulation, early diet, postoperative analgesia, and health guidance before discharge.

General anesthesia

General anesthesia was performed by one of six trained surgeons, who had at least 5 years of experience. Patients were assigned to each anesthesia group by the random number table. When the procedure began, the peripheral vein was opened, and the patients' electrocardiogram, heart rate, and blood oxygen saturation were monitored routinely. Anesthesia induction was performed by intravenous injection of propofol 1.5-2.5 mg/kg, fentanyl 2-3 μg/kg, and atracurium besylate 0.3-0.6 mg/kg. Mechanical ventilation was also performed after tracheal intubation. The conditions for mechanical ventilation were as follows: Tidal volume, 8-12 mL/kg; positive end-expiratory pressure ventilation, 2-4 cm H_2O; ventilation frequency, 12-20 times/min; inspired oxygen concentration, 30-60%; gas flow rate, 2 L/min; and end-tidal partial pressure of carbon dioxide, 35-45 mmHg. The nasopharyngeal temperature probe was used to monitor the patient's intraoperative temperature.

Table 1 All ingredients of the different treatment group

Group	Ingredient
Control	Warm boiled water
XD	Dahuang (Rhubarb) 6 g, Houbu (Magnolia officinalis) 6 g and Zhishi (Immature Bitter Orange) 12 g
MXD	Dahuang (Rhubarb) 6 g, Houbu (Magnolia officinalis) 6 g, Zhishi (Immature Bitter Orange) 12 g, Huangqi (Astragalus) 20 g, Ruxiang (Frankincense) 6 g and Moyao (Myrrh) 6 g

XD: Xiao-Cheng-Qi decoction; MXD: Modified Xiao-Cheng-Qi decoction.

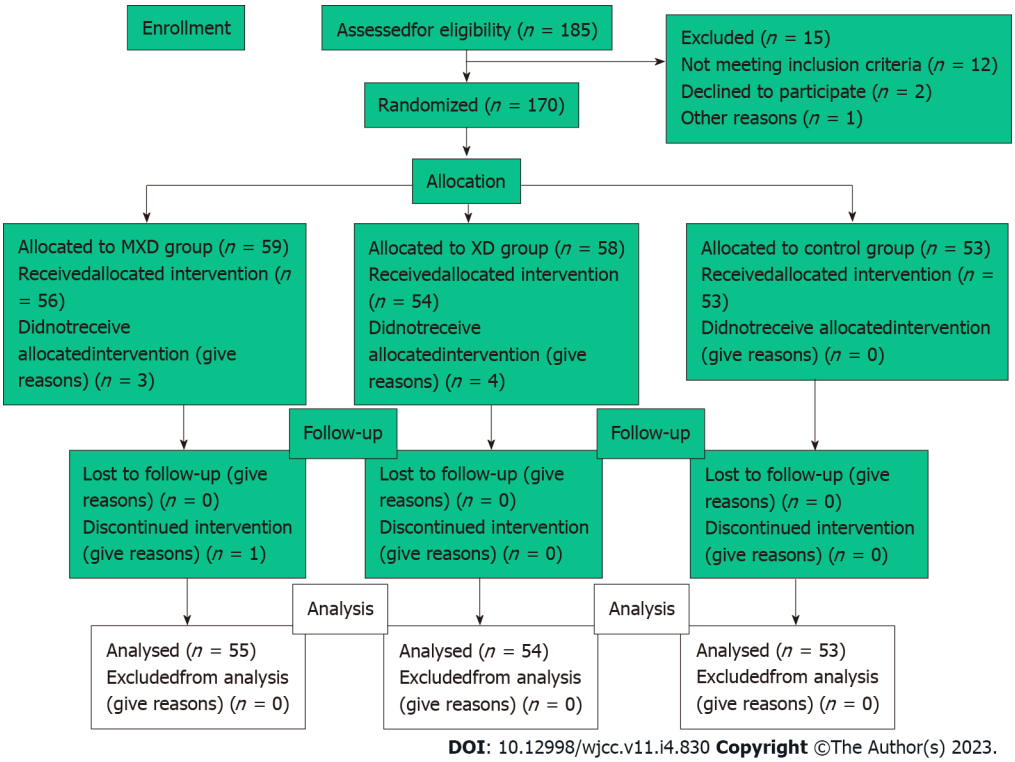

DOI: 10.12998/wjcc.v11.i4.830

Figure 1 Patients' flowchart. XD: Xiao-Cheng-Qi decoction; MXD: Modified Xiao-Cheng-Qi decoction.

Meanwhile, the thermal insulation blanket and infusion heater were used to keep the patient warm during the operation. To anesthetize the patients, remifentanil (0.25-0.5 μg/kg·min) was infused intravenously and sevoflurane was inhaled. It is notable that the inhalation concentration was adjusted according to the patients' vital signs. During the operation, atracurium besylate 0.05 mg/kg was injected intravenously, meanwhile anesthesiologists performed radial artery catheterization to continuously monitor the invasive blood pressure. At that time, anesthesiologists also performed right central venous catheterization to continuously monitor the pressure of the central vein, guide fluid input, maintain hemodynamic stability, and administer vasoactive drugs when necessary. Respiratory parameters were adjusted according to the results of the blood gas analyses.

Operation mode

Biliary surgery was performed by one of four trained surgeons, each of whom has at least 10 years of experience. Patients were assigned to each surgical group by the random number table. The general tasks included checking the status of patients before surgery, disinfecting patient's skin, and laying sterile sheets on the skin. A small arc-shaped incision of about 1.5 cm in length was made under the umbilicus, and then a pneumoperitoneum needle was inserted into the abdominal cavity. Carbon dioxide gas was injected into the pneumoperitoneum to 15 mmgh, followed by insertion of a 10 mm trocar into the abdominal cavity through direct trocar puncture and laparoscopy to explore the abdominal cavity. Two more cannulas were used to puncture under the xiphoid process, the intersection of the right costal margin and the middle clavicular line. Another trocar was inserted under the intersection of the right costal margin and axillary line under laparoscopic surveillance if needed. Laparoscopic choledocholithotomy and cholecystectomy were performed in patients with choledocholithiasis and cholecystolithiasis, while laparoscopic cholecystectomy was done in patients with cholecys-

tolithiasis. The abovementioned patients were randomly assigned to each group according to the mode of operation.

Outcome measures

The outcome measures were: The frequency of bowel sounds, time of first flatus and defecation, time of drinking and eating, and the amount of activity after surgery. The frequency of bowel sounds was observed at 2 h before surgery and at 0, 6, 12, and 24 h after surgery. Thus, stethoscope was performed for 2 min at several points, including McBurney point, anti McBurney's point, and 5 cm below the left and right costal margin; thus, the quality of intestinal sound was recorded. The mean value was calculated and recorded. The time to first passage of flatus, first defecation, first postoperative drinking time, first postoperative liquid diet time, first postoperative semi-liquid diet time, and first post-operative normal diet time were recorded in detail. Physical activity time and distance were assessed using the Mi Band activity monitor (MB4; Xiaomi Technology Co., Ltd., Beijing, China) on days 1, 2, 3, 4, and 5 (from 08:00 to 08:00) after surgery.

The complications were also monitored based on "Evidence-based clinical practice guidelines for cholelithiasis 2016"[18] and "Nurse's guide to common postoperative complications"[19]. Incision complications include surgical site infections, dehiscence, seromas, and hematomas[20]. Intra-abdominal infection is a common disease process after operation, which is associated with substantial morbidity and death[21]. Deep-vein thrombosisa is a condition in which a blood clot forms in a deep vein and causes a blockage[22]. Bile leakage originates from the cut surface of the liver, from injury of the bile ducts, or from anastomotic leakage after bilioenteric anastomosis[23]. Nausea is the unpleasant sensation of being about to vomit and is often associated with mouth watering. Vomiting is the forceful expulsion of gastric contents *via* the mouth[24]. Bloating has been defined as a feeling of increased abdominal pressure that may or may not be accompanied by objective abdominal distension, *i.e.,* visible enlargement of the waist[25]. In addition, the adverse reactions of TCM were observed in detail. Adverse drug reactions are described as "an appreciably harmful or unpleasant reaction, resulting from an intervention related to the use of a medicinal product, which predicts hazard from future administration and warrants prevention or specific treatment, or alteration of the dosage regimen, or withdrawal of the product"[26].

A comparison of the serum levels of C-reactive protein (CRP), interleukin-6 (IL-6), IL-10, serum amyloid A protein (SAA) and substance P among the three different groups was performed by the enzyme-linked immunosorbent assay at different time points, namely on the first day before surgery as well as on days 1, 2, and 5 after surgery. Besides, substance P is a member of the family of mammalian tachykinin peptides, which is predominantly released by enteric neurons, and exert a potent contractile effect on GI smooth muscle through tachykinin receptors by modulating ionic channels and by producing second messengers[27].

Statistical analyses

SPSS software version 24.0 was used to analyze the data obtained from this study. The Pearson's chi-squared test was applied to categorical variables such as sex and operation type. Normality distribution of data was first determined by the Kolmogorov-Smirnov test and accordingly, groups were compared using one-way analysis of variance, student's *t*-test or Mann-Whitney *U* test. The spearman cor-relation coefficient was used to analyze the relationship between the indicators of inflammation and GI function. $P < 0.05$ was considered statistically significant.

RESULTS

Baseline characteristics

The protocol of this study was approved by the ethics committee of Binzhou Medical University Hospital (No. Ethical research 2017-026-01). All participants provided written informed consent. The basic characteristics of the patients in the three groups are described in Table 2, in which there were no significant differences among the three groups in age, sex, body mass index, concomitant disease, surgery type, operation time, or intraoperative blood loss ($P < 0.05$; Table 2).

Recovery of GI function after biliary surgery

Our study found that there was a greater frequency of bowel sounds in the MXD and XD groups compared to the control group at 6, 12, and 24 h after surgery ($P < 0.05$). There was a greater frequency of bowel sounds in the MXD group as compared to that in the control group at 0 h after surgery ($P < 0.05$). The first exhaust time and first defecation time after surgery were earlier in both the MXD and XD groups compared to the control group ($P < 0.05$; Table 3).

Diet after biliary surgery

Compared to the control group, the time of drinking water, liquid diet, and half-liquid diet in either the

Table 2 Basic characteristics of the participants

Characteristics/group	Control (*n* = 53)	XD (*n* = 54)	MXD (*n* = 55)	*P* value
Age (yr)	57.19 ± 13.19	55.44 ± 15.75	54.53 ± 15.36	0.640
Sex				0.782
Male	23 (43.4%)	26 (48.1%)	24 (43.6%)	
Female	30 (56.6%)	28 (51.9%)	31 (56.4%)	
BMI (kg/m^2)	23.84 ± 1.85	23.78 ± 2.01	24.06 ± 1.64	0.701
Concomitant disease				0.917
Yes	30 (56.6%)	28 (51.9%)	29 (52.7%)	
No	23 (43.4%)	26 (48.1%)	26 (47.3%)	
Operation mode				0.997
Laparoscopic cholecystectomy	45 (84.9%)	46 (85.2%)	47 (85.5%)	
Laparoscopic cholecystectomy and choledocholithotomy	8 (15.1%)	8 (14.85%)	8 (14.5%)	
Operation time (min)	176.70 ± 47.02	178.89 ± 47.13	173.09 ± 49.36	0.816
Intraoperative blood loss (mL)	37.36 ± 22.80	37.04 ± 19.97	36.36 ± 19.94	0.969

XD: Xiao-Cheng-Qi decoction; MX: Modified Xiao-Cheng-Qi decoction; BMI: Body mass index.

Table 3 Recovery of gastrointestinal function after biliary surgery

Parameters	Control (*n* = 53)	XD (*n* = 54)	MXD (*n* = 55)	*P* value
Bowel sounds (times/min)				
2 h before surgery	4.66 ± 0.68	4.39 ± 0.86	4.42 ± 0.79	0.144
0 h after surgery	0.02 ± 0.14[1]	0.06 ± 0.23[1]	0.15 ± 0.36[1,2]	0.035
6 h after surgery	2.21 ± 1.32[1]	3.11 ± 1.57[1,2]	3.24 ± 1.62[1,2]	0.001
12 h after surgery	3.77 ± 1.66[1]	6.74 ± 1.99[1,2]	7.65 ± 2.15[1,2,3]	0.000
24 h after surgery	3.95 ± 1.14[1]	4.85 ± 1.39[1,2]	5.18 ± 1.53[1,2]	0.000
Time of first flatus (h)	24.00 ± 11.03	19.70 ± 10.21[2]	17.40 ± 5.31[2]	0.003
Time of first defecation (h)	55.75 ± 26.95	36.91 ± 15.20[2]	34.42 ± 12.9[2]	0.000

[1]$P < 0.05$ *vs* the same group 2 h before surgery.
[2]$P < 0.05$ *vs* the control group.
[3]$P < 0.05$ *vs* Xiao-Cheng-Qi decoction.
XD: Xiao-Cheng-Qi decoction; MXD: Modified Xiao-Cheng-Qi decoction.

MXD group or XD group was shorter ($P < 0.05$). After surgery, the half-liquid diet time in the MXD group was shorter than that in the XD group ($P < 0.05$; Table 4).

Physical activity after biliary surgery

On days 1 and 2 after surgery, the physical activity time and distance in the MXD group were greater than those in the XD group or control group ($P < 0.05$). On day 3 after surgery, the practice time of physical activity of the patients in MXD group was longer than that in the control group, meanwhile, the activity distance of patients in the MXD group was much farther than that in both the XD and control groups ($P < 0.05$; Table 5).

Complications after biliary surgery

Compared with the control group, the incidence of nausea, vomiting, and bloating in either the MXD group or XD group was reduced ($P < 0.05$). There were no serious adverse reactions in the three groups (Table 6).

Table 4 Diet after biliary surgery

Parameters	Control (*n* = 53)	XD (*n* = 54)	MXD (*n* = 55)	*P* value
Postoperative drinking time (h)	11.11 ± 7.26	8.88 ± 3.93[1]	7.21 ± 3.20[1]	0.076
Postoperative liquid diet time (h)	15.72 ± 8.98	12.74 ± 5.47[1]	10.35 ± 4.24[1]	0.049
Postoperative semi-liquid diet time (h)	27.92 ± 15.16	22.53 ± 9.33[1]	17.98 ± 6.83[1,2]	0.028
Postoperative normal diet time (h)	100.94 ± 39.04	94.80 ± 35.86	81.69 ± 29.07	0.333

[1]$P < 0.05$ *vs* the control group.
[2]$P < 0.05$ *vs* Xiao-Cheng-Qi decoction.
XD: Xiao-Cheng-Qi decoction; MXD: Modified Xiao-Cheng-Qi decoction.

Table 5 Physical activity after biliary surgery

Activity indicators	Control (*n* = 53)	XD (*n* = 54)	MXD (*n* = 55)	*P* value
Activity time (min)				
1 d after surgery	27.06 ± 8.29	28.50 ± 8.95	33.76 ± 12.41[1,2]	0.107
2 d after surgery	41.73 ± 11.59	48.07 ± 14.57[1]	57.02 ± 19.91[1,2]	0.157
3 d after surgery	50.94 ± 12.00	61.91 ± 21.73[1]	63.64 ± 19.63[1]	0.201
4 d after surgery	59.24 ± 12.81	68.75 ± 19.54	78.08 ± 35.14[1]	0.130
5 d after surgery	77.40 ± 21.77	85.17 ± 27.81	88.80 ± 22.32	0.481
Activity distance (m)				
1 d after surgery	256.70 ± 94.97	284.57 ± 80.77	344.35 ± 134.01[1,2]	0.127
2 d after surgery	397.19 ± 123.24	480.70 ± 163.85[1]	630.60 ± 177.83[1,2]	0.050
3 d after surgery	505.19 ± 151.09	571.75 ± 177.87	730.21 ± 200.95[1,2]	0.013
4 d after surgery	651.82 ± 181.59	742.75 ± 195.40	782.69 ± 159.86	0.219
5 d after surgery	788.27 ± 236.58	792.50 ± 195.48	937.10 ± 145.73	0.162

[1]$P < 0.05$ *vs* the control group.
[2]$P < 0.05$ *vs* Xiao-Cheng-Qi decoction.
XD: Xiao-Cheng-Qi decoction; MXD: Modified Xiao-Cheng-Qi decoction.

Table 6 Incidence of complications after biliary surgery

Parameters	Control (*n* = 53)	XD (*n* = 54)	MXD (*n* = 55)	*P* value
Incision complications	2 (3.77%)	1 (1.85%)	1 (1.82%)	0.761
Intra-abdominal infection	1 (1.89%)	0 (0%)	0 (0%)	0.761
Deep-vein thrombosis	0 (0%)	0 (0%)	0 (0%)	1.000
Bile leakage	1 (1.89%)	1 (1.85%)	0 (0%)	0.599
Nausea and vomiting	12 (22.64%)	3 (5.56%)[1]	2 (3.64%)[1]	0.001
Bloating	11 (20.75%)	4 (7.41%)[1]	3 (5.45%)[1]	0.009

[1]$P < 0.05$ *vs* the control group.
XD: Xiao-Cheng-Qi decoction; MXD: Modified Xiao-Cheng-Qi decoction.

Adverse reactions of the investigational remedy

Functional diarrhea occurred in both MXD and XD groups without any other adverse effects, toxic reactions, and allergic reactions. The main symptoms of functional diarrhea were the increased fecal frequency (> 3 times/d), increased fecal volume (> 200 g/d), thin fecal quality (> 85%), and no abdominal pain (> 75%)[28,29]. Based on these symptoms, the number of cases with diarrhea was

Table 7 Incidence of functional diarrhea in perioperative period

Parameters	Control (*n* = 53)	XD (*n* = 54)	MXD (*n* = 55)	*P* value
1d before surgery	2 (3.77%)	14 (25.93%)[1]	6 (10.91%)[1,2]	0.003
1d after surgery	1 (1.89%)	9 (16.67%)[1]	6 (10.91%)[1]	0.035
2 d after surgery	0 (0%)	8 (14.81%)[1]	5 (9.09%)[1]	0.017
3 d after surgery	2 (3.77%)	4 (7.41%)	2 (3.64%)	0.595
4 d after surgery	1 (1.89%)	2 (3.70%)	1 (1.82%)	0.777
5 d after surgery	2 (3.77%)	1 (1.85%)	2 (3.64%)	0.816

[1]$P < 0.05$ *vs* the control group.
[2]$P < 0.05$ *vs* Xiao-Cheng-Qi decoction.
XD: Xiao-Cheng-Qi decoction; MXD: Modified Xiao-Cheng-Qi decoction.

counted. Diarrhea was relieved after the discontinuation of the investigational remedies. The incidence of diarrhea in the MXD group and the XD group was significantly higher than that in the control group on the 1st before surgery and 1st, 2nd d after surgery ($P < 0.05$). There was no significant difference among the three groups on the 3rd, 4th and 5th d after surgery ($P > 0.05$) (Table 7).

Inflammatory indicators and substance P

IL-6: On the 1st, 2nd, and 5th d after surgery, the serum concentrations of IL-6 in the three groups were higher than that on the 1st d before operation ($P < 0.05$). It is notable that on the 1st d after surgery, the serum levels of IL-6 in both MXD and XD groups were lower than that in the control group ($P < 0.05$). While, on the 2nd d after surgery, the serum level of IL-6 in MXD group was significantly lower than that in both XD group and control group ($P < 0.05$). However, there was no statistical difference in the serum level of IL-6 between the three groups on the 1st d before surgery and 5th d after surgery ($P > 0.05$) (Table 8).

IL-10: Compared with the 1st d before surgery, there was no statistically significant difference in the serum concentrations of IL-10 between the three groups on the 1st, 2nd, and 5th d after surgery ($P > 0.05$). While there was also no statistical difference in the serum levels of IL-10 between the three groups on the 1st day before surgery and 1st, 2nd, and 5th d after surgery ($P > 0.05$) (Table 8).

CRP and SAA: On the 1st and 2nd d after surgery, the serum concentrations of CRP and SAA in the three groups were higher than that on the 1st d before surgery ($P < 0.05$). It is notable that on the 5th d after surgery, the serum levels of CRP in the control group and SSA in MXD and XD groups were higher than that on the 1st d before surgery ($P < 0.05$). On the 1st d after surgery, the serum levels of CRP and SAA in both the MXD group and XD group were lower than that in the control group ($P < 0.05$), and the serum level of SAA in MXD group was significantly lower than that in the XD group ($P < 0.05$). While on the 2nd d after surgery, the serum level of CRP in MXD group was lower than that in either the XD group or the control group ($P < 0.05$), while SAA in the MXD group was lower than that in the control group ($P < 0.05$). There was no statistically significant difference in the serum levels of CRP and SAA between the three groups on the 1st d before surgery and 5th d after surgery ($P > 0.05$) (Table 8).

Substance P: On the 1st and 2nd d after surgery, the serum concentration of substance P in the MXD group was higher than that on the 1st d before surgery ($P < 0.05$). Our study also found that on the 1st d after surgery, the serum level of substance P in the MXD group was higher than that in both the XD and control groups ($P < 0.05$). Moreover, on the 2nd d after surgery, the serum levels of substance P in the MXD and XD groups were higher than that in the control group ($P < 0.05$; Table 8).

Spearman correlation analysis between indicators of the inflammation and GI function

In terms of correlations, bowel sounds at 12 h after surgery were significantly correlated with the levels of IL-6, CRP and SAA on the 2nd d after surgery (r = -0.25, -0.22, -0.33; $P \leq 0.001$, $P \leq 0.001$, and $P \leq 0.001$, respectively). The occurring time of the first flatus was correlated significantly with the levels of IL-6 and CRP (r = 0.20, 0.35; $P \leq 0.001$, $P = 0.01$, respectively), While the occurring time of the first defecation showed its correlation with CRP and SAA levels on the 2nd d after surgery (r = 0.30, 0.24; $P \leq 0.001$, $P \leq 0.001$, respectively). Similarly, the time of the postoperative liquid diet and the postoperative semi-liquid diet were correlated significantly with CRP levels on the 2nd d after surgery (r = 0.27, 0.29; $P \leq 0.001$, $P \leq 0.001$, respectively). In addition, the level of substance P and SAA on the 2nd d after surgery showed a significant correlation (r = -0.24; $P \leq 0.001$). Bowel sounds at 12 h after surgery, the occurring time of first flatus, and that of the first defecation were significantly correlated with substance P (r = 0.31, -0.23, -025; $P \leq 0.001$, $P \leq 0.001$, and $P \leq 0.001$, respectively). Other correlations were not significant

Table 8 Levels of the indicators for acute inflammatory stress response and substance P in the perioperative period of biliary tract surgery

Indicators	Control (*n* = 53)	XD (*n* = 54)	MXD (*n* = 55)	*P* value
IL-6 (pg/mL)				
1 d before surgery	4.89 ± 1.24	4.43 ± 1.46	4.26 ± 2.62	0.203
1 d after surgery	17.42 ± 6.67[1]	10.63 ± 9.99[1,2]	9.08 ± 8.63[1,2]	0.000
2 d after surgery	11.09 ± 3.57[1]	9.80 ± 6.51[1]	6.13 ± 3.60[1,2,3]	0.000
5 d after surgery	8.49 ± 2.31[1]	7.22 ± 2.17[1]	7.22 ± 3.39[1]	0.487
IL-10 (pg/mL)				
1 d before surgery	1.29 ± 0.50	1.25 ± 0.46	1.24 ± 0.23	0.798
1 d after surgery	1.27 ± 0.49	1.20 ± 0.61	1.21 ± 0.50	0.761
2 d after surgery	1.21 ± 0.51	1.23 ± 0.50	1.19 ± 0.37	0.942
5 d after surgery	1.33 ± 0.55	1.45 ± 0.53	1.39 ± 0.42	0.865
CRP (ng/mL)				
1 d before surgery	6.19 ± 1.77	5.69 ± 2.40	5.59 ± 1.87	0.273
1 d after surgery	16.85 ± 7.73[1]	10.84 ± 8.38[1,2]	8.02 ± 3.44[1,2,3]	0.000
2 d after surgery	17.90 ± 17.36[1]	14.41 ± 11.36[1]	8.83 ± 2.84[1,2,3]	0.001
5 d after surgery	10.33 ± 3.11[1]	10.49 ± 1.45	8.52 ± 2.68	0.170
SAA (ng/mL)				
1 d before surgery	426.21 ± 48.96	415.64 ± 40.60	411.00 ± 47.39	0.214
1 d after surgery	9492.64 ± 1738.16[1]	7807.52 ± 936.93[1,2]	6953.98 ± 1228.38[1,2,3]	0.000
2 d after surgery	14792.13 ± 6501.47[1]	10573.74 ± 4074.71[1,2]	9341.03 ± 1888.41[1,2]	0.000
5 d after surgery	7817.09 ± 550.52[1]	7396.66 ± 611.02[1]	6911.41 ± 1464.14[1]	0.132
Substance P (pg/mL)				
1 d before surgery	40.73 ± 21.53	35.61 ± 19.79	36.14 ± 31.12	0.501
1 d after surgery	33.60 ± 16.05[1]	37.30 ± 16.07	49.25 ± 41.49[1,2,3]	0.009
2 d after surgery	28.23 ± 11.12[1]	45.58 ± 24.07[1,2]	51.73 ± 26.87[1,2]	0.000
5 d after surgery	28.29 ± 11.90	27.55 ± 23.99	35.48 ± 23.70	0.653

[1]$P < 0.05$ *vs* the same group before surgery.
[2]$P < 0.05$ *vs* the control group.
[3]$P < 0.05$ *vs* Xiao-Cheng-Qi decoction.
XD: Xiao-Cheng-Qi decoction; MXD: Modified Xiao-Cheng-Qi decoction; IL: Interleukin; CRP: C-reactive protein; SAA: Serum amyloid A.

(Table 9).

DISCUSSION

In the perioperative period of biliary surgery, various injury factors can activate immune cells through different ways, such as damage-associated molecular patterns and pathogen-associated molecular patterns, and cause excessive release of pro-inflammatory factors, which then lead to local inflammatory response and participate in the body's defense response[10,11]. Moderate inflammatory response in the perioperative period is associated with the defense response and maintenance of homeostasis[30]. However, in the case of an excessive inflammatory response, a large number of inflammatory cells are activated, resulting in a continuous inflammatory response and immune activation. The associated release of a large number of pro-inflammatory mediators[31] and the imbalance between pro-inflammatory mediators and anti-inflammatory mediators eventually lead to systemic inflammatory response syndrome and GI dysfunction[32-35].

Table 9 Spearman correlation between indicators of gastrointestinal function and inflammation on the second day after surgery (r, p)

Parameters	IL-6	IL-10	CRP	SAA	Substance P
Bowel sounds at 12 h after surgery	(0.25, ≤ 0.001)	(-0.03, 0.74)	(-0.22, ≤ 0.001)	(-0.33, ≤ 0.001)	(0.31, ≤ 0.001)
Time of first flatus	(0.20, 0.01)	(0.05, 0.55)	(0.35, ≤ 0.001)	(0.16, 0.04)	(-0.23, ≤ 0.001)
Time of first defecation	(0.14, 0.07)	(0.04, 0.59)	(0.30, ≤ 0.001)	(0.24, ≤ 0.001)	(-0.25, ≤ 0.001)
Postoperative liquid diet time	(0.19, 0.01)	(-0.02, 0.81)	(0.27, ≤ 0.001)	(0.08, 0.33)	(-0.10, 0.23)
Postoperative semi-liquid diet time	(0.09, 0.25)	(-0.00, 0.98)	(0.29, ≤ 0.001)	(0.11, 0.15)	(-0.15, 0.06)
Substance P	(-0.20, 0.01)	(-0.15, 0.06)	(-0.15, 0.05)	(-0.24, ≤ 0.001)	(1.00, ≤ 0.001)

XD: Xiao-Cheng-Qi decoction; MXD: Modified Xiao-Cheng-Qi decoction; IL: Interleukin; CRP: C-reactive protein; SAA: Serum amyloid A.

IL-6 is a main postoperative proinflammatory factor and a reliable predictor of systemic inflammatory response syndrome[36], which is also positively correlated with the severity of surgical trauma [37]. In the randomized controlled trials, Wang *et al*[38] and Chen *et al*[39] confirmed that IL-6 was positively correlated with surgical trauma and acute inflammation, so that IL-6 can be used as a predictor of postoperative inflammatory response. Moreover, IL-10 can negatively regulate the inflammatory response and contributes to the maintenance of pro-inflammatory and anti-inflammatory homeostasis[40]. For example, Rahr *et al*[41] and Oldenburg *et al*[42] revealed that IL-10 may maintain the balance of inflammatory response. In this study, we found that the decrease of IL-6 after surgery in MXD group was more obvious than that in the control group, and the level of IL-10 was more stable before and after surgery. To some extent, MXD is helpful to reduce the inflammatory response, in order to maintain the balance of pro-inflammatory and anti-inflammatory. Except for the inflammatory response during surgical trauma, the body also synthesizes a large number of acute-phase proteins, which inhibit the release of proteolytic enzymes, cytokines, vasoactive substances, and repair damaged tissues[43]. Among the acute phase proteins, CRP and SAA are mainly regulated by cytokines, and their dynamic changes might reflect the degree of trauma and stress response[44,45], so that both of them can be used as the main indicators for evaluating postoperative trauma, detecting septic shock and predicting organ failure[46]. Actually, Li *et al*[47] and Jung *et al*[48] confirmed by randomized controlled trials that CRP and SAA are positively correlated with the degree of trauma and stress response. In our study, the levels of IL-6, CRP and SAA on the 1st and 2nd d after surgery were significantly higher than those before surgery. While their serum level in MXD group was significantly lower than that in the control group. Taken together, MXD can reduce the response to postoperative inflammatory stress to some extent.

According to historical literature, XD was selected from "Treatise on Febrile and Miscellaneous Diseases" written by Zhang Zhong-Jing, a famous TCM doctor of the Han Dynasty in China. The composition of XD includes Dahuang (rhubarb), Houbu (Magnolia officinalis) and Zhishi (Immature Bitter Orange)[49]. MXD is a modified version of XD, with the addition of three components: Astragalus, Frankincense, and Myrrh on the basis of XD. Rhubarb[50-53], Astragalus[54-58], and Magnolia officinalis[59-61] have immune protection effects and reduce the inflammatory stress response. MXD may improve the recovery of GI function of patients with cholelithiasis in the perioperative period under ERAS. All of these results suggested the role of MXD in the improvement of the recovery of GI function, as evidenced by a patients' early exhaust and defecation, early recovery of GI peristalsis, early feeding, and reduced incidence of nausea, vomiting, and bloating. Optimized treatment accelerates the postoperative recovery, which is consistent with the ERAS concept. In addition, regulation of the substance P level by MXD occurs in patients with cholelithiasis during the perioperative period, as substance P can increase the calcium transfer of Cajal interstitial cells in the small intestine to enhance the excitatory neuron response and promote GI peristalsis[27,62]. The serum level of substance P is significantly increased after the application of Betel nut, thereby promoting GI activity [63]. In our study, the serum level of substance P in the MXD group was significantly higher than that in the control group on days 1 and 2 after surgery. Moreover, bowel sounds at 12 h after surgery, the time of both first flatus and first defecation was significantly correlated with substance P, suggesting that MXD may increase the secretion of substance P, thereby promoting the recovery of GI function. Furthermore, on the 1st and 2nd d after surgery, the levels of IL-6, CRP, and SAA in MXD group were lower than that in placebo control, but substance P level was higher, compared to control. In addition, there are significant correlations between indicators of GI function and inflammation. Therefore, it is further confirmed that postoperative inflammatory response may lead to GI dysfunction. Treatment with MXD can reduce postoperative inflammatory stress response, and further promote the recovery of GI function. Because the specific mechanism related to the improvement of recovery of GI function is still not fully clear, further investigation is required. Since this study had some limitations, more indicators for detection and data analyses with large samples collected from multicenter studies are also

needed and are ongoing from our group.

CONCLUSION

Treatment with MXD can reduce the inflammatory response and improve GI function after surgery. Moreover, a close correlation between inflammatory response and GI function was found in our study, however, the pathophysiological relationship between them remains unclear. Furthermore, there is no serious adverse reactions in MXD treatment. Our observations provide insights into the possible role of inflammatory stress response in the pathogenesis of PGID and support the development of novel therapeutic strategies for the prevention and treatment of postoperative inflammatory stress response and PGID.

ARTICLE HIGHLIGHTS

Research background

In the perioperative period of biliary surgery, various factors can induce the release of a large number of inflammatory factors, leading to an imbalance in pro-inflammatory and anti-inflammatory responses and resulting in gastrointestinal (GI) dysfunction. It is crucial to reduce the inflammatory response and promote the recovery of GI function after biliary surgery, both of which are the basis and key for perioperative care and postoperative recovery.

Research motivation

Since lack of effective measures to reduce inflammatory response and promote the recovery of GI function after biliary surgery; therefore, it is necessary to develop novel interventions to reduce the stress response and accelerate postoperative recovery.

Research objectives

To better understand the effects of Modified Xiao-Cheng-Qi decoction (MXD) on the inflammatory response and GI function in perioperative of cholelithiasis, also their correlation, we conducted this study.

Research methods

This was a prospective randomized placebo-controlled trial, in which 162 patients who received biliary tract surgery, were randomly assigned to three groups: MXD group, XD group, and placebo-control group. The parameters included frequency of bowel sounds, time of first flatus and defecation, time of diet, and amount of activity after surgery. The serum levels of C-reactive protein (CRP), interleukin-6 (IL-6), IL-10, serum amyloid A (SAA) protein, and substance P were measured.

Research results

Compared to the placebo-control, improvements in GI function were observed in the MXD groups, such as reduced incidence of nausea, vomiting, and bloating, and the earlier first exhaust time, first defecation time, and feeding time after surgery ($P < 0.05$). On the 1st and 2nd d after surgery, serum levels of IL-6, CRP, and SAA in MXD group were lower than that in placebo control, but substance P level was higher, compared to the control ($P < 0.05$).

Research conclusions

Treatment with MXD can relieve inflammatory response and improve GI function after surgery. Moreover, there are significant correlations between them.

Research perspectives

The future research project will focus on the mechanism of MXD to reduce inflammatory reaction and improve GI function.

FOOTNOTES

Author contributions: Chen QP and Sun BF designed the study and developed the concept; Sun BF, Zhang F, Wei Q, Zhu WT, Ji HB, Zhang XY performed the experiments; Chen QP performed the statistical analysis, revised and finalized the manuscript; Sun BF wrote the manuscript; and all authors read and approved the final version of the manuscript.

Institutional review board statement: The study was reviewed and approved by the Institutional Review Board of Binzhou Medical University Hospital [No. Ethical research (2017-026-01)].

Clinical trial registration statement: This study is registered at ClinicalTrials.gov. The registration identification number is ChiCTR2000033125.

Informed consent statement: All study participants, or their legal guardian, provided informed written consent prior to study enrollment.

Conflict-of-interest statement: All the authors report no relevant conflicts of interest for this article.

Data sharing statement: Technical appendix, statistical code, and dataset are available from the corresponding author at chenqiangpu@bzmc.edu.cn. Participants gave informed consent for data sharing.

CONSORT 2010 statement: The authors have read the CONSORT 2010 statement, and the manuscript was prepared and revised according to the CONSORT 2010 statement.

Country/Territory of origin: China

ORCID number: Bao-Fang Sun 0000-0003-3499-6611; Fan Zhang 0000-0001-8151-6137; Qiang-Pu Chen 0000-0002-1941-3572; Qiang Wei 0000-0003-0668-6579; Wen-Tao Zhu 0000-0002-3432-0606; Hai-Bin Ji 0000-0001-6606-4929; Xing-Yuan Zhang 0000-0003-1613-7274.

S-Editor: Wang JJ
L-Editor: A
P-Editor: Wang JJ

REFERENCES

1 **Hossain M**, Kubes P. Innate immune cells orchestrate the repair of sterile injury in the liver and beyond. *Eur J Immunol* 2019; **49**: 831-841 [PMID: 31001813 DOI: 10.1002/eji.201847485]
2 **Dobson GP**. Addressing the Global Burden of Trauma in Major Surgery. *Front Surg* 2015; **2**: 43 [PMID: 26389122 DOI: 10.3389/fsurg.2015.00043]
3 **O'Dwyer MJ**, Owen HC, Torrance HD. The perioperative immune response. *Curr Opin Crit Care* 2015; **21**: 336-342 [PMID: 26103142 DOI: 10.1097/MCC.0000000000000213]
4 **McDonald B**, Kubes P. Innate Immune Cell Trafficking and Function During Sterile Inflammation of the Liver. *Gastroenterology* 2016; **151**: 1087-1095 [PMID: 27725145 DOI: 10.1053/j.gastro.2016.09.048]
5 **Margraf A**, Ludwig N, Zarbock A, Rossaint J. Systemic Inflammatory Response Syndrome After Surgery: Mechanisms and Protection. *Anesth Analg* 2020; **131**: 1693-1707 [PMID: 33186158 DOI: 10.1213/ANE.0000000000005175]
6 **Alazawi W**, Pirmadjid N, Lahiri R, Bhattacharya S. Inflammatory and Immune Responses to Surgery and Their Clinical Impact. *Ann Surg* 2016; **264**: 73-80 [PMID: 27275778 DOI: 10.1097/SLA.0000000000001691]
7 **Alhayyan A**, McSorley S, Roxburgh C, Kearns R, Horgan P, McMillan D. The effect of anesthesia on the postoperative systemic inflammatory response in patients undergoing surgery: A systematic review and meta-analysis. *Surg Open Sci* 2020; **2**: 1-21 [PMID: 32754703 DOI: 10.1016/j.sopen.2019.06.001]
8 **Kehlet H**. Enhanced Recovery After Surgery (ERAS): good for now, but what about the future? *Can J Anaesth* 2015; **62**: 99-104 [PMID: 25391731 DOI: 10.1007/s12630-014-0261-3]
9 **Page AJ**, Ejaz A, Spolverato G, Zavadsky T, Grant MC, Galante DJ, Wick EC, Weiss M, Makary MA, Wu CL, Pawlik TM. Enhanced recovery after surgery protocols for open hepatectomy--physiology, immunomodulation, and implementation. *J Gastrointest Surg* 2015; **19**: 387-399 [PMID: 25472030 DOI: 10.1007/s11605-014-2712-0]
10 **Taurchini M**, Del Naja C, Tancredi A. Enhanced Recovery After Surgery: a patient centered process. *J Vis Surg* 2018; **4**: 40 [PMID: 29552522 DOI: 10.21037/jovs.2018.01.20]
11 **Carli F**. Physiologic considerations of Enhanced Recovery After Surgery (ERAS) programs: implications of the stress response. *Can J Anaesth* 2015; **62**: 110-119 [PMID: 25501695 DOI: 10.1007/s12630-014-0264-0]
12 **Kapritsou M**. Impact of the Enhanced Recovery Program after Hepato-Pancreato-Biliary Surgery. *Asia Pac J Oncol Nurs* 2019; **6**: 333-335 [PMID: 31572751 DOI: 10.4103/apjon.apjon_15_19]
13 **Ljungqvist O**. ERAS--enhanced recovery after surgery: moving evidence-based perioperative care to practice. *JPEN J Parenter Enteral Nutr* 2014; **38**: 559-566 [PMID: 24567343 DOI: 10.1177/0148607114523451]
14 **Peng H**, Zhang Q, Qian J, Ruan F, Mai H, Wang Z, Liu M, Chen H, Li J, Zhu B, Li C, Wang K, Zhou J. Electrolyte disorders are ERAS-associated in patients undergoing hepato-pancreato-biliary surgery. *Langenbecks Arch Surg* 2020; **405**:

603-611 [PMID: 32710380 DOI: 10.1007/s00423-020-01922-y]
15 **Lau CS**, Chamberlain RS. Enhanced Recovery After Surgery Programs Improve Patient Outcomes and Recovery: A Meta-analysis. *World J Surg* 2017; **41**: 899-913 [PMID: 27822725 DOI: 10.1007/s00268-016-3807-4]
16 **Gentile LF**, Cuenca AG, Efron PA, Ang D, Bihorac A, McKinley BA, Moldawer LL, Moore FA. Persistent inflammation and immunosuppression: a common syndrome and new horizon for surgical intensive care. *J Trauma Acute Care Surg* 2012; **72**: 1491-1501 [PMID: 22695412 DOI: 10.1097/TA.0b013e318256e000]
17 **Chao A**, Chou WH, Chang CJ, Lin YJ, Fan SZ, Chao AS. The admission systemic inflammatory response syndrome predicts outcome in patients undergoing emergency surgery. *Asian J Surg* 2013; **36**: 99-103 [PMID: 23810158 DOI: 10.1016/j.asjsur.2013.01.001]
18 **Tazuma S**, Unno M, Igarashi Y, Inui K, Uchiyama K, Kai M, Tsuyuguchi T, Maguchi H, Mori T, Yamaguchi K, Ryozawa S, Nimura Y, Fujita N, Kubota K, Shoda J, Tabata M, Mine T, Sugano K, Watanabe M, Shimosegawa T. Evidence-based clinical practice guidelines for cholelithiasis 2016. *J Gastroenterol* 2017; **52**: 276-300 [PMID: 27942871 DOI: 10.1007/s00535-016-1289-7]
19 **Dennison RD**. Nurse's guide to common postoperative complications. *Nursing* 1997; **27**: 56-59 [PMID: 9397833 DOI: 10.1097/00152193-199711000-00027]
20 **Scalise A**, Calamita R, Tartaglione C, Pierangeli M, Bolletta E, Gioacchini M, Gesuita R, Di Benedetto G. Improving wound healing and preventing surgical site complications of closed surgical incisions: a possible role of Incisional Negative Pressure Wound Therapy. A systematic review of the literature. *Int Wound J* 2016; **13**: 1260-1281 [PMID: 26424609 DOI: 10.1111/iwj.12492]
21 **Mazuski JE**, Tessier JM, May AK, Sawyer RG, Nadler EP, Rosengart MR, Chang PK, O'Neill PJ, Mollen KP, Huston JM, Diaz JJ Jr, Prince JM. The Surgical Infection Society Revised Guidelines on the Management of Intra-Abdominal Infection. *Surg Infect (Larchmt)* 2017; **18**: 1-76 [PMID: 28085573 DOI: 10.1089/sur.2016.261]
22 **Wade R**, Sideris E, Paton F, Rice S, Palmer S, Fox D, Woolacott N, Spackman E. Graduated compression stockings for the prevention of deep-vein thrombosis in postoperative surgical patients: a systematic review and economic model with a value of information analysis. *Health Technol Assess* 2015; **19**: 1-220 [PMID: 26613365 DOI: 10.3310/hta19980]
23 **Koch M**, Garden OJ, Padbury R, Rahbari NN, Adam R, Capussotti L, Fan ST, Yokoyama Y, Crawford M, Makuuchi M, Christophi C, Banting S, Brooke-Smith M, Usatoff V, Nagino M, Maddern G, Hugh TJ, Vauthey JN, Greig P, Rees M, Nimura Y, Figueras J, DeMatteo RP, Büchler MW, Weitz J. Bile leakage after hepatobiliary and pancreatic surgery: a definition and grading of severity by the International Study Group of Liver Surgery. *Surgery* 2011; **149**: 680-688 [PMID: 21316725 DOI: 10.1016/j.surg.2010.12.002]
24 **Metz A**, Hebbard G. Nausea and vomiting in adults--a diagnostic approach. *Aust Fam Physician* 2007; **36**: 688-692 [PMID: 17885699]
25 **Malagelada JR**, Accarino A, Azpiroz F. Bloating and Abdominal Distension: Old Misconceptions and Current Knowledge. *Am J Gastroenterol* 2017; **112**: 1221-1231 [PMID: 28508867 DOI: 10.1038/ajg.2017.129]
26 **Edwards IR**, Aronson JK. Adverse drug reactions: definitions, diagnosis, and management. *Lancet* 2000; **356**: 1255-1259 [PMID: 11072960 DOI: 10.1016/S0140-6736(00)02799-9]
27 **Kim BJ**, Chang IY, Choi S, Jun JY, Jeon JH, Xu WX, Kwon YK, Ren D, So I. Involvement of Na(+)-leak channel in substance P-induced depolarization of pacemaking activity in interstitial cells of Cajal. *Cell Physiol Biochem* 2012; **29**: 501-510 [PMID: 22508057 DOI: 10.1159/000338504]
28 **Holtmann GJ**, Talley NJ. Inconsistent symptom clusters for functional gastrointestinal disorders in Asia: is Rome burning? *Gut* 2018; **67**: 1911-1915 [PMID: 29921653 DOI: 10.1136/gutjnl-2017-314775]
29 **Hou ZK**, Hu W, Liu FB, Xiao JX, Lyu ZP. [Inspirations of Rome IV on clinical evaluation of traditional Chinese medicine for functional gastrointestinal disease]. *Zhongguo Zhong Yao Za Zhi* 2018; **43**: 2168-2176 [PMID: 29933688 DOI: 10.19540/j.cnki.cjcmm.20180307.007]
30 **Shankar Hari M**, Summers C. Major surgery and the immune system: from pathophysiology to treatment. *Curr Opin Crit Care* 2018; **24**: 588-593 [PMID: 30299310 DOI: 10.1097/MCC.0000000000000561]
31 **Kimura F**, Shimizu H, Yoshidome H, Ohtsuka M, Miyazaki M. Immunosuppression following surgical and traumatic injury. *Surg Today* 2010; **40**: 793-808 [PMID: 20740341 DOI: 10.1007/s00595-010-4323-z]
32 **Binkowska AM**, Michalak G, Słotwiński R. Current views on the mechanisms of immune responses to trauma and infection. *Cent Eur J Immunol* 2015; **40**: 206-216 [PMID: 26557036 DOI: 10.5114/ceji.2015.52835]
33 **Hill TL**. Gastrointestinal Tract Dysfunction With Critical Illness: Clinical Assessment and Management. *Top Companion Anim Med* 2019; **35**: 47-52 [PMID: 31122688 DOI: 10.1053/j.tcam.2019.04.002]
34 **Li H**, He T, Xu Q, Li Z, Liu Y, Li F, Yang BF, Liu CZ. Acupuncture and regulation of gastrointestinal function. *World J Gastroenterol* 2015; **21**: 8304-8313 [PMID: 26217082 DOI: 10.3748/wjg.v21.i27.8304]
35 **Reintam Blaser A**, Preiser JC, Fruhwald S, Wilmer A, Wernerman J, Benstoem C, Casaer MP, Starkopf J, van Zanten A, Rooyackers O, Jakob SM, Loudet CI, Bear DE, Elke G, Kott M, Lautenschläger I, Schäper J, Gunst J, Stoppe C, Nobile L, Fuhrmann V, Berger MM, Oudemans-van Straaten HM, Arabi YM, Deane AM; Working Group on Gastrointestinal Function within the Section of Metabolism, Endocrinology and Nutrition (MEN Section) of ESICM. Gastrointestinal dysfunction in the critically ill: a systematic scoping review and research agenda proposed by the Section of Metabolism, Endocrinology and Nutrition of the European Society of Intensive Care Medicine. *Crit Care* 2020; **24**: 224 [PMID: 32414423 DOI: 10.1186/s13054-020-02889-4]
36 **Fink-Neuboeck N**, Lindenmann J, Bajric S, Maier A, Riedl R, Weinberg AM, Smolle-Juettner FM. Clinical impact of interleukin 6 as a predictive biomarker in the early diagnosis of postoperative systemic inflammatory response syndrome after major thoracic surgery: A prospective clinical trial. *Surgery* 2016; **160**: 443-453 [PMID: 27206334 DOI: 10.1016/j.surg.2016.04.004]
37 **Jawa RS**, Anillo S, Huntoon K, Baumann H, Kulaylat M. Interleukin-6 in surgery, trauma, and critical care part II: clinical implications. *J Intensive Care Med* 2011; **26**: 73-87 [PMID: 21464062 DOI: 10.1177/0885066610384188]
38 **Wang G**, Jiang Z, Zhao K, Li G, Liu F, Pan H, Li J. Immunologic response after laparoscopic colon cancer operation within an enhanced recovery program. *J Gastrointest Surg* 2012; **16**: 1379-1388 [PMID: 22585532 DOI:

10.1007/s11605-012-1880-z]
39 **Chen L**, Sun L, Lang Y, Wu J, Yao L, Ning J, Zhang J, Xu S. Fast-track surgery improves postoperative clinical recovery and cellular and humoral immunity after esophagectomy for esophageal cancer. *BMC Cancer* 2016; **16**: 449 [PMID: 27401305 DOI: 10.1186/s12885-016-2506-8]
40 **Bedke T**, Muscate F, Soukou S, Gagliani N, Huber S. Title: IL-10-producing T cells and their dual functions. *Semin Immunol* 2019; **44**: 101335 [PMID: 31734129 DOI: 10.1016/j.smim.2019.101335]
41 **Rahr HB**, Bendix J, Ahlburg P, Gjedsted J, Funch-Jensen P, Tønnesen E. Coagulation, inflammatory, and stress responses in a randomized comparison of open and laparoscopic repair of recurrent inguinal hernia. *Surg Endosc* 2006; **20**: 468-472 [PMID: 16437269 DOI: 10.1007/s00464-005-0305-4]
42 **Oldenburg HS**, Siroen MP, Boelens PG, Sluijter BJ, Pruitt JH, Naseri AH, Rauwerda JA, Meijer S, Cuesta MA, van Leeuwen PA, Moldawer LL. Aortic aneurysm repair is associated with a lower inflammatory response compared with surgery for inflammatory bowel disease. *Eur Surg Res* 2004; **36**: 266-273 [PMID: 15359089 DOI: 10.1159/000079911]
43 **Strnad P**, Tacke F, Koch A, Trautwein C. Liver - guardian, modifier and target of sepsis. *Nat Rev Gastroenterol Hepatol* 2017; **14**: 55-66 [PMID: 27924081 DOI: 10.1038/nrgastro.2016.168]
44 **Pathak A**, Agrawal A. Evolution of C-Reactive Protein. *Front Immunol* 2019; **10**: 943 [PMID: 31114584 DOI: 10.3389/fimmu.2019.00943]
45 **Sun L**, Ye RD. Serum amyloid A1: Structure, function and gene polymorphism. *Gene* 2016; **583**: 48-57 [PMID: 26945629 DOI: 10.1016/j.gene.2016.02.044]
46 **Wierdak M**, Pisarska M, Kuśnierz-Cabala B, Witowski J, Major P, Ceranowicz P, Budzyński A, Pędziwiatr M. Serum Amyloid A as an Early Marker of Infectious Complications after Laparoscopic Surgery for Colorectal Cancer. *Surg Infect (Larchmt)* 2018; **19**: 622-628 [PMID: 30004836 DOI: 10.1089/sur.2018.105]
47 **Li L**, Chen J, Liu Z, Li Q, Shi Y. Enhanced recovery program versus traditional care after hepatectomy: A meta-analysis. *Medicine (Baltimore)* 2017; **96**: e8052 [PMID: 28930840 DOI: 10.1097/MD.0000000000008052]
48 **Jung IK**, Kim MC, Kim KH, Kwak JY, Jung GJ, Kim HH. Cellular and peritoneal immune response after radical laparoscopy-assisted and open gastrectomy for gastric cancer. *J Surg Oncol* 2008; **98**: 54-59 [PMID: 18521842 DOI: 10.1002/jso.21075]
49 **Fan MX**, Wang HJ, Li XM, Li PY, Bian BL. [Studies on chemical constituents and volatile oil of Xiaochengqi decoction]. *Zhongguo Zhong Yao Za Zhi* 2008; **33**: 1027-1031 [PMID: 18652350]
50 **Chen X**, Yang K, Jing G, Yang J, Li K. Meta-Analysis of Efficacy of Rhubarb Combined With Early Enteral Nutrition for the Treatment of Severe Acute Pancreatitis. *JPEN J Parenter Enteral Nutr* 2020; **44**: 1066-1078 [PMID: 32187391 DOI: 10.1002/jpen.1789]
51 **Cao YJ**, Pu ZJ, Tang YP, Shen J, Chen YY, Kang A, Zhou GS, Duan JA. Advances in bio-active constituents, pharmacology and clinical applications of rhubarb. *Chin Med* 2017; **12**: 36 [PMID: 29299052 DOI: 10.1186/s13020-017-0158-5]
52 **Liu X**, Wu J, Tian R, Su S, Deng S, Meng X. Targeting foam cell formation and macrophage polarization in atherosclerosis: The Therapeutic potential of rhubarb. *Biomed Pharmacother* 2020; **129**: 110433 [PMID: 32768936 DOI: 10.1016/j.biopha.2020.110433]
53 **Cai J**, Xuan ZR, Wei YP, Yang HB, Wang H. [Effects of perioperative administration of Rhubarb on acute inflammatory response in patients with gastric cancer]. *Zhong Xi Yi Jie He Xue Bao* 2005; **3**: 195-198 [PMID: 15885167 DOI: 10.3736/jcim20050309]
54 **Ghasemian-Yadegari J**, Hamedeyazdan S, Nazemiyeh H, Fathiazad F. Evaluation of Phytochemical, Antioxidant and Antibacterial Activity on Astragalus Chrysostachys Boiss. Roots. *Iran J Pharm Res* 2019; **18**: 1902-1911 [PMID: 32184856 DOI: 10.22037/ijpr.2019.1100855]
55 **Li W**, Sun YN, Yan XT, Yang SY, Kim S, Lee YM, Koh YS, Kim YH. Flavonoids from Astragalus membranaceus and their inhibitory effects on LPS-stimulated pro-inflammatory cytokine production in bone marrow-derived dendritic cells. *Arch Pharm Res* 2014; **37**: 186-192 [PMID: 23771500 DOI: 10.1007/s12272-013-0174-7]
56 **Adesso S**, Russo R, Quaroni A, Autore G, Marzocco S. Astragalus membranaceus Extract Attenuates Inflammation and Oxidative Stress in Intestinal Epithelial Cells *via* NF-κB Activation and Nrf2 Response. *Int J Mol Sci* 2018; **19** [PMID: 29534459 DOI: 10.3390/ijms19030800]
57 **Clement-Kruzel S**, Hwang SA, Kruzel MC, Dasgupta A, Actor JK. Immune modulation of macrophage pro-inflammatory response by goldenseal and Astragalus extracts. *J Med Food* 2008; **11**: 493-498 [PMID: 18800897 DOI: 10.1089/jmf.2008.0044]
58 **Wang X**, Li Y, Yang X, Yao J. Astragalus polysaccharide reduces inflammatory response by decreasing permeability of LPS-infected Caco2 cells. *Int J Biol Macromol* 2013; **61**: 347-352 [PMID: 23916649 DOI: 10.1016/j.ijbiomac.2013.07.013]
59 **Poivre M**, Duez P. Biological activity and toxicity of the Chinese herb Magnolia officinalis Rehder & E. Wilson (Houpo) and its constituents. *J Zhejiang Univ Sci B* 2017; **18**: 194-214 [PMID: 28271656 DOI: 10.1631/jzus.B1600299]
60 **Shih HC**, Kuo PC, Wu SJ, Hwang TL, Hung HY, Shen DY, Shieh PC, Liao YR, Lee EJ, Gu Q, Lee KH, Wu TS. Anti-inflammatory neolignans from the roots of Magnolia officinalis. *Bioorg Med Chem* 2016; **24**: 1439-1445 [PMID: 26928286 DOI: 10.1016/j.bmc.2016.01.049]
61 **Li CY**, Chao LK, Wang SC, Chang HZ, Tsai ML, Fang SH, Liao PC, Ho CL, Chen ST, Cheng WC, Chiang CS, Kuo YH, Hua KF, Hsu IC. Honokiol inhibits LPS-induced maturation and inflammatory response of human monocyte-derived dendritic cells. *J Cell Physiol* 2011; **226**: 2338-2349 [PMID: 21660957 DOI: 10.1002/jcp.22576]
62 **Baker SA**, Drumm BT, Skowronek KE, Rembetski BE, Peri LE, Hennig GW, Perrino BA, Sanders KM. Excitatory Neuronal Responses of Ca(2+) Transients in Interstitial Cells of Cajal in the Small Intestine. *eNeuro* 2018; **5** [PMID: 29632869 DOI: 10.1523/ENEURO.0080-18.2018]
63 **Zhang S**, Yang P, Li X, Wang X, Song J, Peng W, Wu C. Comparative Researches of Semen Arecae and Charred Semen Arecae on Gastrointestinal Motility, Motilin, Substance P, and CCK in Chronically Stressed Rats. *Evid Based Complement Alternat Med* 2017; **2017**: 1273561 [PMID: 29375638 DOI: 10.1155/2017/1273561]

World Journal of Clinical Cases

Submit a Manuscript: https://www.f6publishing.com

World J Clin Cases 2023 February 6; 11(4): 844-851

DOI: 10.12998/wjcc.v11.i4.844

ISSN 2307-8960 (online)

CASE REPORT

Metagenomic next-generation sequencing for pleural effusions induced by viral pleurisy: A case report

Xue-Ping Liu, Chen-Xue Mao, Guan-Song Wang, Ming-Zhou Zhang

Specialty type: Respiratory system

Provenance and peer review: Unsolicited article; Externally peer reviewed.

Peer-review model: Single blind

Peer-review report's scientific quality classification

Grade A (Excellent): 0
Grade B (Very good): B
Grade C (Good): 0
Grade D (Fair): 0
Grade E (Poor): 0

P-Reviewer: Kirkik D, Turkey

Received: August 24, 2022
Peer-review started: August 24, 2022
First decision: December 13, 2022
Revised: December 31, 2022
Accepted: January 16, 2023
Article in press: January 16, 2023
Published online: February 6, 2023

Xue-Ping Liu, Guan-Song Wang, Ming-Zhou Zhang, Institute of Respiratory Disease, Xinqiao Hospital, Third Military Medical University, Chongqing 400037, China

Chen-Xue Mao, Department of Laboratory Diagnosis, Chongqing KingMed Center for Clinical Laboratory Co., Ltd, Chongqing 400050, China

Corresponding author: Ming-Zhou Zhang, PhD, Professor, Institute of Respiratory Disease, Xinqiao Hospital, Third Military Medical University, No. 183 Xinqiaozheng Street, Chongqing 400037, China. mingzhou06@tmmu.edu.cn

Abstract

BACKGROUND

Viral pleurisy is a viral infected disease with exudative pleural effusions. It is one of the causes for pleural effusions. Because of the difficult etiology diagnosis, clinically pleural effusions tend to be misdiagnosed as tuberculous pleurisy or idiopathic pleural effusion. Here, we report a case of pleural effusion secondary to viral pleurisy which is driven by infection with epstein-barr virus. Viral infection was identified by metagenomic next-generation sequencing (mNGS).

CASE SUMMARY

A 40-year-old male with a history of dermatomyositis, rheumatoid arthritis, and secondary interstitial pneumonia was administered with long-term oral prednisone. He presented with fever and chest pain after exposure to cold, accompanied by generalized sore and weakness, night sweat, occasional cough, and few sputums. The computed tomography scan showed bilateral pleural effusions and atelectasis of the partial right lower lobe was revealed. The pleural fluids were found to be yellow and slightly turbid after pleural catheterization. Thoracoscopy showed fibrous adhesion and auto-pleurodesis. Combining the results in pleural fluid analysis and mNGS, the patient was diagnosed as viral pleuritis. After receiving Aciclovir, the symptoms and signs of the patient were relieved.

CONCLUSION

Viral infection should be considered in cases of idiopathic pleural effusion unexplained by routine examination. mNGS is helpful for diagnosis.

Key Words: Pleural effusions; Viral pleurisy; Metagenomic next-generation sequencing; Epstein-barr virus; Infection; Case report

Core Tip: Pleural effusion is a common clinical symptom, and infectious pleurisy is one of the reasons. Its pathogen is difficult to be found by microbiological examination, and the diagnosis of viral pleural effusion is particularly difficult. Epstein-barr virus is latent infection in most adults, and it is easy to be reactivated in people with immune deficiency, which may cause infection in all parts of the body. When idiopathic pleural effusion is not clearly diagnosed through routine examination, the possibility of viral infection should be considered, and early improvement of metagenomic next-generation sequencing examination is helpful for the diagnosis.

Citation: Liu XP, Mao CX, Wang GS, Zhang MZ. Metagenomic next-generation sequencing for pleural effusions induced by viral pleurisy: A case report. *World J Clin Cases* 2023; 11(4): 844-851
URL: https://www.wjgnet.com/2307-8960/full/v11/i4/844.htm
DOI: https://dx.doi.org/10.12998/wjcc.v11.i4.844

INTRODUCTION

Pleural effusion is a relatively common clinical condition. Even after invasive procedures, such as thoracoscopy, are used, the cause of the pleural effusion cannot be established in up to 15% of patients [1]. It has been reported that virus infection is one of the causes of pleural effusion. Due to the difficulty in virus separation and culture, clinical diagnosis is challenged. Next-generation sequencing (NGS) technology makes it possible to comprehensively analyze the sequence data of nucleic acids in samples in a single assay. Therefore, untargeted metagenomic NGS (mNGS) of clinical samples has been applied for the comprehensive diagnosis of infections, including viruses, bacteria, fungi, and parasites. To our knowledge, this is the first report of diagnosis of pleural effusion induced by viral pleurisy by mNGS.

CASE PRESENTATION

Chief complaints

In May, 2021, a male, 40-year-old was transferred to the Institute of Respiratory Disease of Xinqiao Hospital, Third Military Medical University for pleural effusion of unknown etiology.

History of present illness

On May 6, he had fever after exposure to cold, accompanied by generalized sore and weakness, night sweats, sometimes cough, and few sputums. He felt chest tightness and shortness of breath after exercise. The symptoms were improved after infusion in a local clinic. On May 10, COVID-19 vaccine was administered, and he then developed fever with the highest temperature of 38 ℃. In the meantime, the above symptoms relapsed, along with the concomitant chest pain. There was no evidence of chills, purulent sputum, bloody expectoration, headache, dizziness, abdominal pain or diarrhea.

On May 14, he visited the local hospital. Blood routine tests showed white blood cell (WBC) 9.41 × 10^9 /L, hemoglobin 146 g/L, platelet 279 × 10^9/L, neutrophils (NEUT) 92.5%, lymphocytes (LYM) 4.1% and eosinophil (EO) 0.2%. Inflammatory indices increased, as demonstrated by C-reactive protein (CRP) 74.96 mg/L, erythrocyte sedimentation rate (ESR) 64 mm/H and procalcitonin 0.24 ng/mL. On chest computed tomography (CT) (plain scan), there was bilateral pleural effusions, with more effusions on the right side, and atelectasis of the partial right lower lobe was revealed (Figure 1A and B). Right pleural catheterization was performed. Approximately 600 mL effusions were drained, and they were in yellow and slightly cloudy with some clots. Pleural fluid routine examination revealed positive Rivalta test, red blood cell (RBC) 0, WBC 3292 × 10^6/L, multinuclear cells 44.7%, monocyte 55.3%, adenosine deaminase (ADA) 55 U/L, lactate dehydrogenase (LDH) 1132U/L, carcinoembryonic antigen (CEA) 3.3 ng/mL, neuron-specificenolase (NSE) 43.39 ng/mL, cytokeratin-19-fragment 56.4 ng/mL, and squamous cell carcinoma associated antigen 2.1 ng/mL. Antibody negative for Mycobacterium tuberculosis was obtained. The patient was assigned to take symptomatic treatment. Cough remained to occur intermittently while the feelings of tired and panting after exercise were milder.

History of past illness

The patient was diagnosed with dermatomyositis, rheumatoid arthritis, and secondary interstitial pneumonia one year before and had a long-term history of oral Prednison Tablet (12.5 mg). He was diagnosed with hypothyroidism 5 years before and confirmed to have autoimmune thyroiditis 4 years

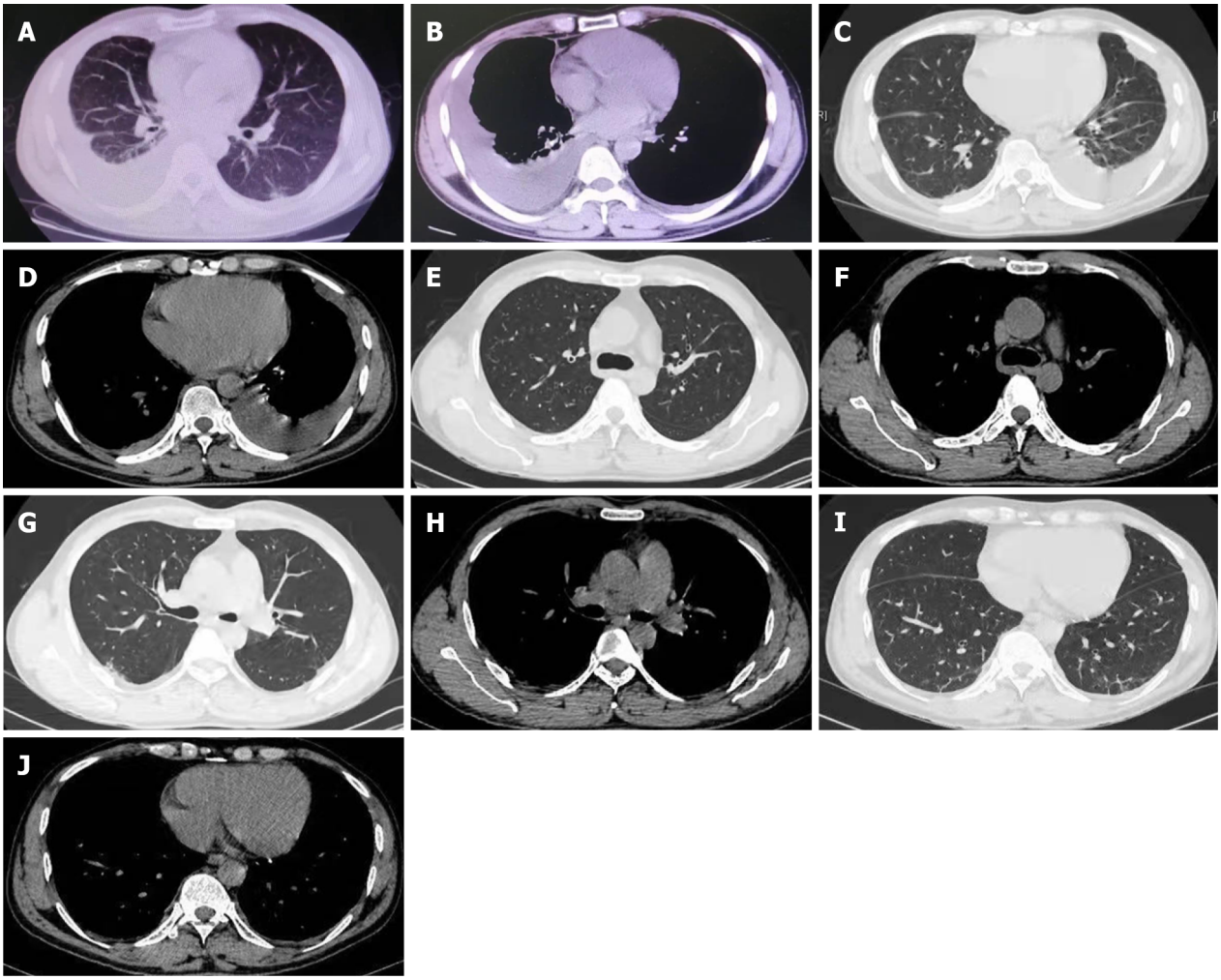

DOI: 10.12998/wjcc.v11.i4.844

Figure 1 Chest computed tomography image. A and B: Chest computed tomography (CT) scan performed on May 14; C and D: Chest CT scan performed on May 26; E-J: Chest CT scan performed on June 22.

later. Long-term oral Euthyrox at 100 μg once daily was understood. Additionally, he was diagnosed with vitiligo 2 mo before the admission.

Personal and family history

He had a 20-year history of smoking (1 packet daily) and had no history of alcohol abuse.

Physical examination

Physical examination was insignificant.

Laboratory examinations

Blood routine presented increasing WBC count (WBC 12.84 × 10^9/L, NEUT% 90.4%, LYM% 5.5%, and EO% 0.1%). Inflammatory indices were CRP 70.4 mg/L and ESR 19 mm/H. Positive Rivalta test was obtained in pleural fluid analysis, along with proteins 54.90 g/L, WBC 10141 × 10^6/L (NEUT% 68.40%, LYM% 21.90%, monocyte-macrophage 8.80%, EO% 0.90%), multinuclear cells 54.0%, monocyte 46.0%, ADA 53U/L, LDH 1717.4 U/L, and CEA 3.79 ng/mL. Acid-fast staining, bacterial culture and fungal culture in pleural fluid were all negative.

Imaging examinations

On May 26, he was transferred to the Respiratory Department of our hospital. Chest CT revealed bilateral pleural thickening and adhesion, bilateral pleural effusions while with more effusions on the left side (Figure 1C and D). Left pleural catheterization was therefore scheduled to find light yellow and slightly cloudy fluid. On the thoracoscopy, the left pleural cavity had more fibrillar adhesion bands, extensive auto-pleurodesis, cavity wall pleural surface thickening, and dispersed carbon deposition on the visceral pleural surface (Figure 2A and B).

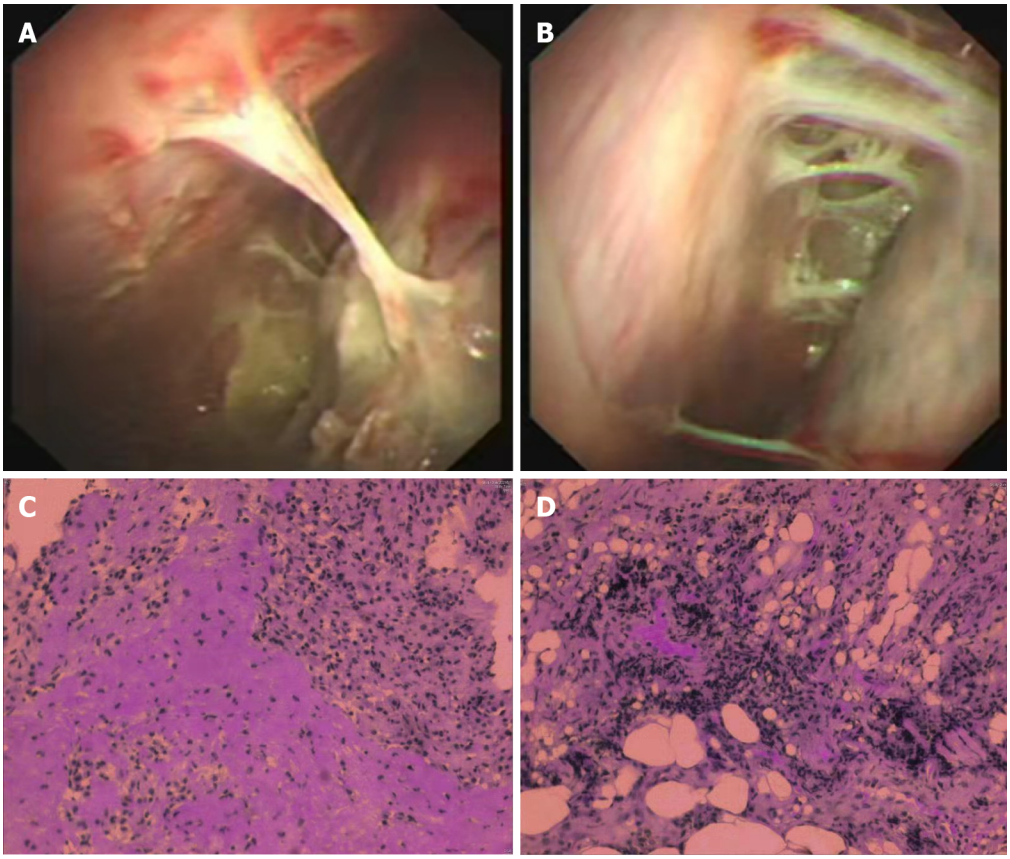

DOI: 10.12998/wjcc.v11.i4.844 **Copyright** ©The Author(s) 2023.

Figure 2 Thoracoscopy and pathologic image. A and B: Thoracoscopy image performed on May 28; C and D: Pathologic findings of the pleural biopsy on May 30.

FURTHER DIAGNOSTIC WORK-UP

The pleural fluid was sent to an independent clinical laboratory (ChongQing KingMed Center for Clinical Laboratory) for mNGS analysis using Illumina platform. There was one sequencing read of epstein-barr virus (EBV) and one sequencing read of *Staphylococcus epidermidis* (*S. epidermidis*) detected.

FINAL DIAGNOSIS

The empyema caused by infection with *S. epidermidis* was not supported by the patient clinical symptoms and thoracoscopic findings. Combining the results in pleural fluid analysis and mNGS, and the previous long-term use of prednison which could induce immunosuppression, the patient was diagnosed as viral infection-induced pleural effusion.

TREATMENT

Oral routine dose aciclovir tablet was scheduled on May 30.

OUTCOME AND FOLLOW-UP

On May 30, blood routine tests showed WBC 11.16 × 10^9/L, NEUT% 79.5%, LYM% 10.8%, EO% 0.6%, and CRP 50.3 mg/L. On June 1, pleural biopsy was performed and revealed dominant infiltration of lymphocytes (major in small B lymphocytes) and tissue cells, slightly increasing $CD8^+$ T lymphocytes and no natural killer (NK) cells (Figure 2C and D). Immunohistochemistry for cytomegalovirus and *in situ* hybridization for EBV were negative. Given the remarkably decreasing pleural effusions and the self-limited property of viral pleurisy, the patient was allowed to discharge on June 3.

On June 22, the blood routine examination showed that the WBC decreased: WBC 7.72 × 10^9/L, NEUT% 77.7%, LYM% 13.9%, and EO% 1.4%. On July 20, the blood routine tests showed WBC 8.91 × 10^9/L, NEUT% 89.0%, LYM% 6.6%, EO% 0.4%, CRP 2.5 mg/L. Chest CT plain scan showed decreasing bilateral pleural effusions and reducing atelectasis of the left lower lobe (Figure 1E-J). The results of blood routine examination on August 25 returned to normal levels: WBC 6.69 × 10^9/L, NEUT% 66.9%, LYM% 23.7%, and EO% 1.5% (Figure 3).

DISCUSSION

Pleural effusion is a common clinical manifestation of multiple diseases involved in pleura, the lung and the whole body. Predisposing factors mainly include heart failure, infectious causes, malignancy, pulmonary embolism, liver cirrhosis, subdiaphragmatic abscess and pancreatitis. Due to the non-specific symptoms, such as cough, dyspnoea and chest pain, the diagnosis of pleural effusion is required by both physical examination and laboratory tests[2]. In most cases, the etiology can be identified by clinical information, imaging techniques and pleural fluid analysis[3]. However, there is still a part that cannot be explained, despite extensive workup, including thoracoscopy or invasive tests (such as pleural biopsy)[1]. Generally, cases which fail to be explained by routine clinical evaluation is defined as idiopathic pleural effusions. Infectious pleurisy is the most common cause of exudative pleural effusion, while the responsible pathogen might be hard to detect by routine microbiologic test.

The viral infection-associated pleural effusion can be a result of the viral inflammation in adjacent tissue which extends to the pleura or the allergic reaction induced by viral infection. In those ways, the pleural effusions associated with viral pleurisy can occur independently without intrapulmonary infiltrates foci. As viral pleurisy is self-limited, the related pleural effusion can resolve spontaneously within two weeks. Additionally, some cases have less effusion, which can be absorbed rapidly, making it relatively concealed in clinic. Cohen *et al*[4] reported that the incidence of pleural effusion after viral pneumonia was 18% according to the radiological findings in the lateral recumbent position, while 2%-9% as recognized.

It has been reported that a variety of viruses could induce viral pleurisy, especially in immunocompromised patients, including influenza viruses[5], coxsackievirus, respiratory syncytial virus[6], cytomegalovirus[7], herpes simplex virus[8], EBV, adenovirus[9], human herpesvirus-8. In this viral-infected population of pleural effusion, clinical diagnosis is challenged. Reasons can be the wide variety of viruses, and difficulty in virus separation and culture. Under these limitations, only a small number of viruses are detectable in specific antibody test and nucleic acid PCR, which, to some extent, makes clinical diagnosis harder. In a prospective study[10], the authors reported that the EBV-positive rate was 40% in the pleural fluid samples of patients with pleural effusions, and the EBV-positive rate reached 59% among patients with unexplained effusions according to the PCR tests.

EBV is widespread, and more than 90% of the worldwide adult population are infected with EBV [11]. EBV is mostly transmitted through saliva, and it could establish a lifelong latent infection that reactivates intermittently to lytic replication. Infancy and childhood are usually the times when EBV primary infections occur subclinically. After primary infection, EBV uses latent infection as an immune evasion strategy to prevent cytotoxic T-cell elimination of infected cells[12]. The amount of EBV latently infected cells remains stable over years, but may vary depending on the individuals[13]. EBV viral loads in normal adults (healthy carriers) are usually undetectable, with 0.1-24.0 Latently infected B-cells per million peripheral blood mononuclear cells (PBMC) in the circulation[14] and low numbers of viral genomes per infected cell[15].

EBV systemic reactivation is possible when the cellular immune response is compromised, for example, in patients who are given bone marrow transplantation[16], patients with solid transplants [17], patients infected with HIV[18] or patients with chronic active EBV infections[19]. In addition, local reactivation of EBV takes place periodically in the oropharynx in EBV-infected healthy individuals[10], this is probably due to insufficient T-cell control in the saliva[20]. It is possible for EBV to infect almost any organ, and complications may result from infection. EBV infection has been found in the pleural space in association with B-cell lymphomas, including primary effusion lymphoma[21,22] and phyotorax-associated lymphoma[23]. However, the role of EBV in nonlymphoma pleural effusions has not been extensively studied. Interstitial pneumonitis has been associated with chronic active EBV infection and primary infection, both in children and in adults, and pleural effusion has been observed as a rare complication of EBV infection[24,25].

In the present case, mNGS detected one EBV sequence whereas the *in situ* hybridization test for EBV in pleural tissue was negative. Possible reason might be the low viral load in pleural fluid and the limited diagnostic sensitivity of the *in situ* hybridization test. According to the previous report, the majority of EBV-positive pleural fluid has a low viral load[10]. Here, the pleural effusion in the patient was gradually resolved in 1 mo, along with recovered WBC and CRP levels, consistent with the self-limited characteristic of the viral pleurisy.

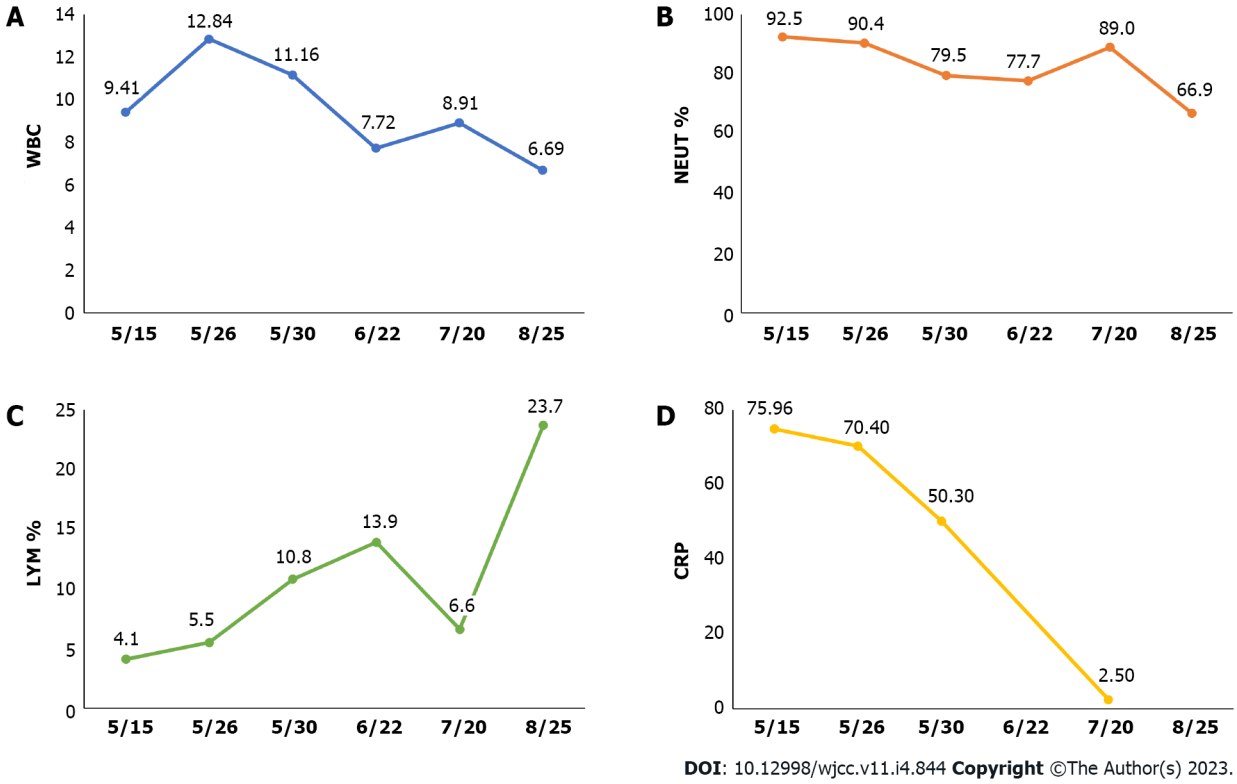

DOI: 10.12998/wjcc.v11.i4.844

Figure 3 Course of some laboratory results of this patient over time. A: The course of white blood cell over time; B: The course of neutrophils % over time; C: The course of lymphocytes % over time; D: The course of C-reactive protein over time. WBC: White blood cell; NEUT: Neutrophils; LYM: Lymphocytes; CRP: C-reactive protein.

CONCLUSION

Current reports have shown that viral infection might be the main culprit of unexplained pleural effusion. Hence, viral infection should be considered in cases of idiopathic pleural effusion unexplained by routine examination, so as to prevent misdiagnosis and missed diagnosis, in the meantime, decrease repeated pleural fluid analysis and avoid additional invasive tests.

FOOTNOTES

Author contributions: Liu XP and Wang GS collected the clinical information; the manuscript was written by Liu XP and Mao CX, and revised by Zhang MZ.

Informed consent statement: Informed written consent was obtained from the patients for the publication of this report and any accompanying images.

Conflict-of-interest statement: Author Chen-Xue Mao is employed by ChongQing KingMed Center for Clinical Laboratory Co., Ltd. The remaining authors declare that the research was conducted in the absence of any commercial or financial relationships that could be construed as a potential conflict of interest.

CARE Checklist (2016) statement: The authors have read the CARE Checklist (2016), and the manuscript was prepared and revised according to the CARE Checklist (2016).

Country/Territory of origin: China

ORCID number: Xue-Ping Liu 0000-0002-0218-0602; Chen-Xue Mao 0000-0003-0631-9998; Guan-Song Wang 0000-0002-

5184-0777; Ming-Zhou Zhang 0000-0001-8879-6426.

S-Editor: Chen YL
L-Editor: A
P-Editor: Chen YL

REFERENCES

1 **Light RW**. Clinical practice. Pleural effusion. *N Engl J Med* 2002; **346**: 1971-1977 [PMID: 12075059 DOI: 10.1056/nejmcp010731]
2 **Rahman NM**, Chapman SJ, Davies RJ. Pleural effusion: a structured approach to care. *Br Med Bull* 2004; **72**: 31-47 [PMID: 15767562 DOI: 10.1093/bmb/Ldh040]
3 **Collins TR**, Sahn SA. Thoracocentesis. Clinical value, complications, technical problems, and patient experience. *Chest* 1987; **91**: 817-822 [PMID: 3581930 DOI: 10.1378/chest.91.6.817]
4 **Cohen M**, Sahn SA. Resolution of pleural effusions. *Chest* 2001; **119**: 1547-1562 [PMID: 11348966 DOI: 10.1378/chest.119.5.1547]
5 **Choi MJ**, Lee YS, Lee JY, Lee KS. Novel influenza A (H1N1) virus infection in children: chest radiographic and CT evaluation. *Korean J Radiol* 2010; **11**: 656-664 [PMID: 21076592 DOI: 10.3348/kjr.2010.11.6.656]
6 **Vieira SE**, Stewien KE, Queiroz DA, Durigon EL, Török TJ, Anderson LJ, Miyao CR, Hein N, Botosso VF, Pahl MM, Gilio AE, Ejzenberg B, Okay Y. Clinical patterns and seasonal trends in respiratory syncytial virus hospitalizations in São Paulo, Brazil. *Rev Inst Med Trop Sao Paulo* 2001; **43**: 125-131 [PMID: 11452319 DOI: 10.1590/s0036-46652001000300002]
7 **Franquet T**, Lee KS, Müller NL. Thin-section CT findings in 32 immunocompromised patients with cytomegalovirus pneumonia who do not have AIDS. *AJR Am J Roentgenol* 2003; **181**: 1059-1063 [PMID: 14500230 DOI: 10.2214/ajr.181.4.1811059]
8 **Aquino SL**, Dunagan DP, Chiles C, Haponik EF. Herpes simplex virus 1 pneumonia: patterns on CT scans and conventional chest radiographs. *J Comput Assist Tomogr* 1998; **22**: 795-800 [PMID: 9754119 DOI: 10.1097/00004728-199809000-00024]
9 **Hong JY**, Lee HJ, Piedra PA, Choi EH, Park KH, Koh YY, Kim WS. Lower respiratory tract infections due to adenovirus in hospitalized Korean children: epidemiology, clinical features, and prognosis. *Clin Infect Dis* 2001; **32**: 1423-1429 [PMID: 11317242 DOI: 10.1086/320146]
10 **Thijsen SF**, Luderer R, van Gorp JM, Oudejans SJ, Bossink AW. A possible role for Epstein-Barr virus in the pathogenesis of pleural effusion. *Eur Respir J* 2005; **26**: 662-666 [PMID: 16204598 DOI: 10.1183/09031936.05.00131204]
11 **Cohen JI**. Epstein-Barr virus infection. *N Engl J Med* 2000; **343**: 481-492 [PMID: 10944566 DOI: 10.1056/nejm200008173430707]
12 **Thorley-Lawson DA**, Gross A. Persistence of the Epstein-Barr virus and the origins of associated lymphomas. *N Engl J Med* 2004; **350**: 1328-1337 [PMID: 15044644 DOI: 10.1056/nejmra032015]
13 **Wagner HJ**, Bein G, Bitsch A, Kirchner H. Detection and quantification of latently infected B lymphocytes in Epstein-Barr virus-seropositive, healthy individuals by polymerase chain reaction. *J Clin Microbiol* 1992; **30**: 2826-2829 [PMID: 1333480 DOI: 10.1128/jcm.30.11.2826-2829.1992]
14 **Yang J**, Tao Q, Flinn IW, Murray PG, Post LE, Ma H, Piantadosi S, Caligiuri MA, Ambinder RF. Characterization of Epstein-Barr virus-infected B cells in patients with posttransplantation lymphoproliferative disease: disappearance after rituximab therapy does not predict clinical response. *Blood* 2000; **96**: 4055-4063 [DOI: 10.1182/blood.v96.13.4055]
15 **Miyashita EM**, Yang B, Lam KM, Crawford DH, Thorley-Lawson DA. A novel form of Epstein-Barr virus latency in normal B cells in vivo. *Cell* 1995; **80**: 593-601 [PMID: 7532548 DOI: 10.1016/0092-8674(95)90513-8]
16 **van Esser JW**, van der Holt B, Meijer E, Niesters HG, Trenschel R, Thijsen SF, van Loon AM, Frassoni F, Bacigalupo A, Schaefer UW, Osterhaus AD, Gratama JW, Löwenberg B, Verdonck LF, Cornelissen JJ. Epstein-Barr virus (EBV) reactivation is a frequent event after allogeneic stem cell transplantation (SCT) and quantitatively predicts EBV-lymphoproliferative disease following T-cell--depleted SCT. *Blood* 2001; **98**: 972-978 [PMID: 11493441 DOI: 10.1182/blood.v98.4.972]
17 **Baldanti F**, Grossi P, Furione M, Simoncini L, Sarasini A, Comoli P, Maccario R, Fiocchi R, Gerna G. High levels of Epstein-Barr virus DNA in blood of solid-organ transplant recipients and their value in predicting posttransplant lymphoproliferative disorders. *J Clin Microbiol* 2000; **38**: 613-619 [PMID: 10655355 DOI: 10.1128/jcm.38.2.613-619.2000]
18 **Ling PD**, Vilchez RA, Keitel WA, Poston DG, Peng RS, White ZS, Visnegarwala F, Lewis DE, Butel JS. Epstein-Barr virus DNA loads in adult human immunodeficiency virus type 1-infected patients receiving highly active antiretroviral therapy. *Clin Infect Dis* 2003; **37**: 1244-1249 [PMID: 14557970 DOI: 10.1086/378808]
19 **Kimura H**, Hoshino Y, Kanegane H, Tsuge I, Okamura T, Kawa K, Morishima T. Clinical and virologic characteristics of chronic active Epstein-Barr virus infection. *Blood* 2001; **98**: 280-286 [PMID: 11435294 DOI: 10.1182/blood.v98.2.280]
20 **van Kooij B**, Thijsen SF, Meijer E, Niesters HG, van Esser JW, Cornelissen JJ, Verdonck LF, van Loon AM. Sequence analysis of EBV DNA isolated from mouth washings and PBMCs of healthy individuals and blood of EBV-LPD patients. *J Clin Virol* 2003; **28**: 85-92 [PMID: 12927755 DOI: 10.1016/s1386-6532(02)00269-x]
21 **Cesarman E**, Chang Y, Moore PS, Said JW, Knowles DM. Kaposi's sarcoma-associated herpesvirus-like DNA sequences in AIDS-related body-cavity-based lymphomas. *N Engl J Med* 1995; **332**: 1186-1191 [PMID: 7700311 DOI: 10.1056/nejm199505043321802]
22 **Renne R**, Zhong W, Herndier B, McGrath M, Abbey N, Kedes D, Ganem D. Lytic growth of Kaposi's sarcoma-associated

herpesvirus (human herpesvirus 8) in culture. *Nat Med* 1996; **2**: 342-346 [PMID: 8612236 DOI: 10.1038/nm0396-342]

23 **Androulaki A**, Drakos E, Hatzianastassiou D, Vgenopoulou S, Gazouli M, Korkolopoulou P, Patsouris E, Dosios T. Pyothorax-associated lymphoma (PAL): a western case with marked angiocentricity and review of the literature. *Histopathology* 2004; **44**: 69-76 [PMID: 14717672 DOI: 10.1111/j.1365-2559.2004.01737.x]

24 **Cloney DL**, Kugler JA, Donowitz LG, Lohr JA. Infectious mononucleosis with pleural effusion. *South Med J* 1988; **81**: 1441-1442 [PMID: 3187635 DOI: 10.1097/00007611-198811000-00025]

25 **Chen J**, Konstantinopoulos PA, Satyal S, Telonis J, Blair DC. Just another simple case of infectious mononucleosis? *Lancet* 2003; **361**: 1182 [PMID: 12686041 DOI: 10.1016/s0140-6736(03)12953-4]

World Journal of Clinical Cases

Submit a Manuscript: https://www.f6publishing.com

World J Clin Cases 2023 February 6; 11(4): 852-858

DOI: 10.12998/wjcc.v11.i4.852

ISSN 2307-8960 (online)

CASE REPORT

Clostridium perfringens gas gangrene caused by closed abdominal injury: A case report and review of the literature

He-Yun Li, Zhi-Xiang Wang, Jian-Chun Wang, Xiao-Di Zhang

Specialty type: Surgery

Provenance and peer review: Unsolicited article; Externally peer reviewed.

Peer-review model: Single blind

Peer-review report's scientific quality classification

Grade A (Excellent): 0
Grade B (Very good): B
Grade C (Good): 0
Grade D (Fair): D, D
Grade E (Poor): 0

P-Reviewer: Demetrashvili Z, Georgia; Musa Y, Canada; Palacios Huatuco RM, Argentina

Received: August 12, 2022
Peer-review started: August 12, 2022
First decision: October 21, 2022
Revised: November 28, 2022
Accepted: January 9, 2023
Article in press: January 9, 2023
Published online: February 6, 2023

He-Yun Li, Department of Intensive Care Unit, Shaanxi Nuclear Industry 215 Hospital, Xianyang 712000, Shaanxi Province, China

Zhi-Xiang Wang, Xiao-Di Zhang, Department of General Surgery, Shaanxi Nuclear Industry 215 Hospital, Xianyang 712000, Shaanxi Province, China

Jian-Chun Wang, Department of Healthcare-associate Infection Management, Shaanxi Nuclear Industry 215 Hospital, Xianyang 712000, Shaanxi Province, China

Corresponding author: Xiao-Di Zhang, BSc, Chief Physician, Department of General Surgery, Shaanxi Nuclear Industry 215 Hospital, No. 52 Weiyang West Road, Qindu District, Xianyang 712000, Shaanxi Province, China. zhangxd215@163.com

Abstract

BACKGROUND

Abdominal *Clostridium perfringens* (*C. perfringens*) gas gangrene is a rare infection that has been described in the literature as most frequently occurring in postoperative patients with open trauma. Intra-abdominal gas gangrene caused by *C. perfringens* infection after closed abdominal injury is extremely rare, difficult to diagnose, and progresses rapidly with high mortality risk. Here, we report a case of *C. perfringens* infection caused by closed abdominal injury.

CASE SUMMARY

A 54-year-old male suffered multiple intestinal tears and necrosis after sustaining an injury caused by falling from a high height. These injuries and the subsequent necrosis resulted in intra-abdominal *C. perfringens* infection. In the first operation, we removed the necrotic intestinal segment, kept the abdomen open and covered the intestine with a Bogota bag. A vacuum sealing drainage system was used to cover the outer layer of the Bogota bag, and the drainage was flushed under negative pressure. The patient was transferred to the intensive care unit for supportive care and empirical antibiotic treatment. The antibiotics were not changed until the results of bacterial culture and drug susceptibility testing were obtained. Two consecutive operations were then performed due to secondary intestinal necrosis. After three definitive operations, the patient successfully survived the perioperative period. Unfortunately, he died of complications related to Guillain-Barre syndrome 75 d after the first surgery. This paper presents this case of intra-abdominal gas gangrene infection and analyzes the diagnosis and treatment based on a review of current literature.

CONCLUSION
When the intestines rupture leading to contamination of the abdominal cavity by intestinal contents, *C. perfringens* bacteria normally present in the intestinal tract may proliferate in large numbers and lead to intra-abdominal infection. Prompt surgical intervention, adequate drainage, appropriate antibiotic therapy, and intensive supportive care comprise the most effective treatment strategy. If the abdominal cavity is heavily contaminated, an open abdominal approach may be a beneficial treatment.

Key Words: *Clostridium perfringens*; Intra-abdominal infection; Gas gangrene; Open abdomen; Case report

Core Tip: Intra-abdominal gas gangrene caused by closed abdominal injury is extremely rare. When using laparotomy and vacuum sealed drainage combined with intensive care and antibiotic treatment, patients passed the perioperative period smoothly. The diagnosis and treatment of this case is of guiding clinical significance.

Citation: Li HY, Wang ZX, Wang JC, Zhang XD. *Clostridium perfringens* gas gangrene caused by closed abdominal injury: A case report and review of the literature. *World J Clin Cases* 2023; 11(4): 852-858
URL: https://www.wjgnet.com/2307-8960/full/v11/i4/852.htm
DOI: https://dx.doi.org/10.12998/wjcc.v11.i4.852

INTRODUCTION

Gas gangrene is a serious infection caused by *Clostridium* spp., which can be divided into *Clostridium perfringens* (*C. perfringens*), *Clostridium sordelli*, *Clostridium novyi*, and *Clostridium putrificum*. It occurs more frequently in skin and soft tissue infections. The first case of gas gangrene in a solid organ was reported by Fraenkel in 1881.

Generally, gas gangrene can be classified into three types: Posttraumatic, postoperative, and spontaneous[1]. Both in the past and at present, trauma caused by war and natural disasters has been the main cause of gas gangrene[2-4]. Postoperative gas gangrene has been reported in hilar cholangiocarcinoma, duodenal papillary carcinoma, bladder cancer, cholecystectomy, and even after implant removal[1,5-8]. Spontaneous gas gangrene is commonly seen in immunosuppressed patients, including those with diabetes, tumors, chemotherapy, and ulcerative colitis[9-14]. Gas gangrene has also been observed after colonoscopy, and in the setting of intrapartum drug abuse. Uterine gangrene caused by endometrial cancer, gas gangrene after intramuscular injection[15-19], and even spontaneous abdominal gas gangrene[20] have also been reported. However, intra-abdominal gas gangrene infection after closed abdominal trauma is extremely rare[21].

Cline and Turnbull summarized the symptoms of superficial gas gangrene[3,22], and its diagnosis is relatively simple. The symptoms of uterine gas gangrene have also been summarized[5,7,8]. Because abdominal gas gangrene is difficult to diagnose due to the lack of specific symptoms, it is rarely diagnosed preoperatively and thus carries a high mortality risk. For patients diagnosed with abdominal gas gangrene, very few can be treated conservatively, and timely surgical intervention is usually necessary to reduce the risk of death[3,22-24].

In the past, an open abdominal approach (open abdomen) has been used to treat severe abdominal infection and abdominal compartment syndrome, and vacuum sealing drainage (VSD) was generally only used to treat trunk and extremity infections. Here, we present a case of intra-abdominal gas gangrene following intestinal laceration caused by closed abdominal injury. In this case, we used open abdomen and VSD together as a comprehensive treatment for severe intra-abdominal gas gangrene infection.

CASE PRESENTATION

Chief complaints

A 54-year-old male presented to the emergency department with complaints of "lower back pain, abdominal pain, and extreme abdominal distension for 24 h after falling from height".

History of present illness

Twenty-four hours before presenting to the emergency department, the patient fell from a height of approximately 3 meters causing lower back pain, and was treated in another hospital. An X-ray showed 12 thoracic vertebral compression fractures. After hospitalization, the patient experienced unbearable severe abdominal distension and abdominal pain and was transferred to our hospital for escalation of care.

History of past illness

The patient had no relevant surgical or medical history.

Personal and family history

The patient had no relevant family medical history.

Physical examination

Temperature 36 °C, blood pressure 85/60 mmHg, respiration rate 30 breaths per minute, heart rate 145 beats per minute, blurred consciousness, flat abdomen, abdominal rigidity, obvious abdominal tenderness with rebound, absent liver dullness, and absent bowel sounds.

Laboratory examinations

A complete blood analysis was performed with the following pertinent results: White blood cell count 4800/mm^3; neutrophils 75.3%; hemoglobin 143 g/L; C-reactive protein 130 mg/L; Po_2 54.5 mmHg; and Pco_2 26 mmHg.

Imaging examinations

Abdominal computed tomography (CT) showed pneumoperitoneum, ascites, and portal venous gas (Figure 1A and B).

FINAL DIAGNOSIS

A large number of Gram-positive bacilli were found in the abdominal pus smear, and the results of bacterial identification by gas chromatography and culture of the pus were consistent with *C. perfringens* infection. The patient was diagnosed with closed abdominal injury complicated by intestinal necrosis and gas gangrene.

TREATMENT

After aggressive fluid resuscitation, emergency laparotomy was performed. A large amount of foul-smelling gas was released during laparotomy, and there were 1.5 L of purulent liquid in the abdominal cavity. The jejunum was transected 100 cm away from the ligament of Treitz, and a length of approximately 40 cm from the upper end was necrotic. The remaining intestine demonstrated multiple contusions. The left colon showed necrosis and a large amount of gas could be seen in the intestinal wall. Crepitus and snowball crepitation were also obvious between the greater omentum layers. The necrotic small intestine and left colon were removed, and transverse colostomy and upper jejunostomy were performed. The abdomen was kept open, the intestine was covered with a Bogota bag, and a gap was left in the middle to facilitate drainage. A VSD device was used to cover the outer layer of the Bogota bag and flush the drainage under negative pressure (Figure 1C and D). After the operation, the patient was transferred to the ICU negative pressure ward, strictly isolated in a single room, and intubated and started on mechanical ventilation. The patient was given 8 million U penicillin, 3 times/d, as well as sulperazon as antibiotic treatment. Colonies of *C. perfringens* were found to be sensitive to penicillin G, ampicillin, rifampicin, levofloxacin, linezolid, ceftriaxone, ceftazidime, cefepime, and cefazolin and resistant to teicoplanin, vancomycin, erythromycin, and clindamycin.

On postoperative day (POD) 6, intestinal contents were found in the abdominal drainage tube. Exploratory reoperation revealed ileal necrosis and a perforation 100 cm away from the ileocecal part and multiple lamellar necrosis of the transverse colon. However, the colon was not perforated. Because the intestinal loop was uncultivated, we repaired the seromuscular layer of the transverse colon at the necrotic mucosa. The transverse colon necrosis was repaired and terminal ileostomy was performed. On POD 10, jejunal necrosis and perforations were found 150 cm from the ligament of Treitz. Debridement and drainage were adopted, and the abdomen was kept open. The bacteria cultured for 3 consecutive days were *Escherichia coli* rather than *C. perfringens*. Accordingly, the antibiotics were changed, and the patient was released from isolation. On POD 12, the patient was removed from the ventilator, and enteral nutrition was restored. On POD 20, fascial closure was performed. We summarize the timeline

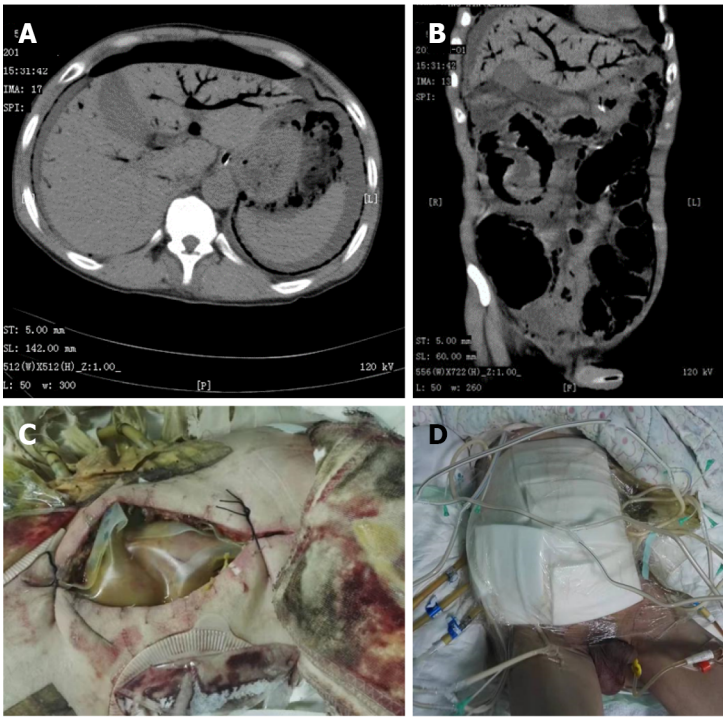

DOI: 10.12998/wjcc.v11.i4.852 **Copyright** ©The Author(s) 2023.

Figure 1 Image examination and treatment. A: Preoperative computed tomography (CT) showing pneumoperitoneum and portal venous gas; B: Coronal view of abdominal CT showing extensive portal venous gas; C: Bogota bag before the second surgery; D: Vacuum sealing drainage.

of information from this case report in Table 1.

OUTCOME AND FOLLOW-UP

The patient was able to move with protective gear 30 d after the operation and was discharged after recovery. Unfortunately, 3 wk after discharge, the patient developed limb weakness, which worsened progressively, and was hospitalized again. After admission, nutrition improved but the patient had difficulty breathing. He was transferred to the ICU again and restarted on mechanical ventilation to assist breathing. Electromyography demonstrated widespread nerve damage throughout the body. Lumbar puncture revealed normal cerebrospinal fluid pressure. Routine tests of cerebrospinal fluid showed that the number of cells was 7/L, and biochemical tests showed that the protein level was 2734 mg/L The department of neurology was consulted to consider Guillain-Barre syndrome after trauma and severe infection. The patient's muscle strength did not recover significantly after methylprednisolone pulse therapy. Seven days later, the patient and his family asked to discontinue treatment. On POD 75, he died of respiratory failure.

DISCUSSION

C. perfringens spores are widely distributed in nature, routinely found on clothing, and known to colonize the biliary, intestinal, and female reproductive tracts[22]. If there is an appropriate growth environment, such as in the settings of closed abdominal trauma or abdominal tissue or organ ischemia and necrosis, *C. perfringens* bacteria in the intestine will multiply in large numbers and may lead to intra-abdominal gas gangrene infection.

The diagnosis of abdominal organ gas gangrene is based on the symptoms described in uterine gas gangrene; however, in the case of abdominal organ gas gangrene, Gram-positive bacteria would be found in peritoneal fluid rather than vaginal secretions. X-ray is useful for the diagnosis of soft tissue gas gangrene but is limited to the abdomen[4]; CT and magnetic resonance (MR) methods can clearly illustrate the presence of interstitial gas, with MR taking longer[4,11]. Portal venous gas was once an indicator of poor prognosis[5,25]. With the advancement of imaging technologies, mortality has decreased significantly. In any case, the presence of gas in solid organs and walls of hollow organs is abnormal and should be considered red flags[26]. Surgical exploration is the main method for follow-up of gas in organs discovered by imaging. If the gas and liquid in the abdominal cavity are foul-smelling

Table 1 Timeline of information from this case report

Date	Time	Major event	Treatment
3/31/2017	-	Fall from a high height	Admitted to another hospital
4/1/2017	-	Severe abdominal distension and unbearable abdominal pain	Transferred to our hospital
	14:30	Shock	Anti-shock therapy
	18:00	Abdominal CT showed pneumoperitoneum, ascites and portal venous gas	Emergency laparotomy
	18:00-23:50	First operation; crepitus and snow-ball crepitation were obvious between the greater omentum layers	Intraoperative bacterial smear; ICU life support after surgery
4/2/2017	1:00	Suspected gas gangrene	Antibiotic therapy with penicillin, sulperazon and ornidazole
	1:20	Critical values in coagulation tests were reported	Plasma transfusion
	10:00	A large number of Gram-positive bacilli found in pus smear	Open abdomen
4/3/2017	7:30	Critical values in coagulation tests were reported	Plasma transfusion
4/4/2017	10:00	*Clostridium perfringens* cultured in drainage fluid	Continued antibiotic therapy
4/7/2017	9:00	Intestinal contents were found in abdominal drainage fluid	Second operation
4/11/2017	9:00	Multidrug-resistant bacteria were found in sputum culture	Added imipenem to antibiotic therapy
	10:00	*Clostridium perfringens* culture negative	-
	12:00	Intestinal contents found in abdominal drainage fluid	Third operation
4/12/2017	10:00	*Clostridium perfringens* culture negative; patient regained consciousness	-
4/13/2017	10:00	*Clostridium perfringens* culture negative; restored enteral nutrition; SBT experiment implemented	Discontinued penicillin; extubated
4/14/2017	10:00	*Enterococcus faecium* found in sputum culture	Replaced other antibiotics with vancomycin
4/21/2017	15:30	Fascial closure	-
4/24/2017	15:00	Patient transferred to general ward	Antibiotics downgraded to Cefoxitin
4/27/2017	10:00	*Escherichia coli* cultured from peritoneal drainage fluid	Antibiotics replaced with sulperazon and amikacin
5/1/2017	10:00	Patient able to move with protective gear	Removed abdominal drainage tube
5/12/2017	10:00	Patient discharged	-
5/30/2017	-	Patient developed progressive myasthenia	Diagnosed with Guillain-Barre syndrome
6/14/2017	-	Patient died of respiratory failure	-

CT: Computed tomography; ICU: Intensive care unit; SBT: Small bowel transit.

and accompanied by gas accumulation in the tissue space and obvious snowball crepitation, gas gangrene infection should be suspected. Bacterial culture of *C. perfringens* from paracentesis fluid or pus is the definitive method of diagnosis, but the positive rate is not high[2,4]. In our case described above, *C. perfringens* was cultured from peritoneal drainage fluid.

For patients who are diagnosed with intra-abdominal gas gangrene, the removal of necrotic tissue and effective drainage are both key to successful treatment. Open abdomen, although controversial for the treatment of severe abdominal infection, is part of the damage control strategy and is considered beneficial[27-29]. Temporary closure of the abdominal cavity and the use of VSD meet the requirements of negative pressure therapy[12,19,30] and can be applied to the open abdomen until the requirements of abdominal fascia closure are met[28,29,31,32]. Negative pressure drainage in the treatment of soft tissue gas gangrene has also been reported[31]. Hyperbaric oxygen therapy is also recommended for the treatment of gas gangrene[3,4,22], but was not used in our case. To our knowledge, we are the first to successfully apply the open abdominal approach and Bogota bag with VSD in the treatment of intra-abdominal gas gangrene.

The use of antibiotics is critical, and penicillin is the first choice. Although some experiments have proven that clindamycin is more active than penicillin in experimental gas gangrene[3,22,33,34], other broad-spectrum antibiotics should be used in combination to treat possible concurrent infections, and empirical drugs are also recommended before diagnosis[4,34]. Appropriate antibiotics should not be selected until the drug susceptibility results are obtained. In the case above, the patient was resistant to

clindamycin.

CONCLUSION

Closed abdominal injury may cause intra-abdominal gas gangrene infection. Timely diagnosis, surgery, and appropriate antibiotic therapy are keys to treatment, and intensive care is necessary. If the abdominal cavity is heavily contaminated, open abdomen is a beneficial treatment.

FOOTNOTES

Author contributions: Zhang XD and Li HY were responsible for patient treatment and case analysis; Wang ZX and Wang JC were responsible for consulting the literature and writing articles.

Informed consent statement: Informed written consent was obtained from the patients for the publication of this report and any accompanying images.

Conflict-of-interest statement: The authors declare that they have no conflicts of interest.

CARE Checklist (2016) statement: The authors have read the CARE Checklist (2016), and the manuscript was prepared and revised according to the CARE Checklist (2016).

Country/Territory of origin: China

ORCID number: Xiao-Di Zhang 0000-0002-6028-1014.

S-Editor: Chen YL
L-Editor: Filipodia
P-Editor: Chen YL

REFERENCES

1 **Bergert H**, Illert T, Friedrich K, Ockert D. Fulminant liver failure following infection by Clostridium perfringens. *Surg Infect (Larchmt)* 2004; **5**: 205-209 [PMID: 15353119 DOI: 10.1089/sur.2004.5.205]
2 **Chen E**, Deng L, Liu Z, Zhu X, Chen X, Tang H. Management of gas gangrene in Wenchuan earthquake victims. *J Huazhong Univ Sci Technolog Med Sci* 2011; **31**: 83-87 [PMID: 21336729 DOI: 10.1007/s11596-011-0155-3]
3 **Stevens DL**, Aldape MJ, Bryant AE. Life-threatening clostridial infections. *Anaerobe* 2012; **18**: 254-259 [PMID: 22120198 DOI: 10.1016/j.anaerobe.2011.11.001]
4 **Leiblein M**, Wagner N, Adam EH, Frank J, Marzi I, Nau C. Clostridial Gas Gangrene - A Rare but Deadly Infection: Case series and Comparison to Other Necrotizing Soft Tissue Infections. *Orthop Surg* 2020; **12**: 1733-1747 [PMID: 33015993 DOI: 10.1111/os.12804]
5 **Miyata Y**, Kashiwagi H, Koizumi K, Kawachi J, Kudo M, Teshima S, Isogai N, Miyake K, Shimoyama R, Fukai R, Ogino H. Fatal liver gas gangrene after biliary surgery. *Int J Surg Case Rep* 2017; **39**: 5-8 [PMID: 28783522 DOI: 10.1016/j.ijscr.2017.07.049]
6 **Takazawa T**, Ohta J, Horiuchi T, Hinohara H, Kunimoto F, Saito S. A case of acute onset postoperative gas gangrene caused by Clostridium perfringens. *BMC Res Notes* 2016; **9**: 385 [PMID: 27488346 DOI: 10.1186/s13104-016-2194-0]
7 **Qandeel H**, Abudeeb H, Hammad A, Ray C, Sajid M, Mahmud S. Clostridium perfringens sepsis and liver abscess following laparoscopic cholecystectomy. *J Surg Case Rep* 2012; **2012**: 5 [PMID: 24960720 DOI: 10.1093/jscr/2012.1.5]
8 **Wang S**, Liu L. Gas gangrene following implant removal after the union of a tibial plateau fracture: a case report. *BMC Musculoskelet Disord* 2018; **19**: 254 [PMID: 30045706 DOI: 10.1186/s12891-018-2186-4]
9 **Gray KM**, Padilla PL, Sparks B, Dziewulski P. Distant myonecrosis by atraumatic Clostridium septicum infection in a patient with metastatic breast cancer. *IDCases* 2020; **20**: e00784 [PMID: 32420030 DOI: 10.1016/j.idcr.2020.e00784]
10 **Akagawa M**, Kobayashi T, Miyakoshi N, Abe E, Abe T, Kikuchi K, Shimada Y. Vertebral osteomyelitis and epidural abscess caused by gas gangrene presenting with complete paraplegia: a case report. *J Med Case Rep* 2015; **9**: 81 [PMID: 25888739 DOI: 10.1186/s13256-015-0567-y]
11 **Dontchos BN**, Ricca R, Meehan JJ, Swanson JO. Spontaneous Clostridium perfringens myonecrosis: Case report, radiologic findings, and literature review. *Radiol Case Rep* 2013; **8**: 806 [PMID: 27330636 DOI: 10.2484/rcr.v8i3.806]

12 **Ball CG**, Ouellet JF, Anderson IB, Kirkpatrick AW. Avoidance of total abdominal wall loss despite torso soft tissue clostridial myonecrosis: a case report. *J Med Case Rep* 2013; **7**: 5 [PMID: 23298523 DOI: 10.1186/1752-1947-7-5]

13 **Kiel N**, Ho V, Pascoe A. A case of gas gangrene in an immunosuppressed Crohn's patient. *World J Gastroenterol* 2011; **17**: 3856-3858 [PMID: 21987630 DOI: 10.3748/wjg.v17.i33.3856]

14 **Nanjappa S**, Shah S, Pabbathi S. Clostridium septicum Gas Gangrene in Colon Cancer: Importance of Early Diagnosis. *Case Rep Infect Dis* 2015; **2015**: 694247 [PMID: 26793397 DOI: 10.1155/2015/694247]

15 **Fairley LJ**, Smith SL, Fairley SK. A case report of iatrogenic gas gangrene post colonoscopy successfully treated with conservative management- is surgery always necessary? *BMC Gastroenterol* 2020; **20**: 163 [PMID: 32460761 DOI: 10.1186/s12876-020-01314-y]

16 **Christie B**. Gangrene bug "killed 35 heroin users". *BMJ* 2000; **320**: 1690 [PMID: 10864534]

17 **De Angelis B**, Cerulli P, Lucilla L, Fusco A, Di Pasquali C, Bocchini I, Orlandi F, Agovino A, Cervelli V. Spontaneous clostridial myonecrosis after pregnancy - emergency treatment to the limb salvage and functional recovery: a case report. *Int Wound J* 2014; **11**: 93-97 [PMID: 22973988 DOI: 10.1111/j.1742-481X.2012.01072.x]

18 **Kashan D**, Muthu N, Chaucer B, Davalos F, Bernstein M, Chendrasekhar A. Uterine Perforation with Intra-Abdominal Clostridium perfringens Gas Gangrene: A Rare and Fatal Infection. *J Gynecol Surg* 2016; **32**: 182-184 [PMID: 27274183 DOI: 10.1089/gyn.2015.0115]

19 **Paquier L**, Mihanović J, Counil A, Karlo R, Bačić I, Dželalija B. Extensive clostridial myonecrosis after gluteal intramuscular injection in immunocompromised patient treated with surgical debridement and negative-pressure wound therapy. *Trauma Case Rep* 2021; **32**: 100469 [PMID: 33842680 DOI: 10.1016/j.tcr.2021.100469]

20 **Wion D**, Le Bert M, Brachet P. Messenger RNAs of beta-amyloid precursor protein and prion protein are regulated by nerve growth factor in PC12 cells. *Int J Dev Neurosci* 1988; **6**: 387-393 [PMID: 2903615 DOI: 10.1016/0736-5748(88)90021-4]

21 **Zhen BL**. Abdominal wall gas gangrene caused by closed small intestinal injury: a case report. *Qinghai Yixue Zazhi* 1987; **6**: 55

22 **Cline KA**, Turnbull TL. Clostridial myonecrosis. *Ann Emerg Med* 1985; **14**: 459-466 [PMID: 3885807 DOI: 10.1016/s0196-0644(85)80292-4]

23 **MacLennan JD**, MacFarlane RG. Toxin and antitoxin studies of gas gangrene in man. *Lancet* 1945; **246**: 301-305 [DOI: 10.1016/s0140-6736(45)90918-4]

24 **Potts WJ**. Battle Casualties in a South Pacific Evacuation Hospital. *Ann Surg* 1944; **120**: 886-890 [PMID: 17858541 DOI: 10.1097/00000658-194412000-00007]

25 **Alqahtani S**, Coffin CS, Burak K, Chen F, MacGregor J, Beck P. Hepatic portal venous gas: a report of two cases and a review of the epidemiology, pathogenesis, diagnosis and approach to management. *Can J Gastroenterol* 2007; **21**: 309-313 [PMID: 17505567 DOI: 10.1155/2007/934908]

26 **Nepal P**, Ojili V, Kaur N, Tirumani SH, Nagar A. Gas Where It Shouldn't Be! *AJR Am J Roentgenol* 2021; **216**: 812-823 [PMID: 33439049 DOI: 10.2214/AJR.20.23545]

27 **Robledo FA**, Luque-de-León E, Suárez R, Sánchez P, de-la-Fuente M, Vargas A, Mier J. Open versus closed management of the abdomen in the surgical treatment of severe secondary peritonitis: a randomized clinical trial. *Surg Infect (Larchmt)* 2007; **8**: 63-72 [PMID: 17381398 DOI: 10.1089/sur.2006.8.016]

28 **Kirkpatrick AW**, Coccolini F, Ansaloni L, Roberts DJ, Tolonen M, McKee JL, Leppaniemi A, Faris P, Doig CJ, Catena F, Fabian T, Jenne CN, Chiara O, Kubes P, Manns B, Kluger Y, Fraga GP, Pereira BM, Diaz JJ, Sugrue M, Moore EE, Ren J, Ball CG, Coimbra R, Balogh ZJ, Abu-Zidan FM, Dixon E, Biffl W, MacLean A, Ball I, Drover J, McBeth PB, Posadas-Calleja JG, Parry NG, Di Saverio S, Ordonez CA, Xiao J, Sartelli M; Closed Or Open after Laparotomy (COOL) after Source Control for Severe Complicated Intra-Abdominal Sepsis Investigators. Closed Or Open after Source Control Laparotomy for Severe Complicated Intra-Abdominal Sepsis (the COOL trial): study protocol for a randomized controlled trial. *World J Emerg Surg* 2018; **13**: 26 [PMID: 29977328 DOI: 10.1186/s13017-018-0183-4]

29 **Sharafuddin MJ**, Kresowik TF. Commentary. Pawaskar M, Satiani B, Balkrishnan R, Starr JE. Economic evaluation of carotid artery stenting versus carotid endarterectomy for the treatment of carotid artery stenosis. J Am Coll Surg. 2007;205:413-419. *Perspect Vasc Surg Endovasc Ther* 2008; **20**: 385-387 [PMID: 19095640 DOI: 10.1177/1531003508322393]

30 **Coccolini F**, Roberts D, Ansaloni L, Ivatury R, Gamberini E, Kluger Y, Moore EE, Coimbra R, Kirkpatrick AW, Pereira BM, Montori G, Ceresoli M, Abu-Zidan FM, Sartelli M, Velmahos G, Fraga GP, Leppaniemi A, Tolonen M, Galante J, Razek T, Maier R, Bala M, Sakakushev B, Khokha V, Malbrain M, Agnoletti V, Peitzman A, Demetrashvili Z, Sugrue M, Di Saverio S, Martzi I, Soreide K, Biffl W, Ferrada P, Parry N, Montravers P, Melotti RM, Salvetti F, Valetti TM, Scalea T, Chiara O, Cimbanassi S, Kashuk JL, Larrea M, Hernandez JAM, Lin HF, Chirica M, Arvieux C, Bing C, Horer T, De Simone B, Masiakos P, Reva V, DeAngelis N, Kike K, Balogh ZJ, Fugazzola P, Tomasoni M, Latifi R, Naidoo N, Weber D, Handolin L, Inaba K, Hecker A, Kuo-Ching Y, Ordoñez CA, Rizoli S, Gomes CA, De Moya M, Wani I, Mefire AC, Boffard K, Napolitano L, Catena F. The open abdomen in trauma and non-trauma patients: WSES guidelines. *World J Emerg Surg* 2018; **13**: 7 [PMID: 29434652 DOI: 10.1186/s13017-018-0167-4]

31 **Liu Z**, Zhao D, Wang B. Improved vacuum sealing drainage in the treatment of gas gangrene: a case report. *Int J Clin Exp Med* 2015; **8**: 19626-19628 [PMID: 26770624]

32 **Huang Q**, Li J, Lau WY. Techniques for Abdominal Wall Closure after Damage Control Laparotomy: From Temporary Abdominal Closure to Early/Delayed Fascial Closure-A Review. *Gastroenterol Res Pract* 2016; **2016**: 2073260 [PMID: 26819597 DOI: 10.1155/2016/2073260]

33 **Stevens DL**, Maier KA, Laine BM, Mitten JE. Comparison of clindamycin, rifampin, tetracycline, metronidazole, and penicillin for efficacy in prevention of experimental gas gangrene due to Clostridium perfringens. *J Infect Dis* 1987; **155**: 220-228 [PMID: 2879873 DOI: 10.1093/infdis/155.2.220]

34 **Aldape MJ**, Bayer CR, Rice SN, Bryant AE, Stevens DL. Comparative efficacy of antibiotics in treating experimental Clostridium septicum infection. *Int J Antimicrob Agents* 2018; **52**: 469-473 [PMID: 30012441 DOI: 10.1016/j.ijantimicag.2018.07.009]

World Journal of Clinical Cases

Submit a Manuscript: https://www.f6publishing.com

World J Clin Cases 2023 February 6; 11(4): 859-865

DOI: 10.12998/wjcc.v11.i4.859

ISSN 2307-8960 (online)

CASE REPORT

Is lymphatic invasion of microrectal neuroendocrine tumors an incidental event?: A case report

Jing-Xue Ran, Liang-Bi Xu, Wan-Wei Chen, Hao-Yi Yang, Yan Weng, Yong-Mei Peng

Specialty type: Gastroenterology and hepatology

Provenance and peer review: Unsolicited article; Externally peer reviewed.

Peer-review model: Single blind

Peer-review report's scientific quality classification

Grade A (Excellent): A
Grade B (Very good): 0
Grade C (Good): 0
Grade D (Fair): D
Grade E (Poor): 0

P-Reviewer: Cerwenka H, Austria; Haddadi S, Algeria

Received: August 30, 2022
Peer-review started: August 30, 2022
First decision: December 9, 2022
Revised: January 2, 2023
Accepted: January 16, 2023
Article in press: January 16, 2023
Published online: February 6, 2023

Jing-Xue Ran, Yan Weng, Yong-Mei Peng, Clinical Medical School, Guizhou Medical University, Guiyang 550000, Guizhou Province, China

Liang-Bi Xu, Wan-Wei Chen, Hao-Yi Yang, Endoscopy Center, Affiliated Hospital of Guizhou Medical University, Guiyang 550000, Guizhou Province, China

Corresponding author: Liang-Bi Xu, MA, Chief Physician, Endoscopy Center, Affiliated Hospital of Guizhou Medical University, No. 9 Beijing Road, Guiyang 550000, Guizhou Province, China. gzxlb@sina.com

Abstract

BACKGROUND

A rectal neuroendocrine tumor (rNET) is a malignant tumor originating from neuroendocrine cells. Currently, tumor size is the primary basis for assessing tumor risk.

CASE SUMMARY

This article reports the case of a 46-year-old male patient who underwent a colonoscopy that found a 3 mm rectal polypoid bulge. The pathological examination of a sample collected with biopsy forceps revealed a neuroendocrine tumor. Further endoscopic submucosal dissection rescue therapy was used. The presence of lymphatic vessels indicated that the tumor had infiltrated the negative resection margin. The lesion was located in the distal rectum near the anal canal. Therefore, to ensure the patient's quality of life, follow-up observation was conducted after full communication with the patient. No tumor recurrence or distant metastasis has been found during the 13-mo follow-up after surgery.

CONCLUSION

Despite the presence of lymphatic invasion and extremely small diameter rNETs in our case, this phenomenon may not imply a higher risk of distant lymph node and organ metastasis.

Key Words: Rectal neuroendocrine tumor; Tumor size; Lymphatic invasion; Case report

Core Tip: Due to the heterogeneity and atypical symptoms of rectal neuroendocrine tumors, in the process of clinical diagnosis and treatment, it is not sufficient to judge the risk of tumor metastasis based only on tumor size and lymphovascular invasion. Therefore, during treatment, it is necessary to formulate an individualized plan, undertake close follow-up observation, and try to improve the quality of life and disease prognosis of patients while reducing the burden of treatment.

Citation: Ran JX, Xu LB, Chen WW, Yang HY, Weng Y, Peng YM. Is lymphatic invasion of microrectal neuroendocrine tumors an incidental event?: A case report. *World J Clin Cases* 2023; 11(4): 859-865
URL: https://www.wjgnet.com/2307-8960/full/v11/i4/859.htm
DOI: https://dx.doi.org/10.12998/wjcc.v11.i4.859

INTRODUCTION

A rectal neuroendocrine tumor (rNET) is a rectal malignancy that originates from neuroendocrine cells with an insidious onset and a lack of specific first symptoms[1]. In recent years, with the extensive development of colon cancer screening programs and the improvement of endoscopic diagnosis and treatment techniques, the incidence of rNET has increased annually[2]. The incidence of rNET has increased nearly 10 times in the past 30 years, indicating that this type of tumor may not be uncommon [3]. Clinically, rNETs are usually found during endoscopy, the vast majority are 10 mm or less in diameter[4]. According to the European Neuroendocrine Tumor Society guidelines, tumor size greater than 20 mm is a risk factor for tumor invasion and metastasis, but vascular invasion, lymph node metastasis, and distant metastasis may also occur in the case of smaller tumors[5,6]. Currently, for rNETs with a tumor size of 10 mm or less, existing treatment guidelines recommend radical surgery and, in the presence of definite vascular invasion, additional lymph node dissection[7,8]. Here, we report a case of a 3 mm rNET located in the distal rectum with lymphatic invasion after endoscopic resection.

CASE PRESENTATION

Chief complaints

Polypoid bulge found on colonoscopy.

History of present illness

A 46-year-old male patient underwent colonoscopy and was found to have a 3-mm-sized polypoid bulge with a smooth surface in the rectum 3 cm from the anus. After sample collection with biopsy forceps, the pathological diagnosis was neuroendocrine tumor (NET) (Figure 1).

History of past illness

No special history of past illness.

Personal and family history

The patient's father had a history of colon cancer. His Personal history has nothing notable.

Physical examination

No special.

Laboratory examinations

No special.

Imaging examinations

Before endoscopic submucosal dissection (ESD), computed tomography (CT) showed no abnormalities in the enhancement of the chest and abdomen.

To clarify whether additional surgery was required, further assessment by 68Gallium labeled somatostatin analogues-positron emission tomography (68Ga-SSA-PET)/CT was used, but the results showed no abnormalities.

Pathological examinations

The pathological diagnosis of the specimen after ESD rescue therapy was rNET G1. The lesion

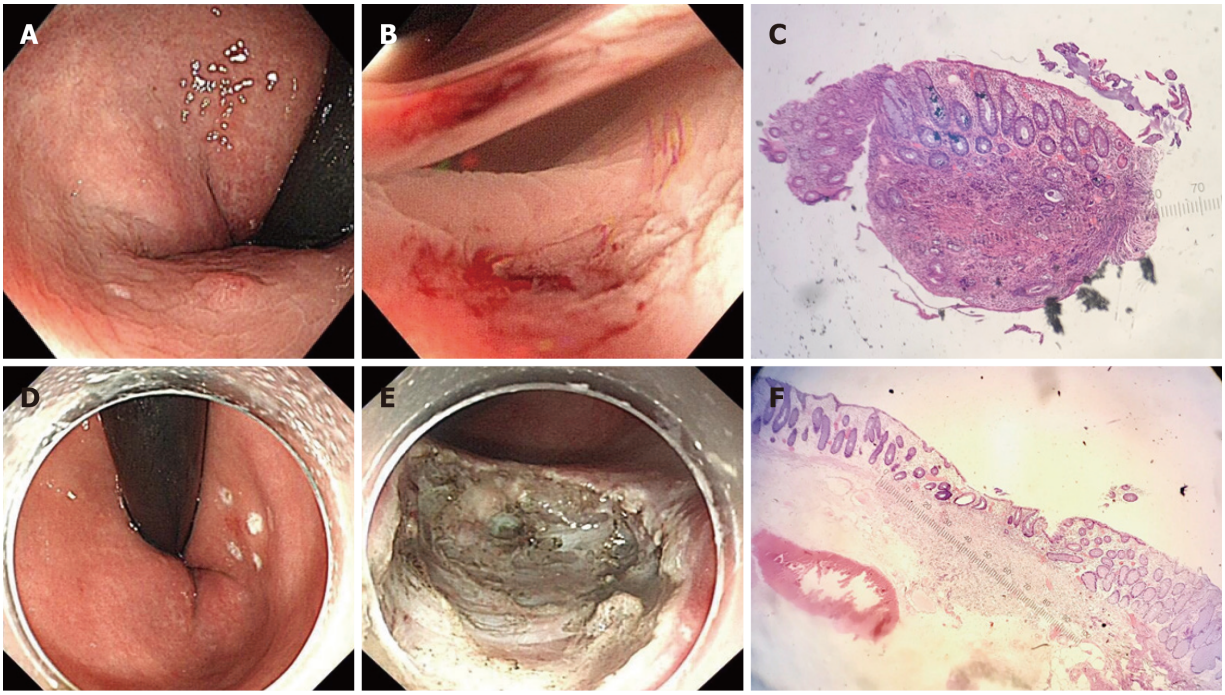

DOI: 10.12998/wjcc.v11.i4.859

Figure 1 The endoscopic manifestation of the rectal neuroendocrine tumor. A-C: Rectal neuroendocrine tumor (rNET): under a white light endoscope, the surface is smooth, sessile, and the same color as the surrounding mucosa (A); after biopsy forceps (B); the first hematoxylin and eosin (H&E) stained pathological smear after the tumor was removed by biopsy forceps (C, × 40). Endoscopic submucosal dissection (ESD) remedial treatment; D-F: Under white light endoscope, before ESD (D); after additional ESD (E); HE stained pathological smears of specimens after ESD (F, × 40).

infiltrated into the submucosa. The depth of submucosal infiltration was 1000 μm. The distance between the deepest infiltration of the lesion and the basal incision margin was 500 μm. The lesion size was 2550 μm. The horizontal and vertical resection margins were negative (Figure 1). Immunohistochemical (IHC) results were as follows: CK (weak +), Vim (-), Syn (+), CD56 (strong +), CgA (strong +), CK7 (-), CK20 (weak +), Villin (+), CEA (focal+), and Ki-67 (2%; Figure 2). The lymphatic invasion was confirmed by D2-40 and CD31 staining (Figure 3).

MULTIDISCIPLINARY EXPERT CONSULTATION

After the pathological examination of the biopsy clamped specimen suggested neuroendocrine tumor, the patient underwent multidisciplinary consultation with oncology, surgery and nuclear medicine, and finally decided to complete 68Ga-SSA-PET/CT, and no distant metastasis was found. Therefore, we decided to perform ESD after consulting the patient's consent and followed up regularly after the operation.

FINAL DIAGNOSIS

The pathological diagnosis of the specimen after ESD rescue therapy was rNET G1.

TREATMENT

ESD salvage therapy was applied.

OUTCOME AND FOLLOW-UP

No tumor recurrence or distant metastasis was detected at 13 mo postoperative follow-up using endoscopy and CT-enhanced scans of the whole abdomen (including the pelvis).

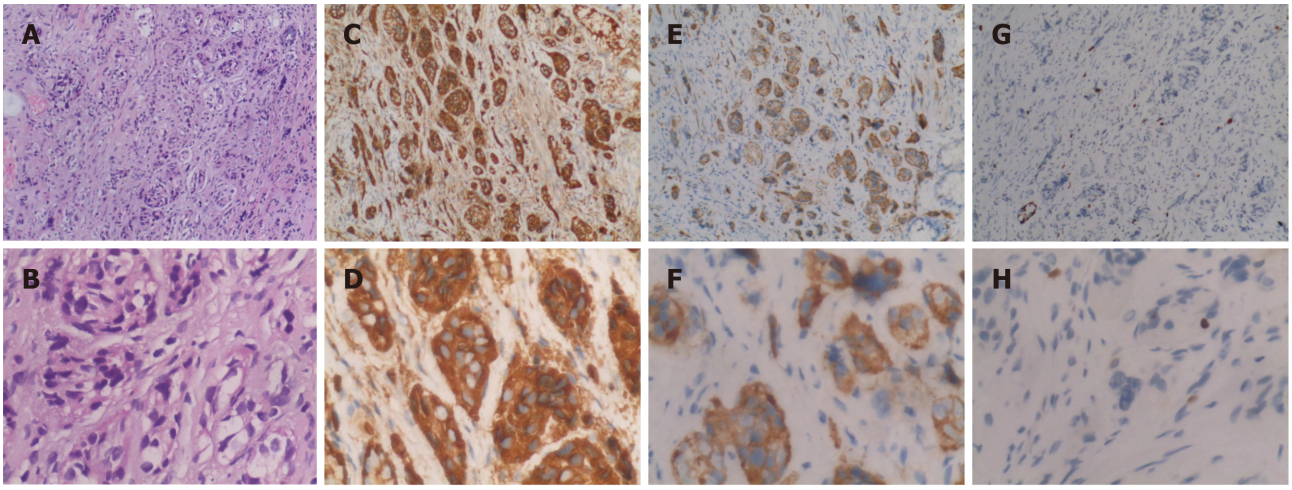

DOI: 10.12998/wjcc.v11.i4.859 **Copyright** ©The Author(s) 2023.

Figure 2 Pathological smears of tumor tissue after various immunohistochemical staining. A-H: HE (A, × 100; B, × 400); CgA (C, × 100; D, × 400); Syn (E, × 100; F, × 400); and ki67 (G, × 100; H, × 400).

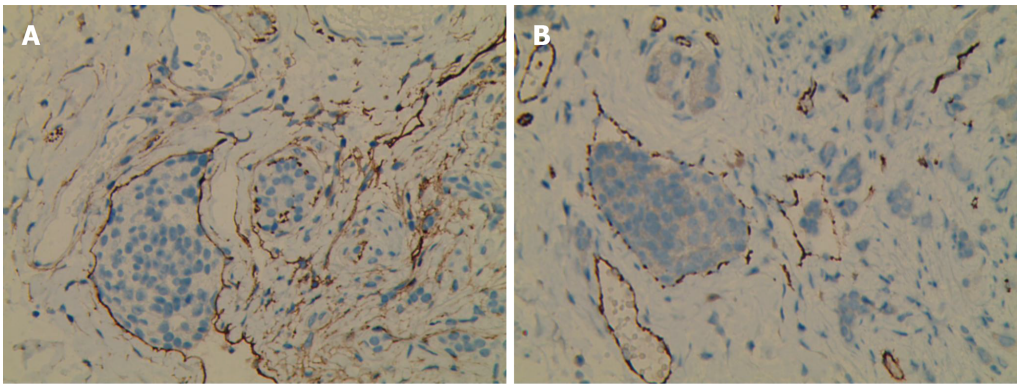

DOI: 10.12998/wjcc.v11.i4.859 **Copyright** ©The Author(s) 2023.

Figure 3 The tumor was found to have lymphatic invasion after staining with CD31 (A) and D2-40 (B). A and B: × 200.

DISCUSSION

Gastroenteropancreatic neuroendocrine tumors (GEP-NETs) are the most common type of NETs[9]. The rectum is the most common site for GEP-NETs in Asian populations[10]. In recent years, with the extensive development of colorectal cancer screening programs and the improvement of endoscopic diagnosis and treatment techniques, the incidence of rNET has continued to rise.

Lymphovascular invasion (LVI) refers to the presence of tumor cells in blood vessels and lymphatic channels. LVI is closely related to tumor metastasis in distant organs and lymph nodes. A meta-analysis found that LVI was associated with an increased risk of distant lymph node metastasis (LNM) after local resection of rNETs[11]. Therefore, LVI is a risk factor for LNM. Another meta-analysis found that, for small rNETs with a tumor size of 10 mm or less, even in the presence of LVI, the prognosis was good after endoscopic resection, with a 5-year follow-up recurrence rate of only 0.3%. In addition, tiny rNETs smaller than 5 mm had a lower incidence of LVI than rNETs with a tumor size of 5-10 mm[12].

In recent years, the detection rate of LVI in rNETs has increased significantly due to immunohistochemical detection methods[12-14]. This increasing trend is proportional to tumor size, even in the fraction of rNETs less than or equal to 5 mm, the detection rate is still about 50%[13]. One study reported that the detection rate of LVI by IHC staining (56.9%) was 6 times higher than that of hematoxylin and eosin (HE) staining alone (8.8%)[15]. This result suggests that the possibility of LVI in small rNETs was underestimated prior to using IHC staining. Both vascular and lymphatic invasion are included in LVI and usually need to be distinguished by IHC detection. Vascular invasion and lymphatic invasion have different effects on LNM. In small rNETs, vascular invasion may have a greater impact on LNM than lymphatic invasion[11].

In this rNET patient, the endoscopic tumor size was 3 mm with lymphatic invasion, the smallest rNET with LVI reporting in all existing research. At the same time, no instances of LNM or distant metastasis were found after the enhanced chest and total abdominal CT and 68G-SSA-PET/CT. During

the 13-mo follow-up after ESD, we did not find tumor recurrence or distant metastasis using endoscopy at the 6-mo and 1-year postoperative follow-up. Whole abdominal CT-enhanced scans did not show tumor recurrence or distant metastasis. These findings suggest that, in small (< 10 mm) or even tiny (< 5 mm) rNETs, although there is lymphatic invasion, lymphatic invasion may not be a determinant of LNM.

A cohort study found that after 6 years of follow-up in patients with rNETs who underwent endoscopic resection, about 1% of the patients developed LNM or distant metastasis, and the tumor grades were G2. In contrast, patients with grade G1 rNETs whose tumor size was less than 20 mm and who underwent endoscopic resection did not develop lymph node or distant metastasis[16]. Therefore, the risk factors for lymph node and distant metastasis of rNETs with a tumor size less than 20 mm need further study.

Although this patient had lymphatic invasion, no lymph node or distant metastasis was found. Therefore, in the absence of a well-established correlation between LVI and LNM of rNETs with a tumor size less than 20 mm, additional surgery may not benefit all patients with LVI. The tumor grade, tumor size, LVI, and depth of invasion may still need to be comprehensively considered to determine whether to perform additional surgery. In addition, imaging studies and radionuclide scintigraphy can be considered when it is unclear whether additional surgery is required[15].

In this patient, the tumor surface was smooth, and endoscopy showed that the tumor size was small. The tumor was misdiagnosed as a hyperplastic polyp and was subjected to examination with biopsy forceps. The size of the lesion was 1500 μm. Residual lesions were found after ESD salvage surgery, in which the tumor size was found to be 1050 μm. These results indicated that simple biopsy forceps were insufficient for such rNETs, and ESD salvage was a suitable option. For hyperplastic polyps of the left colon and rectum with a tumor size of 5 mm or less, both the Japanese Society of Gastroenterology and the European Society for Gastrointestinal Endoscopy recommend endoscopic follow-up only[17,18]. The rectum is a high-incidence site of NETs. Therefore, we suggest that, if the lesions are smooth and bulging, especially when the margins of the lesions are not clear, the possibility of NETs should be considered. The possibility of NETs should be excluded by forceps and biopsy.

For this patient, to ensure his quality of life, we did not choose to conduct surgical intervention, but rather continued with follow-up observation. According to previous literature reports, the metastasis of rNETs can occur after more than 10 years[19,20]. Although no LNM and distant metastasis were found in the short-term follow-up of this patient, long-term follow-up is extremely important, especially for lymph node and liver metastasis. Therefore, this patient's end point of follow-up should be at least 10 years. In the subsequent follow-up schedule, we will perform endoscopy and CT-enhanced scans of the whole abdomen (including the pelvis) once a year, with an additional 68Ga-SSA-PET/CT if abnormalities are detected during the follow-up.

CONCLUSION

rNETs have heterogeneity and atypical symptoms. Therefore, it is not sufficient to judge the risk of tumor metastasis during clinical diagnosis and treatment based only on tumor size and LVI. Instead, during treatment, it is necessary to formulate an individualized plan, undertake close follow-up observation, and try to improve the quality of life and disease prognosis of patients while reducing the burden of treatment.

FOOTNOTES

Author contributions: Ran JX was responsible for writing the paper; Xu LB was responsible for patient treatment and study design; Chen WW and Yang HY were responsible for collecting and analyzing data; Weng Y and Peng YM were responsible for patient follow-up.

Supported by Guizhou Science and Technology Plan Project, No. ZK2022-General-443; and Science and Technology Fund of Guizhou Provincial Health and Health Commission, No. gzwkj2023-135.

Informed consent statement: Written informed consent was obtained from the patient for publication of this report and all accompanying images.

Conflict-of-interest statement: The authors have no conflicts of interest to declare.

CARE Checklist (2016) statement: The authors have read the CARE Checklist (2016), and the manuscript was prepared and revised according to the CARE Checklist (2016).

Country/Territory of origin: China

ORCID number: Jing-Xue Ran 0000-0002-0042-7325; Liang-Bi Xu 0000-0002-3877-0719; Yan Weng 0000-0001-6389-8231.

S-Editor: Gong ZM
L-Editor: A
P-Editor: Gong ZM

REFERENCES

1 **Soga J**. Carcinoids of the rectum: an evaluation of 1271 reported cases. *Surg Today* 1997; **27**: 112-119 [PMID: 9017986 DOI: 10.1007/BF02385898]
2 **Tsikitis VL**, Wertheim BC, Guerrero MA. Trends of incidence and survival of gastrointestinal neuroendocrine tumors in the United States: a seer analysis. *J Cancer* 2012; **3**: 292-302 [PMID: 22773933 DOI: 10.7150/jca.4502]
3 **Dasari A**, Shen C, Halperin D, Zhao B, Zhou S, Xu Y, Shih T, Yao JC. Trends in the Incidence, Prevalence, and Survival Outcomes in Patients With Neuroendocrine Tumors in the United States. *JAMA Oncol* 2017; **3**: 1335-1342 [PMID: 28448665 DOI: 10.1001/jamaoncol.2017.0589]
4 **Scherübl H**. Rectal carcinoids are on the rise: early detection by screening endoscopy. *Endoscopy* 2009; **41**: 162-165 [PMID: 19214898 DOI: 10.1055/s-0028-1119456]
5 **Hyun JH**, Lee SD, Youk EG, Lee JB, Lee EJ, Chang HJ, Sohn DK. Clinical impact of atypical endoscopic features in rectal neuroendocrine tumors. *World J Gastroenterol* 2015; **21**: 13302-13308 [PMID: 26715813 DOI: 10.3748/wjg.v21.i47.13302]
6 **Shinohara T**, Hotta K, Oyama T. Rectal carcinoid tumor, 6 mm in diameter, with lymph node metastases. *Endoscopy* 2008; **40** Suppl 2: E40-E41 [PMID: 18302079 DOI: 10.1055/s-2007-966849]
7 **Ramage JK**, De Herder WW, Delle Fave G, Ferolla P, Ferone D, Ito T, Ruszniewski P, Sundin A, Weber W, Zheng-Pei Z, Taal B, Pascher A; Vienna Consensus Conference participants. ENETS Consensus Guidelines Update for Colorectal Neuroendocrine Neoplasms. *Neuroendocrinology* 2016; **103**: 139-143 [PMID: 26730835 DOI: 10.1159/000443166]
8 **Expert Committee on Neuroendocrine Tumors**, Chinese Society of Clinical Oncology. Expert consensus on gastroenteropancreatic neuroendocrine tumors in China. *Linchuang Zhongliuxue Zazhi* 2016; **21**: 927-946 [DOI: 10.3969/j.issn.1009-0460.2016.10.013]
9 **Bornschein J**, Kidd M, Malfertheiner P, Modlin IM. [Gastrointestinal neuroendocrine tumors]. *Dtsch Med Wochenschr* 2008; **133**: 1505-1510 [PMID: 18597210 DOI: 10.1055/s-2008-1081099]
10 **Gastrointestinal Pathology Study Group of Korean Society of Pathologists**, Cho MY, Kim JM, Sohn JH, Kim MJ, Kim KM, Kim WH, Kim H, Kook MC, Park DY, Lee JH, Chang H, Jung ES, Kim HK, Jin SY, Choi JH, Gu MJ, Kim S, Kang MS, Cho CH, Park MI, Kang YK, Kim YW, Yoon SO, Bae HI, Joo M, Moon WS, Kang DY, Chang SJ. Current Trends of the Incidence and Pathological Diagnosis of Gastroenteropancreatic Neuroendocrine Tumors (GEP-NETs) in Korea 2000-2009: Multicenter Study. *Cancer Res Treat* 2012; **44**: 157-165 [PMID: 23091441 DOI: 10.4143/crt.2012.44.3.157]
11 **Kang HS**, Kwon MJ, Kim TH, Han J, Ju YS. Lymphovascular invasion as a prognostic value in small rectal neuroendocrine tumor treated by local excision: A systematic review and meta-analysis. *Pathol Res Pract* 2019; **215**: 152642 [PMID: 31585816 DOI: 10.1016/j.prp.2019.152642]
12 **Sekiguchi M**, Sekine S, Sakamoto T, Otake Y, Nakajima T, Matsuda T, Taniguchi H, Kushima R, Ohe Y, Saito Y. Excellent prognosis following endoscopic resection of patients with rectal neuroendocrine tumors despite the frequent presence of lymphovascular invasion. *J Gastroenterol* 2015; **50**: 1184-1189 [PMID: 25936647 DOI: 10.1007/s00535-015-1079-7]
13 **Kitagawa Y**, Ikebe D, Hara T, Kato K, Komatsu T, Kondo F, Azemoto R, Komoda F, Tanaka T, Saito H, Itami M, Yamaguchi T, Suzuki T. Enhanced detection of lymphovascular invasion in small rectal neuroendocrine tumors using D2-40 and Elastica van Gieson immunohistochemical analysis. *Cancer Med* 2016; **5**: 3121-3127 [PMID: 27748061 DOI: 10.1002/cam4.935]
14 **Kwon MJ**, Kang HS, Soh JS, Lim H, Kim JH, Park CK, Park HR, Nam ES. Lymphovascular invasion in more than one-quarter of small rectal neuroendocrine tumors. *World J Gastroenterol* 2016; **22**: 9400-9410 [PMID: 27895428 DOI: 10.3748/wjg.v22.i42.9400]
15 **Carideo L**, Prosperi D, Panzuto F, Magi L, Pratesi MS, Rinzivillo M, Annibale B, Signore A. Role of Combined [(68)Ga]Ga-DOTA-SST Analogues and [(18)F]FDG PET/CT in the Management of GEP-NENs: A Systematic Review. *J Clin Med* 2019; **8** [PMID: 31337043 DOI: 10.3390/jcm8071032]
16 **Kuiper T**, van Oijen MGH, van Velthuysen MF, van Lelyveld N, van Leerdam ME, Vleggaar FD, Klümpen HJ. Endoscopically removed rectal NETs: a nationwide cohort study. *Int J Colorectal Dis* 2021; **36**: 535-541 [PMID: 33230657 DOI: 10.1007/s00384-020-03801-w]
17 **Tanaka S**, Saitoh Y, Matsuda T, Igarashi M, Matsumoto T, Iwao Y, Suzuki Y, Nozaki R, Sugai T, Oka S, Itabashi M, Sugihara KI, Tsuruta O, Hirata I, Nishida H, Miwa H, Enomoto N, Shimosegawa T, Koike K. Evidence-based clinical practice guidelines for management of colorectal polyps. *J Gastroenterol* 2021; **56**: 323-335 [PMID: 33710392 DOI: 10.1007/s00535-021-01776-1]
18 **Ferlitsch M**, Moss A, Hassan C, Bhandari P, Dumonceau JM, Paspatis G, Jover R, Langner C, Bronzwaer M, Nalankilli K,

Fockens P, Hazzan R, Gralnek IM, Gschwantler M, Waldmann E, Jeschek P, Penz D, Heresbach D, Moons L, Lemmers A, Paraskeva K, Pohl J, Ponchon T, Regula J, Repici A, Rutter MD, Burgess NG, Bourke MJ. Colorectal polypectomy and endoscopic mucosal resection (EMR): European Society of Gastrointestinal Endoscopy (ESGE) Clinical Guideline. *Endoscopy* 2017; **49**: 270-297 [PMID: 28212588 DOI: 10.1055/s-0043-102569]

19 **Shigematsu Y**, Kanda H, Konishi T, Takazawa Y, Inoue Y, Muto T, Ishikawa Y, Takahashi S. Recurrence 30 Years after Surgical Resection of a Localized Rectal Neuroendocrine Tumor. *Intern Med* 2017; **56**: 1521-1525 [PMID: 28626177 DOI: 10.2169/internalmedicine.56.7547]

20 **Kwaan MR**, Goldberg JE, Bleday R. Rectal carcinoid tumors: review of results after endoscopic and surgical therapy. *Arch Surg* 2008; **143**: 471-475 [PMID: 18490556 DOI: 10.1001/archsurg.143.5.471]

World Journal of Clinical Cases

Submit a Manuscript: https://www.f6publishing.com

World J Clin Cases 2023 February 6; 11(4): 866-873

DOI: 10.12998/wjcc.v11.i4.866

ISSN 2307-8960 (online)

CASE REPORT

Pneumocystis jirovecii diagnosed by next-generation sequencing of bronchoscopic alveolar lavage fluid: A case report and review of literature

Qing-Wei Cheng, Hong-Li Shen, Zhi-Hui Dong, Qian-Qian Zhang, Ya-Fen Wang, Jin Yan, Yu-Sheng Wang, Ning-Gang Zhang

Specialty type: Medicine, research and experimental

Provenance and peer review: Unsolicited article; Externally peer reviewed.

Peer-review model: Single blind

Peer-review report's scientific quality classification

Grade A (Excellent): 0
Grade B (Very good): B
Grade C (Good): C
Grade D (Fair): D
Grade E (Poor): 0

P-Reviewer: Cabezuelo AS, Spain; Soewondo W, Indonesia

Received: September 19, 2022
Peer-review started: September 19, 2022
First decision: December 13, 2022
Revised: December 22, 2022
Accepted: January 9, 2023
Article in press: January 9, 2023
Published online: February 6, 2023

Qing-Wei Cheng, Hong-Li Shen, Zhi-Hui Dong, Qian-Qian Zhang, Ya-Fen Wang, Jin Yan, Department of Oncology, The Sixth Division Hospital, Xinjiang Production and Construction Corps, Wujiaqu 831300, Xinjiang Uygur Autonomous Regions, China

Yu-Sheng Wang, Ning-Gang Zhang, Department of Gastrointestinal Oncology, Shanxi Province Cancer Hospital/Shanxi Hospital Affiliated to Cancer Hospital, Chinese Academy of Medical Sciences/Cancer Hospital Affiliated to Shanxi Medical University, Taiyuan 030013, Shanxi Province, China

Corresponding author: Ning-Gang Zhang, MD, Associate Chief Physician, Department of Gastrointestinal Oncology, Shanxi Province Cancer Hospital/Shanxi Hospital Affiliated to Cancer Hospital, Chinese Academy of Medical Sciences/Cancer Hospital Affiliated to Shanxi Medical University, No. 3 Zhigong Xincun Street, Xinhualing District, Taiyuan 030013, Shanxi Province, China. zng1120@163.com

Abstract

BACKGROUND

The advent of molecular targeted agents and immune checkpoint inhibitors has greatly improved the treatment of advanced renal cell carcinoma (RCC), thus significantly improving patient survival. The incidence of rare drug-related adverse events has gained increased attention.

CASE SUMMARY

We report a patient with advanced RCC treated with multiple lines of molecular targeted agents and immune checkpoint inhibitors, who developed a pulmonary infection after treatment with everolimus in combination with lenvatinib. Determining the pathogenic organism was difficult, but it was eventually identified as *Pneumocystis jirovecii* by next-generation sequencing (NGS) of bronchoscopic alveolar lavage fluid (BALF) and successfully treated with trimethoprim-sulfamethoxazole.

CONCLUSION

Rare pulmonary infections caused by molecular targeted agents are not uncommon in clinical practice, but their diagnosis is difficult. Evaluating BALF with NGS is a good method for rapid diagnosis of such infections.

Key Words: Renal cell carcinoma; Everolimus; Pneumocystis jirovecii pneumonia; Next-generation sequencing; Bronchoscopic alveolar lavage fluid; Case report

Core Tip: The application of molecular targeted agents and immune checkpoint inhibitors have greatly improved the prognosis of advanced renal cell carcinoma (RCC). We report a patient with advanced RCC treated with multiple lines of molecular targeted agents, who developed a *Pneumocystis jirovecii* pneumonia after treatment with everolimus in combination with lenvatinib. The pathogenic organism was identified by next-generation sequencing (NGS) of bronchoscopic alveolar lavage fluid (BALF) and successfully treated with trimethoprim-sulfamethoxazole. Evaluating BALF with NGS technology might be used to detect pathogens and determine the correct treatment plan for patients with rare infections caused by the use of molecular targeted agents.

Citation: Cheng QW, Shen HL, Dong ZH, Zhang QQ, Wang YF, Yan J, Wang YS, Zhang NG. *Pneumocystis jirovecii* diagnosed by next-generation sequencing of bronchoscopic alveolar lavage fluid: A case report and review of literature. *World J Clin Cases* 2023; 11(4): 866-873
URL: https://www.wjgnet.com/2307-8960/full/v11/i4/866.htm
DOI: https://dx.doi.org/10.12998/wjcc.v11.i4.866

INTRODUCTION

Renal cell carcinoma (RCC) is a malignant tumor originating from the renal tubular epithelium and accounts for 80% to 90% of renal malignancies[1]. According to GLOBOCAN 2020 global cancer statistics, RCC was the 14th most prevalent and the 15th most deadly malignancy[2]. Radical surgical resection is the mainstay treatment for localized renal cancer, while a combination of systemic drugs is preferred for advanced renal cancer. Sorafenib was first approved for the treatment of metastatic renal cancer in 2005[3], followed by the approval of targeted drugs such as pegaptanib, sunitinib, axitinib, sorafenib, and everolimus[4-7]; while immune checkpoint inhibitors such as navulizumab, pablizumab, and ipilimumab have also been licensed for use[8-10]. The combination of various molecular targeted drugs and immune checkpoint inhibitors has resulted in a rise in rare adverse effects.

Herein, we report a case of RCC that progressed after multiple lines of therapy and improved with the mammalian target of rapamycin (mTOR) inhibitor, everolimus in combination with lenvatinib; however, the patient complained of a dry cough that developed into a lung infection. Due to difficulty in identifying the infection, empirical anti-bacterial treatment was initially administered, with unsatisfactory results. Eventually, this rare case of *Pneumocystis jirovecii* infection was confirmed using next-generation sequencing (NGS) of bronchoscopic alveolar lavage fluid (BALF), and the infection improved after appropriate treatment.

CASE PRESENTATION

Chief complaints

A 61-year-old man diagnosed with RCC for nearly 3 years presented to our department because of a dry cough with occasional expectoration on February 22, 2022.

History of present illness

The patient was admitted to our hospital with "hematuria for 7 d" on August 5, 2019. A computed tomography (CT) scan on admission revealed right kidney and right renal pelvis occupancy, suggestive of malignancy. In addition, multiple nodules in both lungs were seen, and metastasis was suspected. A timeline of the episode of treatment is shown in Figure 1. After consultation and discussion, the patient agreed to undergo a laparoscopic radical right nephrectomy. Postoperative pathology revealed clear cell RCC of the right kidney. Following surgery, he was treated with oral sunitinib. A follow-up CT scan after 9 mo revealed metastases in the right adrenal gland, and axitinib was given to the patient. Three months later, CT imaging found that the metastases in the right adrenal gland and both lungs were significantly larger than before. He was thus treated with nine cycles of the immune checkpoint inhibitor sintilimab. However, a subsequent CT scan showed that the right adrenal metastasis was slightly enlarged, with multiple metastases appearing in the abdominal cavity, while the size of the lung

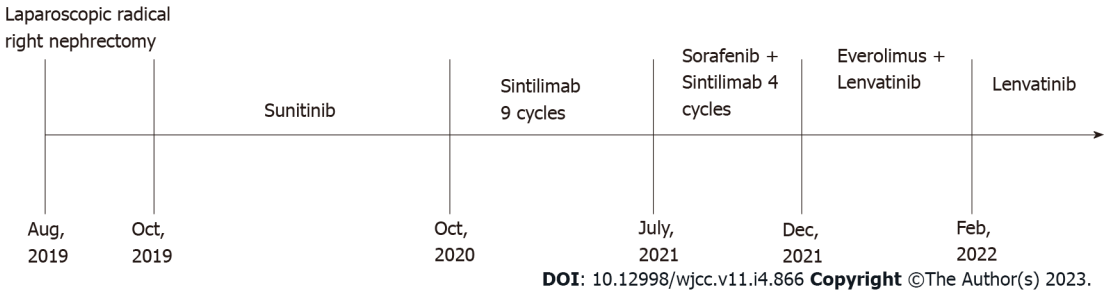

DOI: 10.12998/wjcc.v11.i4.866 **Copyright** ©The Author(s) 2023.

Figure 1 Patient treatment timeline.

metastases was unchanged. On July 19, 2021, four cycles of sorafenib in combination with sintilimab were administered. CT scanning revealed that the lung and abdominal cavity metastases were slightly larger than before, and new subcapsular metastases were detected on the right lobe of the liver. On December 14, 2021, he was switched to everolimus 10 mg once daily in combination with lenvatinib 8 mg once daily. However, on February 22, 2022, the patient developed a dry cough with occasional and little sputum, accompanied by mild dyspnea after activity. No fever or other discomfort was observed.

History of past illness

The patient had no past illness.

Personal and family history

The patient had no specific personal and family history.

Physical examination

On physical examination, the patient's basic vital signs were within normal limits, and his respiratory sounds were rough on both lungs, without dry or wet rales.

Laboratory examinations

The initial blood investigations revealed the following: Leukocytes 5.17 × 10^9/L (reference range: 4.0-11.0), hemoglobin 121.0 g/L, platelet count 400 × 10^9/L, lymphocytes 15.9%, monocytes 6.8%, neutrophils 76.3%, eosinophils 0.6%, basophils 0.4%, high sensitivity C-reactive protein 37.0 mg/L (reference range: 0-5 mg/L), and procalcitonin 0.07 ng/mL (normal value < 0.052 ng/mL). Liver and kidney functions were normal, and sputum culture revealed normal oral flora.

Imaging examinations

CT scan on February 23, 2022 (Figure 2A) identified multiple patches and ground glass shadows in both lungs and scattered soft tissue nodules of different sizes in both lungs, suggestive of a pulmonary infection. The lung and peritoneal metastases were slightly smaller in size. The infection was treated with cefuroxime sodium, piperacillin sulbactam, and moxifloxacin injections, but the patient's condition did not improve, and he still had a persistent dry cough. Another CT scan on the March 21, 2022 (Figure 2B) showed little to no resolution of the lung infection.

FINAL DIAGNOSIS

A bronchoscopy lavage fluid NGS test was performed on March 25, 2022. The patient underwent bronchoscopy, and the fiberoptic bronchoscope reached the trachea and bronchi of both lungs. Irrigation with sterile saline was performed repeatedly in the left lower lobe bronchus and right lower lobe bronchus. The collected samples were then sent to the laboratory for NGS testing and analysis, which revealed *Pneumocystis jirovecii* infection.

TREATMENT

Two cotrimoxazole tablets (sulfamethoxazole 0.4 g, trimethoprim 80 mg/tablet) were given every 6 h and 40 mg methylprednisolone succinate was given twice a day for 5 d, followed by 40 mg once daily for 5 d.

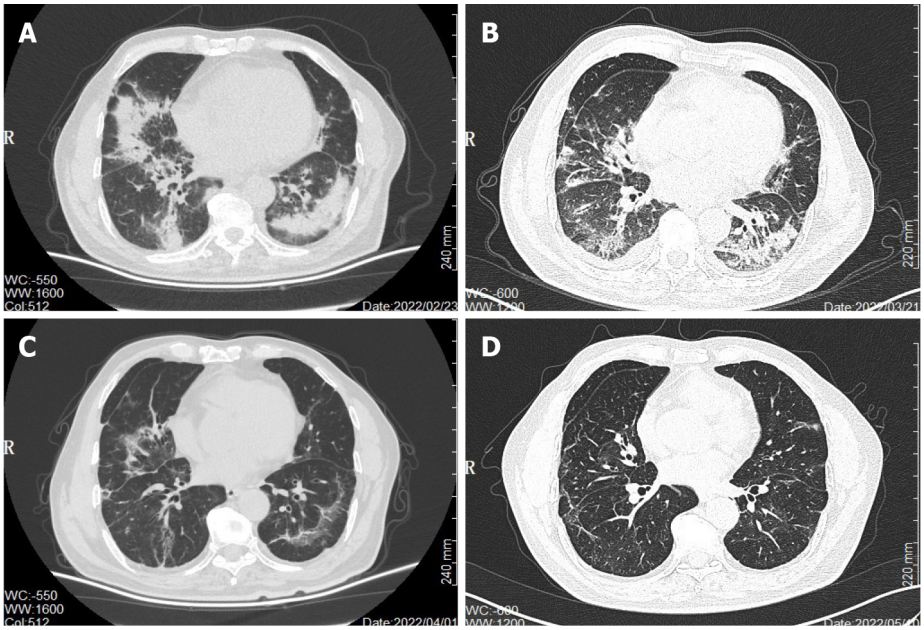

DOI: 10.12998/wjcc.v11.i4.866

Figure 2 Chronological computed tomography of the chest demonstrating changes in the lungs. A: Multiple patches and ground glass shadows in both lungs and scattered soft tissue nodules of different sizes in both lungs in February 2022; B: There was no significant change in pulmonary inflammation after empirical anti-infective treatment in March 2022; C: Pulmonary infection was significantly improved and resolved in both lungs in April 2022; D: Pulmonary infection almost completely disappeared in May 2022.

OUTCOME AND FOLLOW-UP

Following treatment, the patient's cough disappeared. Cotrimoxazole tablets were continued for 3 wk, and the repeat CT on April 1, 2022 (Figure 2C) and May 10, 2022 (Figure 2D) showed significant improvement and resolution in both lungs. There were no treatment-related adverse effects. At present, the patient is well and has not complained of symptoms such as cough and dyspnea.

DISCUSSION

Kidney cancer is the third most prevalent urogenital tumor in China, accounting for 2%-3% of adult malignant tumors, and its incidence is increasing annually[11]. Targeted therapy is the primary treatment strategy for advanced renal cancer. According to their targets, these drugs can be divided into two main categories: Vascular endothelial growth factor (VEGF)/VEGF receptor inhibitors and mTOR inhibitors. VEGF, a major factor in the angiogenesis process in RCC, is a primary target of anti-angiogenic treatments[12,13]. Additionally, mTOR, which is positioned downstream of phosphoinositide 3-kinase and protein kinase B and is regulated by phosphatase and tensin homolog, is heavily involved in RCC development[14]. Inhibition of the mTOR pathway can inhibit both angiogenesis and tumor cell proliferation. Everolimus, an mTOR inhibitor, has been found to improve survival in metastatic RCC patients after TKI-targeted drug therapy failure[15,16].

Everolimus is not only approved for use in advanced RCC but also for the treatment of advanced breast cancer[17], pancreatic neuroendocrine tumor[18], subependymal giant cell astrocytoma associated with tuberous sclerosis[19], and other tumors. It can also prevent immunological rejection after kidney, liver, or heart transplantation[20]. The adverse reactions of everolimus mainly affect the digestive system, respiratory system, endocrine system, and skin mucosa[21,22], with interstitial lung disease (ILD) being the most common pulmonary associated toxicity[23-25]. The incidence of non-infectious pneumonia of metastatic RCC treated with everolimus can reach up to 14%[16]. Following everolimus administration, our patient developed a dry cough, with the CT scan revealing a pulmonary infection. Repeated sputum culture and sputum smear showed no clear evidence of microbial infection. After empirical anti-bacterial treatment, the therapeutic outcome was poor. We thus suspected an uncommon bacterial or fungal infection, but identifying the pathogen was challenging. Therefore, we resorted to BALF NGS testing and revealed that *Pneumocystis jirovecii* was the cause of the infection. Prior to the lung infection, the patient had been treated with many lines of targeted treatments and immune checkpoint inhibitors, and his immune function was compromised. Following treatment with everolimus in combination with lenvatinib, he acquired a rare *Pneumocystis jirovecii* infection. Given that lenvatinib is a multi-targeted anti-angiogenic agent, its common adverse effects include hypertension,

fatigue, diarrhea, palmoplantar erythroderma syndrome, proteinuria and hemorrhagic events, while everolimus is immune-suppressive, making patients susceptible to opportunistic pulmonary infections [26]. Loron *et al*[27] found that the use of everolimus in patients with advanced RCC can lead to rare pathogenic infections, including *Pneumocystis jirovecii* infections. As a result, we speculate that the *Pneumocystis jirovecii* infection in this patient was associated with the use of everolimus.

Pneumocystis jirovecii can accumulate on the surface of the respiratory tract of healthy humans and can proliferate when the immune system is weakened, leading to opportunistic infections[28]. In the 1980s, with the emergence of the human immunodeficiency virus (HIV), *Pneumocystis jirovecii* pneumonia (PJP) became more prevalent in HIV patients[29]. With the increased use of immunosuppressive drugs, the incidence of PJP has gradually increased in non-HIV-infected patients, especially in those with malignant tumors who are treated with immunosuppressants[30,31]. The early stage of infection in non-HIV-infected patients is characterized by a repeated low-grade fever and dry cough without characteristic symptoms, and the disease can advance rapidly to fever and respiratory failure. The mortality rate of non-HIV patients with PJP is 30% to 50%, higher than that of HIV patients[32].

The clinical features of PJP are not specific, and the diagnosis mainly depends on the detection of pathogens. Normal or reduced white blood cells are often seen while serum lactate dehydrogenase and blood fungal (1-3)-β-d-glucan are elevated, and the G test is positive; however, these markers have limited specificity and clinical translational value[33]. X-ray and CT chest examinations lack specificity in the early stage of infection, while after disease progression, CT imaging usually shows diffuse, bilateral pulmonary "ground glass" interstitial infiltrates, which may also appear as pulmonary nodules. Nonetheless, these imaging changes are not specific, especially as they are identical to the presentation of ILD in everolimus-induced interstitial pneumonia, which can easily lead to misdiagnosis [34]. Unlike bacterial and other fungal infections, most non-HIV individuals have a low PJP load, and standard smear microscopy has a low sensitivity; thus, early PJP diagnosis is difficult. Microscopic inspection is commonly utilized to confirm PJP, and clinical specimens typically employed include induced sputum, bronchoalveolar lavage fluid, and lung tissue biopsy, but induced sputum culture has a low positive rate, and lung tissue biopsy is traumatic and difficult to carry out clinically. The BALF technique allows targeted sampling of the lower respiratory tract with a diagnostic positivity rate of 90% to 99% compared to sputum analysis[35]. Polymerase chain reaction (PCR) of alveolar lavage fluid samples is a reliable method for diagnosing PJP, with some studies indicating that PCR has a sensitivity of ≥ 97% and a negative predictive value of ≥ 99%[36]. If the BALF PCR test is negative, PJP can be ruled out, while a positive PCR makes distinguishing between colonization and active infection difficult[37].

Traditional diagnostic methods, such as smear microscopy and induced sputum culture, have a low positive rate for the diagnosis of *Pneumocystis jirovecii* infection. Lung tissue biopsy is a traumatic examination. BALF test has a higher positive rate. As a new detection method independent of microbial culture, NGS is a second-generation gene sequencing technology with the advantages of high throughput, wide coverage and high accuracy[38,39]. NGS can directly detect the nucleic acid sequence of pathogenic bacteria in the samples and determine their type and proportion[40]. It can be used for the detection of not only a variety of pathogens, such as bacteria, fungi, viruses, and parasites, but also a variety of specimens, such as sputum, blood, cerebrospinal fluid, alveolar lavage fluid, and tissue. Compared with the traditional culture method, NGS has higher detection rate and higher negative predictive value. At present, NGS has been successfully used to diagnose and treat difficult and critical infectious diseases, identify unknown pathogens, monitor drug-resistant genes, carry out epidemiological follow-up investigations, *etc*[41,42]. While identifying rare pathogens (*e.g.*, *Legionella pneumophila*, *Corynebacterium striatum*, *Listeria spp.*, *Pneumocystis jirovecii*, *cryptococcus*, *Chlamydia pinioticus*) is challenging clinically, NGS detection of alveolar lavage fluid can offer a rapid diagnosis and determine a correct anti-infection treatment. Notably, NGS of BALF is more sensitive and specific than the traditional approaches in diagnosing HIV-negative PJP[43]. However, NGS still faces many problems with a widespread application. Diagnosis by NGS testing needs to be combined with host factors, and chest CT findings. NGS pathogen test can only identify the pathogen, but cannot detect antimicrobial susceptibility. In addition, the current research on NGS testing of atypical respiratory pathogens is mostly in the form of case reports and clinical studies with a small sample size. Further clinical studies with a larger sample size are required to compare its sensitivity and specificity with traditional detection methods.

Trimethoprim-sulfamethoxazole (TMP/SMZ) is the preferred drug for the treatment of PJP, and it is emphasized that early and adequate dosage yields the best outcome[44], and the standard course to treat PJP is 3 wk[45]. The main side effects of TMP/SMZ include skin rash, drug fever, leukopenia, renal dysfunction, electrolyte disorder, and hepatotoxicity. Patients with renal insufficiency should lower their TMP dosage according to the creatinine clearance rate. For some patients with ineffective TMP/SMZ treatment or intolerable side effects, in recent years, caspofungin combined with low-dose TMP/SMZ has been used in patients with PJP infection following organ transplant. These two drugs have a synergistic effect, achieving satisfactory efficacy and a low incidence of adverse reactions[44,46].

CONCLUSION

With the widespread use of anti-tumor immunosuppressants, the risks of lung infection with atypical bacteria or fungi in cancer patients have increased, and existing traditional diagnostic procedures make such infections difficult to diagnose. Therefore, in the event that tumor patients experience lung infection after anti-tumor treatment and the effect of conventional diagnosis and treatment are unsatisfactory, evaluating BALF with NGS technology can be used to detect pathogens and determine the correct treatment plan for such patients. Collectively, we believe that this approach is promising in the early diagnosis of such infections and deserves more clinical attention.

ACKNOWLEDGEMENTS

We sincerely thank the patient involved in this report.

FOOTNOTES

Author contributions: Cheng QW and Shen HL contributed to the manuscript writing; Dong ZH, Yan J, Zhang QQ, and Wang YS followed the patient during treatment; Wang YS and Zhang NG revised the manuscript; and all authors granted final approval for the version to be submitted.

Informed consent statement: Informed written consent was obtained from the patient for publication of this report and any accompanying images.

Conflict-of-interest statement: All the authors report no relevant conflicts of interest for this article.

CARE Checklist (2016) statement: The authors have read the CARE Checklist (2016), and the manuscript was prepared and revised according to the CARE Checklist (2016).

Country/Territory of origin: China

ORCID number: Ning-Gang Zhang 0000-0002-6640-3617.

S-Editor: Wang JJ
L-Editor: Filipodia
P-Editor: Wang JJ

REFERENCES

1 **Cai Q**, Chen Y, Qi X, Zhang D, Pan J, Xie Z, Xu C, Li S, Zhang X, Gao Y, Hou J, Guo X, Zhou X, Zhang B, Ma F, Zhang W, Lin G, Xin Z, Niu Y, Wang Y. Temporal trends of kidney cancer incidence and mortality from 1990 to 2016 and projections to 2030. *Transl Androl Urol* 2020; **9**: 166-181 [PMID: 32420123 DOI: 10.21037/tau.2020.02.23]
2 **Sung H**, Ferlay J, Siegel RL, Laversanne M, Soerjomataram I, Jemal A, Bray F. Global Cancer Statistics 2020: GLOBOCAN Estimates of Incidence and Mortality Worldwide for 36 Cancers in 185 Countries. *CA Cancer J Clin* 2021; **71**: 209-249 [PMID: 33538338 DOI: 10.3322/caac.21660]
3 **Liu XL**, Xue HY, Chu Q, Liu JY, Li J. Comparative efficacy and safety of sunitinib *vs* sorafenib in renal cell carcinoma: A systematic review and meta-analysis. *Medicine (Baltimore)* 2020; **99**: e19570 [PMID: 32221075 DOI: 10.1097/MD.0000000000019570]
4 **Cai W**, Yuan YC, Li MY, Kong W, Dong BJ, Chen YH, Zhang J, Xue W, Huang YR, Zhou LX, Huang JW. [Comparison of efficacy between sorafenib and sunitinib as first-line therapy for metastatic renal cell carcinoma and analyze prognostic factors for survival]. *Zhonghua Zhong Liu Za Zhi* 2018; **40**: 384-389 [PMID: 29860767 DOI: 10.3760/cma.j.issn.0253-3766.2018.05.012]
5 **Sheng X**, Jin J, He Z, Huang Y, Zhou A, Wang J, Ren X, Ye D, Zhang X, Qin S, Zhou F, Wang B, Guo J. Pazopanib versus sunitinib in Chinese patients with locally advanced or metastatic renal cell carcinoma: pooled subgroup analysis from the randomized, COMPARZ studies. *BMC Cancer* 2020; **20**: 219 [PMID: 32171288 DOI: 10.1186/s12885-020-6708-8]
6 **Motzer RJ**, Hutson TE, Glen H, Michaelson MD, Molina A, Eisen T, Jassem J, Zolnierek J, Maroto JP, Mellado B, Melichar B, Tomasek J, Kremer A, Kim HJ, Wood K, Dutcus C, Larkin J. Lenvatinib, everolimus, and the combination in

patients with metastatic renal cell carcinoma: a randomised, phase 2, open-label, multicentre trial. *Lancet Oncol* 2015; **16**: 1473-1482 [PMID: 26482279 DOI: 10.1016/S1470-2045(15)00290-9]

7 **Motzer R**, Alekseev B, Rha SY, Porta C, Eto M, Powles T, Grünwald V, Hutson TE, Kopyltsov E, Méndez-Vidal MJ, Kozlov V, Alyasova A, Hong SH, Kapoor A, Alonso Gordoa T, Merchan JR, Winquist E, Maroto P, Goh JC, Kim M, Gurney H, Patel V, Peer A, Procopio G, Takagi T, Melichar B, Rolland F, De Giorgi U, Wong S, Bedke J, Schmidinger M, Dutcus CE, Smith AD, Dutta L, Mody K, Perini RF, Xing D, Choueiri TK; CLEAR Trial Investigators. Lenvatinib plus Pembrolizumab or Everolimus for Advanced Renal Cell Carcinoma. *N Engl J Med* 2021; **384**: 1289-1300 [PMID: 33616314 DOI: 10.1056/NEJMoa2035716]

8 **Ning K**, Wu Z, Zou X, Liu H, Wu Y, Xiong L, Yu C, Guo S, Han H, Zhou F, Dong P, Zhang Z. Immune checkpoint inhibitors further aggravate proteinuria in patients with metastatic renal cell carcinoma after long-term targeted therapy. *Transl Androl Urol* 2022; **11**: 386-396 [PMID: 35402197 DOI: 10.21037/tau-21-1015]

9 **Motzer RJ**, Rini BI, McDermott DF, Arén Frontera O, Hammers HJ, Carducci MA, Salman P, Escudier B, Beuselinck B, Amin A, Porta C, George S, Neiman V, Bracarda S, Tykodi SS, Barthélémy P, Leibowitz-Amit R, Plimack ER, Oosting SF, Redman B, Melichar B, Powles T, Nathan P, Oudard S, Pook D, Choueiri TK, Donskov F, Grimm MO, Gurney H, Heng DYC, Kollmannsberger CK, Harrison MR, Tomita Y, Duran I, Grünwald V, McHenry MB, Mekan S, Tannir NM; CheckMate 214 investigators. Nivolumab plus ipilimumab versus sunitinib in first-line treatment for advanced renal cell carcinoma: extended follow-up of efficacy and safety results from a randomised, controlled, phase 3 trial. *Lancet Oncol* 2019; **20**: 1370-1385 [PMID: 31427204 DOI: 10.1016/S1470-2045(19)30413-9]

10 **Gil L**, Alves FR, Silva D, Fernandes I, Fontes-Sousa M, Alves M, Papoila A, Da Luz R. Prognostic Impact of Baseline Neutrophil-to-Eosinophil Ratio in Patients With Metastatic Renal Cell Carcinoma Treated With Nivolumab Therapy in Second or Later Lines. *Cureus* 2022; **14**: e22224 [PMID: 35340486 DOI: 10.7759/cureus.22224]

11 **Zheng RS**, Zhang SW, Zeng HM, Wang SM, Sun KX, Chen R, Li L, Wei WQ, He J. Cancer incidence and mortality in China, 2016. *J Nat Cancer Cent* 2022; **2**: 1-9 [DOI: 10.1016/j.jncc.2022.02.002]

12 **Rini BI**, Escudier B, Tomczak P, Kaprin A, Szczylik C, Hutson TE, Michaelson MD, Gorbunova VA, Gore ME, Rusakov IG, Negrier S, Ou YC, Castellano D, Lim HY, Uemura H, Tarazi J, Cella D, Chen C, Rosbrook B, Kim S, Motzer RJ. Comparative effectiveness of axitinib versus sorafenib in advanced renal cell carcinoma (AXIS): a randomised phase 3 trial. *Lancet* 2011; **378**: 1931-1939 [PMID: 22056247 DOI: 10.1016/S0140-6736(11)61613-9]

13 **Wolf MM**, Kimryn Rathmell W, Beckermann KE. Modeling clear cell renal cell carcinoma and therapeutic implications. *Oncogene* 2020; **39**: 3413-3426 [PMID: 32123314 DOI: 10.1038/s41388-020-1234-3]

14 **Miricescu D**, Balan DG, Tulin A, Stiru O, Vacaroiu IA, Mihai DA, Popa CC, Papacocea RI, Enyedi M, Sorin NA, Vatachki G, Georgescu DE, Nica AE, Stefani C. PI3K/AKT/mTOR signalling pathway involvement in renal cell carcinoma pathogenesis (Review). *Exp Ther Med* 2021; **21**: 540 [PMID: 33815613 DOI: 10.3892/etm.2021.9972]

15 **Motzer RJ**, Escudier B, Oudard S, Hutson TE, Porta C, Bracarda S, Grünwald V, Thompson JA, Figlin RA, Hollaender N, Urbanowitz G, Berg WJ, Kay A, Lebwohl D, Ravaud A; RECORD-1 Study Group. Efficacy of everolimus in advanced renal cell carcinoma: a double-blind, randomised, placebo-controlled phase III trial. *Lancet* 2008; **372**: 449-456 [PMID: 18653228 DOI: 10.1016/S0140-6736(08)61039-9]

16 **Motzer RJ**, Escudier B, Oudard S, Hutson TE, Porta C, Bracarda S, Grünwald V, Thompson JA, Figlin RA, Hollaender N, Kay A, Ravaud A; RECORD-1 Study Group. Phase 3 trial of everolimus for metastatic renal cell carcinoma : final results and analysis of prognostic factors. *Cancer* 2010; **116**: 4256-4265 [PMID: 20549832 DOI: 10.1002/cncr.25219]

17 **Vernieri C**, Corti F, Nichetti F, Ligorio F, Manglaviti S, Zattarin E, Rea CG, Capri G, Bianchi GV, de Braud F. Everolimus versus alpelisib in advanced hormone receptor-positive HER2-negative breast cancer: targeting different nodes of the PI3K/AKT/mTORC1 pathway with different clinical implications. *Breast Cancer Res* 2020; **22**: 33 [PMID: 32252811 DOI: 10.1186/s13058-020-01271-0]

18 **Ma ZY**, Gong YF, Zhuang HK, Zhou ZX, Huang SZ, Zou YP, Huang BW, Sun ZH, Zhang CZ, Tang YQ, Hou BH. Pancreatic neuroendocrine tumors: A review of serum biomarkers, staging, and management. *World J Gastroenterol* 2020; **26**: 2305-2322 [PMID: 32476795 DOI: 10.3748/wjg.v26.i19.2305]

19 **Bakhtiary H**, Barzegar M, Shiva S, Poorshiri B, Hajalioghli P, Herizchi Ghadim H. The Effect of Everolimus on Subependymal Giant Cell Astrocytoma (SEGA) in Children with Tuberous Sclerosis Complex. *Iran J Child Neurol* 2021; **15**: 15-25 [PMID: 34782838 DOI: 10.22037/ijcn.v15i4.30591]

20 **Paoletti E**, Citterio F, Corsini A, Potena L, Rigotti P, Sandrini S, Bussalino E, Stallone G; ENTROPIA Project. Everolimus in kidney transplant recipients at high cardiovascular risk: a narrative review. *J Nephrol* 2020; **33**: 69-82 [PMID: 31028549 DOI: 10.1007/s40620-019-00609-y]

21 **Chang SC**, Tsai CY, Liu KH, Wang SY, Hsu JT, Yeh TS, Yeh CN. Everolimus Related Fulminant Hepatitis in Pancreatic Neuroendocrine Tumor With Liver Metastases: A Case Report and Literature Review. *Front Endocrinol (Lausanne)* 2021; **12**: 639967 [PMID: 33868173 DOI: 10.3389/fendo.2021.639967]

22 **Ruiz-Falcó Rojas ML**, Feucht M, Macaya A, Wilken B, Hahn A, Maamari R, Hirschberg Y, Ridolfi A, Kingswood JC. Real-World Evidence Study on the Long-Term Safety of Everolimus in Patients With Tuberous Sclerosis Complex: Final Analysis Results. *Front Pharmacol* 2022; **13**: 802334 [PMID: 35462939 DOI: 10.3389/fphar.2022.802334]

23 **Lee L**, Ito T, Jensen RT. Everolimus in the treatment of neuroendocrine tumors: efficacy, side-effects, resistance, and factors affecting its place in the treatment sequence. *Expert Opin Pharmacother* 2018; **19**: 909-928 [PMID: 29757017 DOI: 10.1080/14656566.2018.1476492]

24 **Porta C**, Osanto S, Ravaud A, Climent MA, Vaishampayan U, White DA, Creel P, Dickow B, Fischer P, Gornell SS, Meloni F, Motzer RJ. Management of adverse events associated with the use of everolimus in patients with advanced renal cell carcinoma. *Eur J Cancer* 2011; **47**: 1287-1298 [PMID: 21481584 DOI: 10.1016/j.ejca.2011.02.014]

25 **Akata K**, Yatera K, Ishimoto H, Kozaki M, Yamasaki K, Nagata S, Nishida C, Yoshida T, Kawanami T, Matsumoto T, Mukae H. Two cases of everolimus-associated interstitial pneumonia in patients with renal cell carcinoma. *Intern Med* 2011; **50**: 3013-3017 [PMID: 22185995 DOI: 10.2169/internalmedicine.50.6133]

26 **Mauro C**, de Jesus VHF, Barros M, Costa FP, Weschenfelder RF, D'Agustini N, Angel M, Luca R, Nuñez JE, O'Connor JM, Riechelmann RP. Opportunistic and Serious Infections in Patients with Neuroendocrine Tumors Treated with

Everolimus: A Multicenter Study of Real-World Patients. *Neuroendocrinology* 2021; **111**: 631-638 [PMID: 32403102 DOI: 10.1159/000508632]

27 **Loron MC**, Grange S, Guerrot D, Di Fiore F, Freguin C, Hanoy M, Le Roy F, Poussard G, Etienne I, Legallicier B, Pfister C, Godin M, Bertrand D. Pneumocystis jirovecii pneumonia in everolimus-treated renal cell carcinoma. *J Clin Oncol* 2015; **33**: e45-e47 [PMID: 24638002 DOI: 10.1200/JCO.2013.49.9277]

28 **Braga BP**, Prieto-González S, Hernández-Rodríguez J. Pneumocystis jirovecii pneumonia prophylaxis in immunocompromised patients with systemic autoimmune diseases. *Med Clin (Barc)* 2019; **152**: 502-507 [PMID: 30853123 DOI: 10.1016/j.medcli.2019.01.010]

29 **Huang YS**, Yang JJ, Lee NY, Chen GJ, Ko WC, Sun HY, Hung CC. Treatment of Pneumocystis jirovecii pneumonia in HIV-infected patients: a review. *Expert Rev Anti Infect Ther* 2017; **15**: 873-892 [PMID: 28782390 DOI: 10.1080/14787210.2017.1364991]

30 **Avino LJ**, Naylor SM, Roecker AM. Pneumocystis jirovecii Pneumonia in the Non-HIV-Infected Population. *Ann Pharmacother* 2016; **50**: 673-679 [PMID: 27242349 DOI: 10.1177/1060028016650107]

31 **Echavarria I**, Carrión Galindo JR, Corral J, Diz Taín MP, Henao Carrasco F, Iranzo González-Cruz V, Mielgo-Rubio X, Quintanar T, Rivas Corredor C, Pérez Segura P. SEOM clinical guidelines for the prophylaxis of infectious diseases in cancer patients (2021). *Clin Transl Oncol* 2022; **24**: 724-732 [PMID: 35230619 DOI: 10.1007/s12094-022-02800-3]

32 **White PL**, Backx M, Barnes RA. Diagnosis and management of Pneumocystis jirovecii infection. *Expert Rev Anti Infect Ther* 2017; **15**: 435-447 [PMID: 28287010 DOI: 10.1080/14787210.2017.1305887]

33 **Bateman M**, Oladele R, Kolls JK. Diagnosing Pneumocystis jirovecii pneumonia: A review of current methods and novel approaches. *Med Mycol* 2020; **58**: 1015-1028 [PMID: 32400869 DOI: 10.1093/mmy/myaa024]

34 **Kloth C**, Thaiss WM, Beck R, Haap M, Fritz J, Beer M, Horger M. Potential role of CT-textural features for differentiation between viral interstitial pneumonias, pneumocystis jirovecii pneumonia and diffuse alveolar hemorrhage in early stages of disease: a proof of principle. *BMC Med Imaging* 2019; **19**: 39 [PMID: 31113389 DOI: 10.1186/s12880-019-0338-0]

35 **Liu L**, Yuan M, Shi Y, Su X. Clinical Performance of BAL Metagenomic Next-Generation Sequence and Serum (1,3)-β-D-Glucan for Differential Diagnosis of Pneumocystis jirovecii Pneumonia and Pneumocystis jirovecii Colonisation. *Front Cell Infect Microbiol* 2021; **11**: 784236 [PMID: 35004353 DOI: 10.3389/fcimb.2021.784236]

36 **Fan LC**, Lu HW, Cheng KB, Li HP, Xu JF. Evaluation of PCR in bronchoalveolar lavage fluid for diagnosis of Pneumocystis jirovecii pneumonia: a bivariate meta-analysis and systematic review. *PLoS One* 2013; **8**: e73099 [PMID: 24023814 DOI: 10.1371/journal.pone.0073099]

37 **Sivaraj V**, Cliff P, Douthwaite S, Smith M, Kulasegaram R. Pneumocystis jirovecii pneumonia PCR test on upper respiratory tract swab. *HIV Med* 2021; **22**: 321-324 [PMID: 33230932 DOI: 10.1111/hiv.13014]

38 **Qian YY**, Wang HY, Zhou Y, Zhang HC, Zhu YM, Zhou X, Ying Y, Cui P, Wu HL, Zhang WH, Jin JL, Ai JW. Improving Pulmonary Infection Diagnosis with Metagenomic Next Generation Sequencing. *Front Cell Infect Microbiol* 2020; **10**: 567615 [PMID: 33585263 DOI: 10.3389/fcimb.2020.567615]

39 **Chen Y**, Feng W, Ye K, Guo L, Xia H, Guan Y, Chai L, Shi W, Zhai C, Wang J, Yan X, Wang Q, Zhang Q, Li C, Liu P, Li M. Application of Metagenomic Next-Generation Sequencing in the Diagnosis of Pulmonary Infectious Pathogens From Bronchoalveolar Lavage Samples. *Front Cell Infect Microbiol* 2021; **11**: 541092 [PMID: 33777827 DOI: 10.3389/fcimb.2021.541092]

40 **Chiu CY**, Miller SA. Clinical metagenomics. *Nat Rev Genet* 2019; **20**: 341-355 [PMID: 30918369 DOI: 10.1038/s41576-019-0113-7]

41 **Wang J**, Han Y, Feng J. Metagenomic next-generation sequencing for mixed pulmonary infection diagnosis. *BMC Pulm Med* 2019; **19**: 252 [PMID: 31856779 DOI: 10.1186/s12890-019-1022-4]

42 **Lu X**, Zhang J, Ma W, Xing L, Ning H, Yao M. Pneumocystis Jirovecii Pneumonia Diagnosis *via* Metagenomic Next-Generation Sequencing. *Front Med (Lausanne)* 2022; **9**: 812005 [PMID: 35372422 DOI: 10.3389/fmed.2022.812005]

43 **Zhang Y**, Ai JW, Cui P, Zhang WH, Wu HL, Ye MZ. A cluster of cases of pneumocystis pneumonia identified by shotgun metagenomics approach. *J Infect* 2019; **78**: 158-169 [PMID: 30149030 DOI: 10.1016/j.jinf.2018.08.013]

44 **Wu HH**, Fang SY, Chen YX, Feng LF. Treatment of Pneumocystis jirovecii pneumonia in non-human immunodeficiency virus-infected patients using a combination of trimethoprim-sulfamethoxazole and caspofungin. *World J Clin Cases* 2022; **10**: 2743-2750 [PMID: 35434110 DOI: 10.12998/wjcc.v10.i9.2743]

45 **Maschmeyer G**, Helweg-Larsen J, Pagano L, Robin C, Cordonnier C, Schellongowski P; 6th European Conference on Infections in Leukemia (ECIL-6), a joint venture of The European Group for Blood and Marrow Transplantation (EBMT), The European Organization for Research and Treatment of Cancer (EORTC), the International Immunocompromised Host Society (ICHS) and The European LeukemiaNet (ELN). ECIL guidelines for treatment of Pneumocystis jirovecii pneumonia in non-HIV-infected haematology patients. *J Antimicrob Chemother* 2016; **71**: 2405-2413 [PMID: 27550993 DOI: 10.1093/jac/dkw158]

46 **Jin F**, Liu XH, Chen WC, Fan ZL, Wang HL. High initial (1, 3) Beta-d-Glucan concentration may be a predictor of satisfactory response of c aspofungin combined with TMP/SMZ for HIV-negative patients with moderate to severe Pneumocystis jirovecii pneumonia. *Int J Infect Dis* 2019; **88**: 141-148 [PMID: 31442630 DOI: 10.1016/j.ijid.2019.08.015]

World Journal of Clinical Cases

Submit a Manuscript: https://www.f6publishing.com

World J Clin Cases 2023 February 6; 11(4): 874-882

DOI: 10.12998/wjcc.v11.i4.874

ISSN 2307-8960 (online)

CASE REPORT

Identification of 1q21.1 microduplication in a family: A case report

Ting-Ting Huang, Hai-Feng Xu, Shang-Yu Wang, Wen-Xin Lin, Yie-Hen Tung, Kaleem Ullah Khan, Hui-Hui Zhang, Hu Guo, Guo Zheng, Gang Zhang

Specialty type: Neurosciences

Provenance and peer review: Unsolicited article; Externally peer reviewed.

Peer-review model: Single blind

Peer-review report's scientific quality classification

Grade A (Excellent): 0
Grade B (Very good): B
Grade C (Good): 0
Grade D (Fair): 0
Grade E (Poor): 0

P-Reviewer: Dokponou YCH, Morocco

Received: August 17, 2022
Peer-review started: August 17, 2022
First decision: November 11, 2022
Revised: December 21, 2022
Accepted: January 12, 2023
Article in press: January 12, 2023
Published online: February 6, 2023

Ting-Ting Huang, Hai-Feng Xu, Shang-Yu Wang, Wen-Xin Lin, Yie-Hen Tung, Kaleem Ullah Khan, Hu Guo, Guo Zheng, Gang Zhang, Department of Neurology, Children's Hospital of Nanjing Medical University, Nanjing 210000, Jiangsu Province, China

Hui-Hui Zhang, Nanjing Medical University, Nanjing 210000, Jiangsu Province, China

Hui-Hui Zhang, Nanjing Xiaozhuang University Experimental Primary School, Nanjing 210000, Jiangsu Province, China

Corresponding author: Gang Zhang, MD, PhD, Doctor, Department of Neurology, Children's Hospital of Nanjing Medical University, No. 72 Guangzhou Road, Nanjing 210000, Jiangsu Province, China. zhanggangnjmu@126.com

Abstract

BACKGROUND

Copy number variation (CNV) has become widely recognized in recent years due to the extensive use of gene screening in developmental disorders and epilepsy research. 1q21.1 microduplication syndrome is a rare CNV disease that can manifest as multiple congenital developmental disorders, autism spectrum disorders, congenital malformations, and congenital heart defects with genetic heterogeneity.

CASE SUMMARY

We reported a pediatric patient with 1q21.1 microduplication syndrome, and carried out a literature review to determine the correlation between 1q21.1 microduplication and its phenotypes. We summarized the patient's medical history and clinical symptoms, and extracted genomic DNA from the patient, her parents, elder brother, and sister. The patient was an 8-mo-old girl who was hospitalized for recurrent convulsions over a 2-mo period. Whole exon sequencing and whole genome low-depth sequencing (CNV-seq) were then performed. Whole exon sequencing detected a 1.58-Mb duplication in the CHR1:145883867-147465312 region, which was located in the 1q21.1 region. Family analysis showed that the pathogenetic duplication fragment, which was also detected in her elder brother's DNA originated from the mother.

CONCLUSION

Whole exon sequencing combined with quantitative polymerase chain reaction can provide an accurate molecular diagnosis in children with 1q21.1 microduplication syndrome, which is of great significance for genetic counseling and early intervention.

Key Words: 1q21.1 microduplication syndrome; Epilepsy; Copy number variation; Familial; Whole exon sequencing; Congenital developmental disorders; Case report

Core Tip: We reported an 8-mo-old girl with 1q21.1 microduplication syndrome, and review the literature to determine the correlation between 1q21.1 microduplication and its phenotypes. Whole exon sequencing and whole genome low-depth sequencing (Copy number variation -seq) were performed on the patient and her family members. This case shows that whole exon sequencing combined with quantitative polymerase chain reaction can provide an accurate molecular diagnosis in children with 1q21.1 microduplication syndrome, which is important for genetic counseling and early intervention in the patients.

Citation: Huang TT, Xu HF, Wang SY, Lin WX, Tung YH, Khan KU, Zhang HH, Guo H, Zheng G, Zhang G. Identification of 1q21.1 microduplication in a family: A case report. *World J Clin Cases* 2023; 11(4): 874-882
URL: https://www.wjgnet.com/2307-8960/full/v11/i4/874.htm
DOI: https://dx.doi.org/10.12998/wjcc.v11.i4.874

INTRODUCTION

Copy number variation (CNV) has become widely recognized in recent years due to the extensive use of gene screening in developmental disorders and epilepsy research[1]. In this study, we performed molecular genetic analysis on a child admitted to the hospital in October 2019 with unexplained seizures and found approximately 1.58 Mb of duplication in the 1q21.1-1q21.2 (CHR1:145883867-147465312 *3) region. Previous literature reported that epilepsy was associated with CNV of region 1q21.1, but it is mainly seen in microdeletion syndrome and rarely in microduplication syndrome[2,3]. The existing reports show that 1q21.1 microduplication syndrome leads to a phenotype that includes developmental delays, autism spectrum disorders, congenital malformations, and congenital heart defects (typically, tetralogy of Fallot) along with characteristic facial dysmorphic signs[4-6]. Here, we describe a 1q21.1 microduplication in a patient with a 1.58 Mb duplication. The patient experienced seizures, developmental delay, and congenital heart disease in the form of ventricular septal defect. In addition, we summarized and analyzed the clinical characteristics and CNV regions of children with 1q21.1 microduplication syndrome in order to further illustrate the correlation between the duplication region and phenotype.

CASE PRESENTATION

Chief complaints

The patient was an 8-mo-old girl who was hospitalized for recurrent convulsions over a 2-mo period.

History of present illness

She presented with repeated convulsions after admission to the hospital that manifested as upturned eyes, followed by involuntary blinking, cyanosis of the lips and hands and confusion. This was not considered a tonic seizure, and she had no limb shaking. The convulsions occurred approximately 10 times a day, each lasting about 30 s; some episodes were self-relieving. The patient did not present with fever before the convulsions and there was no history of birth asphyxia or trauma. The convulsions were relieved after treatment with sodium valproate. The patient also suffered from developmental retardation as she could not lift her head in the prone position until 6 mo old, and was unable to sit independently at admission (age: 8 mo). Her gross and fine motor skills were poor, but her language and speech skills seemed to be fine. The patient had clear consciousness. Her weight was in the normal range, and she did not show macrocephaly or short stature.

History of past illness

Ventricular septal defect (VSD) was found when she was 4 mo old, and she underwent open-heart repair of the VSD.

Personal and family history

She delivered naturally at term. There was no hypoxia or suffocation or intraventricular hemorrhage

during birth. Her parents denied any family history of developmental disorders, mental disorders, or genetic disorders. Both parents were in good health and are unrelated. The mother claimed that she developed a cold in the first 3 mo of the pregnancy. The mother denied any possible exposure to toxic substances such as alcohol, drugs, or other harmful environmental factors during the pregnancy and perinatal period. The child has a 5-year-old sister in good health and a 2.5-year-old brother who has language developmental delay and a two-time history of febrile convulsions. The patient's brother had no hypoxia or asphyxia or intraventricular hemorrhage at birth, has poor gross and fine motor skills, and he also appeared to have poor speech and language skills. He did not present with macrocephaly or short stature.

Physical examination

On physical examination, there was no remarkable dysmorphism in the patient's appearance. A 6-cm-long surgical scar was observed on the anterior chest. She had normal limb muscle strength and muscle tone, and her physiological reflexes were normal, with no evidence of any pathological signs.

Laboratory examinations

Routine blood, urine, and stool tests showed no abnormalities. Her thyroid hormone and growth hormone profiles were normal.

Imaging examinations

Electrocardiography showed sinus rhythm, left atrial burden, and T-wave changes in partial leads (V5). Chest radiography revealed increased pulmonary vascular markings, enlarged heart shadow, right upper mediastinal widening, and a thymus. Her video electroencephalography (VEEG) detected sharp slow wave release in the mid-line CZ (central midline point) and PZ (parietal midline point) zone during the sleep course. Cranial magnetic resonance imaging (MRI) showed left lateral ventricle enlargement and dysgenesis of the corpus callosum.

Further diagnostic work-up

Genomic DNA extraction: Briefly, 2 mL peripheral blood was drawn from the patient, her parents, and siblings, and sent to Kaiumph Medical Diagnosis (Beijing, China) for molecular karyotyping. We used a blood genomic DNA extraction kit (QIAamp DNA Blood Mini Kit, Qiagen) to extract genomic DNA.

Chromosome microarray: We first extracted DNA from peripheral blood and then processed the DNA samples by CMA using whole-genome bacterial artificial chromosome (BAC) microarrays, in accordance with the protocol. Data analysis was performed using algorithm fixed settings. The genomic coverage resolution of this microarray platform is up to 1 Mb. There were a minimum of 3 consecutive BAC clones used for microarray probes to determine copy number variation. We compared the detected CNVs with the known CNVs in the public database, and also classified detected CNVs as "Clinically Significant," "Likely Benign," or as "Variants Of Uncertain Clinical Significance (VOUS)." The result of the chromosome microarray test was negative.

Whole exome sequencing: Genomic DNA was quantified using Nanodrop 2000 (Thermal Fisher Scientific, United States). We used the NEXT flex Rapid DNA-Seq Kit to construct a genomic DNA library, used xGen Exome Research Panel v2 (IDT, United States) to capture the constructed libraries, and then used Novaseq 6000 (Illumina, United States) to sequence for 10–12 GB. We screened for variants based on minor allele frequencies in the normal population and performed variant function and prediction by Mutation Tester, Polyphen2, and SIFT. The mutant pathogenicity was assessed in accordance with guidelines of the American College of Medical Genetics and Genomics. We carried out analysis of CNV of patient's total exome detection results based on Cap CNV (capture copy number variation) analysis which was published in previous articles[1]. The results of gene sequencing and analysis with seizure-related genes such as *AAAS, AARS, AASS,* and *ABAT*, and another 1254 genes failed to show any pathogenic variation at the exon region.

Cap CNV analysis: We calculated the depth of each exon using bedtools-2.16.2 coverage for the same batch of samples. The sequencing quantity ratio of the sample and the batch mean was calculated to obtain the corrected depth in order to correct the bias in the sequencing data quantity. The depth ratio is used to determine whether a potential CNV exists in an exonic area, obtained from the corrected sample depth over the batch mean depth. A potential deletion is judged by a depth ratio of less than 0.7, and a potential duplication is judged by a depth ratio of greater than 1.3. The criterion for judging the low-quality area is that the rate of abnormal depth ratio in this area exceeds 20% in this batch, and then it is filtered.

The criteria for screening candidate CNV regions are as follows: (1) It is required that at least two consecutive exons have abnormal depth ratio for OMIM disease-related gene exon regions; and (2) It is required that at least ten consecutive exons have abnormal depth ratio for non OMIM disease-related gene exon regions. Then the regions of candidate CNV were annotated with Decipher and DGV.

The analysis of CNVs based on the depth of the exon captured sequence showed that there was a 1.58 Mb duplication of heterozygosity in the 1q21.1 region, which included the following 11 genes *GJA5*, *FMO5*, *CHD1L*, *PRKAB2*, *BCL9*, *BNBPF11*, *BNBPF12*, *BNBPF24*, *GJA8*, *GPR89B*, *GPR89C* (Figure 1, Table 1).

SYBR green fluorescent quantitative polymerase chain reaction: Primers for fluorescent quantitative polymerase chain reaction (qPCR) were designed for *FMO5*, *CHD1L*, *GJA5*, and *ABL1* genes in the microduplication region. *ABL1*, as a housekeeping gene, is used as an internal reference. The relative quantitative values (RQ values) of *FMO5* (forward, GAGCCCCATCCCACTTTCC; reverse, CCAACGCCATACCATTCAGG), *CHD1L* (forward, CCTCCTCAAGACAGCTGGTG; reverse, GCCCACCAGATCCTGATTCC) and *GJA5* (forward, CAGAGCCCCGGACCTCTTT; reverse, TCCCCATCTCCCACATTCG) genes were calculated with *ABL1* (forward, CTAAAGGTGAAAGCTCCG; reverse, GACTGTTGACTGGCGTGAT) as the internal reference gene by an ABI QuantStudioTM 6 Flex fluorescence quantitative analyzer for statistical analysis. Fluorescence qPCR was performed to determine the expression of related genes in duplicate regions of the genomic DNA from the patient, her parents, and normal controls. We purchased the PCR reaction reagents from Cowin Biosciences Company (Beijing, China), and the primer sequences were synthesized by Shanghai Sangon Biotech Company (Shanghai, China). We randomly selected exons from the *FMO5*, *CHD1L*, and *GJA5* genes in the 1.58 Mb heterozygous duplication region, which was detected by CNV analysis, according to the results of whole exome sequencing (WES) to design the fluorescent quantitative PCR primers with the *ABL* as the internal reference gene. The results showed that the patient and her mother were carriers of a heterozygous duplication in *FMO5*, *CHD1L*, and *GJA5* genes (the patient's RQ was approximately 1.5, and the mother's RQ was between 1.4 and 1.8). The father, however, did not show microduplication of *FMO5*, *CHD1L*, and *GJA5* genes (RQ: approximately 1), which indicated that the mutation originated from the mother (Figure 2).

Familial analysis of low-depth whole genome sequencing: Low-depth whole genome sequencing detected a duplication of 2.096 Mb of heterozygosity in chromosome 1q (CHR1:145828373-147924436). The region has not yet been reported in the Decipher database. Low-depth whole genome sequencing, which was performed on the DNA of the patient's mother and brother, also revealed a 2.096 Mb duplication of heterozygosity in the CHR1:145828373-147924436 region (as shown in Figure 3). These results indicated that the duplicate fragment originated from the mother and was also carried by the brother.

The patient's family tree: The patient, her brother and mother had a duplication of heterozygosity in the 1q21.1 region, her father and sister did not (Figure 4).

FINAL DIAGNOSIS

The patient was diagnosed with 1q21.1 microduplication syndrome.

TREATMENT

During the hospital stay, the patient had no epileptic seizures. The convulsions were relieved after treatment with sodium valproate.

OUTCOME AND FOLLOW-UP

Detailed history-taking and follow-up examinations showed that the patient and her brother are currently lagging behind in motor development and have language developmental delay and are likely on the autistic spectrum.

DISCUSSION

The 1q21.1 region is considered the most genetically unstable fragment due to multiple low-copy duplication, and one of the largest regions in the human genome that carries repeated duplication, thereby making it prone to CNV[2,4]. CNVs in the region are associated with developmental disorders, feeding problems, intellectual disability (ID), developmental delays (DD), congenital heart defects, behavioral problems (including autistic disorder and attention deficit hyperactivity disorder), and various other congenital deformities. There are 20-40 genes in the 1q21.1 region. The CNV of 1q21.1 can present as two main types: The one containing only the distal end region of 1q21.1 is called type I

Table 1 Genes contained in the 1.58 Mb duplication region and their functions

Gene	Phenotype	Inheritance	Gene function
GJA5	Atrial Fibrillation, Familial, 11; Atrial Standstill 1; Tetralogy of Fallot; Chromosome 1q21.1 deletion syndrome, 1.35-MB	AD	The *GJA5* gene encodes gap junction protein 40 (CX40), a cardiac gap junction protein expressed in the right ventricular outflow tract, which plays a key role in cell adhesion and intercellular communication
FMO5	Duodenal Atresia; Jacobsen Syndrome; Mowat-Wilson Syndrome	AD	The gene acts as Baeyer-Villiger monooxygenase on a broad range of substrates. Catalyzes the insertion of an oxygen atom into a carbon-carbon bond adjacent to a carbonyl, which converts ketones to esters
CHD1L	Postcholecystectomy Syndrome; Prostate Calculus; Chromosome 1q21.1 Duplication Syndrome	AD	DNA helicase which plays a role in chromatin-remodeling following DNA damage, targeted to sites of DNA damage through interaction with poly (ADP-ribose) and functions to regulate chromatin during DNA repair. Able to catalyze nucleosome sliding in an ATP-dependent manner. Helicase activity is strongly stimulated upon poly (ADP-ribose)-binding
NBPF12	Amelogenesis Imperfecta, Type Ia; Neuroblastoma; Microcephaly; Autism	Unknown	No data available for molecular function
NBPF11	Neuroblastoma; Duodenal Atresia	Unknown	Predicted to be located in the cytoplasm. No data available for molecular function
NBPF24	Also known asNBPF11	Unknown	No data available for molecular function
PRKAB2	Chromosome 1q21.1 Duplication Syndrome; Type 2 Diabetes Mellitus	Unknown	Non-catalytic subunit of AMP-activated protein kinase (AMPK), an energy sensor protein kinase that plays a key role in regulating cellular energy metabolism
BCL9	Chromosome 1q21.1 Duplication Syndrome; Lymphoma; Leukemia; Retinitis Pigmentosa	Unknown	Involved in signal transduction through the Wnt pathway. Promotes beta-catenin's transcriptional activity. Gene coding for a large proline-rich protein with two transcripts, expressed in all tissues and a third expressed only in thymus, spleen, small intestine, involved in translocation t(1;14) and t(1;22)
GJA8	Chromosome 1q21.1 Duplication Syndrome; Cataract 1, Multiple Types; Cataract Microcornea Syndrome; Early-Onset Sutural Cataract	AD	Structural component of eye lens gap junctions. Gap junctions are dodecameric channels that connect the cytoplasm of adjoining cells. They are formed by the docking of two hexameric hemichannels, one from each cell membrane. Small molecules and ions diffuse from one cell to a neighboring cell *via* the central pore
GPR89B	Thrombocytopenia-Absent Radius Syndrome; Hypothyroidism, Congenital, Nongoitrous, 1	Unknown	Voltage dependent anion channel required for acidification and functions of the Golgi apparatus that may function in counter-ion conductance. Plays a role in lymphocyte development, probably by acting as a RABL3 effector in hematopoietic cells
GPR89C	Also known as, *GPR89B*	Unknown	The function of the gene is the same as *GPR89B*

ADP: Adenosine diphosphate; AD: Autosomal dominant; AMP: Adenosine monophosphate; DNA: Deoxyribonucleic acid.

(approximately 1.8 Mb), and the one extending proximally to encompass the thrombocytopenia absent radius syndrome region is called type 2 (approximately 2.7 Mb)[4,5].

1q21.1 microduplication syndrome is a rare chromosome 1 mutation. It can be an autosomal dominant inheritance or a novel mutation. There is no significant difference in the sex ratio. Microduplication of 1q21.1 is observed in approximately 0.03% adults, and the frequency in live births is estimated to be 1/6309. It presents with variable and partially explicit phenotypes; the common clinical manifestations are multiple congenital developmental disorders, which include DD, autism spectrum disorders, congenital malformations, and congenital heart defects, wherein tetralogy of Fallot is the most common. It can also be seen in normal individuals[4,6-8]. In 2017, Busè *et al*[9] expanded the phenotype of the 1q21.1 syndrome and suggested that the 1q21.1 microduplication syndrome showed special facial features such as macrocephaly or relative macrocephaly, prominent forehead, and widening of the eye distance. The relationship between triangular head deformity and 1q21.1 microduplication syndrome was also mentioned[9]. Some researchers believed that it is a predisposing locus instead of a clinically distinct syndrome, given its incomplete dominance and variable phenotype[10]. With the development of genome microarray and other methods for detecting CNVs, the improved accuracy of CNVs detection, and the widespread use of gene screening in the study of DD and epilepsy, an increasing number of cases of 1q21.1 microduplication have been reported.

1q21.1 microduplication has been linked to a range of neurodevelopmental disorders, including autism spectrum disorders, ID, and even epilepsy, although there is no known gene for neurological disorders in this region[11]. The UCSC Genome Browser lists two genes located in the distal microduplication region, *CHD1L* and *PRKAB2*, which may be associated with epilepsy[2]. The *CHD1L* gene is also a candidate gene for attention deficit hyperactivity disorder and autism spectrum disorders, and the repetition of *CHD1L* is implicated in delayed language development[10]. The *CHD1L* gene, which is associated with a variety of cancers, encodes a helicase responsible for DNA repair. It comes from the same family as *CHD2*, which is related to epileptic encephalopathy and various generalized epilepsy syndromes[2]. *PRKAB2* acts as a regulator of cellular responses to numerous stimuli, encodes the β2

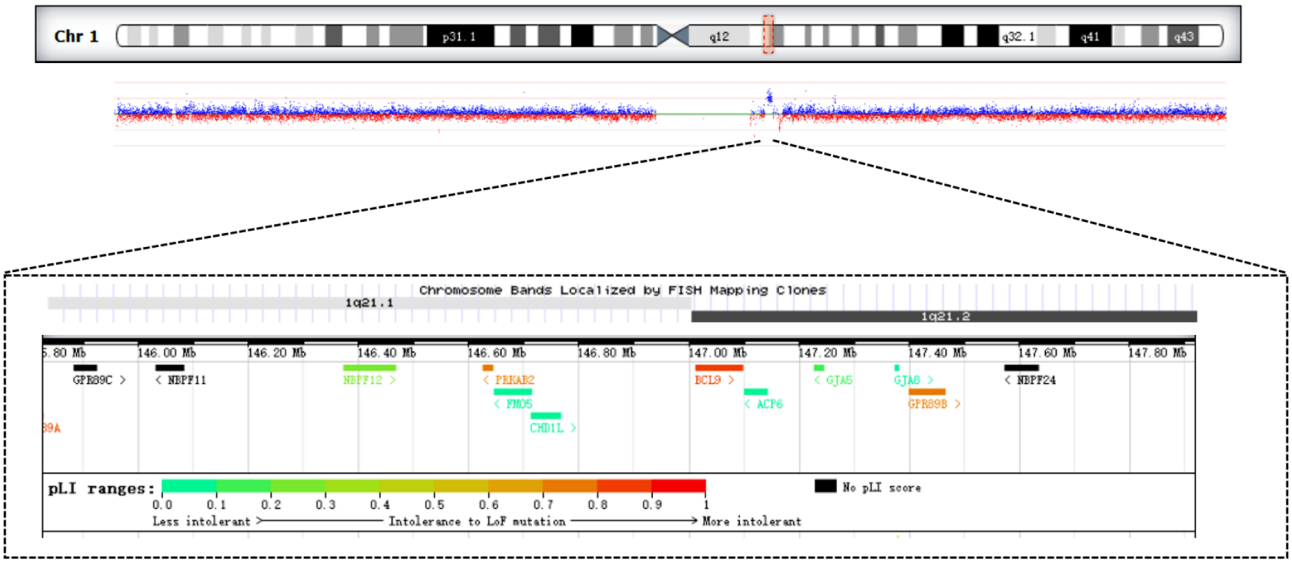

DOI: 10.12998/wjcc.v11.i4.874 **Copyright** ©The Author(s) 2023.

Figure 1 Patient's chromosome 1 duplication.

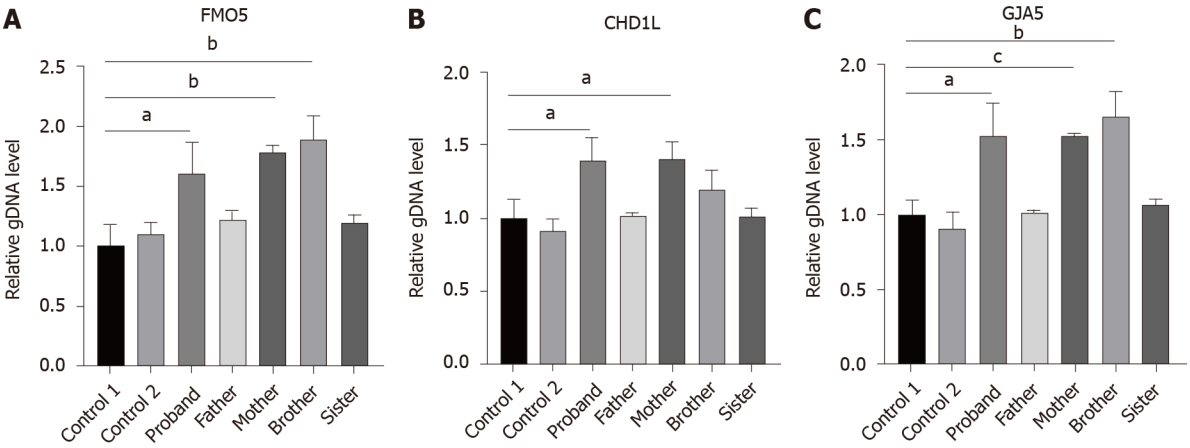

DOI: 10.12998/wjcc.v11.i4.874 **Copyright** ©The Author(s) 2023.

Figure 2 Fluorescent quantitative polymerase chain reaction showed that the patient and her mother were carriers of heterozygous duplication in *FMO5*, *CHD1L*, and *GJA5* genes. A: gDNA level of *FMO5* in 1q21 region; B: gDNA level of *CHD1L* in 1q21 region; C: gDNA level of *GJA5* in 1q21 region. $^{a}P \leq 0.05$; $^{b}P \leq 0.01$; $^{c}P \leq 0.001$.

subunits of AMP-activated protein kinase, and appears to play an important role in brain function[12]. With regard to the previously mentioned macrocephaly, it has been reported that it may be related to *DUF1220* in this region, because the deletion of *DUF1220* was found to be associated with microcephaly in 1q21.1 microdeletion syndrome. *HYDIN2*, in region 1q21.1, is a gene involved in the *DUF1220* protein domain, and a homolog of the *HYDIN* gene in region 16q22.2. *HYDIN*, expressed only in the brain, is associated with hydrocephalus, so it may affect head circumference[13-15]. Regarding congenital heart defect, the *GJA5* gene is believed to play an important role in the heart phenotype in the 1q21.1 region. It encodes gap junction protein 40 (CX40), a cardiac gap junction protein expressed through the right ventricular outflow tract, which plays a key role in intercellular communication and cellular adhesion and makes *GJA5* gene a major candidate for congenital heart defect phenotype in this region[5,16-18].

At present, the sample size of 1q21.1 microduplication syndrome is limited, and the reported phenotypes are different. Using "1q21.1 microduplication syndrome" as the key word, we searched the biomedical literature database (PubMed) for nearly 10 years of literature, and we counted the 1q21.1 duplication regions and the genes contained in the region (Supplementary Table 1). Therefore, we still need more research to clarify the connection between genotype and specific phenotype of 1q21.1 microduplication syndrome. In our case, the result of the patient's gene analysis detected microduplication which contained both the *GJA5* and *CHD1L* genes in the 1q21.1 region. This might explain her seizures and congenital heart disease. In the familial analysis, her mother and brother both carried microduplication of the *GJA5* and *CHD1L* genes. However, her brother, who had a heterozygous

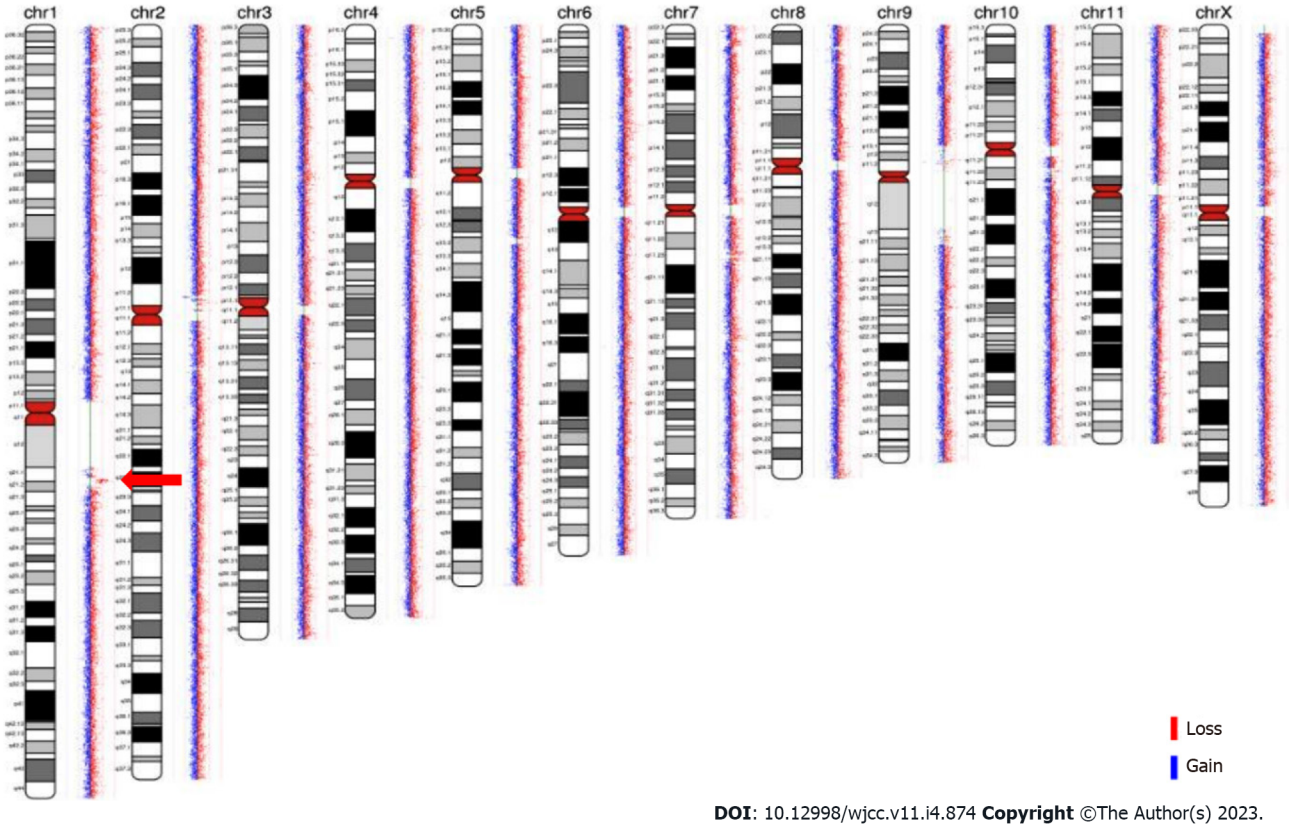

Figure 3 The patient's mother and brother chromosome 1 duplication marked by a red arrow.

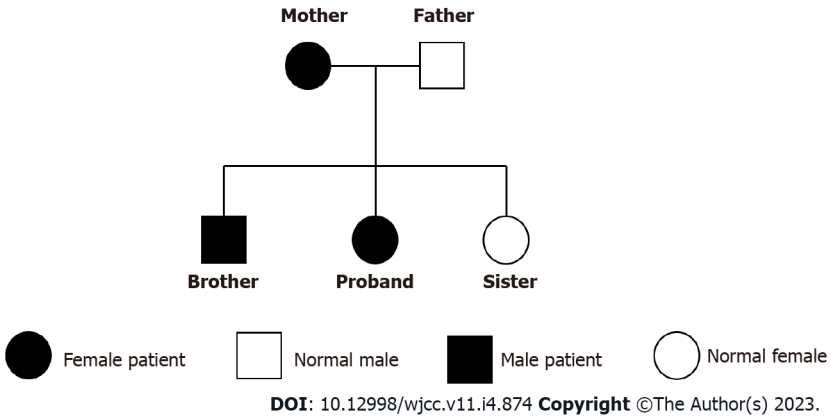

Figure 4 The patient's family tree.

duplication of about 2.096 Mb in the CHR1:145826755-147924436 region, showed symptoms presenting with language DD and febrile convulsions, while her mother showed no abnormalities. VEEG and cranial MRI of the patient's mother did not show any abnormalities, and the language ability and reading ability of her mother were normal as assessed by the simple Wechsler Adult Intelligence Scale-Revised in China. In 2015, Judith and Verhagen *et al*[17] reported a case of 1q21.1 microduplication in a family of 11 people over three generations. Their patient suffered from severe learning difficulties and was diagnosed with chronic depression and anxiety at the age of 18. All carriers in her family showed hypertelorism and other facial dysmorphism but no congenital heart defect. At the first pregnancy of the proband, ultrasound examination at 20 wk of gestation revealed excessive fetal growth and a complex congenital heart defect, the pregnancy was terminated on the advice of her obstetrician. With these two reports of the same genotype but different phenotypes, we could speculate that the same genetic changes may result in different phenotypes. The phenotypes of our patient and her relatives still require long-term follow-up, for any new potential phenotypes.

The development of the nervous system is a complex process involving nearly 70% gene expression, which may explain why different CNVs have common clinical features. However, there is no explanation as to why the same position and CNV would result in a different phenotype[19]. Genes are epigenetically inherited and subject to environmental modifications; genetic alterations may make CNV carriers more susceptible to environmental influences, which can lead to different phenotypes, depending on the severity of the environmental impact[20,21]. Furthermore, the variable expressivity and incomplete penetrance suggest that the influence of CNV is modified by other genetic loci or environmental factors[22]. Xu *et al*[23] suggested that women have a higher tolerance for pathogenicity/potential CNVs and have an inclination to pass these CNVs on to their offspring of males. At present, all CNVs studies of the Chinese population are concentrated on describing the genotype-phenotype correlation and explaining the mechanism of pathogenesis. Therefore, understanding the clinical significance of CNVs or offering optimum treatment options to CNV carriers at prenatal consultation continues to remain challenging.

CONCLUSION

1q21.1 microduplication syndrome is a rare CNV disease. This finding has extended our knowledge of the clinical manifestations of 1q21.1 microduplication syndrome and enhanced our understanding of CNV. However, further research is required to clarify the connection between genotype and specific phenotype of 1q21.1 microduplication syndrome. WES combined with qPCR can provide an accurate molecular diagnosis for children carrying this genetic mutation, which is of great significance for genetic counseling and early intervention.

FOOTNOTES

Author contributions: Zhang G designed and performed the study; Huang TT, Xu HF, and Wang SY wrote the draft manuscript; Lin WX, Tung YH and Zhang HH collected the data; Khan KU, Guo H and Zheng G carried out language revision; All authors approved the submission of the final manuscript.

Informed consent statement: Written informed consent for publication was obtained from the parents.

Conflict-of-interest statement: All the authors have no financial relationship with any commercial entity with a potential interest in the subject of this manuscript.

CARE Checklist (2016) statement: The authors have read the CARE Checklist (2016), and the manuscript was prepared and revised according to the CARE Checklist (2016).

Country/Territory of origin: China

ORCID number: Ting-Ting Huang 0000-0001-5177-416X; Wen-Xin Lin 0000-0003-0591-3880; Guo Zheng 0000-0001-7525-9680; Gang Zhang 0000-0001-5729-7667.

S-Editor: Liu JH
L-Editor: A
P-Editor: Liu JH

REFERENCES

1 **Tung Y**, Lu H, Lin W, Huang T, Kim S, Hu G, Zhang G, Zheng G. Case Report: Identification of a de novo Microdeletion 1q44 in a Patient With Seizures and Developmental Delay. *Front Genet* 2021; **12**: 648351 [PMID: 34093647 DOI: 10.3389/fgene.2021.648351]
2 **Gourari I**, Schubert R, Prasad A. 1q21.1 Duplication syndrome and epilepsy: Case report and review. *Neurol Genet* 2018; **4**: e219 [PMID: 29379884 DOI: 10.1212/NXG.0000000000000219]
3 **Seo HS**, Jung YJ, Kim JH, Lee HH, Park CH. The Effect of Metformin on Prognosis in Patients With Locally Advanced Gastric Cancer Associated With Type 2 Diabetes Mellitus. *Am J Clin Oncol* 2019; **42**: 909-917 [PMID: 31693512 DOI: 10.1097/COC.0000000000000627]

4 **Dolcetti A**, Silversides CK, Marshall CR, Lionel AC, Stavropoulos DJ, Scherer SW, Bassett AS. 1q21.1 Microduplication expression in adults. *Genet Med* 2013; **15**: 282-289 [PMID: 23018752 DOI: 10.1038/gim.2012.129]

5 **Sun G**, Tan Z, Fan L, Wang J, Yang Y, Zhang W. 1q21.1 microduplication in a patient with mental impairment and congenital heart defect. *Mol Med Rep* 2015; **12**: 5655-5658 [PMID: 26238956 DOI: 10.3892/mmr.2015.4166]

6 **Xavier J**, Zhou B, Bilan F, Zhang X, Gilbert-Dussardier B, Viaux-Savelon S, Pattni R, Ho SS, Cohen D, Levinson DF, Urban AE, Laurent-Levinson C. 1q21.1 microduplication: large verbal-nonverbal performance discrepancy and ddPCR assays of HYDIN/HYDIN2 copy number. *NPJ Genom Med* 2018; **3**: 24 [PMID: 30155272 DOI: 10.1038/s41525-018-0059-2]

7 **Gillentine MA**, Lupo PJ, Stankiewicz P, Schaaf CP. An estimation of the prevalence of genomic disorders using chromosomal microarray data. *J Hum Genet* 2018; **63**: 795-801 [PMID: 29691480 DOI: 10.1038/s10038-018-0451-x]

8 **Veerapandiyan A**, Oh D, Kornitzer J. Distal 1q21.1 and proximal 1q21.2 microduplication in a child with attention-deficit hyperactivity disorder. *Acta Neurol Belg* 2019; **119**: 289-290 [PMID: 30120686 DOI: 10.1007/s13760-018-1002-0]

9 **Busè M**, Cuttaia HC, Palazzo D, Mazara MV, Lauricella SA, Malacarne M, Pierluigi M, Cavani S, Piccione M. Expanding the phenotype of reciprocal 1q21.1 deletions and duplications: a case series. *Ital J Pediatr* 2017; **43**: 61 [PMID: 28724436 DOI: 10.1186/s13052-017-0380-x]

10 **Benítez-Burraco A**, Barcos-Martínez M, Espejo-Portero I, Fernández-Urquiza M, Torres-Ruiz R, Rodríguez-Perales S, Jiménez-Romero MS. Narrowing the Genetic Causes of Language Dysfunction in the 1q21.1 Microduplication Syndrome. *Front Pediatr* 2018; **6**: 163 [PMID: 29922639 DOI: 10.3389/fped.2018.00163]

11 **Dougherty ML**, Nuttle X, Penn O, Nelson BJ, Huddleston J, Baker C, Harshman L, Duyzend MH, Ventura M, Antonacci F, Sandstrom R, Dennis MY, Eichler EE. The birth of a human-specific neural gene by incomplete duplication and gene fusion. *Genome Biol* 2017; **18**: 49 [PMID: 28279197 DOI: 10.1186/s13059-017-1163-9]

12 **Harvard C**, Strong E, Mercier E, Colnaghi R, Alcantara D, Chow E, Martell S, Tyson C, Hrynchak M, McGillivray B, Hamilton S, Marles S, Mhanni A, Dawson AJ, Pavlidis P, Qiao Y, Holden JJ, Lewis SM, O'Driscoll M, Rajcan-Separovic E. Understanding the impact of 1q21.1 copy number variant. *Orphanet J Rare Dis* 2011; **6**: 54 [PMID: 21824431 DOI: 10.1186/1750-1172-6-54]

13 **Dumas LJ**, O'Bleness MS, Davis JM, Dickens CM, Anderson N, Keeney JG, Jackson J, Sikela M, Raznahan A, Giedd J, Rapoport J, Nagamani SS, Erez A, Brunetti-Pierri N, Sugalski R, Lupski JR, Fingerlin T, Cheung SW, Sikela JM. DUF1220-domain copy number implicated in human brain-size pathology and evolution. *Am J Hum Genet* 2012; **91**: 444-454 [PMID: 22901949 DOI: 10.1016/j.ajhg.2012.07.016]

14 **Brunetti-Pierri N**, Berg JS, Scaglia F, Belmont J, Bacino CA, Sahoo T, Lalani SR, Graham B, Lee B, Shinawi M, Shen J, Kang SH, Pursley A, Lotze T, Kennedy G, Lansky-Shafer S, Weaver C, Roeder ER, Grebe TA, Arnold GL, Hutchison T, Reimschisel T, Amato S, Geragthy MT, Innis JW, Obersztyn E, Nowakowska B, Rosengren SS, Bader PI, Grange DK, Naqvi S, Garnica AD, Bernes SM, Fong CT, Summers A, Walters WD, Lupski JR, Stankiewicz P, Cheung SW, Patel A. Recurrent reciprocal 1q21.1 deletions and duplications associated with microcephaly or macrocephaly and developmental and behavioral abnormalities. *Nat Genet* 2008; **40**: 1466-1471 [PMID: 19029900 DOI: 10.1038/ng.279]

15 **O'Bleness M**, Searles VB, Varki A, Gagneux P, Sikela JM. Evolution of genetic and genomic features unique to the human lineage. *Nat Rev Genet* 2012; **13**: 853-866 [PMID: 23154808 DOI: 10.1038/nrg3336]

16 **Soemedi R**, Topf A, Wilson IJ, Darlay R, Rahman T, Glen E, Hall D, Huang N, Bentham J, Bhattacharya S, Cosgrove C, Brook JD, Granados-Riveron J, Setchfield K, Bu'lock F, Thornborough C, Devriendt K, Breckpot J, Hofbeck M, Lathrop M, Rauch A, Blue GM, Winlaw DS, Hurles M, Santibanez-Koref M, Cordell HJ, Goodship JA, Keavney BD. Phenotype-specific effect of chromosome 1q21.1 rearrangements and GJA5 duplications in 2436 congenital heart disease patients and 6760 controls. *Hum Mol Genet* 2012; **21**: 1513-1520 [PMID: 22199024 DOI: 10.1093/hmg/ddr589]

17 **Verhagen JM**, de Leeuw N, Papatsonis DN, Grijseels EW, de Krijger RR, Wessels MW. Phenotypic Variability Associated with a Large Recurrent 1q21.1 Microduplication in a Three-Generation Family. *Mol Syndromol* 2015; **6**: 71-76 [PMID: 26279651 DOI: 10.1159/000431274]

18 **Wang HD**, Liu L, Wu D, Li T, Cui CY, Zhang LZ, Wang CZ. Clinical and molecular cytogenetic analyses of four families with 1q21.1 microdeletion or microduplication. *J Gene Med* 2017; **19** [PMID: 28220983 DOI: 10.1002/jgm.2948]

19 **Deshpande A**, Weiss LA. Recurrent reciprocal copy number variants: Roles and rules in neurodevelopmental disorders. *Dev Neurobiol* 2018; **78**: 519-530 [PMID: 29575775 DOI: 10.1002/dneu.22587]

20 **Rosenfeld JA**, Coe BP, Eichler EE, Cuckle H, Shaffer LG. Estimates of penetrance for recurrent pathogenic copy-number variations. *Genet Med* 2013; **15**: 478-481 [PMID: 23258348 DOI: 10.1038/gim.2012.164]

21 **Qiao Y**, Badduke C, Tang F, Cowieson D, Martell S, Lewis SME, Peñaherrera MS, Robinson WP, Volchuk A, Rajcan-Separovic E. Whole exome sequencing of families with 1q21.1 microdeletion or microduplication. *Am J Med Genet A* 2017; **173**: 1782-1791 [PMID: 28475290 DOI: 10.1002/ajmg.a.38247]

22 **Maher BS**, Riley BP, Kendler KS. Psychiatric genetics gets a boost. *Nat Genet* 2008; **40**: 1042-1044 [PMID: 19165917 DOI: 10.1038/ng0908-1042]

23 **Xu M**, Ji Y, Zhang T, Jiang X, Fan Y, Geng J, Li F. Clinical Application of Chromosome Microarray Analysis in Han Chinese Children with Neurodevelopmental Disorders. *Neurosci Bull* 2018; **34**: 981-991 [PMID: 29948840 DOI: 10.1007/s12264-018-0238-2]

World Journal of Clinical Cases

Submit a Manuscript: https://www.f6publishing.com

World J Clin Cases 2023 February 6; 11(4): 883-887

DOI: 10.12998/wjcc.v11.i4.883

ISSN 2307-8960 (online)

CASE REPORT

Double pigtail catheter reduction for seriously displaced intravenous infusion port catheter: A case report

Yu Liu, Duan-Ming Du

Specialty type: Surgery

Provenance and peer review: Unsolicited article; Externally peer reviewed.

Peer-review model: Single blind

Peer-review report's scientific quality classification

Grade A (Excellent): 0
Grade B (Very good): B
Grade C (Good): 0
Grade D (Fair): 0
Grade E (Poor): 0

P-Reviewer: Dragonieri S, Italy

Received: August 25, 2022
Peer-review started: August 25, 2022
First decision: December 20, 2022
Revised: December 29, 2022
Accepted: January 10, 2023
Article in press: January 10, 2023
Published online: February 6, 2023

Yu Liu, Duan-Ming Du, Department of Interventional Therapy, Shenzhen Second People's Hospital, The First Affiliated Hospital of Shenzhen University, Shenzhen 518035, Guangdong Province, China

Corresponding author: Duan-Ming Du, PhD, Chief Doctor, Department of Interventional Therapy, Shenzhen Second People's Hospital, The First Affiliated Hospital of Shenzhen University, No. 3002 Sungang Road, Futian District, Shenzhen 518035, Guangdong Province, China. dmdu69@163.com

Abstract

BACKGROUND

Implanted intravenous infusion port (TIAP) is mainly used for patients who need central venous infusion and poor peripheral vascular conditions. With the advantages of easy to carry, long maintenance cycle, few complications and excellent quality of life, it has been widely used in the fields of malignant tumor chemotherapy, parenteral nutrition support and repeated blood collection. Implanted intravenous infusion port (IVAP) dislocation can have significant complications if not recognised and reinstated immediately.

CASE SUMMARY

A 24-year-old man was treated with adjuvant chemotherapy for osteosarcoma. Severe displacement of IVAP catheter was found by chest X-ray examination. The IVAP cannot be used normally. Therefore, we conducted an emergency procedure to reset the catheter through double pigtail catheters, the operation was successful and the infusion port was restored.

CONCLUSION

When IVAP catheter displacement cannot be reset by conventional techniques, two pigtail catheters can be successfully used instead.

Key Words: Catheter; Displaced catheter; Implantable; Implanted intravenous infusion port; Pigtail catheter; Case report

Core Tip: In the face of serious ectopic infusion port, we successfully solved the problem with double pig tail catheter.

Citation: Liu Y, Du DM. Double pigtail catheter reduction for seriously displaced intravenous infusion port catheter: A case report. *World J Clin Cases* 2023; 11(4): 883-887
URL: https://www.wjgnet.com/2307-8960/full/v11/i4/883.htm
DOI: https://dx.doi.org/10.12998/wjcc.v11.i4.883

INTRODUCTION

Implanted intravenous infusion port (IVAP) catheters are mainly used for patients who need central venous infusion therapy and have poor peripheral vascular conditions. It has been widely used in malignant tumour chemotherapy, parenteral nutrition support treatment, and repeated blood collection in various nations because of the benefits of easy carrying, extended maintenance time, few complications, and excellent quality of life. Inadequate care can lead to complications such as catheter displacement, obstruction, infection, pneumothorax, haemothorax, vascular damage, thrombus, and catheter rupture[1-4]. Among them, catheter displacement of the infusion port has become a critical complication as it affects the chemotherapy effect on patients and it can be life-threatening if the displacement is not recognised and repositioned promptly.

We describe a case with catheter displacement that could not be solved by conventional procedures which is a single pig tail catheter reduction or surgical removal of the port. Hence, we used the double pigtail catheters to reset the displaced catheter. Such interventional reduction surgery is rarely reported.

CASE PRESENTATION

Chief complaints

Our patient was a 24-year-old male with osteosarcoma at the distal end of the left calf. After the second chemotherapy round, the patient developed severe cough and vomiting, and it was difficult to push the catheter when using normal saline. Chest X-ray showed that the catheter had been displaced into a loop.

History of present illness

Osteosarcoma following chemotherapy.

History of past illness

On December 23, 2021, the patient experienced resection of a lesion of the distal left fibula, ankle fusion and microwave ablation.

Personal and family history

The patient denied having any specific family or personal history of any illnesses.

Physical examination

The patient's vital signs at the point of presentation were 36.4°C for body temperature, 114/73 mmHg for blood pressure, 96 beats per minute for pulse, and 20 breaths per minute for respiratory rate. During the physical examination, the patient cooperated and was conscious. A 15-cm surgical incision in the left leg was visible, skin temperature was normal, the plantar flexion and extension of the left ankle were limited, and movement and sensation of the left lower limb were normal.

Laboratory examinations

D-dimer dynamic: 0.57 mg/L.

Imaging examinations

Chest X-ray indicated that the catheter was displaced into a loop (Figure 1A).

FINAL DIAGNOSIS

The final diagnosis result is that ectopic catheter in infusion port.

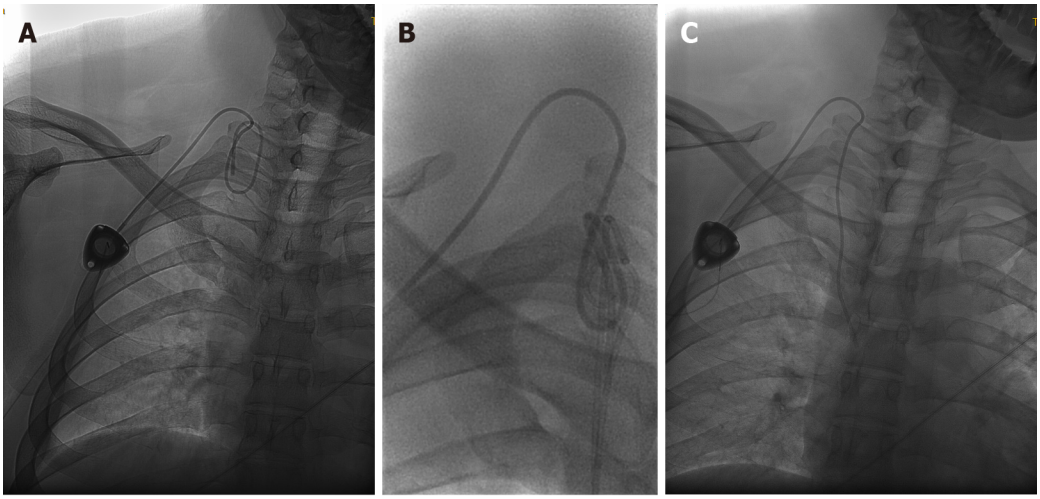

DOI: 10.12998/wjcc.v11.i4.883

Figure 1 X-ray found severe ectopic infusion port. A: Preoperative examination revealed severe ectopic infusion port; B: Intraoperative film, two 5F pigtail catheters used to reposition the ectopic infusion port catheter; C: The ectopic infusion port catheter has been successfully reset, and the end of the catheter in the inferior margin of the 5th posterior rib.

TREATMENT

After consulting with the appropriate departments, we prepared to reset the IVAP using an interventional approach. The patient lay flat on the digital subtraction angiography examination bed during the procedure. Digital subtraction angiography fluoroscopy showed that the catheter was displaced into a loop. We used the modified Seldinger puncture to puncture the right femoral vein, and 5F vascular sheath was successfully implanted. Using a long exchange guide wire, we guided the 5F pigtail catheter (Yixinda SCW-StraightPigtail-05110) to the right jugular vein, through the natural bending at the front end of the catheter, trapped the middle and long section of the infusion port catheter, and reset the infusion port catheter by slightly rotating and pulling down[5,6]. Due to the severe displacement of the infusion tube, we failed to reset the catheter using one pigtail. Therefore, we used the same method to puncture the left femoral vein and successfully reset the displaced infusion port catheter using the double pigtail catheter (Figure 1B and C).

OUTCOME AND FOLLOW-UP

Post-operation, the patient did not complain of discomfort and successfully completed the third chemotherapy in the ward.

DISCUSSION

IVAP chemotherapy can give patients continuous venous access and shield their peripheral blood vessels from harm from irritating medications[7]. Because of the benefits of easy carrying, long maintenance period, few complications and high quality of life of patients, it has been widely used in malignant tumour chemotherapy, parenteral nutrition support treatment and repeated blood collection. Increased attention has been paid to complications related to transfusion port such as thrombosis, infection, displacement, pneumothorax and others. Among them, the displacement of transfusion port pipeline is a significant complication of transfusion port implantation, as it affects chemotherapy effectivity and can be life threatening[8]. Catheter displacement may be caused by: (1) A catheter that is too short, and its end position is 1/3 above the superior vena cava; (2) strenuous exercise of the arm or shoulder; (3) severe cough; and (4) repeated vomiting. The catheter displacement in our patient may have been due to repeated vomiting during the second chemotherapy session[9,10].

CONCLUSION

When the catheter is displaced into a loop, the general interventional reduction surgery may not be sufficient to reset the displaced catheter. Thus, we can adopt the method of co-reduction using double

pigtails to increase the traction force of the catheter reduction and make the pull-down force stronger.

ACKNOWLEDGEMENTS

We thank the patient for participating in the study and for agreeing to undergo follow-ups.

FOOTNOTES

Author contributions: Liu Y carried out the study, participated in data collection, and drafted the manuscript; Du DM performed statistical analysis and participated in study design and participated in the acquisition, analysis, and interpretation of the data, and drafted the manuscript; all authors read and approved the final manuscript.

Supported by Shenzhen Key Medical Discipline Construction Fund, No. SZXK052.

Informed consent statement: Informed written consent was obtained from the patient for publication of this report and any accompanying images.

Conflict-of-interest statement: All the authors declare that they have no conflict of interest.

CARE Checklist (2016) statement: The authors have read the CARE Checklist (2016), and the manuscript was prepared and revised according to the CARE Checklist (2016).

Country/Territory of origin: China

ORCID number: Yu Liu 0000-0001-9528-4728; Duan-Ming Du 0000-0002-3360-9563.

S-Editor: Liu JH
L-Editor: A
P-Editor: Liu JH

REFERENCES

1 **Chou PL**, Fu JY, Cheng CH, Chu Y, Wu CF, Ko PJ, Liu YH, Wu CY. Current port maintenance strategies are insufficient: View based on actual presentations of implanted ports. *Medicine (Baltimore)* 2019; **98**: e17757 [PMID: 31689833 DOI: 10.1097/MD.0000000000017757]
2 **Ding X**, Ding F, Wang Y, Wang L, Wang J, Xu L, Li W, Yang J, Meng X, Yuan M, Chu J, Ge F, Dong W, Xue M; Shanghai Cooperation Group on Central Venous Access Vascular Access Committee of the Solid Tumor Theranostics Committee, Shanghai Anti-Cancer Association. Shanghai expert consensus on totally implantable access ports 2019. *J Interv Med* 2019; **2**: 141-145 [PMID: 34805890 DOI: 10.1016/j.jimed.2019.10.008]
3 **Xu L**, Qin W, Zheng W, Sun X. Ultrasound-guided totally implantable venous access ports *via* the right innominate vein: a new approach for patients with breast cancer. *World J Surg Oncol* 2019; **17**: 196 [PMID: 31767003 DOI: 10.1186/s12957-019-1727-0]
4 **Marcy PY**, Schiappa R, Ferrero JM, Dahlet C, Brenet O, Yazbec G, Dubois PY, Salm B, Fouche Y, Mari V, Montastruc M, Lebrec N, Ancel B, Paillocher N, Dupoiron D, Rangeard O, Gal J, Ettaiche M, Chateau Y, Chamorey E. Patient satisfaction and acceptance of their totally implanted central venous catheter: a French prospective multicenter study. *J Vasc Access* 2017; **18**: 390-395 [PMID: 28731491 DOI: 10.5301/jva.5000744]
5 **Chen GQ**, Wu Y, Zhao KF, Shi RS. Removal of "ruptured" pulmonary artery infusion port catheter by pigtail catheter combined with gooseneck trap: A case report. *World J Clin Cases* 2021; **9**: 8820-8824 [PMID: 34734061 DOI: 10.12998/wjcc.v9.i29.8820]
6 **Letachowicz K**, Gołębiowski T, Miś M, Wolańczyk M, Zmonarski S, Krajewska M. Partial breakage of a tunneled dialysis catheter: An uncommon finding. *Hemodial Int* 2021; **25**: E15-E17 [PMID: 33073510 DOI: 10.1111/hdi.12894]
7 **Nagasawa Y**, Shimizu T, Sonoda H, Mekata E, Wakabayashi M, Ohta H, Murata S, Mori T, Naka S, Tani T. A comparison of outcomes and complications of totally implantable access port through the internal jugular vein versus the subclavian vein. *Int Surg* 2014; **99**: 182-188 [PMID: 24670030 DOI: 10.9738/INTSURG-D-13-00185.1]
8 **Shankar G**, Jadhav V, Ravindra S, Babu N, Ramesh S. Totally Implantable Venous Access Devices in Children Requiring Long-Term Chemotherapy: Analysis of Outcome in 122 Children from a Single Institution. *Indian J Surg Oncol* 2016; **7**: 326-331 [PMID: 27651694 DOI: 10.1007/s13193-015-0485-x]

9 **Lv DN**, Xu HZ, Zheng LL, Chen LL, Ling Y, Ye AQ. Extravasation of chemotherapeutic drug from an implantable intravenous infusion port in a child: A case report. *World J Clin Cases* 2021; **9**: 7840-7844 [PMID: 34621835 DOI: 10.12998/wjcc.v9.i26.7840]

10 **Miao J**, Ji L, Lu J, Chen J. Randomized clinical trial comparing ultrasound-guided procedure with the Seldinger's technique for placement of implantable venous ports. *Cell Biochem Biophys* 2014; **70**: 559-563 [PMID: 24748179 DOI: 10.1007/s12013-014-9956-x]

World Journal of Clinical Cases

Submit a Manuscript: https://www.f6publishing.com

World J Clin Cases 2023 February 6; 11(4): 888-895

DOI: 10.12998/wjcc.v11.i4.888

ISSN 2307-8960 (online)

CASE REPORT

Thyroid storm in a pregnant woman with COVID-19 infection: A case report and review of literatures

Hyo-Eun Kim, Juseok Yang, Ji-Eun Park, Jong-Chul Baek, Hyen-Chul Jo

Specialty type: Obstetrics and gynecology

Provenance and peer review: Unsolicited article; Externally peer reviewed.

Peer-review model: Single blind

Peer-review report's scientific quality classification

Grade A (Excellent): 0
Grade B (Very good): B
Grade C (Good): C
Grade D (Fair): 0
Grade E (Poor): 0

P-Reviewer: Freund O, Israel; Magalhães JE, Brazil

Received: October 27, 2022
Peer-review started: October 27, 2022
First decision: November 11, 2022
Revised: November 24, 2022
Accepted: January 5, 2023
Article in press: January 5, 2023
Published online: February 6, 2023

Hyo-Eun Kim, Juseok Yang, Ji-Eun Park, Jong-Chul Baek, Hyen-Chul Jo, Department of Obstetrics and Gynecology, Gyeongsang National University Changwon Hospital, Changwon 51472, South Korea

Corresponding author: Hyen-Chul Jo, MD, PhD, Assistant Professor, Department of Obstetrics and Gynecology, Gyeongsang National University Changwon Hospital, Samjunga Street 11, Sungsan Gu, Changwon 51472, South Korea. cholida73@naver.com

Abstract

BACKGROUND

The severe acute respiratory syndrome coronavirus-2 (SARS-CoV-2) has been found to be responsible for the recent global pandemic known as coronavirus disease 2019 (COVID-19). SARS-CoV-2 infections not only result in significant respiratory symptoms but also cause several extrapulmonary manifestations, such as thrombotic complications, myocardial dysfunction and arrhythmia, thyroid dysfunction, acute kidney injury, gastrointestinal symptoms, neurological symptoms, ocular symptoms, and dermatological complications. We present the first documented case of thyroid storm in a pregnant woman precipitated by SARS-CoV-2.

CASE SUMMARY

A 42-year-old multiparous woman at 35 + 2 wk of gestation visited the emergency room (ER) with altered mentation, seizures, tachycardia, and high fever. The patient showed no remarkable events in the prenatal examination, and the nasopharyngeal COVID-19 polymerase chain reaction (PCR) test was positive two days before the ER visit. The results of laboratory tests, such as liver function test, serum electrolytes, blood glucose, blood urea nitrogen, and creatinine, were all within the normal ranges. However, the thyroid function test showed hyperthyroidism, and the nasopharyngeal COVID-19 PCR test was positive, as expected. No specific findings were observed on the brain computed tomography, and there were no signs of lateralization on neurological examination. Fetal heartbeat and movement were good, and there were no significant uterine contractions. The initial impression was atypical eclampsia. However, the patient's condition worsened, and a cesarean section was performed under general anesthesia; a healthy boy was delivered, and 12 h after delivery, the patient's seizures disappeared and consciousness was restored. The patient was referred to an endocrinologist for hyperthyroidism, and a thyroid storm with Graves' disease was diagnosed. Here, SARS-CoV-2 was believed to be the trigger

for the thyroid storm, considering that the patient tested positive for COVID-19 two days before the seizures.

CONCLUSION
In pregnant women presenting with seizures or changes in consciousness, the possibility of a thyroid storm should be considered. There are various causes for a thyroid storm, but given the recent pandemic, it is necessary to bear in mind that the thyroid storm may be precipitated by COVID-19.

Key Words: COVID-19; Hyperthyroidism; Pregnancy; Thyroid storm; Thyrotoxicosis; Case report

Core Tip: Coronavirus disease 2019 (COVID-19) is a pandemic disease. For pregnant women presenting with emergency symptoms, clinicians should consider the possibility of a thyroid storm caused by COVID-19.

Citation: Kim HE, Yang J, Park JE, Baek JC, Jo HC. Thyroid storm in a pregnant woman with COVID-19 infection: A case report and review of literatures. *World J Clin Cases* 2023; 11(4): 888-895
URL: https://www.wjgnet.com/2307-8960/full/v11/i4/888.htm
DOI: https://dx.doi.org/10.12998/wjcc.v11.i4.888

INTRODUCTION

The incidence of hyperthyroidism in pregnancy is about 0.2% and is mostly subclinical[1]. A thyroid storm (TS) is a rare but serious complication in patients with hyperthyroidism (1%-2% of cases of hyperthyroidism)[2-4]. The symptoms of a TS are similar to those of hyperthyroidism, but they are more sudden, severe, and extreme. We report a case in which a pregnant woman who visited the emergency room (ER) with altered mentation, seizures, and high fever was initially misdiagnosed as eclampsia and eventually diagnosed to have a TS because of coronavirus disease 2019 (COVID-19) infection.

CASE PRESENTATION

Chief complaints

A 42-year-old multiparous woman with a gestational age of 35 + 2 wk presented to the ER with altered mentation, seizures, and a high fever of 38.3 °C.

History of present illness

The patient tested positive for the nasopharyngeal COVID-19 polymerase chain reaction (PCR) test with symptoms of throat pain two days before her ER visit. Upon arrival at the ER, endotracheal intubation was performed immediately, and an emergency call was made to the obstetrics and gynecology department. According to the widely accepted severity scale of COVID-19 (Table 1), illness of severity was critical requiring mechanical ventilation[5].

History of past illness

The patient had previously delivered a healthy baby by cesarean section two years ago. According to the statements of the guardians obtained in the ER, the patient did not have any specific underlying diseases, and there were no remarkable events during the prenatal examinations in the current pregnancy.

Personal and family history

The patient had no history of drug abuse, smoking, or drinking. Further, there was no family history of genetic, autoimmune, or thyroid diseases.

Physical examination

The seizure was a generalized tonic-clonic type, and the patient presented with drooling and continuous upper eyeball deviation. The pupillary reflex was prompt, symmetric, and consensual. Vital signs

Table 1 Illness severity for coronavirus disease 2019

Severity	Signs and symptoms
Asymptomatic/presymptomatic	Positive for SARS-CoV-2 using a test but no symptoms that are consistent with COVID-19
Mild illness	Signs and symptoms of COVID-19 but no shortness of breath, dyspnea, or abnormal chest imaging
Moderate illness	Signs and symptoms of lower respiratory disease or abnormal imaging and $SpO_2 \geq 94\%$ on room air at sea level
Severe illness	$SpO_2 \leq 94\%$ on room air at sea level, $PaO_2/FiO_2 < 300$ mmHg, respiratory frequency > 30 breaths/min, or lung infiltrates > 50%
Critical illness	Respiratory failure, septic shock, and/or multiple organ dysfunction

From the American college of emergency physicians field guide. COVID-19: Coronavirus disease 2019; SARS-CoV-2: Severe acute respiratory syndrome coronavirus-2.

revealed a blood pressure of 121/71 mmHg and heart rate of 115 beats per minute.

Laboratory examinations

The nasopharyngeal COVID-19 test performed in the ER was positive. Laboratory results at the emergency unit showed increased C-reactive protein of 15.7 mg/L [reference range (RR): 0-5 mg/L], erythrocyte sedimentation rate of 37 mm/h (RR: 0-20 mm/h), and D-dimer of 2.7 μg/mL (RR: 0.0-0.5 μg/mL). There was no proteinuria or other abnormality in the urine protein-to-creatinine ratio, which could be considered a sign of eclampsia. The results of the laboratory tests, such as liver function test, serum electrolytes, blood glucose, blood urea nitrogen, and creatinine, were all normal. The thyroid function test showed a thyroid stimulating hormone (TSH) level of < 0.01 mIU/L [3rd trimester-specific reference range (3TRR): 0.38-4.04 mIU/L[6]], free T4 level of 1.95 ng/dL (3TRR: 0.5-0.8 ng/dL[6]), and total T3 level of 183.9 ng/dL (3TRR: 123-162 ng/dL[6]), which reflect overt hyperthyroidism. According to the Burch-Wartofsky Point Scale (BWPS)[2], the score was 65, which was highly suggestive of a TS.

Imaging examinations

Brain computed tomography revealed no acute intracranial hemorrhage, focal parenchymal lesions, or visible causes of seizure. In addition, there were no focal neurological signs, and the neurologist underestimated the likelihood of seizures owing to the central nervous system lesions.

Further diagnostic work-up

No noteworthy findings were obtained from the chest X-ray and electrocardiogram. On ultrasonography, the fetal growth was noted to be appropriate for the gestational age, and the fetal heartbeat and movements were normal. No significant uterine contractions were observed in the tocomonitor.

Initial diagnosis

The initial impression was eclampsia because of the seizures and altered consciousness. However, there were several points that were not suitable for a diagnosis of eclampsia. For example, the maternal blood pressure was normal, and there was no proteinuria, fetal growth restriction, thrombocytopenia, kidney failure, or hepatic dysfunction. Thus, we arrived at a diagnosis of atypical eclampsia.

FINAL DIAGNOSIS

The final diagnosis was status epilepticus (SE) due to a TS from a preexisting Graves' disease. Given that the patient tested positive for COVID-19 two days before admission to the ER, the trigger for the TS is believed to be SARS-CoV-2.

TREATMENT

For the primary treatment of eclampsia, labetalol, magnesium sulfate, and midazolam were used to control the seizures. However, the seizures persisted, and consciousness was not restored. Thus, a cesarean section was performed under general anesthesia because it was judged that both the mother and fetus could be at risk if the seizures continued.

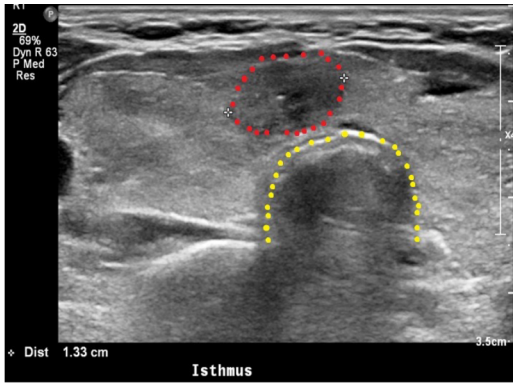

DOI: 10.12998/wjcc.v11.i4.888

Figure 1 Thyroid ultrasonography. Diffusely enlarged thyroid gland with rounded lobes showing the diffusely heterogeneous and coarse echotexture of the thyroid gland. The isthmus nodule was suspected to be malignant owing to its ill-defined margin. The red dots indicate the isthmus nodule; this nodule was identified as a papillary carcinoma by fine-needle aspiration cytology. The yellow dots indicate the trachea.

OUTCOME AND FOLLOW-UP

The seizures continued until general anesthesia was administered, and the cesarean section was performed without any special events. The newborn infant weighed 2680 g, with 1 min and 5 min Apgar scores of 8 and 8, respectively. After delivery by cesarean section, the intensity of the seizures decreased but persisted. Therefore, low-level sedation was maintained with midazolam for about 12 h in the intensive care unit. Over time, the intensity of the seizures decreased, and consciousness was restored. The newborn's nasopharyngeal COVID-19 PCR test was negative and thyroid function tests were within the normal ranges. Magnetic resonance imaging and electroencephalogram were performed on the infant in consultation with the neurologist, and no specific findings were observed.

The patient was then referred to an endocrinologist for evaluation and treatment of hyperthyroidism. In the serological test, TSH (< 0.01 mIU/L) was suppressed, but the free T4 (1.86 ng/dL), total T3 (175.3 ng/dL), and TSH receptor antibody (2.44 IU/L; RR: 0.0-1.750 IU/L[6]) were all elevated with respect to the reference values. Thyroid ultrasonography showed a diffusely enlarged thyroid gland with round-shaped lobes as well as diffusely heterogeneous and coarse echotexture (Figure 1). The isthmus nodule was suspected to be malignant, and fine-needle aspiration was performed (Figure 1). The cytology result showed a papillary carcinoma, and a thyroidectomy was scheduled. The endocrinologist thus concluded that a TS may have been a complication of preexisting Graves' disease and prescribed methimazole, methylprednisolone, and propranolol. The patient was discharged in a healthy condition ten days after the cesarean section. After approximately one month of using methimazole, the thyroid function test results were close to normal values.

DISCUSSION

Hyperthyroidism can develop in about 0.2% of pregnant women, and Graves' disease is responsible for almost 95% of the cases of hyperthyroidism during pregnancy. A TS is a rare condition that affects about 1% of pregnant women with hyperthyroidism. A TS is a severe exacerbation of thyrotoxicosis, which is an emergency disease that causes tachycardia, hyperthermia, agitation, and altered mental status[2]. It is known that TS has a variety of causes. For example, a TS may occur with an acute disease, such as acute myocardial infarction, stroke, congestive heart failure, or trauma[7]. It is also known that infection or pregnancy itself can trigger a TS[2]. There are several case reports of TS caused by SARS-CoV-2 infection[2,3,8,9]. However, this is the first report of a TS in a pregnant woman with a SARS-CoV-2 infection.

Etiology

How does SARS-CoV-2 trigger a TS? Recent studies have answered this question in two ways. First, angiotensin-converting enzyme 2 receptor and transmembrane protease serine 2, which are known to play important roles in SARS-CoV-2 invasion of the human host cells, are more highly expressed in thyroid cells than in the lungs, oral cavity, pharynx, and larynx, which may cause a TS[10-12]. Second, Lania *et al*[8] suggested that SARS-CoV-2 could affect the thyroid cells indirectly through a cytokine storm. This cytokine storm is characterized by hyperactivity of the Th1/Th17 immune response, with increased production of several proinflammatory cytokines, including interleukin-6 and tumor necrosis factor α[13,14]. Several proinflammatory cytokines can cause excessive and uncontrolled immune responses, eventually leading to a TS.

Pregnancy itself can cause hyperthyroidism, which can eventually lead to a TS. As the circulating estrogen increases during pregnancy, the thyroxine-binding globulin (TBG) increases. TBG binds to the circulating T4, reducing the free T4 levels. To compensate for this, the size of the thyroid gland increases, and the production of T4 and T3 increases by 50%[15-17]. Owing to the homogeneity of human chorionic gonadotropin (hCG) and TSH, elevated hCG levels can stimulate the thyroid gland, resulting in further elevation of free T4[17,18]. Millar *et al*[19] reported that patients with hyperthyroidism during pregnancy were 10 times more likely to develop a TS than during non-pregnancy.

Symptoms

A TS typically manifests clinically as a combination of the following signs and symptoms: Fever, tachycardia, cardiac dysrhythmia, and central nervous system dysfunction[20]. Our patient had a generalized tonic-clonic type of seizure, SE. Specifically, recurrent seizures occurred despite the use of appropriate doses of midazolam, and these were classified as refractory SE (RSE)[21]. According to reports, about 9%-43% of SE cases show a clinical course of RSE[21,22], and the in-hospital mortality of RSE has been reported to be about 15%-33%[23-25]. In the present case, the RSE was classified as new-onset RSE (NORSE) because there were no previous neurological diseases and no preexisting toxic and metabolic causes[26]. In the case of our patient, the fever may have been caused by not only COVID-19 but also by the TS induced by COVID-19. Thus, if SE is caused by the fever of COVID-19, it can also be classified as febrile infection-related epilepsy syndrome, which is a subset of NORSE[26].

SARS-CoV-2 can also cause a wide variety of extrapulmonary symptoms owing to its inflammatory effects. For example, cardiac (myocarditis, pericardial effusion, shock), renal (glomerulonephritis), hematological (thrombocytopenic purpura, anemia), neurological (Guillain–Barré syndrome, meningoencephalitis, optic neuritis), and musculoskeletal (myositis, arthritis) complications have been reported [10,27-31].

Diagnosis

There are studies recommending routine thyroid function tests in patients with SARS-CoV-2 infection[3,8,32]. In our opinion, if the abovementioned symptoms, namely fever, tachycardia, cardiac dysrhythmia, and central nervous system dysfunction, are observed in pregnant women, it is necessary to conduct routine thyroid function tests.

Additionally, the BWPS is the most widely used criterion for diagnosing a TS. The BWPS is a score that helps to assess the probability of a TS independent of the level of thyroid hormones; it is based solely on clinical and physical criteria[2,4]. The BWPS considers body temperature, central nervous effects, hepatogastrointestinal symptoms, and cardiovascular dysfunction, along with the patient's prior history[33].

There are several neurological diseases that must be differentiated from the perspective of accompanying SE with the help of neurologists. In consideration of the patient's condition, neurological examinations and brain imaging studies should be performed to differentiate intracranial diseases. Among these, the differential diagnoses for cerebral venous sinus thrombosis, meningoencephalitis, and posterior reversible encephalopathy syndrome should be included.

Because the pregnant woman had seizures, eclampsia was suspected initially. Therefore, it is necessary to identify the symptoms and signs of eclampsia accurately. For example, it is important to identify pretibial pitting edema, visual disturbances, and epigastric pain. In our case, the patient showed no such signs. In addition, the patient was normotensive, and there was no proteinuria, fetal growth restriction, thrombocytopenia, kidney failure, hepatic dysfunction, or liver failure. In conclusion, the possibility of eclampsia was judged to be low.

Paraneoplastic neurologic syndrome (PNS) also needs to be differentially diagnosed as an additional disease. PNS is an autoimmune disease and may present with several clinical manifestations, such as encephalitis, autonomic dysfunction, peripheral neuropathy, cerebellar ataxia, and visual disturbances [34]. Clinicians should be hence alert to the possibility of PNS if the patient has a past or family history of cancer or an autoimmune disease[34].

Treatment

An appropriate treatment plan should be developed by evaluating the symptoms of thyrotoxicosis, gestational age, and fetal condition. Treatment of mild thyrotoxicosis in COVID-19 patients without an underlying thyroid disease does not necessitate thionamides, and most of these patients will recover spontaneously[6]. However, patients with a TS should receive prompt treatment with fluids, antithyroid drugs (ATD), steroids, and beta blockers in conjunction with consultation with an endocrinologist.

ATD is the most crucial treatment for TS; it inhibits the synthesis of thyroid hormone by blocking the organification of iodine within the thyroid gland and eventually reducing the amount of thyroid hormone released into circulation. Pregnant women with hyperthyroidism should also be treated with ATD. Either propylthiouracil or methimazole, which are both thionamides, can be used to treat pregnant women with hyperthyroidism. However, methimazole is typically avoided in the first trimester because it has been associated with rare embryopathy, such as esophageal or choanal atresia and aplasia cutis, a congenital skin defect[1]. After the first trimester, either methimazole or propylthiouracil can be used to treat hyperthyroidism. In rare cases, propylthiouracil has been reported to

result in clinically significant hepatotoxicity[16]. Therefore, patients should be given information about the risks and benefits of ATD. Fortunately, several published articles suggest that antithyroid treatment carries minimal risk to the fetus during early pregnancy. This risk is lower than is commonly perceived and less than that of untreated thyrotoxicosis[17,18].

However, in our case, it was practically challenging to wait for the effects of ATD to manifest in a state where the change of consciousness was accompanied by continued seizures and the fetal well-being could not be guaranteed. In such cases, if the gestational age is close to term, a cesarean section to terminate the pregnancy may be a good solution. Beta blockers can be used as adjunctive therapy for symptomatic palpitations. Corticosteroids inhibit the peripheral conversion of T4 to T3 and have been shown to improve outcomes in patients with TS[1].

CONCLUSION

Clinicians should always bear in mind that SARS-CoV-2 infections can cause a TS and must routinely perform thyroid function tests in the infected patients. When a TS occurs in a pregnant woman infected with SARS-CoV-2, a treatment plan should be established in consideration of the symptoms of thyrotoxicosis, gestational age, and fetal condition. In the case of a TS occurring at an early gestational age, ATD can be used, and the progression can be monitored. However, if the woman is near the term of gestational age and has multi-organ failure or neurological symptoms, termination of pregnancy by cesarean section may be a good choice.

A TS in a pregnant woman is a very serious and life-threatening emergency. Thus, an urgent multidisciplinary approach involving collaboration among the emergency physician, endocrinologist, obstetrician, neurologist, neonatologist, and anesthesiologist is essential for successful management of the patient.

ACKNOWLEDGEMENTS

We gratefully acknowledge the kind cooperation of the patient, the family members, and the staff for their assistance in conducting this study.

FOOTNOTES

Author contributions: Jo HC suggested the initial idea and designed this study; Yang J, Park JE, and Baek JC collected the relevant data; Kim HE analyzed the data and prepared the manuscript.

Informed consent statement: Informed written consent was obtained from the patient for publication of this report and any accompanying images.

Conflict-of-interest statement: The authors declare that they have no conflict of interest to disclose.

CARE Checklist (2016) statement: The authors have read the CARE Checklist (2016), and the manuscript was prepared and revised accordingly.

Country/Territory of origin: South Korea

ORCID number: Hyo-Eun Kim 0000-0002-7985-509X; Hyen-Chul Jo 0000-0001-9943-2863.

S-Editor: Zhang H
L-Editor: A
P-Editor: Zhang H

REFERENCES

1 Thyroid Disease in Pregnancy: ACOG Practice Bulletin, Number 223. *Obstet Gynecol* 2020; **135**: e261-e274 [PMID:

32443080 DOI: 10.1097/AOG.0000000000003893]
2 **Rao AN**, Al-Ward RY, Gaba R. Thyroid Storm in a Patient With COVID-19. *AACE Clin Case Rep* 2021; **7**: 360-362 [PMID: 34250225 DOI: 10.1016/j.aace.2021.06.011]
3 **Sullivan K**, Helgeson J, McGowan A. COVID-19 Associated Thyroid Storm: A Case Report. *Clin Pract Cases Emerg Med* 2021; **5**: 412-414 [PMID: 34813431 DOI: 10.5811/cpcem.2021.5.52692]
4 **Swee du S**, Chng CL, Lim A. Clinical characteristics and outcome of thyroid storm: a case series and review of neuropsychiatric derangements in thyrotoxicosis. *Endocr Pract* 2015; **21**: 182-189 [PMID: 25370315 DOI: 10.4158/EP14023.OR]
5 **ACEP**. American College of Emergency Physicians COVID-19 Field Guide. [cited 24 November 2022]. Available from: https://www.acep.org/corona/covid-19-field-guide/diagnosis/diagnosis-when-there-is-no-testing/
6 **Cunningham F**, Leveno K, Bloom S, Dashe J, Hoffman B, Casey B, Spong C. Williams Obstetrics. 25th ed. New York: McGraw Hill Education, 2018: 1258
7 **Nai Q**, Ansari M, Pak S, Tian Y, Amzad-Hossain M, Zhang Y, Lou Y, Sen S, Islam M. Cardiorespiratory Failure in Thyroid Storm: Case Report and Literature Review. *J Clin Med Res* 2018; **10**: 351-357 [PMID: 29511425 DOI: 10.14740/jocmr3106w]
8 **Lania A**, Sandri MT, Cellini M, Mirani M, Lavezzi E, Mazziotti G. Thyrotoxicosis in patients with COVID-19: the THYRCOV study. *Eur J Endocrinol* 2020; **183**: 381-387 [PMID: 32698147 DOI: 10.1530/EJE-20-0335]
9 **Pastor S**, Molina Á Sr, De Celis E. Thyrotoxic Crisis and COVID-19 Infection: An Extraordinary Case and Literature Review. *Cureus* 2020; **12**: e11305 [PMID: 33282582 DOI: 10.7759/cureus.11305]
10 **Pranasakti ME**, Talirasa N, Rasena HA, Purwanto RY, Anwar SL. Thyrotoxicosis occurrence in SARS-CoV-2 infection: A case report. *Ann Med Surg (Lond)* 2022; **78**: 103700 [PMID: 35505686 DOI: 10.1016/j.amsu.2022.103700]
11 **Hoffmann M**, Kleine-Weber H, Schroeder S, Krüger N, Herrler T, Erichsen S, Schiergens TS, Herrler G, Wu NH, Nitsche A, Müller MA, Drosten C, Pöhlmann S. SARS-CoV-2 Cell Entry Depends on ACE2 and TMPRSS2 and Is Blocked by a Clinically Proven Protease Inhibitor. *Cell* 2020; **181**: 271-280.e8 [PMID: 32142651 DOI: 10.1016/j.cell.2020.02.052]
12 **Lazartigues E**, Qadir MMF, Mauvais-Jarvis F. Endocrine Significance of SARS-CoV-2's Reliance on ACE2. *Endocrinology* 2020; **161** [PMID: 32652001 DOI: 10.1210/endocr/bqaa108]
13 **Wu D**, Yang XO. TH17 responses in cytokine storm of COVID-19: An emerging target of JAK2 inhibitor Fedratinib. *J Microbiol Immunol Infect* 2020; **53**: 368-370 [PMID: 32205092 DOI: 10.1016/j.jmii.2020.03.005]
14 **Prompetchara E**, Ketloy C, Palaga T. Immune responses in COVID-19 and potential vaccines: Lessons learned from SARS and MERS epidemic. *Asian Pac J Allergy Immunol* 2020; **38**: 1-9 [PMID: 32105090 DOI: 10.12932/AP-200220-0772]
15 **Moleti M**, Di Mauro M, Sturniolo G, Russo M, Vermiglio F. Hyperthyroidism in the pregnant woman: Maternal and fetal aspects. *J Clin Transl Endocrinol* 2019; **16**: 100190 [PMID: 31049292 DOI: 10.1016/j.jcte.2019.100190]
16 **Sarkar S**, Bischoff LA. Management of Hyperthyroidism during the Preconception Phase, Pregnancy, and the Postpartum Period. *Semin Reprod Med* 2016; **34**: 317-322 [PMID: 27741549 DOI: 10.1055/s-0036-1593489]
17 **Cooper DS**, Laurberg P. Hyperthyroidism in pregnancy. *Lancet Diabetes Endocrinol* 2013; **1**: 238-249 [PMID: 24622372 DOI: 10.1016/S2213-8587(13)70086-X]
18 **Stagnaro-Green A**, Dong A, Stephenson MD. Universal screening for thyroid disease during pregnancy should be performed. *Best Pract Res Clin Endocrinol Metab* 2020; **34**: 101320 [PMID: 31530447 DOI: 10.1016/j.beem.2019.101320]
19 **Millar LK**, Wing DA, Leung AS, Koonings PP, Montoro MN, Mestman JH. Low birth weight and preeclampsia in pregnancies complicated by hyperthyroidism. *Obstet Gynecol* 1994; **84**: 946-949 [PMID: 7970474]
20 **Ross DS**, Burch HB, Cooper DS, Greenlee MC, Laurberg P, Maia AL, Rivkees SA, Samuels M, Sosa JA, Stan MN, Walter MA. 2016 American Thyroid Association Guidelines for Diagnosis and Management of Hyperthyroidism and Other Causes of Thyrotoxicosis. *Thyroid* 2016; **26**: 1343-1421 [PMID: 27521067 DOI: 10.1089/thy.2016.0229]
21 **Rossetti AO**, Lowenstein DH. Management of refractory status epilepticus in adults: still more questions than answers. *Lancet Neurol* 2011; **10**: 922-930 [PMID: 21939901 DOI: 10.1016/S1474-4422(11)70187-9]
22 **Mayer SA**, Claassen J, Lokin J, Mendelsohn F, Dennis LJ, Fitzsimmons BF. Refractory status epilepticus: frequency, risk factors, and impact on outcome. *Arch Neurol* 2002; **59**: 205-210 [PMID: 11843690 DOI: 10.1001/archneur.59.2.205]
23 **Strzelczyk A**, Ansorge S, Hapfelmeier J, Bonthapally V, Erder MH, Rosenow F. Costs, length of stay, and mortality of super-refractory status epilepticus: A population-based study from Germany. *Epilepsia* 2017; **58**: 1533-1541 [PMID: 28681418 DOI: 10.1111/epi.13837]
24 **Delaj L**, Novy J, Ryvlin P, Marchi NA, Rossetti AO. Refractory and super-refractory status epilepticus in adults: a 9-year cohort study. *Acta Neurol Scand* 2017; **135**: 92-99 [PMID: 27080243 DOI: 10.1111/ane.12605]
25 **Ferlisi M**, Shorvon S. The outcome of therapies in refractory and super-refractory convulsive status epilepticus and recommendations for therapy. *Brain* 2012; **135**: 2314-2328 [PMID: 22577217 DOI: 10.1093/brain/aws091]
26 **Hirsch LJ**, Gaspard N, van Baalen A, Nabbout R, Demeret S, Loddenkemper T, Navarro V, Specchio N, Lagae L, Rossetti AO, Hocker S, Gofton TE, Abend NS, Gilmore EJ, Hahn C, Khosravani H, Rosenow F, Trinka E. Proposed consensus definitions for new-onset refractory status epilepticus (NORSE), febrile infection-related epilepsy syndrome (FIRES), and related conditions. *Epilepsia* 2018; **59**: 739-744 [PMID: 29399791 DOI: 10.1111/epi.14016]
27 **Ramos-Casals M**, Brito-Zerón P, Mariette X. Systemic and organ-specific immune-related manifestations of COVID-19. *Nat Rev Rheumatol* 2021; **17**: 315-332 [PMID: 33903743 DOI: 10.1038/s41584-021-00608-z]
28 **Gupta A**, Madhavan MV, Sehgal K, Nair N, Mahajan S, Sehrawat TS, Bikdeli B, Ahluwalia N, Ausiello JC, Wan EY, Freedberg DE, Kirtane AJ, Parikh SA, Maurer MS, Nordvig AS, Accili D, Bathon JM, Mohan S, Bauer KA, Leon MB, Krumholz HM, Uriel N, Mehra MR, Elkind MSV, Stone GW, Schwartz A, Ho DD, Bilezikian JP, Landry DW. Extrapulmonary manifestations of COVID-19. *Nat Med* 2020; **26**: 1017-1032 [PMID: 32651579 DOI: 10.1038/s41591-020-0968-3]
29 **Maev IV**, Shpektor AV, Vasilyeva EY, Manchurov VN, Andreev DN. [Novel coronavirus infection COVID-19: extrapulmonary manifestations]. *Ter Arkh* 2020; **92**: 4-11 [PMID: 33346454 DOI: 10.26442/00403660.2020.08.000767]

30 **Laya BF**, Cledera THC, Lim TRU, Baluyut JMP, Medina JMP, Pasia NV. Cross-sectional Imaging Manifestations of Extrapulmonary Involvement in COVID-19 Disease. *J Comput Assist Tomogr* 2021; **45**: 253-262 [PMID: 33186179 DOI: 10.1097/RCT.0000000000001120]

31 **Freund O**, Eviatar T, Bornstein G. Concurrent myopathy and inflammatory cardiac disease in COVID-19 patients: a case series and literature review. *Rheumatol Int* 2022; **42**: 905-912 [PMID: 35275269 DOI: 10.1007/s00296-022-05106-3]

32 **Muller I**, Cannavaro D, Dazzi D, Covelli D, Mantovani G, Muscatello A, Ferrante E, Orsi E, Resi V, Longari V, Cuzzocrea M, Bandera A, Lazzaroni E, Dolci A, Ceriotti F, Re TE, Gori A, Arosio M, Salvi M. SARS-CoV-2-related atypical thyroiditis. *Lancet Diabetes Endocrinol* 2020; **8**: 739-741 [PMID: 32738929 DOI: 10.1016/S2213-8587(20)30266-7]

33 **Burch HB**, Wartofsky L. Life-threatening thyrotoxicosis. Thyroid storm. *Endocrinol Metab Clin North Am* 1993; **22**: 263-277 [PMID: 8325286]

34 **Kannoth S**. Paraneoplastic neurologic syndrome: A practical approach. *Ann Indian Acad Neurol* 2012; **15**: 6-12 [PMID: 22412264 DOI: 10.4103/0972-2327.93267]

World Journal of Clinical Cases

Submit a Manuscript: https://www.f6publishing.com

World J Clin Cases 2023 February 6; 11(4): 896-902

DOI: 10.12998/wjcc.v11.i4.896

ISSN 2307-8960 (online)

CASE REPORT

Computed tomography diagnosed left ovarian venous thrombophlebitis after vaginal delivery: A case report

Jin-Jin Wang, Chu-Chu Hui, Yi-Ding Ji, Wei Xu

Specialty type: Radiology, nuclear medicine and medical imaging

Provenance and peer review: Unsolicited article; Externally peer reviewed.

Peer-review model: Single blind

Peer-review report's scientific quality classification

Grade A (Excellent): 0
Grade B (Very good): B
Grade C (Good): C
Grade D (Fair): 0
Grade E (Poor): 0

P-Reviewer: Hatipoglu S, Turkey; Naem AA, Germany

Received: September 6, 2022
Peer-review started: September 6, 2022
First decision: December 13, 2022
Revised: December 21, 2022
Accepted: January 12, 2023
Article in press: January 12, 2023
Published online: February 6, 2023

Jin-Jin Wang, Yi-Ding Ji, Department of Radiology, The Ninth People's Hospital of Suzhou City, Suzhou 215200, Jiangsu Province, China

Chu-Chu Hui, Department of Ultrasound, The Ninth People's Hospital of Suzhou City, Suzhou 215200, Jiangsu Province, China

Wei Xu, Department of Emergency Medicine, The Ninth People's Hospital of Suzhou City, Suzhou 215200, Jiangsu Province, China

Corresponding author: Wei Xu, MD, Academic Editor, Department of Emergency Medicine, The Ninth People's Hospital of Suzhou City, No. 2666 Ludang Road, Suzhou 215200, Jiangsu Province, China. szjyxw82@126.com

Abstract

BACKGROUND

Postpartum ovarian vein thrombophlebitis (POVT) is a rare but serious postpartum complication that affects mostly postpartum women. A high index of suspicion is required when faced with sudden postpartum abdominal pain.

CASE SUMMARY

A 25-year-old healthy woman who accepted a vaginal delivery procedure suffered fever (temperature 39.6℃) one day after delivery, accompanied with left lower abdominal pain. Physical examination indicated mild tenderness in the left lower abdomen, accompanied with rebound pain. The patient was confirmed to have left ovarian venous thrombosis with inflammation after receiving a multi-detector row computed tomography scan.

CONCLUSION

POVT is a rare and dangerous postpartum complication. A high index of suspicion is required for the occurrence of ovarian venous thrombosis when faced with postpartum abdominal pain and fever. Early application of Doppler ultrasound, computed tomography, magnetic resonance imaging and other auxiliary examinations is conducive to timely and accurate diagnosis of POVT, thus reducing maternal mortality.

Key Words: Ovarian venous thrombosis; Postpartum; Multi-detector row computed tomography; Case report

Core Tip: Postpartum ovarian vein thrombophlebitis (POVT) is a rare but serious postpartum complication that affects mostly postpartum women. POVT is more likely to occur in patients after cesarean section and in the right ovarian vein. However, in our case, POVT occurred in the left ovarian vein, which is rare.

Citation: Wang JJ, Hui CC, Ji YD, Xu W. Computed tomography diagnosed left ovarian venous thrombophlebitis after vaginal delivery: A case report. *World J Clin Cases* 2023; 11(4): 896-902
URL: https://www.wjgnet.com/2307-8960/full/v11/i4/896.htm
DOI: https://dx.doi.org/10.12998/wjcc.v11.i4.896

INTRODUCTION

Postpartum ovarian vein thrombophlebitis (POVT) is a rare clinical disease with an incidence of only about 0.05%-0.18%, which is related to pregnancy, pelvic inflammation, malignant tumors, and pelvic surgeries[1]. The clinical manifestations of POVT are non-specific and usually include lower abdominal pain, fever, and elevated leukocyte count, which is difficult to distinguish from acute appendicitis, pelvic infectious lesions, tubal and ovary abscess, ovarian torsion, abdominal abscess, postpartum endometritis, and urinary tract infection[2]. In postpartum patients, any abnormal abdominal pain should be highly suspected with POVT when usual causes of abdominal pain are excluded. The combination of anticoagulation and intravenous antibiotics is the preferred treatment for POVT. In June 2019, a 25-year-old woman with natural delivery was admitted to our hospital as she developed fever and left lower abdominal pain one day after delivery. She was diagnosed to have left ovarian venous thrombosis after accepting a multi-detector computed tomography (MDCT) scan. Here, we report this rare case and performed a review of the relevant literature.

CASE PRESENTATION

Chief complaints

A 25-year-old woman presented to our emergency department with left lower abdominal pain accompanied by nausea, high fever (39.6°C), and chills for one day. She was postpartum for only 24 h and gave birth to a viable full-term male infant (G1P0) *via* a successful vaginal delivery. During the vaginal delivery, the patient vomited a small amount of dark fluid.

History of present illness

A 25-year-old woman presented to our emergency department with left lower abdominal pain accompanied by nausea, high fever (39.6°C), and chills for one day.

History of past illness

The patient has no history of smoking or previous thrombotic accidents. She also denied having any cardiovascular or haematological disease.

Personal and family history

The patient had no smoking history or any special family history.

Physical examination

The physical examination revealed an obvious tenderness in the left middle and lower abdomen, accompanied by rebound pain, while with no swelling in both lower limbs and no massive vaginal bleeding.

Laboratory examinations

Laboratory examinations showed an elevated white blood cell (WBC) count at 14.25 × 10^9/L with significantly increased C-reactive protein (CRP; 98.01 mg/L). The WBC count increased to 24.75 × 10^9/L and CRP rose to 166 mg/L 12 h later.

Imaging examinations

We arranged an emergency MDCT scan for the patient, which showed a tubular high density shadow

on the left side of the abdomen from the left ovary zone to the left renal hulum. Ureteral stone or swelling of the change on the left side of the intestinal wall was not presented in the CT scan (Figure 1A and B). An enhanced CT scan (ioversol 80 mL, injection at 3.5 mL/s *via* the left elbow vein) was performed immediately and showed an enlarged left ovary with a low density shadow in the left ovarian vein extending to the left renal vein. Fortunately, the left renal vein was not invaded (Figure 1C and D).

FINAL DIAGNOSIS

The patient was confirmed to have left ovarian venous embolism.

TREATMENT

The patient underwent anticoagulation (low molecular weight heparin 4100 IU HD qd) and anti-infection (cefoperazone sodium and sulbactam sodium 3.0 g ivd q8h) therapy for 10 d, followed by oral anticoagulant therapy with rivaroxaban (20 mg qd for 6 mo). After 14 d of hospitalization, the patient recovered and was discharged without any uncomfortable feeling.

OUTCOME AND FOLLOW-UP

The patient underwent a B-ultrasound scan one month postpartum with no abnormalities in bilateral ovaries and uterus (Figure 2). In the outpatient follow-up at 3 mo postpartum, the patient had no recurrent abdominal pain and fever, and no abnormal oral mucosa, nosebleed, vaginal bleeding, chest tightness, hemoptysis, or other manifestations during the administration of anticoagulants. A plain CT scan of the whole abdomen was reexamined 6 mo postpartum, which showed that the left renal vein developed well without thickening or exudation (Figure 3).

DISCUSSION

POVT is very rare and was first reported by Al-toma *et al*[3] in 1956. Less than 200 cases have been reported globally so far, and 90% occurred within 10 d after delivery. This case also developed within 24 h after vaginal delivery. Research by Jenayah *et al*[4] found that the incidence of POVT in cesarean section women is higher than that in women with a natural vaginal delivery, while the incidence in twin pregnancy is higher than that in singleton pregnancy. In addition, studies have shown that POVT is closely related to maternal hypercoagulability and venous congestion. The risk of venous thrombosis during pregnancy and puerperium is 5 times that in non-pregnant women of the same age. However, the real cause of the disease is still unknown[5,6]. Several scholars believe that POVT is also related to the increase in venous pressure during pregnancy. The increase in blood volume and endocrine changes during pregnancy lead to increased pressure on the blood vessel wall and venous valve, which in turn leads to insufficiency of venous valve function and pelvic venous stasis, finally promoting the formation of thrombus[7]. Relevant studies have shown that POVT occurred in the right ovarian vein in about 90% of cases, which may result from the compression and expansion of the right ovarian vein and fallopian tube due to dextrorotation of the uterus during pregnancy. Meanwhile, the right ovarian vein flows downstream, which is more likely to be infected than the left ovarian vein with venous reflux[8]. Furthermore, the small angle between the right ovarian vein and the inferior vena cava makes it more easily affected by changes in blood pressure[9]. In this case, the left ovarian vein thrombosis occurred, which is also rare in POVT cases.

The clinical symptoms of POVT are not specific, generally manifesting as localized abdominal pain and nausea or vomiting in the right lower abdomen, with or without fever. There are no obvious specific changes in laboratory tests[1,3,5]. Our patient was characterized by high fever, chills, and tenderness in the left lower abdomen. Combined with the results of abdominal CT scan, ovarian vein thrombophlebitis can be diagnosed. Relevant data show that POVT can spread and involve the inferior vena cava, and in severe cases, it can lead to life-threatening pulmonary embolism. However, the incidence of this disease is extremely low, with no specific clinical manifestations and sensitive laboratory tests, and clinicians often lack the knowledge of the disease. Therefore, in daily clinical work, it is necessary to suspect this disease for women who have recurrent high fever and abdominal pain after delivery.

Nowadays, non-invasive examinations such as Doppler ultrasound, magnetic resonance imaging (MRI), or enhanced MDCT are the main methods for diagnosing POVT, with a sensitivity of 52%, 92%,

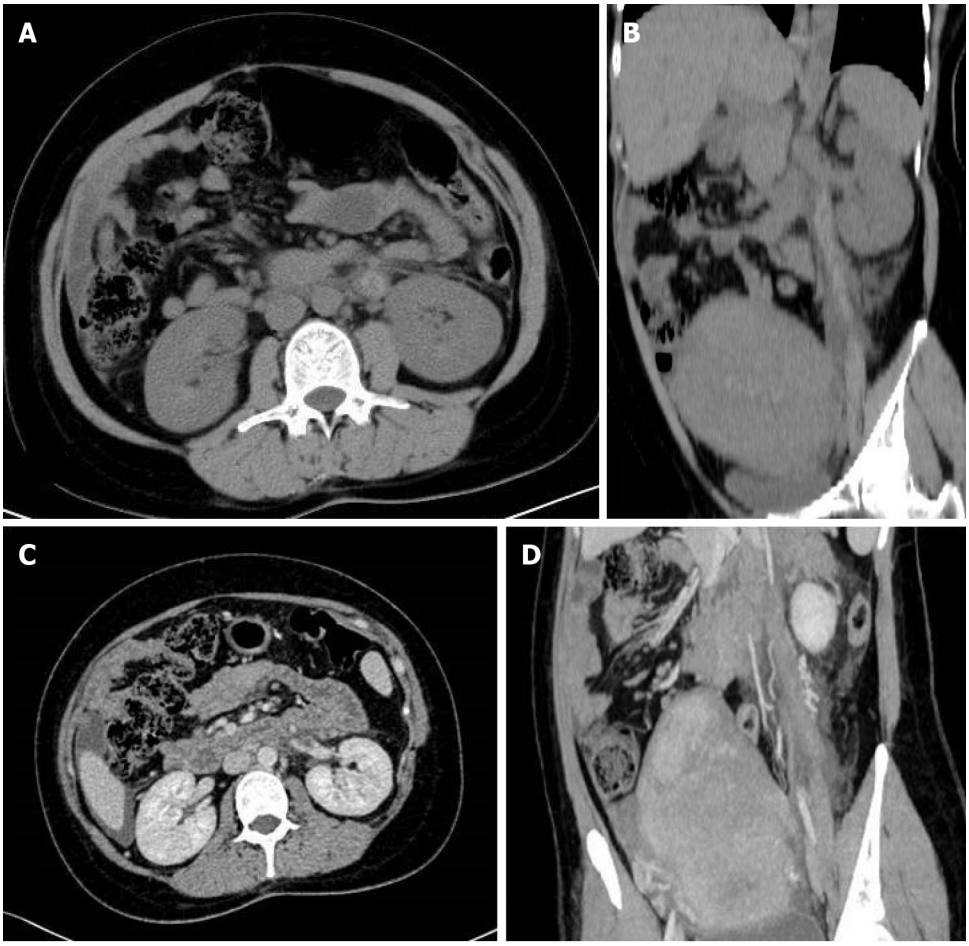

DOI: 10.12998/wjcc.v11.i4.896 **Copyright** ©The Author(s) 2023.

Figure 1 Computed tomography images. A and B: Plain computed tomography images; C and D: Enhanced computed tomography images.

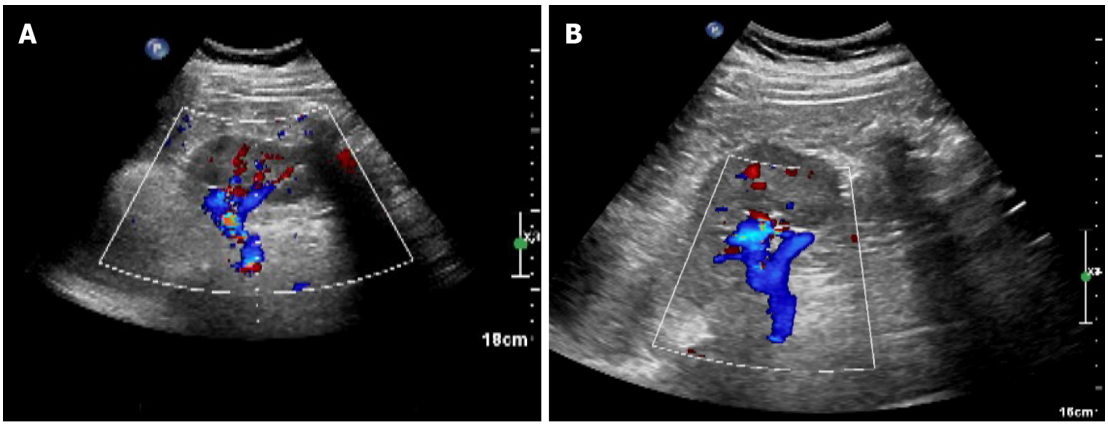

DOI: 10.12998/wjcc.v11.i4.896 **Copyright** ©The Author(s) 2023.

Figure 2 B-ultrasound performed at one month postpartum showed no abnormalities in bilateral ovaries and uterus. A: Sagittal view 1; B: Sagittal view 2.

and 100%, respectively[5,6,10-13]. Ultrasound is considered to be the preferred method of obstetric examination due to its flexible and real-time characteristics; however, its accuracy often depends on the operator's experience and operating skills[13,14]. With the development of ultrasound technology and the improvement of the diagnostic level of sonographers, reports of ultrasound diagnosis of POVT have appeared one after another. POVT appears on ultrasound as an abnormal echo between the ovarian venous plexus and the inferior vena cava[15]. However, abdominal ultrasound is easily affected by intestinal gas, and is difficult to distinguish it from enlarged appendix or hydroureter, making it limited in the diagnosis of POVT[16]. On the other hand, color Doppler ultrasound is still considered as one of

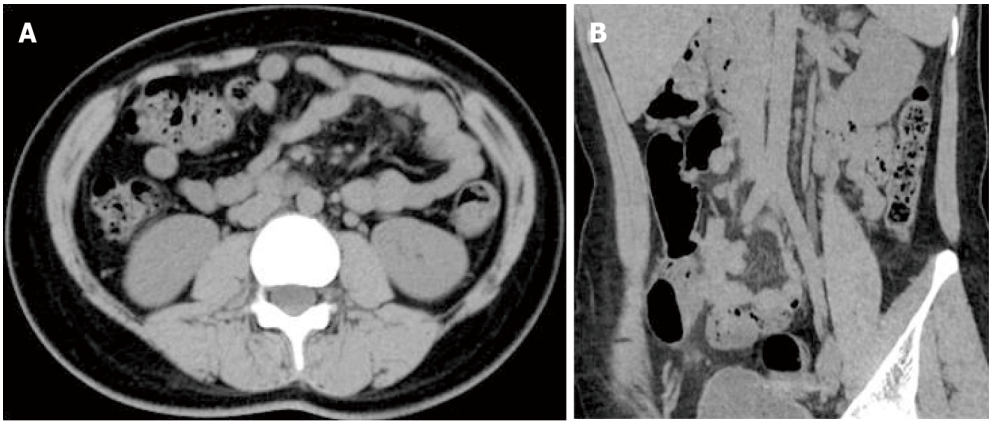

DOI: 10.12998/wjcc.v11.i4.896

Figure 3 Plain computed tomography images six months postpartum. A: Coronal view; B: Sagittal view.

the best choices for monitoring the blood flow of the inferior vena cava and ovarian vein in the follow-up procedure of PVOT. With the advancement of science and technology, MRI is increasingly used in clinical diagnosis and treatment. Advantages of MRI have been recognized in diagnosing vascular thrombosis, while certain limitations were also confirmed. Its advantages include that: The airflow effect of blood vessels in both the T2WI sequence and the DWI sequence of MRI can show the thrombus without contrast medium; MRI can protect the patients from X-ray radiation exposure; MRI scans can provide better and more reliable visualization and multi-plane display images. One of the limitations of MRI is that it is not available 24 h in most hospitals. The scanning range of a single procedure is also limited with a long scanning time. Furthermore, the pictures of MRI are greatly affected by the patient's breathing and bowel movements. Some patients are also not suitable for MRI examination (metal implantation in the body, patients with claustrophobia, *etc.*).

CT examination is mostly used when the ultrasound examination gives a negative result while the clinician highly suspects this disease. A whole abdomen CT scan can efficiently detect abnormal conditions specially. In this case, the MDCT scan revealed that a long tubular high-density shadow in the front of the left renal hilus, which extended to the left appendage with exudation around the tube wall. A wide range of tubular high-density shadow in the non-aortic region with or without an uneven density of the surrounding fat gap, suggested the formation of fresh intravenous thrombus. A dilated left ovarian vein and the ascending lumbar vein without contrast agent on the image of a dynamic-enhanced CT scan was usually considered to be the most important evidence for the diagnosis of POVT. Most cases of ovarian vein thrombophlebitis are diagnosed by CT scans. The increased density of fat spaces around the blood vessel wall as well as the blood vessel cavity in CT images reminds the diagnostician to determine the location of the lesion quickly and accurately. MDCT scanning is fast and less affected by breathing. The visualized image of MDCT scan can be post-processed in multiple planes, and abdominal pain in postpartum patients resulting from other diseases can be excluded (such as urinary calculi, appendicitis, gastrointestinal perforation, endometritis, *etc.*) by CT scanning. In addition, when POVT is suspected or the cause of postpartum abdominal pain is identified, the specificity and sensitivity of enhanced CT scans could be almost 100%[17]. Therefore, we believe that the high efficiency and convenience of CT make it the most preferred non-invasive inspection method for POVT. Indeed, we recommend that clinicians choose enhanced CT scan when POVT is suspected. The DWI sequence and T2WI sequence of MRI can be used as one of the methods of follow-up examinations for patients to avoid multiple X-rays exposure.

Once POVT has been diagnosed, patients need to be given active treatments as soon as possible in case of systemic sepsis caused by ovarian vein thrombosis. Pulmonary embolism is the most severe complication of ovarian thrombosis. In POVT patients, the incidence of pulmonary embolism is about 13.2%, while the mortality rate of POVT is less than 5%, which is mostly caused by pulmonary embolism. A venous filter can usually prevent the pulmonary embolism clinically[13]. Due to the scarce incidence of POVT, there has been no standard treatment for POVT, and treatment for deep vein thrombosis is often adopted. At present, heparin anticoagulation and intravenous antibiotics are the main non-invasive treatments for POVT in clinical practice. However, domestic and foreign experts still have disputes about whether POVT needs anticoagulation therapy or not. Most experts advocate anticoagulation to prevent the further formation and spreading of thrombus[7]. There is no recommended standard for the duration of anticoagulation so far. It depends on the changes in the patient's condition during follow-up. Some scholars believe that anticoagulation is required for 3 mo, while others considered that it should be maintained for at least 2 wk. For those with extensive pelvic thrombosis, the anticoagulation procedure should be administered for at least 6 wk, and whether to continue anticoagulation is based on subsequent imaging evaluation. The treatment time of broad-spectrum antibiotics is

generally recommended to be 7 to 10 d, and it is usually recommended to use it until the infection indicators return to normal and the fever is cured for 48 to 72 h[12]. Moreover, Salomon *et al*[1] reported that for some POVT patients without fever, elevated WBC count, and other infection symptoms, antibiotics could not be used. Our patient was treated with heparin anticoagulation for 2 wk and then it was switched to rivaroxaban to continue anticoagulation for 6 mo. During the hospitalization, she accepted cefoperazone sodium and sulbactam sodium for 10 d. The patient did not have abnormal bleeding in the oral mucosa or other locations, and the reexamination CT indicated that the thrombus disappeared. Brown *et al*[18] found that when compared to combined use of heparin and antibiotics, no significant difference in fever and hospital stay could be found in the group of patients using antibiotics alone. However, they only assessed the cure time of fever but did not assess the risk of thrombosis, pulmonary embolism, *etc.* The serious consequences are mostly caused by its complications, therefore, we believe that anticoagulation therapy is still necessary. The anticoagulants such as heparin, warfarin, and rivaroxaban are safe in the postpartum period, but their application in patients with postpartum POVT should be studied further. Furthermore, the choice of antibiotics should cover both aerobes and anaerobes. In addition, there are very few reports on the surgical treatment of POVT. Shi *et al*[19] reported a 35-year-old G3P2 woman who suffered high fever after C-section, and anti-inflammatory treatment was not effective within one week. An abdominal wall incision haematoma was found, and a second surgery was performed later. The patient was ultimately diagnosed with abdominal incision haematoma and right ovarian vein infectious thrombophlebitis after C-section. They used imipenem and tigecycline to strengthen the anti-inflammatory effects, simultaneously administrating low-molecular-weight heparin and warfarin as anticoagulant therapy. On the 30th day after C-section, the right ovarian vein thrombus disappeared. Some surgical options used in the past, including ligation of the ovarian vein or inferior vena cava and even removal of the uterus, have been abandoned[10,16,17,20].

CONCLUSION

POVT is a rare complication after delivery without typical clinical manifestation or any specific laboratory examination results. Early and accurate diagnosis of POVT is particularly important since it may result in life-threatening pulmonary embolism. Even in patients with a low risk of deep vein thrombosis, POVT should be considered when faced with postpartum fever and abdominal pain. To conclude, we recommend MDCT scan as the preferred noninvasive method for the clinical diagnosis of POVT.

ACKNOWLEDGEMENTS

We thank the obstetric and radiology teams of the centers who helped to recruit the women to the study.

FOOTNOTES

Author contributions: Wang JJ, Ji YD, and Xu W designed the study; Wang JJ and Hui CC wrote the manuscript; Wang JJ and Hui CC collected and input the data; Xu W carried out the statistical analysis; all authors reviewed the manuscript.

Informed consent statement: Written informed consent was obtained from the patient for the publication of this case report and any accompanying images.

Conflict-of-interest statement: All the authors have no conflicts of interest to disclose.

CARE Checklist (2016) statement: The authors have read the CARE Checklist (2016), and the manuscript was prepared and revised according to the CARE Checklist (2016).

Country/Territory of origin: China

ORCID number: Jin-Jin Wang 0000-0001-9514-408X; Chu-Chu Hui 0000-0003-2992-1877; Yi-Ding Ji 0000-0002-0111-7724;

Wei Xu 0000-0001-8683-0467.

S-Editor: Liu JH
L-Editor: Wang TQ
P-Editor: Liu JH

REFERENCES

1 **Salomon O**, Dulitzky M, Apter S. New observations in postpartum ovarian vein thrombosis: experience of single center. *Blood Coagul Fibrinolysis* 2010; **21**: 16-19 [PMID: 19587586 DOI: 10.1097/MBC.0b013e32832f2ada]
2 **Yildirim E**, Kanbay M, Ozbek O, Coskun M, Boyacioglu S. Isolated idiopathic ovarian vein thrombosis: a rare case. *Int Urogynecol J Pelvic Floor Dysfunct* 2005; **16**: 308-310 [PMID: 16211369 DOI: 10.1007/s00192-004-1247-4]
3 **Al-toma A**, Heggelman BG, Kramer MH. Postpartum ovarian vein thrombosis: report of a case and review of literature. *Neth J Med* 2003; **61**: 334-336 [PMID: 14708913]
4 **Jenayah AA**, Saoudi S, Boudaya F, Bouriel I, Sfar E, Chelli D. Ovarian vein thrombosis. *Pan Afr Med J* 2015; **21**: 251 [PMID: 26526119 DOI: 10.11604/pamj.2015.21.251.6908]
5 **Khishfe BF**, Sankovsky A, Nasr I. Idiopathic ovarian vein thrombosis: a rare cause of abdominal pain. *Am J Emerg Med* 2016; **34**: 935.e1-935.e2 [PMID: 26475360 DOI: 10.1016/j.ajem.2015.09.022]
6 **Adesiyun AG**, Samaila MO, Ojabo A. Postpartum ovarian vein thrombosis: incidental diagnosis at surgery. *Case Rep Obstet Gynecol* 2014; **2014**: 898342 [PMID: 24523973 DOI: 10.1155/2014/898342]
7 **Cao W**, Ni X, Wang Q, Li J, Li Y, Chen T, Wang X. Early diagnosis and precision treatment of right ovarian vein and inferior vena cava thrombosis following caesarean section: A case report. *Exp Ther Med* 2020; **19**: 2923-2926 [PMID: 32256777 DOI: 10.3892/etm.2020.8548]
8 **Scarsbrook AF**, Evans AL, Owen AR, Gleeson FV. Diagnosis of suspected venous thromboembolic disease in pregnancy. *Clin Radiol* 2006; **61**: 1-12 [DOI: 10.1016/j.crad.2005.08.015]
9 **Kearon C**, de Wit K, Parpia S. Diagnosis of Pulmonary Embolism with d-Dimer Testing. Reply. *N Engl J Med* 2020; **382**: 1075 [PMID: 32160676 DOI: 10.1056/NEJMc1917227]
10 **Daaloul W**, El Bekri S, Ouerdiane N, Masmoudi A, Ben Hamouda S, Bouguerra B, Sfar R. [Postpartum ovarian vein thrombophlebitis]. *Tunis Med* 2013; **91**: 158-159 [PMID: 23526286]
11 **Pak BK**, Sun IO, Kang DM. Unusual Ovarian Vein Thrombosis Associated with Urinary Tract Infection: A Case Report. *J Belg Soc Radiol* 2022; **106**: 24 [PMID: 35581984 DOI: 10.5334/jbsr.2810]
12 **Parino E**, Mulinaris E, Saccomano E, Gallo JC, Kohan G. Postpartum Ovarian Vein Thrombophlebitis with Staphylococcal Bacteremia. *Case Rep Infect Dis* 2015; **2015**: 589436 [PMID: 26221549 DOI: 10.1155/2015/589436]
13 **Fei Z**, Peng A, Wang L, Zhang L. Pulmonary embolism caused by postpartum ovarian vein thrombophlebitis after vaginal delivery: Case report and brief review of the literature. *J Clin Ultrasound* 2020; **48**: 291-293 [PMID: 31930727 DOI: 10.1002/jcu.22814]
14 **Johnson SC**, Esclapes M. Sonography of postpartum ovarian vein thrombophlebitis. *J Clin Ultrasound* 1998; **26**: 143-149 [PMID: 9502037 DOI: 10.1002/(sici)1097-0096(199803/04)26:3<143::aid-jcu6>3.0.co;2-m]
15 **Pumtako M**, Pumtako C. Septic pulmonary embolism caused by postpartum ovarian vein thrombophlebitis: A case report. *Case Rep Womens Health* 2022; **36**: e00445 [PMID: 36061333 DOI: 10.1016/j.crwh.2022.e00445]
16 **Nagayama M**, Watanabe Y, Okumura A, Amoh Y, Nakashita S, Dodo Y. Fast MR imaging in obstetrics. *Radiographics* 2002; **22**: 563-80; discussion 580 [PMID: 12006687 DOI: 10.1148/radiographics.22.3.g02ma03563]
17 **Abrantes J**, Teixeira E, Gomes F, Fernandes C. Postpartum ovarian vein thrombosis and venous anatomical variation. *BMJ Case Rep* 2019; **12** [PMID: 31229971 DOI: 10.1136/bcr-2018-228399]
18 **Brown CEL**, Cunningham FG. Ovarian Vein Thrombosis: Incidence of Recurrent Venous Thromboembolism and Survival. *Obstet Gynecol* 2018; **131**: 740-741 [PMID: 29578969 DOI: 10.1097/AOG.0000000000002550]
19 **Shi Q**, Gandi DS, Hua Y, Zhu Y, Yao J, Yang X, Xu Y, Zhang Y. Postpartum septic pelvic thrombophlebitis and ovarian vein thrombosis after caesarean section: a rare case report. *BMC Pregnancy Childbirth* 2021; **21**: 561 [PMID: 34404357 DOI: 10.1186/s12884-021-04037-4]
20 **Stafford M**, Fleming T, Khalil A. Idiopathic ovarian vein thrombosis: a rare cause of pelvic pain - case report and review of literature. *Aust N Z J Obstet Gynaecol* 2010; **50**: 299-301 [PMID: 20618252 DOI: 10.1111/j.1479-828X.2010.01159.x]

World Journal of Clinical Cases

Submit a Manuscript: https://www.f6publishing.com

World J Clin Cases 2023 February 6; 11(4): 903-908

DOI: 10.12998/wjcc.v11.i4.903

ISSN 2307-8960 (online)

CASE REPORT

Preoperative 3D reconstruction and fluorescent indocyanine green for laparoscopic duodenum preserving pancreatic head resection: A case report

Xiao-Li Li, Lian-Sheng Gong

Specialty type: Medicine, research and experimental

Provenance and peer review: Unsolicited article; Externally peer reviewed.

Peer-review model: Single blind

Peer-review report's scientific quality classification

Grade A (Excellent): 0
Grade B (Very good): B
Grade C (Good): C
Grade D (Fair): 0
Grade E (Poor): 0

P-Reviewer: Casella C, Italy; Cianci P, Italy

Received: September 9, 2022
Peer-review started: September 9, 2022
First decision: October 12, 2022
Revised: October 21, 2022
Accepted: January 10, 2023
Article in press: January 10, 2023
Published online: February 6, 2023

Xiao-Li Li, Lian-Sheng Gong, Department of General Surgery, Xiangya Hospital, Central South University, Changsha 410008, Hunan Province, China

Corresponding author: Lian-Sheng Gong, MD, PhD, Professor, Department of General Surgery, Xiangya Hospital, Central South University, No. 87 Xiangya Road, Kaifu District, Changsha 410008, Hunan Province, China. 13973169263@163.com

Abstract

BACKGROUND

Duodenum-preserving pancreatic head resection (DPPHR) is the choice of surgery for benign or low-grade malignant tumors of the pancreatic head. Laparoscopic DPPHR (LDPPHR) procedure can be improved by preoperative 3D model reconstruction and the use of intravenous indocyanine green fluorescent before surgery for real-time navigation with fluorescent display to guide the surgical dissection and prevention of from injury to vessels and biliary tract.

CASE SUMMARY

Here we report the successful short- and long-term outcomes after one year following LDPPHR for a 60-year lady who had an uneventful recovery and was discharged home one week after the surgery.

CONCLUSION

There was no bile leakage or pancreatic leakage or delayed gastric emptying. The histopathology report showed multiple cysts in the pancreatic head and localized pancreatic intraepithelial tumor lesions. The resected margin was free of tumor.

Key Words: Duodenum-preserving pancreatic head resection; Fluorescent navigation; Laparoscopic 3D model reconstruction; Case report

Core Tip: Duodenum-preserving pancreatic head resection (DPPHR) is the choice of surgery for benign or low-grade malignant tumors of the pancreatic head. Laparoscopic DPPHR (LDPPHR) procedure can be improved by preoperative 3D model reconstruction and the use of intravenous indocyanine green fluorescent before surgery for real-time navigation with fluorescent display to guide the surgical dissection and prevention of from injury to vessels and biliary tract. Here we report the successful short- and long-term outcomes after one year following LDPPHR for a 60-year lady who had an uneventful recovery and was discharged home one week after the surgery. There was no bile leakage or pancreatic leakage or delayed gastric emptying. The histopathology report showed multiple cysts in the pancreatic head and localized pancreatic intraepithelial tumor lesions. The resected margin was free of tumor.

Citation: Li XL, Gong LS. Preoperative 3D reconstruction and fluorescent indocyanine green for laparoscopic duodenum preserving pancreatic head resection: A case report. *World J Clin Cases* 2023; 11(4): 903-908
URL: https://www.wjgnet.com/2307-8960/full/v11/i4/903.htm
DOI: https://dx.doi.org/10.12998/wjcc.v11.i4.903

INTRODUCTION

Duodenum-preserving pancreatic head resection (DPPHR) is the choice of surgery for benign or low-grade malignant tumors of the pancreatic head. The most common benign and borderline pancreatic neoplastic lesions include Cystic Tumor, Neuroendocrine Tumor, Solid Pseudopapillary Tumor and Intraductal Papillary Mucinous Neoplasm (IPMN). The DPPHR was first reported in 1972 by Beger for the treatment of the inflammatory mass caused by chronic pancreatitis[1]. Compared with traditional pancreatic surgery, this procedure retains the gastroduodenal continuity, reduces the extent of pancreatic resection, retains the pancreatic intestinal axis, and help preserve normal anatomical and physiological structures with good short- and long-term outcome. A variety of modifications in surgical techniques have been proposed, such as Frey's operation, Berne's operation, Takada's operation, *etc*[2-5].

With the development of minimally invasive and precision medicine, laparoscopic DPPHR (LDPPHR) has become a better option, but it is less practiced and rarely reported because of the complexity of the operation. Combined with fluorescence technology and preoperative 3D model reconstruction, the LDPPHR under fluorescence navigation is beneficial. The fluorescence dye, indocyanine green (ICG) used intravenously during surgery is excreted through the bile, showing green fluorescence under near-infrared light excitation[6]. The use of fluorescence navigation technology greatly improves the visualization of biliary anatomy for accurate planning and resection and prevents intraoperative bile duct injury. In extrahepatic biliary fluorescence imaging, Vlek *et al*[7] used the method of injecting ICG through peripheral vein 15~60 min before operation. After ICG was injected into peripheral vein, the liver could fluoresce within 2-5 min, and the biliary tract could fluoresce within 8-10 min. The concentration in bile reached its peak 30 min to 2 h after ICG intravenous injection.

CASE PRESENTATION

Chief complaints

A female patient, aged 60 years, was admitted with a pancreatic head mass found during the physical check-up.

History of present illness

A female patient, aged 60 years, was admitted with a pancreatic head mass found during the physical check-up. The blood routine, coagulation profile, liver function, renal function, serum electrolyte, the markers of HBV, and tumor antigen screening tests were normal. Endoscopic ultrasonography showed multiple mixed-echo nodules in the head and neck of the pancreas, with irregular shape and clear boundary, and mainly a hypoechoic parenchyma. The computed tomography (CT) scan showed cystic lesions in the head and neck of the pancreas. Some lesions were connected to the main pancreatic duct, suspicious of IPMN. The CT angiography (CTA) and venous-phase imaging (CTV) of peripancreatic vessels were normal (Figure 1A).

Laboratory examinations

The blood routine, coagulation profile, liver function, renal function, serum electrolyte, the markers of HBV, and tumor antigen screening tests were normal.

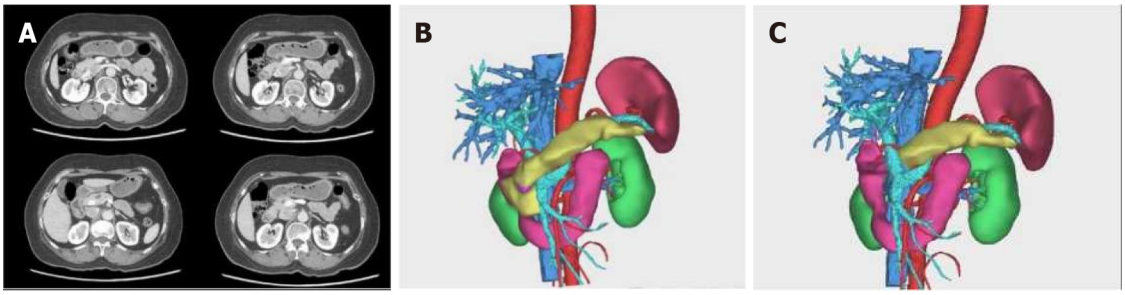

DOI: 10.12998/wjcc.v11.i4.903

Figure 1 Preoperative examination and surgical planning. A: Multiple cystic lesions with septum seen in the head and neck of the pancreas. The computer tomography value is 20 Hu. The lesions are connected to the main pancreatic duct; B: preoperative 3D reconstruction; C: plan of surgical resection with postoperative pancreatic changes are visualized in 3D reconstruction.

Imaging examinations

Endoscopic ultrasonography showed multiple mixed-echo nodules in the head and neck of the pancreas, with irregular shape and clear boundary, and mainly a hypoechoic parenchyma. The CT scan showed cystic lesions in the head and neck of the pancreas. Some lesions were connected to the main pancreatic duct, suspicious of IPMN. The CTA and CTV of peripancreatic vessels were normal (Figure 1A).

The 3D reconstruction preoperatively (Figure 1B), and plan of surgical resection with postoperative pancreatic changes are visualized (Figure 1C).

FINAL DIAGNOSIS

Multiple cysts in pancreatic head and localized pancreatic intraepithelial tumor lesions (PanIN-2).

TREATMENT

15 min Before operation, one ml (2.5 mg) ICG was injected into the peripheral vein (if the biliary tract development is not satisfactory during operation, the additional dose can be continued). The gastrocolonic ligament was dissected with an ultrasonic knife under laparoscopy, multiple cystic tumors in the pancreatic head were noted. The ultrasonic knife was used for dissection of duodenum and pancreatic head. The superior mesenteric vein was dissected at the lower edge of the pancreas. The tunnel behind the pancreatic neck was established. The pancreatic neck was taped and transected. The bile duct was evaluated in fluorescence laparoscopic mode (Figure 2A). Under fluorescent navigation, dissection of the uncinate process of the pancreas was continued from the lower border and upward under the postpancreatic head capsule. The anterior and posterior inferior pancreaticoduodenal vessels were exposed, and the branches of vessels entering the pancreas were severed keeping the integrity of the posterior fascia of the pancreas. Gastroduodenal artery was dissected. The superior anterior pancreaticoduodenal artery branches entering the pancreatic head were cut, retaining the blood supply of the duodenum. With fluorescent display, the pancreatic tissue was dissected off along the posterior fascial plane of the pancreatic head, protect the common bile duct, duodenum and its blood supply. There was no bile leakage and bleeding detected under fluorescent laparoscopy (Figure 2B and C). For digestive tract reconstruction, the jejunum was severed at 15 cm from the Treitz ligament, the distal jejunum was pulled out from behind the colon, the pancreatic duct was cannulated with a silicone tube, and end-to-side pancreatojejunostomy was performed using continuous 3-0 absorbable suture (Vicryl®). Roux-Y jejuno-jejunostomy was performed about 45 cm away from the pancreatojejunostomy. There was no bleeding, bile leakage and pancreatic leakage. An abdominal drainage tube was placed behind the pancreatojejunostomy (Video).

OUTCOME AND FOLLOW-UP

Results

Post-operative recovery was uneventful. On the 4th day white blood cell: 7.7 x 10^{9}/L. Percentage of neutrophils: 82%, hemoglobin: 114 g/L. Serum albumin: 34 g/L, Serum total bilirubin: 10.3 μmol/L, Serum direct bilirubin: 5.2 μmol/L, ascites amylase: 149 U/L. Postoperative pathological report showed

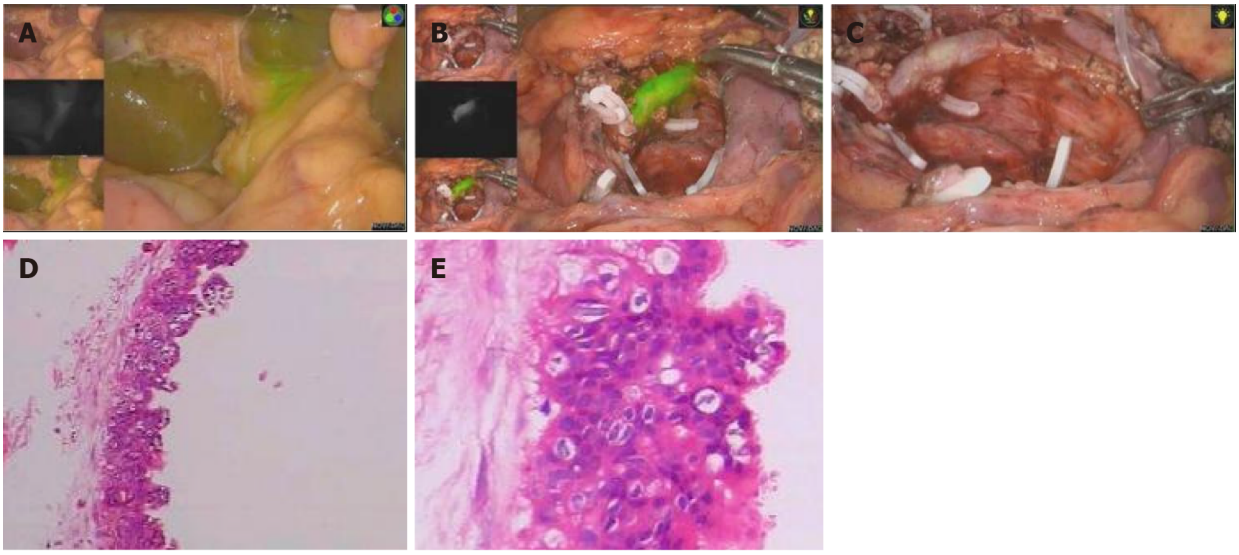

DOI: 10.12998/wjcc.v11.i4.903

Figure 2 Intraoperative operation and postoperative pathological examination. A: Bile duct display after 40 min of fluorescence injection; B: Surgical wound after complete resection of pancreatic head tissue under fluorescence laparoscopy; C: Surgical wound after laparoscopic complete resection of pancreatic head; D: Postoperative pathological 1; E: Postoperative pathological 2.

multiple cysts in pancreatic head and localized pancreatic intraepithelial tumor lesions (PanIN-2). Resected margin was free of tumor (Figure 2D and E).

Follow-ups

Follow up CT after 5 mo (Figure 3A), 11 mo (Figure 3B) and 17 mo (Figure 3C) were normal. The follow-up hepatorenal function and blood sugar were normal.

DISCUSSION

In our case the outcome of LDPPHR was satisfactory without biliary or pancreatic leakage, and at one-year follow-up the CT scan, liver function and blood sugar tests were normal. The preoperative 3D reconstruction and intraoperative use of ICG fluorescent was helpful in anatomical dissection, avoiding injury to important vessels and biliary tract.

The traditional pancreaticoduodenectomy (PD) for benign or low-grade malignant tumors of the head of the pancreas, is now performed by laparoscopic PD (LPD) with overall mortality reduced to about 1% in large volume centers. However, postoperative morbidity and complications is still as high as 40%-60%, including malnutrition and pancreatic dysfunction[8]. Patients with benign tumors or low-grade malignant tumors of the pancreatic head will survive for a long time after surgical treatment, If LPD is performed, it may seriously affect the safety and quality of life of the patients after operation. DPPHR with various modifications is a more reasonable procedure for patients with benign and low-grade malignant tumors of the pancreatic head removes the tumor of the pancreatic head, retaining the continuity of gastro-duodenum and biliary tract anatomy and physiological functions. The minimally invasive laparoscopy resection LDPPHR has gained acceptance[9,10].

Intraoperative use of ICG fluorescent has added advantage in dissection and preservation of important vessels, for example, the blood supply of the duodenal papilla and the intrapancreatic part of the bile duct mainly comes from the supply of the posterior pancreaticoduodenal artery arch[11,12], the duodenal papilla is mainly supplied by the papillary artery from the superior posterior pancreaticoduodenal artery, protecting the posterior pancreaticoduodenal artery arch is particularly important for maintaining a good blood supply to the duodenum, the intrapancreatic part of the bile duct and the duodenal papilla. During the LDPPHR procedure in our case, the posterior fascia of the pancreatic head was preserved to avoid damaging the posterior pancreaticoduodenal artery arch, and the anterior pancreaticoduodenal artery arch was preserved as much as possible.

The application of 3D visualization technology combined with 3D printing technology in liver cancer and hilar cholangiocarcinoma has been reported in the literature. The variation of bile duct and blood vessel and the transverse and longitudinal infiltration of tumor can be observed clearly and stereoscopically from multiple dimensions to judge whether the tumor invades blood vessels and the resectability of the tumor. Preoperative 3D model reconstruction can plan different surgical approaches and resection ranges, select the best individualized surgical scheme, and achieve the purpose of accurate

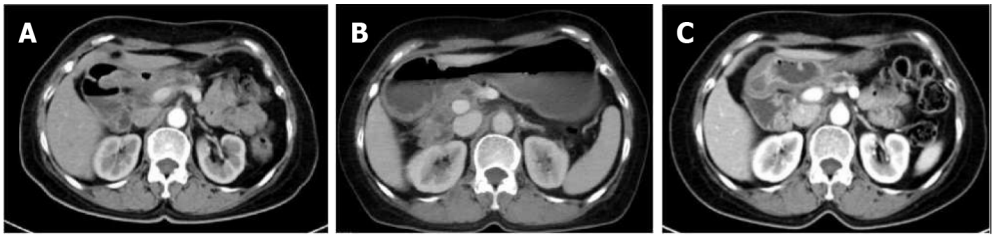

DOI: 10.12998/wjcc.v11.i4.903

Figure 3 Postoperative follow-up. A: Follow-up computer tomography (CT) after 5 mo; B: Follow-up CT after 11 mo; C: Follow-up CT after 17 mo.

lesion resection [13,14]. In this case, the application of 3D visualization technology to LDPPHR has achieved satisfactory results in preoperative diagnosis, surgical planning and intraoperative real-time navigation. By constructing a 3D model before operation, we can more intuitively observe the scope of pancreatic lesions, observe that there is no vascular anatomical variation in this case, and preserve the anterior and posterior pancreaticoduodenal arterial arches to the greatest extent during the operation. In this way, we can "have a clear mind" before operation and "skill and ease" during operation. It laid the foundation for the success of the operation.

ICG, as a water-soluble dye for intravenous injection, can be selectively absorbed by the liver and excreted through the bile. After binding with mucin in the bile, ICG presents green fluorescence under near-infrared light excitation, which provides the possibility for fluorescence visualization of bile duct [15]. In a study by Wikner *et al*[16], it is easier to expose the common bile duct in ICG fluorescence mode than in traditional mode. The exposure of the intrapancreatic part of the bile duct and blood supply protection are a major difficulty in this operation. If the intrapancreatic part of the bile duct was difficult to be exposed due to inflammation or other factors, ICG fluorescence technology could achieve accurate navigation, and greatly reduces the difficulty of common bile duct exposure.

CONCLUSION

Use of preoperative 3D was helpful in precise planning, and the intraoperative fluorescent navigation aided in the surgical dissection, preserving the important vessels and biliary anatomy during LDPPHR. This procedure is worthy of promotion hospitals with such facilities.

FOOTNOTES

Author contributions: Li XL, Gong LS contributed to the study conception and design; Material preparation, data collection and analysis were performed by Li XL, Gong LS; The first draft of the manuscript was written by Gong LS, and all authors commented on previous versions of the manuscript. All authors read and approved the final manuscript.

Informed consent statement: Written informed consent was obtained from the patient for the publication of this case report.

Conflict-of-interest statement: All the authors report no relevant conflicts of interest for this article.

CARE Checklist (2016) statement: The authors have read the CARE Checklist (2016), and the manuscript was prepared and revised according to the CARE Checklist (2016).

Country/Territory of origin: China

ORCID number: Xiao-Li Li 0000-0002-0717-3575; Lian-Sheng Gong 0000-2392-1839-1933.

S-Editor: Liu GL
L-Editor: A
P-Editor: Liu GL

REFERENCES

1 **Beger HG**, Kunz R, Poch B. The Beger procedure--duodenum-preserving pancreatic head resection. *J Gastrointest Surg* 2004; **8**: 1090-1097 [PMID: 15702531 DOI: 10.1016/j.gassur.2003.12.001]

2 **Frey CF**, Smith GJ. Description and rationale of a new operation for chronic pancreatitis. *Pancreas* 1987; **2**: 701-707 [PMID: 3438308 DOI: 10.1097/00006676-198711000-00014]

3 **Gloor B**, Friess H, Uhl W, Büchler MW. A modified technique of the Beger and Frey procedure in patients with chronic pancreatitis. *Dig Surg* 2001; **18**: 21-25 [PMID: 11244255 DOI: 10.1159/000050092]

4 **Takada T**, Yasuda H, Uchiyama K, Hasegawa H. Duodenum-preserving pancreatoduodenostomy. A new technique for complete excision of the head of the pancreas with preservation of biliary and alimentary integrity. *Hepatogastroenterology* 1993; **40**: 356-359 [PMID: 8406305]

5 **Lu C**, Jin WW, Mou YP, Zhou YC, Wang YY, Xia T, Zhu QC, Xu BW, Ren YF, Meng SJ, He YH, Jiang QT. [Clinical effect of minimally invasive duodenum preserving pancreatic head resection for benign and pre-malignant lesions of pancreatic head]. *Zhonghua Waike Zazhi* 2022; **60**: 39-45 [PMID: 34954945 DOI: 10.3760/cma.j.cn112139-20211104-00516]

6 **Hong D**, Cheng J, Wu W, Liu X, Zheng X. How to Perform Total Laparoscopic Duodenum-Preserving Pancreatic Head Resection Safely and Efficiently with Innovative Techniques. *Ann Surg Oncol* 2021; **28**: 3209-3216 [PMID: 33123857 DOI: 10.1245/s10434-020-09233-8]

7 **Vlek SL**, van Dam DA, Rubinstein SM, de Lange-de Klerk ESM, Schoonmade LJ, Tuynman JB, Meijerink WJHJ, Ankersmit M. Biliary tract visualization using near-infrared imaging with indocyanine green during laparoscopic cholecystectomy: results of a systematic review. *Surg Endosc* 2017; **31**: 2731-2742 [PMID: 27844236 DOI: 10.1007/s00464-016-5318-7]

8 **He K**, Hong X, Chi C, Cai C, Wang K, Li P, Liu X, Li J, Shan H, Tian J. A new method of near-infrared fluorescence image-guided hepatectomy for patients with hepatolithiasis: a randomized controlled trial. *Surg Endosc* 2020; **34**: 4975-4982 [PMID: 32020287 DOI: 10.1007/s00464-019-07290-z]

9 **Stauffer JA**, Coppola A, Villacreses D, Mody K, Johnson E, Li Z, Asbun HJ. Laparoscopic versus open pancreaticoduodenectomy for pancreatic adenocarcinoma: long-term results at a single institution. *Surg Endosc* 2017; **31**: 2233-2241 [PMID: 27604369 DOI: 10.1007/s00464-016-5222-1]

10 **Beger HG**. Benign Tumors of the Pancreas-Radical Surgery Versus Parenchyma-Sparing Local Resection-the Challenge Facing Surgeons. *J Gastrointest Surg* 2018; **22**: 562-566 [PMID: 29299757 DOI: 10.1007/s11605-017-3644-2]

11 **Prete FP**, Di Meo G, Liguori P, Gurrado A, De Luca GM, De Leo V, Testini M, Prete F. Modified "Blumgart-Type" Suture for Wirsung-Pancreaticogastrostomy: Technique and Results of a Pilot Study. *Eur Surg Res* 2021; **62**: 105-114 [PMID: 33975310 DOI: 10.1159/000515987]

12 **Liang B**, Chen Y, Li M, Dong X, Yao S, Liu T. Total laparoscopic central pancreatectomy with Roux-Y pancreaticojejunostomy for solid pseudopapillary neoplasm of pancreas: A case report. *Medicine (Baltimore)* 2019; **98**: e15495 [PMID: 31045833 DOI: 10.1097/MD.0000000000015495]

13 **Beger HG**, Mayer B, Rau BM. Parenchyma-Sparing, Limited Pancreatic Head Resection for Benign Tumors and Low-Risk Periampullary Cancer--a Systematic Review. *J Gastrointest Surg* 2016; **20**: 206-217 [PMID: 26525207 DOI: 10.1007/s11605-015-2981-2]

14 **Bai RJ**, Wang JE, Jiang HJ, Hao XJ, Dong XP, Huang YH, Wei L. Investigation on the optical scan condition for imaging of multi-slice spiral CT liver perfusion in rats. *Chin Med J (Engl)* 2013; **126**: 4742-4746 [PMID: 24342322]

15 **Dîrzu DS**, Dicu C, Dîrzu N. Urinary retention: a possible complication of unilateral continuous quadratus lumborum analgesia - a case report. *Rom J Anaesth Intensive Care* 2019; **26**: 75-78 [PMID: 31111099 DOI: 10.2478/rjaic-2019-0011]

16 **Wikner M**. Unexpected motor weakness following quadratus lumborum block for gynaecological laparoscopy. *Anaesthesia* 2017; **72**: 230-232 [PMID: 27891579 DOI: 10.1111/anae.13754]

World Journal of Clinical Cases

Submit a Manuscript: https://www.f6publishing.com

World J Clin Cases 2023 February 6; 11(4): 909-917

DOI: 10.12998/wjcc.v11.i4.909

ISSN 2307-8960 (online)

CASE REPORT

Unusual presentation of systemic lupus erythematosus as hemophagocytic lymphohistiocytosis in a female patient: A case report

Li-Yuan Peng, Jing-Bo Liu, Hou-Juan Zuo, Gui-Fen Shen

Specialty type: Immunology

Provenance and peer review: Unsolicited article; Externally peer reviewed.

Peer-review model: Single blind

Peer-review report's scientific quality classification

Grade A (Excellent): 0
Grade B (Very good): B, B
Grade C (Good): C
Grade D (Fair): 0
Grade E (Poor): 0

P-Reviewer: Dauyey K, Kazakhstan; El Chazli Y, Egypt; Tanaka H, Japan

Received: October 13, 2022
Peer-review started: October 13, 2022
First decision: November 30, 2022
Revised: December 29, 2022
Accepted: January 12, 2023
Article in press: January 12, 2023
Published online: February 6, 2023

Li-Yuan Peng, Jing-Bo Liu, Hou-Juan Zuo, Division of Cardiology, Department of Internal Medicine, Tongji Hospital, Tongji Medical College, Huazhong University of Science and Technology, Wuhan 430030, Hubei Province, China

Gui-Fen Shen, Department of Rheumatology and Immunology, Tongji Hospital, Tongji Medical College, Huazhong University of Science and Technology, Wuhan 430030, Hubei Province, China

Corresponding author: Gui-Fen Shen, MD, Doctor, Department of Rheumatology and Immunology, Tongji Hospital, Tongji Medical College, Huazhong University of Science and Technology, No. 1095 Jiefang Avenue, Wuhan 430030, Hubei Province, China.
guifenshen@126.com

Abstract

BACKGROUND

Hemophagocytic lymphohistiocytosis (HLH) is a rare life-threatening disorder, often resulting in the immune-mediated injury of multiple organ systems, including primary HLH and secondary HLH (sHLH). Among them, sHLH results from infections, malignant, or autoimmune conditions, which have quite poor outcomes even with aggressive management and are more common in adults.

CASE SUMMARY

We report a rare case of a 36-year-old female manifested with sHLH on background with systemic lupus erythematosus (SLE). During hospitalization, the patient was characterized by recurrent high-grade fever, petechiae and ecchymoses of abdominal skin, and pulmonary infection. Whole exon gene sequencing revealed decreased activity of natural killer cells. She received systematic treatment with Methylprednisolone, Etoposide, and anti-infective drugs. Intravenous immunoglobulin and plasmapheresis were applied when the condition was extremely acute and progressive. The patient recovered and did not present any relapse of the HLH for one year of follow-up.

CONCLUSION

The case showed sHLH, thrombotic microvascular, and infection in the whole course of the disease, which was rarely reported by now. The treatment of the patient emphasizes that early recognition and treatment of sHLH in SLE patients was of utmost importance to improve the prognosis and survival rate of patients.

Key Words: Hemophagocytic lymphohistiocytosis; Systemic lupus erythematosus; Autoimmune abnormalities; Case report

Core Tip: Hemophagocytic lymphohistiocytosis (HLH) is a rare life-threatening disorder, including primary HLH and secondary HLH (sHLH). We report a rare case of a 36-year-old female manifested with sHLH on background with systemic lupus erythematosus (SLE) and related with decreased activity of natural killer cells according to whole exon gene sequencing. Our study expanded the thoughts on the diagnosis and treatment of HLH in SLE patients.

Citation: Peng LY, Liu JB, Zuo HJ, Shen GF. Unusual presentation of systemic lupus erythematosus as hemophagocytic lymphohistiocytosis in a female patient: A case report. *World J Clin Cases* 2023; 11(4): 909-917
URL: https://www.wjgnet.com/2307-8960/full/v11/i4/909.htm
DOI: https://dx.doi.org/10.12998/wjcc.v11.i4.909

INTRODUCTION

Hemophagocytic lymphohistiocytosis (HLH) is a rare potentially life-threatening disorder, resulting in pathologic immune activation mediated multi-organ dysfunction[1,2]. It can be divided into primary HLH and secondary HLH. Primary HLH is an inherited autosomal recessive disorder that often manifests in the pediatric population[2]. Secondary HLH (sHLH) results from infections, malignancy, or autoimmune condition, and more commonly manifests among adults[3]. The clinical characteristics of HLH vary, but can include prolonged fever, lymphadenopathy, hepatosplenomegaly, and elevated levels of alanine aminotransferase, aspartate aminotransferase, triglyceride, and ferritin[4,5].

Systemic lupus erythematosus (SLE) is an autoimmune condition that is strongly associated with HLH[6]. In SLE patients, the estimated prevalence of co-occurrence of sHLH has been reported to be 0.9%-4.6%[7,8]. Here, we report a rare case of a young female with SLE accompanied by HLH. The patient's symptoms and laboratory abnormalities improved dramatically after two hospital admissions to our department, and no relapse of HLH symptoms was detected during the 1-year follow-up.

CASE PRESENTATION

Chief complaints

The 36-year-old Han Chinese woman was admitted to our hospital following two-month recurrent high-grade fever (> 39°C).

History of present illness

The patient initially presented to our hospital with Intermittent high-grade fever on January 4, 2021. The fever lasted for more than 20 d peaking at 40.4°C. She previously visited a local hospital and the laboratory results showed a reduced total white blood cells (WBC) count (1.8×10^9/L), and reduced counts of lymphocytes (0.4×10^9/L) and neutrophils (1.24×10^9/L). Dramatically increased C-reactive protein (CRP) levels (54.4 mg/L) were also detected. The patient was treated with broad-spectrum antibiotics (detailed drug names, duration, and dosages were not known). However, after the symptoms did not improve, the patient was finally admitted to our hospital for further treatment.

History of past illness

The patient had been diagnosed with SLE for more than 9 years and was treated with prednisone (10 mg per day). She did not report any history of chronic respiratory disease or surgical procedures. No travel history, infectious exposure was reported. She was allergic to quinolones.

Personal and family history

There was nothing of note in the patient's personal or family history.

Physical examination

Upon admission, the patient was conscious and her temperature was 39.5°C, her heart rate was 119 beats/min, and her blood pressure was 111/86 mmHg. No enlarged lymph nodes were found. Systemic

examination found no signs of hepatosplenomegaly, abdominal tenderness, or rebound pain.

Laboratory examinations

Laboratory results on admission revealed decreased levels of WBCs (2.41× 10^9/L), neutrophils (1.68 × 10^9/L), red blood cells (RBCs, 2.71 × 10^{12}/L), hemoglobin (Hb, 80 g/L), and serum calcium (CA, 2.00 mmol/L), and increased levels of ferritin (1835.3 μg/L), CRP (62.04 mg/L), procalcitonin (0.71 ng/mL), erythrocyte sedimentation rate (138 mm/h), interleukin (IL)-10 (5.9 pg/mL), IL-6 (328.56 pg/mL), IL-2R (1060 U/mL), and interferon (IFN)-γ (65.29 pg/mL). The patient tested positive for anti-nuclear antibody (ANA) (titer > 1:1000) and anti-SSA antibody (> 400.00 RU/mL), but negative for other antibodies including anti-dsDNA antibody, anti-Smith antibody, and antiphospholipid antibody. Hypertriglyceridemia was also detected in the patient. The results of other investigations are shown in Figure 1A-D.

Imaging examinations

Computed tomography (CT) of the chest revealed patchy shadows in the lower lobe of the left lung (Figure 2B). Ultrasound of the abdomen and pelvis showed no sign of hepatosplenomegaly.

Further diagnostic work-up

After 3-d of anti-infective treatment (injection of dexamethasone and cefoperazone sodium), the patient's temperature decreased to 37.4°C. To investigate the cause of the persistent high fever in this patient, bone marrow aspiration was performed three days after admission (day 3) and showed normal with no significant hemophagocytosis (Supplementary Figure 1A). Examination of the peripheral blood revealed an increased proportion of neutrophils, toxic particles within the cytoplasm, variation in the size of mature red blood cells, with some arranged in straight lines, and clearly visible platelets that appeared both scattered and aggregated (Supplementary Figure 1B).

In addition, we performed the whole exon gene sequencing to screen for genetic diseases and revealed missense mutations in the LYST gene [c.910G>A (p.D304N)], ATM gene [c.8071C>T (p.R2691C)], and FERMT1 gene [c.1590A>T (p.K530N)]. Among them, LYST gene is involved in lysosomal transport regulation. The abnormality mutation in LYST gene may cause lysosomal membrane fusion disorder, deposition of giant cytoplasmic particles, inducing immunodeficiency syndrome-related HLH. ATM gene encodes a key kinase of cell cycle checkpoint, which plays an important role in cell cycle regulation and DNA damage response. Abnormality of ATM gene may lead to Ataxia-telangiectasia (A-T), which is characterized by immune deficiency, ataxia, telangiectasia, chromosome instability, tumor susceptibility. The protein encoded by FERMT1 gene is involved in integrin signal transmission and the linkage between actin skeleton and outer matrix. Genetic abnormalities of FERMT1 can lead to FERMT1-related immunodeficiency characterized by skin diseases, photosensitivity, and autoimmune diseases. Next-generation sequencing of microorganism infection in peripheral blood also showed negative results.

FINAL DIAGNOSIS

The patient was diagnosed with SLE according to clinical guidelines[9], with an SLE Disease Activity Score (SLE- DAS) of 55[10] indicating that she was in the active stage of SLE after a 9-year disease duration. On evaluation, altogether four of the eight diagnostic criteria of HLH were fulfilled[11], although her bone marrow biopsy showed no hemophagocytosis. A diagnosis of HLH secondary to SLE was made (Table 1). The diagnosis of the patient also included thrombotic microangiopathy and severe pulmonary infection. Thrombotic microangiopathy was diagnosed according to a combination of symptoms and signs, including scattered petechiae and ecchymoses over her abdomen and extremities. Severe pulmonary infection was diagnosed based on uncontrolled recurrent fever and chest CT findings. Recovered infection foci in the lungs after continuous antimicrobial treatment also aided the diagnosis of severe pulmonary infection.

TREATMENT

Control of sHLH caused by SLE

Initially, the patient received broad-spectrum antimicrobial treatment at a local hospital with no significant improvement in symptom. Then, the patient was admitted to our hospital and after an extensive medical examination diagnosed with systemic autoimmune abnormalities induced by sHLH. She was treated with methylprednisolone (6 d), immunosuppressants (tacrolimus), and antimicrobial therapy. Plasmapheresis and etoposide were applied when the condition was extremely acute and progressive. Along with gamma globulin and leukocyte raising therapy, the patient's temperature returned to normal. Then methylprednisolone was maintained at 50 mg/d (Figure 1E).

Table 1 Baseline characteristics and hemophagocytic lymphohistiocytosis diagnosis of patient

Variables	Patient
Baseline characteristics	
Age (yr)	36
Etiology/Trigger	SLE and multiple infections
HLH- directed therapies	VP16 and methylprednisolone
HLH- 2004 criteria at diagnosis (ref.: Henter-2007)	
Fever	Y
Splenomegaly	N
Cytopenia, affecting 2 of 3 lineages in the peripheral blood	
Hemoglobin concentration < 9 g/dL	Y
Neutrophil count < 1.0×10^9/L	Y
Platelet count < 100×10^9/L	Y
Hypertriglyceridemia (fasting ≥ 3.0 mmol/L) and/or hypofibrinogenemia (≤ 150 mg/dL)	Y
Hemophagocytosis in bone marrow or spleen or lymph nodes (no evidence of malignancy)	N
Low or absent natural killer cell activity	N/A
Ferritin ≥ 500 ng/mL	Y
Soluble cluster of differentiation 25 (*i.e.* soluble interleukin 2 receptor) ≥ 2400 U/mL	N

HLH: Hemophagocytic lymphohistiocytosis; N/A: Not applicable; Y: Yes; N: No; ref.: References.

Thrombotic microvascular disease

As the disease rapidly progressed, several scattered petechiae and ecchymoses were detected over the patient's abdomen and extremities (Figure 2A). Besides, patient showed decrease levels of platelet and hemoglobin, and severe abdominal pain. Platelet and plasma transfusions were performed in response to coagulation dysfunction.

Anti-infective therapy

Because of methylprednisolone and immunosuppressant treatment, the patient presented with infection. As a result of granulocyte deficiency and the absence of a definite etiological diagnosis, the infection was difficult to control and, following recurrent episodes of fever, the patient was re-admitted to our hospital. After continuous antimicrobial treatment, infection foci in the lungs were eventually confined (Figure 2B-E).

OUTCOME AND FOLLOW-UP

The patient was discharged after her temperature normalized for 6 d and laboratory abnormalities and the patient's condition had improved. After 1 year of follow-up, no episodes of fever were reported, and laboratory findings were normal. Chest CT showed that the shadow on the lungs had diminished (Figure 2F).

DISCUSSION

In this study, we report a case of a young female SLE patient who developed sHLH, thrombotic microvascular disease, and infection of the lungs during the course of the disease. As far as we know, this is the first case of an SLE patient with a disease course accompanied by sHLH, thrombotic microvascular disease, and infection. As a rare case of a young female with SLE accompanied by HLH. The patient presented with thrombotic microangiopathy (TMA) and infection on second admission to our hospital, which was an essential reminder for clinicians during treatment of SLE patients complicated with HLH. Besides, we also did whole exon gene sequencing to screen for genetic diseases.

Primary HLH is generated from genetic mutations disrupting cytotoxic effects such as the normal assembly of perforins and granzymes, proper trafficking and targeting of cells, and the timely cessation of the immune response. sHLH results from a malignant, infectious, or autoimmune stimulus. The

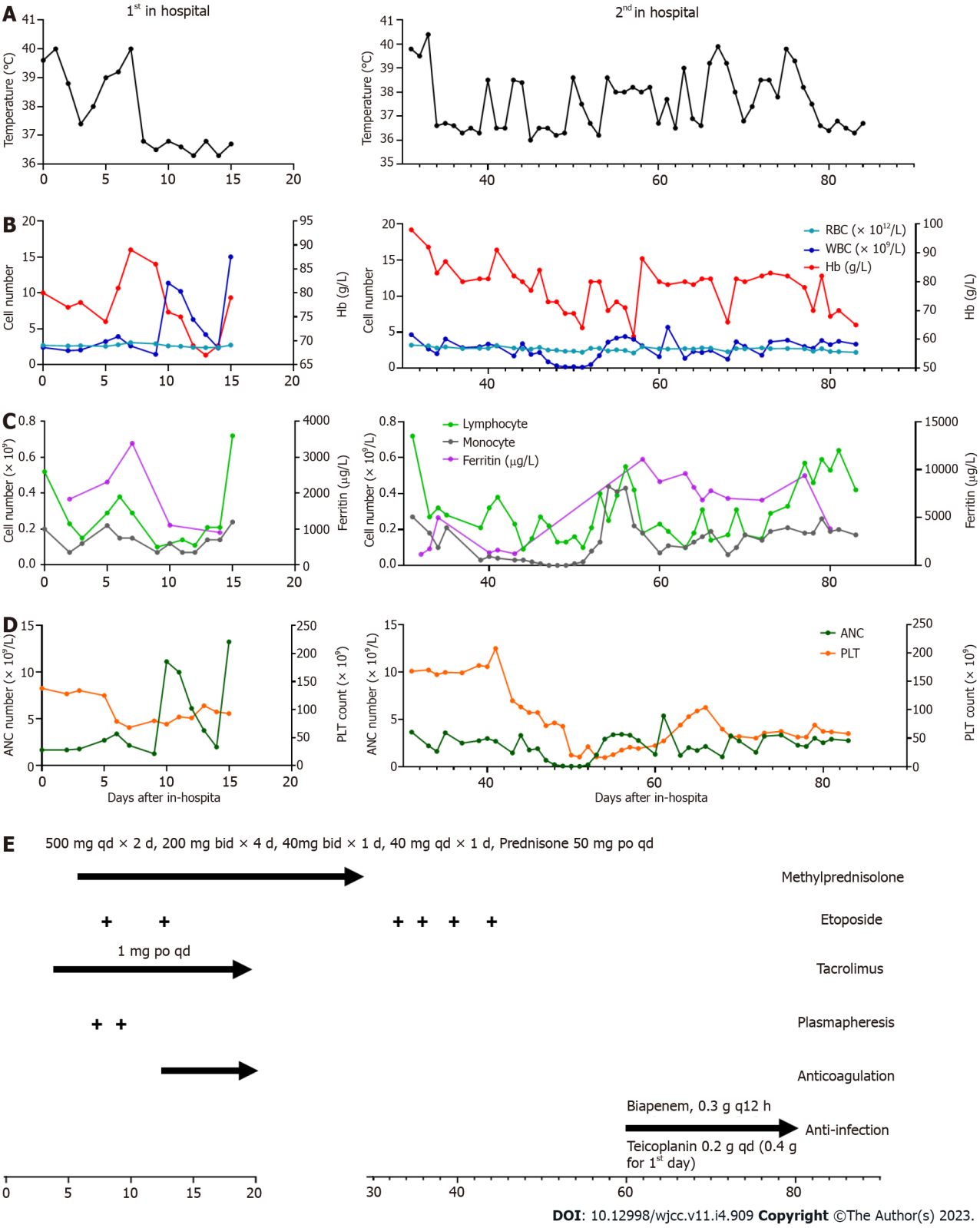

DOI: 10.12998/wjcc.v11.i4.909 **Copyright** ©The Author(s) 2023.

Figure 1 Inflammatory and hematologic results during hospitalization. A: Body temperature of the patients; B-C: the count of blood cells, including red blood cells (RBC), white blood cells (WBC), lymphocyte and monocyte; D: The concentration of hemoglobin and ferritin; E: Treatment schedule, lines and arrows represent continuous therapy. RBC: Red blood cell; WBC: White blood cell; Hb: Hemoglobin; PLT: Platelet; ANC: Absolute neutrophilic count.

pathophysiology of HLH is characterized by abnormal reciprocal activation of cytotoxic T lymphocytes, natural killer cells, and macrophages, and dramatic elevations in cytokine levels. sHLH is also referred to as macrophage activation syndrome (MAS) or more recently MAS-HLH[12]. Nearly 25% of SLE-associated MAS-HLH cases occurred when the first manifestation of the underlying disease was detected with no identifiable trigger[12]. The patient in our study had been diagnosed with SLE for 9 years and had no obvious causes for MAS-HLH, indicating that sHLH may not only accompany the first

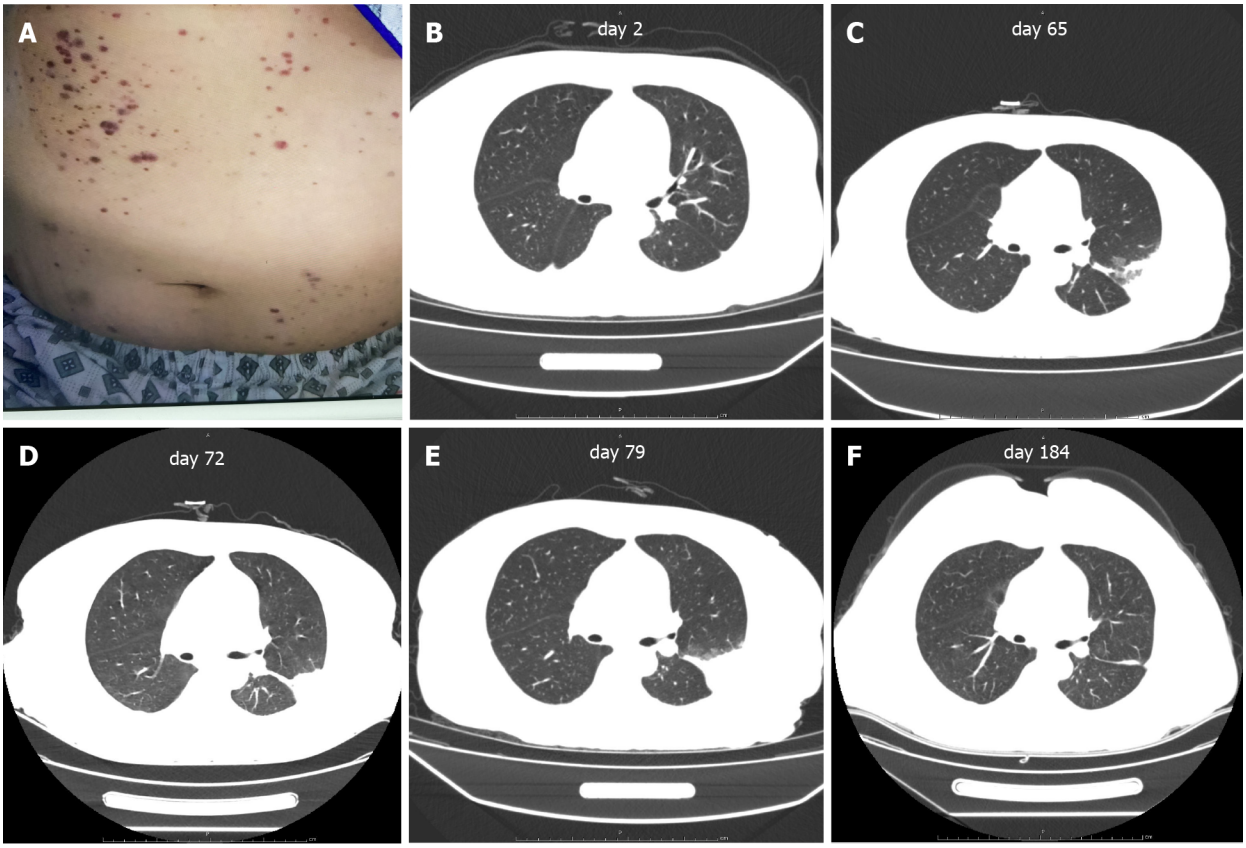

DOI: 10.12998/wjcc.v11.i4.909

Figure 2 Abdominal skin and scan of chest computed tomography. A: Scattered petechiae and ecchymoses were detected over the patient's abdomen and extremities during hospitalization; B-F: Chest computed tomography showed the recovery of infection foci in the lungs.

manifestation of symptoms but may also arise after long-term SLE. Clinicians should therefore be vigilant with patients suffering from intermittent fever regarding infections, malignant lymphoid tumors, and febrile recessive diseases[11]. Tuberculosis, for which there are more than 10 million new cases each year, should be ruled out as almost half of the patients present exclusively with extrapulmonary disease[13]. Our patient received empirical treatment for tuberculosis after several negative attempts to gain laboratory evidence. However, no clinical improvement was observed. Bone marrow biopsy was also performed and showed no involvement of the marrow due to lymphoma.

The previous study systematically reviewed the characteristics of patients with SLE and MAS[14]. Aziz *et al*[14] demonstrated that MAS development in SLE patients led to highly intensive care unit admissions and in-hospital mortalities with the presence of infection, and thrombocytopenia. Similar to the review, the patient in our case report showed dramatically increased levels of ferritin, which formed an important part of the diagnostic criteria[14]. Despite MAS-HLH being a life-threatening disorder, the complexity of the underlying diseases, triggers, and associated symptoms means that there is currently no standardized treatment protocol for HLH in adults[15]. Patients have shown the beneficial effects of treatment with a combination of corticosteroids with other immunosuppressive medications compared with corticosteroids alone[8,16]. In our case study, we used a combination treatment strategy and received a satisfactory therapeutic effect. However, there is no clear conclusion on which immunosuppressant is preferable for MAS-HLH in SLE patients[8]. Further studies are needed to investigate the detailed treatment strategies for MAS-HLH secondary to SLE.

TMA is a rare and fatal complication in SLE patients[17], occurring in 3%-9% cases of SLE cases[18]. The pathology of TMA in SLE patients is that endothelial injury results in thrombosis in capillaries and arterioles[19]. The trigger factors of TMA in SLE patients included lupus flare, infection, pregnancy, and medication non-compliance[17]. TMA has been divided into thrombotic thrombocytopenic purpura (TTP) and hemolytic uremic syndrome. The triggering factor in our case was severe infection. TTP has been associated with more deleterious outcomes in patients with SLE[17]. Importantly, no standardized clinical treatment guideline has been reported for TMA secondary to SLE[17]. The basic treatment strategies currently employed, which include glucocorticoids, immunosuppressive therapy, anticoagulation, anti-platelet agents, and plasmapheresis, result in treatment failure in half of all patients[20]. Our patient was treated on coagulation dysfunction and a positive therapeutic effect was observed. A combination of multiple treatment strategies, including basic treatment and supportive treatment, would maximize the therapeutic effect and improve the prognosis of patients.

Pulmonary manifestations of SLE normally include disorders of the lung parenchyma, pleura, and pulmonary vasculature[21]. Furthermore, immunosuppressive treatment, which is routinely used during SLE management, predisposes to an increased risk of respiratory infections[22]. Respiratory infection often mimics acute pulmonary manifestations secondary to SLE[21]. Pulmonary infection in SLE patients presents with a wide array of symptoms and is difficult to differentiate from other pulmonary disorders related to SLE[23]. Our patient presented with infection foci in the lungs. After timely anti-infection treatment, her body temperature returned to normal, and the lung infection foci were absorbed. Careful screening of complications in SLE patients should be undertaken by clinicians to improve the prognosis of patients.

Our study had some limitations. We did not check nature killer cell activity. These are not routine tests, and it is difficult to rely on such test results to determine HLH diagnosis, as this condition occurs at such low incidence rate. Furthermore, our patient did not have continuous clinical examination data because she was admitted to hospital on two separate occasions.

CONCLUSION

This case study examines the characteristics of sHLH, infection, and the thrombotic microvascular during the course of sHLH disease in an SLE patient, which has rarely been reported to date. Our findings highlight the importance of the early recognition and treatment of sHLH in SLE cases to improve the prognosis and survival rate of MAS-HLH patients.

This case report also highlights that fever and pancytopenia acted as important clinical features of SLE and sHLH. The features that prompted consideration of sHLH in this patient were fever, pancytopenia, hypertriglyceridemia, and hyperferritinemia coupled with her 9-year history of SLE. Timely recognition, early and effective interventions to treat the triggers and pathological processes, and systematic symptomatic treatment are crucial in curbing the rapid progressive disease course. Although significant advances have been made, much work is still needed in the HLH field to deepen our understanding of this condition and improve patient outcomes.

ACKNOWLEDGEMENTS

The authors thank the patient for her cooperation.

FOOTNOTES

Author contributions: Peng LY and Liu JB reviewed the literature and drafted the manuscript; Zuo HJ and Shen GF were responsible for the revision of the manuscript for important intellectual content; all authors issued final approval for the version to be submitted.

Informed consent statement: Written informed consent was obtained from the patient's legal guardian(s) for publication of this case report and any accompanying images.

Conflict-of-interest statement: We all declare that we have no conflicts of interest.

CARE Checklist (2016) statement: The authors have read the CARE Checklist (2016), and the manuscript was prepared and revised according to the CARE Checklist (2016).

Country/Territory of origin: China

ORCID number: Li-Yuan Peng 0000-0002-0813-1449; Gui-Fen Shen 0000-0002-3040-4482.

S-Editor: Liu JH
L-Editor: A
P-Editor: Liu JH

REFERENCES

1 **Jordan MB**, Allen CE, Weitzman S, Filipovich AH, McClain KL. How I treat hemophagocytic lymphohistiocytosis. *Blood* 2011; **118**: 4041-4052 [PMID: 21828139 DOI: 10.1182/blood-2011-03-278127]

2 **La Rosée P**, Horne A, Hines M, von Bahr Greenwood T, Machowicz R, Berliner N, Birndt S, Gil-Herrera J, Girschikofsky M, Jordan MB, Kumar A, van Laar JAM, Lachmann G, Nichols KE, Ramanan AV, Wang Y, Wang Z, Janka G, Henter JI. Recommendations for the management of hemophagocytic lymphohistiocytosis in adults. *Blood* 2019; **133**: 2465-2477 [PMID: 30992265 DOI: 10.1182/blood.2018894618]

3 **Ramos-Casals M**, Brito-Zerón P, López-Guillermo A, Khamashta MA, Bosch X. Adult haemophagocytic syndrome. *Lancet* 2014; **383**: 1503-1516 [PMID: 24290661 DOI: 10.1016/S0140-6736(13)61048-X]

4 **Weitzman S**. Approach to hemophagocytic syndromes. *Hematology Am Soc Hematol Educ Program* 2011; **2011**: 178-183 [PMID: 22160031 DOI: 10.1182/asheducation-2011.1.178]

5 **Chen WT**, Liu ZC, Li MS, Zhou Y, Liang SJ, Yang Y. Tuberculosis-associated hemophagocytic lymphohistiocytosis misdiagnosed as systemic lupus erythematosus: A case report. *World J Clin Cases* 2022; **10**: 3178-3187 [PMID: 35647112 DOI: 10.12998/wjcc.v10.i10.3178]

6 **Patel AR**, Desai PV, Banskota SU, Edigin E, Manadan AM. Hemophagocytic Lymphohistiocytosis Hospitalizations in Adults and Its Association With Rheumatologic Diseases: Data From Nationwide Inpatient Sample. *J Clin Rheumatol* 2022; **28**: e171-e174 [PMID: 33337810 DOI: 10.1097/RHU.0000000000001670]

7 **Gupta D**, Mohanty S, Thakral D, Bagga A, Wig N, Mitra DK. Unusual Association of Hemophagocytic Lymphohistiocytosis in Systemic Lupus Erythematosus: Cases Reported at Tertiary Care Center. *Am J Case Rep* 2016; **17**: 739-744 [PMID: 27733745 DOI: 10.12659/ajcr.899433]

8 **Dall'Ara F**, Cavazzana I, Frassi M, Taraborelli M, Fredi M, Franceschini F, Andreoli L, Rossi M, Cattaneo C, Tincani A, Airò P. Macrophage activation syndrome in adult systemic lupus erythematosus: report of seven adult cases from a single Italian rheumatology center. *Reumatismo* 2018; **70**: 100-105 [PMID: 29976044 DOI: 10.4081/reumatismo.2018.1023]

9 **Aringer M**, Costenbader K, Daikh D, Brinks R, Mosca M, Ramsey-Goldman R, Smolen JS, Wofsy D, Boumpas DT, Kamen DL, Jayne D, Cervera R, Costedoat-Chalumeau N, Diamond B, Gladman DD, Hahn B, Hiepe F, Jacobsen S, Khanna D, Lerstrøm K, Massarotti E, McCune J, Ruiz-Irastorza G, Sanchez-Guerrero J, Schneider M, Urowitz M, Bertsias G, Hoyer BF, Leuchten N, Tani C, Tedeschi SK, Touma Z, Schmajuk G, Anic B, Assan F, Chan TM, Clarke AE, Crow MK, Czirják L, Doria A, Graninger W, Halda-Kiss B, Hasni S, Izmirly PM, Jung M, Kumánovics G, Mariette X, Padjen I, Pego-Reigosa JM, Romero-Diaz J, Rúa-Figueroa Fernández Í, Seror R, Stummvoll GH, Tanaka Y, Tektonidou MG, Vasconcelos C, Vital EM, Wallace DJ, Yavuz S, Meroni PL, Fritzler MJ, Naden R, Dörner T, Johnson SR. 2019 European League Against Rheumatism/American College of Rheumatology classification criteria for systemic lupus erythematosus. *Ann Rheum Dis* 2019; **78**: 1151-1159 [PMID: 31383717 DOI: 10.1136/annrheumdis-2018-214819]

10 **Jesus D**, Larosa M, Henriques C, Matos A, Zen M, Tomé P, Alves V, Costa N, Le Guern V, Iaccarino L, Costedoat-Chalumeau N, Doria A, Inês LS. Systemic Lupus Erythematosus Disease Activity Score (SLE-DAS) enables accurate and user-friendly definitions of clinical remission and categories of disease activity. *Ann Rheum Dis* 2021; **80**: 1568-1574 [PMID: 34407927 DOI: 10.1136/annrheumdis-2021-220363]

11 **Henter JI**, Horne A, Aricó M, Egeler RM, Filipovich AH, Imashuku S, Ladisch S, McClain K, Webb D, Winiarski J, Janka G. HLH-2004: Diagnostic and therapeutic guidelines for hemophagocytic lymphohistiocytosis. *Pediatr Blood Cancer* 2007; **48**: 124-131 [PMID: 16937360 DOI: 10.1002/pbc.21039]

12 **Lorenz G**, Schul L, Schraml F, Riedhammer KM, Einwächter H, Verbeek M, Slotta-Huspenina J, Schmaderer C, Küchle C, Heemann U, Moog P. Adult macrophage activation syndrome-haemophagocytic lymphohistiocytosis: 'of plasma exchange and immunosuppressive escalation strategies' - a single centre reflection. *Lupus* 2020; **29**: 324-333 [PMID: 32013725 DOI: 10.1177/0961203320901594]

13 **Furin J**, Cox H, Pai M. Tuberculosis. *Lancet* 2019; **393**: 1642-1656 [PMID: 30904262 DOI: 10.1016/S0140-6736(19)30308-3]

14 **Aziz A**, Castaneda EE, Ahmad N, Veerapalli H, Rockferry AG, Lankala CR, Hamid P. Exploring Macrophage Activation Syndrome Secondary to Systemic Lupus Erythematosus in Adults: A Systematic Review of the Literature. *Cureus* 2021; **13**: e18822 [PMID: 34804679 DOI: 10.7759/cureus.18822]

15 **Schram AM**, Berliner N. How I treat hemophagocytic lymphohistiocytosis in the adult patient. *Blood* 2015; **125**: 2908-2914 [PMID: 25758828 DOI: 10.1182/blood-2015-01-551622]

16 **Kumakura S**, Murakawa Y. Clinical characteristics and treatment outcomes of autoimmune-associated hemophagocytic syndrome in adults. *Arthritis Rheumatol* 2014; **66**: 2297-2307 [PMID: 24756912 DOI: 10.1002/art.38672]

17 **Kello N**, Khoury LE, Marder G, Furie R, Zapantis E, Horowitz DL. Secondary thrombotic microangiopathy in systemic lupus erythematosus and antiphospholipid syndrome, the role of complement and use of eculizumab: Case series and review of literature. *Semin Arthritis Rheum* 2019; **49**: 74-83 [PMID: 30598332 DOI: 10.1016/j.semarthrit.2018.11.005]

18 **Magil AB**, McFadden D, Rae A. Lupus glomerulonephritis with thrombotic microangiopathy. *Hum Pathol* 1986; **17**: 192-194 [PMID: 3512413 DOI: 10.1016/s0046-8177(86)80293-3]

19 **Benz K**, Amann K. Thrombotic microangiopathy: new insights. *Curr Opin Nephrol Hypertens* 2010; **19**: 242-247 [PMID: 20186056 DOI: 10.1097/MNH.0b013e3283378f25]

20 **Pattanashetti N**, Anakutti H, Ramachandran R, Rathi M, Sharma A, Nada R, Gupta KL. Effect of Thrombotic Microangiopathy on Clinical Outcomes in Indian Patients With Lupus Nephritis. *Kidney Int Rep* 2017; **2**: 844-849 [PMID: 29270491 DOI: 10.1016/j.ekir.2017.04.008]

21 **Amarnani R**, Yeoh SA, Denneny EK, Wincup C. Lupus and the Lungs: The Assessment and Management of Pulmonary Manifestations of Systemic Lupus Erythematosus. *Front Med (Lausanne)* 2020; **7**: 610257 [PMID: 33537331 DOI: 10.3389/fmed.2020.610257]

22 **Cuchacovich R**, Gedalia A. Pathophysiology and clinical spectrum of infections in systemic lupus erythematosus. *Rheum Dis Clin North Am* 2009; **35**: 75-93 [PMID: 19480998 DOI: 10.1016/j.rdc.2009.03.003]

23 **Hannah JR**, D'Cruz DP. Pulmonary Complications of Systemic Lupus Erythematosus. *Semin Respir Crit Care Med* 2019; **40**: 227-234 [PMID: 31137062 DOI: 10.1055/s-0039-1685537]

World Journal of Clinical Cases

Submit a Manuscript: https://www.f6publishing.com

World J Clin Cases 2023 February 6; 11(4): 918-921

DOI: 10.12998/wjcc.v11.i4.918

ISSN 2307-8960 (online)

CASE REPORT

Polyarteritis nodosa presenting as leg pain with resolution of positron emission tomography-images: A case report

Ji-Hyoun Kang, Jahae Kim

Specialty type: Medicine, research and experimental

Provenance and peer review: Unsolicited article; Externally peer reviewed.

Peer-review model: Single blind

Peer-review report's scientific quality classification

Grade A (Excellent): 0
Grade B (Very good): 0
Grade C (Good): C
Grade D (Fair): 0
Grade E (Poor): 0

P-Reviewer: Wang T, China

Received: September 27, 2022
Peer-review started: September 27, 2022
First decision: December 13, 2022
Revised: December 13, 2022
Accepted: January 12, 2023
Article in press: January 12, 2023
Published online: February 6, 2023

Ji-Hyoun Kang, Division of Rheumatology, Department of Internal Medicine, Chonnam National University Medical School & Hospital, Gwangju 61469, South Korea

Jahae Kim, Department of Nuclear Medicine, Chonnam National University Hospital & Medical School, Gwangju 61469, South Korea

Corresponding author: Ji-Hyoun Kang, MD, PhD, Associate Professor, Division of Rheumatology, Department of Internal Medicine, Chonnam National University Medical School & Hospital, 42 Jebong-ro, Dong-gu, Gwangju 61469, South Korea.
romi918@naver.com

Abstract

BACKGROUND

Although fluorodeoxyglucose-positron emission tomography/computed tomography (FDG-PET/CT) is widely used for diagnosis and follow-up of large sized vessel vasculitis, it is still not widely used for small to medium sized vessel vasculitis.

CASE SUMMARY

This is the case of a 68-year-old male who presented at the emergency department complaining of fever, myalgia, and bilateral leg pain of over two weeks duration, with elevated levels of C-reactive protein. He was subsequently admitted and despite the absence of clinically significant findings, the patient continued to exhibit recurrent fever. A fever of unknown origin workup, which included imaging studies using FDG-PET/CT, revealed vasculitis involving small to medium-sized vessels of both lower extremities, demonstrated by linear hypermetabolism throughout the leg muscles. The patient was treated with methylprednisolone and methotrexate after diagnosis leading to the gradual resolution of the patient's symptoms. Three weeks later, a follow-up FDG-PET/CT was performed. Previously hypermetabolic vessels were markedly improved.

CONCLUSION

Our case report demonstrated that FDG-PET/CT has tremendous potential to detect medium-sized vessel inflammation; it can also play a crucial role in prognosticating outcomes and monitoring therapeutic efficacy.

Key Words: Positron emission tomography-computed tomography; Polyarteritis nodosa;

Case report

Core Tip: The fluorodeoxyglucose-positron emission tomography/computed tomography can be an option to diagnose small to medium-sized vessel vasculitis and follow-up to assess on the extent and improvement of inflammation in patients with polyarteritis nodosa.

Citation: Kang JH, Kim J. Polyarteritis nodosa presenting as leg pain with resolution of positron emission tomography-images: A case report. *World J Clin Cases* 2023; 11(4): 918-921
URL: https://www.wjgnet.com/2307-8960/full/v11/i4/918.htm
DOI: https://dx.doi.org/10.12998/wjcc.v11.i4.918

INTRODUCTION

Polyarteritis nodosa (PAN) is characterized by systemic necrotizing vasculitis which can involve medium-sized vessels. This vasculitis is usually difficult to diagnose, thus, imaging study including fluorodeoxyglucose-positron emission tomography/ computed tomography (FDG-PET/CT) would be a possible role to identify this disease.

CASE PRESENTATION

Chief complaints

A 68-year-old male visited to emergency department complaining fever, myalgia, and both leg pain during more than two weeks.

History of present illness

Although he was treated with administered ceftriaxone and metronidazole in other hospital for a week.

History of past illness

There was no specific past illness.

Personal and family history

There was no specific personal and family history.

Physical examination

However, his C-reactive protein (CRP) was still high (37.71 mg/dL) and complaining symptoms such as fever, both leg pain was still remained. Therefore, he was admitted to our hospital for further assessment.

Laboratory examinations

His blood, urine culture findings were all negative. And his serologic results such as hepatitis viral marker, rheumatoid factor, anti-cyclic citrullinated peptide antibody, antineutrophil cytoplasmic antibody and anti-nuclear antibody were negative. Because he complained daily fever after admission, fever of unknown origin work up was needed.

Imaging examinations

There were no clinically significant findings without two small hemangiomas in the liver on contrast enhanced computed tomography in whole body including neck, chest, and abdomen-pelvic cavity. FDG-PET/CT on day 5 showed vasculitis involving small to medium vessels of both lower extremities by showing somewhat linear hypermetabolism through the muscles (Figure 1).

FINAL DIAGNOSIS

Finally, he was diagnosed PAN according to criteria by showing satisfied with unexplained more than 4

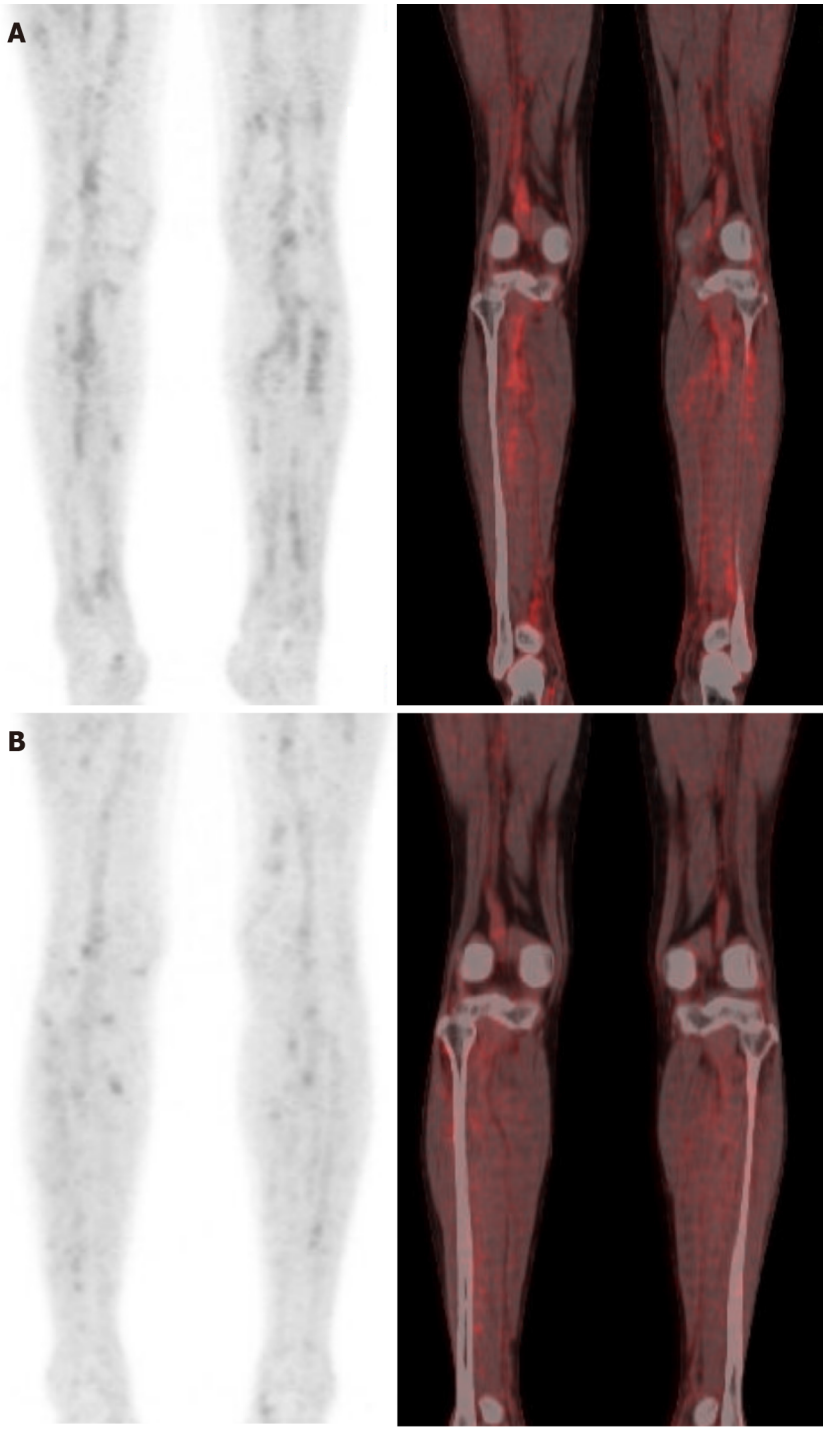

DOI: 10.12998/wjcc.v11.i4.918

Figure 1 Fluorodeoxyglucose-positron emission tomography/computed tomography. A: Fluorodeoxyglucose-positron emission tomography/computed tomography image showed hypermetabolism in both lower extremities; B: After treatment 3 wk later, lesion was markedly improved.

kg of weight loss, myalgia, new onset more than 90 mmHg of diastolic blood pressure and elevated of blood urea nitrogen > 40mg/dL according to the American College of Rheumatology proposed classification criteria for PAN in 1990[1].

TREATMENT

The patient was treated with more than 1mg/kg dosage of methylprednisolone intravenously and immunosuppressants. The patient was treated with high dosage of prednisolone, and methotrexate after diagnosis.

OUTCOME AND FOLLOW-UP

Then, his symptoms were resolved, and his CRP level was 1.19 mg/dL. After 3 wk later, he was performed FDG-PET/CT again to identify his vasculitis state. As a result, previous hypermetabolism of vessels were markedly improved. After resolution of his symptoms, the patient was tapered glucocorticoids and methotrexate and maintained improved status in outpatient clinic.

DISCUSSION

It is already known that FDG-PET/CT has new diagnostic tool to detect large vessel vasculitis, with its high sensitivity for vessel inflammation[2]. And FDG-PET/CT was shown possibility as a promising prognostic marker by identification of patients having risk of vascular complications. In addition, prior report suggests that FDG-PET/CT can be a role of showing therapeutic efficacy[3].

CONCLUSION

This patient's finding indicates that FDG-PET/CT can be an option to diagnose small to medium vessels vasculitis and follow-up to evaluated on the extent and improvement of vessel inflammation in patients with PAN to show therapeutic effects.

FOOTNOTES

Author contributions: Kang JH designed the research study, performed the research, analyzed the data and wrote the manuscript; Kim JH performed the research; All authors have read and approve the final manuscript.

Informed consent statement: Informed written consent was obtained from the patient for publication of this report and any accompanying images.

Conflict-of-interest statement: The authors declare that they have no conflict of interest to disclose.

CARE Checklist (2016) statement: The authors have read the CARE Checklist (2016), and the manuscript was prepared and revised according to the CARE Checklist (2016).

Country/Territory of origin: South Korea

ORCID number: Ji-Hyoun Kang 0000-0003-1113-2001.

S-Editor: Liu GL
L-Editor: A
P-Editor: Liu GL

REFERENCES

1 **Lightfoot RW Jr**, Michel BA, Bloch DA, Hunder GG, Zvaifler NJ, McShane DJ, Arend WP, Calabrese LH, Leavitt RY, Lie JT. The American College of Rheumatology 1990 criteria for the classification of polyarteritis nodosa. *Arthritis Rheum* 1990; **33**: 1088-1093 [PMID: 1975174 DOI: 10.1002/art.1780330805]

2 **Slart RHJA**; Writing group; Reviewer group; Members of EANM Cardiovascular; Members of EANM Infection & Inflammation; Members of Committees, SNMMI Cardiovascular; Members of Council, PET Interest Group; Members of ASNC; EANM Committee Coordinator. FDG-PET/CT(A) imaging in large vessel vasculitis and polymyalgia rheumatica: joint procedural recommendation of the EANM, SNMMI, and the PET Interest Group (PIG), and endorsed by the ASNC. *Eur J Nucl Med Mol Imaging* 2018; **45**: 1250-1269 [PMID: 29637252 DOI: 10.1007/s00259-018-3973-8]

3 **Pelletier-Galarneau M**, Ruddy TD. PET/CT for Diagnosis and Management of Large-Vessel Vasculitis. *Curr Cardiol Rep* 2019; **21**: 34 [PMID: 30887249 DOI: 10.1007/s11886-019-1122-z]

World Journal of Clinical Cases

Submit a Manuscript: https://www.f6publishing.com

World J Clin Cases 2023 February 6; 11(4): 922-930

DOI: 10.12998/wjcc.v11.i4.922

ISSN 2307-8960 (online)

CASE REPORT

Easily misdiagnosed complex Klippel-Trenaunay syndrome: A case report

Ling-Li Li, Rui Xie, Fu-Qing Li, Cheng Huang, Bi-Guang Tuo, Hui-Chao Wu

Specialty type: Gastroenterology and hepatology

Provenance and peer review: Unsolicited article; Externally peer reviewed.

Peer-review model: Single blind

Peer-review report's scientific quality classification

Grade A (Excellent): 0
Grade B (Very good): 0
Grade C (Good): C
Grade D (Fair): 0
Grade E (Poor): 0

P-Reviewer: Kumar S, India

Received: September 29, 2022
Peer-review started: September 29, 2022
First decision: December 13, 2022
Revised: December 31, 2022
Accepted: January 10, 2023
Article in press: January 10, 2023
Published online: February 6, 2023

Ling-Li Li, Rui Xie, Fu-Qing Li, Cheng Huang, Bi-Guang Tuo, Hui-Chao Wu, Department of Gastroenterology, Digestive Disease Hospital, Affiliated Hospital of Zunyi Medical University, Zunyi 563003, Guizhou Province, China

Corresponding author: Hui-Chao Wu, MM, Chief Physician, Department of Gastroenterology, Digestive Disease Hospital, Affiliated Hospital of Zunyi Medical University, No. 149 Dalian Street, Huichuan District, Zunyi 563003, Guizhou Province, China. wuhuichao985@163.com

Abstract

BACKGROUND

Klippel-Trenaunay syndrome (KTS) is a congenital vascular malformation with a complicated etiology. It is sporadic and clinically rare in occurrence. The typical characteristics are capillary malformation (also known as port-wine stain), varicose veins and malformations, and bony and/or soft tissue hypertrophy with or without lymphatic malformation, which are known as the "classic clinical triad". Herein, a rare case of KTS characterized by crossed-bilateral limb hypertrophy accompanied by intermittent hematochezia and hematuria is reported.

CASE SUMMARY

We described a 37-year-old female with KTS. She was admitted to our hospital owing to the gradual enlargement of the left lower extremity along with intermittent hematochezia and hematuria. The patient was diagnosed to have hemorrhoid bleeding by other hospitals and treated with conventional hemostatic drugs, but continued to have intermittent gastrointestinal bleeding and hematuria. Therefore, she visited our hospital to seek further treatment. During hospitalization, relevant imaging and laboratory examinations and colonoscopy were performed. In combination with the patient's history and relevant examinations, we considered that the patient had a complex form of KTS. We recommended a combined diagnosis and treatment from the vascular, interventional, anorectal, and other departments, although she declined any further treatment for financial reasons.

CONCLUSION

The clinical manifestations of KTS are extensive and diverse and chiefly include the typical triad. However, Vascular malformations of KTS can also involve several parts and systems such as digestive and urogenital systems. Therefore, the atypical manifestations and rare complications necessitate the clinician's attention and are not to be ignored.

Key Words: Gross hematuria; Hematochezia; Klippel-Trenaunay syndrome; Limb hypertrophy; Vascular malformation; Case report

Core Tip: Klippel-Trenaunay syndrome (KTS) is a complicated, mixed, low-flow vascular malformation syndrome. Vessels that show abnormalities include skin capillaries, veins, and lymphatic vessels. Vascular malformation can lead to soft tissue and/or bony hypertrophy and, hence, KTS is also known as venous malformation and bone hypertrophy syndrome. However, Vascular malformations of KTS can also involve several parts and systems such as digestive and urogenital systems. KTS is a rare congenital disease and the clinical manifestations of it are extensive and diverse. This patient that we reported was initially misdiagnosed to have filariasis and hemorrhoid bleeding. Therefore, the atypical manifestations and rare complications necessitate the clinician's attention and are not to be ignored.

Citation: Li LL, Xie R, Li FQ, Huang C, Tuo BG, Wu HC. Easily misdiagnosed complex Klippel-Trenaunay syndrome: A case report. *World J Clin Cases* 2023; 11(4): 922-930
URL: https://www.wjgnet.com/2307-8960/full/v11/i4/922.htm
DOI: https://dx.doi.org/10.12998/wjcc.v11.i4.922

INTRODUCTION

First described by the French physicians Klippel and Trénaunay in 1900, Klippel-Trenaunay syndrome (KTS) is also known as congenital venous malformation and bone hypertrophy syndrome. KTS is a rare disease with an incidence rate of 2-5/100000[1], involving multiple factors and its pathogenesis is not well understood. It exhibits a series of clinical symptoms and complications, including capillary malformation, varicose veins and malformations, and bony and/or soft tissue hypertrophy with or without lymphatic malformation, which often affects only one lower extremity. These symptoms are denoted as the "classic clinical triad"[2]. The clinical diagnosis of KTS is based on the presence of two of these features[3]. Moreover, some atypical KTS cases need to be diagnosed based on a detailed medical history combined with physical and imaging examinations. The disease is sporadic and rare and lacks any obvious aggregation tendencies of family, sex, and race[1,4]. In addition, the clinical manifestations are extensive and vary immensely. Therefore, there is no standard treatment for KTS. Because the syndrome often presents with swelling and varicose veins in the lower extremities, it is imperative to distinguish it from non-gene related diseases, such as filariasis and varicose veins that are not induced by vascular malformations, to avoid misdiagnosis. Vascular malformations associated with KTS can affect the extremities, particularly one lower extremity and, rarely, bilateral or upper extremities. In addition to the extremities, the splanchnic system can be involved. The involvement of the gastrointestinal tract may appear in the form of intermittent or continuous bleeding in the digestive tract, whereas the involvement of the urogenital system may appear in the form of life-threatening hematuria with massive bleeding[5]. According to the literature, KTS marked by the involvement of both the gastrointestinal and urogenital systems is rare (about 1%) and only one case of KTS with crossed-bilateral extremity involvement has been reported[6]. Herein, we have reported a case of KTS characterized by crossed-bilateral extremity involvement combined with lower gastrointestinal hemorrhage and hematuria. Based on our literature search, we could not find any other similar case. This patient was initially misdiagnosed in other hospitals to have filariasis and hemorrhoid bleeding.

CASE PRESENTATION

Chief complaints

A 37-year-old female presented to the gastroenterology clinic because of the gradual enlargement of the left lower extremity along with intermittent hematochezia and hematuria for 5 mo.

History of present illness

The patient had repeated hematochezia with intermittent gross hematuria for 5 mo, and the symptoms gradually worsened.

History of past illness

The female patient was found to have several port wine stains on the skin of her left lower extremity and hip after birth. In addition, her left lower extremity was found to be larger than the right lower extremity since childhood, which gradually increased with age and was accompanied with pain and heaviness. At the age of 14 years, she was diagnosed with "filariasis" by other hospitals; however, no improvement was noted after the anti-filarial treatment. Repeated hematochezia began to appear at the age of 7 years. The bleeding frequency was low (3-5 times/mo), and the amount was small. As the problem was self-limiting and did not affect her normal life, the patient did not undergo enteroscopy or professional treatment. However, the hematochezia gradually worsened and intermittent gross hematuria appeared. She was admitted to another hospital and was diagnosed to have hemorrhoid bleeding. She was treated with conventional hemostatic drugs, but continued to have intermittent gastrointestinal bleeding and hematuria.

Personal and family history

Her parents did not have a consanguineous marriage, and nobody else in the family had a similar medical history.

Physical examination

The patient walked with asymmetry in both lower extremities and mild claudication. Her skin and sclera were pale. There was a mild enlargement in the right arm, and her fingers were thickened. There was a small piece of port-wine stain on the back of her hand (Figure 1A and B), and the varicose veins were seen on the forearm (black arrows in Figure 1C). Furthermore, there were several map-like port wine stains on the left lower extremity, hip, and trunk (Figure 1D-H). The left hip and the left extremity were obviously enlarged, with giant deformed toes (Figure 1E-H) and atypical varicose veins on the outside of the leg (black arrows in Figure 1G).

Laboratory examinations

Blood routine: Hemoglobin 88g/L. Liver function was normal.

Imaging examinations

Abdominal computed tomography (CT)-plain scan + enhancement: The spleen was large, with multiple low-density shadows, which were considered to be vascular lesions (hemangioma). The rectal wall was unevenly thickened, and the enhancement was not uniform. The left ovarian vein was thickened, with a filling-defect area. The left iliac vein and pelvic floor vein were slightly thickened and tortuous. Multiple speckled calcium density shadows were observed in the pelvic cavity. The bladder wall was slightly thickened, and venous stones were detected (Figure 2). Left lower extremity magnetic resonance imaging (MRI)-plain scan + enhancement: There was an obvious enlargement in the left lower extremity, with multiple tortuous strip long T1/T2 and enhanced signals in the subcutaneous soft tissues, muscle space, and the muscle soft tissue area. Subcutaneous varicose veins were prominent on the left leg, with an obvious enhancement. Multiple reticular long T2WI signal shadows were observed in the surrounding muscles and soft tissues, with mild enhancement (Figure 3). X-ray of both lower extremities: The spine exhibited a slight compensatory deviation to the left. The soft tissue of the left lower extremity was thickened, with nonuniform density and a normal bone structure (Figure 4).

FINAL DIAGNOSIS

Based on the patient's medical history and the various clinical presentation and related examinations and tests, she was diagnosed with a complex form of KTS.

TREATMENT

As the patient was currently not showing any symptoms of hematuria and no active colonic bleeding was observed in the colonoscopy, no other drug or treatment was administered. However, in order to prevent the aggravation of the patient's condition and avoid gastrointestinal rebleeding, we recommended a combined diagnosis and treatment from the vascular, interventional, anorectal, and other departments, although she declined any further treatment for financial reasons. Presently, the patient is on conventional hemostatic drugs and iron treatment.

DOI: 10.12998/wjcc.v11.i4.922

Figure 1 Physical examination. A and B: There was a mild enlargement in the right arm and the right fingers; C: Varicose veins was observed on the right forearm (black arrows); D-H: There were several map-like port wine stains on the left lower extremity, hip, and trunk (E); there was an obvious enlargement in the left hip (F-H); there was an obvious enlargement in the left extremity with atypical varicose (Servelle veins) veins outside the leg (G, black arrows); the left toe was extremely enlarged and deformed (H).

OUTCOME AND FOLLOW-UP

The patient continues to experience intermittent and a small amount of hematochezia (similar to hemorrhoid bleeding), which is not life-threatening. The patient has accordingly been advised regular medical consultation. If the bleeding worsens, surgery can be considered.

DISCUSSION

KTS is a complicated, mixed, and low-flow vascular malformation syndrome. The vessels that displayed abnormalities include skin capillaries, veins, and lymphatic vessels. Vascular malformation can lead to soft tissues and/or bony hypertrophy; hence, KTS is also known as venous malformation and bone hypertrophy syndrome[7]. The etiology of KTS is complex and controversial. The somatic *PIK3CA* mutation is believed to cause abnormal hyperplasia of the blood vessels, bone, and soft tissues[6-8]. Furthermore, chromosome translocation may be involved[9]. A recent theory suggested that this disease is related to mesodermal dysplasia acting on angiogenesis[10].

The clinical manifestations of KTS are extensive and diverse and chiefly include the typical triad (port-wine stains, varicose veins with or without venous malformations, and bony and/or soft tissue hypertrophy). The complete triad occurs in 63% of the patients and is either found at birth or develops during infancy and becomes more and more evident with age[11,12]. The patient reported in this study also exhibited similar findings. Port-wine stain is considered to be caused by skin capillary malformation, while some scholars claim that it is related to lymphoid malformation[13]. The stain has a map-like, segmental distribution.

Sreekar *et al*[14] demonstrated that venous malformations in patients with KTS can involve multiple parts and systems. Nonetheless, most of the extremity involvement is unilateral (approximately 85%) [15], especially unilateral lower extremity. In rare cases, the upper extremities, trunk, head, and neck can be involved and is usually manifested as varicose veins. Two persistent embryonic veins are common in the abnormal veins of patients with KTS: The lateral marginal vein (or the Servelle vein) and the sciatic vein. The servelle vein is present on the outside of the thigh and displays obvious varicose and malformations. There is a controversy regarding whether patients with KTS exhibit deep venous

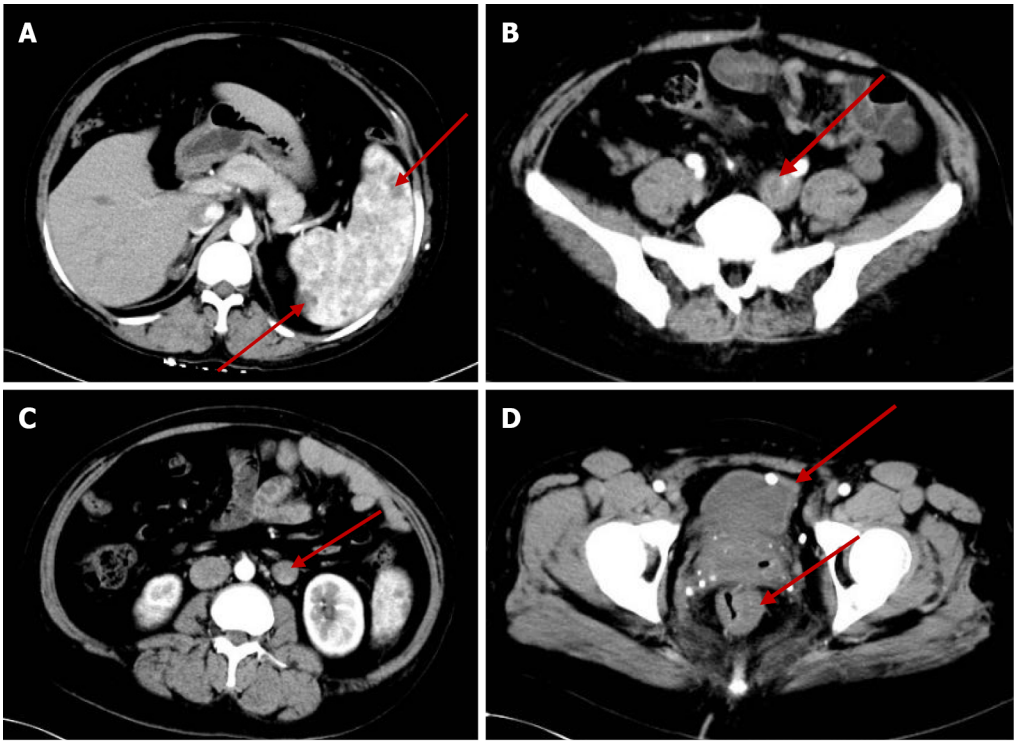

DOI: 10.12998/wjcc.v11.i4.922 **Copyright** ©The Author(s) 2023.

Figure 2 Abdominal computed tomography plain scan + enhancement. A: The spleen is large with multiple low-density shadows (hemangioma); B: The left iliac vein is thickened; C: The left ovarian vein is thickened with a filling defect area (thrombosis); D: The rectal wall is unevenly thickened. The bladder wall is slightly thickened and venous stones can be observed.

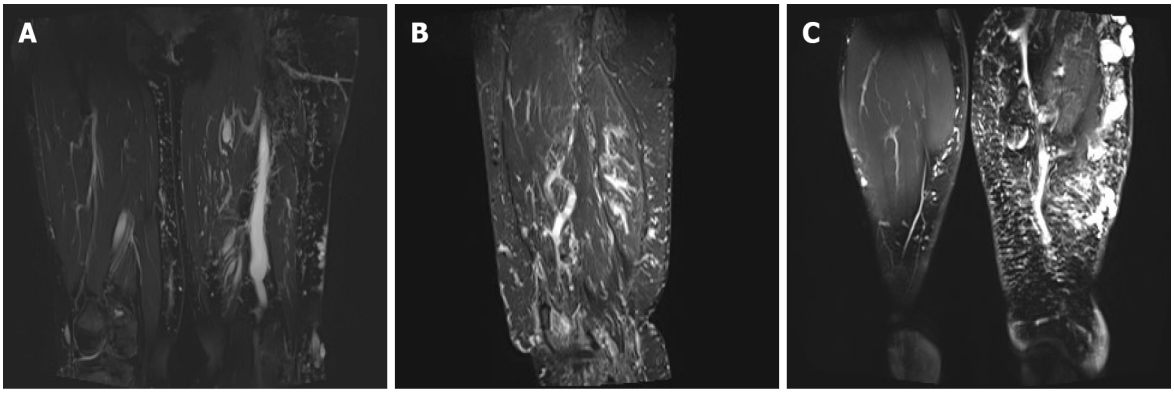

DOI: 10.12998/wjcc.v11.i4.922 **Copyright** ©The Author(s) 2023.

Figure 3 Left lower extremity magnetic resonance imaging plain scan + enhancement. A-C: Obvious enlargement, swelling, and extensive reticular signal abnormality can be seen in the left lower extremity (Lymphadenopathy). The subcutaneous varicose veins can be noted on the left leg.

abnormalities. In this case, Port-wine stain was observed in the trunk, left lower extremity, hip, and the back of the right hand (Figure 1). Mild varicose veins were observed on the right arm (Figure 1C). Obvious varicose Servelle veins were detected on the outside of the left lower extremity (Figure 1G). The right hip was more hypertrophic than the left one. This case demonstrated cross bilateral hypertrophy of the left lower and right upper extremities (Figure 1), which is quite rare and has only been reported once[6]. In addition, the patient's left toe was giant and deformed (Figure 1H), possibly related to KTS[16]. Meanwhile, the MRI of the lower extremity demonstrated significant enlargement, varicose veins and malformations, and lymphatic abnormality in the left lower extremity (Figure 3), which is consistent with the clinical characteristics of KTS. In addition to the extremity involvement, the splanchnic system can be rarely involved in patients with KTS, including the gastrointestinal tract, urogenital tract, liver, and spleen. In this case, the patient displayed intermittent hematochezia and hematuria. The relevant examination, that is, abdominal CT splenomegaly, exhibited splenic hemangioma, thickened rectal wall, thickened bladder wall, venous stone, and thickened iliac vein and ovarian vein (Figure 2). Colonoscopy revealed extensive varicose vein malformations of the intestinal

DOI: 10.12998/wjcc.v11.i4.922

Figure 4 X-ray of both the lower extremities. The spine showing a compensatory slight deviation to the left. The soft tissues of the left lower extremity were thickened with a nonuniform density.

wall (Figure 5). All these findings proved that the patient had involvement of the intestine, urogenital tract, and spleen as well as a wide range of vascular lesions. Therefore, her condition was complex and serious, for which she needed active treatment. Intestinal involvements are mostly observed in the sigmoid colon and rectum, and only a few were recorded in the entire intestine. This problem is often manifested as asymptomatic-repeated hematochezia, which can, occasionally, be life-threatening and cause massive bleeding. In case of no bleeding, the intestinal involvement may be ignored. Bleeding often occurs in the first 10 years of life[5,17]. As for the involvement of the genitourinary system, it is often manifested in the form of bleeding, such as hematuria, increased menstruation, and massive uterine bleeding during childbirth. However, the splenic involvement may be more serious because the spontaneous rupture of splenic hemangioma is life-threatening and requires emergency surgery[18,19]. Although our patient showed abnormal blood vessels in the spleen, no such acute bleeding occurred.

The most common symptoms of KTS are swelling and pain in the extremity, accompanied by obvious heaviness caused by venous disfunction and abnormal lymphatic drainage[20,21]. Other atypical manifestations include infectious cellulitis, extremity ulcer, headache, intracerebral hemorrhage, hydrocephalus, seizures[14,22,23], and even poor vision when the eyes are involved[24]. In addition, other rare complications, such as deep venous thrombosis, venous thromboembolism, pulmonary embolism, thrombophlebitis, and gangrene, may occur in the patients[25]. The abovementioned atypical manifestations and rare complications necessitate the clinician's attention and are not to be ignored.

Being a rare disease with a complex etiology, KTS can only be diagnosed clinically as no universal diagnostic criteria have been reported and pathological diagnosis is barely possible. When the patients display some atypical symptoms, the diagnosis is made based on medical history and related examinations. Based on the clinical characteristics of KTS, noninvasive imaging is the first choice to facilitate the diagnosis. Lower extremity ultrasound is the preferred modality as it can clearly display the blood flow characteristics as well as venous malformations and exhibits high sensitivity and specificity[7]. Moreover, X-ray can judge the length of bones as well as bony hypertrophy and reveal the hypertrophy of the soft tissues. CT venography or magnetic resonance venography was performed when deep vein abnormalities were considered. Most scholars believe that MRI is necessary for the diagnosis of KTS owing to its high resolution for the soft tissues and its ability to demonstrate abnormalities in the lymphatic vessels. CT can also be employed for the diagnosis of KTS, albeit it is not the first choice and not employed in routine examination. The method should be avoided in children and patients with KTS who exhibited renal disfunction because of radiation hazard and possible renal damage. When

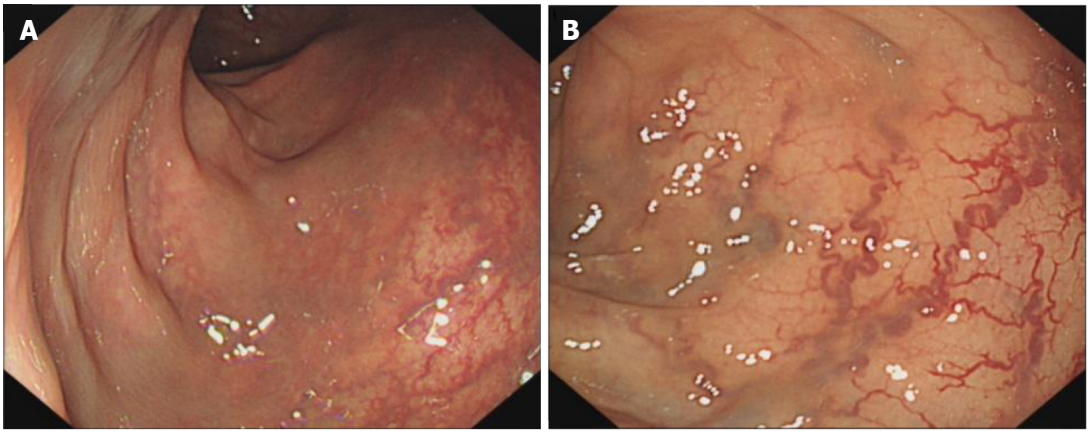

DOI: 10.12998/wjcc.v11.i4.922

Figure 5 Colonoscopy. A and B: The intestinal mucosal veins are displayed and varicosed. The intestinal wall can be observed in cyan.

considering KTS combined with pulmonary embolism, pulmonary CT angiography is preferred. If the gastrointestinal tract is involved or if the patient has hemochezia, endoscopy is essential because it can help directly visualize the blood vessels of the digestive tract and judge the bleeding site. If necessary, local hemostasis can also be performed and is of a high diagnostic value. In the present case, the patient underwent colonoscopy, which exhibited clustered abnormal expansion of the blood vessels in the intestinal wall below the descending colon (Figure 5). This finding suggested unique vascular manifestations and helped avoid misdiagnosis.

The mutations of somatic *PIK3CA* are considered to be one of the causes of vascular malformation and limb hypertrophy of KTS. Therefore, KTS is included in the PIK3CA-related overgrowth spectrum (PROS)[26]. PROS is defined as a series of rare congenital disease syndromes due to mutations in *PIK3CA*. PROS is one of the subcategories in the latest (2018) ISSVA classification, which, in addition, to including KTS, it also includes fibroadipose hyperplasia or overgrowth; congenital lipomatous overgrowth, vascular malformations, epidermal nevi, scoliosis/skeletal and spinal (CLOVES) syndrome; fibroadipose infiltrating lipomatosis/facial infiltrative lipomatosis; hemihyperplasia multiple lipomatosis; macrodactyly; megalencephaly-capillary malformation (MCAP/M-CM); fibro-adipose vascular anomaly (FAVA); capillary, lymphatic, and venous malformations and lymphatic malformation (LM). These diseases are characterized by vascular malformations and tissue overgrowth. Because KTS has several overlapping clinical features with other syndromes such as CLOVES syndrome and FAVA[27], it needs to be distinguished from these diseases. Meanwhile, according to the ISSVA classification, the clinical features of Parkes-Weber Syndrome are the same as those of KTS; the difference is that Parkes-Weber syndrome also includes arterial malformations, which are manifested as arteriovenous fistula. Moreover, while the vascular malformation is high flow in the Parkes-Weber Syndrome, it is low flow in KTS. Furthermore, KTS needs to be differentiated from non-gene related diseases, such as common pressure varicose veins and late filariasis. Filariasis is caused by the parasitism of adults in the lymphatic vessels, which blocks lymphatic circulation and results in subcutaneous tissue swelling, hypertrophy, and deformity without vascular malformation. The patient reported in this study was once misdiagnosed to have filariasis. In addition, the patients with gastrointestinal bleeding or hematuria should be distinguished from bleeding caused by simple hemorrhoids or other gastrointestinal diseases or urinary diseases with hematuria. Overall, the clinicians should bear in mind the characteristics of KTS.

Until date, there is no consensus available on the treatment of KTS. The syndrome cannot be completely cured, and symptomatic treatment is mostly given. The disease is characterized by multiple involvements, which have enormous physical and mental impacts. Lameness due to limb deformity and hypertrophy poses inconvenience in daily living and mars the appearance, which may cause psychological disorders accompanied by long-term recurrent pain[26]. Therefore, multidisciplinary cooperative treatment aimed at alleviating the symptoms, delaying disease progression as well as treatment complications, and improving the quality of life of the patients is essential in managing KTS[3,25,28]. Varicose veins can be treated by methods such as compression with elastic socks, raising the affected extremity, and other physical therapies as well as changing the lifestyle and keeping the affected extremity clean. Port-wine stain can be treated with a laser. Infectious cellulitis and thrombophlebitis are usually treated with antibiotics and symptomatic analgesic treatment in case of pain. Anticoagulant therapy is used to treat acute thrombosis, and prophylactic medications are given before operation[29]. In some cases, surgery is needed; for instance, surgical treatment is required in case of life-threatening gastrointestinal and urogenital bleeding or splenic rupture and bleeding. To manage hypertrophy of the extremity, it is possible to reduce weight *via* surgery. Nevertheless, symptomatic treatment combined with psychotherapy is the best approach for KTS[30].

CONCLUSION

KTS is a congenital vascular malformation with a complicated etiology. The somatic *PIK3CA* mutation is believed to cause abnormal hypertrophy of the blood vessels, bone, and soft tissues. The clinical manifestations of KTS are extensive and diverse and chiefly include the typical triad. However, vascular malformations of KTS can also involve several parts and systems such as digestive and urogenital systems, which increases the complexity and severity of the disease. Therefore, the atypical manifestations and rare complications necessitate the clinician's attention and are not to be ignored.

FOOTNOTES

Author contributions: Li LL and Wu HC wrote the manuscript; Tuo BG contributed to the diagnosis; Li FQ and Huang C performed literature review and followed-up; Xie R revised the manuscript; all authors have read and approved the final manuscript.

Supported by the Basic Research Projects of Science and Technology Department of Guizhou Province, No. Qian Ke He-zk[2022]-646; Master Start-up Foundation of Affiliated Hospital of Zunyi Medical College, No. 2016-45; and Collaborative Innovation Center of Chinese Ministry of Education, No. 2020-39.

Informed consent statement: Informed written consent was obtained from the patient for publication of this report and any accompanying images.

Conflict-of-interest statement: The authors declare that they have no conflict of interest.

CARE Checklist (2016) statement: The authors have read the CARE Checklist (2016), and the manuscript was prepared and revised according to the CARE Checklist (2016).

Country/Territory of origin: China

ORCID number: Ling-Li Li 0000-0002-0208-1364; Rui Xie 0000-0001-7970-5916; Fu-Qing Li 0000-0003-4447-3021; Cheng Huang 0000-0003-1882-828X; Bi-Guang Tuo 0000-0003-3147-3487; Hui-Chao Wu 0000-0002-7385-095X.

S-Editor: Chen YL
L-Editor: A
P-Editor: Chen YL

REFERENCES

1 **Permatananda PANK**, I Gusti Agung Made Adnyana Putra. Klippel Trenaunay Syndrome: A Brief Overview. *Bsm* 2021; **5**: 387-394 [DOI: 10.32539/bsm.v5i2.231]
2 **Marvin EK**, Schoch JJ, Nguyen H, Anderson KR, Driscoll DJ, Rose CH, Bendel EC, Tollefson MM. Venous thromboembolic and bleeding complications among pregnant women with Klippel-Trenaunay syndrome. *J Am Acad Dermatol* 2019; **81**: 1277-1282 [PMID: 30991120 DOI: 10.1016/j.jaad.2019.04.018]
3 **Lee A**, Driscoll D, Gloviczki P, Clay R, Shaughnessy W, Stans A. Evaluation and management of pain in patients with Klippel-Trenaunay syndrome: a review. *Pediatrics* 2005; **115**: 744-749 [PMID: 15741381 DOI: 10.1542/peds.2004-0446]
4 **Wang ZK**, Wang FY, Zhu RM, Liu J. Klippel-Trenaunay syndrome with gastrointestinal bleeding, splenic hemangiomas and left inferior vena cava. *World J Gastroenterol* 2010; **16**: 1548-1552 [PMID: 20333801 DOI: 10.3748/wjg.v16.i12.1548]
5 **Samo S**, Sherid M, Husein H, Sulaiman S, Yungbluth M, Vainder JA. Klippel-Trenaunay Syndrome Causing Life-Threatening GI Bleeding: A Case Report and Review of the Literature. *Case Rep Gastrointest Med* 2013; **2013**: 813653 [PMID: 23862081 DOI: 10.1155/2013/813653]
6 **Al-Najjar RM**, Fonseca R. An atypical case of Klippel-Trénaunay syndrome presenting with crossed-bilateral limb hypertrophy and postaxial polydactyly: a case report. *BMC Pediatr* 2019; **19**: 95 [PMID: 30954069 DOI: 10.1186/s12887-019-1480-0]
7 **Deka JB**, Deka NK, Shah MV, Bhatnagar N, Nanni AL, Jimenez F. Intraneural hemangioma in Klippel-Trenaunay syndrome: role of musculo-skeletal ultrasound in diagnosis-case report and review of the literature. *J Ultrasound* 2020; **23**: 435-442 [PMID: 32078146 DOI: 10.1007/s40477-020-00434-1]
8 **John PR**. Klippel-Trenaunay Syndrome. *Tech Vasc Interv Radiol* 2019; **22**: 100634 [PMID: 31864529 DOI:

10.1016/j.tvir.2019.100634]
9 **Oduber CE**, van der Horst CM, Hennekam RC. Klippel-Trenaunay syndrome: diagnostic criteria and hypothesis on etiology. *Ann Plast Surg* 2008; **60**: 217-223 [PMID: 18216519 DOI: 10.1097/SAP.0b013e318062abc1]
10 **Oluwafemi A**, Omokafe L, Maduka Ogechi C, Ganiyu A, Bako I, Oluleke I, Ifeoma I. Klippel-trenaunay syndrome: A rare case presenting in a 5-year-old girl. *West Afr J Radiol* 2016; **23**: 136 [DOI: 10.4103/1115-1474.164870]
11 **Kocaman O**, Alponat A, Aygün C, Gürbüz Y, Sarisoy HT, Celebi A, Sentürk O, Hülagü S. Lower gastrointestinal bleeding, hematuria and splenic hemangiomas in Klippel-Trenaunay syndrome: a case report and literature review. *Turk J Gastroenterol* 2009; **20**: 62-66 [PMID: 19330738]
12 **Harna B**, Tomar S. Klippel Trenaunay Syndrome. *Indian J Pediatr* 2020; **87**: 966-967 [PMID: 32036598 DOI: 10.1007/s12098-019-03178-x]
13 **Maari C**, Frieden IJ. Klippel-Trénaunay syndrome: the importance of "geographic stains" in identifying lymphatic disease and risk of complications. *J Am Acad Dermatol* 2004; **51**: 391-398 [PMID: 15337982 DOI: 10.1016/j.jaad.2003.12.017]
14 **Sreekar H**, Dawre S, Petkar KS, Shetty RB, Lamba S, Naik S, Gupta AK. Diverse manifestations and management options in Klippel-Trenaunay syndrome: a single centre 10-year experience. *J Plast Surg Hand Surg* 2013; **47**: 303-307 [PMID: 23710784 DOI: 10.3109/2000656X.2013.766201]
15 **Baba A**, Yamazoe S, Okuyama Y, Shimizu K, Kobashi Y, Nozawa Y, Munetomo Y, Mogami T. A rare presentation of Klippel-Trenaunay syndrome with bilateral lower limbs. *J Surg Case Rep* 2017; **2017**: rjx024 [PMID: 28458832 DOI: 10.1093/jscr/rjx024]
16 **Redondo P**, Bastarrika G, Aguado L, Martínez-Cuesta A, Sierra A, Cabrera J, Alonso-Burgos A. Foot or hand malformations related to deep venous system anomalies of the lower limb in Klippel-Trénaunay syndrome. *J Am Acad Dermatol* 2009; **61**: 621-628 [PMID: 19577333 DOI: 10.1016/j.jaad.2009.04.027]
17 **Shaikh OH**, Kumbhar US, Jain A, Chakkalakkoombil SV. Klippel-Trenaunay syndrome in a young patient with the involvement of gastrointestinal and genitourinary tracts: an unusual and rare presentation. *BMJ Case Rep* 2021; **14** [PMID: 33653847 DOI: 10.1136/bcr-2020-239420]
18 **Karakayali F**, Basaran C, Soy EA, Karakus S, Yabanoglu H, Moray G, Haberal M. Spontaneous spleen rupture and rectus sheath hematoma in a patient with Klippel-Trenaunay syndrome: report of a case. *Surg Today* 2010; **40**: 154-157 [PMID: 20107956 DOI: 10.1007/s00595-008-4008-z]
19 **de Luna Díaz Mdel M**, de Laguno de Luna A, Osorio D, Arenzana LM, Eslava Y. [Spontaneous spleen rupture in a patient with Klippel-Trenaunay syndrome]. *Cir Esp* 2011; **89**: 64-66 [PMID: 20510400 DOI: 10.1016/j.ciresp.2010.03.022]
20 **Cohen MM Jr**. Klippel-Trenaunay syndrome. *Am J Med Genet* 2000; **93**: 171-175 [PMID: 10925375 DOI: 10.1002/1096-8628(20000731)93:3<171::aid-ajmg1>3.0.co;2-k]
21 **Hale EK**. Klippel-Trenaunay syndrome. *Dermatol Online J* 2002; **8**: 13 [PMID: 12546768]
22 **Anlar B**, Yalaz K, Erzen C. Klippel-Trenaunay-Weber syndrome: a case with cerebral and cerebellar hemihypertrophy. *Neuroradiology* 1988; **30**: 360 [PMID: 2845296 DOI: 10.1007/BF00328192]
23 **Gupte GL**, Deshmukh CT, Bharucha BA, Irani SF. Klippel-Trenaunay-Weber syndrome with hydrocephalus: an unusual association. *Pediatr Neurosurg* 1995; **22**: 328-329 [PMID: 7577668 DOI: 10.1159/000120924]
24 **Olcaysu OO**, Altun A, Olcaysu E, Marzıoğlu Ozdemır E, Demır B. Unilateral cataract and vitreoretinopathy in a case with klippel-trenaunay syndrome. *Case Rep Ophthalmol Med* 2014; **2014**: 312030 [PMID: 25031878 DOI: 10.1155/2014/312030]
25 **Asghar F**, Aqeel R, Farooque U, Haq A, Taimur M. Presentation and Management of Klippel-Trenaunay Syndrome: A Review of Available Data. *Cureus* 2020; **12**: e8023 [PMID: 32528762 DOI: 10.7759/cureus.8023]
26 **Vahidnezhad H**, Youssefian L, Uitto J. Klippel-Trenaunay syndrome belongs to the PIK3CA-related overgrowth spectrum (PROS). *Exp Dermatol* 2016; **25**: 17-19 [PMID: 26268729 DOI: 10.1111/exd.12826]
27 **Bertino F**, Braithwaite KA, Hawkins CM, Gill AE, Briones MA, Swerdlin R, Milla SS. Congenital Limb Overgrowth Syndromes Associated with Vascular Anomalies. *Radiographics* 2019; **39**: 491-515 [PMID: 30844349 DOI: 10.1148/rg.2019180136]
28 **Harvey JA**, Nguyen H, Anderson KR, Schoch JJ, Bendel EC, Driscoll DJ, Palmer BA, Tollefson MM. Pain, psychiatric comorbidities, and psychosocial stressors associated with Klippel-Trenaunay syndrome. *J Am Acad Dermatol* 2018; **79**: 899-903 [PMID: 29883592 DOI: 10.1016/j.jaad.2018.05.1245]
29 **Redondo P**, Bastarrika G, Sierra A, Martínez-Cuesta A, Cabrera J. Efficacy and safety of microfoam sclerotherapy in a patient with Klippel-Trenaunay syndrome and a patent foramen ovale. *Arch Dermatol* 2009; **145**: 1147-1151 [PMID: 19841402 DOI: 10.1001/archdermatol.2009.210]
30 **Noel AA**, Gloviczki P, Cherry KJ Jr, Rooke TW, Stanson AW, Driscoll DJ. Surgical treatment of venous malformations in Klippel-Trénaunay syndrome. *J Vasc Surg* 2000; **32**: 840-847 [PMID: 11054214 DOI: 10.1067/mva.2000.110343]

World Journal of Clinical Cases

Submit a Manuscript: https://www.f6publishing.com

World J Clin Cases 2023 February 6; 11(4): 931-937

DOI: 10.12998/wjcc.v11.i4.931

ISSN 2307-8960 (online)

CASE REPORT

Benign lymphoepithelial cyst of parotid gland without human immunodeficiency virus infection: A case report

Yan Liao, Yan-Jie Li, Xian-Wen Hu, Rui Wen, Pan Wang

Specialty type: Medicine, research and experimental

Provenance and peer review: Unsolicited article; Externally peer reviewed.

Peer-review model: Single blind

Peer-review report's scientific quality classification

Grade A (Excellent): 0
Grade B (Very good): B
Grade C (Good): C
Grade D (Fair): 0
Grade E (Poor): 0

P-Reviewer: ISHIDA T, Japan; liu H, United States

Received: October 1, 2022
Peer-review started: October 1, 2022
First decision: November 30, 2022
Revised: December 13, 2022
Accepted: January 10, 2023
Article in press: January 10, 2023
Published online: February 6, 2023

Yan Liao, Xian-Wen Hu, Rui Wen, Pan Wang, Department of Nuclear Medicine, Affiliated Hospital of Zunyi Medical University, Zunyi 563003, Guizhou Province, China

Yan-Jie Li, Department of Critical Care Medicine, The Second Affiliated Hospital of Zunyi Medical University, Zunyi 563003, Guizhou Province, China

Corresponding author: Pan Wang, MD, Chief Doctor, Director, Professor, Department of Nuclear Medicine, Affiliated Hospital of Zunyi Medical University, No. 149 Dalian Road, Huichuan District, Zunyi 563003, Guizhou Province, China. 1298178828@qq.com

Abstract

BACKGROUND

Benign lymphoepithelial cyst (BLEC) of the parotid gland is a rare benign embryonic-dysplastic cystic tumor in the anterolateral neck that occurs most commonly in human immunodeficiency virus (HIV)-positive adults and rarely in non-acquired immune deficiency syndrome patients. The main presentation is a slow-growing, painless mass, and secondary infection may cause acute inflammatory symptoms.

CASE SUMMARY

A 44-year-old Chinese male patient presented with a 1-year history of a mass in the left side of the neck. On physical examination, a mass similar in size and shape to a quail egg was found in the left parotid gland. The mass was tough, without tenderness, and easily moveable. The results of HIV tests, including antibody and nucleic acid tests and CD4+ T cell examination, were negative. Imaging examination revealed a left parotid gland mass. The patient underwent surgical treatment, and BLEC was diagnosed based on postoperative pathology. After 2 years of follow-up, the patient survived well without related discomfort.

CONCLUSION

The detailed characteristics of a BLEC in a patient without HIV infection contribute to an improved understanding of this rare disease.

Key Words: Benign lymphoepithelial cyst; Parotid gland; Human immunodeficiency virus; Case report

Core Tip: Benign lymphoepithelial cyst (BLEC) of the parotid gland is a rare lesion seldom found in non-acquired immune deficiency syndrome patients. BLECs are benign embryonic dysplastic cystic tumors that typically occur in the anterolateral part of the neck. We present a case of BLEC of the parotid gland in a non-human immunodeficiency virus -infected patient in order to improve clinicians' understanding of the disease.

Citation: Liao Y, Li YJ, Hu XW, Wen R, Wang P. Benign lymphoepithelial cyst of parotid gland without human immunodeficiency virus infection: A case report. *World J Clin Cases* 2023; 11(4): 931-937
URL: https://www.wjgnet.com/2307-8960/full/v11/i4/931.htm
DOI: https://dx.doi.org/10.12998/wjcc.v11.i4.931

INTRODUCTION

Benign lymphoepithelial cyst (BLEC) of the parotid gland, which is also known as branchial cleft cyst, is a rare benign cystic neoplasm of embryonic dysplasia. It usually occurs in the anterolateral region of the neck but has been reported in the oral cavity or parotid gland in rare cases[1,2]. This disease mainly presents as a slow-growing tumor and is not associated with recurrence or metastasis. These tumors usually occur in patients with human immunodeficiency virus (HIV) infection and are rarely encountered in non-HIV-infected patients[3]. To improve clinicians' understanding of this rare disease, the present report describes the imaging, histopathological, and diagnostic characteristics of a parotid gland BLEC found in a 44-year-old, non-HIV-infected patient. The case description is followed by a review of the relevant literature.

CASE PRESENTATION

Chief complaints

A 44-year-old Chinese man was admitted to the hospital on September 1, 2020, due to a painless mass on the left side of the neck that had been present for 1 year.

History of present illness

One year previously, the patient incidentally noticed a painless mass on the left side of his neck approximately 2.0 cm × 2.0 cm in size. The patient had neck swelling occasionally, and the severity of these symptoms gradually increased over the course of the disease. The patient reported no tenderness, redness, swelling, or heat pain at the mass; no earache, swelling, or pain around the ear; and no cheek pain, numbness or difficulty when opening the mouth.

History of past illness

The patient had a history of hypertension for 1 month and was regularly taking nifedipine sustained release tablets and Irbesartan tablets as antihypertensive treatment.

Personal and family history

The patient had no personal or family history of benign or malignant tumors.

Physical examination

Physical examination on admission revealed a temperature of 36.5°C, resting respiratory rate of 20 breaths/min, heart rate of 80 bpm, and blood pressure of 117/70 mmHg. On physical examination, a mass similar in size and shape to a quail egg was found in the left parotid gland, measuring about 2.0 cm × 2.0 cm in size. The mass felt tough, without tenderness and was easily movable with no local redness, swelling, heat or pain. No abnormalities were observed in the contralateral parotid gland.

Laboratory examinations

The laboratory test results showed a white blood cell count of 6.16 × 10^9/L, with 74% neutrophils, 135 g/L hemoglobin, and a platelet count of 277 × 10^9/L. The erythrocyte sedimentation rate was 2 mm/h, and all results for routine urine, stool, liver and kidney function tests as well as electrolyte and blood biochemical index levels were within normal ranges. The results of HIV tests, including antibody and nucleic acid tests as well as CD4+ T cell examination, were negative. Furthermore, all results of testing for carcinoembryonic antigen, neuron-specific enolase, cytokeratin 19 fragment, squamous cell carcinoma antigen, blood coagulation, and immune indexes were negative.

Imaging examinations

On August 31, 2020, ultrasound of the neck recognized a 2.2 cm × 2.2 cm hypoechoic mass in the left parotid gland, with a clear boundary, coarse calcification foci, and no blood flow signal (Figure 1). On September 2, 2020, neck computed tomography (CT) showed a round cystic lesion in the left parotid gland, with a maximum cross-sectional area of approximately 2.3 cm × 2.2 cm, uneven density, small patches with slightly high-density shadows, and clear boundaries (Figure 2A). On contrast-enhanced CT, the cyst wall was slightly enhanced in the arterial phase, but no obvious enhancement was observed in the cyst (Figure 2B). The enhancement degree in the venous phase was similar to that in the arterial phase (Figure 2C). No abnormality was found in the right parotid gland.

PATHOLOGY

In general, the lesion was a pale round nodule with a complete capsule and small volume, accompanied by a small amount of parotid tissue attachment. The size was about 2.2 cm × 2.0 cm × 1.8 cm. The surface of the tumor was smooth and soft, and the surface skin mucosa was not abnormal, and the color was not special. The section was cystic, and the cyst was soybean dreg-like material with a wall thickness of 0.1 cm. Under light microscopy, the cyst wall was laminated squamous epithelium without epithelial nail process and the surface layer was mostly incomplete keratosis. The epithelium was surrounded by a large number of lymphoid stromata with lymphoid follicular formation and a center of occurrence (Figure 3). The histological features of the tumor were consistent with a diagnose of BLEC. The clinical and pathological data of this case are presented in Table 1.

FINAL DIAGNOSIS

The patient was diagnosed with a non-HIV-infected BLEC of the parotid gland on the basis of history, clinical features, and ancillary examination (imaging and histopathology).

TREATMENT

Because BLECs are benign, most cases of BLEC have a good prognosis. The principles of treatment are early diagnosis, infection control, and complete resection of the lesion without facial nerve injury. Treatment options include observation, repeat aspiration, sclerotherapy, radiotherapy, and surgery.

During the treatment period, the patient in the present case did not stop Nifedipine and Irbesartan for treatment of hypertension. Blood pressure and electrocardiography were normal at admission, and surgical treatment was possible under close monitoring of blood pressure. During surgery, care must be taken to identify the internal and external carotid arteries and vagus nerve, hypoglossal nerve, glossopharyngeal nerve, and superior laryngeal nerve to avoid injury to these structures. Finally, the patient and his family members chose surgical treatment (the specific surgical method was termed left parotid gland tumor + partial superficial lobectomy + facial nerve exploration and protection + fascia flap plasty). The operation was successful, and the patient returned to the ward safely after surgery.

OUTCOME AND FOLLOW-UP

The patient was followed up for 2 years. CT/magnetic resonance imaging (MRI) and color ultrasound were not performed during follow-up, because the patient felt no obvious symptoms.

DISCUSSION

BLEC is a rare cystic neoplasm with benign embryonic dysplasia. The first case of BLEC was reported by Hildebrandt in 1895, but only 21 cases were published by researchers through 1981. With the emergence of the HIV epidemic, the incidence of BLEC in the parotid gland gradually increased, and researchers found that BLECs were closely related to HIV infection in most cases, with BLEC as one of the early clinical manifestations. Around 3%-6% of HIV-positive adults and 1%-10% of HIV-positive children experience BLEC symptoms. In sharp contrast, BLECs are rarely found in non-HIV-infected patients, and the exact prevalence of BLEC in this population has not been reported[1-4]. In the present case, the results of HIV tests, including antibody and nucleic acid tests as well as CD4+ T cell examination, were negative. In previous reports, the disease was also known as branchial cleft cyst and usually observed in either the mandibular angle at the bottom of the outer regions or in the anterior

Table 1 Clinical and pathological data of this case of benign lymphoepithelial cyst of the parotid gland

	Finding
Age, sex	44 years, male
Family history	None
Personal history	None
Chief complaint	Left neck painless mass present for 1 year
Physical examination	A quail egg-shaped mass on the left parotid gland, about 2.0 cm × 2.0 cm in size, tough, without tenderness, easily moveable, no local redness, swelling, heat or pain, and no abnormalities in the contralateral parotid gland
Laboratory examinations	HIV tests, including antibody and nucleic acid tests and CD4+ T cell examination, were negative
Ultrasound of the neck	A 2.2 cm × 2.2 cm hypoechoic mass in the left parotid gland, with a clear boundary, coarse calcification foci, and no blood flow signal (Figure 1)
Neck CT	A round cystic lesion in the left parotid gland, with a maximum cross-sectional area of 2.3 cm × 2.2 cm, uneven density, small patches with slightly high-density shadows, and clear boundaries (Figure 2A). On enhanced scanning, the cyst wall was slightly enhanced in the arterial phase, but no obvious enhancement was observed in the cyst (Figure 2B). The enhancement degree in the venous phase was similar to that in the arterial phase (Figure 2C)
Pathology	The cyst wall was laminated squamous epithelium without epithelial nail process and the surface layer was mostly incomplete keratosis (Figure 3A); The epithelium was surrounded by a large number of lymphoid stromata with lymphoid follicular formation and a center of occurrence (Figure 3B)
Final diagnosis	Non-HIV-infected BLEC of parotid gland
Treatment	Surgical treatment (specific surgical method was termed left parotid gland tumor + partial superficial lobectomy + facial nerve exploration and protection + fascia flap plasty)
Follow-up	No recurrence of symptoms in 2-year clinical follow-up

HIV: Human immunodeficiency virus; CT: Computed tomography; BLEC: Benign lymphoepithelial cyst.

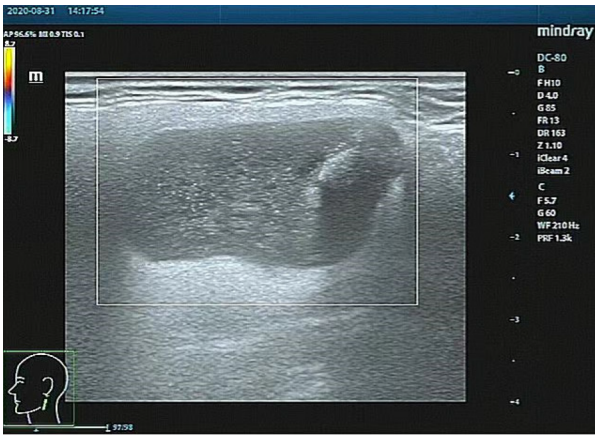

DOI: 10.12998/wjcc.v11.i4.931

Figure 1 Color ultrasound of the neck. It reveals a 2.2 cm × 2.2 cm hypoechoic mass in the left parotid gland, with a clear boundary, coarse calcification foci, and no blood flow signal.

portion of the sternocleidomastoid. It was found to occur less frequently in the mouth or parotid gland. In addition, its distribution in men and women is uniform. Although catheter jam seems to be a cause, the source of the blockage is often not obvious. Furthermore, its pathogenesis remains unclear. Currently, the majority of researchers believe that extraglandular lymphoid infiltration and/or intraglandular lymphoid hyperplasia with duct obstruction and/or epithelial embedding is the main cause.

BLEC is a slow-growing tumor not associated with recurrence or metastasis[5-8]. The main symptom of this disease is a slowly growing, painless swollen mass, often combined with local symptoms such as dysphagia, dysphagia, dyspnea and stridor, and secondary infection can manifest as acute inflammatory symptoms, such as redness, swelling and fever[3,8]. The diagnosis of BLEC mainly depends on history, clinical manifestations, and preoperative auxiliary examination. Preoperative auxiliary diagnostic procedures include CT, MRI, ultrasound and fine needle aspiration (FNA)[9]. To date, imaging characteristics of this disease have been rarely reported. By reviewing the relevant literature[1,

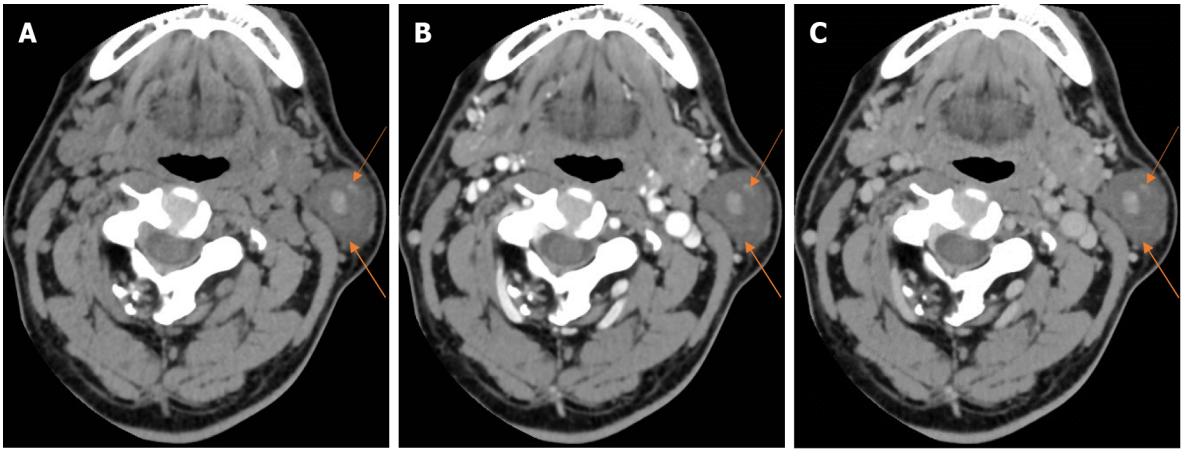

DOI: 10.12998/wjcc.v11.i4.931 **Copyright** ©The Author(s) 2023.

Figure 2 Neck computed tomography. A: Plain computed tomography scan. A round cystic lesion was seen in the left parotid gland, with a maximum cross-sectional area of about 2.3 cm × 2.2 cm, uneven density, small patches with slightly high-density shadow, and clear boundary; B: Arterial phase. On enhanced scanning, the cyst wall was slightly enhanced in the arterial phase, but no obvious enhancement was observed in the cyst; C: Venous phase. The enhancement degree in the venous phase was similar to that in the arterial phase (orange arrows).

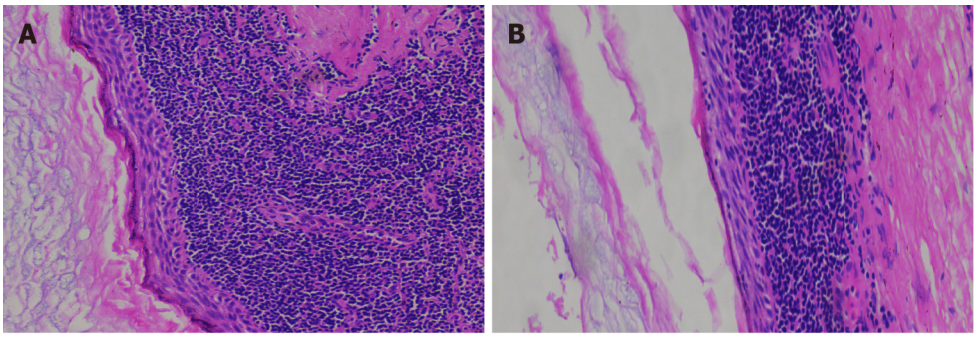

DOI: 10.12998/wjcc.v11.i4.931 **Copyright** ©The Author(s) 2023.

Figure 3 Histopathology of benign lymphoepithelial cyst of the parotid gland. A: The cyst wall was laminated squamous epithelium without epithelial nail process and the surface layer was mostly incomplete keratosis; B: The epithelium was surrounded by a large number of lymphoid stromata with lymphoid follicular formation and a center of occurrence (hematoxylin–eosin staining, magnification × 200).

9], we found that the CT manifestations of a typical BLEC are a single, thin-walled round or oval cystic foci in the parotid gland, with clear boundaries and low density in the cyst. On enhanced scanning, only the cyst wall shows mild to moderate enhancement, and no enhancement is seen in the cyst. In the present case, CT showed that the small patches with slightly high-density in the parotid gland were caused by viscous fluid in the capsule or lesions complicated with infection. MRI mainly showed a single thin-walled cystic lesion in the parotid gland, which was round or oval in shape, with a clear boundary, and the cyst wall showed a low signal. Intracystic T1 weighted imaging showed low signal, while T2 weighted imaging showed high signal. Moreover, the cyst wall was significantly enhanced on enhanced scanning, but no enhancement was found in the cyst[2]. Ultrasonic features of the lesions included a circular shape with a complete capsule and smooth lining, and cystic wall blood flow signals were not rich. The epithelial cells in a BLEC may contain keratin, and shed inflammatory cells can form a viscous gel-like yellowish-white liquid[10,11]. The internal echo of the cyst can generally appear as one of three types, including coarse granular hyperecho and cloud weak echo mixed signal, clear cystic echo through sound, and cluster weak echo and cystic echo mixed. In this case, ultrasound showed typical mixed signals including coarse granular hyperechoic signal and cloud weak echo signal. FNA can be used as an important auxiliary method for the clinical diagnosis of lateral cervical lesions. The criteria for FNA cytological diagnosis of BLEC include thick, yellow, pustular fluid; non-nucleated cells; keratinocytes; and squamous epithelial cells of varying maturity[1]. Histologically, the walls of BLEC cysts are usually covered with squamous epithelium and/or, in some cases, columnar or cuboidal cells. Lymphoid tissue with or without germinal centers in subepithelial connective tissue is the most prominent morphological feature[12]. Histological examination of the mass case showed that the cyst wall was laminated squamous epithelium without epithelial nail process and the surface layer was mostly incomplete keratosis, surrounded by a large number of lymphoid stromata with lymphoid follicular formation and a center of occurrence. Differential diagnoses include: (1) Warthin tumor[2],

which is more common in middle-aged and elderly patients and more likely to occur in the posterior lower pole of the parotid gland, with uneven internal density; (2) Intramuscular benign hemangioma [13], which is a fast-flowing intramuscular mass with uneven density and visible fat density in children that requires pathological examination for diagnosis; (3) Lymphoma[14], which is more common in men over 50 years old and appears as irregular soft tissue masses with a large range and uniform density on CT, without obvious calcification, cystic degeneration or necrosis, with diffuse growth to the surrounding area and mostly without adjacent bone destruction, and mild to moderate enhancement on enhanced scanning; (4) Thyroglossal duct cysts[15], which present as a painless mass in the front of the neck and are usually dumbbell shaped and movable when the tongue is extended or swallowed; CT shows a low-density, usually monocular parenchyma lesion during embryonic thyroid migration, mostly located in the midline and associated with the hyoid bone; (5) Lymphocele[16], which typically manifest as a cystic density focus with uniform density, clear boundary, thin cyst wall, no obvious exudation and calcification, and after enhancement, the cyst wall can present slightly uniform enhancement, with no enhancement in the cyst; (6) Metastatic lymph nodes[17], which are accompanied by a history of primary tumor, and on CT exhibit uneven density, calcification, cystic or necrotizing changes, uneven edges, adhesion to surrounding tissues, and obvious annular or peripheral enhancement; and (7) Lymphadenitis[18], which is more common in children and present with local redness, swelling, heat and pain while appearing mostly oval with a thick wall and ring and uniform enhancement without obvious wall nodules and calcification, but with a blurred surrounding fat space. The current treatment principles for this disease include early diagnosis, infection control, and cyst removal, and the treatment options include observation, repeated aspiration, sclerotherapy, radiotherapy, and surgical treatment[4]. Observation in asymptomatic patients shows that repeated aspiration therapy is generally ineffective, and cysts will recur within weeks to months. Sclerotherapy is limited in scope and is generally only used for cases in which the cystic fluid can be aspirated, while radiotherapy is mostly used for HIV-infected BLEC[3]. For our patient, surgery was the best treatment at present, and attention was paid to identify and avoid injury to adjacent blood vessels and nerves during surgery. In this case, surgical treatment was chosen by the patient, and the specific surgical procedure was termed left parotid gland tumor + partial superficial lobectomy + facial nerve exploration and protection + fascia flap plasty. The potential complications of surgical treatment include recurrence, the formation of persistent fistula, and cranial nerve injury, which require close follow-up. In this case, the patient survived well with no related discomfort after 2 years of follow-up.

CONCLUSION

BLEC in the absence of HIV infection is a rare benign cystic tumor of embryonic dysplasia, known as a branchial cleft cyst. The disease progresses slowly. Because the imaging, histopathology, and diagnosis and treatment characteristics of non-HIV-infected BLEC are poorly understood, the present case is reported to increase readers' awareness of the disease.

ACKNOWLEDGEMENTS

We thank Medjaden Inc. for scientific editing of this manuscript.

FOOTNOTES

Author contributions: Liao Y and Li YJ contributed to the study conception and writing; Liao Y and Hu XW contributed to the collection of pathological findings; Hu XW and Wen R contributed to the analysis; Li YJ collected data; Wang P reviewed and revised the first draft; all authors read and approved the final version of the manuscript.

Supported by Zunyi Medical College Research Start Fund, No. 2017CK-1130-038.

Informed consent statement: Informed written consent was obtained from the patient for publication of this report and any accompanying images.

Conflict-of-interest statement: The authors declare that they have no conflict of interest to disclose.

CARE Checklist (2016) statement: The authors have read the CARE Checklist (2016), and the manuscript was prepared and revised according to the CARE Checklist (2016).

Country/Territory of origin: China

ORCID number: Yan Liao 0000-0001-9799-9954; Yan-Jie Li 0000-0003-3650-8052; Xian-Wen Hu 0000-0001-7251-2329; Rui Wen 0000-0002-8522-2053; Pan Wang 0000-0001-7083-0016.

S-Editor: Liu GL
L-Editor: A
P-Editor: Liu GL

REFERENCES

1 **Najib Z**, Berrada O, Lahjaouj M, Oukessou Y, Rouadi S, Abada RA, Roubal M, Mahtar M. Cervical lymphoepithelial cyst: Case report and literature review. *Ann Med Surg (Lond)* 2021; **61**: 185-187 [PMID: 33489106 DOI: 10.1016/j.amsu.2020.12.041]
2 **Joshi J**, Shah S, Agarwal D, Khasgiwal A. Benign lymphoepithelial cyst of parotid gland: Review and case report. *J Oral Maxillofac Pathol* 2018; **22**: S91-S97 [PMID: 29491615 DOI: 10.4103/jomfp.JOMFP_252_17]
3 **Pillai S**, Agarwal AC, Mangalore AB, Ramaswamy B, Shetty S. Benign Lymphoepithelial Cyst of the Parotid in HIV Negative Patient. *J Clin Diagn Res* 2016; **10**: MD05-MD06 [PMID: 27190845 DOI: 10.7860/JCDR/2016/17915.7609]
4 **Dave SP**, Pernas FG, Roy S. The benign lymphoepithelial cyst and a classification system for lymphocytic parotid gland enlargement in the pediatric HIV population. *Laryngoscope* 2007; **117**: 106-113 [PMID: 17202938 DOI: 10.1097/01.mlg.000024]
5 **Nahata V**. Branchial Cleft Cyst. *Indian J Dermatol* 2016; **61**: 701 [PMID: 27904209 DOI: 10.4103/0019-5154.193718]
6 **Zimmerman KO**, Hupp SR, Bourguet-Vincent A, Bressler EA, Raynor EM, Turner DA, Rehder KJ. Acute upper-airway obstruction by a lingual thyroglossal duct cyst and implications for advanced airway management. *Respir Care* 2014; **59**: e98-e102 [PMID: 24170914 DOI: 10.4187/respcare.02513]
7 **Fujibayashi T**, Itoh H. Lymphoepithelial (so-called branchial) cyst within the parotid gland. Report of a case and review of the literature. *Int J Oral Surg* 1981; **10**: 283-292 [PMID: 6809660 DOI: 10.1016/s0300-9785(81)80073-7]
8 **Chavan S**, Deshmukh R, Karande P, Ingale Y. Branchial cleft cyst: A case report and review of literature. *J Oral Maxillofac Pathol* 2014; **18**: 150 [PMID: 24959062 DOI: 10.4103/0973-029X.131950]
9 **Glosser JW**, Pires CA, Feinberg SE. Branchial cleft or cervical lymphoepithelial cysts: etiology and management. *J Am Dent Assoc* 2003; **134**: 81-86 [PMID: 12555960 DOI: 10.14219/jada.archive.2003.0020]
10 **da Silva KD**, Coelho LV, do Couto AM, de Aguiar MCF, Tarquínio SBC, Gomes APN, Mendonça EF, Batista AC, Nonaka CFW, de Sena LSB, Alves PM, Libório-Kimura TN, Louredo BVR, Câmara J, Caldeira PC. Clinicopathological and immunohistochemical features of the oral lymphoepithelial cyst: A multicenter study. *J Oral Pathol Med* 2020; **49**: 219-226 [PMID: 31782199 DOI: 10.1111/jop.12978]
11 **Reynolds JH**, Wolinski AP. Sonographic appearance of branchial cysts. *Clin Radiol* 1993; **48**: 109-110 [PMID: 8004887 DOI: 10.1016/s0009-9260(05)81082-7]
12 **Hirota J**, Maeda Y, Ueta E, Osaki T. Immunohistochemical and histologic study of cervical lymphoepithelial cysts. *J Oral Pathol Med* 1989; **18**: 202-205 [PMID: 2475614 DOI: 10.1111/j.1600-0714.1989.tb00763.x]
13 **Wee SJ**, Park MC, Chung CM, Tak SW. Intramuscular hemangioma in the zygomaticus minor muscle: a case report and literature review. *Arch Craniofac Surg* 2021; **22**: 115-118 [PMID: 33957738 DOI: 10.7181/acfs.2021.00087]
14 **Thanarajasingam G**, Bennani-Baiti N, Thompson CA. PET-CT in Staging, Response Evaluation, and Surveillance of Lymphoma. *Curr Treat Options Oncol* 2016; **17**: 24 [PMID: 27032646 DOI: 10.1007/s11864-016-0399-z]
15 **Corvino A**, Pignata S, Campanino MR, Corvino F, Giurazza F, Tafuri D, Pinto F, Catalano O. Thyroglossal duct cysts and site-specific differential diagnoses: imaging findings with emphasis on ultrasound assessment. *J Ultrasound* 2020; **23**: 139-149 [PMID: 32052384 DOI: 10.1007/s40477-020-00433-2]
16 **Hekiert A**, Newman J, Sargent R, Weinstein G. Spontaneous cervical lymphocele. *Head Neck* 2007; **29**: 77-80 [PMID: 17103412 DOI: 10.1002/hed.20484]
17 **Suh CH**, Baek JH, Choi YJ, Lee JH. Performance of CT in the Preoperative Diagnosis of Cervical Lymph Node Metastasis in Patients with Papillary Thyroid Cancer: A Systematic Review and Meta-Analysis. *AJNR Am J Neuroradiol* 2017; **38**: 154-161 [PMID: 27789450 DOI: 10.3174/ajnr.A4967]
18 **Desai S**, Shah SS, Hall M, Richardson TE, Thomson JE; Pediatric Research in Inpatient Settings (PRIS) Network. Imaging Strategies and Outcomes in Children Hospitalized with Cervical Lymphadenitis. *J Hosp Med* 2020; **15**: 197-203 [PMID: 31891560 DOI: 10.12788/jhm.3333]

World Journal of Clinical Cases

Submit a Manuscript: https://www.f6publishing.com

World J Clin Cases 2023 February 6; 11(4): 938-944

DOI: 10.12998/wjcc.v11.i4.938

ISSN 2307-8960 (online)

CASE REPORT

Epithelioid trophoblastic tumor of the lower uterine segment and cervical canal: A case report

Ling-Qin Yuan, Ting Hao, Guo-You Pan, Hui Guo, Da-Peng Li, Nai-Fu Liu

Specialty type: Medicine, research and experimental

Provenance and peer review: Unsolicited article; Externally peer reviewed.

Peer-review model: Single blind

Peer-review report's scientific quality classification

Grade A (Excellent): 0
Grade B (Very good): 0
Grade C (Good): C, C
Grade D (Fair): 0
Grade E (Poor): 0

P-Reviewer: Aniţei MG, Romania; Zhang X, United States

Received: October 21, 2022
Peer-review started: October 21, 2022
First decision: November 16, 2022
Revised: November 29, 2022
Accepted: January 9, 2023
Article in press: January 9, 2023
Published online: February 6, 2023

Ling-Qin Yuan, Guo-You Pan, Hui Guo, Da-Peng Li, Nai-Fu Liu, Department of Gynecologic Oncology, Shandong Cancer Hospital and Institute, Shandong First Medical University and Shandong Academy of Medical Sciences, Jinan 250117, Shandong Province, China

Ting Hao, Department of Pathology, Shandong Cancer Hospital and Institute, Shandong First Medical University and Shandong Academy of Medical Sciences, Jinan 250117, Shandong Province, China

Corresponding author: Ling-Qin Yuan, MD, PhD, Chief Physician, Department of Gynecologic Oncology, Shandong Cancer Hospital and Institute, Shandong First Medical University and Shandong Academy of Medical Sciences, No. 440, Jiyan Road, Jinan 250117, Shandong Province, China. ylqsd@aliyun.com

Abstract

BACKGROUND

Epithelioid trophoblastic tumor (ETT) is the rarest type of gestational trophoblastic tumor (GTT). It has been reported that more than 50% of ETTs arise in the uterine cervix or the lower uterine segment. Here, we report a case of ETT within the lower uterine segment and cervical canal and discuss its manifestations, possible causes, and related influencing factors.

CASE SUMMARY

A 35-year-old woman (gravida 7, miscarriage 3, induction 2 with 1 being twins, para 2 of cesarean section, live 2), who had amenorrhea for 9 mo after breastfeeding for 22 mo after the last cesarean section, was diagnosed with ETT. The lesion was present in the lower uterine segment and endocervical canal with severe involvement of the anterior wall of the lower uterine segment and the front wall of the lower uterine segment where the cesarean incisions were made. Laboratory tests showed slight elevation of serum beta-human chorionic gonadotropin. Intraoperative exploration showed the presence of a normal-sized uterus body with an enlarged tumor in the lower uterine segment. The surface of the lower uterine segment was light blue, the entire lesion was approximately about 8 cm × 8 cm × 9 cm, with compression and displacement of the surrounding tissue. Histological examination diagnosed ETT. Immunohistochemical analysis showed positive expression of p63, with a Ki-67 proliferation index of 40%.

CONCLUSION

A search of the PubMed database using the search terms "cesarean section" and "epithelioid trophoblastic tumor" retrieved nine articles, including 13 cases of ETT

and ETT-related lesions, all 13 cases had a history of cesarean section, and the lesions were all located at the cesarean section incision on the anterior wall of the lower uterine segment. The present case is the 14th reported case of ETT after cesarean section. Therefore, we deduced that cesarean section trauma had an important effect on the occurrence of ETT at this site.

Key Words: Epithelioid trophoblastic tumor; Lower uterine segment; Cervical canal; p63; Gestational trophoblastic tumor; Case report

Core Tip: Epithelioid trophoblastic tumor (ETT) is rare clinically. we describe a case of ETT in the lower uterine segment and cervical canal. The lesion was present in the lower uterine segment and endocervical canal where the cesarean incisions were made. A search of the PubMed database using the search terms "cesarean section" and "ETT" retrieved 13 cases of ETT, all of which had a history of cesarean section, and the lesions were located in the cesarean incision of the uterus. Therefore, we deduced that cesarean section trauma had an important effect on the occurrence of ETT at this site.

Citation: Yuan LQ, Hao T, Pan GY, Guo H, Li DP, Liu NF. Epithelioid trophoblastic tumor of the lower uterine segment and cervical canal: A case report. *World J Clin Cases* 2023; 11(4): 938-944
URL: https://www.wjgnet.com/2307-8960/full/v11/i4/938.htm
DOI: https://dx.doi.org/10.12998/wjcc.v11.i4.938

INTRODUCTION

Epithelioid trophoblastic tumor (ETT) is a rare form of gestational trophoblastic tumor (GTT) and is clinically uncommon. It arises from the malignant transformation of intermediate trophoblastic cells at the chorionic leave. Transformation of placental site nodules to ETT has been observed on histological examination of surgical specimens[1]. ETT tends to be diagnosed after pathological assessment of curettage or surgical specimens. There are no specific symptoms or signs and the reported interval between the antecedent pregnancy and the clinical manifestation ranges from 1 to 15 years, with an average of 6.2 years. Specifically, over 50% of ETTs arise in the cervix or low uterine segment[2]. Here, we report a case of ETT within the lower uterine segment and cervical canal and discuss its manifestations, possible causes, and related influencing factors.

CASE PRESENTATION

Chief complaints

A 35-year-old woman presented to our hospital after 9 mo of amenorrhea and 10 d after hysteroscopy.

History of present illness

She went to the local county hospital because after 22 mo of breastfeeding, she had amenorrhea for 2 mo. She had experienced no discomfort. She was scheduled for an ultrasound that showed a suspected 2 cm uterine fibroid or uterine cyst and was followed up regularly. Seven months later, menstruation had still not commenced. During the follow-up consultation, a 5.0 cm x 4.5 cm x 3.1 cm inhomogeneous echo was observed in the lower uterine cavity and cervix, adjacent to a 2.9 cm x 1.7 cm liquid dark area with poor sound transmission. A hysteroscopy was performed with the removal of a large amount of blood clot-like tissue. The histochemical and immunohistochemical (IHC) pathological diagnosis was ETT.

History of past illness

The patient had no past illness. In terms of her pregnancy history, she had a total of seven pregnancies, of which three were miscarriages, two midterm induction, one resulted in twins, and two full-term cesarean sections for the first and last pregnancies.

Personal and family history

No other special circumstances.

Physical examination

Specialist examination on admission showed a small amount of dark red bloody fluid in the vagina and no purplish-blue nodules in the vulva, vagina, or cervix. The appearance of the cervix was normal. The uterus was the size of a uterus at 12 wk of pregnancy and was irregular in shape, slightly soft in texture, movable, and slightly tender. No obvious mass was found in the bilateral adnexal areas.

Laboratory examinations

The laboratory investigations showed beta-human chorionic gonadotropin (βHCG) levels of 64.30 mIU/mL [normal range (NR): 0-3] and cytokeratin 19 fragment levels of 3.94 ng/mL (NR: 0-3.3). No abnormalities in other tumor markers were seen: Squamous-cell carcinoma, 0.33 ng/mL (NR: 0-2.7); carcinoembryonic antigen, 0.61 ng/mL (NR: 0-3.4); carbohydrate antigen (CA) 125, 22.60 U/mL (NR: 0-35); CA 19-9, 13.70 U/mL (NR: 0-39); CA 15-3, 11.10 U/mL (NR: 0-25); CA 72-4, 3.0 U/mL (NR: 0-6.9); neuron-specific enolase, 12.3 ng/mL (NR: 0-17); human epididymal protein 4, 28.8 pmol/L (NR: 0-140).

Imaging examinations

On admission, 16 d after her previous hysteroscopy, ultrasonography revealed a 7.1 cm × 6.3 cm anechoic mass in the lower segment of the uterus, with blurred margins, solid cyst-like appearance, and reduced blood flow signals. Computerized tomography (CT) imaging of the chest, abdomen, and pelvis showed significant enlargement of the uterine cavity, with a large-scale high-density shadow with punctate gas and unclear edges visible in the plain scan. The enhancement was not significant after application of contrast agent, and the muscle layer was compressed and thinned. No other abnormalities were seen. The CT imaging findings indicated that, after hysteroscopy, part of the hematoma should be considered in the operation area (Figure 1).

FINAL DIAGNOSIS

Postoperative histological examination of the tumor showed that it was composed of mononuclear intermediate trophoblast cells with vacuoles and prominent nucleoli and "geographic" necrosis (Figure 2A and B). IHC analysis showed positive expression of HCG, epithelial membrane antigen (EMA), inhibin-alpha, p63, and human placental alkaline phosphatase (PLAP), with a Ki-67 proliferation index of 40% (Figure 3A-F). The final diagnosis was lower uterine segment and cervical canal ETT.

TREATMENT

On March 11, a total abdominal hysterectomy and bilateral salpingectomy were performed. During the operation, a normal-sized uterus was seen with an enlarged tumor in the lower uterine segment, together with severe involvement of the anterior wall of the lower uterine segment. The surface of the anterior wall of the lower uterine segment was light blue and thin, the entire enlarged lower uterine segment with the cervical canal was about 8 cm × 8 cm × 9 cm in size, with compression and displacement of the surrounding tissues (Figure 4A and B). Other organs and tissues were normal. Postoperatively, the uterus was dissected through an anterior wall incision, showing that the walls of the lower uterine segment and cervical canal were 2 mm in thickness, with black blood clot-like tissue visible inside (Figure 4C).

OUTCOME AND FOLLOW-UP

The patient recovered smoothly after surgery. After three days, the βHCG level had decreased to 5.53 mIU/mL and the cytokeratin 19 fragments had returned to the normal range of 1.22 ng/mL, while after another seven days, the βHCG level returned to the normal range of 0.48 mIU/mL.

DISCUSSION

ETT is the rarest form of GTT and was previously known as atypical choriocarcinoma. It was first described by Mazur in 1989, and the term "ETT" has become widely used since the detailed documentation of its clinicopathological and IHC features by Shih and Kurman in 1998[3-6]. It primarily affects women of reproductive age, although there have been reported cases of postmenopausal patients, with a reported age range from 15 to 66 years[7,8].

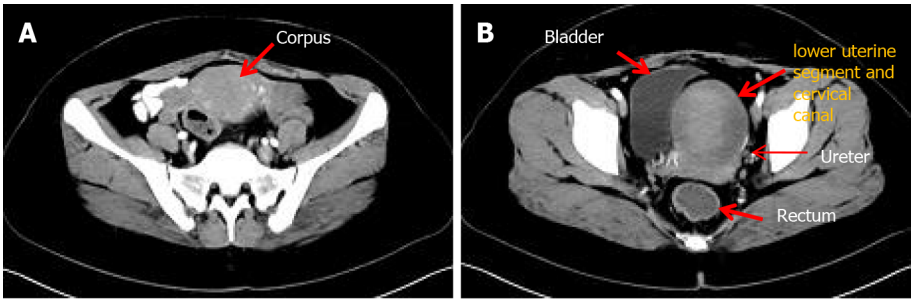

DOI: 10.12998/wjcc.v11.i4.938 **Copyright** ©The Author(s) 2023.

Figure 1 Computerized tomography imaging. A: Uterine body; B: Lower uterine segment and cervical canal lesion.

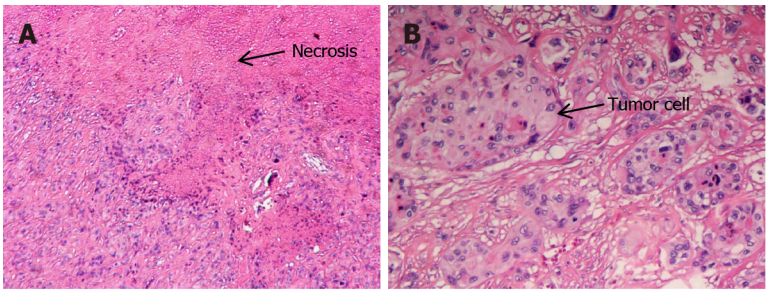

DOI: 10.12998/wjcc.v11.i4.938 **Copyright** ©The Author(s) 2023.

Figure 2 Histological analysis: Hematoxylin-eosin stain. A: Geographical necrosis of tumors (×40); B: Mononuclear intermediate trophoblast cells with vacuoles and prominent nucleoli (×100).

ETT mostly arises within the uterine cavity, although this may vary. Stănculescu *et al*[9] reported cervical occurrence of ETT in 31% of cases, while Hui *et al*[2] reported that 50% of ETTs arise within the uterine cervix or lower uterine segment. The lower uterine segment is derived from the extension of the uterine isthmus during pregnancy, that is, the junction between the uterus and the cervix. The incision for cesarean section is in the lower uterine segment. The present case had had seven pregnancies, three miscarriages: Two midterm inductions, one for twins, and two term cesarean sections. The final diagnosis was lower uterine segment and cervical canal ETT. Her last pregnancy had resulted in a full-term cesarean section 31 mo previously. The tumor made a large, tree stump-like swelling in the lower uterine segment and cervical canal, while the uterus was normal-sized and rested on top of the swelling (Figure 4A). Trauma to the continuity and integrity of the uterine tissue after surgical incision and wound healing in the lower uterine segment may be associated with the development of ETT, and this may be part of the reason why ETTs appear in the lower uterine segment and cervical canal. There have been reports of ETT occurring at and around the uterine incision scar[10,11]. A search of the PubMed database using the search terms "cesarean section" and "epithelioid trophoblastic tumor" retrieved nine articles, including 13 cases of ETT and ETT-related lesions[12]. All 13 cases had a history of cesarean section, and the lesions were all located at the cesarean section incision on the anterior wall of the lower uterine segment. The present case is the 14th reported case of ETT after cesarean section. Therefore, we deduced that cesarean section trauma was an important influencing factor of ETT at this site.

ETT is usually associated with a prior gestational event. The antecedent gestations can be term pregnancy, abortion, hydatidiform mole, and ectopic pregnancy. Phippen *et al*[13] reported a case of ETT that occurred in the cervix after an ectopic pregnancy. There are even reported cases of isolated lung ETT, where microsatellite genotyping of the tumor cells at informative microsatellite loci revealed the biparental origin of the tumors, with the presence of paternal alleles at each locus, and confirmed their placental origin[14]. Thus, a history of pregnancy is a prerequisite for ETT, although the preceding gestation may be sometimes remote. Vaginal bleeding or menometrorrhagia is the most common symptom but amenorrhea can also occur, and in our case, amenorrhea was the only presenting complaint. The patient had experienced amenorrhea for nine months before her second visit to the local hospital for hysteroscopy. It was after the hysteroscopy that the patient developed vaginal bleeding. ETT tumor cells express both HCG and keratin, and laboratory tests showed that the serum βHCG levels were slightly elevated to 64.30 mIU/mL, while the cytokeratin 19 fragment was 3.94 ng/mL, which is consistent with literature reports[2,4,6]. The cytokeratin level decreased to the normal range three days postoperatively, and the βHCG returned to the normal range 10 d postoperatively.

Immunohistochemistry, in this case, showed that the ETT tumor cells typically expressed HCG, inhibin-alpha, EMA, and p63, with locally expressed PLAP and a Ki-67 nuclear labeling index of 40%;

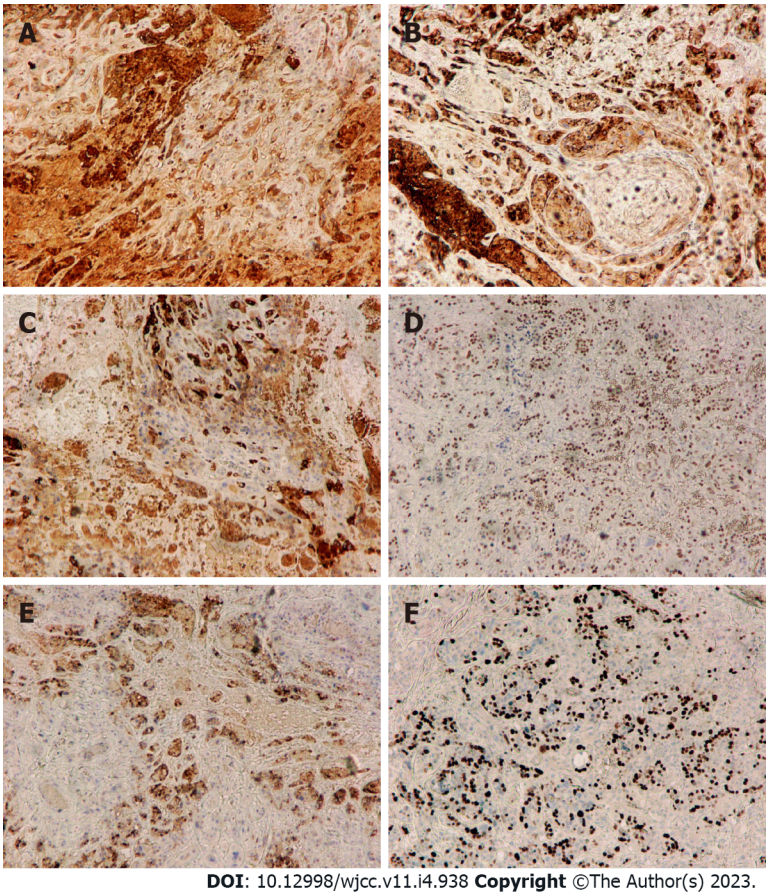

DOI: 10.12998/wjcc.v11.i4.938 **Copyright** ©The Author(s) 2023.

Figure 3 Immunohistochemistry assay (×40). A: Human chorionic gonadotropin -positive; B: Epithelial membrane antigen -positive; C: Inhibin-alpha-positive; D: p63-positive; E: Placental alkaline phosphatase -positive; F: Ki-67 proliferation index of 40%.

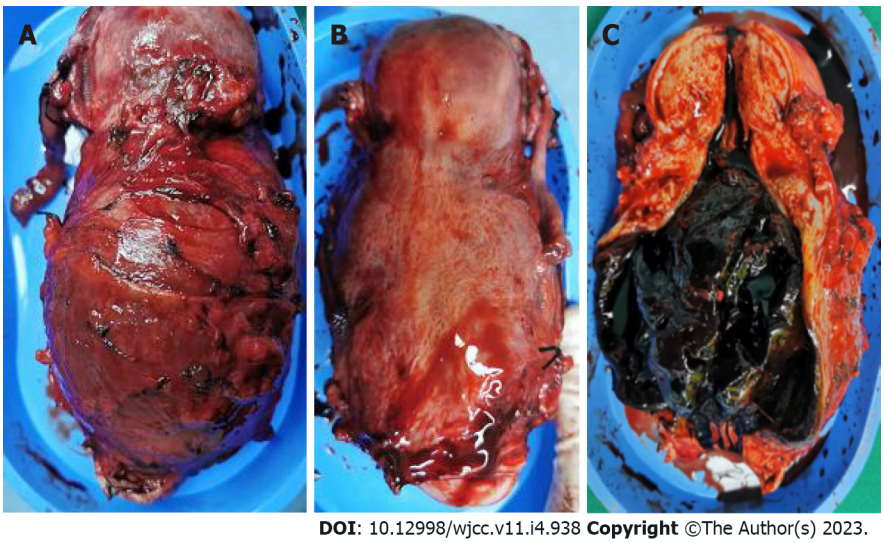

DOI: 10.12998/wjcc.v11.i4.938 **Copyright** ©The Author(s) 2023.

Figure 4 Surgical specimen. A: Front view; B: Rear view; C: Anterior wall section.

this is consistent with literature reports. The expression of p63 is helpful for the differential diagnosis of ETT and placental site reaction and placental site trophoblastic tumor, as the latter two are negative and ETT is positive[15]. Most reports have found a Ki-67 nuclear labeling index of approximately 17%, with a few reports describing significant elevation[2,14,16].

ETT is a relatively indolent malignancy that, in our case, persisted for seven months without extrauterine invasion and metastasis. Clinicians tend to be unaware of the existence of this lesion. It can occur many years after the previous pregnancy; Keser *et al*[4] reported a case of ETT that occurred 16 years after the previous pregnancy, and Hsiue *et al*[17] reported a case of ETT that occurred 23 years

after the previous pregnancy. For uncertain uterine and extrauterine lesions that do not conform to the general rules, low blood βHCG levels combined with histopathology, immunohistochemistry, and genetic testing of the diseased tissue are of great significance for the diagnosis and treatment of the disease.

CONCLUSION

ETT is not benign, but it is an indolent tumor. ETT patients do not present any specific symptoms or signs. A commonly used treatment strategy is surgical resection, which is effective when there is no extrauterine spread or metastasis of the tumor cells. The ETT case discussed in the present report would help enhance the understanding of the disease from a clinician's perspective. Importantly, the present report identified cesarean section trauma was an important influencing factor of ETT that occurred in the patient's cervical canal and lower uterine segment.

FOOTNOTES

Author contributions: Yuan LQ contributed to conceptualization; Pan GY and Guo H contributed to data curation and visualization; Yuan LQ, Hao T, Li DP, Liu NF contributed to formal analysis; Yuan LQ, Hao T contributed to writing-original draft preparation; Yuan LQ contributed to writing-review and editing; Yuan LQ contributed to manuscript revision; All authors have read and approved the final manuscript.

Informed consent statement: Written informed consent was obtained from the patient for the publication of this case report.

Conflict-of-interest statement: All the authors report no relevant conflicts of interest for this article.

CARE Checklist (2016) statement: The authors have read the CARE Checklist (2016), and the manuscript was prepared and revised according to the CARE Checklist (2016).

Country/Territory of origin: China

ORCID number: Ling-Qin Yuan 0000-0002-6555-1239.

S-Editor: Liu GL
L-Editor: A
P-Editor: Liu GL

REFERENCES

1 **Tsai HW**, Lin CP, Chou CY, Li CF, Chow NH, Shih IM, Ho CL. Placental site nodule transformed into a malignant epithelioid trophoblastic tumour with pelvic lymph node and lung metastasis. *Histopathology* 2008; **53**: 601-604 [PMID: 18983471 DOI: 10.1111/j.1365-2559.2008.03145.x]
2 **Hui P**. Gestational Trophoblastic Tumors: A Timely Review of Diagnostic Pathology. *Arch Pathol Lab Med* 2019; **143**: 65-74 [PMID: 30407075 DOI: 10.5858/arpa.2018-0234-RA]
3 **Bell SG**, Uppal S, Sakala MD, Sciallis AP, Rolston A. An extrauterine extensively metastatic epithelioid trophoblastic tumor responsive to pembrolizumab. *Gynecol Oncol Rep* 2021; **37**: 100819 [PMID: 34258359 DOI: 10.1016/j.gore.2021.100819]
4 **Keser SH**, Kokten SC, Cakir C, Sensu S, Buyukbayrak EE, Karadayi N. Epithelioid trophoblastic tumor. *Taiwan J Obstet Gynecol* 2015; **54**: 621-624 [PMID: 26522123 DOI: 10.1016/j.tjog.2015.08.020]
5 **Mazur MT**. Metastatic gestational choriocarcinoma. Unusual pathologic variant following therapy. *Cancer* 1989; **63**: 1370-1377 [PMID: 2465817 DOI: 10.1002/1097-0142(19890401)63:7<1370::aid-cncr2820630723>3.0.co;2-g]
6 **Shih IM**, Kurman RJ. Epithelioid trophoblastic tumor: a neoplasm distinct from choriocarcinoma and placental site trophoblastic tumor simulating carcinoma. *Am J Surg Pathol* 1998; **22**: 1393-1403 [PMID: 9808132 DOI: 10.1097/00000478-199811000-00010]
7 **Zhang X**, Shi H, Chen X. Epithelioid trophoblastic tumor after induced abortion with previous broad choriocarcinoma: a case report and review of literature. *Int J Clin Exp Pathol* 2014; **7**: 8245-8250 [PMID: 25550880]
8 **Yigit S**, Gun E, Yilmaz B, Kolsuz Z. Epithelioid trophoblastic tumor in a postmenopausal woman: A case report and

review of the literature in the postmenopausal group. *Indian J Pathol Microbiol* 2020; **63**: S98-S101 [PMID: 32108639 DOI: 10.4103/IJPM.IJPM_656_18]

9 **Stănculescu RV**, Bauşic V, Vlădescu TC, Vasilescu F, Brătilă E. Epithelioid trophoblastic tumor: a case report and literature review. *Rom J Morphol Embryol* 2016; **57**: 1365-1370 [PMID: 28174805]

10 **Black KA**, Simone K, Hirt-Walsh C, Sabourin J. Epithelioid trophoblastic tumor presenting as a Caesarean scar defect: A case report. *Gynecol Oncol Rep* 2021; **36**: 100715 [PMID: 33604444 DOI: 10.1016/j.gore.2021.100715]

11 **Yang C**, Li J, Zhang Y, Xiong H, Sheng X. Epithelioid trophoblastic tumor coexisting with choriocarcinoma around an abdominal wall cesarean scar: a case report and review of the literature. *J Med Case Rep* 2020; **14**: 178 [PMID: 33012293 DOI: 10.1186/s13256-020-02485-8]

12 **Zhou F**, Lin K, Shi H, Qin J, Lu B, Huang L. Atypical postcesarean epithelioid trophoblastic lesion with cyst formation: a case report and literature review. *Hum Pathol* 2015; **46**: 1036-1039 [PMID: 25907864 DOI: 10.1016/j.humpath.2014.10.031]

13 **Phippen NT**, Lowery WJ, Leath CA 3rd, Kost ER. Epithelioid trophoblastic tumor masquerading as invasive squamous cell carcinoma of the cervix after an ectopic pregnancy. *Gynecol Oncol* 2010; **117**: 387-388 [PMID: 20223511 DOI: 10.1016/j.ygyno.2010.02.013]

14 **Fénichel P**, Rouzier C, Butori C, Chevallier P, Poullot AG, Thyss A, Mouroux J. Extragestational βHCG secretion due to an isolated lung epithelioid trophoblastic tumor: microsatellite genotyping of tumoral cells confirmed their placental origin and oriented specific chemotherapy. *J Clin Endocrinol Metab* 2014; **99**: 3515-3520 [PMID: 25029419 DOI: 10.1210/jc.2014-1460]

15 **Houghton O**, McCluggage WG. The expression and diagnostic utility of p63 in the female genital tract. *Adv Anat Pathol* 2009; **16**: 316-321 [PMID: 19700941 DOI: 10.1097/PAP.0b013e3181b507c6]

16 **Zhang T**, Zeng X, Xu H, Gao L, Xiong L, An R, Xue Y. Clinical characteristics and outcomes of extrauterine epithelioid trophoblastic tumors. *Arch Gynecol Obstet* 2019; **300**: 725-735 [PMID: 31312959 DOI: 10.1007/s00404-019-05239-0]

17 **Hsiue EH**, Hsu C, Tseng LH, Lu TP, Kuo KT. Epithelioid Trophoblastic Tumor Around an Abdominal Cesarean Scar: A Pathologic and Molecular Genetic Analysis. *Int J Gynecol Pathol* 2017; **36**: 562-567 [PMID: 28134666 DOI: 10.1097/PGP.0000000000000366]

World Journal of Clinical Cases

Submit a Manuscript: https://www.f6publishing.com

World J Clin Cases 2023 February 6; 11(4): 945-951

DOI: 10.12998/wjcc.v11.i4.945

ISSN 2307-8960 (online)

CASE REPORT

Treatment of portosystemic shunt-borne hepatic encephalopathy in a 97-year-old woman using balloon-occluded retrograde transvenous obliteration: A case report

Akihiro Nishi, Tsuneaki Kenzaka, Misa Sogi, Shuichiro Nakaminato, Takahiro Suzuki

Specialty type: Gastroenterology and hepatology

Provenance and peer review: Unsolicited article; Externally peer reviewed.

Peer-review model: Single blind

Peer-review report's scientific quality classification

Grade A (Excellent): 0
Grade B (Very good): B, B
Grade C (Good): 0
Grade D (Fair): D
Grade E (Poor): 0

P-Reviewer: Methawasin K, Thailand; Wang YT, China

Received: October 17, 2022
Peer-review started: October 17, 2022
First decision: December 26, 2022
Revised: December 30, 2022
Accepted: January 12, 2023
Article in press: January 12, 2023
Published online: February 6, 2023

Akihiro Nishi, Misa Sogi, General Medicine, Awa Regional Medical Center, Tateyama 2940014, Chiba, Japan

Tsuneaki Kenzaka, Division of Community Medicine and Career Development, Kobe University Graduate School of Medicine, Kobe 6500017, Hyogo, Japan

Shuichiro Nakaminato, Takahiro Suzuki, Department of Radiology, Kameda Medical Center, Kamogawa 2968602, Chiba, Japan

Corresponding author: Akihiro Nishi, MD, Doctor, General Medicine, Awa Regional Medical Center, 1155 Yamamoto, Tateyama 2940014, Chiba, Japan. akihiro.nishi24@gmail.com

Abstract

BACKGROUND

Hyperammonemia and hepatic encephalopathy are common in patients with portosystemic shunts. Surgical shunt occlusion has been standard treatment, although recently the less invasive balloon-occluded retrograde transvenous obliteration (B-RTO) has gained increasing attention. Thus far, there have been no reports on the treatment of portosystemic shunts with B-RTO in patients aged over 90 years. In this study, we present a case of hepatic encephalopathy caused by shunting of the left common iliac and inferior mesenteric veins, successfully treated with B-RTO.

CASE SUMMARY

A 97-year-old woman with no history of liver disease was admitted to our hospital because of disturbance of consciousness. She had no jaundice, spider angioma, palmar erythema, hepatosplenomegaly, or asterixis. Her blood tests showed hyperammonemia, and abdominal contrast-enhanced computed tomography revealed a portosystemic shunt running between the left common iliac vein and the inferior mesenteric vein. She was diagnosed with hepatic encephalopathy secondary to a portosystemic shunt. The patient did not improve with conservative treatment: Lactulose, rifaximin, and a low-protein diet. B-RTO was performed, which resulted in shunt closure and improvement in hyperammonemia and disturbance of consciousness. Moreover, there was no abdominal pain or elevated levels of liver enzymes due to complications. The patient was discharged without further consciousness disturbance.

CONCLUSION
Portosystemic shunt-borne hepatic encephalopathy must be considered in the differential diagnosis for consciousness disturbance, including abnormal behavior and speech.

Key Words: Hepatic encephalopathy; Hyperammonemia; Portosystemic shunt; Balloon-occluded retrograde transvenous obliteration; Elderly; Case report

Core Tip: Hyperammonemia and hepatic encephalopathy are common with portosystemic shunts. In this case, hepatic encephalopathy caused by shunting of the left common iliac and inferior mesenteric veins was successfully treated with balloon-occluded retrograde transvenous obliteration (B-RTO). A 97-year-old woman was diagnosed with hepatic encephalopathy secondary to a portosystemic shunt. The patient did not improve with conservative treatment: Lactulose, rifaximin, and a low-protein diet. B-RTO was performed, resulting in shunt closure and improvement in hyperammonemia and disturbance of consciousness. The patient was discharged without further consciousness disturbance.Portosystemic shunt-borne hepatic encephalopathy must be considered in the differential diagnosis for consciousness disturbance, including abnormal behavior and speech.

Citation: Nishi A, Kenzaka T, Sogi M, Nakaminato S, Suzuki T. Treatment of portosystemic shunt-borne hepatic encephalopathy in a 97-year-old woman using balloon-occluded retrograde transvenous obliteration: A case report. *World J Clin Cases* 2023; 11(4): 945-951
URL: https://www.wjgnet.com/2307-8960/full/v11/i4/945.htm
DOI: https://dx.doi.org/10.12998/wjcc.v11.i4.945

INTRODUCTION

Hepatic encephalopathy is defined as impaired brain function caused by liver insufficiency and/or portosystemic shunt[1]. Portosystemic shunts are known to cause hyperammonemia without liver dysfunction[2]. A portosystemic shunt is a condition in which portal blood flows directly into the systemic circulatory system. In such a condition, ammonia produced in the digestive tract is not metabolized in the liver, resulting in hyperammonemia and hepatic encephalopathy. Treatment methods include medical therapy, surgical shunt occlusion, and shunt embolization with interventional radiology (IVR)[2]. Surgical shunt occlusion or IVR is the treatment of choice when there is no improvement with medical treatment, or when complete cure is desired. In recent years, balloon-occluded retrograde transvenous obliteration (B-RTO) has attracted attention owing to its less invasive nature. However, thus far, there have been no reports of B-RTO treatment for cases of portosystemic shunts in very elderly patients, *i.e.*, those aged above 90 years.

In this study, we report a case of hepatic encephalopathy caused by shunting of the left common iliac and inferior mesenteric veins in a 97-year-old patient whose condition improved after B-RTO treatment.

CASE PRESENTATION

Chief complaints

A 97-year-old Japanese woman exhibited abnormal behavior and disorganized speech for 10 d before admission.

History of present illness

Ten days prior to admission, the patient was agitated and spoke incomprehensible words to a neighbor. Her family met her 6 d prior to admission but noticed no unusual behavior or speech. Four days prior to admission, she exhibited strange behavior, saying that she did not know how to eat eggs and walking out with an egg clutched in her hand. Two days prior to admission, she lost spontaneity and had urinary incontinence, which she normally does not have. On the day of admission, her speech was impaired, and her family admitted her to the emergency room of our hospital.

History of past illness

She had a medical history of cholecystectomy and distal gastrectomy for gastric cancer, with no history

of liver disease or cognitive dysfunction.

Personal and family history

She did not take any medications or consume alcohol. She lived alone and had independent activities of daily living; her food intake and defecation status were unknown.

Physical examination

Upon examination, she was disorientated, only answered "yes" to questions, and could not follow directions. Her vital signs were as follows: Glasgow Coma Scale score, 13 (E4V4M5); blood pressure, 157/111 mmHg; body temperature, 36.6 °C; pulse rate, 100 beats/min; respiratory rate, 20 breaths/min; and oxygen saturation, 99% on ambient air. Physical examination revealed no jaundice, spider angioma, palmar erythema, hepatosplenomegaly, or asterixis.

Laboratory examinations

Blood test results showed elevated serum ammonia levels at 125 μg/dL (normal range: 12-66 μg/dL) (Table 1). Cerebrospinal fluid examination results were normal, and blood cultures were negative.

Imaging examinations

Computed tomography (CT) of the head and magnetic resonance imaging showed no abnormalities.

FURTHER DIAGNOSTIC WORK-UP

On day 2 after admission, her serum ammonia levels were further elevated to 251 μg/dL and electroencephalography showed triphasic waves. On day 3, an abdominal contrast-enhanced CT scan revealed shunting between the left common iliac vein and the inferior mesenteric vein (Figure 1).

FINAL DIAGNOSIS

Based on the extent of hyperammonemia and abdominal contrast-enhanced CT findings, a diagnosis of hepatic encephalopathy due to an extrahepatic portosystemic shunt was made.

TREATMENT

As conservative therapy, 39 g/d oral lactulose was started on day 4, and 1200 mg/d oral rifaximin and a low-protein diet were started on day 13. Her serum ammonia levels decreased to 80 μg/dL on day 14. However, there was little improvement in the patient's level of consciousness. Therefore, B-RTO was performed under local anesthesia on day 20, and coils were placed in the shunts between the left common iliac vein and the inferior mesenteric vein (Figure 2). On day 21, contrast-enhanced CT confirmed no coil displacement, and shunt closure was achieved. By contrast, mild edematous changes were observed in the descending and sigmoid colons. Moreover, there was a partial thrombus in the inferior mesenteric vein; however, anticoagulants were not administered because of the patient's advanced age. We followed the patient carefully, noting abdominal pain and elevated liver enzymes.

OUTCOME AND FOLLOW-UP

Her level of consciousness improved on day 21 (the day after B-RTO). Her serum ammonia levels were 21 μg/dL on day 28 and remained within the normal range throughout subsequent hospitalizations. There was no abdominal pain or elevated levels of liver enzymes due to complications. The patient was discharged on day 65 without any further disturbance of consciousness.

DISCUSSION

We report the case of a 97-year-old patient with hepatic encephalopathy due to shunting of the left common iliac and inferior mesenteric veins. To the best of our knowledge, this is the first case in which B-RTO was performed for a portosystemic shunt in a very elderly patient aged above 90 years.

On the basis of physical examination, hematology, and imaging findings, this case had no liver dysfunction or cirrhosis. The imaging findings showed shunting of the left common iliac vein and the

Table 1 Laboratory data on admission

Parameter	Recorded value	Standard value
White blood cell count	8500/μL	3500-8500/μL
Hemoglobin	14.5 g/dL	12-16 g/dL
Platelet count	16.5 × 10^4/μL	12-28 × 10^4/μL
Prothrombin time	15.2 s	10-13 s
Prothrombin time	60.8%	70-130%
Activated partial thromboplastin time	30.8 s	25.3-37.6 s
C-reactive protein	0.1 mg/L	≤ 0.5 mg/dL
Total protein	7.1 g/dL	6.5-8.3 g/dL
Albumin	4.2 g/dL	3.8-5.3 g/dL
Total bilirubin	1.4 mg/dL	0.2-1.2 mg/dL
Aspartate aminotransferase	35 U/L	7-34 U/L
Alanine aminotransferase	22 U/L	4-43 U/L
Lactase dehydrogenase	299 U/L	119-229 U/L
Alkaline phosphatase	128 U/L	38-113 U/L
γ-Glutamyl transpeptidase	16 U/L	6-30 U/L
Blood urea nitrogen	24 mg/dL	8-20 mg/dL
Creatinine	0.66 mg/dL	≤ 0.80 mg/dL
Sodium	145 mEq/L	139-146 mEq/L
Potassium	4.1 mEq/L	3.7-4.8 mEq/L
Chloride	109 mEq/L	101-109 mEq/L
Calcium	9.3 mg/dL	8.6-10.2 mg/dL
Glucose	102 mg/dL	70-109 mg/dL
TSH	1.06 μIU/mL	0.35-4.94 μIU/mL
Free T4	1.24 ng/dL	0.70-1.48 ng/dL
Cortisol	20.8 μg/dL	5.6-21.3 μg/dL
Vitamin B1	3.0 μg/dL	2.6-5.8 μg/dL
Ammonia	125 μg/dL	12-66 μg/dL
HBs-Ag	(-)	
HCV-Ab	(-)	

TSH: Thyroid-stimulating hormone; HBs-Ag: Hepatitis B virus surface antigen; HCV-Ab: Hepatitis C virus antibody.

inferior mesenteric vein, suggesting that the portosystemic shunt was the cause of hepatic encephalopathy. Portosystemic shunts are classified according to their location as type I (intrahepatic), type II (intrahepatic and extrahepatic), type III (extrahepatic), type IV (extrahepatic, portal hypertension), and type V (extrahepatic, absence of the portal vein)[2]. A type III (extrahepatic) portosystemic shunt, to which this case belongs, is the most frequent, accounting for 48.9% of all types, with an average age of onset of 57.4 years[2]. There are congenital and acquired causes of this type of shunt formation, with congenital causes being malformations or retained embryonal vascular vessels and the acquired causes being complications related to abdominal surgery[2]. The patient in this case had a history of cholecystectomy and distal gastrectomy, which may have resulted in the formation of an acquired shunt; however, the cause was difficult to determine because of the lack of comparative images from the past.

Surgical shunt occlusion is the curative treatment for portosystemic shunts; however, it is generally invasive and does not necessarily provide good outcomes[1]. In our case, complications and prolonged hospitalization were concerning. In such cases, IVR is an alternative treatment, and recently cases wherein patients were treated with B-RTO have been reported[3-6]. B-RTO is considered less invasive

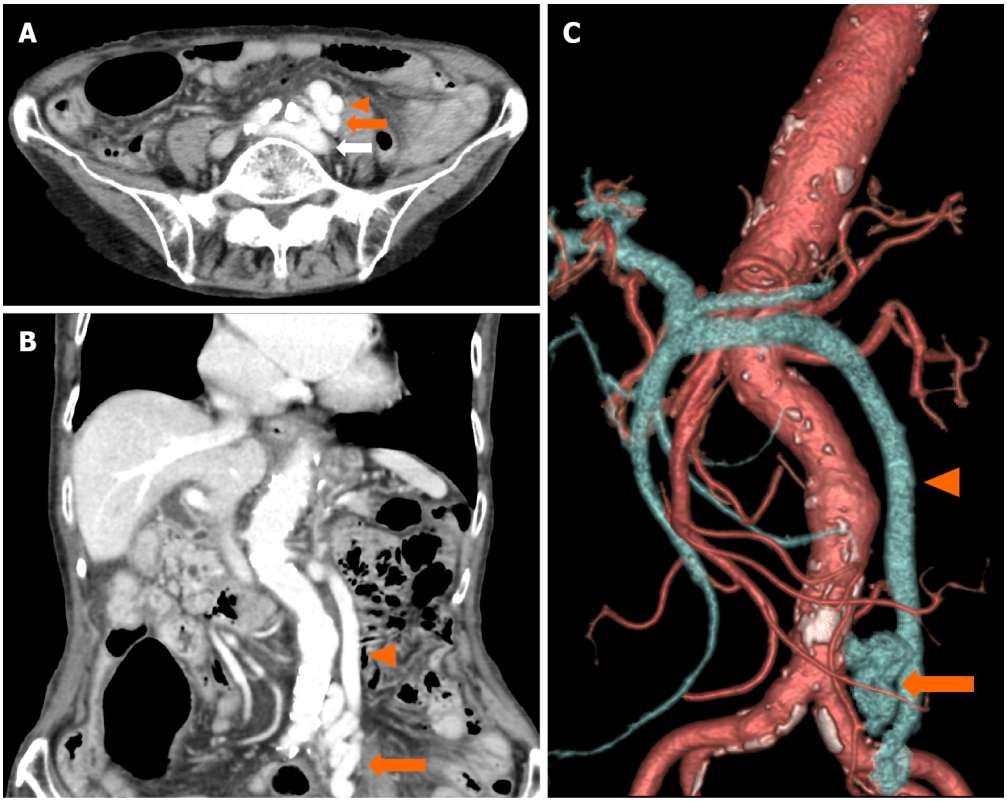

DOI: 10.12998/wjcc.v11.i4.945 **Copyright** ©The Author(s) 2023.

Figure 1 Abdominal computed tomography scan with contrast enhancement. A-C: Images showing a portosystemic shunt (orange arrow) running between the left common iliac vein (white arrow) and the inferior mesenteric vein (arrowhead).

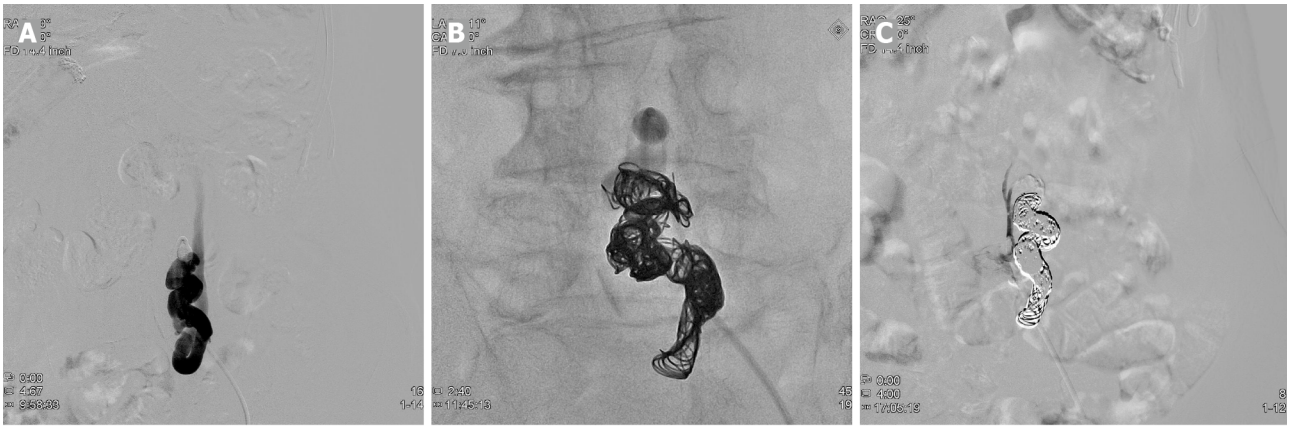

DOI: 10.12998/wjcc.v11.i4.945 **Copyright** ©The Author(s) 2023.

Figure 2 Angiography images before and after embolization. A: A balloon catheter is advanced into the portosystemic shunt through the left femoral vein; B: The shunt is filled with the coil; C: The shunt is completely obliterated.

than surgical treatment, although it may cause complications, such as pleural effusion, ascites, thrombosis, pulmonary embolism, and worsening of esophageal varices[2,7-9]. Anticoagulant administration to elderly patients is particularly challenging owing to the risk of bleeding, and indications should be carefully considered. To the best of our knowledge, the oldest patient who underwent B-RTO for a portosystemic shunt was 86 years old[5]. B-RTO has no age-related restrictions on its indications and does not require special treatment on account of patients' advanced age[10]. Although this patient was 97 years old, she had no serious comorbidities and was able to perform her daily activities. Therefore, we thought that there was great merit in performing curative treatment and B-RTO.

Hepatic encephalopathy is one of the differential diagnoses of disturbance of consciousness, and it is common to measure serum ammonia levels when there is a history of liver disease or physical findings suggestive of liver dysfunction[11]. By contrast, shock, gastrointestinal bleeding, vesicorectal fistulas, drugs such as valproic acid, and obstructive urinary tract infections caused by urease-producing

bacteria may lead to hyperammonemia, even in the absence of liver diseases[12,13]. Portosystemic shunts also cause hyperammonemia[14].

Although there was no history of liver disease or findings suggestive of liver dysfunction in this case, measurement of serum ammonia levels led to diagnosis and subsequent treatment.

CONCLUSION

This is the first report of B-RTO performed in a patient aged > 90 years with a portosystemic shunt. It is important to consider hepatic encephalopathy due to a portosystemic shunt as a differential diagnosis of disturbance of consciousness, including abnormal behavior and disorganized speech.

FOOTNOTES

Author contributions: Nishi A managed the case and wrote and revised the manuscript; Kenzaka T, Sogi M, Nakaminato S, and Suzuki T assisted with the preparation and revision of the manuscript; all authors read and approved the final manuscript.

Informed consent statement: Informed written consent was obtained from the patients for the publication of this report and any accompanying images.

Conflict-of-interest statement: The authors declare that they have no competing interests.

CARE Checklist (2016) statement: The authors have read the CARE Checklist (2016), and the manuscript was prepared and revised according to the CARE Checklist (2016).

Country/Territory of origin: Japan

ORCID number: Akihiro Nishi 0000-0003-4140-4880; Tsuneaki Kenzaka 0000-0002-3120-6605; Misa Sogi 0000-0001-6555-2015; Shuichiro Nakaminato 0000-0003-3413-1941; Takahiro Suzuki 0000-0003-2126-5959.

S-Editor: Chen YL
L-Editor: A
P-Editor: Chen YL

REFERENCES

1 **Vilstrup H**, Amodio P, Bajaj J, Cordoba J, Ferenci P, Mullen KD, Weissenborn K, Wong P. Hepatic encephalopathy in chronic liver disease: 2014 Practice Guideline by the American Association for the Study of Liver Diseases and the European Association for the Study of the Liver. *Hepatology* 2014; **60**: 715-735 [PMID: 25042402 DOI: 10.1002/hep.27210]

2 **Watanabe A**. Portal-systemic encephalopathy in non-cirrhotic patients: classification of clinical types, diagnosis and treatment. *J Gastroenterol Hepatol* 2000; **15**: 969-979 [PMID: 11059925 DOI: 10.1046/j.1440-1746.2000.02283.x]

3 **Asakura T**, Ito N, Sohma T, Mori N. Portosystemic Encephalopathy without Liver Cirrhosis Masquerading as Depression. *Intern Med* 2015; **54**: 1619-1622 [PMID: 26134193 DOI: 10.2169/internalmedicine.54.3800]

4 **Yamagami T**, Yoshimatsu R, Miura H, Hasebe T, Koide K. Hepatic encephalopathy due to intrahepatic portosystemic venous shunt successfully treated by balloon occluded retrograde transvenous embolization with GDCs. *Acta Radiol Short Rep* 2012; **1** [PMID: 23986827 DOI: 10.1258/arsr.2012.120041]

5 **Miyata K**, Tamai H, Uno A, Nakao R, Muroki T, Nasu T, Kawashima A, Nakao T, Kondo M, Ichinose M. Congenital portal systemic encephalopathy misdiagnosed as senile dementia. *Intern Med* 2009; **48**: 321-324 [PMID: 19252354 DOI: 10.2169/internalmedicine.48.1777]

6 **Tanaka O**, Ishihara K, Oyamada H, Harusato A, Yamaguchi T, Ozawa M, Nakano K, Yamagami T, Nishimura T. Successful portal-systemic shunt occlusion with balloon-occluded retrograde transvenous obliteration for portosystemic encephalopathy without liver cirrhosis. *J Vasc Interv Radiol* 2006; **17**: 1951-1955 [PMID: 17185692 DOI: 10.1097/01.RVI.0000250890.38012.38]

7 **Shimoda R**, Horiuchi K, Hagiwara S, Suzuki H, Yamazaki Y, Kosone T, Ichikawa T, Arai H, Yamada T, Abe T, Takagi H, Mori M. Short-term complications of retrograde transvenous obliteration of gastric varices in patients with portal hypertension: effects of obliteration of major portosystemic shunts. *Abdom Imaging* 2005; **30**: 306-313 [PMID: 15688111

DOI: 10.1007/s00261-004-0270-8]

8 **Cho SK**, Shin SW, Do YS, Park KB, Choo SW, Kim SS, Choo IW. Development of thrombus in the major systemic and portal veins after balloon-occluded retrograde transvenous obliteration for treating gastric variceal bleeding: its frequency and outcome evaluation with CT. *J Vasc Interv Radiol* 2008; **19**: 529-538 [PMID: 18375297 DOI: 10.1016/j.jvir.2007.10.012]

9 **Yoshimatsu R**, Yamagami T, Tanaka O, Miura H, Okuda K, Hashiba M, Nishimura T. Development of thrombus in a systemic vein after balloon-occluded retrograde transvenous obliteration of gastric varices. *Korean J Radiol* 2012; **13**: 324-331 [PMID: 22563270 DOI: 10.3348/kjr.2012.13.3.324]

10 **Saad WE**, Kitanosono T, Koizumi J, Hirota S. The conventional balloon-occluded retrograde transvenous obliteration procedure: indications, contraindications, and technical applications. *Tech Vasc Interv Radiol* 2013; **16**: 101-151 [PMID: 23830671 DOI: 10.1053/j.tvir.2013.02.003]

11 **Han JH**, Wilber ST. Altered mental status in older patients in the emergency department. *Clin Geriatr Med* 2013; **29**: 101-136 [PMID: 23177603 DOI: 10.1016/j.cger.2012.09.005]

12 **Hawkes ND**, Thomas GA, Jurewicz A, Williams OM, Hillier CE, McQueen IN, Shortland G. Non-hepatic hyperammonaemia: an important, potentially reversible cause of encephalopathy. *Postgrad Med J* 2001; **77**: 717-722 [PMID: 11677282 DOI: 10.1136/pmj.77.913.717]

13 **Kenzaka T**, Kato K, Kitao A, Kosami K, Minami K, Yahata S, Fukui M, Okayama M. Hyperammonemia in Urinary Tract Infections. *PLoS One* 2015; **10**: e0136220 [PMID: 26292215 DOI: 10.1371/journal.pone.0136220]

14 **Walker V**. Severe hyperammonaemia in adults not explained by liver disease. *Ann Clin Biochem* 2012; **49**: 214-228 [PMID: 22349554 DOI: 10.1258/acb.2011.011206]

World Journal of Clinical Cases

Submit a Manuscript: https://www.f6publishing.com

World J Clin Cases 2023 February 6; 11(4): 952-961

DOI: 10.12998/wjcc.v11.i4.952

ISSN 2307-8960 (online)

CASE REPORT

Development of Henoch-Schoenlein purpura in a child with idiopathic hypereosinophilia syndrome with multiple thrombotic onset: A case report

Yan-Yan Xu, Xiao-Bi Huang, Yun-Gong Wang, Li-Yun Zheng, Min Li, Yu Dai, Sheng Zhao

Specialty type: Immunology

Provenance and peer review: Unsolicited article; Externally peer reviewed.

Peer-review model: Single blind

Peer-review report's scientific quality classification

Grade A (Excellent): 0
Grade B (Very good): B
Grade C (Good): C, C
Grade D (Fair): 0
Grade E (Poor): 0

P-Reviewer: Dragonieri S, Italy; Ji X, China

Received: November 16, 2022
Peer-review started: November 16, 2022
First decision: November 25, 2022
Revised: December 11, 2022
Accepted: January 9, 2023
Article in press: January 9, 2023
Published online: February 6, 2023

Yan-Yan Xu, Xiao-Bi Huang, Yun-Gong Wang, Li-Yun Zheng, Sheng Zhao, Department of Pediatric Cardiovascular, Anhui Province Children's Hospital, Anhui Hospital of Children's Hospital Affiliated with Fudan University, Hefei 230051, Anhui Province, China

Min Li, Department of Pediatric Intensive Care Unit, Anhui Province Children's Hospital, Anhui Hospital of Children's Hospital affiliated with Fudan University, Hefei 230051, Anhui Province, China

Yu Dai, Department of Pediatrics, The Fourth Affiliated Hospital of Anhui Medical University, Hefei 230032, Anhui Province, China

Corresponding author: Sheng Zhao, MMed, Chief Doctor, Department of Pediatric Cardiovascular, Anhui Province Children's Hospital, Anhui Hospital of Children's Hospital affiliated with Fudan University, No. 39 Wangjiang East Road, Hefei 230051, Anhui Province, China. 382877830@qq.com

Abstract

BACKGROUND

The incidence of pulmonary embolism (PE) in children is low, but its mortality is high. Hypereosinophilic syndrome (HES) is a group of diseases caused by an abnormal increase in eosinophilic granulocytes resulting in multiple-organ dysfunction. The urgent event of thromboembolism in the pulmonary region provoked by eosinophils in idiopathic HES (IHES) is relatively unusual. This article reports a case of IHES with multiple PEs and left leg venous thrombosis as the first manifestation. One month later, the patient developed Henoch-Schonlein purpura (HSP), which is very rare.

CASE SUMMARY

We report the case of a 12-year-old boy who was admitted to the hospital with dyspnea, left leg pain, and aggravation. He had bilateral PE and left leg venous embolism with mild eosinophilia. Low-molecular-weight heparin and urokinase were given. At the same time, the interventional department was contacted about filter implantation, followed by urokinase thrombolysis. The left leg thrombus was aspirated under ultrasound guidance. He was discharged from the hospital on rivaroxaban. One month later, he developed a rash on both legs and ankle pain consistent with HSP, with severe eosinophilia and motor and sensory distu-

rbances. The patient was diagnosed with IHES with multiple embolisms complicated by HSP after excluding other causes of the eosinophil elevation. After glucocorticoid treatment, the symptoms were relieved, but the patient later developed purpura nephritis.

CONCLUSION
We report a rare and life-threatening case of IHES with multiple embolisms associated with HSP. A mild elevation of eosinophils early in the disease leads to difficulties in diagnosis and delayed treatment.

Key Words: Eosinophil; Hypereosinophilic syndrome; Henoch-Schoenlein purpura; Thrombosis; Case report

Core Tip: Pulmonary embolism (PE) in children usually occurs in the presence of an underlying condition, systemic disease, or other risk factors. Idiopathic PE accounts for less than 4% of these. The child has no risk factors for thrombosis other than obesity at the first hospitalization. A month later, he developed a purpuric rash on both legs, and pain in his ankles consistent with Henoch-Schönlein purpura (HSP) was accompanied by severe eosinophilia and motor and sensory impairments. Persistent eosinophilia in peripheral blood can lead to tissue infiltration and even organ damage. If end-organ damage occurs, hypereosinophilic syndrome (HES) can be diagnosed immediately. According to monist principles, patients are diagnosed with idiopathic HES with multiple embolisms complicated by HSP. After glucocorticoids, eosinophils quickly return to normal, neurological symptoms gradually improve, and the rash disappears. Eosinophils are only mildly elevated in PE, making clinical diagnosis more difficult.

Citation: Xu YY, Huang XB, Wang YG, Zheng LY, Li M, Dai Y, Zhao S. Development of Henoch-Schoenlein purpura in a child with idiopathic hypereosinophilia syndrome with multiple thrombotic onset: A case report. *World J Clin Cases* 2023; 11(4): 952-961
URL: https://www.wjgnet.com/2307-8960/full/v11/i4/952.htm
DOI: https://dx.doi.org/10.12998/wjcc.v11.i4.952

INTRODUCTION

Hypereosinophilic syndrome (HES) is a group of clinical syndromes characterized by a persistent and significant increase in eosinophilic granulocytes in the peripheral blood and surrounding tissues, resulting in organ dysfunction. This condition, which has an unknown cause, is called idiopathic HES (IHES). This disease mostly occurs in people between 20 years and 50 years of age, with an incidence rate of 0.04/100000 and a mortality rate of 9.3%[1]. It is rare in children, in whom its incidence is unknown. Pulmonary embolism (PE) caused by IHES is even rarer. Patients with HES also have autoimmune diseases such as ulcerative colitis, autoimmune hepatitis, autoimmune thyroiditis, multiple sclerosis, systemic lupus erythematosus, antiphospholipid syndrome, myasthenia gravis, and rheumatoid arthritis[2-4]. Henoch-Schoenlein purpura (HSP) is a common vasculitis in school-aged children that can affect the skin, joints, kidneys, and other organs. Children diagnosed with IHES with multiple embolisms complicated by HSP are very rare. This case extends the list of HES patients with autoimmune diseases. To improve the understanding of this disease among pediatric clinicians, a case of IHES with dyspnea and leg pain as the initial presentation and subsequent concomitant HSP was reported in our hospital.

CASE PRESENTATION

Chief complaints

A 12-year-old boy was admitted to our hospital for the first time on January 11, 2021 because of dyspnea for 2 wk, left leg pain for 1 wk, and aggravation for 3 d. He also had a fever and occasional cough. On February 24 and April 2, 2021, the patient was admitted to the hospital with a symmetrical, dark red rash on both legs that did not face when pressed, accompanied by ankle swelling and pain.

History of present illness

The child had a history of respiratory infections prior to labored breathing.

History of past illness

The child was previously healthy.

Physical examination

First hospital admission: The patient was 168 cm tall, weighed 76 kg, and had a body mass index (BMI) of 26.9 kg/m^2. His vital signs were as follows: Body temperature, 37.4 °C; blood pressure 128/81 mmHg; heart rate, 104 beats per min; respiratory rate 32/min; and SpO_2 92% (room air). The patient's skin was normal, but he displayed slight shortness and exertion of breath. The circumference of his left leg was 39.5 cm and right leg 37.5 cm, and his limb muscle tension was normal.

Second and third admissions: His legs showed a scattered, symmetrical, pressing dark red rash that did not fade, and both ankles were swollen and painful. On April 4, 2021, the child had decreased pain and temperature sensation in the right plantar, the toe could not bend to the ventral side, and the skin temperature of the right plantar was higher than that of the opposite side.

Laboratory examinations

His platelet count was 50 × 10^9/L, and his eosinophil count (EC) was slightly high at 0.63 × 10^9/L (Figure 1). On the other hand, his D-dimer level was 11.12 μg/mL (Figure 2). Serum potassium was 3.32 mmol/L. On day 8, blood tests showed normal levels of potassium. C4 was slightly high at 0.46 g/L (normal: 0-0.4). Protein C was 50.2% (normal: 75-130). Neuronal enolase was slightly high at 21.96 μg/L (normal: 0-16.3). N-terminal pro-brain natriuretic peptide (NT-proBNP) and troponin I (TnI) were high at 3116 pg/mL and 0.145 ng/mL, respectively, on January 11, 2021. No abnormalities were found in TnI on January 16, 2021 or in NT-proBNP on January 19, 2021. On February 24, 2021, the patient's IgE level was significantly high at 531 IU/mL (normal: 0-52). No abnormalities were found in hemoglobin, glucose, lipid, liver function, renal function parameters, C-reactive protein, activated partial thromboplastin time, or protein C. Anti-neutrophil cytoplasmic antibody, antinuclear antibodies, anticardiolipin antibody, HIV tests, hepatitis B, hepatitis C, mycoplasma pneumonia antibody, borrelia, and treponema pallidum were negative. Chlamydia pneumoniae IgG was positive. Human chorionic gonadotropin, alpha-fetoprotein, carcinoembryonic antigen, ferritin, and C3 were within the reference ranges. Allergen IgE detection, food intolerance, stool for Giardia lamblia, cryptosporidium, pinworm, and genetics were negative. On February 26, 2021, the microalbumin level in urine was 13.01 mg/L, but total urinary protein was not found due to the problem of specimen retention. The 24-h urinary total protein and microalbumin levels reviewed at later stages are shown in Figure 3.

Imaging examinations

On January 11, 2021, color Doppler echocardiography revealed right atria and ventricle enlargement, mild tricuspid regurgitation with insufficiency, and pulmonary hypertension. Color Doppler ultrasonography of the blood vessels of the legs showed thrombosis of the superficial femoral vein, popliteal vein, and posterior tibial vein of the left leg (Figure 4A). The lung computed tomography (CT) showed scattered wedge-shaped consolidation of both lungs with an outward-facing base and apex pointing to the hilum, a relatively widened pulmonary artery, and pulmonary infarction cannot be excluded. CT angiography of the pulmonary artery showed extensive embolization of both pulmonary arteries with enlargement of the pulmonary artery and the right heart (Figure 4B). On February 4, 2021, color Doppler ultrasound of the left lower extremity vein showed patency of blood flow. On April 6, 2021, color Doppler echocardiography showed a plump right atrium, mild tricuspid regurgitation with regurgitation insufficiency, and mild pulmonary hypertension. Bone marrow puncture and cranial and spinal MRI were not performed.

MULTIDISCIPLINARY EXPERT CONSULTATION

HSP was diagnosed given the child's typical symmetry of the two legs, nonfading compression, dark-red rash, and ankle swelling and pain. Symptomatic treatment was recommended, and glucocorticoids were added when necessary.

FINAL DIAGNOSIS

The patient was diagnosed with IHES with multiple embolisms complicated by HSP.

TREATMENT

First hospital admission: Immediately afterward, he was given low-molecular-weight heparin and

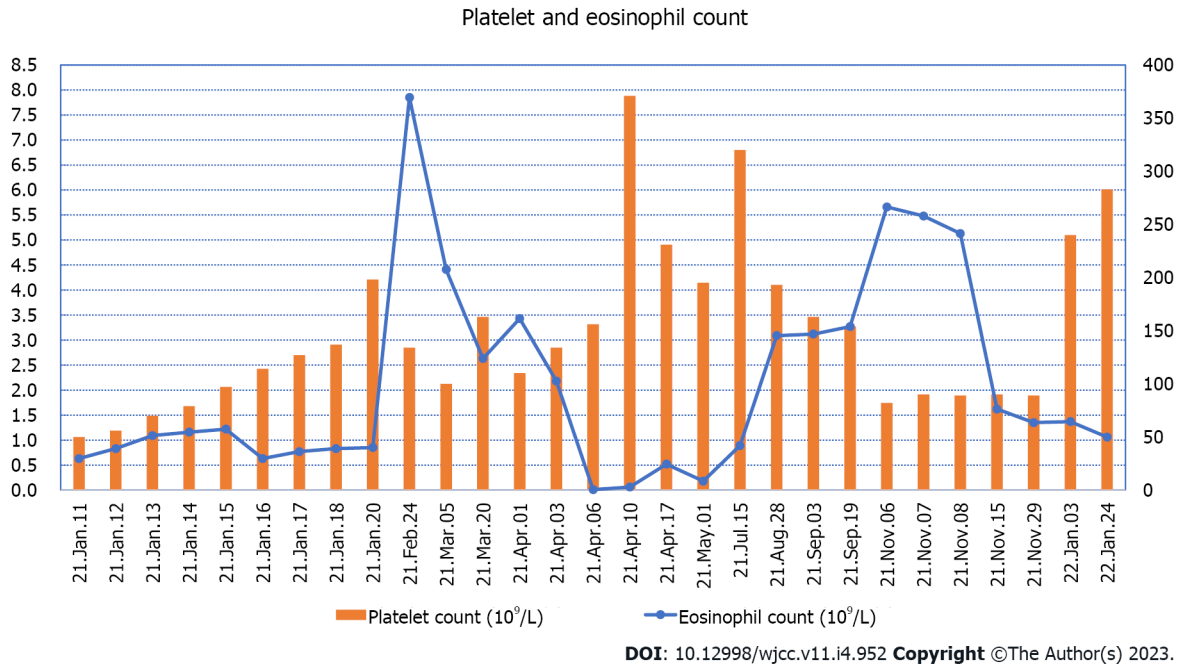

DOI: 10.12998/wjcc.v11.i4.952 **Copyright** ©The Author(s) 2023.

Figure 1 Changes in platelet and eosinophil count from the first hospitalization to the end of follow-up.

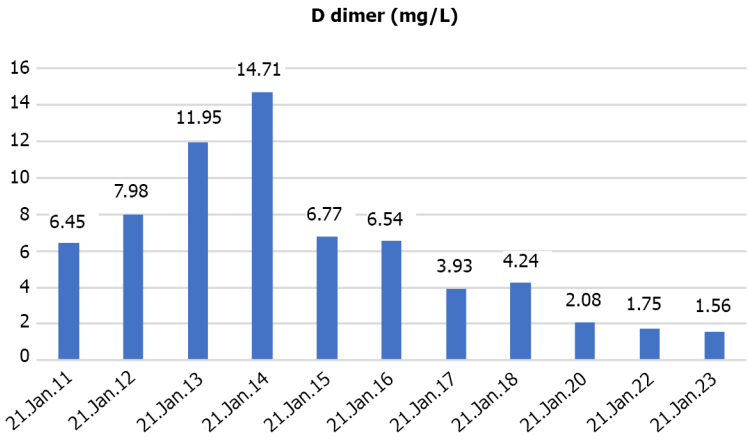

DOI: 10.12998/wjcc.v11.i4.952 **Copyright** ©The Author(s) 2023.

Figure 2 D dimer changes during the child's first hospitalization.

urokinase. At the same time, the interventional department was contacted for inferior vena cava filter implantation followed by urokinase thrombolysis. Angiography showed a marked reduction in filling defects. Rivaroxaban tablets were taken orally after the operation. On January 15, 2021, the left leg thrombus was aspirated under ultrasound guidance, and numerous long strips of thrombus were extracted (Figure 4C). Postoperative angiography showed that the filling defect had disappeared. On January 21, 2021, the filter was removed, and a thrombosis was attached to the filter (Figure 4D). He was discharged from the hospital on rivaroxaban.

Second hospital admission: He was given anti-anaphylactic treatment while rivaroxaban was continued orally.

Third hospital admission: Methylprednisolone sodium succinate (2.0 mg/kg/d) was administered. Prednisone (0.5 mg/kg/d) and rivaroxaban were administered orally at discharge. Prednisone and rivaroxaban were gradually discontinued over 3 mo.

OUTCOME AND FOLLOW-UP

After methylprednisolone sodium succinate treatment was administered, EC decreased significantly,

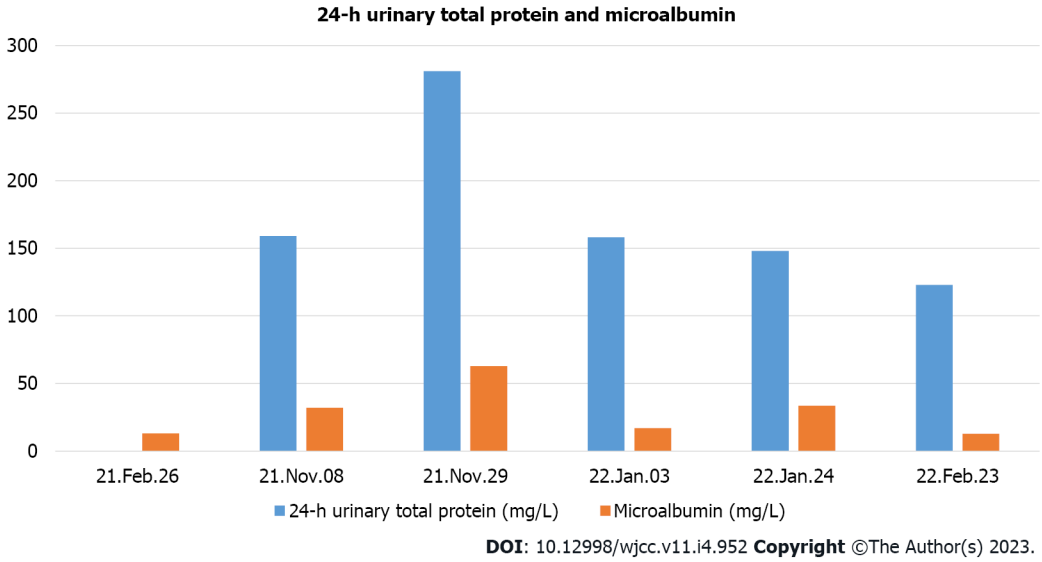

DOI: 10.12998/wjcc.v11.i4.952 **Copyright** ©The Author(s) 2023.

Figure 3 The 24-h urinary total protein and microalbumin levels reviewed at later stages.

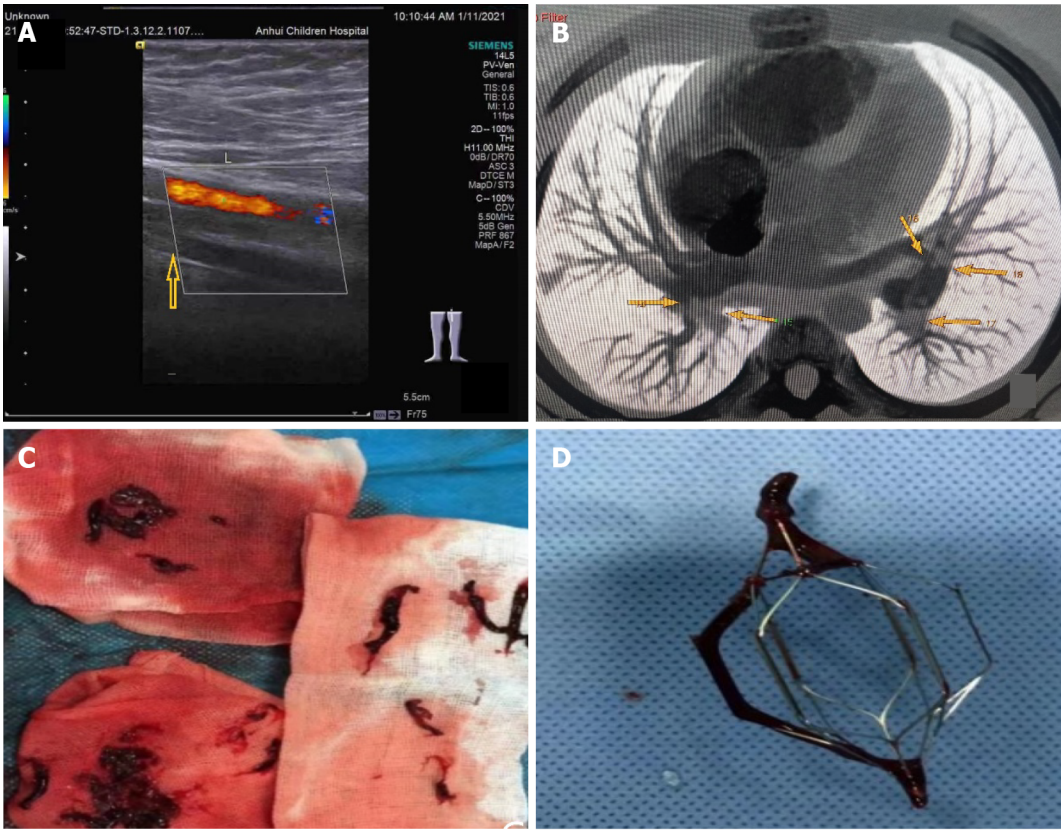

DOI: 10.12998/wjcc.v11.i4.952 **Copyright** ©The Author(s) 2023.

Figure 4 The 24-h urinary total protein and microalbumin levels reviewed at later stages. A: The arrow in the figure indicates the superficial femoral vein of the left lower extremity, through which no blood flow passes. The color flow is the superficial femoral artery of the left lower extremity; B: The arrows in the figure indicate multiple filling defects in the main pulmonary arteries of both lobes and segments; C: Many long thrombi aspirated from the left leg; D: When the filter was removed, a thrombosis was attached to the filter.

and the patient's skin rash, arthralgia, pain, temperature sensation, and toe activity gradually recovered. After following the child for one year, on November 8, 2021, the child showed signs of respiratory tract infection, skin rash in the legs again, and ankle pain. On November 10, 2021, purpura nephritis was diagnosed, and prednisone was given (0.2 mg/kg/d). The child has no symptoms at present, and his EC has decreased. His total urinary protein and micro urinary albumin levels gradually returned to normal. Presently, prednisone is being gradually reduced.

DISCUSSION

A 30% mortality rate in patients with PE was reported in some studies that included autopsy-based PE diagnosis[5]. PE in children is associated with central venous catheterization, malignancy, congenital heart disease, systemic lupus erythematosus, trauma, surgery, long-term total parenteral nutrition, dehydration, infection, hospitalization with a state of acquired or congenital hypercoagulability, oral contraceptive usage, and inactivity. There were no risk factors in our patient. One month later, the child had significantly elevated eosinophils (EOSs) and a symmetrical, dark-red rash on both legs that did not fade when pressed, accompanied by ankle swelling and pain. The rash was diagnosed as HSP after consultation with the nephrology department. HES can cause thrombi. A retrospective review of the English literature (Table 1) found 16 articles[6-21], a total of 21 patients were diagnosed with HES and complicated with thrombotic events, of which deep venous thrombosis accounted for 38%, and PE 33%. The mortality rate was 19%. HES is characterized by a consistently elevated EC of 1.5×10^9/L or more that lasts for at least 6 mo or across 2 examinations (≥ 1 mo between tests) and can be diagnosed immediately in the event of life-threatening end-organ injuries, such as PE and cerebrovascular thromboembolism, to avoid delayed treatment[22]. HES is more common in men than in women, and fever is the most common symptom, which can cause functional impairment of the skin, heart, nerves, lungs, digestive tract, and other organs. Thrombotic events are rare. The patient reported here presented with PE and left leg venous thrombosis as the first manifestation, and the peripheral blood eosinophil level was only slightly elevated at this time. Rato reported a case of IHES with a maximum peripheral eosinophil count of 0.83×10^9/L, but the pleural pathological examination was consistent with eosinophil pleurisy. Bronchoalveolar lavage revealed EOSs with a large pericardial effusion and left ventricular perforation. A pericardial biopsy indicated the presence of many EOSs[23]. According to the principles of monism, HES was considered likely in this case. HES has a complex etiology and can be divided into primary (mainly hematological tumors), secondary (allergic diseases such as asthma, parasitic or fungal infections, drugs, and rheumatic diseases), and idiopathic[24]. Our patient was negative for HES-related etiology and screening indicators, including infection, allergens, rheumatic diseases, immune deficiency, and tumors. The child was healthy and showed normal growth and development. He denied a history of rhinitis, asthma, intractable eczema, or repeated bacterial infections. He did not lose weight recently, nor did he have an enlargement of the liver, spleen, or lymph nodes, so primary HES was not supported. The onset age was young, there was no history of thrombotic disease in his lineal or collateral relatives, and no positive results were found in the genetic test. The diagnosis was IHES with multiple embolisms associated with HSP.

In most cases, PE originates from deep vein thrombosis of the legs. The child first had dyspnea, followed by left leg pain. PE may come from in situ thrombosis. In HES, symptoms similar to PE are usually caused by a large increase in EOSs in the pulmonary vasculature. Thus, this "thrombus" that is subsequently detected clinically is not a true thrombus but rather an accumulation of EOSs[25]. This pulmonary accumulation leaves fewer EOSs in peripheral blood, which may explain the EOS reduction in the PE with leg thrombosis in the present case. Furthermore, EOS release eosinophilic cationic protein (ECP), EOS peroxidase (EPO), major basic protein (MBP), and EOS-derived neurotoxin (EDN) to damage vascular endothelial cells through degranulation. MBP, ECP, and EPO can also improve the activity of tissue factors. Coagulation factors VI and X activate the endogenous coagulation pathway, inhibit the production of activated protein C, and cause hypercoagulability. In addition, EOSs can directly activate tissue factor, platelet-activating factor, and leukotriene; activate the exogenous coagulation pathway; activate and aggregate platelets; and promote thrombosis, while direct EC infiltration leads to vascular endothelial cell injury[26]. These mechanisms suggest that IHES may involve blood vessels and cause thrombi. The child's EC fluctuated between 2.63×10^9/L-7.85×10^9/L in the late stage, and neurological damage occurred. EOS particles contain EDN and MBP, which may be associated with neurological damage[27].

Glucocorticoids (0.5-1.0 mg/kg/d) are currently recommended as the mainstream treatment for IHES. It has been reported all patients' EC decreased, and 98.3% achieved complete remission after treatment with glucocorticoids. Standard anticoagulation treatments also effectively prevented the recurrence of venous thromboembolism, and no severe bleeding events were observed during the short-term follow-up. There is no published information about the long-term outcomes of glucocorticoids and anticoagulant therapy in patients with idiopathic eosinophilia (including HES) and venous thromboembolism[28]. Glucocorticoids inhibit EOS maturation and the production of cytokines and chemokines, induce EOS apoptosis, and reduce tissue and organ damage. Interferon-α, imatinib, hydroxyurea, or mepolizumab is recommended for glucocorticoid deficiency, intolerance, or long-term maintenance therapy[24]. In the case of thrombosis, anticoagulation, catheter interventional thrombolytic therapy, and surgical treatment can be selected, according to the location of the thrombosis, the time of embolization, and the specific situation of the patient[29]. The first symptom in the present child was multiple systemic embolisms. After the elimination of anticoagulant contraindications, anticoagulant and thrombolytic therapy were administered, and catheter interventional thrombolytic therapy was performed simultaneously. When IHES was combined with HSP, there was no recurrence of the rash after glucocorticoid administration. With anticoagulant therapy, the neurological damage gradually recovered, and the EOSs quickly returned to normal.

Table 1 Before and after are different patients

No.	Ref.	Number of cases	Symptom	Thrombotic events	Treat	Prognosis
1	[6]	2	Papules/multiple painful, papules and; plaques over both legs	DVT of the lower extremities, PE, left renal vein thrombosis/dermal microthrombi	Prednisolone and anticoagulants/unknown	Died/unknown
2	[7]	1	Pain and swelling of both legs accompanied with fever	DVT of the lower extremities, PE, portal thrombosis, mesenteric venous thrombosis	Prednisone, coumadin	Improved
3	[8]	2	Progressive chest pain, cough, hemoptysis, painless right leg swelling and 10 d history of intermittent diarrhea/pain and swelling of right leg, hemoptysis	DVT of the right lower extremity, PE	Anticoagulant, corticosteroids	Improved
4	[9]	1	Shortness of breath, chest pain, digital ischaemia	DVT of the lower extremities, PE, portal vein; thrombus, vena cava thrombus	Inferior vena cava filter insertion, thrombolysis, prednisolone, antico-agulation	Improved
5	[10]	1	Distal lower extremity paresthesias and fatigue	Cerebral arteriolar thromboembolism	Methylprednisolone	Died
6	[11]	1	Headaches, vomiting, a rise in blood pressure	Sagittal sinus vein thrombosis	Anticoagulation	Died
7	[12]	1	Fever, respiratory distress	Right atrial and ventricular thrombosis	Anticoagulation	Improved
8	[13]	2	Pain in the left inguinal region/palsy and pain in the right middle finger	Thrombus formation from the trunk of the portalvein, superior mesenteric vein, splenic vein, and right hepatic vein to deep veins in the lower extremities/A thrombus of the muscular artery in the subcutaneous region	Splenectomy, prednisolone, anticoagu-lation/prednisolone, cyclosporin A, prostaglandin E1, the finger was amputated	Improved
9	[14]	1	Left upper abdominal pain, dry cough, a painful, swollen left leg	DVT of the left lower extremity	Prednisolone, anticoagulation	Improved
10	[15]	1	Headache, vomiting	Superior sagittal sinus thrombosis	Anticoagulation	Improved
11	[16]	1	Fever	Portal vein thrombosis	Corticosteroids, anticoagulation	Improved
12	[17]	1	Disorientation, decreased muscle strength in the upper limbs, nonspecific chest pain	Arch of the aorta thrombus	Corticosteroids, anticoagulation	Aggravation
13	[18]	1	Cough, malaise, loss of appetite, and fever	DVT of the lower extremities, PE, and both right and left biventricular mural thrombi	Glucocorticoids	Improved
14	[19]	1	Swelling in the right parotid gland	Transverse and sigmoid sinuses thrombosis	Methylprednisolone	Died
15	[20]	1	Fever, hemoptysis, and chest pain	DVT of the lower extremities, PE	Dexamethasone, anticoagulation	Improved
16	[21]	3	Unknown	Superficial venous thrombophlebitis of the lower extremities	Prednisone, anticoagulation	Improved

DVT: Deep venous thrombosis; PE: Pulmonary embolism.

HSP, also known as IgA vasculitis, is the most common small vasculitis in childhood. It may affect the skin, joints, gastrointestinal tract, and kidneys. HSP can be complicated by venous thrombosis[30,31], but there was no evidence of HSP before the occurrence of thrombosis in this child. It is not clear whether IHES and HSP have a common pathogenesis. Interleukin-4 (IL-4) and IL-5 are cytokines secreted by Th2 cells. IL-5 specifically promotes terminal differentiation and proliferation of EOSs and is an important chemokine in EOSs. When inflammation occurs, EOSs aggregate and become activated, and a large amount of IL-5 is secreted, which leads to increased EOS proliferation and infiltration and leukotriene synthesis, resulting in a self-amplification effect and aggravation of the inflammatory response[32,33]. IL-5 and IL-4 can promote the expression of vascular endothelial cell adhesion molecules, thereby enhancing EOS, basophil, and endothelial cell binding and causing inflammatory cells to infiltrate local tissues. IL-5 not only activates EOSs but can also recruit transforming growth

factor β and various cytokines to promote IgA production in B lymphocytes, all of which play an important role in the pathogenesis of HSP[34]. IL-5 and ECP-activated EOSs may be factors in the pathogenesis of purpura nephritis[35]. The serum ECP of children with HSP during the acute episode was significantly higher than that of healthy children and children in remission with hormone therapy. The serum ECP of those with kidney involvement was significantly higher than that of those without kidney involvement. Late respiratory tract infection in children leads to recurrent rash, joint pain, increased urinary protein, and EC. This leads to the progression of purpura nephritis, in which IL-5, ECP, and mast cells also play a certain role[36]. The current case was isolated, and whether there are other pathways between eosinophilia and HSP needs to be further investigated.

CONCLUSION

In this case, a 12-year-old boy diagnosed with IHES presented with dyspnea and lower limb pain as the first presentation, with only mild eosinophilia, and later developed HSP. Respiratory infections can cause recurrence of HSP and an increase in eosinophils. For atypical rare diseases with multidisciplinary treatment and poor prognosis, clinical expertise should be paid more attention.

FOOTNOTES

Author contributions: Xu YY contributed to manuscript writing and editing and data collection; Wang YG, Zheng LY, Li M, and Dai Y contributed to data analysis; Huang XB and Zhao S contributed to conceptualization and supervision; all authors have read and approved the final manuscript.

Informed consent statement: Informed written consent was obtained from the patient for publication of this report and any accompanying images.

Conflict-of-interest statement: The authors declare that they have no conflict of interest to disclose.

CARE Checklist (2016) statement: The authors have read the CARE Checklist (2016), and the manuscript was prepared and revised according to the CARE Checklist (2016).

Country/Territory of origin: China

ORCID number: Yan-Yan Xu 0000-0001-9808-5927; Xiao-Bi Huang 0000-0002-8827-6145; Sheng Zhao 0000-0002-4116-8403.

S-Editor: Chen YL
L-Editor: A
P-Editor: Chen YL

REFERENCES

1 **Shomali W**, Gotlib J. World Health Organization-defined eosinophilic disorders: 2022 update on diagnosis, risk stratification, and management. *Am J Hematol* 2022; **97**: 129-148 [PMID: 34533850 DOI: 10.1002/ajh.26352]
2 **Markusse HM**, Schravenhoff R, Beerman H. Hypereosinophilic syndrome presenting with diarrhoea and anaemia in a patient with systemic lupus erythematosus. *Neth J Med* 1998; **52**: 79-81 [PMID: 9557531 DOI: 10.1016/s0300-2977(97)00086-7]
3 **Kane SP**. Ulcerative colitis with chronic liver disease, eosinophilia and auto-immune thyroid disease. *Postgrad Med J* 1977; **53**: 105-108 [PMID: 876921 DOI: 10.1136/pgmj.53.616.105]
4 **Chaudhuri K**, Dubey S, Zaphiropoulos G. Idiopathic hypereosinophilic syndrome in a patient with long-standing rheumatoid arthritis: a case report. *Rheumatology (Oxford)* 2002; **41**: 349-350 [PMID: 11934978 DOI: 10.1093/rheumatology/41.3.349]
5 **Heit JA**, Silverstein MD, Mohr DN, Petterson TM, O'Fallon WM, Melton LJ 3rd. Predictors of survival after deep vein thrombosis and pulmonary embolism: a population-based, cohort study. *Arch Intern Med* 1999; **159**: 445-453 [PMID: 10074952 DOI: 10.1001/archinte.159.5.445]
6 **Liao YH**, Su YW, Tsay W, Chiu HC. Association of cutaneous necrotizing eosinophilic vasculitis and deep vein thrombosis in hypereosinophilic syndrome. *Arch Dermatol* 2005; **141**: 1051-1053 [PMID: 16103348 DOI:

10.1001/archderm.141.8.1051]
7 **Sui T**, Li Q, Geng L, Xu X, Li Y. A case of hypereosinophilic syndrome presenting with multiorgan thromboses associated with intestinal obstruction. *Turk J Haematol* 2013; **30**: 311-314 [PMID: 24385812 DOI: 10.4274/Tjh.2012.0141]
8 **Li D**, Xu L, Lin D, Jiang S, Feng S, Zhu L. Acute pulmonary embolism and deep vein thrombosis secondary to idiopathic hypereosinophilic syndrome. *Respir Med Case Rep* 2018; **25**: 213-215 [PMID: 30237972 DOI: 10.1016/j.rmcr.2018.09.006]
9 **Todd S**, Hemmaway C, Nagy Z. Catastrophic thrombosis in idiopathic hypereosinophilic syndrome. *Br J Haematol* 2014; **165**: 425 [PMID: 24456103 DOI: 10.1111/bjh.12729]
10 **Grigoryan M**, Geisler SD, St Louis EK, Baumbach GL, Davis PH. Cerebral arteriolar thromboembolism in idiopathic hypereosinophilic syndrome. *Arch Neurol* 2009; **66**: 528-531 [PMID: 19364940 DOI: 10.1001/archneurol.2009.36]
11 **Schulman H**, Hertzog L, Zirkin H, Hertzanu Y. Cerebral sinovenous thrombosis in the idiopathic hypereosinophilic syndrome in childhood. *Pediatr Radiol* 1999; **29**: 595-597 [PMID: 10415185 DOI: 10.1007/s002470050656]
12 **Tai CP**, Chung T, Avasarala K. Endomyocardial fibrosis and mural thrombus in a 4-year-old girl due to idiopathic hypereosinophilia syndrome described with serial cardiac magnetic resonance imaging. *Cardiol Young* 2016; **26**: 168-171 [PMID: 25683059 DOI: 10.1017/S1047951115000013]
13 **Fujita K**, Ishimaru H, Hatta K, Kobashi Y. Hypereosinophilic syndrome as a cause of fatal thrombosis: two case reports with histological study. *J Thromb Thrombolysis* 2015; **40**: 255-259 [PMID: 25388084 DOI: 10.1007/s11239-014-1151-9]
14 **Gao SJ**, Wei W, Chen JT, Tan YH, Yu CB, Litzow MR, Liu QJ. Hypereosinophilic syndrome presenting with multiple organ infiltration and deep venous thrombosis: A case report and literature review. *Medicine (Baltimore)* 2016; **95**: e4658 [PMID: 27583887 DOI: 10.1097/MD.0000000000004658]
15 **Sakuta R**, Tomita Y, Ohashi M, Nagai T, Murakami N. Idiopathic hypereosinophilic syndrome complicated by central sinovenous thrombosis. *Brain Dev* 2007; **29**: 182-184 [PMID: 16996710 DOI: 10.1016/j.braindev.2006.08.004]
16 **Yamada Y**, Hoshino K, Shimojima N, Shinoda M, Obara H, Kawachi S, Fuchimoto Y, Tanabe M, Kitagawa Y, Morikawa Y. Idiopathic hypereosinophilic syndrome in a case with ABO-incompatible liver transplantation for biliary atresia complicated by portal vein thrombosis. *Pediatr Transplant* 2010; **14**: e49-e53 [PMID: 20042017 DOI: 10.1111/j.1399-3046.2009.01170.x]
17 **Silva MS**, Ramalho C, Ferreira F, Maia I, Joosten A. Idiopathic Hypereosinophilic Syndrome Presenting With Embolic Stroke. *Cureus* 2021; **13**: e19307 [PMID: 34900483 DOI: 10.7759/cureus.19307]
18 **Eisa N**, Shaheen K, Alraiyes AH, Alraies MC. Loeffler's endocarditis with biventricular mural thrombi. *BMJ Case Rep* 2013; **2013** [PMID: 24081624 DOI: 10.1136/bcr-2013-009609]
19 **Numagami Y**, Tomita T, Murakami K, Masaki I, Kubo K, Michiharu N. Sinus thrombosis in idiopathic hypereosinophilic syndrome causing fatal cerebral haemorrhage. *J Clin Neurosci* 2008; **15**: 585-587 [PMID: 18308571 DOI: 10.1016/j.jocn.2006.12.021]
20 **Chen TS**, Xing LH, Wang SL, Liu QH, Zhao SL, Yuan CC. Pulmonary embolism, deep vein thrombosis and recurrent bone cysts in a patient with hypereosinophilic syndrome. *Blood Coagul Fibrinolysis* 2016; **27**: 831-834 [PMID: 26780165 DOI: 10.1097/MBC.0000000000000501]
21 **Terrier B**, Piette AM, Kerob D, Cordoliani F, Tancrède E, Hamidou L, Lebbé C, Blétry O, Kahn JE. Superficial venous thrombophlebitis as the initial manifestation of hypereosinophilic syndrome: study of the first 3 cases. *Arch Dermatol* 2006; **142**: 1606-1610 [PMID: 17178987 DOI: 10.1001/archderm.142.12.1606]
22 **Akuthota P**, Weller PF. Spectrum of Eosinophilic End-Organ Manifestations. *Immunol Allergy Clin North Am* 2015; **35**: 403-411 [PMID: 26209892 DOI: 10.1016/j.iac.2015.04.002]
23 **Rueff Rato I**, Rigor J, Ferreira P, Laranjinha J, Santos-Silva G, Martins-Mendes D. Investigating Febrile Polyserositis: An Unusual Case of Idiopathic Hypereosinophilic Syndrome. *Eur J Case Rep Intern Med* 2021; **8**: 002426 [PMID: 33987122 DOI: 10.12890/2021_002426]
24 **Butt NM**, Lambert J, Ali S, Beer PA, Cross NC, Duncombe A, Ewing J, Harrison CN, Knapper S, McLornan D, Mead AJ, Radia D, Bain BJ; British Committee for Standards in Haematology. Guideline for the investigation and management of eosinophilia. *Br J Haematol* 2017; **176**: 553-572 [PMID: 28112388 DOI: 10.1111/bjh.14488]
25 **Karnak D**, Kayacan O, Beder S, Delibalta M. Hypereosinophilic syndrome with pulmonary and cardiac involvement in a patient with asthma. *CMAJ* 2003; **168**: 172-175 [PMID: 12538545]
26 **Noh HR**, Magpantay GG. Hypereosinophilic syndrome. *Allergy Asthma Proc* 2017; **38**: 78-81 [PMID: 28052805 DOI: 10.2500/aap.2017.38.3995]
27 **Moertel CL**, Kazacos KR, Butterfield JH, Kita H, Watterson J, Gleich GJ. Eosinophil-associated inflammation and elaboration of eosinophil-derived proteins in 2 children with raccoon roundworm (Baylisascaris procyonis) encephalitis. *Pediatrics* 2001; **108**: E93 [PMID: 11694677 DOI: 10.1542/peds.108.5.e93]
28 **Liu Y**, Meng X, Feng J, Zhou X, Zhu H. Hypereosinophilia with Concurrent Venous Thromboembolism: Clinical Features, Potential Risk Factors, and Short-term Outcomes in a Chinese Cohort. *Sci Rep* 2020; **10**: 8359 [PMID: 32433573 DOI: 10.1038/s41598-020-65128-4]
29 **Kearon C**, Akl EA, Comerota AJ, Prandoni P, Bounameaux H, Goldhaber SZ, Nelson ME, Wells PS, Gould MK, Dentali F, Crowther M, Kahn SR. Antithrombotic therapy for VTE disease: Antithrombotic Therapy and Prevention of Thrombosis, 9th ed: American College of Chest Physicians Evidence-Based Clinical Practice Guidelines. *Chest* 2012; **141**: e419S-e496S [PMID: 22315268 DOI: 10.1378/chest.11-2301]
30 **Diana A**, Gaze H, Laubscher B, De Meuron G, Tschantz P. A case of pediatric Henoch-Schönlein purpura and thrombosis of spermatic veins. *J Pediatr Surg* 2000; **35**: 1843 [PMID: 11101753 DOI: 10.1053/jpsu.2000.9293]
31 **Dhaliwal KK**, Lile NA, Tan CL, Lim CH. Life-threatening complications of Henoch-Schönlein purpura: diffuse alveolar haemorrhage, venous thrombosis and bowel ischaemia. *BMJ Case Rep* 2020; **13** [PMID: 32994270 DOI: 10.1136/bcr-2020-235905]
32 **Horii Y**, Muraguchi A, Iwano M, Matsuda T, Hirayama T, Yamada H, Fujii Y, Dohi K, Ishikawa H, Ohmoto Y. Involvement of IL-6 in mesangial proliferative glomerulonephritis. *J Immunol* 1989; **143**: 3949-3955 [PMID: 2592764]
33 **Yamaguchi Y**, Suda T, Suda J, Eguchi M, Miura Y, Harada N, Tominaga A, Takatsu K. Purified interleukin 5 supports the

terminal differentiation and proliferation of murine eosinophilic precursors. *J Exp Med* 1988; **167**: 43-56 [PMID: 3257253 DOI: 10.1084/jem.167.1.43]

34 **Sonoda E**, Matsumoto R, Hitoshi Y, Ishii T, Sugimoto M, Araki S, Tominaga A, Yamaguchi N, Takatsu K. Transforming growth factor beta induces IgA production and acts additively with interleukin 5 for IgA production. *J Exp Med* 1989; **170**: 1415-1420 [PMID: 2677210 DOI: 10.1084/jem.170.4.1415]

35 **Kawasaki Y**, Hosoya M, Suzuki H. Possible pathologenic role of interleukin-5 and eosino cationic protein in Henoch-Schönlein purpura nephritis. *Pediatr Int* 2005; **47**: 512-517 [PMID: 16190956 DOI: 10.1111/j.1442-200x.2005.02115.x]

36 **Namgoong MK**, Lim BK, Kim JS. Eosinophil cationic protein in Henoch-Schönlein purpura and in IgA nephropathy. *Pediatr Nephrol* 1997; **11**: 703-706 [PMID: 9438647 DOI: 10.1007/s004670050370]

World Journal of Clinical Cases

Submit a Manuscript: https://www.f6publishing.com

World J Clin Cases 2023 February 6; 11(4): 962-971

DOI: 10.12998/wjcc.v11.i4.962

ISSN 2307-8960 (online)

CASE REPORT

Three cases of jejunal tumors detected by standard upper gastrointestinal endoscopy: A case series

Jaesun Lee, Sunmoon Kim, Daesung Kim, Sangeok Lee, Kihyun Ryu

Specialty type: Medicine, research and experimental

Provenance and peer review: Unsolicited article; Externally peer reviewed.

Peer-review model: Single blind

Peer-review report's scientific quality classification

Grade A (Excellent): 0
Grade B (Very good): B, B, B
Grade C (Good): 0
Grade D (Fair): 0
Grade E (Poor): 0

P-Reviewer: Ergenç M, Turkey; Gao C, China; Iwamuro M, Japan

Received: November 22, 2022
Peer-review started: November 22, 2022
First decision: December 19, 2022
Revised: December 27, 2022
Accepted: January 9, 2023
Article in press: January 9, 2023
Published online: February 6, 2023

Jaesun Lee, Sunmoon Kim, Daesung Kim, Kihyun Ryu, Department of Gastroenterology, Konyang University Myunggok Medical Research Institute, Daejeon 35365, South Korea

Sangeok Lee, Department of Surgery, Konyang University Hospital, Konyang University College of Medicine, Daejeon 35365, South Korea

Corresponding author: Kihyun Ryu, MD, PhD, Associate Professor, Department of Gastroenterology, Konyang University Myunggok Medical Research Institute, 158 Gwanjeodong-ro, Seo-gu, Daejeon 35365, South Korea. medidrug@kyuh.ac.kr

Abstract

BACKGROUND

In patients with obscure gastrointestinal bleeding, re-examination with standard upper endoscopes by experienced physicians will identify culprit lesions in a substantial proportion of patients. A common practice is to insert an adult-sized forward-viewing endoscope into the second part of the duodenum. When the endoscope tip enters after the papilla, which is a marker for the descending part of the duodenum, it is difficult to endoscopically judge how far the duodenum has been traversed beyond the second part.

CASE SUMMARY

We experienced three cases of proximal jejunal masses that were diagnosed by standard upper gastrointestinal endoscopy and confirmed with surgery. The patients visited the hospital with a history of melena; during the initial upper gastrointestinal endoscopy and colonoscopy, the bleeding site was not confirmed. Upper gastrointestinal bleeding was suspected; thus, according to guidelines, upper endoscopy was performed again. A hemorrhagic mass was discovered in the small intestine. The lesion of the first patient was thought to be located in the duodenum when considering the general insertion depth of a typical upper gastrointestinal endoscope; however, during surgery, it was confirmed that it was in the jejunum. After the first case, lesions in the second and third patients were detected at the jejunum by inserting the standard upper endoscope as deep as possible.

CONCLUSION

The deep insertion of standard endoscopes is useful for the diagnosis of obscure gastrointestinal bleeding.

Key Words: Esophagogastroduodenoscopy; Obscure gastrointestinal bleeding; Jejunal neoplasm; Case report

Core Tip: In obscure gastrointestinal bleeding, guidelines recommend a second-look endoscopy. If there are negative results, enteroscopy is necessary. However, enteroscope is less commonly used than other endoscopes, and diagnosis may be delayed. We report cases of gastrointestinal stromal tumors in the jejunum diagnosed with standard upper endoscopy and confirmed by surgery. In many cases, we do not know how deep the endoscope was inserted; however, we found the tip of the upper endoscope reached the jejunum and confirmed it through surgery. We recommend inserting an upper gastrointestinal endoscope deeply when performing second-look endoscopy for obscure upper gastrointestinal bleeding.

Citation: Lee J, Kim S, Kim D, Lee S, Ryu K. Three cases of jejunal tumors detected by standard upper gastrointestinal endoscopy: A case series. *World J Clin Cases* 2023; 11(4): 962-971
URL: https://www.wjgnet.com/2307-8960/full/v11/i4/962.htm
DOI: https://dx.doi.org/10.12998/wjcc.v11.i4.962

INTRODUCTION

In clinical practice, many bleeding points can be initially identified by upper gastrointestinal endoscopy and colonoscopy. The small intestine is frequently difficult to approach because of its anatomical structure and location, leading to delayed diagnosis and treatment. Although many types of enteroscopes have been developed, they have difficulty in diagnosing and treating patients with active bleeding, especially regarding cost limitations. Considering the maintenance costs and frequency of use, many centers do not have enteroscopes. However, in clinical settings, since a several cases of small bowel bleeding occur at the proximal jejunum, those cases can be diagnosed and treated by colonoscopy or push enteroscopy[1]. Herein, we report three cases of obscure gastrointestinal bleeding from gastrointestinal stromal tumors in jejunum diagnosed by standard upper gastrointestinal endoscopy.

CASE PRESENTATION

Chief complaints

Case 1: A 55-year-old man presented with a 3 d history of melena.

Case 2: A 74-year-old woman presented with a 3 d history of melena.

Case 3: A 77-year-old woman presented with a 2 d history of melena.

History of present illness

Case 1: The patient visited a regional hospital because of black stools and underwent upper gastrointestinal endoscopy, colonoscopy, and abdominal computed tomography. However, the exact bleeding point was not identified; thus, he was referred to our clinic for further evaluation.

Case 2: The patient visited our emergency center because of black stools. She also presented epigastric pain and general weakness.

Case 3: The patient was referred to our hospital after visiting a regional hospital for black stools. She also presented general weakness.

History of past illness

Case 1: None.

Case 2: The patient was diagnosed with cerebrovascular accident accompanied by hypertension 17 years ago.

Case 3: The patient had been treated for cerebrovascular accidents 6 and 10 years ago.

Personal and family history

Case 1: None.

Case 2: The patient was on antihypertensive drug therapy including aspirin and had gait disturbance because of weakness in the right upper and lower extremities.

Case 3: The patient was on antihypertensive drug therapy including aspirin. She was under rehabilitation for gait disturbance and mostly remained in the lying position.

Physical examination

Case 1: Vital signs were normal. The bowel sounds increased.

Case 2: Vital signs were normal. No abdominal tenderness, rebound tenderness, and palpable mass were noted.

Case 3: Vital signs were normal. The bowel sounds increased.

Laboratory examinations

Case 1: Hemoglobin concentration dropped to 9.6 g/dL. Other results were within normal limits.

Case 2: Hemoglobin concentration dropped to 4.4 g/dL. Biochemical tests revealed blood urea nitrogen, 22.0 mg/dL; serum creatinine, 0.73 mg/dL; total bilirubin, 1.5 mg/dL, and other results were within normal limits.

Case 3: Hemoglobin concentration decreased to 6.0 g/dL, and other laboratory results were relatively in the normal range.

Imaging examinations

Case 1: The bleeding point was evaluated again by upper gastrointestinal endoscopy before the assessment of the small intestine. We used a video Gastroscope GIF-Q260 (working distance, 103 cm; Olympus Corp., Tokyo, Japan). Endoscopy was performed without sedation. After the stomach and the descending(second) part of the duodenum were thoroughly examined, the endoscope was maximally inserted using the axis-maintaining and bowel-shortening method as in the colonoscopy. While inserting the endoscope tip deeper from the third part of the duodenum, the color of the mucosal surface suddenly changed to dark. At that time, a 2.5 cm protruding mass of black mucosa was identified on the transitional area (Figure 1). The surface of the mass was smooth, the center was depressed, and its distal part had exposed blood vessels. Active bleeding was not noted at that time. Secondary reading of abdominal computed tomography from an outside hospital was made by a radiologist who was a subspecialist of gastrointestinal system in our hospital. According to the radiology report, intraluminal mass was noted at the proximal jejunum (Figure 2).

Case 2: Upper gastrointestinal endoscopy was performed to find the bleeding points, but neither active bleeding nor a suspicious lesion was identified. On the following day, colonoscopy was performed, which revealed large amounts of black stools without suspicious bleeding points. Since black blood clots were observed in the terminal portion of the ileum, the patient was scheduled for enteroscopy. Before enteroscopy, upper gastrointestinal endoscopy was performed again without sedation. The stomach and descending part of the duodenum were thoroughly examined with the same endoscope that was used in case 1, but no suspicious bleeding points were identified. The endoscope tip was maximally inserted deeper than the descending part of the duodenum using the axis-maintaining and bowel-shortening method with abdominal compression. During the insertion, the arrangement of the mucosal fold was altered, and a 1.5 cm protruding mass was seen at what appeared to be the jejunum (Figure 3). Abdominal computed tomography detected a 2.0 cm enhanced mass at what appeared to be the proximal jejunum (Figure 4).

Case 3: We performed upper gastrointestinal endoscopy and colonoscopy, but could not find any bleeding points. Abdominal computed tomography revealed a 3.8 cm dumbbell-shaped enhancing mass in the proximal jejunum (Figure 5). To check for active bleeding and perform biopsy, endoscopic examination was decided, and previously described (as in cases 1 and 2) standard upper gastrointestinal endoscopy was performed without sedation. The endoscope was inserted by the technique used in the previous cases. The mass covered with normal mucosa of approximately 3 cm in size was noted at the structure suspected as the proximal jejunum, nearly filling the lumen (Figure 6). Simultaneously with endoscopy, fluoroscopy was performed to confirm the location of the tip of the scope (Figure 7). A small bowel series was conducted to determine the exact location. On small bowel series, a 2.0 cm ellipsoid filling defect lesion was observed in the proximal jejunal loops at a distance of approximately 20 cm from the Treitz ligament (Figure 5).

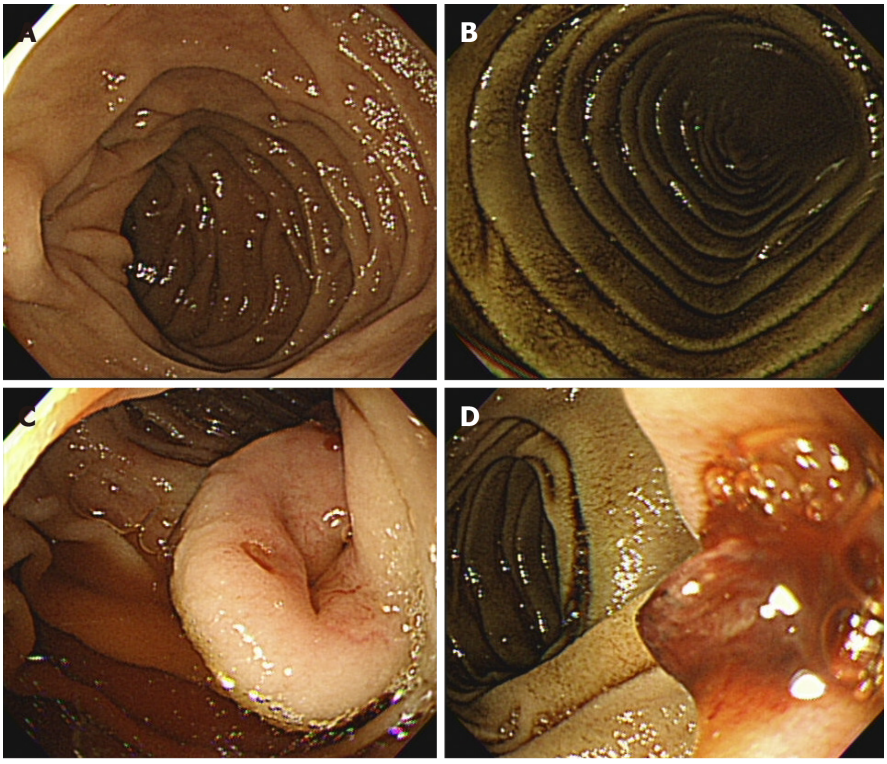

DOI: 10.12998/wjcc.v11.i4.962 **Copyright** ©The Author(s) 2023.

Figure 1 Conventional upper gastrointestinal endoscopy findings. A and B: A dark discoloration is seen in the area which suspected to the third part of the duodenum; C: There is an approximately 2.5 cm central depressed mass in the transitional zone with mucosal color; D: The mass shows a smooth surface and focal bleeding with exposed vessels.

FINAL DIAGNOSIS

Case 1: The tumor measured 2.7 cm × 2 cm, and the mitotic count was low (< 1/50 high-power fields).

Case 2: The tumor measured 3.9 cm × 2.2 cm, and the mitotic count was low (< 1/50 high-power fields).

Case 3: The tumor measured 2.5 cm × 1.6 cm, and the mitotic count was low (< 1/50 high-power fields).

Immunohistochemical studies of all cases showed positive staining for CD 117 (c-kit) in the tumor cells (Figure 8). These findings supported a diagnosis of a gastrointestinal stromal tumor (GIST) having a low risk.

TREATMENT

Case 1: According to the imaging study, the mass was thought to be a submucosal tumor located in the duodenum or jejunum because it is thought that forward-viewing standard upper gastrointestinal endoscopes commonly cannot reach over the distal part of the duodenum. Thus, the tumor location was not accurate, and the patient was scheduled for elective operation, with various possibilities of tumor location. For instance, if the location is retroperitoneal, pancreaticoduodenectomy (Whipple's operation) should be performed, which needs substantial time and skilled surgeons. While waiting for the surgery date, hematochezia suddenly developed, and emergency exploratory laparotomy was performed because of changes in the vital signs while preparing for surgery. The mass was found in the jejunum, 20 cm distal to the Treitz ligament, and segmental resection with end-to-end anastomosis was performed.

Case 2: Laparoscopic segmental small bowel resection was performed, and a protruding tumor in the proximal jejunum was identified.

Case 3: The patient underwent laparoscopic segmental small bowel resection.

DOI: 10.12998/wjcc.v11.i4.962 **Copyright** ©The Author(s) 2023.

Figure 2 Abdominal computed tomography with contrast enhancement. It shows an enhancing mass (arrow) with central depression and luminal narrowing at proximal jejunum. A: Axial view; B: Coronal view.

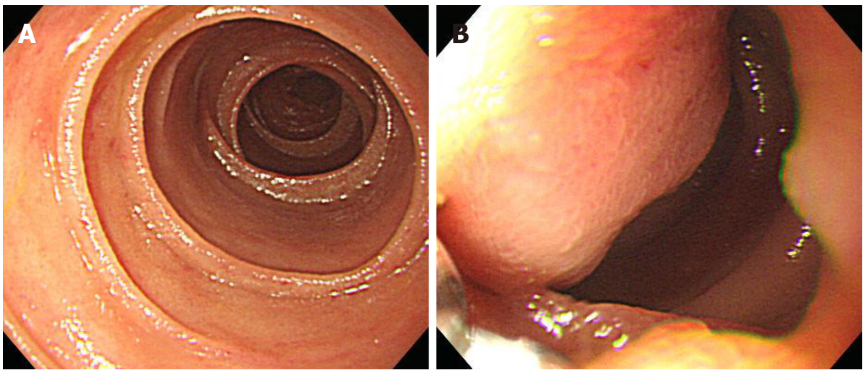

DOI: 10.12998/wjcc.v11.i4.962 **Copyright** ©The Author(s) 2023.

Figure 3 Conventional upper gastrointestinal endoscopy findings. A: The tip of an endoscope is inserted into the area suspected to the fourth part of the duodenum; B: A 1.5 cm sized irregular-shaped protruding mass is seen in the area suspected to the fourth part of the duodenum.

OUTCOME AND FOLLOW-UP

This part is not available.

DISCUSSION

Obscure gastrointestinal bleeding is a case in which bleeding points cannot be identified by initial upper gastrointestinal endoscopy and colonoscopy[2]. Causes of obscure gastrointestinal bleeding include bleeding tumors, such as malignant tumors or large adenomas, inflammatory diseases, vascular diseases, parasitic infestations, pancreaticobiliary tract diseases, and diverticula. Obscure gastrointestinal bleeding occurs mostly in the small intestine; thus, methods for the diagnosis of small intestinal diseases have been extensively studied so far[2].

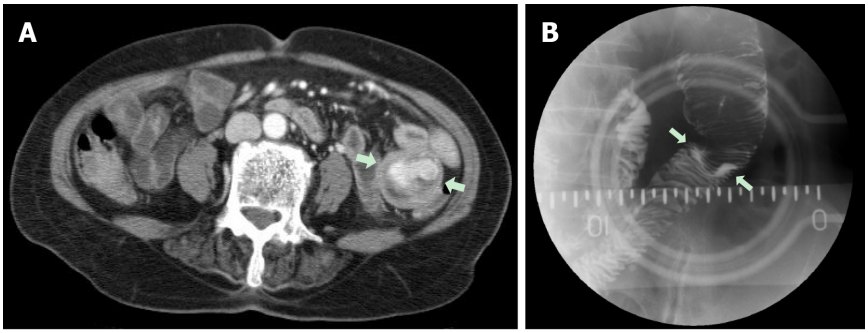

DOI: 10.12998/wjcc.v11.i4.962 **Copyright** ©The Author(s) 2023.

Figure 4 Abdominal computed tomography and small bowel series with barium findings. A: Abdominal computed tomography with contrast enhancement. It shows an enhanced mass(arrow) with luminal narrowing at the proximal jejunum; B: An intraluminal protruding mass is seen in the small bowel series with barium.

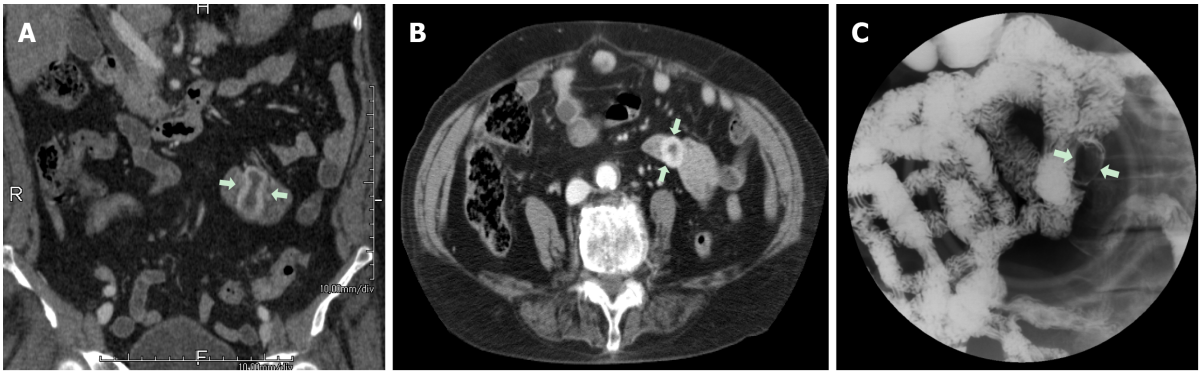

DOI: 10.12998/wjcc.v11.i4.962 **Copyright** ©The Author(s) 2023.

Figure 5 Abdominal computed tomography and small bowel series with barium findings. A and B: Abdominal computed tomography with contrast enhancement. They show a 3.8 cm sized dumbbell-shaped enhanced mass in the proximal jejunum (arrow). A: Coronal view; B: Axial view; C: A 2.0 cm sized filling defect lesion is seen in the small bowel series with barium.

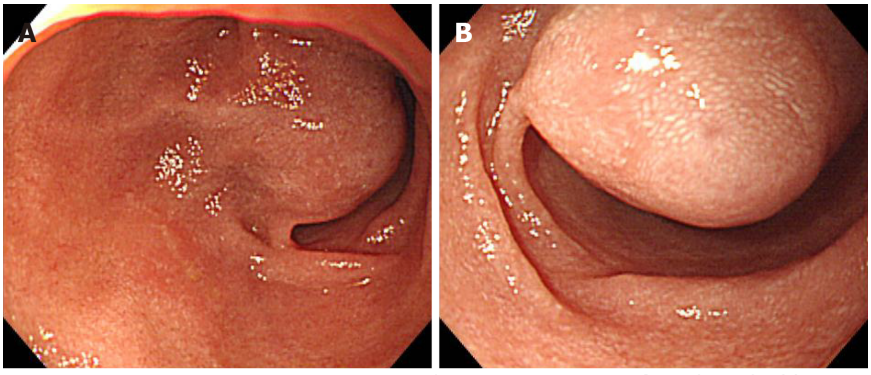

DOI: 10.12998/wjcc.v11.i4.962 **Copyright** ©The Author(s) 2023.

Figure 6 Conventional upper gastrointestinal endoscopy findings. A and B: A 3 cm sized mass covered with normal mucosa was nearly filling the lumen at proximal jejunum.

Numerous small bowel tests are available, and each has its advantages and disadvantages. Video capsule endoscopy has been widely used in clinical practice and has played a crucial role in the evaluation of obscure gastrointestinal bleeding. However, this endoscopy does not allow for tissue biopsy or endoscopic treatment, and some lesions could be missed because it passed through the duodenum and proximal jejunum too rapidly[3]. Thus, enteroscopy is superior to video capsule endoscopy. Enteroscopy includes push enteroscopy that can examine up to 70-150 cm distal to the Treitz ligament and deep enteroscopy. Currently, several techniques of deep enteroscopy that can examine almost the entire small intestine have been developed, such as double-balloon enteroscopy, single-balloon enteroscopy, and spiral enteroscopy[4]. However, these enteroscopic procedures have some

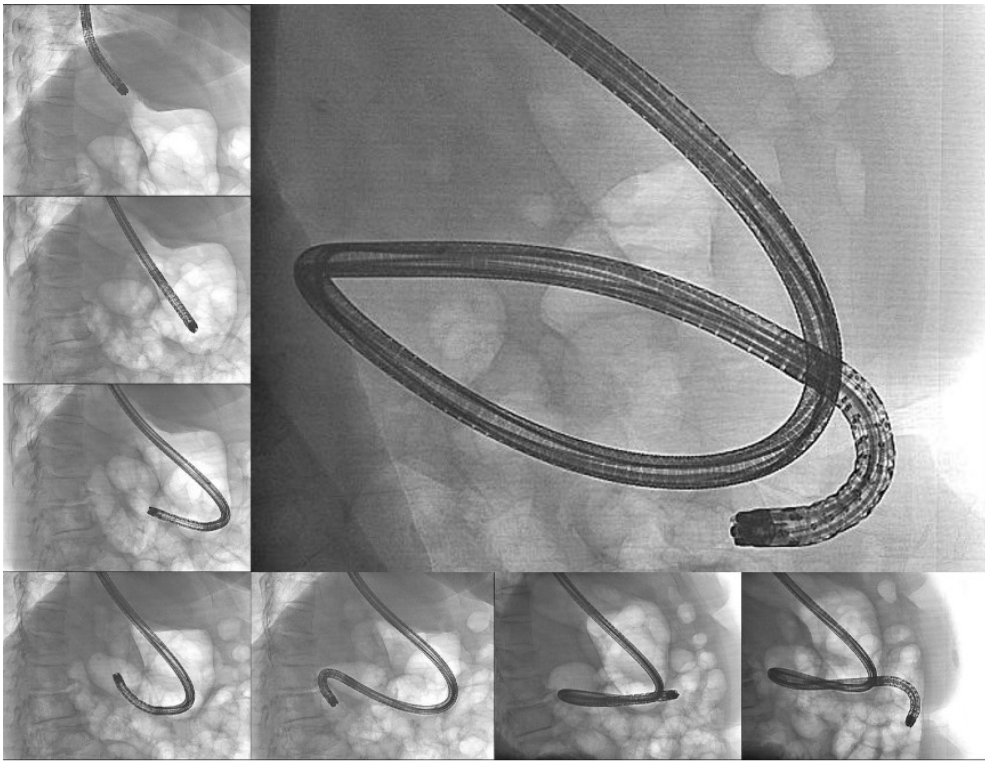

DOI: 10.12998/wjcc.v11.i4.962

Figure 7 Fluoroscopy findings. The largest image shows that the tip of the endoscope is located at proximal jejunum (beyond the Treitz ligament). Counterclockwise from the top left image: The tip of the endoscope is located at the cardia, angle, proximal antrum, distal antrum, bulb, ampulla of Vater, and distal duodenum.

disadvantages because they are expensive, and in some cases, enteroscopic treatment is not feasible. Hemostasis through angiography is necessary when patients' vital signs are unstable or massive active bleeding is suspected, but if there are no overt bleeding, the diagnostic yield is low[5]. Bleeding lesions are most frequently detected immediately after bleeding onset[6]. Bleeding lesions were found within the reach of standard endoscopy in 5%-25% of patients with obscure gastrointestinal bleeding, while bleeding points were not discovered on the first endoscopy[7-9]. Thus, many guidelines, especially the American Society for Gastrointestinal Endoscopy guideline[10] and the American College of Gastroenterology clinical guideline, recommend repeating gastrointestinal endoscopy in patients whose cause is not initially determined[11]. In cases where the aforementioned endoscopic procedures were performed again under the suspicion of upper gastrointestinal bleeding, experienced endoscopists can detect the culprit lesion[12]. Fry *et al*[13] detected potential and definitive bleeding lesions by re-examination within the reach of conventional upper and lower endoscopes in 47.6% and 24.3% of the patients with obscure gastrointestinal bleeding, respectively.

GISTs are rare forms of mesenchymal tumors in the gastrointestinal tract and are commonly discovered in the stomach (50%-60%) and small intestine (30%-35%) and less frequently in the colorectal area (5%) and esophagus (< 1%)[14]. In various studies of small bowel GISTs, tumors were often located in the jejunum[15-17]. Symptoms of GISTs are non-specific and vary in size and location. Small tumors (<2 cm) are mostly asymptomatic, and the most common symptom in symptomatic cases is gastrointestinal bleeding in 50% of the patients, followed by abdominal pain (20%-50%) and gastrointestinal obstruction (10%-30%)[18]. They account for 27% of the causes of small bowel bleeding [19]. According to Sass *et al*[20], gastrointestinal bleeding occurs in 87% of stromal tumors of the duodenum, 64% of stromal tumors of the small bowel except the duodenum, and 45% of stromal tumors of the stomach and colon including the rectum.

Byeon *et al*[21]. reported that double-balloon enteroscopy detected bleeding lesions in the jejunum in 18 of 30 patients with suspected gastrointestinal bleeding. They stated that the incidence of angiodysplasia was not significantly different between the jejunum and ileum (the small bowel distal to the jejunum) and that most of the erosive or ulcerative lesions and stromal tumors were found in the jejunum. In another study, in nine cases of Dieulafoy's lesion-induced small bowel bleeding, most of the lesions were located in the proximal jejunum[22]. Another study showed that stromal tumors were found more frequently in the jejunum than in the ileum (n = 264 *vs* n = 161) [23]. Therefore, meticulous examination of the jejunum is extremely important in patients with obscure gastrointestinal bleeding.

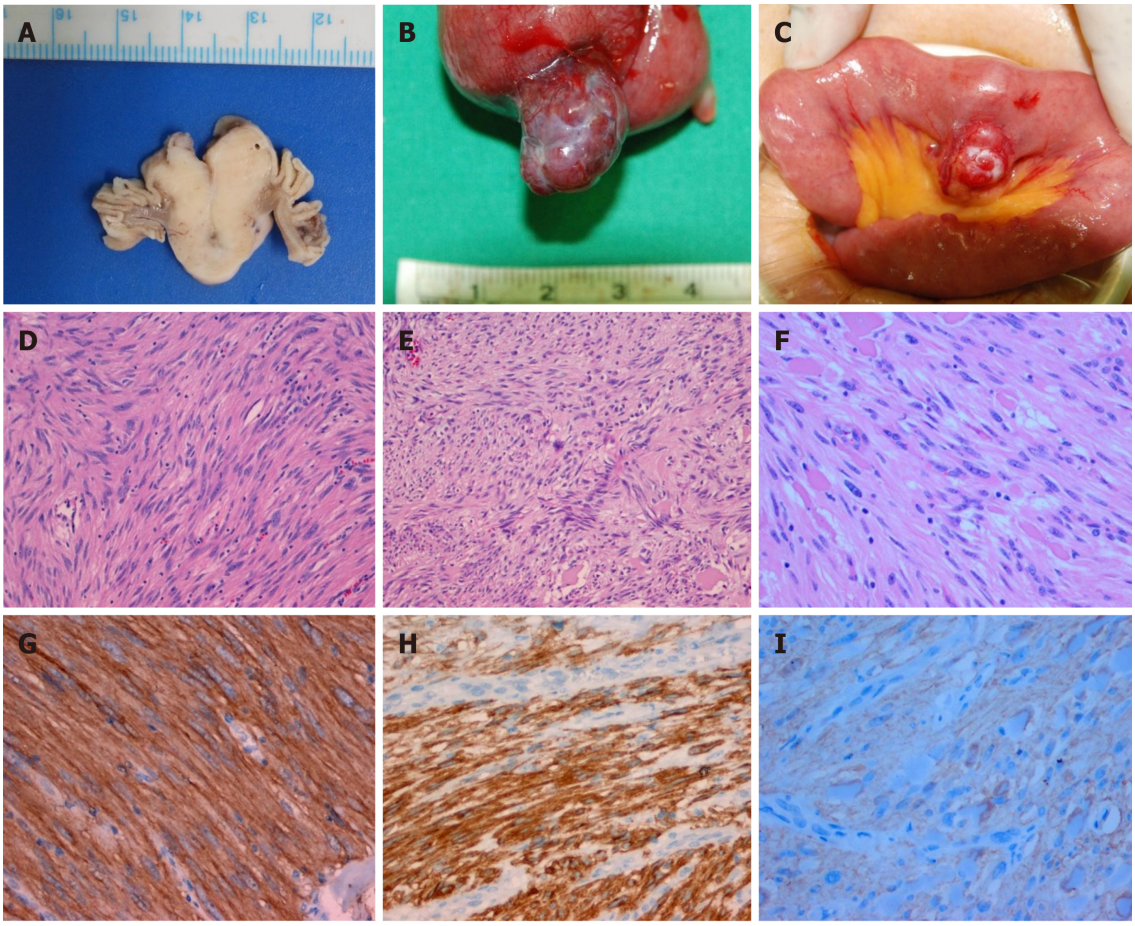

DOI: 10.12998/wjcc.v11.i4.962

Figure 8 Macroscopic and microscopic examination. A: Macroscopic cross section shows a gray-white solid tumor; B: Macroscopic examination shows a 2 cm (longest diameter) encapsulated lobulating mass; C: Macroscopic examination shows a 2.5 cm sized encapsulated round mass; D-F: Microscopic examinations show that the tumors are composed of spindle cells having high cellularity (hematoxylin-eosin staining, × 100); G-I: Immunohistochemically, these tumors are positive for CD117 (c-kit stain, × 200). (A, D, and G: Patient 1; B, E, and H: Patient 2; C, F, and I: Patient 3).

Conventional forward-viewing upper gastrointestinal endoscopy, which is also called esophagogastroduodenoscopy, has been widely used to observe the small intestine up to the descending part of the duodenum. Brady *et al*[24] investigated the maximum reach of a flexible GIF-K2 upper endoscope (working distance, 113 cm; Olympus, Tokyo, Japan) and a TX-8 upper endoscope (working distance, 110 cm; ACMI, Southborough, MA, United States) using X-rays. They stated that the endoscopes reached the second part of the duodenum in 96% of the endoscopic procedures, the third part in 51%, and the small intestine distal to the fourth part in 38%. Moreover, although none of the endoscopists recognized that the endoscope tip had reached the jejunum, X-ray imaging revealed that the endoscope tip had, in fact, reached the jejunum in 6 of 55 (10.9%) patients. This result implies that conventional upper gastrointestinal endoscopy has potential in finding lesions located in the proximal part of the jejunum.

We re-examined three patients with obscure gastrointestinal bleeding by upper gastrointestinal endoscopy using the axis-maintaining and bowel-shortening method as in colonoscopy and detected the bleeding lesions in the proximal part of the jejunum. In case 1, a bleeding lesion was identified by endoscopy, and computed tomography found it in the proximal part of the jejunum. However, considering that the maximum reach of upper gastrointestinal endoscopes is the duodenum, the patient was scheduled for elective operation including Whipple's operation. If partial resection or end-to-end anastomosis of the jejunum had been more quickly performed instead of a relatively invasive retroperitoneal surgery after confirmation of the tumor location in the jejunum, additional interventions, including massive blood transfusion, would not have been required, and the patient's clinical outcome would have become better. Based on this experience, in cases 2 and 3, tumors were detected in the jejunum by second-look upper gastrointestinal endoscopy, and surgery was performed after confirming their location. In case 3, we could intuitively check the location of endoscope tip in real time by performing fluoroscopy simultaneously with endoscopy. Many endoscopists wonder how far the endoscope tip extends during an upper gastrointestinal endoscopy, and our experience provide information.

Standard upper gastrointestinal endoscopy may not be needed in cases where enteroscopic procedures, such as push enteroscopy, are available immediately. In some reports, lesions of the small intestine have been diagnosed through an oral approach using a colonoscope or pediatric colonoscope [25,26]. However, pediatric colonoscopes are often not available in hospitals that do not perform endoscopy frequently for pediatric patients, and an oral approach using a conventional colonoscope can cause discomfort to patients. In a previous report, there were no adverse effects when the upper gastrointestinal endoscope was inserted deep into the duodenum to the fourth part compared with insertion to the second part, and in our case, there were no adverse effects related to deep insertion[27]. Meticulous re-examination by standard upper gastrointestinal endoscopy is usually recommended in patients with obscure gastrointestinal bleeding. In some cases, efforts to maximally insert an endoscope during re-examination by standard upper gastrointestinal endoscopy may be safe and effective for the detection of lesions in the proximal part of the jejunum. As advantages, this standard endoscopy could enable collection of biopsy specimens and perform immediate treatment of bleeding lesions; thus, it should be conducted before small bowel examinations.

CONCLUSION

Inserting a standard upper endoscope into the deeper part of the duodenum than the second part can help diagnose some cases of obscure gastrointestinal bleeding.

FOOTNOTES

Author contributions: Ryu K contributed conceptualization and supervision; Kim S and Ryu K collected and organized the data; Lee J and Ryu K wrote the original draft; Kim S, Kim D and Lee S reviewed and edited the manuscript; all authors have read and agreed to the published version of the manuscript.

Informed consent statement: Written informed consent was not received from the patients, but the reason for the exemption was recognized by the Institutional Review Board of Konyang University Hospital.

Conflict-of-interest statement: All authors declare no conflict of interest.

CARE Checklist (2016) statement: The authors have read the CARE Checklist (2016), and the manuscript was prepared and revised according to the CARE Checklist (2016).

Country/Territory of origin: South Korea

ORCID number: Daesung Kim 0000-0002-4881-7883; Kihyun Ryu 0000-0003-0595-6776.

S-Editor: Wang LL
L-Editor: A
P-Editor: Wang LL

REFERENCES

1 **Foutch PG**, Sawyer R, Sanowski RA. Push-enteroscopy for diagnosis of patients with gastrointestinal bleeding of obscure origin. *Gastrointest Endosc* 1990; **36**: 337-341 [PMID: 2210273 DOI: 10.1016/s0016-5107(90)71060-7]
2 **Raju GS**, Gerson L, Das A, Lewis B; American Gastroenterological Association. American Gastroenterological Association (AGA) Institute medical position statement on obscure gastrointestinal bleeding. *Gastroenterology* 2007; **133**: 1694-1696 [PMID: 17983811 DOI: 10.1053/j.gastro.2007.06.008]
3 **Arakawa D**, Ohmiya N, Nakamura M, Honda W, Shirai O, Itoh A, Hirooka Y, Niwa Y, Maeda O, Ando T, Goto H. Outcome after enteroscopy for patients with obscure GI bleeding: diagnostic comparison between double-balloon endoscopy and videocapsule endoscopy. *Gastrointest Endosc* 2009; **69**: 866-874 [PMID: 19136098 DOI: 10.1016/j.gie.2008.06.008]
4 **Jeon SR**, Kim JO. Deep enteroscopy: which technique will survive? *Clin Endosc* 2013; **46**: 480-485 [PMID: 24143307 DOI: 10.5946/ce.2013.46.5.480]
5 **Murphy B**, Winter DC, Kavanagh DO. Small Bowel Gastrointestinal Bleeding Diagnosis and Management-A Narrative

Review. *Front Surg* 2019; **6**: 25 [PMID: 31157232 DOI: 10.3389/fsurg.2019.00025]
6 **Bresci G**, Parisi G, Bertoni M, Tumino E, Capria A. The role of video capsule endoscopy for evaluating obscure gastrointestinal bleeding: usefulness of early use. *J Gastroenterol* 2005; **40**: 256-259 [PMID: 15830284 DOI: 10.1007/s00535-004-1532-5]
7 **Zaman A**, Sheppard B, Katon RM. Total peroral intraoperative enteroscopy for obscure GI bleeding using a dedicated push enteroscope: diagnostic yield and patient outcome. *Gastrointest Endosc* 1999; **50**: 506-510 [PMID: 10502171 DOI: 10.1016/s0016-5107(99)70073-8]
8 **Descamps C**, Schmit A, Van Gossum A. "Missed" upper gastrointestinal tract lesions may explain "occult" bleeding. *Endoscopy* 1999; **31**: 452-455 [PMID: 10494684 DOI: 10.1055/s-1999-151]
9 **Kitiyakara T**, Selby W. Non-small-bowel lesions detected by capsule endoscopy in patients with obscure GI bleeding. *Gastrointest Endosc* 2005; **62**: 234-238 [PMID: 16046986 DOI: 10.1016/s0016-5107(05)00292-0]
10 **ASGE Standards of Practice Committee**, Gurudu SR, Bruining DH, Acosta RD, Eloubeidi MA, Faulx AL, Khashab MA, Kothari S, Lightdale JR, Muthusamy VR, Yang J, DeWitt JM. The role of endoscopy in the management of suspected small-bowel bleeding. *Gastrointest Endosc* 2017; **85**: 22-31 [PMID: 27374798 DOI: 10.1016/j.gie.2016.06.013]
11 **Gerson LB**, Fidler JL, Cave DR, Leighton JA. ACG Clinical Guideline: Diagnosis and Management of Small Bowel Bleeding. *Am J Gastroenterol* 2015; **110**: 1265-87; quiz 1288 [PMID: 26303132 DOI: 10.1038/ajg.2015.246]
12 **Chak A**, Cooper GS, Canto MI, Pollack BJ, Sivak MV Jr. Enteroscopy for the initial evaluation of iron deficiency. *Gastrointest Endosc* 1998; **47**: 144-148 [PMID: 9512279 DOI: 10.1016/s0016-5107(98)70347-5]
13 **Fry LC**, Bellutti M, Neumann H, Malfertheiner P, Mönkemüller K. Incidence of bleeding lesions within reach of conventional upper and lower endoscopes in patients undergoing double-balloon enteroscopy for obscure gastrointestinal bleeding. *Aliment Pharmacol Ther* 2009; **29**: 342-349 [PMID: 19035975 DOI: 10.1111/j.1365-2036.2008.03888.x]
14 **Joensuu H**, Vehtari A, Riihimäki J, Nishida T, Steigen SE, Brabec P, Plank L, Nilsson B, Cirilli C, Braconi C, Bordoni A, Magnusson MK, Linke Z, Sufliarsky J, Federico M, Jonasson JG, Dei Tos AP, Rutkowski P. Risk of recurrence of gastrointestinal stromal tumour after surgery: an analysis of pooled population-based cohorts. *Lancet Oncol* 2012; **13**: 265-274 [PMID: 22153892 DOI: 10.1016/S1470-2045(11)70299-6]
15 **Zhou L**, Liao Y, Wu J, Yang J, Zhang H, Wang X, Sun S. Small bowel gastrointestinal stromal tumor: a retrospective study of 32 cases at a single center and review of the literature. *Ther Clin Risk Manag* 2018; **14**: 1467-1481 [PMID: 30174429 DOI: 10.2147/TCRM.S167248]
16 **Nakatani M**, Fujiwara Y, Nagami Y, Sugimori S, Kameda N, Machida H, Okazaki H, Yamagami H, Tanigawa T, Watanabe K, Watanabe T, Tominaga K, Noda E, Maeda K, Ohsawa M, Wakasa K, Hirakawa K, Arakawa T. The usefulness of double-balloon enteroscopy in gastrointestinal stromal tumors of the small bowel with obscure gastrointestinal bleeding. *Intern Med* 2012; **51**: 2675-2682 [PMID: 23037455 DOI: 10.2169/internalmedicine.51.7847]
17 **Vij M**, Agrawal V, Kumar A, Pandey R. Gastrointestinal stromal tumors: a clinicopathological and immunohistochemical study of 121 cases. *Indian J Gastroenterol* 2010; **29**: 231-236 [PMID: 21221881 DOI: 10.1007/s12664-010-0079-z]
18 **Marcella C**, Shi RH, Sarwar S. Clinical Overview of GIST and Its Latest Management by Endoscopic Resection in Upper GI: A Literature Review. *Gastroenterol Res Pract* 2018; **2018**: 6864256 [PMID: 30515204 DOI: 10.1155/2018/6864256]
19 **Lahoti S**, Fukami N. The small bowel as a source of gastrointestinal blood loss. *Curr Gastroenterol Rep* 1999; **1**: 424-430 [PMID: 10980982 DOI: 10.1007/s11894-999-0025-3]
20 **Sass DA**, Chopra KB, Finkelstein SD, Schauer PR. Jejunal gastrointestinal stromal tumor: a cause of obscure gastrointestinal bleeding. *Arch Pathol Lab Med* 2004; **128**: 214-217 [PMID: 14736280 DOI: 10.5858/2004-128-214-JGSTAC]
21 **Byeon JS**, Chung JW, Choi KD, Choi KS, Kim B, Myung SJ, Yang SK, Kim JH. Clinical features predicting the detection of abnormalities by double balloon endoscopy in patients with suspected small bowel bleeding. *J Gastroenterol Hepatol* 2008; **23**: 1051-1055 [PMID: 18086108 DOI: 10.1111/j.1440-1746.2007.05270.x]
22 **Dulic-Lakovic E**, Dulic M, Hubner D, Fuchssteiner H, Pachofszky T, Stadler B, Maieron A, Schwaighofer H, Püspök A, Haas T, Gahbauer G, Datz C, Ordubadi P, Holzäpfel A, Gschwantler M; Austrian Dieulafoy-bleeding Study Group. Bleeding Dieulafoy lesions of the small bowel: a systematic study on the epidemiology and efficacy of enteroscopic treatment. *Gastrointest Endosc* 2011; **74**: 573-580 [PMID: 21802676 DOI: 10.1016/j.gie.2011.05.027]
23 **Miettinen M**, Lasota J. Gastrointestinal stromal tumors: review on morphology, molecular pathology, prognosis, and differential diagnosis. *Arch Pathol Lab Med* 2006; **130**: 1466-1478 [PMID: 17090188 DOI: 10.5858/2006-130-1466-GSTROM]
24 **Brady CE 3rd**, Stewart DL, DiPalma JA, Clement DJ, Coleman TW, Rugh KS. Upper gastrointestinal endoscopy--how far does the endoscope go? *Gastrointest Endosc* 1985; **31**: 367-369 [PMID: 4076732 DOI: 10.1016/s0016-5107(85)72249-3]
25 **Jung HS**, Shim KN, Baik SJ, Ryu KH, Song HJ, Cho YK. A case of bleeding from proximal jejunal GIST diagnosed by colonoscopy through the oral approach. *Korean Journal of Gastrointestinal Endoscopy* 2007; 219-222
26 **Parker HW**, Agayoff JD. Enteroscopy and small bowel biopsy utilizing a peroral colonoscope. *Gastrointest Endosc* 1983; **29**: 139-140 [PMID: 6852478 DOI: 10.1016/s0016-5107(83)72558-7]
27 **Qiao WG**, Han ZM, Ren YT, Xing TY, Tan WX, De Liu S, Zhi FC. Role of esophagogastroduodenoscopy in detecting distal duodenal lesions: A single-center pilot study in Southern China. *J Dig Dis* 2017; **18**: 618-624 [PMID: 29024444 DOI: 10.1111/1751-2980.12549]

World Journal of Clinical Cases

Submit a Manuscript: https://www.f6publishing.com

World J Clin Cases 2023 February 6; 11(4): 972-978

DOI: 10.12998/wjcc.v11.i4.972

ISSN 2307-8960 (online)

CASE REPORT

Omental infarction diagnosed by computed tomography, missed with ultrasonography: A case report

Jae Kyoon Hwang, Yu Jeong Cho, Bo Seung Kang, Kyueng-Whan Min, Young Seo Cho, Yong Joo Kim, Kyung Suk Lee

Specialty type: Medicine, research and experimental

Provenance and peer review: Unsolicited article; Externally peer reviewed.

Peer-review model: Single blind

Peer-review report's scientific quality classification

Grade A (Excellent): 0
Grade B (Very good): B, B, B
Grade C (Good): C, C, C, C
Grade D (Fair): 0
Grade E (Poor): 0

P-Reviewer: Gao C, China; Yang L, China; Yao J, China; Fan L, China

Received: December 7, 2022
Peer-review started: December 7, 2022
First decision: December 19, 2022
Revised: December 28, 2022
Accepted: January 12, 2023
Article in press: January 12, 2023
Published online: February 6, 2023

Jae Kyoon Hwang, Kyung Suk Lee, Department of Pediatrics, Hanyang University Guri Hospital, Hanyang University College of Medicine, Guri-si 11923, Gyeonggi-do, South Korea

Yu Jeong Cho, Department of Surgery, Hanyang University Guri Hospital, Hanyang University College of Medicine, Guri-si 11923, Gyeonggi-do, South Korea

Bo Seung Kang, Department of Emergency Medicine, Hanyang University Guri Hospital, Hanyang University College of Medicine, Guri-si 11923, Gyeonggi-do, South Korea

Kyueng-Whan Min, Department of Pathology, Hanyang University Guri Hospital, Hanyang University College of Medicine, Guri-si 11923, Gyeonggi-do, South Korea

Young Seo Cho, Department of Radiology, Hanyang University Guri Hospital, Hanyang University College of Medicine, Guri-si 11923, Gyeonggi-do, South Korea

Yong Joo Kim, Department of Pediatrics, Hanyang University Hospital, Hanyang University College of Medicine, Seoul 04763, South Korea

Corresponding author: Kyung Suk Lee, MD, PhD, Associate Professor, Department of Pediatrics, Hanyang University Guri Hospital, Hanyang University College of Medicine, 153 Gyeongchun-ro, Guri-si 11923, Gyeonggi-do, South Korea. lksallergy@gmail.com

Abstract

BACKGROUND

Omental infarction (OI) is a surgical abdominal disease that is not common in adults and is very rare in children. Similar to various acute abdominal pain diseases including appendicitis, diagnosis was previously achieved by diagnostic laparotomy but more recently, ultrasonography or computed tomography (CT) examination has been used.

CASE SUMMARY

A 6-year-old healthy boy with no specific medical history visited the emergency room with right lower abdominal pain. He underwent abdominal ultrasonography by a radiologist to rule out acute appendicitis. He was discharged with no significant sonographic finding and symptom relief. However, the symptoms persisted for 2 more days and an outpatient visit was made. An outpatient abdominal CT was used to make a diagnosis of OI. After laparoscopic operation, his symptoms resolved.

CONCLUSION
In children's acute abdominal pain, imaging studies should be performed for appendicitis and OI.

Key Words: Omental infarction; Children; Ultrasonography; Computed tomography; Case report

Core Tip: We report the case of a 6-year-old boy with omental infarction (OI) diagnosed by computed tomography (CT) and missed by ultrasonography. The patient who complained of right abdominal pain underwent a laboratory test and ultrasound examination in the emergency room. However, there were no specific findings, so he was discharged. However, the abdominal pain persisted, so a CT scan was performed at the outpatient clinic. Then, OI was diagnosed, and he underwent laparoscopic operation and was discharged after hospitalization. Even if there are no specific findings by ultrasonography, CT examination should be carefully considered.

Citation: Hwang JK, Cho YJ, Kang BS, Min KW, Cho YS, Kim YJ, Lee KS. Omental infarction diagnosed by computed tomography, missed with ultrasonography: A case report. *World J Clin Cases* 2023; 11(4): 972-978
URL: https://www.wjgnet.com/2307-8960/full/v11/i4/972.htm
DOI: https://dx.doi.org/10.12998/wjcc.v11.i4.972

INTRODUCTION

Omental infarction (OI) is a rare disease of acute abdominal pain in children[1]. Abdominal pain is a common cause of emergency department visits and appendicitis is the most common cause of abdomen surgery in children[2]. OI was reported in about 0.1% to 0.5% of children undergoing surgery for appendicitis[3]. Therefore, it is common for many doctors to initially suspect OI as appendicitis or other diseases, and many cases have been diagnosed intraoperatively[2]. Currently, because of advances in imaging technologies, the number of cases diagnosed by abdominal ultrasound and computed tomography (CT), rather than surgery, is increasing[3-5]. Although abdominal ultrasound and CT have high accuracy, CT has higher sensitivity for OI diagnosis[6].

This case was suspected of appendicitis in the emergency department, and an ultrasound examination was performed, but no singularity was found. The patient was discharged but diagnosed by an outpatient CT scan two days later.

CASE PRESENTATION

Chief complaints

A 6-year-old healthy boy with no specific medical history visited the emergency room with right lower abdominal pain that started two days before the visit.

History of present illness

The day before the visit, he received a prescription from the local clinic, but there was no improvement, so he went to the emergency room.

History of past illness

A history of abdominal pain was not presented.

Personal and family history

No family history of abdominal disease.

Physical examination

The patient's height and weight were 115 cm and 29 kg, respectively. His vital signs in the emergency room were as follows: Body temperature, 37 °C; heart rate, 110 beats/min; and respiratory rate, 22 breaths/min. Tenderness of the right lower quadrant (RLQ) was observed, but rebound tenderness, muscle guarding, and rigid abdomen were not observed.

Laboratory examinations

Not performed, because radiological findings were not significantly abnormal and the patient's symptoms were relieved.

Imaging examinations

Abdominal X-ray examination was performed, and gaseous distension was observed (Figure 1A and B). Abdominal ultrasound was performed after being referred to a radiologist to rule out acute appendicitis. Ultrasonography showed the appendix had collapsed and tenderness was not present. In addition, there was no significant wall thickening or tenderness in the scanned bowel loop, and no abnormal fluid collection or enlarged lymph node was seen in the abdominal cavity. There were no abnormal findings on ultrasonography.

Initial diagnosis

Gastrointestinal disease; abdominal pain, right lower quadrant.

Initial treatment

The symptoms improved spontaneously and the patient was discharged.

Clinical course

The patient visited the pediatric outpatient department two days later due to aggravated abdominal pain. At the visit, he had a limp, severe pain around the periumbilical area, no fever, and no symptoms such as nausea, vomiting, or anorexia. On physical examination, tenderness of the RLQ remained. A glycerin enema was performed under the suspicion of fecal impaction on initial X-ray, but there were no feces and no palpable stool by digital rectal examination. An additional physical examination showed rebound tenderness and a laboratory exam was performed. Inflammatory findings were as follows: white blood cell (WBC) 13200/mm^3, absolute neutrophil count (ANC) 9540/mm^3, erythrocyte sedimentation rate 40 mm/hr, and C-reactive protein (CRP) 1.2 mg/dL, but no electrolyte imbalance was observed. The calculated pediatric appendicitis score was 7, which was likely appendicitis, and contrast enhanced abdomen CT scan was examined. The appendix was collapsed, and no evidence of acute appendicitis was found. Abdominal CT scan showed approximately 4 cm of fat lobule below the umbilical ligament of the liver left lobe. A hyperdense halo and surrounding fat stranding were detected in the periphery of the fat lobule. The vessel of the upper portion inside the fat lobule showed a whirling sign. These abdominal CT findings were consistent with OI, and surgery was performed on the same day in consultation with the pediatric surgeon.

FINAL DIAGNOSIS

The final diagnosis was OI.

TREATMENT

The patient underwent laparoscopic surgery (Figure 2) and OI was confirmed by histological examination (Figure 3).

OUTCOME AND FOLLOW-UP

After laparoscopic surgery, the patient's pain improved and he was discharged at POD 5 without any complications.

DISCUSSION

An OI usually affects only one part of the omentum and is commonly seen on the right side[7]. Therefore, it is often necessary to differentiate OI from appendicitis because the side of the abdominal pain is similar[2]. The cause of OI was unclear. Explanations might include abnormal arterial supply to the omentum, torsion around the omental pedicle, or venous torsion usually involving the right epiploic vessels[1,8]. There are several risk factors for OI such as obesity, trauma, coughing, and overeating and such factors can cause thrombosis or infarction[8]. The patient reported that he had recently gained weight rapidly and was obese with a Body Mass Index of 21.9 kg/m^2 (99.5 percentile).

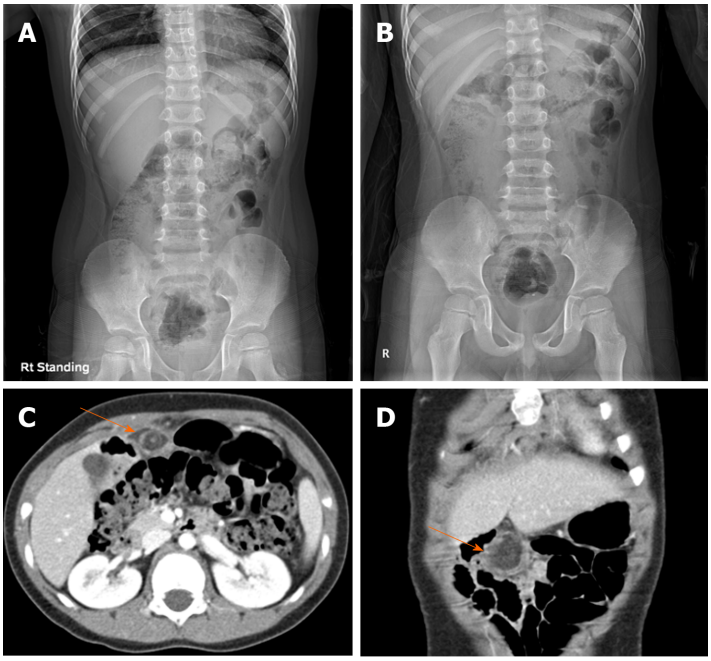

DOI: 10.12998/wjcc.v11.i4.972 **Copyright** ©The Author(s) 2023.

Figure 1 Radiologic study. A and B: Simple abdomen; C and D: Computed tomography. On erect (A) and supine (B) plain radiography, feces and gas are found inside the large bowel, and no other specific findings are shown. Axial (C) and coronal (D) scan of abdominal computed tomography show a fat lobule below the umbilical ligament of the liver left lobe. A hyperdense halo and surrounding fat stranding are in the periphery of the fat lobule (arrow). The vessel of the upper portion inside the fat lobule shows a whirling sign.

DOI: 10.12998/wjcc.v11.i4.972 **Copyright** ©The Author(s) 2023.

Figure 2 Intraoperative photography demonstrating an infarcted omentum adherent to the anterior abdominal wall. The white arrow shows the falciform ligament.

OI occurs in approximately 0.1% to 0.5% of children evaluated for acute appendicitis[3]. The male to female ratio is usually 2:1[9]. OI was reported in 15% of children and 85% of adults, so it is very rare in children and very difficult to diagnose at first examination[10]. Abdominal pain is common in children and most are non-surgical diseases such as constipation and enteritis. Appendicitis is the most common pediatric surgical abdominal disease in children, and it accounts for 20%-30% of children's colic[11,12]. Other surgical abdominal diseases of children are intussusception, Meckel's diverticulum, and so on. Intussusception mainly occurs from 6 mo to 2 years old, and Meckel's diverticulum represents an intestinal obstruction and/or painless gastrointestinal hemorrhage[11,13]. In our patient, considering his age and symptoms, the likelihood of intussusception and Meckel's diverticulum was low, and appendicitis was evaluated. When the patient visited the emergency room, small bowel and appendix ultrasonography were performed by an expert radiologist. The patient, who had no significant abnormal findings by ultrasonography, was discharged.

When he came to the outpatient clinic two days later, an enema was administered first because constipation was suspected by simple abdomen X-ray examination. Because there were no abnormal findings by enema and rectal examination, it was necessary to differentiate other abdominal diseases. Therefore, we performed a laboratory study. Then, we calculated the pediatric appendicitis score as 7

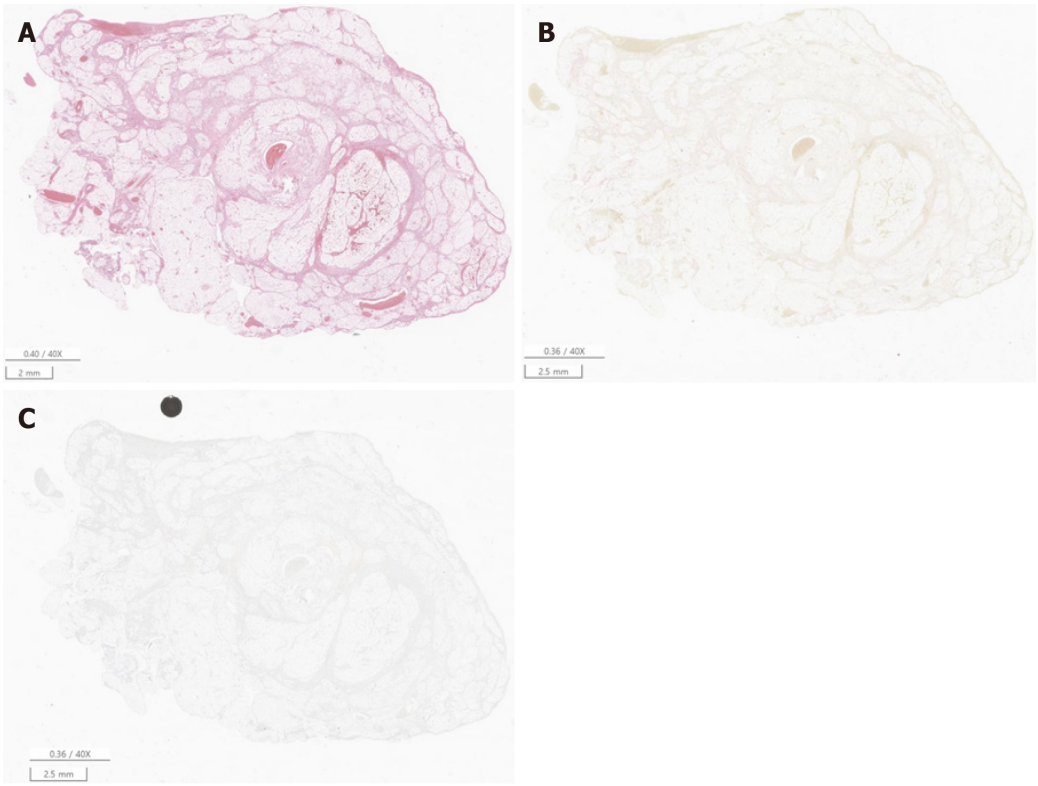

DOI: 10.12998/wjcc.v11.i4.972

Figure 3 Representative microscopic features. A: Omentum is consistent with a hemorrhagic infarction [Hematoxylin & Eosin staining (HE), original magnification × 40]; B: Microorganisms were not identified by Gram staining (HE, original magnification × 40); C: The Ki-67 proliferative index was 5% (HE, original magnification × 40).

points (likely appendicitis), so it was necessary to differentiate other abdominal diseases by CT[14,15]. Previous studies revealed that leukocytosis and fever are minor symptoms of OI[6]. A previous study compared OI and acute appendicitis in children and suggested that OI should be considered in patients with lower right abdominal pain with a neutrophil fraction < 77%[16]. The results showed that WBCs (11928 ± 1042 and 16207 ± 857; *P* value 0.024), neutrophils (8080 ± 832 and 14057 ± 781; *P* value 0.001), and CRP (3.349 ± 1.155 and 9.082 ± 1.659 mg/dL; *P* value 0.008) were significantly different between OI and acute appendicitis[16]. These findings were consistent with our case. Our patient had leukocytosis (WBC > 10000) and neutrophilia (ANC > 7500). In children and adolescents, ultrasonography is preferred over CT because of the risk of exposure to radiation[3]. On ultrasonography, OI shows increased echogenicity of noncompressible omental fat in a painful area[17,18]. In children, OI is difficult to diagnose *via* ultrasound when communication or symptoms are unclear. In this case, the patient was considered to have a negative ultrasound finding because the symptom was unclear and the presentation of abdominal pain was not localized. Clinically, OI is difficult to distinguish from acute appendicitis and often misdiagnosed as acute appendicitis, leading to surgery[19]. Although abdominal ultrasonography is a safe diagnostic method, CT is the gold standard for the diagnosis of OI due to its high specificity and sensitivity[3,20]. Therefore, CT may be considered if acute appendicitis is not clearly ruled out or if abdominal pain persists even after acute appendicitis is excluded. The CT findings of acute appendicitis, which is the most common cause requiring surgery for RLQ pain, include a distended appendix with a diameter of more than 6 mm, wall thickening of more than 3 mm, and secondary inflammatory periappendiceal chances. The sensitivity and specificity of CT for the diagnosis of acute appendicitis are within the range of 94%-98%[21]. However, because children are vulnerable to radiation, the same dose of radiation is more harmful to them than to adults. The abdominal CT scan was examined with a tube voltage of 100 kVp, and the dose length product was 166 mGycm, which was much lesser than the abdominal CT dose for adults. Nevertheless, additional efforts should be devoted to reducing the radiation dose as much as possible in the abdominal CT examination for children. Ultrasonography is more useful for follow-up to check whether OI has resolved after conservative treatment without radiation exposure[3].

As for OI treatment, it has not yet been precisely determined whether surgical or conservative treatment is better[6]. Some recommend conservative treatment because OI is a self-limiting disease that occurs over 10 to 15 days, whereas others insist on surgical treatment for quick recovery and prevention of a secondary abscess[22,23]. This patient complained of severe pain, and with the consent of his parents, the OI was treated with surgery.

CONCLUSION

In conclusion, if a case has right abdominal pain and no specific findings on ultrasonography, a CT examination should be carefully considered if symptoms do not improve by follow-up or other diseases are suspected. However, because there is a risk of radiation exposure, its implementation should be minimized.

FOOTNOTES

Author contributions: Lee KS, Hwang JK, Cho YJ, Kang BS, Min YH and Kim YJ planned and designed the study; Lee KS, Hwang JK, Cho YJ, Min YH and Cho YS wrote the main manuscript text and prepared the figures; Kang BS, Cho YS and Kim YJ supervised this manuscript; Lee KS, Hwang JK, Cho YJ, Kang BS, Min YH, Cho YS and Kim YJ revised the manuscript.

Informed consent statement: We obtained parental consent for this case report.

Conflict-of-interest statement: All authors declare no conflict of interests for this article.

CARE Checklist (2016) statement: The authors have read the CARE Checklist (2016), and the manuscript was prepared and revised according to the CARE Checklist (2016).

Country/Territory of origin: South Korea

ORCID number: Jae Kyoon Hwang 0000-0003-0312-567X; Yu Jeong Cho 0000-0001-6823-2746; Bo Seung Kang 0000-0002-0792-0198; Kyueng-Whan Min 0000-0002-4757-9211; Young Seo Cho 0000-0003-4034-7271; Yong Joo Kim 0000-0002-2654-5397; Kyung Suk Lee 0000-0002-6300-1348.

S-Editor: Wang LL
L-Editor: A
P-Editor: Wang LL

REFERENCES

1 **Arigliani M**, Dolcemascolo V, Nocerino A, Pasqual E, Avellini C, Cogo P. A Rare Cause of Acute Abdomen: Omental Infarction. *J Pediatr* 2016; **176**: 216-216.e1 [PMID: 27289499 DOI: 10.1016/j.jpeds.2016.05.034]
2 **Di Nardo G**, Di Serafino M, Gaglione G, Mercogliano C, Masoni L, Villa MP, Parisi P, Ziparo C, Vassallo F, Evangelisti M, Vallone G, Esposito F. Omental Infarction: An Underrecognized Cause of Right-Sided Acute Abdominal Pain in Children. *Pediatr Emerg Care* 2021; **37**: e1555-e1559 [PMID: 33170567 DOI: 10.1097/PEC.0000000000002114]
3 **Kozłowski M**, Piotrowska O, Giżewska-Kacprzak K. Omental Infarction in a Child-Conservative Management as an Effective and Safe Strategy in Diagnosis and Treatment. *Int J Environ Res Public Health* 2021; **18** [PMID: 34360347 DOI: 10.3390/ijerph18158057]
4 **Tonerini M**, Calcagni F, Lorenzi S, Scalise P, Grigolini A, Bemi P. Omental infarction and its mimics: imaging features of acute abdominal conditions presenting with fat stranding greater than the degree of bowel wall thickening. *Emerg Radiol* 2015; **22**: 431-436 [PMID: 25725796 DOI: 10.1007/s10140-015-1302-0]
5 **McCusker R**, Gent R, Goh DW. Diagnosis and management of omental infarction in children: Our 10 year experience with ultrasound. *J Pediatr Surg* 2018; **53**: 1360-1364 [PMID: 29550035 DOI: 10.1016/j.jpedsurg.2018.02.047]
6 **Rimon A**, Daneman A, Gerstle JT, Ratnapalan S. Omental infarction in children. *J Pediatr* 2009; **155**: 427-431.e1 [PMID: 19540514 DOI: 10.1016/j.jpeds.2009.03.039]
7 **van Breda Vriesman AC**, de Mol van Otterloo AJ, Puylaert JB. Epiploic appendagitis and omental infarction. *Eur J Surg* 2001; **167**: 723-727 [PMID: 11775722 DOI: 10.1080/11024150152707680]
8 **Bachar GN**, Shafir G, Postnikov V, Belenky A, Benjaminov O. Sonographic diagnosis of right segmental omental infarction. *J Clin Ultrasound* 2005; **33**: 76-79 [PMID: 15674838 DOI: 10.1002/jcu.20091]
9 **Coulier B**. Segmental omental infarction in childhood: a typical case diagnosed by CT allowing successful conservative treatment. *Pediatr Radiol* 2006; **36**: 141-143 [PMID: 16328324 DOI: 10.1007/s00247-005-0025-x]
10 **Esposito F**, Ferrara D, Schillirò ML, Grillo A, Diplomatico M, Tomà P. "Tethered Fat Sign": The Sonographic Sign of Omental Infarction. *Ultrasound Med Biol* 2020; **46**: 1105-1110 [PMID: 32035686 DOI: 10.1016/j.ultrasmedbio.2020.01.003]
11 **Nguyen PN**, Petchers A, Choksi S, Edwards MJ. Common Conditions II: Acute Appendicitis, Intussusception, and Gastrointestinal Bleeding. *Surg Clin North Am* 2022; **102**: 797-808 [PMID: 36209746 DOI: 10.1016/j.suc.2022.07.010]

12 **Patterson KN**, Deans KJ, Minneci PC. Shared decision-making in pediatric surgery: An overview of its application for the treatment of uncomplicated appendicitis. *J Pediatr Surg* 2022 [PMID: 36379750 DOI: 10.1016/j.jpedsurg.2022.10.009]

13 **Hansen CC**, Søreide K. Systematic review of epidemiology, presentation, and management of Meckel's diverticulum in the 21st century. *Medicine (Baltimore)* 2018; **97**: e12154 [PMID: 30170459 DOI: 10.1097/MD.0000000000012154]

14 **Goldman RD**, Carter S, Stephens D, Antoon R, Mounstephen W, Langer JC. Prospective validation of the pediatric appendicitis score. *J Pediatr* 2008; **153**: 278-282 [PMID: 18534219 DOI: 10.1016/j.jpeds.2008.01.033]

15 **Samuel M**. Pediatric appendicitis score. *J Pediatr Surg* 2002; **37**: 877-881 [PMID: 12037754 DOI: 10.1053/jpsu.2002.32893]

16 **Yang YL**, Huang YH, Tiao MM, Tang KS, Huang FC, Lee SY. Comparison of clinical characteristics and neutrophil values in omental infarction and acute appendicitis in children. *Pediatr Neonatol* 2010; **51**: 155-159 [PMID: 20675239 DOI: 10.1016/S1875-9572(10)60029-0]

17 **Grattan-Smith JD**, Blews DE, Brand T. Omental infarction in pediatric patients: sonographic and CT findings. *AJR Am J Roentgenol* 2002; **178**: 1537-1539 [PMID: 12034634 DOI: 10.2214/ajr.178.6.1781537]

18 **Schlesinger AE**, Dorfman SR, Braverman RM. Sonographic appearance of omental infarction in children. *Pediatr Radiol* 1999; **29**: 598-601 [PMID: 10415186 DOI: 10.1007/s002470050657]

19 **Lim S**, Hong HS, Kim YT, Lee HK, Lee MH. Computed Tomography and Ultrasound of Omental Infarction in Children: Differential Diagnoses of Right Lower Quadrant Pain. *J Korean Soc Radiol* 2013; **68**: 431-437 [DOI: 10.3348/jksr.2013.68.5.431]

20 **Bianchi F**, Leganés Villanueva C, Brun Lozano N, Goruppi I, Boronat Guerrero S. Epiploic Appendagitis and Omental Infarction as Rare Causes of Acute Abdominal Pain in Children. *Pediatr Rep* 2021; **13**: 76-85 [PMID: 33562670 DOI: 10.3390/pediatric13010010]

21 **Moteki T**, Horikoshi H. New CT criterion for acute appendicitis: maximum depth of intraluminal appendiceal fluid. *AJR Am J Roentgenol* 2007; **188**: 1313-1319 [PMID: 17449776 DOI: 10.2214/AJR.06.1180]

22 **Balthazar EJ**, Lefkowitz RA. Left-sided omental infarction with associated omental abscess: CT diagnosis. *J Comput Assist Tomogr* 1993; **17**: 379-381 [PMID: 8491897 DOI: 10.1097/00004728-199305000-00007]

23 **Loh MH**, Chui HC, Yap TL, Sundfor A, Tan CE. Omental infarction--a mimicker of acute appendicitis in children. *J Pediatr Surg* 2005; **40**: 1224-1226 [PMID: 16080922 DOI: 10.1016/j.jpedsurg.2005.05.002]

Published by **Baishideng Publishing Group Inc**
7041 Koll Center Parkway, Suite 160, Pleasanton, CA 94566, USA
Telephone: +1-925-3991568
E-mail: bpgoffice@wjgnet.com
Help Desk: https://www.f6publishing.com/helpdesk
https://www.wjgnet.com